IAEA-TECDOC-336

TRANSACTINIUM ISOTOPE NUCLEAR DATA – 1984

PROCEEDINGS OF THE THIRD ADVISORY GROUP MEETING
ON TRANSACTINIUM ISOTOPE NUCLEAR DATA
ORGANIZED BY THE
INTERNATIONAL ATOMIC ENERGY AGENCY
AND HELD IN UPPSALA, 21–25 MAY 1984

A TECHNICAL DOCUMENT ISSUED BY THE
INTERNATIONAL ATOMIC ENERGY AGENCY, VIENNA, 1985

PLEASE BE AWARE THAT
ALL OF THE MISSING PAGES IN THIS DOCUMENT
WERE ORIGINALLY BLANK

DISCLAIMER

Portions of this document may be illegible in electronic image products. Images are produced from the best available original document

The IAEA does not maintain stocks of reports in this series. However, microfiche copies of these reports can be obtained from

INIS Clearinghouse
International Atomic Energy Agency
Wagramerstrasse 5
P.O. Box 100
A-1400 Vienna, Austria

Orders should be accompanied by prepayment of Austrian Schillings 80.00 in the form of a cheque or in the form of IAEA microfiche service coupons which may be ordered separately from the INIS Clearinghouse.

TRANSACTINIUM ISOTOPE NUCLEAR DATA – 1984
IAEA, VIENNA, 1985
IAEA-TECDOC-336

Printed by the IAEA in Austria
May 1985

CONTENTS

MEETING SUMMARY

A. Introduction

The third Advisory Group Meeting on Transactinium Isotope Nuclear Data (TND) was convened by the IAEA Nuclear Data Section as a sequel to the first two IAEA Advisory Group Meetings on Transactinium Isotope Nuclear Data, held at the Kernforschungszentrum Karlsruhe, Fed. Rep. of Germany, in November 1975 and in Cadarache, France in May 1979. This meeting was held at the Gustaf Werner Institute of the University of Uppsala, in Uppsala, Sweden, from 21-25 May 1984. The meeting was attended by 32 participants and 5 observers from 15 Member States and 2 international organizations.

B. Objectives

Transactinium isotopes comprise all isotopes heavier than actinium (i.e., Z larger than 89). They play important roles in the nuclear fuel cycles of both thermal and fast reactors, and have found increasing areas of applications in science and industry. The quantitative appraisal of the role and applications of these isotopes can only be done with an adequate knowledge of their nuclear characteristics, that is their nuclear data.

The participants of the first meeting recognized that transactinium isotopes had become more and more important in nuclear technology, and that the knowledge of nuclear data required to evaluate the effects of transactinium isotopes in nuclear technology was not satisfactory. Recommendations of the 1975 meeting led to the formation of two IAEA-sponsored coordinated research programmes: one on the intercomparison of evaluations of transactinium isotope neutron nuclear data, the other on the measurement and evaluation of transactinium isotope decay data.

Since the time of the first meeting, a considerable amount of effort has gone into TND measurements and evaluations aiming specifically to satisfy data requirements which were identified at the first two TND meetings.

The primary objective of this third TND meeting was to review the developments which have taken place in the TND field since then, and to identify those data which are still discrepant or which do not satisfy the required accuracies.

C. Meeting proceedings and achievements

During the first two days of the meeting, eight review papers and seventeen contributed papers were presented. The titles and authors are listed in the Table of Contents. During the following two days, three working groups reviewed the data status and drafted specific conclusions and recommendations in the form of Working Group Reports. The Summary Report of the meeting, including the conclusions and recommendations, and the Working Group reports are published separately in INDC report INDC(NDS)-158/L.

REVIEW PAPERS

Review Paper 1

TESTING OF EVALUATED TRANSACTINIUM ISOTOPE NEUTRON DATA AND REMAINING DATA REQUIREMENTS

H. KÜSTERS
Institute of Neutron Physics and Nuclear Engineering,
Nuclear Research Centre Karlsruhe,
Karlsruhe, Federal Republic of Germany

Abstract

The paper reviews the formation of minor actinides in light water and fast reactors, as well as the current status and recent improvements in the nuclear data for minor actinides, and compares recently evaluated data with experimental results. The paper also describes the qualification of nuclear data by post-irradiation analysis and integral measurements in fast critical assemblies.

1. Introduction

The first international meeting on transactinium isotope nuclear data, held in Karlsruhe in 1975 /1/, mainly dealt with neutron cross-sections and other nuclear properties as e.g. decay constants of minor actinide isotopes, abbreviated in this paper to MINACs. For the plutonium and the thorium fuel cycle, the MINAC isotopes are ^{230}Th up to ^{244}Cm with the exception of the main nuclei ^{232}Th, ^{233}U, ^{235}U, ^{238}U, ^{239}Pu, ^{240}Pu and ^{241}Pu (sometimes the higher Pu isotopes are incorrectly counted as MINACs; for special interests the curium isotopes beyond mass number 244 are also included in the MINAC list).

Minor actinide isotopes are understood to be of "minor importance" in thermal and fast reactor design. This minor importance is regarded with respect to the influence of these nuclei on the reactivity balance or the neutron spectrum of a nuclear plant. However, the MINACs can be of prime importance in the out-of-pile stages of the nuclear fuel cycle, especially in determining the decay heat and the neutron as well as alpha, beta and gamma radiation of spent nuclear fuel after discharge from the reactor. These aspects are essential for designing safe transport casks and intermediate storage facilities, reprocessing units and waste disposal sites.

The intensive discussion on the nuclear data aspects of MINACs originated from the predicted expansion of nuclear energy after the first oil crisis in 1973. Reprocessing units of sizes up to 1500 to/yr throughput were dis-

cussed, recycling of Pu in thermal reactors was, and in some countries is considered as a serious strategy besides the introduction of Pu into fast breeder reactors; also U-recycling came into the discussion. Almost in parallel the problem of safeguarding fissile material became essential, leading to "dirty fuel cycle concepts" in the INFCE discussions. Here minor actinides (mainly those of the thorium cycle) played a major role.

These ambitious plans meanwhile have changed and become more moderate because the nuclear energy demand has not increased as anticipated; reprocessing plants are designed now for a size of about 350 to/yr throughput and alternate fuel cycles are practically out of discussion; direct storage of spent fuel has gained some interest (for economic reasons). Presently extended burn-ups of PWRs up to and even above 50000 MWd/t are under investigation besides recycling of Pu in thermal reactors.

These more "down to earth" projects nevertheless all require a good knowledge of the concentrations of minor actinides in spent fuel, because the concentrations of these isotopes increases both with extending the burn-up and with multiple recycling of fissile material in thermal reactors.

Some studies continue to investigate actinide recycling (Am, Cm) to reduce the hazards in a perpetual storage from the long-lived alpha emitters besides plutonium, or to separate Np from the waste. Also studies on recycling actinides and non-volatile fission products using the AIROX process are performed. To determine the possible risks associated with fuel handling in the various stages of these complex fuel cycles, the radiation level of the MINACs is of prime importance, strongly depending on the corresponding nuclear data in the generation and decay process.

Having observed in 1975 large discrepancies and gaps for the MINAC cross-sections in the data files existing at that time, a fruitful international effort started to improve the data basis of MINACs, both experimentally and theoretically. To test the adequacy of these improved data, C. Reich requested in 1979 /2/ "well-documented benchmark-quality depletion measurements or to identify if they exist".

Although already the second Advisory Group Meeting in 1979 /3/ included also the data status of the main transactinium isotopes, the present paper will summarize the work of testing the minor actinide neutron data only;

the status of the main transactinium isotope nuclear data is well known from the experience in thermal and fast reactors; important long standing discrepancies as e.g. the neutron capture data for ^{238}U could not be removed up to now, and there seems to be little hope that this is possible with the present experimental techniques. These data will not be discussed here.

In this paper, experimental and calculated resonance integrals as well as measured and calculated nuclide concentrations in post-irradiation analyses only for MINAC isotopes are compared. The paper will be restricted to the U-Pu fuel cycles in thermal and fast reactors.

From this intercomparison and from sensitivity studies, remaining data requests are deduced.

2. Formation of Minor Actinides in Light Water Reactors and Fast Reactors, and Related Nuclear Data Requests

As already mentioned in the introduction, the discussion in this paper deals with nuclides in the U-Pu fuel cycle. The importance of the nuclei in question has been discussed in many publications; sensitivity studies have led to data accuracy requirements. Therefore this section summarizes the main aspects of the formation and importance of MINACs in relation to nuclear data, to give an adequate background for the subsequent discussion.

2.1 General Importance of Minor Actinides

The following summary briefly describes the main reactor physics aspects of the MINAC isotopes in the various stages of the nuclear fuel cycle (see e.g. /4/).

General Importance of Minor Actinides (MINACs

Fuel Cycle Stage	Reactor Physics Aspects	Important MINACs
a) In-Pile:	Reactivity ($\frac{\Delta k}{k} > 10^{-3}$) cycle length, (breeding, conversion)	U234, U236 Np237, Pu238(FBR) Pu242, Am241(R)+) Am243(R)+)
With the exception of U236, total reactivity effects are small, partly due to compensation.		
b) Shut-Down:	Reactivity margin, subcriticality, (heat is mainly produced by FP)	U234, U236 Np237, Pu242 Am241 (R) Am243 (R)
c) Transportation and interim storage:	Subcriticality, radiation (n + γ)	U236, Np237 Am241, Cm242 Cm244
d) Reprocessing:	Radiolysis Separation Subcriticality in dissolver (low burn-up) (activity : FP)	Pu238 Cm244 Np237
e) Refabrication:	n + γ radiation Pu-aerosols	Pu236 U232 TL208 Pu238 Am241
f) Waste:	n + γ radiation during vitrification long-term hazard	Pu losses Am241 Am243 Cm244

+) R = Pu recycling, i.e. important in recycling strategies.
FP = Fission products

2.2 The Inventory of Minor Actinide Isotopes in Thermal and Fast Reactors of 1250 MWe at Fuel Discharge

As a measure of practical importance of minor actinides the concentration of these isotopes in actual reactors is presented in this section.

Present-day commercial PWR plants, like the KWU-Biblis reactor, have an electrical output of about 1250 MWe. For this reactor type, the inventory of MINACS is calculated for two burn-up values: for 33 GWd/t and for the extended burn-up of 40 GWd/t (even higher burn-up values are envisaged, but a natural limit lies in the range between 45 - 50 GWd/t, if zircaloy is used as clad material in these reactors). The inventory is calculated at fuel discharge /5, 6/. Major changes in MINAC-concentrations after discharge occur for the following isotopes: Pu236 (2.9y half-life) → U232, Pu241 (14.9y) → Am241 and Cm242 (163d) → Pu238; the corresponding concentrations of these isotopes at any further stage of the fuel cycle (e.g. at reprocessing) can easily be evaluated.

Furthermore, the inventory of the mixed oxide (MOX) fuel part in a mixture of a 70% U- and 30% MOX-fuelled PWR, as foreseen in Pu-recycling /7/ is given; for this type of reactor the burn-up was also calculated to 33 GWd/t to be compared to the results from a usual fuel loading. It should be mentioned that in the Pu-recycling case the MINAC concentration is reduced in the dissolution process of a reprocessing plant, due to common reprocessing of MOX- and uranium fuel elements.

Results are collected in Tab. 2-1. It can be seen that the increase in burn-up mainly influences Pu236, Pu238 and, to a major extent, Cm244; in the case presented here, the Cm244 content is roughly doubled in a MOX- compared to an initial uranium loading.

In Tab. 2-2, the MINAC concentrations in a Fast Reactor of 1250 MWe (Superphénix type) are given at fuel discharge; the core burn-up is 63 GWd/t, the mixed core and axial blanket burn-up in a common reprocessing strategy is 41 MWd/t. For comparison, the inventories are calculated for a start-up loading with PWR-plutonium, and for an equilibrium cycle /8/. As is expected, the MINAC concentrations are all larger for the start-up case with PWR-plutonium fuel; of main importance is the increase in Pu236,

MINAC	3.2% U235 33 GWD/T	3.6% U235 40 GWD/T	B-40 / B-33	PU-RECYCLE (30% MOX,70%U) MOX-FUEL 33 GWD/T	RECYC / NORMAL
U234	145	160	1.1	49	0.3
U236	4050	4820	1.2	762	0.2
NP237	426	552	1.3	170	0.4
PU236	1.6 - 3	2.4 - 3	1.5	1.2 - 3	0.8
PU238	132	195	1.5	997	8
PU242	486	637	1.3	8600	18
AM241	37	39	1.1	569	15
AM242M	0.4	0.41	1	8	20
AM243	84	127	1.5	1670	20
CM242	12	16	1.3	119	10
CM244	24	44	1.8	860	36

Tab. 2-1: Inventory of MINACs in a PWR of 1250 MWe at Discharge [gr/tHM]

MINAC	SPX START WITH PWR-PU: PU238:..:PU242 = 1.7:57:24:11:6	SPX IN EQUILIBRIUM PU238:..:PU242 = 0.15:71:24:3:1.5	START-UP LOAD / EQUIL. LOAD
NP237	181	179	1
PU236	1.1 - 3	5.4 - 4	2
PU238	1580	158	10
PU242	6480	1730	4
AM241	1830	266	7
AM242M	92	8	12
AM243	698	176	4
CM242	160	18	9
CM244	107	27	4

Tab. 2-2: Inventory [gr/tHM] of MINACs at Discharge in a FBR of 1250 MWe (Superphénix-Type) with Core Burn-up 63 GWd/t, Mixed Core and Axial Blanket Burn-up 41 GWd/t

Pu238 and the curia isotopes. The reason for the reduced concentration in the equilibrium case is the common reprocessing of core and axial blanket material, changing mainly the Pu-composition due to the admixture of almost pure Pu239 (i.e. practically no higher plutonia or MINACs) from the blankets.

2.3 Formation Routes of Important Actinides, Related Cross-Sections and their Accuracy Requests

From the previous discussion the most important MINAC isotopes in the U-Pu fuel cycle are: U236, Np237, Pu236, Pu238, Am241, Am243, Cm242 (decreased importance due to short half-life) and Cm244. U236 has a high neutron capture cross-section and influences strongly the reactivity balance end of cycle. Np237 is on the main route in U-fuelled reactors for the build-up of Pu236, which decays finally to Tl208 with a very strong γ-radiation. The strong α-decay of Pu238 is mainly responsible for radiolysis in reprocessing, in addition it forms a relatively intensive source for neutron emission. Gamma radiation from Am241 causes trouble in refabrication units, also neutron emission is important. Neutron capture in Am243 leads to the most intensive long-lived neutron source isotope Cm244; the alpha decay of Am243 produces Pu239, which is of some importance for the alpha activity of nuclear waste. Cm242 is a very strong neutron emitter, but is important only shortly after discharge, when spent fuel is being cooled at the reactor site. The alpha emitters Am241, Am243 and Cm244 contribute essentially to the long-term activity of stored high active waste (besides the losses of plutonium in a reprocessing unit).

If recycling of actinides in thermal or fast reactors is considered, then the Am isotopes also play a greater role in the in-pile reactivity balance, especially if Am-recycling is investigated. Studies on this topic are performed to evaluate a reasonable transmutation process of actinides /9/.

Tab. 2-3 represents the formation routes of important MINACs; the approximate formation rates of these isotopes through the various routes in a Pressurized Water Reactor and a Fast Reactor are also given in this table /10/ (EQUIL means the formation in an equilibrium cycle). From this information the main cross-sections for MINAC isotope generation can be deduced, e.g. by sensitivity studies. This is shown in Tab. 2-4 together with other reactions of prime importance for major actinides.

	APPROXIMATE FORMATION RATE IN A	
	PWR [%]	FBR [%]
U236. NP237. PU236		
U235(N.γ)U236(N.γ)U237(β)NP237(N.2N)NP236(β)PU236	80	10
(N.2N) U238	20	90
AM241. CM242. PU238		
PU241(β)AM241(N.γ)AM242G(β)CM242(α)PU238	~ 9	55 (EQUIL)-70
NP237(N.γ)NP238(β)PU238	91	15 - 30(EQUIL)
PU239(N.2N)PU238	< 0.1	15
AM1243. CM244		
PU242(N.γ)PU243(β)AM243	99.5	95 - 97 (EQUIL)
AM242M(N.γ)AM1243	0.5	5 - 3 (EQUIL)
AM243(N.γ)AM244(β)CM244	99.5	99.6 - 99.8
CM243(N.γ)CM244	0.5	< 0.4

Tab. 2-3: Formation - Routes of Important MINACs

PRIORITY 1 X-SECT. OF MINAC	OTHER REACTIONS OF PRIORITY 1
σ_C (U236)	$\sigma_{C,F}$ (U235)
σ_C (NP237)	$\sigma_{N,2N}$ (U238)
$\sigma_{N,2N}$ (NP237)	$\sigma_{C,F}$ (PU239.240.241)
BRANCHING TO NP236*	$\sigma_{N,2N}$ (PU239)
σ_F (PU238) (FBR)	λ_β (PU241)
σ_C (AM241)	
BRANCHING TO AM242M AM242G	λ_α (CM242)
σ_C (PU238) (FBR)	

Tab. 2-4: Priority I Cross-Sections for MINAC-Formation due to Sensitivity Studies

Besides the (n,2n) cross-section of Np237 the main concern has to be given to the capture data. The fission cross-section is usually much smaller, but in those cases where a fission threshold is used in neutron dosimetry (e.g. Np237), special care has to be taken. Tab. 2-5 lists the average one-group cross-sections for fission and capture processes in a PWR and a FBR /11/.

MINAC	PWR σ_C	PWR σ_F	FBR σ_C	FBR σ_F
U236	6.2	0.2	0.74	0.093
NP237	30	0.6	1.8	0.3
PU236	20.	21.	1.6	1.4
PU238	32	2.4	0.7	1.0
PU242	25	0.5	0.6	0.25
AM241	95	1.1	1.9	0.27
AM242M	155.	770.	0.46	3.9
AM243	46	0.7	1.5	0.2
CM244	17	1.6	0.68	0.42
	$\sigma_C \gtrsim 10.\sigma_F$ (EXC : PU236, AM242M)			

Tab. 2-5: Approximate One-Group Cross-Sections [b] (near EOC)

In 1975, the nuclear data status and the requests for actinide nuclear data were formulated /12/. A comprehensive list of status and accuracy requests is reproduced as Tab. 2-6 from Ref. 13. Most of the requests for the MINAC isotopes were not met, in some cases the status could not even be defined. Two examples of integral tests, one for a PWR, one for a Fast Critical Assembly, are shown in Tab. 2-7 and Tab. 2-8, see e.g. Ref. 14. The integral tests confirm that there exist large uncertainties in the basic nuclear data, leading to corresponding large discrepancies between calculated and measured MINAC concentrations or MINAC reaction rates, even if some adjustment in the cross-sections to meet the experimental U238 concentration is made; this is not surprising at all.

As mentioned earlier, the world-wide effort to improve the nuclear data situation by experiments and evaluations, indeed succeeded quite considerably, as will be discussed in the following chapter.

Isotope	Half-Life $T_{1/2}$	Decay Properties: Type	Decay Properties: Accuracy (%) Requested	Decay Properties: Accuracy (%) Status	Cross Sections: Type Therm. React.	Cross Sections: Type Fast React.	Cross Sections: Accuracy (%) Request Therm.	Cross Sections: Accuracy (%) Request Fast	Cross Sections: Accuracy (%) Status Therm.	Cross Sections: Accuracy (%) Status Fast
Pa231	$1 \cdot 10^4$Y				C/I_c		10/20		10/7	
Pa233	27.d				C/I_c		10/10		12/4	
Th232	$1 \cdot 10^{10}$Y				(n,2n)		50		-	
U232	74Y				$C/I_c/F/I_f$		30/30/30/30		2/6/12/15	
U233	$1.6 \cdot 10^5$Y				(n,2n)		10		-	
U234	$2.5 \cdot 10^5$Y	α-Intensity	1	3	C/I_c		5/5		2/12	
U236	$2.4 \cdot 10^7$Y	λ	1	2	C/I_c		4/4		6/6	
U237	6.7d				C/I_c		100/100		33/18	
Np237	$2.2 \cdot 10^6$Y	α-Intensity	1	20	C/I_c	C,F,(n,2n)	100/10	30/50/50	2/8	50/10/-
Np239	2.3d				C	C/F	100	20/50		/-
Pu236	2.8Y				C/I_c	C/F	100/100	30/50	-/-	-/-
Pu238	86.4Y	λ/ (γ/α)-Int.	0.5/1/0.1	1.5/25/1	$C/I_c/F$	C/F	30/50/50	20/7	4/10/3	30/10
Pu240	$6.6 \cdot 10^3$Y	λ/ (γ/α)-Int.	0.2/1/0.2	5/Fact/1	C/I_c		2/1	•	1/12	
Pu241	13.2Y	λ/γ-Int.	1/1	5/5	$C/I_c/F$		3/10/1	•	3/5/1	
Pu242	$3.8 \cdot 10^5$Y	λ/α-Int.	1/4	5/10	C/I_c		10/5	•	4/4	
Am241	458Y	γ-Intensity	1	2	C/I_c	C/F	10/10	5/15	3/9	30/30?
Am242M	152Y				$C/I_c/F$	C/F	50/50/30	50/15	-/-/4	-/50
Am243	795Y				C/I_c	C/F/(n,2n)	15/10	10/30/50	5/3	-/10/-
Cm242	163d	λ	0.1	1	C/I_c	C/F	50/50	60/25	50/30	-/-
Cm243	35Y				$C/I_c/F$	C/F	50/50/50	30/20	-/-/7	-/-
Cm244	18Y				C/I_c	C/F	50/50	50/50	20/10	-/30?

Tab. 2-6: Comparison of Requested and Achieved Accuracy of TNO (1975)

• Requests according to WRENDA

C : Capture I_c : Resonance Integral for neutron capture

F : Fission I_f : Resonance Integral for neutron fission

NUCLIDE	$\frac{E-C}{E}$ %
U234/U	7.1
U236/U	- 1.4
PU238/PU	15.4
PU242/PU	1.7
AM241/AM	- 5.7
AM242M/AM	FACTORS
AM243/AM	8.8
CM242/CM	70
CM243/CM	88
CM244/CM	- 7.6

Tab. 2-7: Deviation ($\frac{E-C}{E}$ %) of Isotopic MINAC-Compositions for the US-Robinson PWR at Discharge (ORIGEN73, Adjusted to U238)

ISOTOPE I	ZEBRA 1975	SNEAK 1975	
	σ_F^I/σ_F(PU239)	σ_F^I/σ_F(PU239)	$1+\delta_F^I/\delta_F$(PU239)
PU242	1.23 ± 5 %	-	-
AM241	1.26 ± 4 %	1.4 ± 2 %	1.95
AM243	0.88 ± 4 %	-	-
CM244	1.35 ± 8 %	-	-

Tab. 2-8: Calculated and Measured Reaction Rate Ratios in Fast Critical Assemblies (C/E): 1975

3. Some Examples for Recent Improvements in Nuclear Data for Minor Actinides

The main aspect of this chapter is to present some of the features of the KEDAK evaluation for Am and Cm isotope cross-sections /15/, because those Karlsruhe tests on MINAC data in integral experiments, to be discussed in chapter 4 to chapter 6, are based on these data. More examples will be found in the contributions to this conference.

Fig. 3-1 compares the KEDAK evaluation for the total, the fission and capture cross-sections for Am241 with other evaluations and with new measurements on differential data in the keV and MeV neutron energy range /15/. It should be noted that the theoretical KEDAK curves for the total cross-section and for the subthreshold fission are predictions! The agreement between the KEDAK data and the measurements is excellent. A similar good agreement is achieved for low neutron energies.

Fig. 3-2 shows the comparison of the KEDAK capture cross-section for Am243 in the keV range with ENDF/B-V data and very recent measurements from Wisshak and Käppeler /16/. Both the experimental and KEDAK agree well, and are higher by about 50% compared to ENDF/B-V.

Fig. 3-3 gives the evaluation of the KEDAK subthreshold fission data for Am243 in comparison to evaluations in the ENDF/B-V, JENDL-2 and UKNDL data libraries. A wide spread between the different evaluations can be observed. Differential measurements by Behrens and Wisshak in 1981 and 1982 are excellently predicted by the KEDAK evaluation.

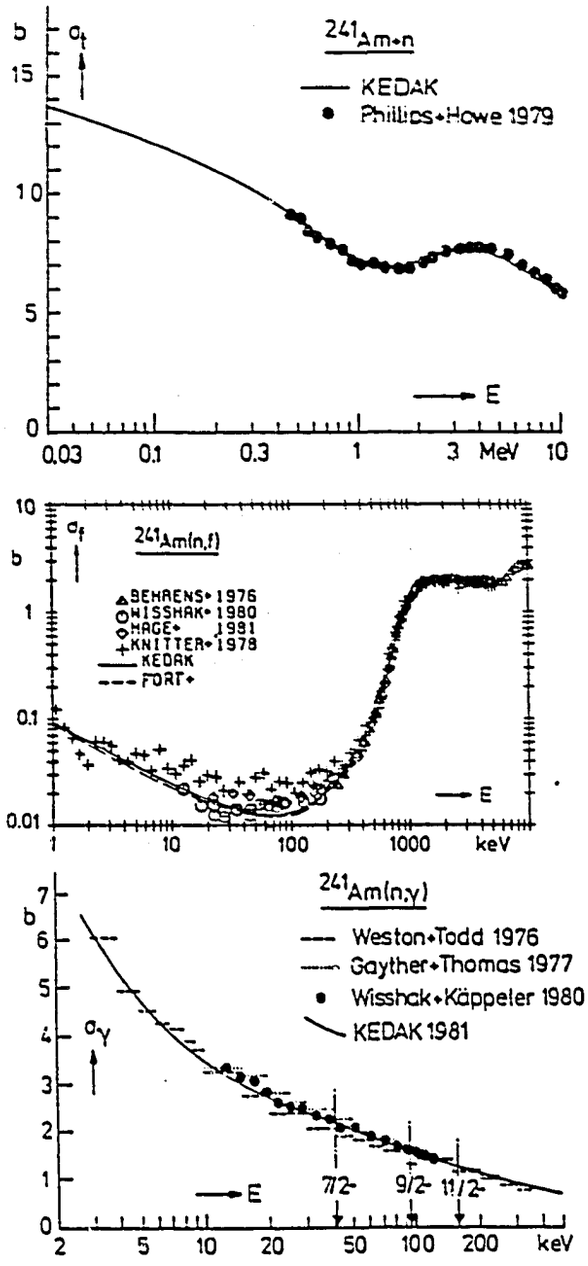

Fig. 3-1:

Calculated and Measured Nuclear Data for the Total, Fission and Capture Cross Section of ^{241}Am.
Note: The Theoretical Curve for the Total and Sub-threshold Fission data are Predictions.

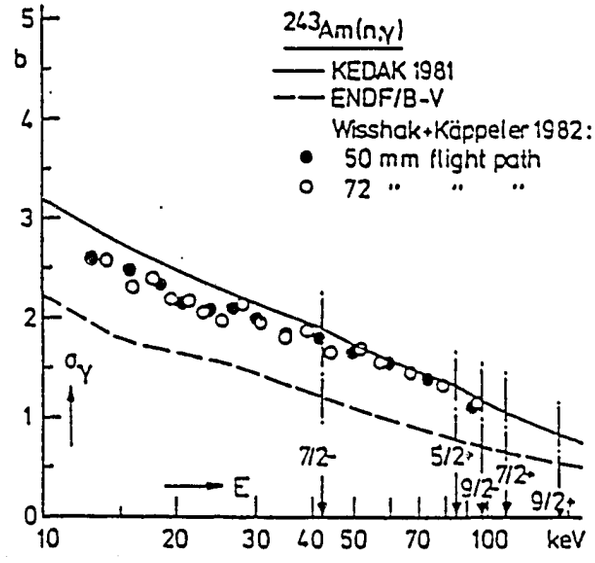

Fig. 3-2: The Capture Cross-Section of ^{243}Am in the keV Energy Range

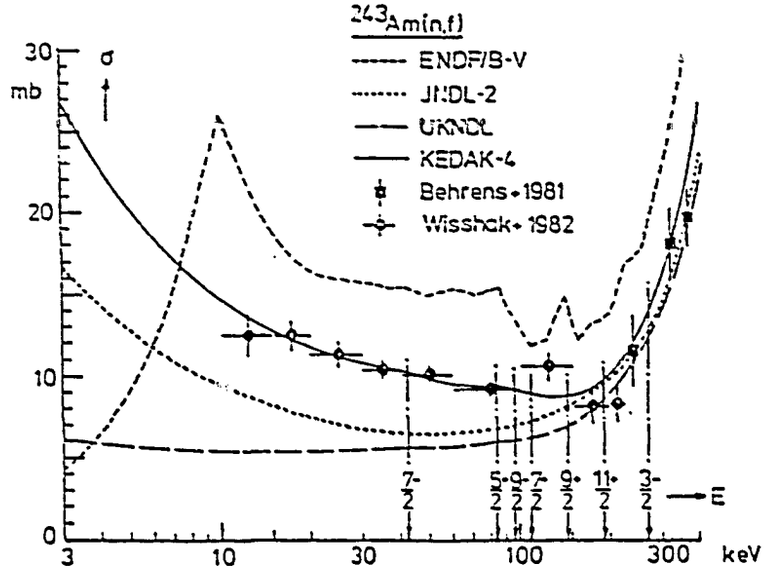

Fig. 3-3: The Fission Cross-Section of ^{243}Am in the keV Energy Range

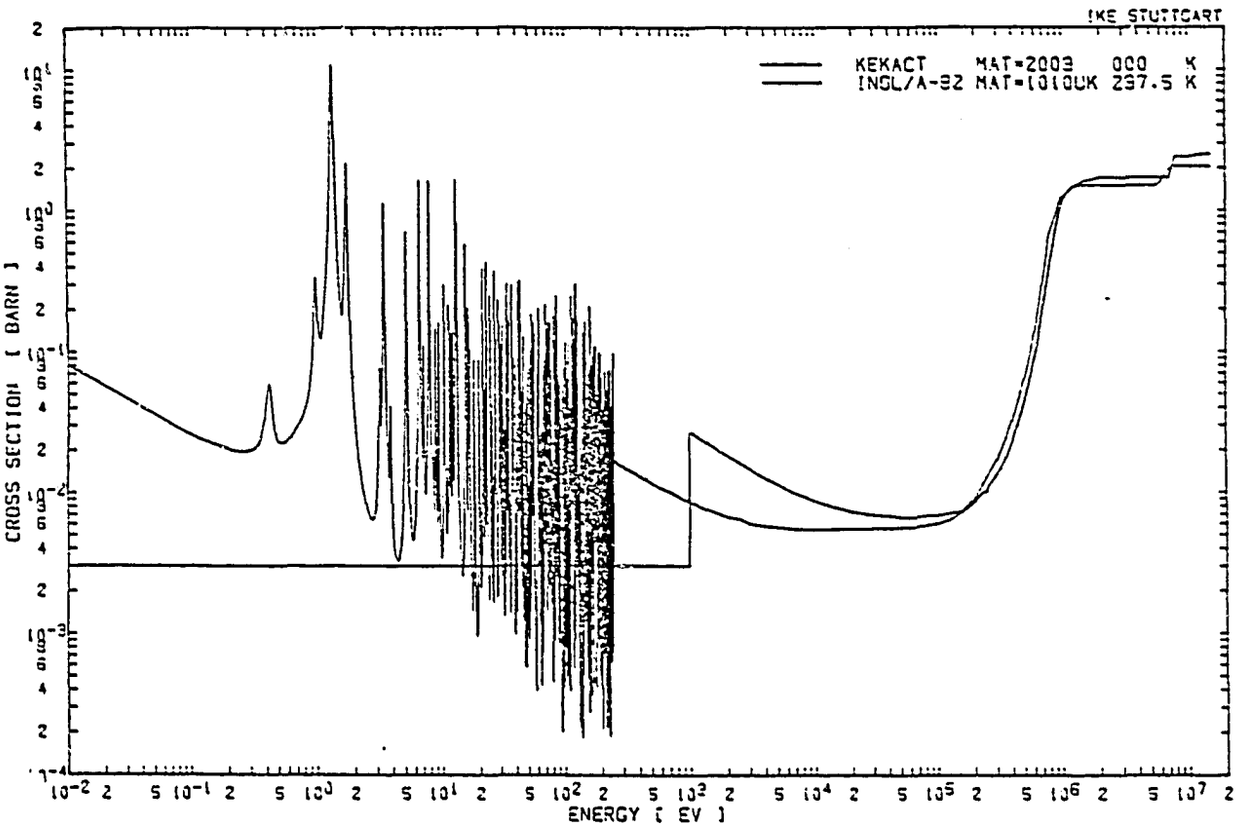

Fig. 3-4: The Fission Cross-Section of ^{243}Am

In the energy region below 1 keV large discrepancies for the fission cross-section of Am243 remain. Due to lack of information, the KEDAK evaluators assumed a constant fission cross-section; an unpublished evaluation performed in Harwell (1983) has a very distinct resonance structure, as shown in Fig. 3-4 /17/. Although the low energy fission cross-section of Am243 is small and of no practical importance, the discrepancy should be resolved.

A similar discrepancy exists for the evaluated fission cross-sections of Cm242 over the whole energy range up to 10 MeV between a Bologna evaluation and ENDF/B-V; this is depicted in Fig. 3-5 /17/.

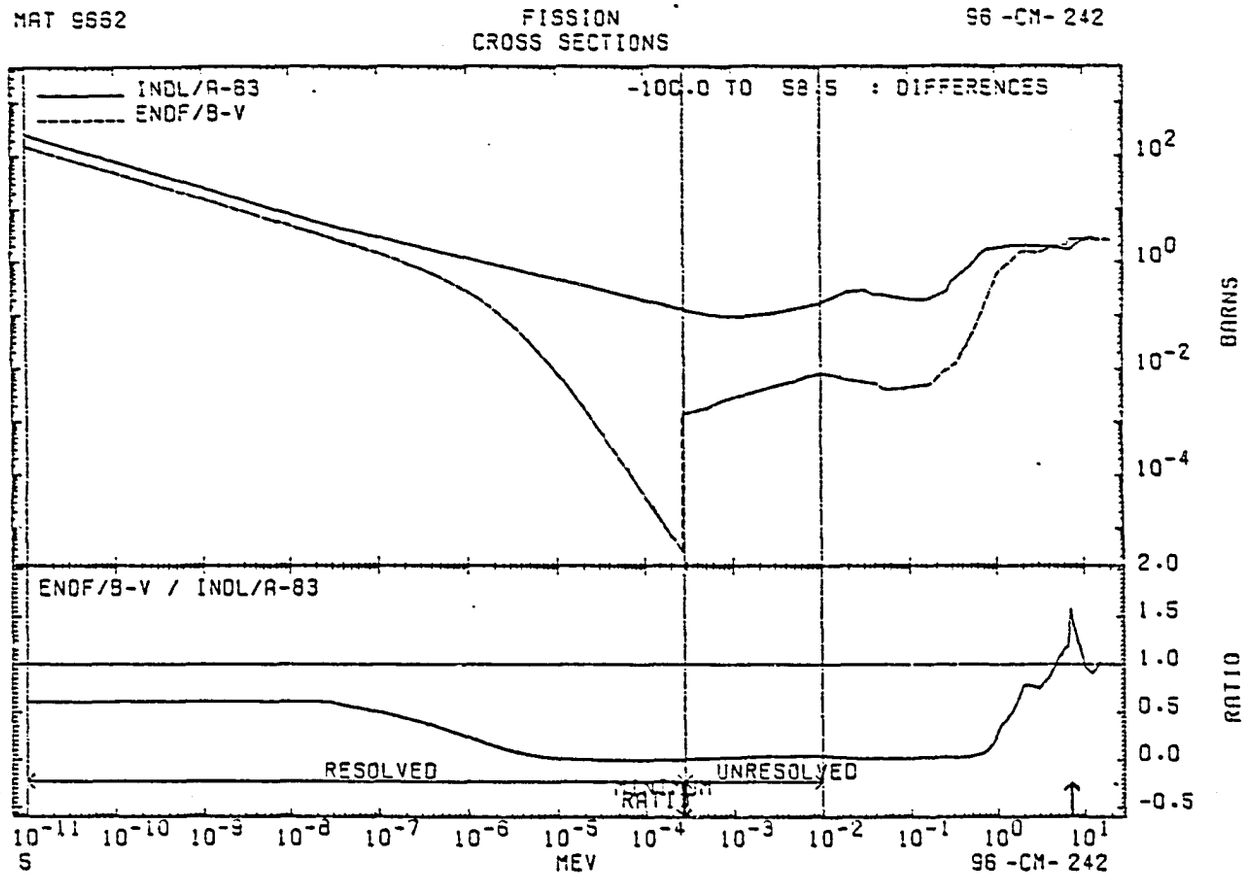

Fig. 3-5: The Fission Cross-Section of ^{242}Cm

As another example the (n,2n) cross-section and corresponding branching ratio of Np237 are discussed. Fig. 3-6 is reproduced from the 1983 NEANDC-INDC joint discrepancy file /18/. Although the notation is somewhat confusing with respect to the build-up of Pu236, the present uncertainties in the cross-section itself and in the branching ratio are clearly seen; a further comparison of various evaluations of the (n,2n) cross-section for Np237 is shown in Fig. 3-7 /17/: large discrepancies exist near the threshold in all evaluations, even the plateau around 12 MeV is very uncertain, about a factor of 2.5 exists between ENDF/B-V and the recent

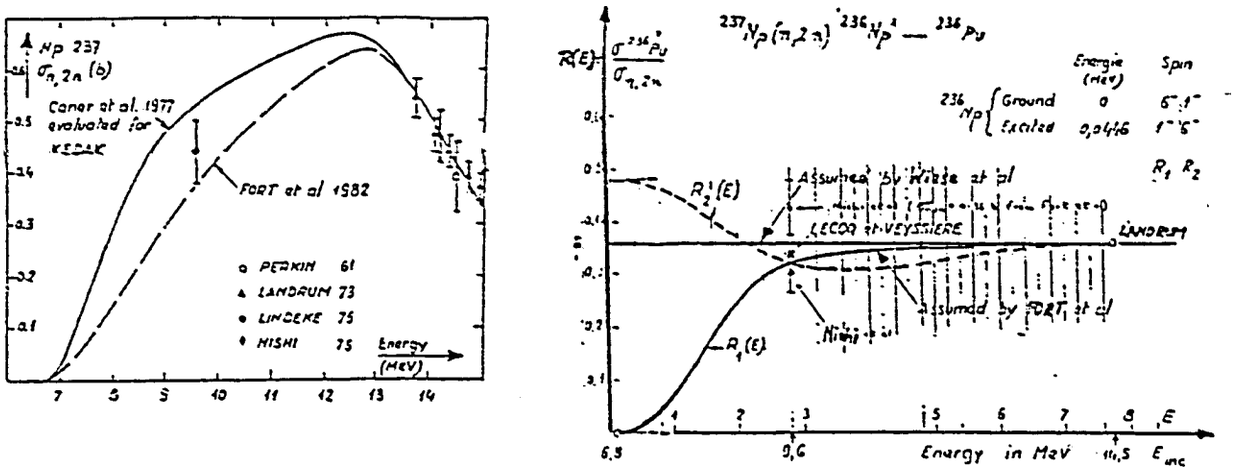

Fig. 3-6: Evaluated and Measured (n,2n) Cross-Sections for Np237 and the Corresponding Branching Ratios

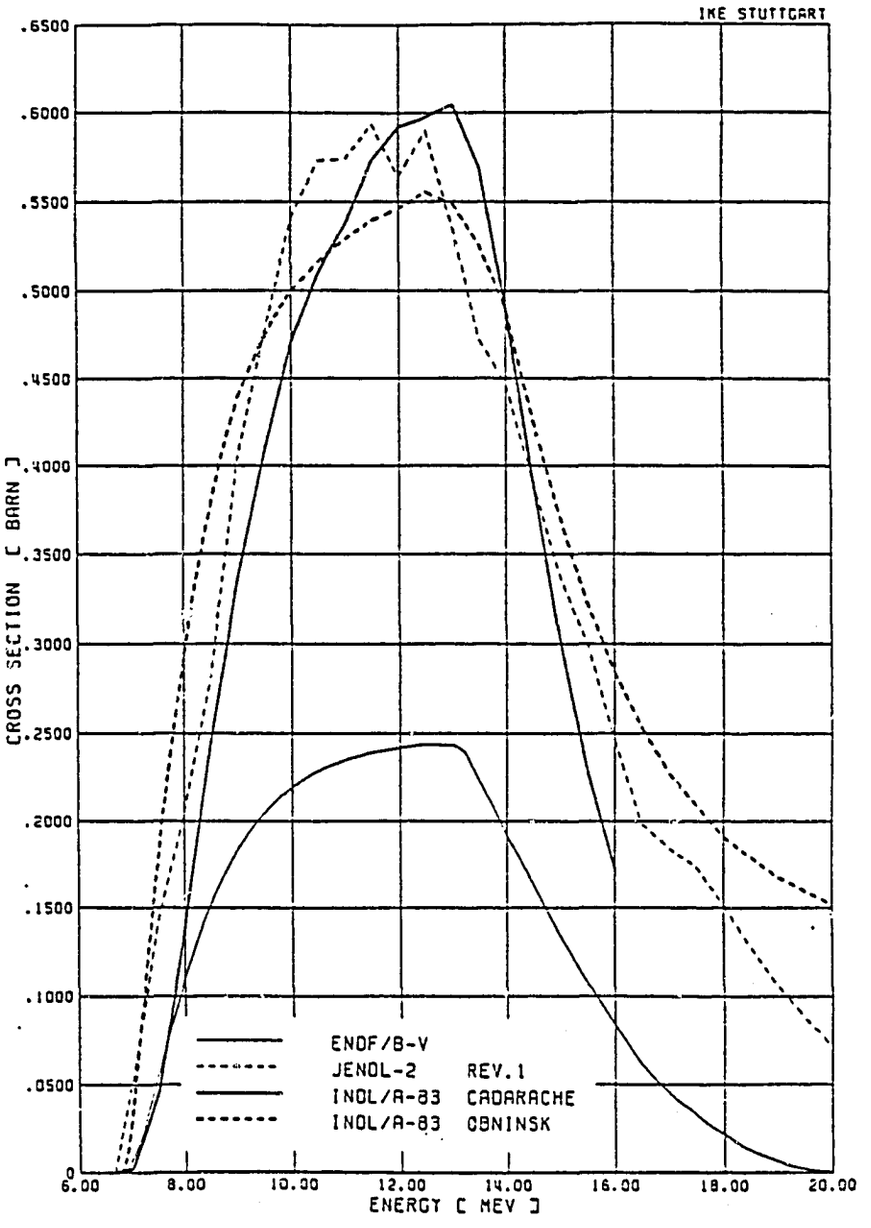

Fig. 3-7: The (n,2n) Cross-Section of ^{237}Np

Cadarache evaluation. This situation renders the prediction of Pu236 in nuclear reactors rather doubtful.+)

From this brief summary follows that with the exception of the (n,2n) reaction cross-section for Np237 most of the discrepancies in the important data of minor actinide isotopes in fission reactor applications have been considerably reduced. Whether these data fit integral experiments, will be shown in the following chapters.

4. Comparison of Recently Evaluated Thermal Neutron Cross-Sections and Resonance Integrals for Minor Actinides with Experimental Results

The quality of evaluated nuclear data in reactor physics applications are tested at first on measurements in a well defined environment: These measurements concern the 2200 m/s values and the resonance integrals for neutron fission and neutron capture. The intercomparison may not be unproblematic, because sometimes no correction has been applied for e.g. the decay of isotopes, and for the resonance integrals the cadmium cut-off energy sometimes is not stated by experimenters, which especially is important if the nucleus in question has resonances in that energy region (as e.g. Am241). There also exists the possibility of comparing calculated and measured cross-sections, averaged over a fission spectrum. The interpretation of the measurements themselves is rather complicated and therefore the results are often uncertain (sophisticated transport theory has to be applied to determine these high leakage measurements). This intercomparison is not performed here.

+) Remark: New measurements of the $^{237}Np(n,2n)\ ^{236}Np(22.5h)$reaction cross-section, which determines the Pu236 build-up, were contributed by N. V. Kornilov et al. to the 1984 IAEA Advisory Group Meeting in these proceedings; the discrepancies now seem to be practically removed; support of the KEDAK data is indicated.

4.1 Preliminary Intercomparison of Nuclear Data for Minor Actinides

For the various evaluations of the Coordinated IAEA Research Programme on Evaluated Neutron Reaction Data for Actinides /19/, M. Mattes and J. Keinert performed an intercomparison for thermal cross-sections and resonance integrals for an interim IAEA-data file (INDL/A-82) in 1982 together with the values given in BNL-325 (1973). The values in Tab. 4-1 are taken from Ref. 20. Although the data of INDL/A-82 meanwhile are partly superseded, and new integral measurements have been conducted since 1973, the table shows the differences in the various evaluations and thus gives an idea of the spread of data in 1982.

Generally, the spread in the thermal data and resonance integrals is rather wide, especially for the resonance integrals of the Am- and Cm-isotopes.

For Am241, the evaluated thermal capture cross-sections of INDL differ by about 5%, BNL-325 is higher by about 30% compared to all the evaluations. As quoted by Lynn et al. in Ref. 21, a proper correction for the half-life of Am241 and Cm242 as well as for the β-decay of Am242g leads to a deduced

Tab. 4-1: Comparison of Thermal Neutron Cross-Sections and Resonance Integrals from Different Evaluations (Mattes, Keinert, Stuttgart 1982)

ISOTOPE	LIBRARY	σ_γ(E=0,0253eV) BARN	σ_F(E=0,0253eV) BARN	I_γ (*) BARN	I_F (*) BARN
^{237}Np	INDL/A-82	181,02	0,018	653,83	5,83
	ENDF/B-V	169,10	0,017	640,43	6,87
	BNL-325	169±3	0,019±0,003	660±50	-
^{242}Pu	INDL/A-82	18,50	-	1126,8	5,34
	" USSR	18,65	0,001	1136,1	5,14
	" BOLOGNA	18,50	0,0010	1102,2	-
	ENDF/B-V	19,17	0,0010	1272,6	5,57
	BNL-325	18,5±0,4	< 0,2	1130±60	5

(*) CD CUTOFF ENERGY 0,5eV

Tab. 4-1: (continued)

ISOTOPE	LIBRARY	σ_γ(E=0.0253eV) BARN	σ_F(E=0.0253eV) BARN	I_γ (*) BARN	I_F (*) BARN
^{241}Am	INDL/A-82				
	UK	600.4	3.10	1414.8	15.0
	KEDAK	609.9	3.15	1438.2	15.6
	Bologna	625.3	3.15	1379.2	-
	Cadarache 83+)	577.3	3.10	1438.9	13.8
	ENDF/B-V	576.5	3.27	1420.5	13.4
	BNL-325	832±20	3.15±0.10	1477±120	21±2
^{242m}Am	INDL/A-82	1343.5	6624.8	206.55	1527.7
	ENDF/B-V	1343.5	6624.8	286.28	1883.4
	BNL-325	1400±860	6600±300	7000±2000	1570±110
^{243}Am	INDL/A-82	74.6	0.0029	1820.3	5.70
	" UK	77.0	0.0500	1845.7	5.95
	" Bologna	59.2	-	1785.	-
	ENDF/B-V	74.8	0.	1818.4	6.15
	BNL-325	79.3±2.0	< 0.07	1820±70	-

+) This evaluation from 1983 was added to the 1982 intercomparison.

(*) Cd Cutoff Energy 0.5eV

Tab. 4-1: (continued)

ISOTOPE	LIBRARY	σ_γ(E=0.0253eV) BARN	σ_F(E=0.0253eV) BARN	I_γ (*) BARN	I_F (*) BARN
^{242}Cm	INDL/A-82	15.93	5.0	116.13	11.09
	" Bologna	16.52	4.97	115.17	11.60
	ENDF/B-V	17.14	3.02	156.08	6.26
	BNL-325	16±5	< 5	150±40	-
^{244}Cm	INDL/A-82	14.41	1.18	593.09	17.80
	" KEDAK	14.41	1.03	632.66	18.96
	ENDF/B-V	10.37	0.60	593.51	18.70
	BNL-325	13.9±1.0	1.2±0.1	650±50	12.5±2.5
^{245}Cm	INDL/A-82	346.5	2001.6	107.71	799.03
	ENDF/B-V	383.0	2161.	117.52	833.18
	BNL-325	345±20	2020±40	101±8	750±150

(*) Cd Cutoff Energy 0.5eV

Tab. 4-1: (continued)

ISOTOPE	LIBRARY	σ_γ(E=0.0253eV) BARN	σ_f(E=0.0253eV) BARN	I_γ (*) BARN	I_f (*) BARN
^{246}Cm	INDL/A-82	1.46	0.140	110.62	6.94
	ENDF/B-V	1.30	0.063	103.81	10.42
	BNL-325	1.3±0.3	0.17±0.10	121±7	10.0±0.4
^{248}Cm	INDL/A-82	9.81	0.397	254.63	12.61
	ENDF/B-V	2.44	0.087	248.34	15.42
	BNL-325	4±1	0.34±0.07	275±75	13.2±0.8

(*) Cd Cutoff Energy 0.5eV

value of 612 25 barn, which is in a satisfactory agreement with the recent evaluations. For Cm248, both the thermal cross-sections for neutron capture and fission are discrepant by factors of more than two; fortunately this isotope has no importance in reactor physics application.

The most striking differences in the resonance integrals of Tab. 4-1 are those of I_γ for Am242m and I_f for Cm242. Although differential data for neutron capture in Am242m are very scarce, the quoted resonance integral must be in error: the measurements of Schuman /27/ coincide with the quoted 7700 barn, but this value corresponds to the resonance integral for neutron absorption, not capture (see section 4.2). In Tab. 4-1, evaluations give $I_\gamma \approx 200 - 300$ barn. For I_f (Cm242), the INDL values are twice the values given in ENDF/B-V; neutron fission in Cm242 is not an important reaction, nevertheless this discrepancy should be resolved.

As a general conclusion to this section, a meaningful comparison of evaluated data with results from integral experiments requires a thorough assessment of the accuracy of the experiments, a trivial statement, but it is not always respected. The following section especially deals with a recent critical assessment of resonance integrals.

4.2 Critical Assessment of Resonance Integrals for Am and Cm Isotopes

This section is based on the investigation of Goel and Fischer /22, 23/.

The review in Ref. 22 and Ref. 23 considers direct measurements of resonance integrals, which use more or less pure isotopes, and those data, which are derived from isotope production measurements in irradiated reactor fuels.

The direct measurement of resonance integrals uses the Cd-difference technique; the thickness of the Cd, covering the probe, determines the lower energy of neutrons which reach the sample. A precise knowledge of this Cd-cutoff energy is a prerequisite for an accurate evaluation of the resonance integral. This is especially important if resonances are near this cutoff.

The derivation of resonance integrals from isotope production measurements is complicated due to mutual resonance shielding effects, which influences the shape of the neutron flux to deviate from a 1/E behaviour. In addition, the accuracy, obtained from isotope production measurements, may be doubtful according to compensation of various uncertainties in the multiple absorption processes.

A brief summary of the critical discussion on the accuracy of resonance integrals is given below.

Am241

Resonance integrals of this isotope are strongly dependent on the Cd-cutoff energy and on impurities in the sample. The best available measurement for the capture resonance integral is that of Harbour et al. /24/. The measurement was performed with a highly pure (> 99.9% Am241) sample; the thermal to epithermal neutron flux ratio and the Cd-cutoff energy have been carefully evaluated. The recommended measured value for the capture resonance integral is I_γ^H = 1538±135 barn for a cutoff energy of 0.369 eV. The corresponding KEDAK-4 value for this cutoff energy is I_γ^K = 1549 barn, in excellent agreement with experiment.

Neutron fission in Am241 is less important than capture. Integral measurements by Gavrilov et al. /25/ are not fully consistent with those of Harbour, cited above. A value for the fission resonance integral is deduced to I_f^G = 22.5±0.25 barn; the corresponding KEDAK-4 value is I_f^K = 14.8 barn, which is lower by almost 40%; other measurements up to 1977 always gave results for I_f above 20 barn. Only very recently Dabbs et al. measured the Am241 fission cross-section at ORELA /26/. The fission resonance integral deduced from this experiment is significantly lower than the older values, namely I_f^D = 14.1±0.9 barn for a cutoff energy of 0.5 eV, which is fairly close to the corresponding theoretical values in Tab. 4-1 with the same cutoff. The discrepancy between the two sets of

experiments should be fully understood to gain more confidence in both experimental and theoretical values.

Am242m

The value of the absorption resonance integral of I_a^S = 7000±2000 barn in BNL-325 was measured by Schuman /27/; the resonance integral was deduced from an isotope production analysis, concurrent to Am241. The value for Am242m depends strongly on the cross-sections adopted for Am241. The large uncertainties in these data in 1969 cause a large error in the absorption resonance integral for Am242m; therefore these data are not reliable; the capture resonance integral should therefore be derived from differential measurements or evaluations. For KEDAK-4 one obtains I_γ^K = 280 barn and I_a^K = 1909 barn.

The fission resonance integrals are very discrepant in evaluations as well as in measurements. In the experiments of Zhuravlev /29/ the data were derived from a sample containing only about 1% Am242m, so that the main contribution to the fission rate came from Am241 and Am243; the result was I_f^Z = 2260±200 barn. Dabbs et al. published new fission cross-sections in 1983 /28/. These authors quote I_f^D = 1800±65 barn with a cutoff energy of 0.5 eV. This value is substantially larger than that of I_f^{BNL} = 1570±110 barn quoted in BNL-325.

Am243

Experimental results for the capture resonance integral from 1957 to 1977 agree within their quoted experimental uncertainties and yield I_γ^{Ex} = 2200 - 2300 barn. The values are not very dependent on the value of the Cd-cut-off energy. However, all evaluations come to values between about I_γ^T = 1800 - 1850 barn, being about 20% lower than the experimental results. An increase in the resonance parameters to match the experimental result cannot be justified at present. This discrepancy has to be resolved.

For the fission resonance integral the differential neutron data are very uncertain due to the lack of reliable experiments for this rather low cross-section of some barn. The available experimental resonance integrals differ by about a factor of two, being 9 barn (Zhuravlev /29/) and 17 barn (Gavrilov /25/). All evaluated values are around 6 barn (Tab. 4-1). Though

σ_f (Am243) is not very important, this large uncertainty should be removed.

Cm244

Experiments for the capture resonance integral are in agreement and give I_γ^{Ex} = 650±50 barn, see e.g. Ref. 30. The evaluation from KEDAK-4 gives I_γ^{K} = 637 barn (the slightly lower value of 633 barn in Tab. 4-1 is due to a slightly different procedure than that used at KfK). A good agreement between experiment and evaluation can be stated.

A critical discussion of the (not important) fission resonance integral recommends the careful measurement of Benjamin with a 99.02% Cm244 sample to I_f^{B} = 18±1 barn /31/. All evaluations give also data very near to 18 barn. Again agreement is achieved. But the deduced result from Thompson et al. /30/ yields a value of 12.5±2.5 barn; this discrepancy should be resolved.

Nuclide	KEDAK-4	Experiment
Am-241	1549	1538 ± 135
Am-243	1847	2210 ± 150
Cm-244	637	650 ± 50

Tab. 4-2: Resonance Integrals for Neutron Capture of Important Am and Cm Isotopes

In summary, Tab. 4-2 gives the intercomparison between calculated and recommended measured capture resonance integrals as the most important integral quantities for the essential isotopes in fuel cycle analyses; the basic differential data are taken from KEDAK-4.

From this table, only the difference of about 20% in the resonance capture data of Am243 needs further clarification, probably on the experimental side.

5. Qualification of Nuclear Data for Actinides by Postirradiation Analysis of Pressurized Water Reactor Fuel

The previous chapter showed that modern nuclear data of important minor actinide isotopes indeed agree satisfactorily well with carefully examined integral experiments for thermal cross-sections and resonance integrals; some further clarification is needed, but the target accuracies have almost been reached.

To broaden the experience, further comparisons between calculations and experiments in postirradiation analyses of PWR fuel were performed. The target quantities are nuclide concentrations of burnt fuel. Concentrations of all actinides have to be considered in postirradiation analyses to avoid any misinterpretation of possible discrepancies for a certain isotope. To judge the quality of both theoretical and experimental results, first the corresponding methods and techniques are investigated.

This chapter is based on studies done at the Nuclear Research Center Karlsruhe; most of the results are taken from Ref. 5 and Ref. 32.

5.1 Theoretical and Experimental Methods Used in Postirradiation Analysis

The general procedure at KfK to predict the nuclear properties of irradiated discharged PWR fuel is outlined in Fig. 5-1.

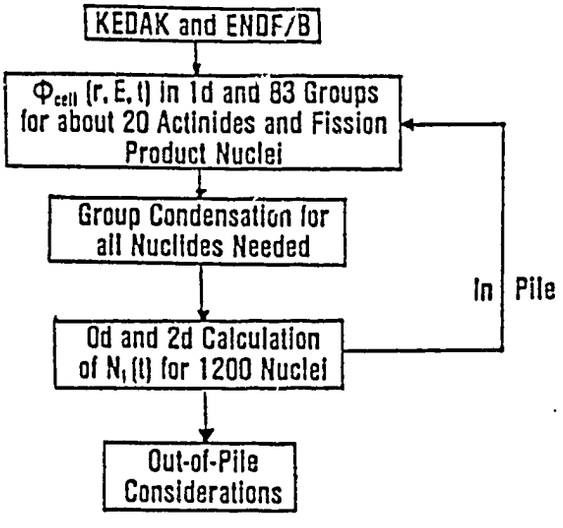

Fig. 5-1: The General Calculational Procedure to Predict the Nuclear Properties of Discharged LWR Fuel

The data base is KEDAK-4 and ENDF/B. The in-pile nuclide transmutations are treated with a time-dependent cell program. Energetic and spatial resonance shielding in the used 83 energy group structure is determined with standard methods for thermal reactor calculations. The time intervals between spectrum recalculations are chosen in accordance with the spectral variations caused by soluble boron burn-up, fission product and transuranium isotope generation. These variations are larger at the beginning than towards the end of each cycle. For the calculation of the neutron spectrum in the unit cell all important nuclei are considered, as usual. The changes in the concentrations of about 1200 nuclei, needed in a full description of the out-of-pile nuclear characteristics of the fuel cycle, are determined by first collapsing the corresponding nuclear data with the cell spectrum and then applying either zero-dimensional or multidimensional neutronic calculations, depending on the purpose of the investigation. The time dependence of the soluble boron is taken into account properly, which is especially important in nuclear data checks. To avoid any ambiguity caused by theoretical methods near boundaries, water gaps or control rods, the experimentally measured power density at the position of the fuel sample to be analysed, is used. Thus a better deduction of nuclear data deficiencies in the postirradiation analysis for the various nuclide concentrations is possible. The accuracy of the theoretical analysis then depends mainly on the accuracy of the measured time dependent pinpower density, usually about 2 - 3 %, and the nuclear data uncertainties, assuming the methods for the cell calculations to be correct. In the calculations, often not the (time dependent) pinpower density is taken from experimental results, but instead the measured burn-up is used in the theoretical investigation, then accordingly the pinpower has to be normalized to give the experimental burn-up. The burn-up value is the most dominant parameter for the amount of fission products and actinides in spent fuel, especially of all transuranium isotopes. In experiment, various methods are used to determine the burn-up of spent fuel from a sample. Usually one can assume an uncertainty of 2 - 5 % /33/.

In conclusion, if nuclear data and theoretical methods are assumed to be correct, the predicted nuclide concentrations are as uncertain as the experimental burn-up value i.e. up to 5%. This is not a very high accuracy, but it is sufficient for the investigations of MINACs. Clearly this uncertainty has to be compared with the uncertainty of the measurements for the determination of the nuclide concentrations; this is discussed subsequently.

Many parameters influence the accuracy of the experimental results for nuclide concentrations in reactor fuel. Generally, the kind of material is important with respect to the analysis method used, whether the sample contains fuel powder, whether it is a solution, or whether the fuel is oxide, carbide or nitrate. The accuracy is increased, if the material to be analysed is a pure material, i.e. without impurities. High burn-up fuel, either from an initial reactor loading with enriched uranium or mixed Pu/U oxide requires special attention in the analytical techniques. The homogeneity of the sample is of prime importance. In addition, different techniques need different amounts of sample material to perform a reliable measurement. A careful investigation of possible perturbations of a measurement for a specific isotope by other constituents of the sample is requested.

The following experimental techniques are used to analyse nuclear fuel: alpha counting, alpha spectrometry, gamma spectrometry, spectrophotometry, thermal ionization mass spectrometry, titrimetry, X-ray fluorenscence, isotope dilution mass spectrometry (IDMS). These methods yield different accuracies in applying them to element or isotope analysis in nuclear material. Any measured result should be given only together with a reliable error analysis. Unfortunately, this clear request is missing in most of the quoted experimental results. For uranium and plutonium isotopes, recently de Bièvre et al. have assessed the achievable uncertainty components in fissile element and isotope assay in destructive analyses of nuclear material /34/. The uncertainties quoted in the upper part of Tab. 5-1, for U and Pu elements in spent fuel and for Pu isotopes from pure plutonium material, are taken from Ref. 34. The accuracy of experimental results in an isotopic analysis of spent fuel is estimated from the spread in the results obtained in various laboratories for alpha spectrometry and isotopic dilution measurements. The estimate for IDMS might be a bit optimistic; however, the experience, obtained in KfK, is very promising /35, 36/.

5.2 Comparison of Calculated and Measured Nuclide Concentrations for PWR Spent Fuel at Discharge

An intercomparison for uranium, plutonium and transplutonium concentrations in spent fuel from PWRs is shown in Fig. 5-2 to Fig. 5-8; all data refer to discharge of the fuel from the reactor. The data are a selection

U, PU ELEMENTS IN SPENT FUEL : 0.5 - 1 %

PU - ISOTOPES FROM PURE PLUTONIUM MATERIAL

PU238 (2 %) PU239 (0.1 - 0.15 %)

PU240 (0.3 %) PU241 (0.3 - 1 %)

PU242 (0.5 %)

SPENT FUEL ISOTOPIC ANALYSIS (BASED ON EXP. INTERCOMPARISONS)

NUCLIDE	α - SPECTROMETRY [%]	IDMS [%]
PU236	20 - 30	
PU238	5 - 15	
PU242	< 5	
AM241	LARGE SCATTER (~50)	~5
AM243	~ 20	~5
CM242	LARGE SCATTER (~50)	
CM244	~ 5	~5

Tab. 5-1: Estimated Experimental Accuracy of Postirradiation Techniques

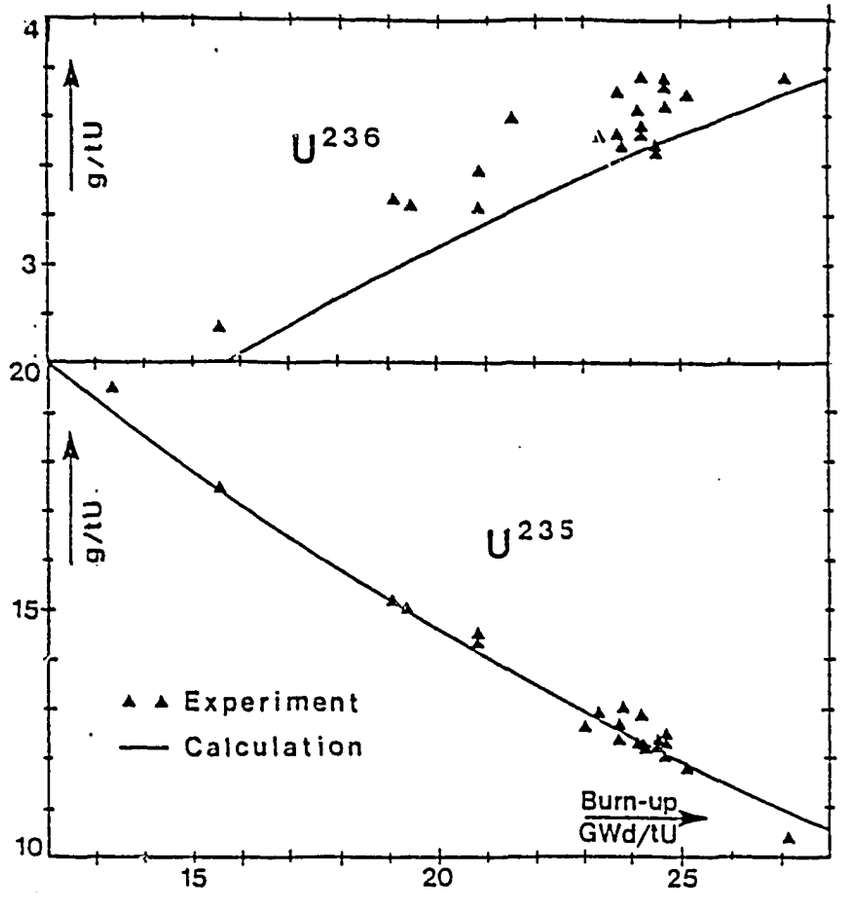

Fig. 5-2: Isotopic Concentrations of U235 and U236 in Spent PWR Fuel from TRINO2 Pellets

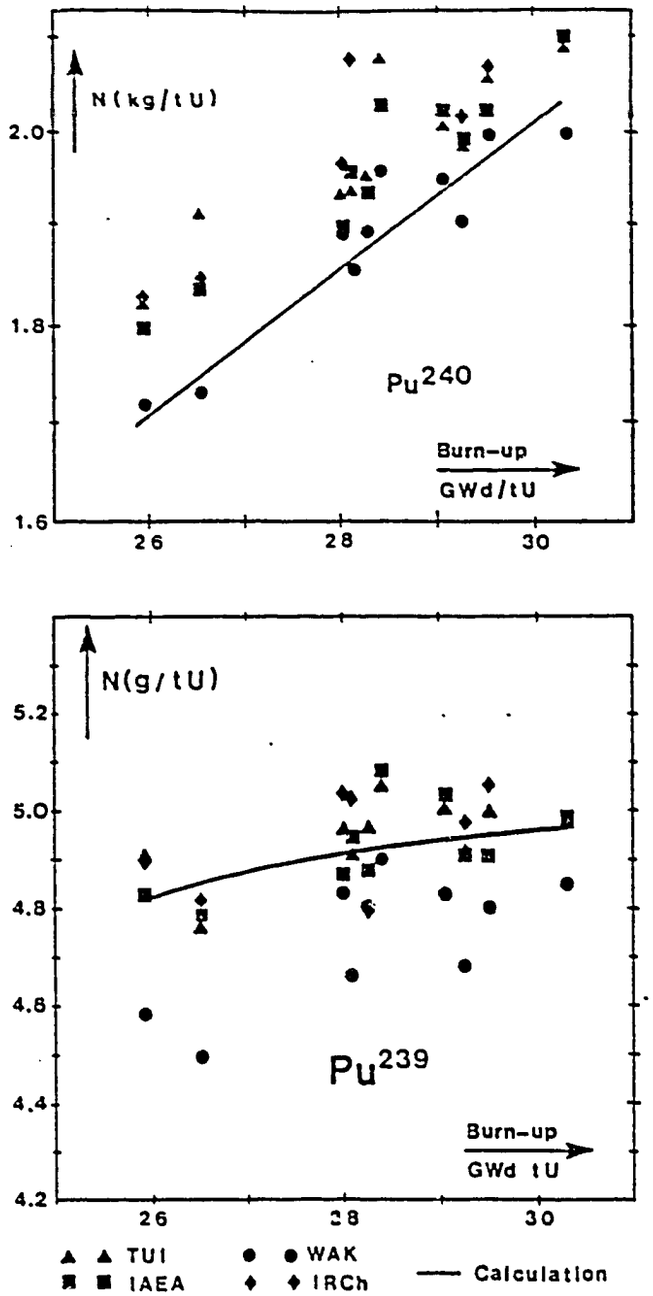

Fig. 5-3: Isotopic Concentrations of Pu239 and Pu240 in Spent PWR Fuel from KWO Batches

from many intercomparisons, which all look very similar. The experimental data are taken from batch and pellet analyses for the fuel from the German PWR Kernkraftwerk Obrigheim (KWO) and the Italian TRINO Vercellese PWR; for further references see Ref. 5.

The figures are self-explanatory. The following comments should be made: The U236 and Pu240 concentrations are slightly underestimated; for Pu239 note the suppressed coordinate zero, nevertheless the experimental data

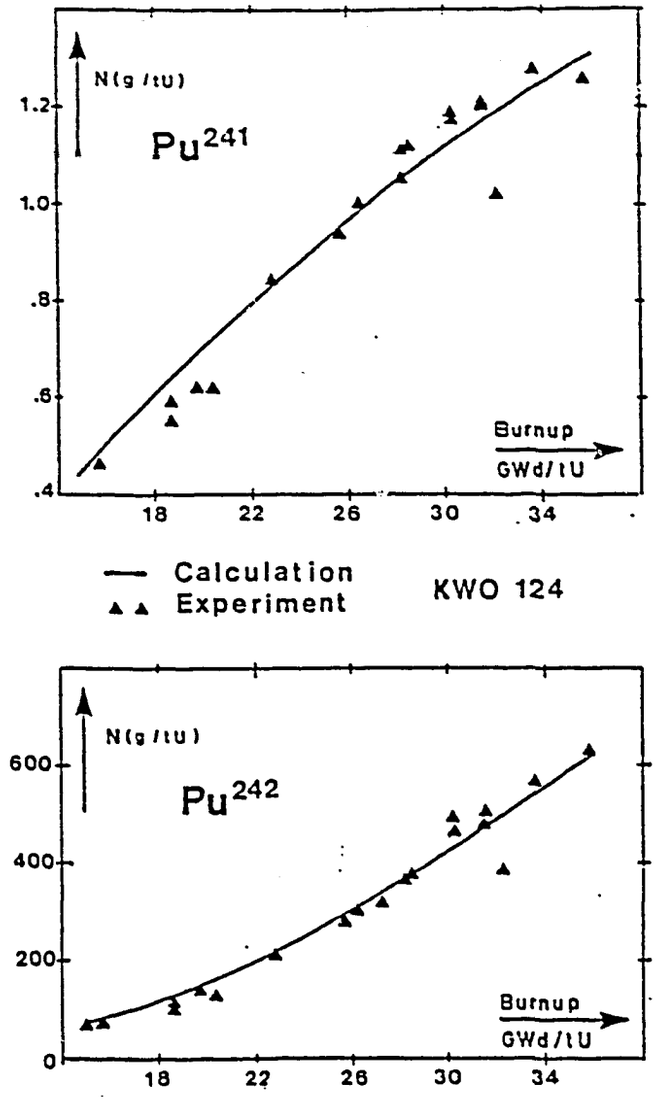

Fig. 5-4: Isotopic Concentrations of Pu241 and Pu242 in Spent PWR Fuel from KWO Pellets

scatter over the investigated region of burn-up by about 3%, if the low data from WAK (routine measurements) are discarded: this is much larger than the quoted accuracy of 0.15% in Tab. 5-1. This could be explained by different techniques used in the various laboratories, perhaps also by a various degree of sophistication in the analysis. The large scatter in the Am241 results of Fig. 5-5 (open triangles) indicates the difficulty to measure the concentration of this isotope with alpha-spectrometry: the alpha spectrum from Am241 is almost completely shadowed by that of Pu238. The IDMS results were obtained in 1982, when the calculations were already completed; an excellent agreement between the theoretical prediction and the IDMS values is observed. It can also be seen that the IDMS results for Am243 are lower by about 20% than the calculations. This is in agreement with the observed underestimation of the capture resonance integral, as

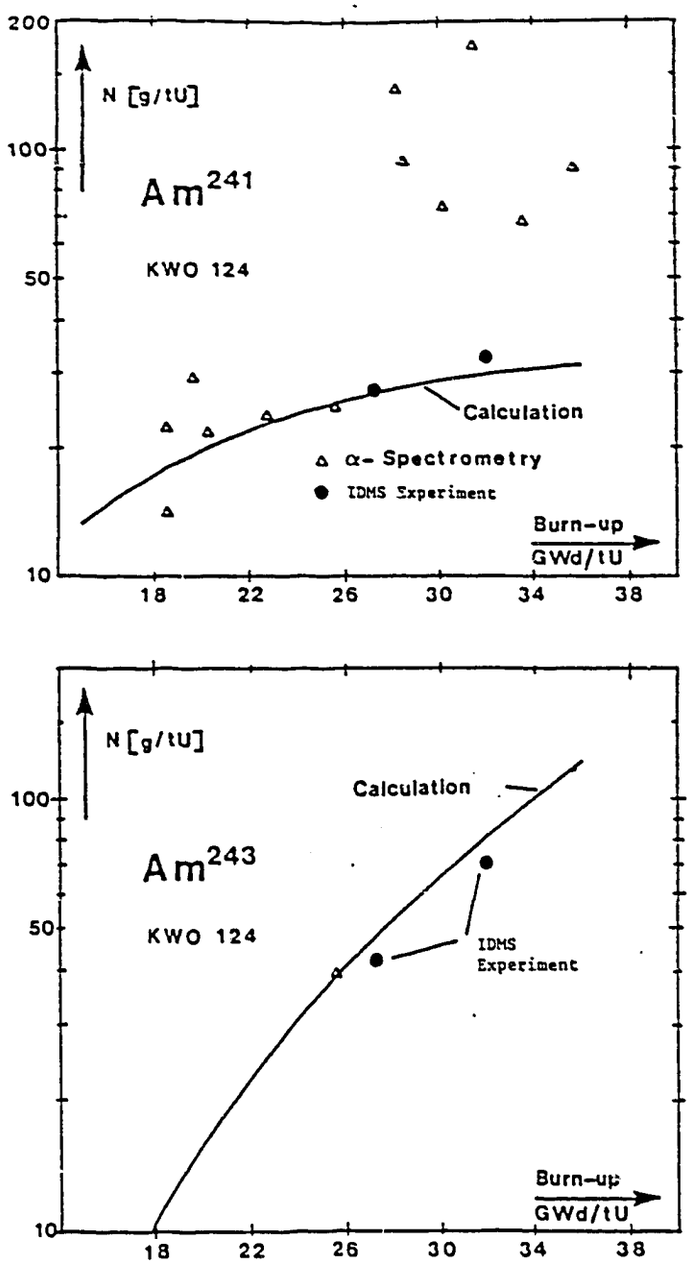

Fig. 5-5: Isotopic Concentrations of Am241 and Am243 from Spent PWR Fuel from KWO Pellets

discussed in section 4.2. Cm242 concentrations, shown in Fig. 5-6, are slightly underpredicted by calculations; however, the experimental uncertainty is rather large. An excellent agreement between theory and measurements is observed for Pu238, also for Cm244 in Fig. 5-7.

According to the discussion in chapter 2, the generation of Pu236 mainly via the (n,2n) reaction on Np237 is of special interest, because of the not yet completely resolved uncertainty of the (n,2n) cross-section and the corresponding branching ratio to the short-lived Np236 isotope. Fig. 5-8 shows that the KEDAK data, based on an evaluation of Caner et al.

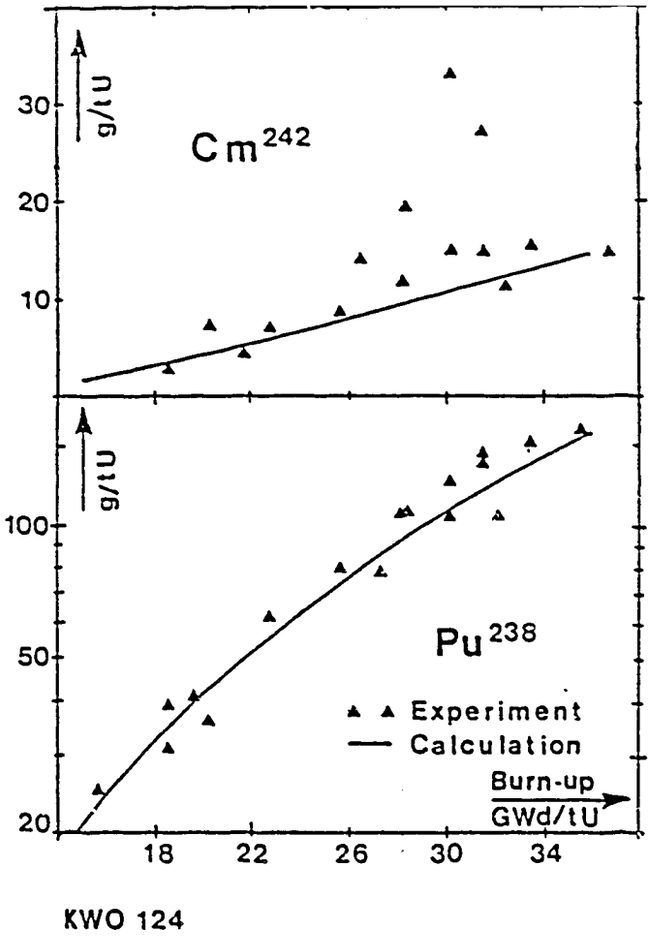

Fig. 5-6: Isotopic Concentrations of Pu238 and Cm242 in Spent PWR Fuel from KWO Pellets

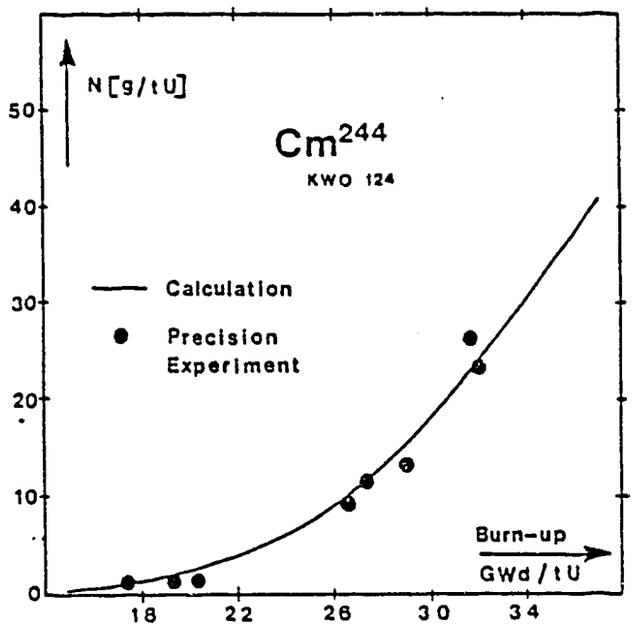

Fig. 5-7: Isotopic Concentration of Cm244 in Spent PWR Fuel from KWO Pellets

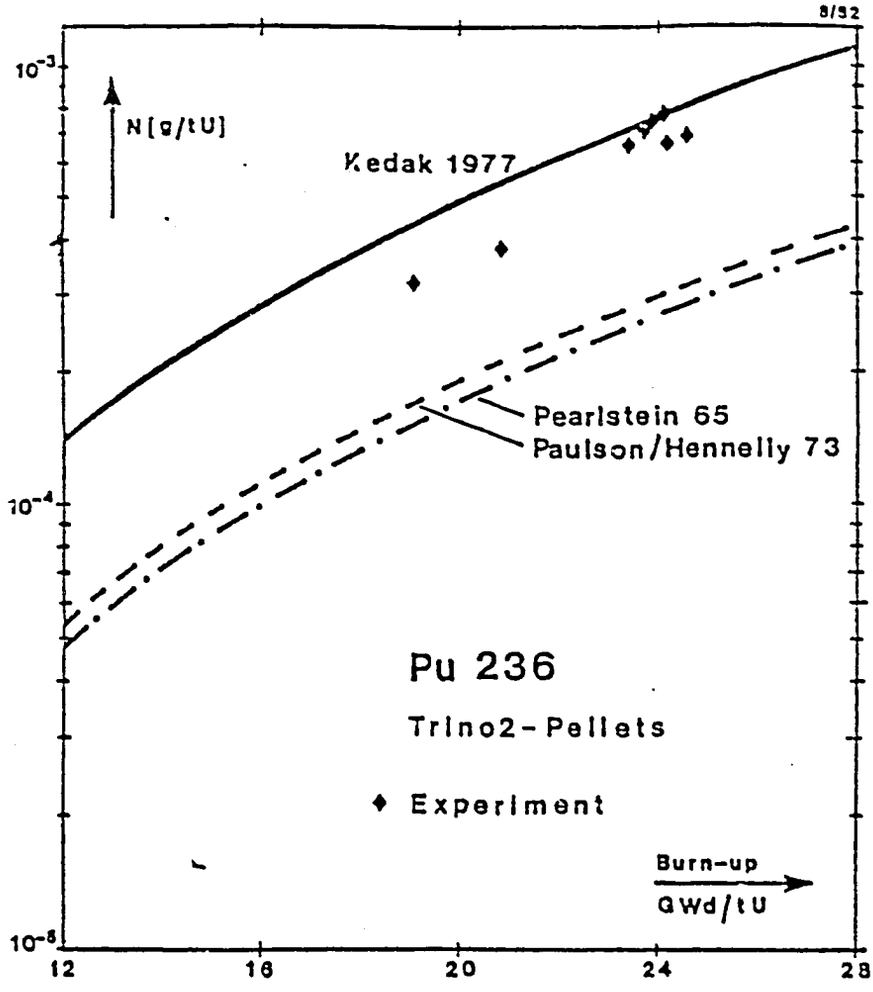

Fig. 5-8: Isotopic Concentration of Pu236 in Spent PWR Fuel from TRINO2 Pellets

/37/ overestimates only slightly the experiments, while Pearlstein (1965) and Paulson/Henelly (1973) data give results which are lower by about a factor of two /5, 38/. This difference needs urgent clarification+), although at KfK the observed agreement between calculations using KEDAK cross-sections with measured values was felt to be satisfactory.

As a conclusion, postirradiation analyses performed at KfK on the basis of KEDAK, gives satisfactory agreement with experiments for almost all actinide isotopes of interest. The observed differences coincide with the findings for resonance integrals in section 4.2, especially for the capture resonance integrals as the most important quantities for the generation of transplutonium isotopes. This conclusion gives confidence in the used data and methods.

+)Remark: The consideration of the new measurements by N. V. Kornilov et al. (submitted to this conference) probably gives a solution to the problem.

6. Qualification of Nuclear Data for Actinides by Integral Measurements in Fast Critical Assemblies and by Postirradiation Analyses of Fast Power Reactor Fuel

The first comparisons between calculations and measurements, done in fast zero power assemblies around 1965, showed large discrepancies for essential integral parameters as k_{eff}, the breeding ratio, reaction rates and reactivity coefficients. Although the mathematical tools at this time were not yet developed to a sufficiently high accuracy, most of the discrepancies were attributed to the very uncertain nuclear data in and above the resonance region of the actinides. The fast reactor design teams therefore tried to overcome the deficiency of nuclear data by adjusting nuclear group constants to results obtained in integral experiments. Presently in use are the following adjusted group constant sets: FGL5 in the UK /39/, the JAERI sets in Japan /40/, the CARNAVAL Formulaire in France /41/, the OSCAR-76 group constants in the USSR /42/ and the KfK-INR set in the Federal Republic of Germany /43/. The adjustment was performed mainly on the essential capture and fission group data for the major actinides as U235, U238, Pu239, Pu240, Pu241, and also for the fission products. A comprehensive review on the present accuracy of physics characteristics in unirradiated fast reactor cores is given in Ref. 44.

Integral tests on minor actinide isotope nuclear data were performed in Phénix in the PROFIL-I irradiation program. Tab. 6-1 compares the deviation of the calculated reaction rates relative to those of U238, as reported in 1978 /45/. The calculations were performed with CARNAVAL-III, which for these isotopes is mainly based on ENDF/B-IV. As can be seen, the differences between experiments and calculations are relatively large, but the experiments are also very uncertain. This observation led to plan for a new irradiation measurement in Phénix, PROFIL-II, especially to test the data of MINACs. The experiments are completed, the evaluation of the results and the comparison with recent calculational methods are underway and will be available in 1985 /46/. In addition, irradiation experiments for minor actinide samples are performed in the Karlsruhe fast reactor test facility KNK-II. Both these experimental investigations will hopefully resolve the remaining uncertainties in the prediction of MINACs in fast reactors.

Tab. 6-1: Deviations of Experimental (E) Reaction Rates for Minor Actinides Relative to U238 from Calculations (C), using CARNAVAL-III

Nuclide	$\frac{E-C}{C}$ (%)	Nuclide	$\frac{E-C}{C}$ (%)
Np237	+ 32 ± 15 %	Am241	- 8 ± 12 %
Np239	- 5 ± 19 %	Am243	- 10 ± 10 %
Pu238	- 22 ± 3 %	Cm244	- 19 ± 15 %
Pu242	- 36 ± 5 %		

But much information on the quality of the nuclear data of MINACs has already been collected since 1978. In late 1979, the author gave a review on available data up to that time at the International Conference on "Nuclear Cross-Sections for Technology" in Knoxville /14/. Already at that time a convergence of various data sets could be observed, demonstrated in Tab. 6-2 and Tab. 6-3, reproduced from Ref. 14. These tables show one-group constants from France (FRA), Germany (GER), Japan, UK and USA (ENDF/B-IV and ENDF/B-V). For completeness, values from the USSR are included, which are not strictly comparable, because these data are based on a simple fast reactor benchmark (often quoted as BAKER-benchmark), while all the other data use the neutron spectrum of a NEACRP benchmark for a 1000 MWe fast reactor /47/. Large data discrepancies, as observed in 1975, do not exist anymore for important actinide nuclei. Even the differences in the capture and fission group cross-sections for Am241, Am243 and Cm244 are relatively small in the various data sets. This was encouraging to perform further integral tests and to consider in the corresponding calculations the most recent data available.

In 1982 Stevenson reported new measurements for the Cm242 and Cm244 production rates in the fast zero energy assembly ZEBRA /48/. Tab. 6-4 shows the comparison of the experimental and calculated one-group cross-sections for curium production. The calculational tools are sophisticated, see also e.g. Ref. 44. The broad-group data for capture in Am241 and Am243 were based on recent Harwell evaluations, for Am241 see Ref. 21. Sensitive radiochemical methods have been used to determine the curium produced in milligram samples of irradiated Am241 and Am243.

Tab. 6-2: Comparison of One-Group Constants for the NEACRP-LMFBR Benchmark: ^{238}Pu to ^{242}Pu

	CAPTURE [b]							FISSION [b]						
COUNTRY	FRA	GER	JAPAN	UK	USA		USSR*)	FRA	GER	JAPAN	UK	USA		USSR*)
BASIS	CARN IV	KEDAK	JAERI	FGL5	ENDF/B IV	ENDF/B V		CARN IV	KEDAK	JAERI	FGL5	ENDF/B IV	ENDF/B V	
^{238}Pu	0.54 A	0.68	0.91	0.45	0.48	0.80	0.90	0.84 A	1.03	1.12	1.13	1.15	1.14	1.16
^{239}Pu	0.57 A	0.57	0.61	0.55	0.56	0.57	-	1.81 A	1.87	1.88	1.83	1.84	1.86	-
^{240}Pu	0.55 A	0.57	0.62	0.63	0.58	0.61	-	0.33 A	0.36	0.37	0.35	0.36	0.36	-
^{241}Pu	0.5 A	0.5	0.55	0.62	0.51	0.50	-	2.53 A	2.54	2.61	2.69	2.61	2.63	-
^{242}Pu	0.63	0.5	0.41	0.39 M	0.39	0.48	-	0.22	0.24	0.28	0.22	0.27	0.25	-

Tab. 6-3: Comparison of One-Group Constants for the NEACRP-LMFBR Benchmark: ^{241}Am to ^{244}Cm

	CAPTURE [b]							FISSION [b]						
COUNTRY	FRA	GER	JAPAN	UK	USA		USSR*)	FRA	GER	JAPAN	UK	USA		USSR*)
BASIS	CARN. IV	KEDAK	JAERI	FGL5	ENDF/B IV	ENDF/B V		CARN IV	KEDAK	JAERI	FGL5	ENDF/B IV	ENDF/B V	
^{241}Am	2.02 A	1.93	1.69	2.01 M	1.37	1.89	1.90	0.29	0.26	0.30	0.31	0.41	0.28	0.31
^{242}Am	0.7	0.46	-	0.11	-	0.097	0.42	3.7	3.86	-	3.33	-	3.61	3.2
^{243}Am	1.6	1.53	1.65	1.73 M	0.86	1.20	1.8	0.2	0.2	0.23	0.19	0.17	0.22	0.20
^{242}Cm	0.59	-	-	0.51	-	-	0.46	2.05	-	-	1.23	-	-	0.16
^{243}Cm	0.5	0.18	-	0.10	-	0.27	0.39	3.39	2.46	-	2.89	-	2.77	2.5
^{244}Cm	0.85	0.65	0.66	0.49 M	0.53	0.91	0.98	0.45	0.43	0.43	0.38	0.52	0.40	0.42

*) not strictly comparable, see text. A: Adjusted; M: Modified FGL5

The calculated to experimental ratios show means of 0.85 for Cm242 production and 0.95 for Cm244 production. These data support the evaluations, which were almost entirely based on theoretical models.

For the ZEBRA core 12 and 14, a comparison of one-group capture cross-sections of Am241 and Am243 between results, deduced from experiments, and calculations, using KEDAK-4 as data basis, was made /49/. This comparison is shown in Tab. 6-5. The obtained C/E accuracy, 5 - 8 % for Am241, and 9% for Am243 (underprediction!) is satisfactory. Tab. 6-6 shows the C/E-comparison for the fission rate ratios relative to Pu239 in ZEBRA core 21;

Tab. 6-4: Experimental and Calculated One-Group Cross-Sections for Cm Production (Stevenson S2) (Data Based on Lynn Evaluation)

Sample Location	Cm242 Production			Cm244 Production		
	Exp (E)	Calc. (C)	C/E	Exp (E)	Calc. C)	C/E
Core Center in						
ZEBRA-12	1.48	1.28	0.85	-	-	-
ZEBRA-14	1.28	1.16	0.91	1.61	1.60	0.99
ZEBRA-16	-	-	-	1.99	1.72	0.86
ZEBRA-21						
Mid-Core	1.18	1.03	0.87	1.34	1.43	1.06
Edge of Breeder	2.20	1.88	0.86	2.79	2.58	0.92
Near Breeder Center	3.92	3.13	0.80	-	-	-
Breeder Center	4.07	3.32	0.82	4.85	4.52	0.93
Mean and Standard Deviation			0.85 ±0.04			0.95±0.08

Tab. 6-5: Comparison of Calculated (C) One-Group Capture Cross Sections (KEDAK-4) with Experiments (E) in ZEBRA

	^{241}Am			^{243}Am		
ZEBRA CORE	C	E	C/E	C	E	C/E
12	1.34	1.46	0.92	—	—	—
14	1.22	1.28	0.95	1.46	1.61	0.91

Tab. 6-6: Calculated Fission Rate Ratios Relative to ^{239}Pu in Comparison to Experiments in ZEBRA

ZEBRA	^{241}Am			^{243}Am		
Core 21	C	E	C/E	C	E	C/E
Fissile Zone	0.204	0.2043	1.0	0.1775	0.1539	1.15
Fertile Zone	0.0303	0.0298	1.02	0.0194	0.0215	0.904

Tab. 6-7: Post Irradiation Analysis of PFR-Fuel, C/E-Comparison for Mass and Activity; Calculational Base: FISPIN (Pickles 82)

Nuclide	Burn-Up (%) 4.63	6.31	8.61	Remarks
U235	0.996	1.004	1.002	Mass Comparison (Mass Spectrometry)
U238	1.04	1.033	1.04	
Pu239	0.997	1.001	0.999	
Pu240	0.89	0.883	0.914	
Pu241	0.8	0.8	0.9	
Pu242	-	0.9	-	
Pu239 / Pu240	1.004	1.003	0.946	Activity Comparison (α-Spectrometry)
Pu238	0.69	0.76	0.85	
Am241	1.04	1.75	1.28	
Pu238 / Am241	0.86	1.06	0.98	
Cm242	1.10	0.95	0.97	

again the data base is KEDAK-4. An excellent agreement is found for Am241, the relative Am243 fission rate is uncertain to about ± 15 %.

These examples show the good quality of the present Am nuclear data. Spent fuel from the fast prototype reactor PFR was analysed and compared with calculations /50/; the measurements concerned concentrations or activities of several isotopes. The experiments used mass spectrometry and alpha spectrometry; the burn-up part of the calculations was based on the FISPIN code /51/. Tab. 6-7 gives the C/E comparisons for actinide isotopes for three different values of reactor burn-up. Larger differences show up for the concentrations of Pu240, Pu241 (to a lesser extent for Pu242), especially for the lower burn-up values of 4-6 a/o and 6.3 a/o. The activity comparisons are unsatisfactory for Pu238 and Am241, the latter is caused very probably by the used alpha spectrometry technique, as discussed already in chapter 5.

As a last example, Tab. 6-8 compares the very recently calculated and measured uranium inventory and the relative plutonium isotope concentrations of reprocessed fuel from two subassemblies (SA) of the fast test facility KNK-II/1 in Karlsruhe /52/. The charged fuel contains 93% enriched U235, U/(U+Pu) is 70%, Pu/(U+Pu) 30%. The uranium inventory and the

Tab. 6-8: Measured and Calculated Uranium and Relative Plutonium Concentrations for a Reprocessed Fast Test Reactor Fuel Assembly (KNK-II/1)

NUCLIDES	SA - 202 BURN-UP CORE: 39 GWD/T		SA - 203 BURN-UP CORE: 76 GWD/T	
	EXPERIMENT	CALCULATION	EXPERIMENT	CALCULATION
U /KG/	29.0	29.9	28.74	29.3
$\frac{PU238}{PU}$ /%/	0.7	0.73	0.77	0.77
$\frac{PU239}{PU}$ /%/	77.6	77.2	78.5	78.2
$\frac{PU240}{PU}$ /%/	14.6	14.7	14.3	15.6
$\frac{PU241}{PU}$ /%/	5.1(A)	6.0	4.9(A)	4.0
$\frac{PU242}{PU}$ /%/	2.0(B)	1.3	1.5(B)	1.4

(A) γ - SPECTROSCOPY (B) ESTIMATED FROM α - SPECTROMETRY

relative Pu-concentrations are considered as reliable measurements. The calculations were performed on the basis of the KfK-INR group set /43/, with updated group data for Pu240. The agreement between calculated and measured quantities is excellent.

As a conclusion to this chapter, integral tests on minor actinide nuclear data in a fast reactor spectrum do not yet exist in a comparable amount as those for PWR fuel. However, the published results, especially for Am241 and Am243 capture and fission data (responsible for the Cm242 and Cm244 production), are very satisfactory. Further information will come up in the near future from the irradiation experiments in Phénix (PROFIL-II) and in KNK-II/2.

7. Remaining Nuclear Data Requirements of High Priority for Minor Actinides in Thermal and Fast Reactor Fuel

The investigations in chapters 4 to 6 allow to deduce data requirements for neutron reactions essential in fuel cycle analysis for thermal and fast reactors. Because the uncertainties of the nuclear data for the major actinide isotopes are well known and probably cannot be improved by the presently used techniques in the differential data measurements, only the requirements for the minor actinide isotopes are given here, which indeed could be fulfilled in the near future.

For applications in fuel cycle analyses of thermal reactors, three uncertainties need improvement with very high priority: Tab. 7-1 quotes the (n,2n) reaction of Np237 and the energy dependence of the corresponding branching ratio of the short- and long-lived isotopes of Np236. As already mentioned in chapter 4 and chapter 5, the studies done at KfK did not request this clarification, because by comparison with postirradiation experiments the data from Paulson/Hennelly and Pearlstein were discarded. The INDC-discrepancy list 1984 quotes the discrepancies as not understood. New measurements on the differential cross-sections and a careful integral measurement are therefore requested.+)

The capture cross-section of Am243 needs re-examination because of a 20% difference between calculated integral parameters (resonance integral, concentration) and corresponding experimental results. There are indications (see Section 4.2) that a careful re-measurement of the capture resonance integral for Am243 might resolve the discrepancy; this measurement therefore is recommended.

Tab. 7-2 summarizes differences in the various evaluations done within the IAEA Co-ordinated Research Programme. These observations are based on graphical representations of the evaluated data, provided by M. Mattes;

+) New differential measurements were reported at this meeting (see contribution from N. V. Kornilov et al. and the review article from J. E. Fréhaut), which very probably resolve the discrepancies; these new data seem to support the KfK-investigations.

Tab. 7-1: Requested Nuclear Data Improvements of Highest Priority in Fuel Cycle Applications for Thermal Reactors

Nuclide	Reaction	Remarks
Np237	a) (n,2n) b) Energy dependence of branching ratio to Np236m and Np236g	Reaction leading to the short-lived Np236 isotope, responsible for Pu236 formation*)
Am243	(nγ)	Unresolved discrepancy between evaluations and resonance integral, important for Cm244 formation

*) Problem Practically Solved at this Meeting

Tab. 7-2: Observed Differences of Low Importance in Fuel Cycle Applications for Thermal Reactors

Nuclide	Reaction	Major Differences in INDL-Evaluations
Am241	(nγ)	thermal data
Am242m	(nγ)	thermal and resolved resonance region
	(nf)	resonance region
Am243	(nγ)	MeV range
	(nf)	below 10 keV
Cm242	(nγ)	above 10 eV
	(nf)	all neutron energies
Cm244	(nf)	thermal and resonance region

Tab. 7-2 does not claim to be complete. All these data are of low importance in fuel cycle analyses, improvements therefore are motivated mainly by scientific interest.

Nuclear data of other isotopes important in fuel cycle analysis of thermal reactors are sufficiently accurate.

For fast reactor fuel cycle analysis, conclusions can be drawn which happen to be almost the same. In 1980, Patrick and Sowerby assessed the accuracy requirements on minor actinide nuclear data for fast reactors /53/. These authors performed a sensitivity analysis, assuming the 1980 uncertainties in the various reactions. The aim of this investigation was to obtain the uncertainty in the formation of minor actinide isotopes,

which are due to the uncertainties of nuclear data only. A selection of the results is reproduced in Tab. 7-3. It should be mentioned that the reaction path Am241(nγ) → Am242g contributes (via decay of Am242g) to the total heat production of irradiated fast reactor fuel. Only the uncertainties of the Np237(n,2n) reaction, the capture cross-section of Am243, and the branching of Am241 capture to Am242g and Am242m lead to possible uncertainties in the predictions of Pu236, Cm244 and Cm242, respectively. Due to the successful test of the Cm242 and Cm244 production in ZEBRA, the modern Am data give sufficiently good agreement with integral tests.

Tab. 7-4 compares the accuracy, which could be achieved in 1980, with the requested accuracy /53/. These neutron reactions, which need definite improvement, are essentially the same as those for thermal reactors, with the addition of the reaction Am241(nγ) → Am242g. Two further processes are noted in Tab. 7-2, which depend on decay properties and on (α,n) reactions. In this study, for fast reactors the Am243 capture values tested in the ZEBRA facility, could be considered already as sufficiently accurate. Thus, if the Np237(n,2n) and the Am243(nγ) discrepancies could be regarded as almost removed, then the most important uncertainties in evaluating fuel cycle properties of fast reactor fuel, which depend on neutron reactions with actinides, would not exist anymore if modern nuclear data are used in the studies. This optimistic conclusion hopefully will be confirmed by the forthcoming results from experiments in Phénix and KNK-II.

8. General Conclusion

The worldwide effort to improve the neutron data base of minor actinide isotopes was very successful. Most of the discrepancies, which were observed in 1975, have been reduced to an acceptable level in 1984. Therefore the uncertainties in evaluating fuel cycle properties of thermal and fast reactors, are reduced correspondingly. Tests of recent nuclear data in thermal and fast reactors before the 1984 Advisory Group Meeting in Uppsala, revealed only very few important discrepancies: the (n,2n) reaction on Np237 and the capture cross-section of Am243 (mainly in thermal reactors). The evaluated modern Am243 capture data in the fast energy range were supported by integral tests. At the Uppsala meeting, N. V. Kornilov et al. presented new measurements on the Np237(n,2n) reaction, which seem to solve most of the discrepancies. If this is confirmed, then

Tab. 7-3: Uncertainty in MINAC Formation in Fast Reactors due to Uncertainties in Present Neutron Data

MINAC Formation	Main Uncertainty Reason	Assumed Uncertainty of Reactions (%)	Uncertainty (%) in MINAC Formation due to Data Uncertainties
Pu236	Np237(n,2n)	100	100 +)
Pu238	Am241(nγ) → Am242g	20	8 - 9
Am241	Am241(nγ) → Am242g	20	4 - 6
	$T_{1/2}$(Pu241)	3.5	
Am243	Pu242(nγ)	10	10
Cm242	Am241(nγ) → Am242g	20	16
	Am241(nγ) → Am242m	20	
Cm244	Am243(nγ)	25	23
	Pu242(nγ)	10	

+) Problem Practically Solved at this Meeting

Tab. 7-4: Remaining Nuclear Data Requirements of Highest Importance in Fuel Cycle Applications for Fast Reactors

REACTION	PRESENT ACCURACY (%)	REQUIRED ACCURACY %	PURPOSE
NP237 (N,2N)	50 - 100 +)	25	PU236 FORMATION
BRANCHING TO NP236M, NP237G	NOT KNOWN+)		
AM243 (Nγ)	25	10	CM244 FORMATION (NEUTRON EMISSION)
AM241 (Nγ) TO AM242G	20	8	TOTAL HEAT
CM242 SPONT.FISSION BRANCHING	10	5	N - EMISSION
(α N)-YIELD	30	10	

+) Problem Practically Solved at this Meeting

only neutron reactions of low importance in fuel cycle analysis remain to be improved.

Acknowledgement

The author appreciates the helpful discussions with U. Fischer and Dr. H. W. Wiese. He is very grateful to Mrs. M. Mattes for providing the graphical intercomparisons of the INDL evaluations. Mrs. G. Bunz is thanked for the effective typing of this report.

References

/1/ Proc. of an Advisory Group Meeting on "Transactinium Isotope Nuclear Data", IAEA-186, Vol. 1 - 3 (1975)

/2/ C. W. Reich, Report on the IAEA Coordinated Research Programme on the Measurement and Evaluation of Transactinium Isotope Nuclear Data, IAEA-TECDOC-232, p. 45 (1979)

/3/ Proc. of the Second Advisory Group Meeting on "Transactinium Isotope Nuclear Data - 1979", IAEA-TECDOC-232 (1979)

/4/ H. Küsters, M. Lalovic, H. W. Wiese, Fuel Handling, Reprocessing, Waste and Related Nuclear Data Aspects, Proc. of Int. Conf. on "Neutron Physics and Nuclear Data", p. 518, Harwell (1978) and Report KfK-2833 (1979)

/5/ U. Fischer, H. W. Wiese, "Verbesserte konsistente Berechnung des nuklearen Inventars abgebrannter DWR-Brennstoffe auf der Basis von Zell-Abbrand-Verfahren mit KORIGEN", Report KfK-3014 (1983). See also the English translation, Report ORNL-tr-5043.

/6/ U. Fischer, Private Communication (1984)

/7/ G. Schlosser, R. Manzel, "Recycling of Plutonium in Light-Water Reactors, Part 1: Demonstration Programs", Siemens Forschungs- und Entwicklungs-Berichte, Bd. 8 (1979), Nr. 2, p. 108, Springer Verlag

G. Schlosser, P. Uttendaele, "Recycling of Plutonium in Light-Water Reactors, Part 2: Prospective Commercial Recycling", Siemens Forschungs- und Entwicklungs-Berichte, Bd. 8 (1979), Nr. 3, p. 153, Springer Verlag

See also:
H. Küsters, in "Recent Reactor Physics and Shielding Investigations in the Federal Republic of Germany", Proc. ANS Topical Meeting on "Progress in Reactor Physics and Shielding", p. 23, Sun Valley (1980)

/8/ H. W. Wiese, in "Technologische Fragen des Brüterkreislaufs" (Editors: Marth/Lahr), Report KfK-3278, p. 125 (1982) and Private Communication (1984)

/9/ See for instance "Second Technical Meeting on the Nuclear Transmutation of Actinides", Joint Research Center Ispra, 21 - 24 April 1980

/10/ J. Bouchard, "Comprehensive Review of TND-Requirements for U and U-Pu Fuelled Thermal and Fast Reactors, and their Associated Fuel Cycles", Proc. of the Second Advisory Group Meeting on Transactinium Nuclear Data, IAEA-TECDOC-232, p. 23, Cadarache (1979)

/11/ For PWRs: see Ref. 5 (1983)
For FBRs: H. W. Wiese, Private Communication (1984)

/12/ See Ref. /1/, Summary Report, p. 1

/13/ H. Küsters, M. Lalovic, "Review on Transactinium Isotope Build-up and Decay in Reactor Fuel and Related Sensitivities to Cross Section Changes
and
Results and Main Conclusions of the IAEA-Advisory Group Meeting on Transactinium Nuclear Data, held at Karlsruhe, November 1975", Report KfK-2283 (1976)

/14/ H. Küsters, "Nuclear Data Needs for the Analysis of Generation and Burn-up of Actinide Isotopes in Nuclear Reactors", Proc. Int. Conf. on "Nuclear Cross Sections for Technology", p. 18, Knoxville (1979)
Also: Report KfK-2917 (1980)

/15/ F. H. Fröhner, B. Goel, U. Fischer, H. Jahn, "Neutron Cross Section Evaluation for ^{241}Am, ^{242m}Am, ^{243}Am and ^{244}Cm", Proc. of Int. Conf. on "Nuclear Data for Science and Technology", p. 211, Antwerp (1982)

/16/ K. Wisshak, F. Käppeler, "The Neutron Capture Section of ^{243}Am in the Energy Range from 5 to 250 keV", Proc. of Int. Conf. on "Nuclear Data for Science and Technology", p. 215, Antwerp (1982)

/17/ The comparisons were provided by M. Mattes, IKE Stuttgart, on the basis of the INDL-Data Library.

/18/ Nuclear Data Discrepancies 1983, NEANDC-INDC Joint Discrepancy File, p. 47, OCDE Paris (1984)

/19/ H. D. Lemmel, The IAEA Nuclear Data Library for Actinides (INDL/A) and the Related Coordinated Research Programmes (CRP), This Conference (1984)

/20/ M. Mattes, J. Keinert, Internal Note of the Institut für Kernenergetik, Stuttgart (1982)

/21/ J. E. Lynn, B. H. Patrick, M. G. Sowerby, E. M. Bowey, "Evaluation of Differential Nuclear Data for Americium Isotopes, Part I: ^{241}Am", Report AERE-R-8528, Harwell (1979)

/22/ B. Goel, U. Fischer, "A Critical Review of Resonance Integrals and Postirradiation Fuel Analysis for Important Isotopes of Am and Cm", Proc. Int. Conf. on "Nuclear Data for Science and Technology", p. 196, Antwerp (1982)

/23/ B. Goel, U. Fischer, "Validation of KEDAK-4 Data for Thermal Reactors: Resonance Integrals and Postirradiation Fuel Analysis", Report KfK-3449 (1983)

/24/ R. M. Harbour, K. W. Macmurdo, F. J. McCrosson, Nucl. Sci. Eng. 50, 364 (1973)

/25/ V. D. Gavrilov, V. A. Goucharev, V. V. Ivanenko, V. N. Kustov, V. P. Smirkov, Sov. At. Energy 4, 808 (1977)

/26/ J. W. T. Dabbs, C. H. Johnson, C. E. Bemis, Nucl. Sci. Eng. 83, 22 (1983)

/27/ R. P. Schuman, WASH-1136, pages 51 and 53 (1969)

/28/ J. W. T. Dabbs, C. E. Bemis, S. Raman (ORNL) and R. W. Hoff (LLNL), Nucl. Sci. Eng. 84, 1 (1983)

/29/ K. D. Zhuravlev, N. I. Kroskin, A. P. Ujetvjerikov, Sov. At. Energy 41, 285 (1975)

/30/ M. C. Thompson, M. L. Hyder, R. J. Reuland, J. Inorg. Nucl. Chem. 33, 1553 (1971)

/31/ R. W. Benjamin, K. M. Macmurdo, J. D. Spencer, Nucl. Sci. Eng. 47, 203 (1972)

/32/ U. Fischer, H. Küsters, H. W. Wiese, "Validation of Methods and Data for Calculating Nuclear Properties of Irradiated PWR Fuel by Comparison to Experimental Postirradiation Results", Trans. Am. Nucl. Soc. 45, 745 (1983)

/33/ M. A. S. Marzo, "Untersuchungen zur Anwendung der Isotopenrelationstechnik bei Nachbestrahlungsuntersuchungen und der Überwachung von Spaltstoffen", Report KfK-3264 (1982)

/34/ P. De Bièvre, S. Baumann, T. Görgenyi, E. Kuhn, S. Deron, P. De Regge, "1983 Target Values for Uncertainty Components in Fissile Element and Isotope Assay", ESARDA Bulletin, No. 6, 1 (1984)

/35/ B. Ganser, "Analyse und ein Gewinnungsverfahren des Americiums im Kernbrennstoffzyklus des Druckwasserreaktors", Report KfK-3380 (1982)

/36/ M. Wantschik, "Bestimmung der Curiumbildung in Leichtwasserreaktoren und Vergleich mit Berechnungen", Report KfK-3316 (1982)

/37/ M. Caner, S. Wechsler, S. Yiftah, "Evaluation of ^{237}Np Microscopic Data", Report IA-1346 (1977)

/38/ H. W. Wiese, U. Fischer, B. Goel, "Analysis of Cross Sections for the Formation of Pu236 and Co58,60 in both Thermal and Fast Reactors", Proc. of Int. Conf. on "Nuclear Data for Science and Technology", p. 202, Antwerp (1982)

/39/ J. L. Rowlands, The Production and Performance of the Adjusted Cross Section Set FGL5, Proc. Int. Conf. on "Physics of Fast Reactors", Tokyo, p. 1133 (1973)

/40/ J. P. Chaudat, J. Y. Barre, A. Khairallah, Improvements of the Predicted Characteristics for Fast Power Reactors from Integral Experiments:
CARNAVAL-III, Proc. Int. Conf. on "Physics of Fast Reactors", Tokyo, p. 1207 (1973)
and
J. P. Chaudat et al., Data Adjustments for Fast Reactor Design, Trans. Am. Nucl. Soc. 27, p. 877, Nov. 1977 (CARNAVAL-IV)

/41/ S. Katsuragi et al., JAERI Fast Reactor Group Constants System, Report JAERI-1199 (1970)
and
T. Kamei, Proc. Int. Conf. on "Fast Reactor Physics", Aix-en-Provence, p. 223 (1979)

/42/ L. N. Usachev, Yu. A. Kazanskij, V. A. Dulin and Yu. Bobkov, Adjustment of Evaluated Microscopic Data on the Basis of Evaluated Integral Experiments, in "Neutron Physics", Moscow, Part I, p. 53 (1977)

/43/ E. Kiefhaber, The KFK-INR-Set of Group Constants, Report KfK-1572 (1972)

/44/ H. Küsters, S. Pilate, "The Present Accuracy of Physics Characteristics of Unirradiated Fast Reactor Cores", Submitted for Publication in "Annals of Nuclear Energy" (1984)

/45/ M. Darrouzet, A. Giacometi, M. Robin, "Formation et Disparition des Actinides Secondaires dans les Réacteurs à Eau et les Réacteurs à Neutrons Rapides", Proc. Int. Conf. on "Neutron Physics and Nuclear Data", p. 597, Harwell (1978)

/46/ M. Salvatores, Private Communication (1984)

/47/ L. G. LeSage, R. D. Knight, D. C. Wade, K. E. Freese, P. J. Collins, "International Comparison Calculation of a Large Sodium Cooled Fast Breeder Reactor", Report ANL-80-78 (1978) and NEA-CRP-L-243 (1978)

/48/ J. M. Stevenson, A. D. Knipe, D. W. Sweep, R. A. P. Wiltshire, K. M. Glover, B. Whittaker, "Integral Experiments to Measure the Production Rates of ^{242}Cm and ^{244}Cm in Fast Reactor Spectra", Proc. Int. Conf. on "Nuclear Data for Science and Technology", p. 178, Antwerp (1982)

/49/ B. Goel, Private Communication (1984)

/50/ S. Pickles, H. J. Powell, "Experimental Validation of Irradiated Fuel Inventories Calculated by the FISPIN Code", Proc. Int. Conf. on "Nuclear Data for Science and Technology", p. 190, Antwerp (1982)

/51/ R. F. Burstall, "FISPIN - A Computer Code for Nuclide Inventory Calculations", Report ND-R-328(R) (1979)

/52/ H. W. Wiese, in "Der Brüterbrennstoffkreislauf - Brennelemente und ihre Wiederaufarbeitung", Report KfK-3775, p. 109 (1984)

/53/ B. H. Patrick, M. G. Sowerby, "An Assessment of the Accuracy Requirements on Higher Actinide Nuclear Data for Fast Reactors", Reports: NEANDC (UK) 174A, NEACRP-A-400, INDC (UK) - 34/G (1980)

REQUIREMENTS AND STATUS OF TRANSACTINIUM ISOTOPE NUCLEAR REACTION DATA

S. IGARASI, T. NAKAGAWA
Nuclear Data Centre,
Japan Atomic Energy Research Institute,
Tokai-mura, Naka-gun, Ibaraki-ken, Japan

Abstract

Status of transactinium isotope nuclear reaction data (TND) is surveyed on the basis of data requirements submitted to the previous advisory group meetings on TND. Insufficient or poor data are sorted out by reviewing the status of the experimental and evaluated data. Better-looking data are examined whether or not they surely satisfy the required accuracy by comparing the evaluated data. Finally, the data which should be more investigated to meet the requirements are pointed out.

I. Introduction

There are many review works and examinations on the requirements for the transactinium nuclear data (TND)[1-6]. Reports on these works collect many requests for TND from the users in the various fields, and show a variety of reasons behind the requests. There is also variety in the required data accuracy. In general, users' requests seem to become more complex, if new requests be added to them. This complexity, however, is not always essential, because almost the same quantities and nuclides appear in each review report. In this sense, the data requirements discussed in the previous meetings[1,2] represent typical users' needs. Hence, it is reasonable to adopt them as an object to see whether users' needs have been satisfied or not.

In this report, we examine the status of the required data which were submitted to the previous two advisory group meetings (AGM) on TND as insufficient data. We also examine the corresponding requirements given in WRENDA 81/82[7], and those surveyed by a Working Group on Nuclear Data for Nuclear Fuel Cycle in Japanese Nuclear Data Committee (JNDC)[8,9].

In Chapter II, we review the status of the measurements and evaluations for the required data, and sort out insufficient or poor data. We examine, in Chapter III, whether or not the remaining data satisfy the required accuracy. Our examination is performed by comparing the evaluated data. This is based on the idea that the evaluated data are much easier for users to handle than the experimental data, and that the reliability of the evaluated data gives direct impact on the users' needs. We check also fitness of the evaluated data to the measurements, and point out the data which meet the requirements. Finally, we indicate the data which should be more investigated.

II. Status of Required TND

In this Chapter, we review the status of the required transactinium neutron reaction data presented at the previous advisory group meetings, together with those given in WRENDA 81/82 and surveyed by the Working Group of JNDC. We summarize these requirements in Appendix, and show required accuracies in Table 1. In order to see the progress of the experiments and evaluations for these required quantities, we list the related literature recorded in CINDA 83 and its supplement which indicate endeavors since 1977, in Appendix. This adoption of 1977 is based on the idea that a part of the endeavors stimulated by the first AGM was discussed in the second meeting but most of them should be reexamined or newly examined. Available main evaluated data libraries are also shown in Appendix.

It is probably reasonable to consider that the status of the new evaluated data or libraries gives a good measure of availability of the data. In the following, we will make a brief survey of the data given in Appendix and pick off the clearly insufficient data. Although we cannot show all the figures of data in this report, the following discussions are based on the graphical comparison of the data. Quantitative examination for the reserved data will be given in the next chapter.

Th and Pa-isotopes

Experimental data of Th-isotopes are absolutely insufficient. Except the thermal value of the ^{230}Th capture cross section and the data below 10 MeV of the ^{232}Th(n,2n) reaction cross section, the evaluated data are very discrepant with each other. Since many experiments had been performed for the ^{232}Th(n,2n) cross section before 1977, endeavor should be concentrated on the evaluation work. Situation of the experimental data for Pa-isotopes is very poor. The evaluated data of the ^{233}Pa capture cross section show good agreement from 1 keV to 10 keV, and in the thermal region. Experimental data which can be compared with them are at least necessary.

U-isotopes

There are no recent experimental data for the ^{232}U fission and capture cross sections. ENDF/B-V is only one available file. A few experimental data of the ^{233}U(n,2n) reaction cross section have been measured, but the evaluated data are very discrepant. The evaluated data for the ^{234}U capture cross section disagree with each other. No experimental data have been given since 1977. The evaluated capture cross section of ^{236}U shows good agreement below 1 eV and from 10 keV to 1 MeV. Large discrepancy exists between 1 eV and 100 eV, and above 1 MeV. For the capture cross section of ^{237}U, no experimental data exist, and the evaluated data are discrepant. There are many experimental data for the ^{238}U(n,2n) reaction cross section, and the evaluated data are relatively in good agreement with each other.

In the next chapter, we will quantitatively examine the ^{238}U(n,2n) reaction cross section and ^{236}U capture cross section further. Except these two, the data of the U-isotopes are still insufficient.

Np-isotopes

No experimental data of the ^{237}Np capture cross section above 200 keV can be found in Appendix. The evaluated data agree with each other below 100 keV. There are many experimental data of the ^{237}Np fission cross section. The evaluated data above threshold are in good agreement, but the data in the subthreshold region are very discrepant. No

data of the ^{237}Np(n,2n) reaction cross section have been measured since 1977. Some experiments had been made before 1977, but the evaluated data show large discrepancy. There are several experimental data of $\bar{\nu}$, but the status of evaluation seems a little poor.

Quantitative examination will be made for the capture cross section below 100 keV, the fission cross section above 100 keV and $\bar{\nu}$.

The data status of ^{239}Np is absolutely insufficient.

Pu-isotopes

No experimental data of the ^{236}Pu capture and fission cross sections have been measured except for the thermal fission. The evaluated data of JENDL-2 and ENDF/B-V show large disagreement. The capture cross section of ^{238}Pu has not been measured since 1977. There are large discrepancies among the evaluated data. The fission cross section of this isotope has been measured recently. Many old experimental data are available. There are, however, discrepancies in the subthreshold region among the evaluated data. No experimental data exist for the (n,3n) cross section and $\bar{\nu}$. The ^{239}Pu(n,2n) reaction cross section is insufficient for both experimental and evaluated data. Some measurements have been performed for the ^{240}Pu capture cross section below a few hundred keV. Many evaluation works have also been made. A little discrepancy is found among the main evaluated data libraries. The status of the experimental data of the ^{241}Pu capture cross section is not necessarily sufficient. Many evaluation works have been made, but apparent discrepancy is found among the data of the main libraries. There are many experiments and evaluations for the ^{241}Pu fission cross section. The data of the main libraries are in good agreement above 100 keV and in the thermal energy region. The data of $\bar{\nu}$ for this isotope have been studied both in experiments and evaluations. Reexamination for this quantity will be made in the next chapter. Some measurements and evaluations have been performed for the ^{242}Pu capture cross section. The data in the thermal energy region are in good agreement among the main libraries.

The fission cross section of ^{238}Pu and ^{241}Pu, the capture cross section of ^{240}Pu and ^{242}Pu, and the $\bar{\nu}$-value of ^{241}Pu will be reexamined later.

Am-isotopes

Several experiments for the ^{241}Am capture cross section have been carried out since the first AGM of TND. Main evaluated data libraries show good agreement below a few hundred keV. Recent data of the fission cross section agree with each other in the subthreshold energy region. Main libraries, however, reveal discrepancy in the resonance region. No experimental data are reported for the $\bar{\nu}$-value. Except for the fission cross section of ^{242m}Am, the experimental data are very scarce for the ^{242}Am ground and meta-stable states. Discrepancies exist between ENDF/B-V and JENDL-2. Some measurements for the ^{243}Am capture and fission cross sections have been reported. The capture cross sections of the main libraries agree fairly well with each other below 200 keV. Large discrepancy is found for the fission cross section in the subthreshold energy region. The (n,2n) reaction cross section and $\bar{\nu}$-value have not been measured yet for ^{243}Am.

The capture cross sections of ^{241}Am and ^{243}Am below a few hundred keV will be reexamined in the next chapter. Also, the fission cross sections for both isotopes will be discussed.

Cm-isotopes

A few experiments have been performed for the total cross section of ^{242}Cm. The main libraries show large discrepancy. The status of the capture and fission cross sections of this isotope is absolutely poor. No data of $\bar{\nu}$ have been measured, except for the spontaneous fission. The experimental data for the capture and fission cross sections of ^{243}Cm are scarce. There are discrepancies between the JENDL-2 and ENDF/B-V data. The status of the ^{244}Cm capture cross section is still poor. The fission cross section above the threshold energy has been measured recently. Main libraries show discrepancies except for the threshold region. The capture cross section of ^{245}Cm has been measured only in the thermal region. There are large discrepancies between the JENDL-2 and ENDF/B-V data. Several measurements for the fission cross section have been reported. The data of JENDL-2 and ENDF/B-V are discrepant below 10 keV. The status of the ^{246}Cm capture cross section is the same as that of ^{245}Cm. The fission cross section has been measured recently, but the evaluated data are very discrepant below 1 MeV. The capture cross section of ^{247}Cm and ^{248}Cm, and the fission cross section of ^{247}Cm are insufficient.

In the next chapter, the fission cross section of ^{244}Cm and ^{245}Cm will be reexamined.

Bk, Cf and Es-isotopes

The data status of these isotopes is still insufficient. ENDF/B-V and/or ENDL-82 are available.

This brief survey proved that many required data are still unsatisfied. They are as follows, exclusive of Bk, Cf and Es-isotopes.

(i) Capture cross section:
^{230}Th, ^{231}Pa, ^{233}Pa, ^{232}U, ^{234}U, ^{237}U, ^{239}Np, ^{236}Pu, ^{238}Pu, ^{241}Pu, ^{242g}Am, ^{242m}Am, ^{242}Cm,

(ii) Fission cross section:
^{232}U, ^{239}Np, ^{236}Pu, ^{242g}Am, ^{242m}Am, ^{242}Cm, ^{243}Cm, ^{246}Cm, ^{247}Cm.

(iii) $\bar{\nu}$:
^{239}Np, ^{238}Pu, ^{241}Am, ^{242m}Am, ^{243}Am, ^{242}Cm.

(iv) (n,2n) cross section:
^{232}Th, ^{233}U, ^{237}Np, ^{239}Np, ^{239}Pu, ^{243}Am.

(v) Total cross section:
^{242g}Am, ^{242m}Am, ^{242}Cm.

(vi) (n,3n) cross section:
^{232}Th, ^{238}Pu.

III. Critical Assessment of the Selected Data

We have examined the status of the experimental and evaluated data, and reserved some data for further examination. In this chapter, we will look into whether or not the reserved quantities satisfy the required accuracy. In Table 1, we list the required accuracy presented in the previous two AGM's on TND together with the accuracy submitted to the WRENDA 81/82. We segment the energy range into four parts tentatively: (i) thermal region below 1 eV, (ii) resonance region between 1 eV and 1 keV, (iii) unresolved resonance or fluctuation region from 1 keV to 1 MeV and (iv) smooth region above 1 MeV. An energy column for 0.0253 eV (Therm.) is set up separately.

In order to compare the required data with the real data, we adopt first the JENDL-2 and ENDF/B-V or -IV data. It is difficult to define a quantity to be compared with the required accuracy from the evaluated data, but we calculate

$$\Delta\sigma_i = |\sigma_i(J) - \sigma_i(B)| \ / \ \bar{\sigma}_i ,$$

at the i-th energy point, where $\sigma_i(J)$, $\sigma_i(B)$ and $\bar{\sigma}_i$ are cross-section values for JENDL-2, ENDF/B-V or -IV and their average value. In Table 2, we give the maximum and minimum values of this quantity for each energy segment, and the average of $\Delta\sigma_i$ in Table 3. Although a direct comparison between Table 1 and Table 3 is probably meaningless, it is indubitable that the values in Table 3 give a measure of discrepancy among the data. In fact, Table 3 numerically justifies the discussion in the previous chapter.

The quantities to be checked here are as follows.

(a) Capture cross section:
^{236}U, ^{237}Np, ^{240}Pu, ^{242}Pu, ^{241}Am, ^{243}Am.

(b) Fission cross section:
^{237}Np, ^{238}Pu, ^{241}Pu, ^{241}Am, ^{243}Am, ^{244}Cm, ^{245}Cm.

(c) $\bar{\nu}$:
^{237}Np, ^{241}Pu.

(d) (n,2n) cross section:
^{238}U.

In the following, we will examine the status of these data by using Table 2, Table 3 and some experimental and evaluated data.

Table 1. Required Accuracies for Transactinium Isotope Nuclear Data

		from '75 and '79 AGM (%)					from WRENDA 81/82 (%)				
		Therm.	≦1eV	1eV∿1keV	1keV∿1MeV	1MeV≦	Therm.	≦1eV	1eV∿1keV	1keV∿1MeV	1MeV≦
Th-230	$\sigma_{n,\gamma}$	50						10	10	10	
Th-232	$\sigma_{n,2n}$					50					5∿20
	$\sigma_{n,3n}$					50					10∿15
Pa-231	$\sigma_{n,\gamma}$	10					5	5∿10	5∿10	10	10
Pa-233	$\sigma_{n,\gamma}$	10					5	5	5∿15	10∿15	10∿15
U -232	$\sigma_{n,\gamma}$	30					2	2∿5	2∿5	50	50
	$\sigma_{n,f}$	30								50	50
U -233	$\sigma_{n,2n}$					10					10
U -234	$\sigma_{n,\gamma}$	5					3	3∿5	5∿15	5∿50	15∿50
U -236	$\sigma_{n,\gamma}$	4					3	10	7∿20	7∿50	7∿50
U -237	$\sigma_{n,\gamma}$	100								50	50
U -238	$\sigma_{n,2n}$					10					5∿20
Np-237	$\sigma_{n,\gamma}$	10		15	15		10	10	10∿15	10∿20	10∿20
	$\sigma_{n,f}$				50	50				1∿10	1∿10
	$\sigma_{n,2n}$					10∿15					10∿15
	$\bar{\nu}$					50					

Table 1. Required Accuracies for Transactinium Isotope Nuclear Data (Contd)

		from '75 and '79 AGM (%)					from WRENDA 81/82 (%)				
		Therm.	≤1eV	1eV~1keV	1keV~1MeV	1MeV≤	Therm.	≤1eV	1eV~1keV	1keV~1MeV	1MeV≤
Np-239	$\sigma_{n,\gamma}$	100		20	20		20	20~30	20~30	20~50	20~50
	$\sigma_{n,f}$				50	50	30	30	30	30~50	30~50
	$\sigma_{n,2n}$					50					50
	$\bar{\nu}$				50	50					
Pu-236	$\sigma_{n,\gamma}$	50		20~50							
	$\sigma_{n,f}$			20	50	50				10	10
Pu-238	$\sigma_{n,\gamma}$	10		20	20		20	20	20	10~20	10~20
	$\sigma_{n,f}$	50		20	7~20	7~20				15~20	15~20
	$\sigma_{n,3n}$					50					
	$\bar{\nu}$				4	4			4	4	4
Pu-239	$\sigma_{n,2n}$					10~50					10~15
Pu-240	$\sigma_{n,\gamma}$	2	5				3	3	3~7	4~10	4~10
Pu-241	$\sigma_{n,\gamma}$	3					3	3	3~10	3~10	7~10
	$\sigma_{n,f}$	1					1	1~5	1~10	1~10	5~10
	$\bar{\nu}$	0.5								2~5	5
Pu-242	$\sigma_{n,\gamma}$	5~50			30	30	3~10	3~10	3~15	5~20	10~20
Am-241	$\sigma_{n,\gamma}$	10~50	10	5~10	5~10	10	10~20	10~20	8~20	5~20	5~20

		from '75 and '79 AGM (%)					from WRENDA 81/82 (%)				
		Therm.	≤1eV	1eV~1keV	1keV~1MeV	1MeV≤	Therm.	≤1eV	1eV~1keV	1keV~1MeV	1MeV≤
Am-241	$\sigma_{n,f}$				15	15	20	20	20	3~20	3~10
	$\bar{\nu}$				10	10	5~20	5~20	5~20	5~20	5~20
Am-242g	σ_{tot}		50	50	50	50	10	10	10	10	10
	$\sigma_{n,\gamma}$		50	50	50	50	10~30	10~30	10~50	10~50	20~50
	$\sigma_{n,f}$		50	50	50	50	10~15	15	15~20	15~20	15~20
Am-242m	σ_{tot}		20	20	20	20	10	10	10	10	10
	$\sigma_{n,\gamma}$	20	20	20~50	20~50	20	10~30	10~30	10~50	10~50	20~50
	$\sigma_{n,f}$	10	20	20	15~20	15~20	10~15	15	15~20	15~20	15~20
	$\bar{\nu}$				10	10	15	15	10~15	10~15	10~15
Am-243	$\sigma_{n,\gamma}$	10		10	10~50	10~50	10~30	10~30	10~30	10~30	10~30
	$\sigma_{n,f}$				30	30	15	15	15	10~15	10~15
	$\sigma_{n,2n}$					50					
	$\bar{\nu}$				10	10	15	15	15~25	15~25	15~25
Cm-242	σ_{tot}		20	20							
	$\sigma_{n,\gamma}$	20	20	20~50	30~50	30	10~30	10~30	10~50	10~50	30
	$\sigma_{n,f}$				20~25	20~25	10~30	10~30	10~30	10~30	10~30
	$\bar{\nu}$				15	15	30	30	30	30	30

Table 1. Required Accuracies for Transactinium Isotope Nuclear Data (Contd)

		from '75 and '79 AGM (%)					from WRENDA 81/82 (%)				
		Therm.	≤1eV	1eV~1keV	1keV~1MeV	1MeV≤	Therm.	≤1eV	1eV~1keV	1keV~1MeV	1MeV≤
Cm-243	$\sigma_{n,\gamma}$	50	30	30	30	30	15~30	15~30	10~50	10~50	10~30
	$\sigma_{n,f}$	50			20	20	50	50	50	50	10~50
Cm-244	$\sigma_{n,\gamma}$	20		50	30~50	30	10~30	10~30	10~30	10~30	10~30
	$\sigma_{n,f}$				20~50	20~50	30	30	10~30	10~30	10~30
Cm-245	$\sigma_{n,\gamma}$	50			50	50	10~30	10~30	10~50	10~50	30
	$\sigma_{n,f}$	50					10~30	10~30	10~50	10~50	30~50
Cm-246	$\sigma_{n,\gamma}$	100	10	10	200	200	10	10	10	10~50	50
	$\sigma_{n,f}$	30								50	50
Cm-247	$\sigma_{n,\gamma}$	30					5~10	5~10	5~10	5~50	50
	$\sigma_{n,f}$	30	5~10	5~10	10	10	5~10	5~10	5~10	5~50	50
Cm-248	$\sigma_{n,\gamma}$	50								50	50
Bk-249	$\sigma_{n,\gamma}$	30								50	50
	$I_{n,\gamma}$		10	10							
Cf-249	$\sigma_{n,\gamma}$	50								50	50
	$\sigma_{n,f}$	30									
Cf-250	$\sigma_{n,\gamma}$	50	10	10			10	10	10	10	
	$\sigma_{n,f}$	30	10	10			10	10	10	10	

		from '75 and '79 AGM (%)					from WRENDA 81/82 (%)				
		Therm.	≤1eV	1eV~1keV	1keV~1MeV	1MeV≤	Therm.	≤1eV	1eV~1keV	1keV~1MeV	1MeV≤
Cf-251	$\sigma_{n,\gamma}$	50					10	10	10	10	
	$\sigma_{n,f}$	30	10	10			10	10	10	10	
Cf-252	$\sigma_{n,\gamma}$	30									
	$\sigma_{n,f}$	30					10	10	10	10	
Cf-253	$\sigma_{n,\gamma}$	100									
	$\sigma_{n,f}$	30									
Es-253	$\sigma_{n,\gamma}$	30									

Table 2 Discrepancies between JENDL-2 and ENDF/B-IV or -V

(in percent)

Quantity	< 1 eV	1 eV - 1 keV	1 keV - 1 MeV	Above 1 MeV
Th-230 (n,γ)	0.15 - 32	4.2 - 79	54 - 130	5.3 - 200
Th-232 (n,2n)				0.0 - 95
Th-232 (n,3n)				0.0 - 36
Pa-231 (n,γ)	(ENDF/B-V only)			
Pa-233 (n,γ)	0.37 - 110	0.05 - 59	4.0 - 100	4.4 - 100
U -232 (n,γ)	(ENDF/B-V only)			
U -232 (n,f)	(ENDF/B-V only)			
U -233 (n,2n)				0.0 - 100
U -234 (n,γ)	7.2 - 23	2.7 - 64	5.9 - 81	14 - 200
U -236 (n,γ)	0.2 - 2.8	0.0 - 58	0.07 - 43	2.7 - 200
U -237 (n,γ)	(ENDF/B-V only)			
U -238 (n,2n)				0.0 - 16
Np-237 (n,γ)	4.7 - 28	0.6 - 7.6	0.09 - 25	2.7- 200
Np-237 (n,f)	9.1 - 40	1.3 - 180	0.9 - 100	1.8 - 25
Np-237 (n,2n)				0.0 - 120
Np-237 $\bar{\nu}$	6.6	6.6	6.4 - 6.6	2.1 - 6.4
Np-239 (n,γ)	(JENDL-2 only)			
Np-239 (n,f)	(JENDL-2 only)			
Np-239 (n,2n)	(JENDL-2 only)			
Np-239 $\bar{\nu}$	(JENDL-2 only)			
Pu-236 (n,γ)	120 - 200	11 - 200	65 - 120	22 - 200
Pu-236 (n,f)	9.1 - 200	120 - 200	19 - 170	8.9 - 43
Pu-238 (n,γ)	2.2 - 2.3	0.2 - 190	0.07- 70	86 - 170
Pu-238 (n,f)	0.6 - 8.3	0.8 - 190	0.5 - 56	0.0 - 5.0
Pu-238 (n,3n)				0.0 - 110
Pu-238 $\bar{\nu}$	0.05	0.05	0.05	0.03 - 0.05
Pu-239 (n,2n)				0.0 -150
Pu-240 (n,γ)	0.0 - 0.9	0.03 - 19	0.6 - 35	2.1- 160
Pu-241 (n,γ)	1.2 - 30	0.4 - 110	1.7 - 59	15 - 200
Pu-241 (n,f)	0.05 - 10	0.3 - 79	0.3 - 12	0.7 - 29
Pu-241 $\bar{\nu}$	0.0	0.0	0.0	0.0
Pu-242 (n,γ)	3.0 - 4.0	0.3 - 14	0.02- 40	15 - 92
Am-241 (n,γ)	0.2 - 48	0.9 - 30	0.4 - 32	6.2 - 200
Am-241 (n,f)	1.0 - 47	0.3 - 160	0.1 - 82	0.3 - 4.9
Am-241 $\bar{\nu}$	4.2	4.2	3.8 - 4.2	0.1 - 3.5
Am-242g total	71 - 110	36 - 120	1.7 - 42	27 - 54
Am-242g(n,γ)	150- 180	81 - 170	81 - 200	200
Am-242g(n,f)	0.3 - 79	28 - 120	49 - 200	200
Am-242m total	0.0 - 0.2	0.3 - 96	0.4 - 25	0.6 - 23
Am-242m(n,γ)	0.0	0.0 - 120	11 - 170	52 - 200
Am-242m(n,f)	0.0	0.0 - 98	0.4 - 43	5.4 - 34
Am-242m $\bar{\nu}$	0.3	0.3	0.3	0.1 - 0.3
Am-243 (n,γ)	0.3 - 5.1	0.1 - 5.7	5.6 - 110	9.1 - 200
Am-243 (n,f)	200	190 - 200	1.5 - 180	3.4 - 12
Am-243 (n,2n)				0.0 - 140
Am-243 $\bar{\nu}$	1.9	1.9	1.9 - 2.5	2.7 - 8.5
Cm-242 total	4.1 - 12	12 - 180	1.7 - 17	1.1 - 8.6
Cm-242 (n,γ)	2.3 - 7.6	0.07- 200	5.8 - 120	35 - 200
Cm-242 (n,f)	48 - 94	110- 200	150 - 190	1.3 - 96
Cm-242 $\bar{\nu}$	1.7	1.7	1.6 - 1.7	0.4 - 1.6
Cm-243 (n,γ)	12 - 81	7.0 - 110	0.03- 110	15 - 200
Cm-243 (n,f)	0.6 - 15	3.9 - 120	0.8 - 49	2.3 - 22
Cm-244 (n,γ)	31 - 33	0.01- 100	6.0 - 65	23 - 200
Cm-244 (n,f)	63 - 110	0.2 - 170	0.1 - 50	1.7 - 21
Cm-245 (n,γ)	1.5 - 91	2.6 - 140	2.9 - 94	12 - 200
Cm-245 (n,f)	0.04- 55	0.3 - 120	0.2 - 22	0.0 - 36
Cm-246 (n,γ)	2.6 - 2.8	0.01 - 24	9.6 - 61	28 - 200
Cm-246 (n,f)	77	1.7 - 150	8.9 - 200	1.7 - 36
Cm-247 (n,γ)	0.7 - 180	2.8 - 200	16 - 89	2.3 - 200
Cm-247 (n,f)	2.4 - 190	1.7 - 200	3.6 - 120	4.5 - 33
Cm-248 (n,γ)	5.0 - 5.6	0.2 - 11	0.2 - 110	3.4 - 200

Table 3 Discrepancies between JENDL-2 and ENDF/B-IV or -V

(in percent)

Quantity	0.0253 eV	< 1 eV	1 eV - 1 keV	1 keV - 1 MeV	Above 1 MeV
Th-230 (n,γ)	2.3	10	32	81	150
Th-232 (n,2n)	-	-	-	-	14
Th-232 (n,3n)	-	-	-	-	7.2
Pa-231 (n,γ)	(ENDF/B-V only)				
Pa-233 (n,γ)	3.2	14	7.3	35	35
U -232 (n,γ)	(ENDF/B-V only)				
U -232 (n,f)	(ENDF/B-V only)				
U -233 (n,2n)	-	-	-	-	60
U -234 (n,γ)	7.7	11	30	26	130
U -236 (n,γ)	2.6	2.0	7.1	11	120
U -237 (n,γ)	(ENDF/B-V only)				
U -238 (n,2n)	-	-	-	-	3.6
Np-237 (n,γ)	6.7	14	3.9	8.9	120
Np-237 (n,f)	14	21	52	24	7.5
Np-237 (n,2n)	-	-	-	-	36
Np-237 $\bar{\nu}$	6.6	6.6	6.6	6.5	4.6
Np-239 (n,γ)	(JENDL-2 only)				
Np-239 (n,f)	(JENDL-2 only)				
Np-239 (n,2n)	(JENDL-2 only)				
Np-239 $\bar{\nu}$	(JENDL-2 only)				
Pu-236 (n,γ)	130	160	90	93	120
Pu-236 (n,f)	85	86	150	130	23
Pu-238 (n,γ)	2.3	2.2	18	16	140
Pu-238 (n,f)	2.8	2.8	40	16	1.6
Pu-238 (n,3n)	-	-	-	-	18
Pu-238 $\bar{\nu}$	0.05	0.05	0.05	0.05	0.04
Pu-239 (n,2n)	-	-	-	-	45
Pu-240 (n,γ)	0.55	0.35	4.5	13	74
Pu-241 (n,γ)	0.96	9.6	41	18	120
Pu-241 (n,f)	0.70	2.2	9.3	3.7	9.2
Pu-241 $\bar{\nu}$	0.0	0.0	0.0	0.0	0.0
Pu-242 (n,γ)	4.0	3.7	4.0	11	49
Am-241 (n,γ)	4.0	11	9.8	12	130
Am-241 (n,f)	8.1	11	43	12	3.0
Am-241 $\bar{\nu}$	4.2	4.2	4.2	4.1	2.0
Am-242g total	100	93	54	26	39
Am-242g(n,γ)	180	180	110	160	220
Am-242g(n,f)	7.7	24	51	150	220
Am-242m total	0.06	0.04	50	8.0	9.9
Am-242m(n,γ)	0.11	0.0	75	70	150
Am-242m(n,f)	0.08	0.0	56	19	15
Am-242m $\bar{\nu}$	0.32	0.32	0.32	0.32	0.23
Am-243 (n,γ)	4.9	3.4	1.1	54	130
Am-243 (n,f)	200	200	200	68	7.4
Am-243 (n,2n)	-	-	-	-	44
Am-243 $\bar{\nu}$	1.9	1.9	1.9	2.0	5.1
Cm-242 total	5.6	7.7	52	11	4.1
Cm-242 (n,γ)	7.4	6.1	5.3	7.3	140
Cm-242 (n,f)	50	60	180	170	23
Cm-242 $\bar{\nu}$	1.7	1.7	1.7	1.7	1.1
Cm-243 (n,γ)	77	57	59	22	150
Cm-243 (n,f)	12	11	32	26	12
Cm-244 (n,γ)	33	33	16	39	100
Cm-244 (n,f)	65	77	43	12	13
Cm-245 (n,γ)	1.2	44	39	49	120
Cm-245 (n,f)	10	23	28	6.4	12
Cm-246 (n,γ)	2.8	2.8	6.8	37	110
Cm-246 (n,f)	71	77	72	150	16
Cm-247 (n,γ)	2.9	50	110	51	110
Cm-247 (n,f)	15	50	120	37	15
Cm-248 (n,γ)	5.0	5.2	4.0	12	110

Capture cross section:

^{236}U (Figure 1): The experimental data covered the energy region below 20 keV[10], and the region between 300 keV and 4 MeV[11,12] before the JENDL-2 evaluation was performed. A recent experiment covers from 100 eV to 50 keV (see Appendix). The difference between JENDL-2 and ENDF/B-V is small in average, below 2 MeV. At 0.0253 eV, their difference is 3%. The experimental uncertainty is 6%.[13] There are still large discrepancies above 2 MeV. Table 2 shows that some differences between the two evaluations exist in the resonance region.

Although these defects must be removed, the requirement to this quantity is almost satisfied. Further endeavors should be made for the data in MeV region and the resonance parameters. The experimental thermal value should also be improved a little.

Figure 1 Capture Cross Section of U-236

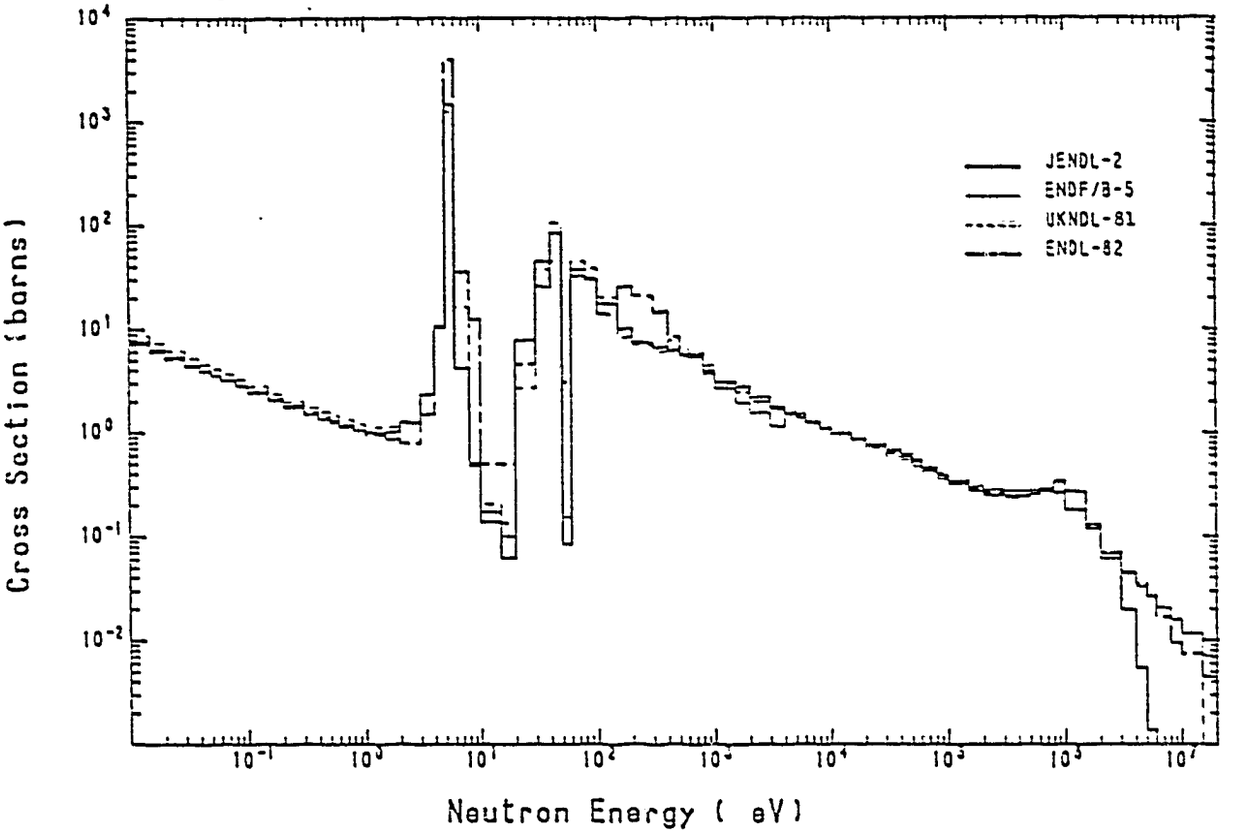

^{237}Np (Figure 2): The experimental data cover the energy range below 3 MeV[14]. The uncertainty of the data at 0.0253 eV is 4% at most[13]. The difference between JENDL-2 and ENDF/B-V is 7% at 0.0253 eV. Hence the requirement for the thermal cross section is fulfilled. Table 2 and 3 show rather large difference between the two evaluated files below 1 eV. This may be due to the different resonance parameters between the two. JENDL-2 adopted the parameters by Weston and Todd[15], together with the fission width by Plattard et al.[16] A recent measurement[17] gave the resonance data up to 600 eV. Including this experiment, evaluation for the resonance parameters may be required. Exclusive of the resonance region and MeV region, the status of the data meets the requirement.

Figure 2 Capture Cross Section of Np-237

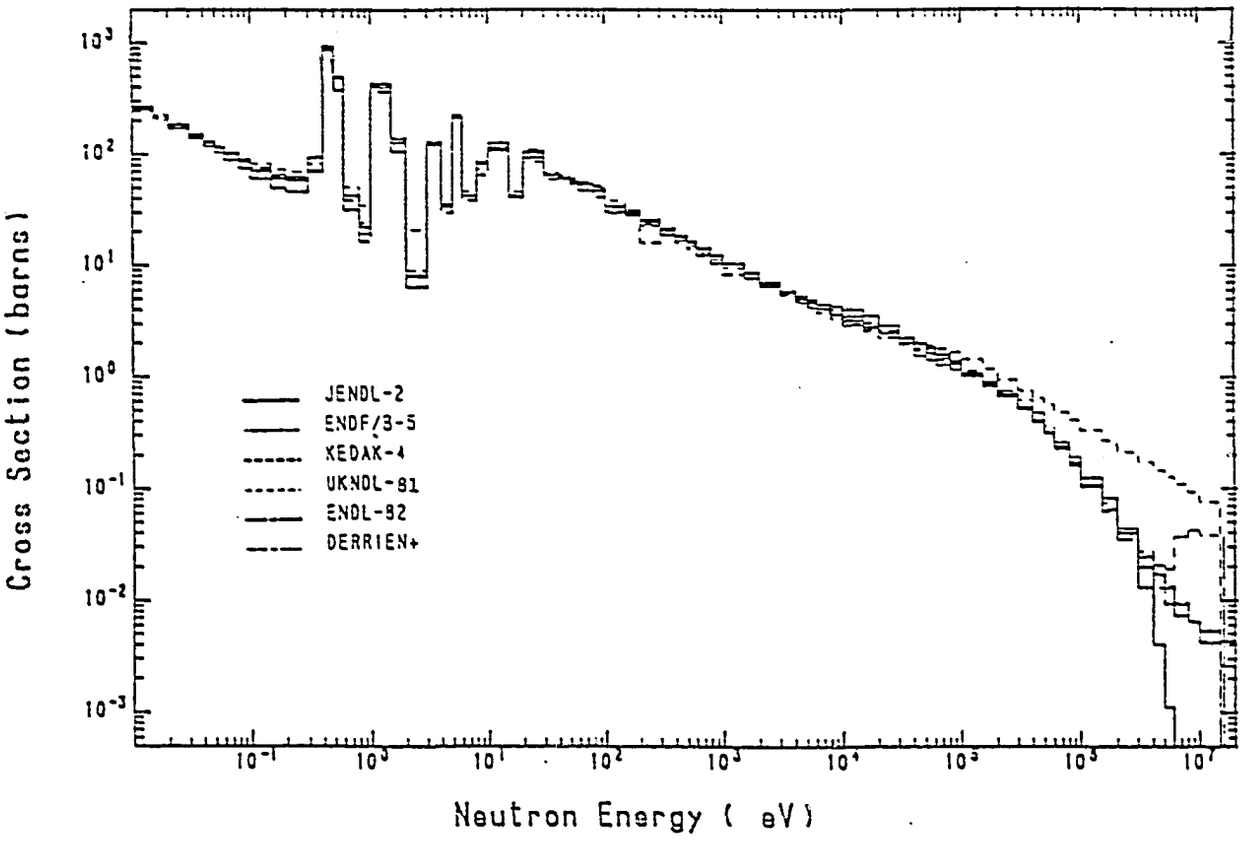

^{240}Pu (Figure 3): The experimental data have been measured below 350 keV. The experimental uncertainty is 0.5% at 0.0253 eV[13]. The JENDL-2 and ENDF/B-IV data are in very good agreement below 1 eV region, and the difference at 0.0253 eV is 0.5%. Agreement between the two evaluated files are fairly good, in average, below a few hundred keV, and the requirement may be fulfilled in this region. Table 2 and Figure 3 show, however, that there are small but some significant differences in the resonance region. High priority request in WRENDA requires the accuracy of 3% for the cross section below 100 eV. Hence, further study may be needed for the resonance parameters. Above several hundred keV, measurement and evaluation seem to be poor.

^{242}Pu (Figure 4): The experimental data have been measured below 250 keV. The uncertainty at 0.025 eV is 2%,[13] and the difference between the JENDL-2 and ENDF/B-IV data is 4% at most. Hence, the status of the data nearly satisfies the requirement for the thermal region. Table 3 shows that the two evaluated files are fairly in good agreement, in average, below 1 MeV. Table 2 reveals that there are large differences in some parts above 1 keV region. Figure 4 shows that these exist around 2-3 keV. Further study should be tried in this region as well as in MeV region.

Figure 3 Capture Cross Section of Pu-240

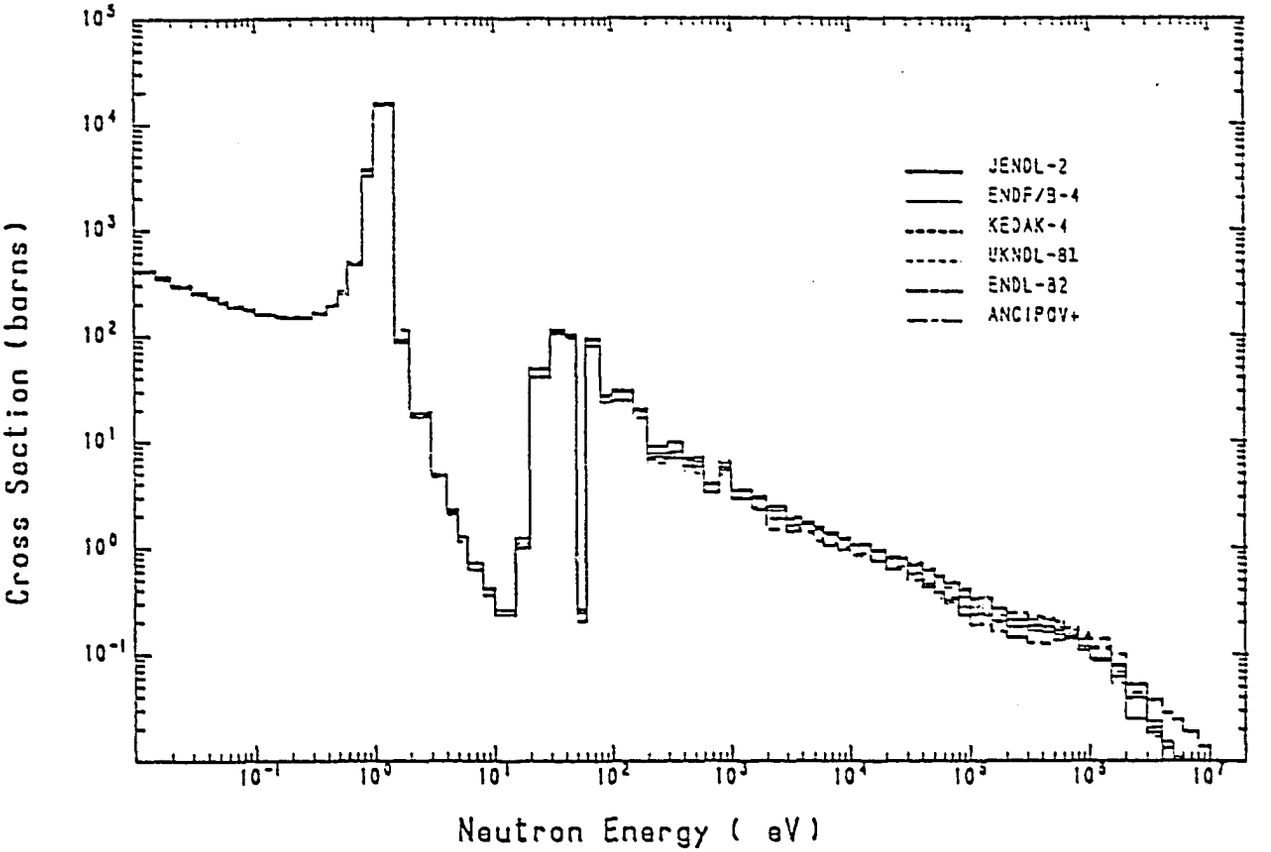

Figure 4 Capture Cross Section of Pu-242

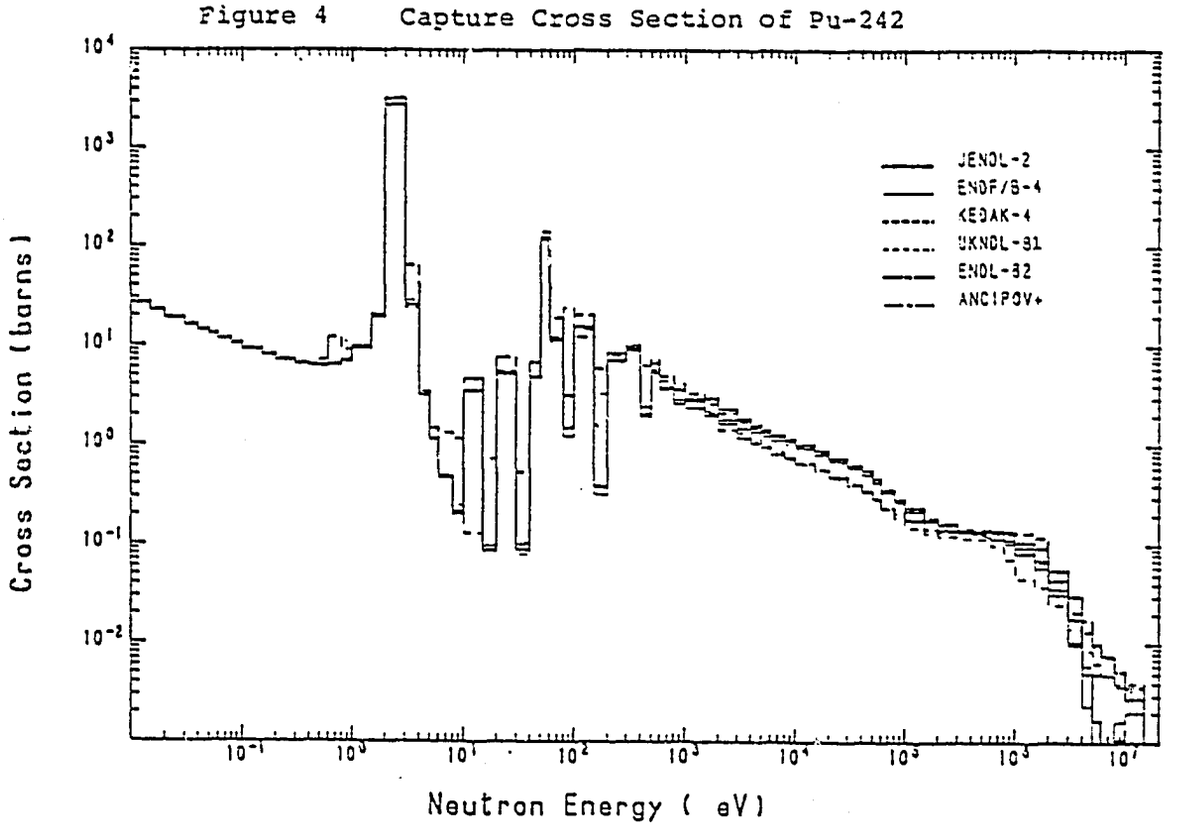

^{241}Am (Figure 5): The measurements have been performed up to 500 keV. The uncertainty at 0.0253 eV is 3.5%.[18] The difference between the JENDL-2 and ENDF/B-V data is 4%. Thus the data status meets the requirement for the thermal cross section. Table 3 shows that the two evaluated data files are nearly in good agreement, in average, below several hundred keV, but Table 2 and Figure 5 reveal that the large differences exist in the resonance region and above 10 keV. Except the region from 1 keV to 10 keV as well as the thermal region, further study should be needed. The resonance integral data are still discrepant in both measurements and evaluations.

Figure 5 Capture Cross Section of Am-241

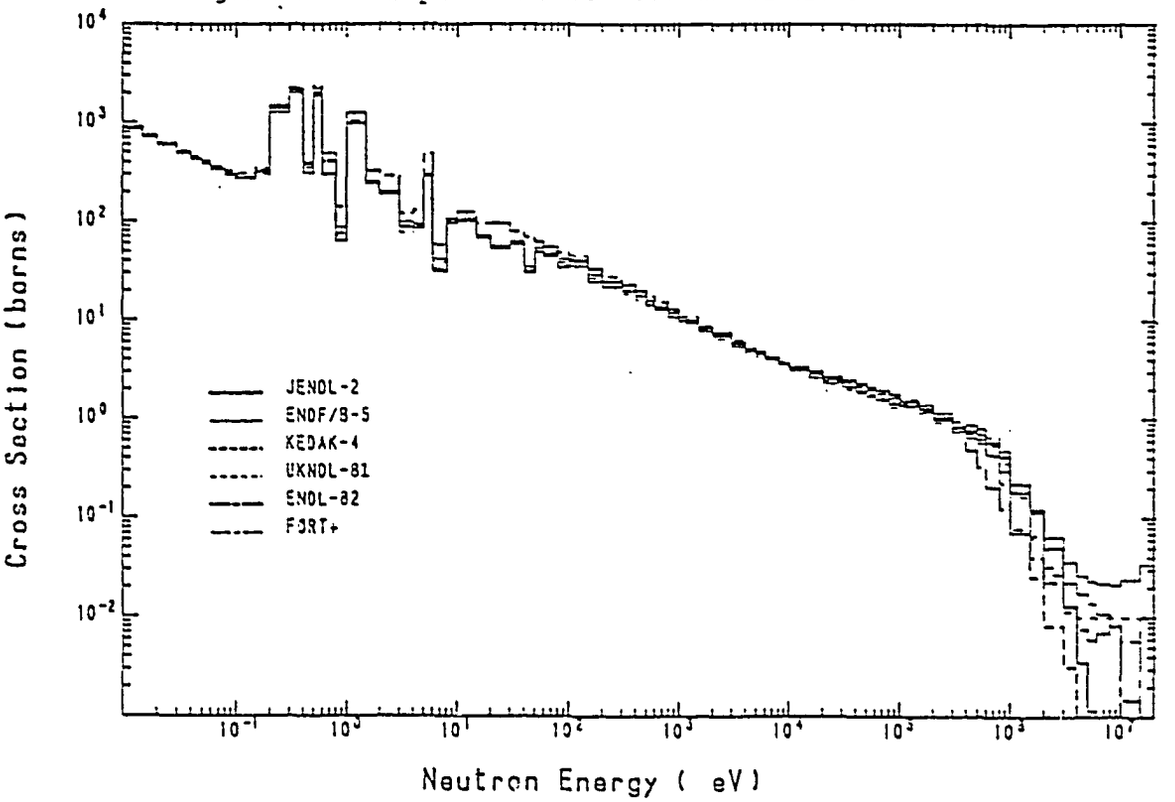

^{243}Am (Figure 6): The experimental data have been obtained up to 250 keV. The uncertainty at 0.0253 eV is 2.5%.[13] The difference between the JENDL-2 and ENDF/B-V data is 5%. Hence the data at 0.0253 eV seems to satisfy the required accuracy. Table 2 and Table 3 show that the agreement between the JENDL-2 and ENDF/B-V data is extremely good below 1 keV, and apparently the requirement seems to be satisfied. However, the resonance integrals manifest very different values between the measurement and evaluation. In this sense, the data status of this quantity must be still insufficient. Above 1 keV, the two evaluated data files disagree with each other.

Fission cross section:

^{237}Np (Figure 7): The experimental data have been measured up to above 40 MeV, and cover the whole energy range from thermal to 20 MeV. The requirements have been made for the data above the threshold energy. The JENDL-2 and ENDF/B-V data agree in average with each other

Figure 6 Capture Cross Section of Am-243

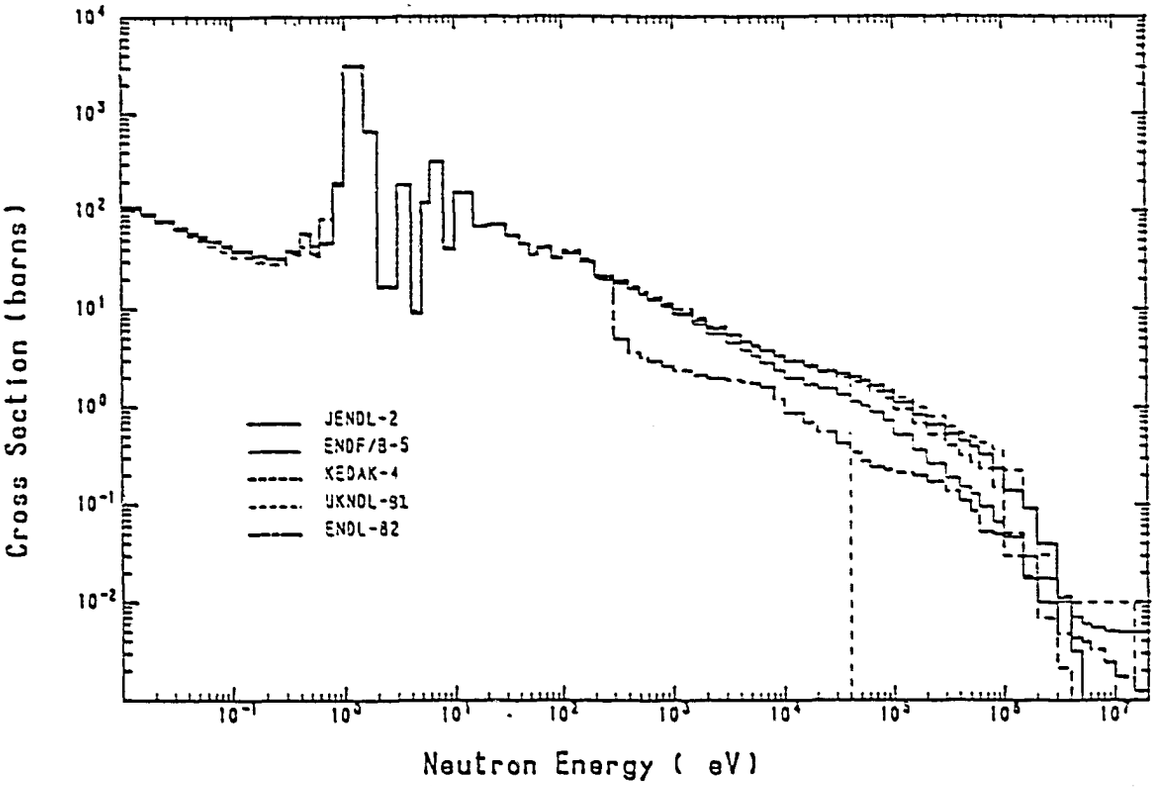

Figure 7 Fission Cross Section of Np-237

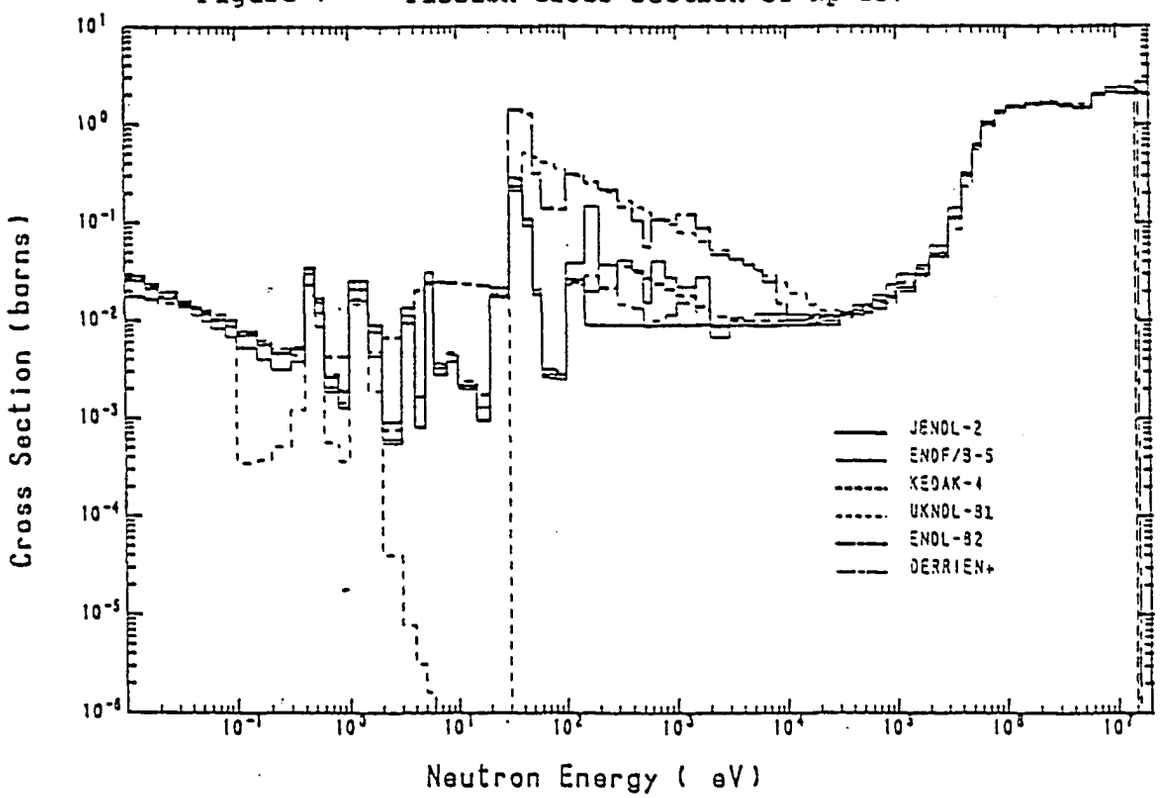

in the plateau region, but some difference is found in the threshold region. Since there are many experimental data, endeavors should be made to obtain reliable evaluated data above the threshold region. For the data in the subthreshold region, there are large discrepancies among the evaluated data.

^{238}Pu (Figure 8): The measurements have been made up to 10 MeV. The experimental uncertainty at 0.0253 eV is 3%.[13] The difference between the JENDL-2 and ENDF/B-V is 3% also. But, the JENDL-2 data deviate 5% from the experimental data. Hence the requirement for the thermal cross section is satisfied, but further evaluation may be required. Table 2 and Table 3 show that the two evaluated data files are very different with each other, except the plateau region. The requirement seems to be fulfilled for the data above 1 MeV, but further endeavors may be needed for the subthreshold region. The JENDL-2 resonance integral is larger than the experimental data.

Figure 8 Fission Cross Section of Pu-238

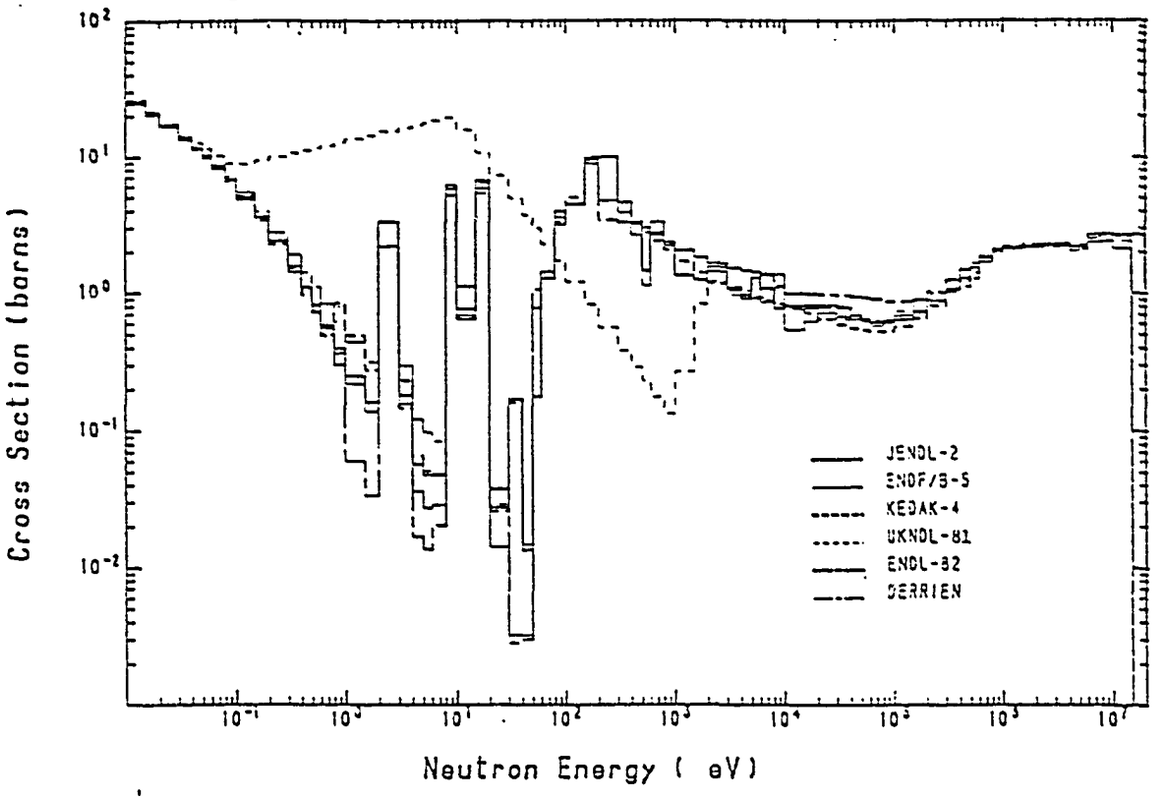

^{241}Pu (Figure 9): The experimental data cover the whole energy region below 30 MeV. The experimental uncertainty at 0.0253 eV is 0.8%.[13] The difference between the JENDL-2 and ENDF/B-IV is 0.1%, and 0.6% between the experimental and evaluated data. Hence the requirement for the thermal cross section is satisfied. Table 3 shows that the two evaluated data files agree well, in average, with each other, and the requirement may be almost satisfied. Table 2 reveals, however, that there are partly some large differences between the evaluated data. Since many experimental data have been obtained, evaluation work should be done further a little.

^{241}Am (Figure 10): There are many new experimental data which cover the energy range up to 20 MeV. The uncertainty of the experimental data at 0.0253 eV is estimated as 6.5%.[18] The difference between the JENDL-2 and ENDF/B-V data is 8%. Since the JENDL-2 value reproduces the experimental data, the requirement seems to be met well. The experimental resonance integral, however, is about twice as large as that of the evaluated data. This means that the status of the data is still unsatisfactory including the thermal cross section. Table 2 shows that there are large differences between the evaluated data below 1 MeV. Hence more endeavors should be made. Above the threshold energy, the status of the data satisfies the requirements.

Figure 9 Fission Cross Section of Pu-241

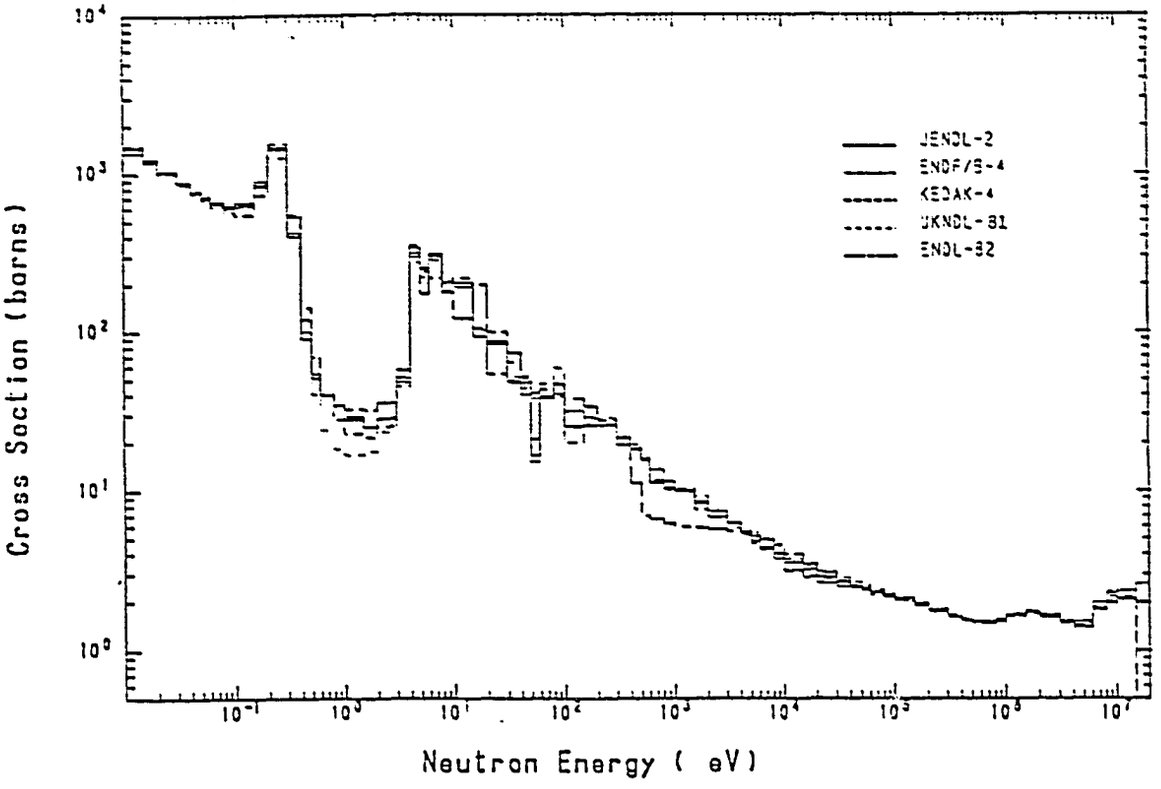

Figure 10 Fission Cross Section of Am-241

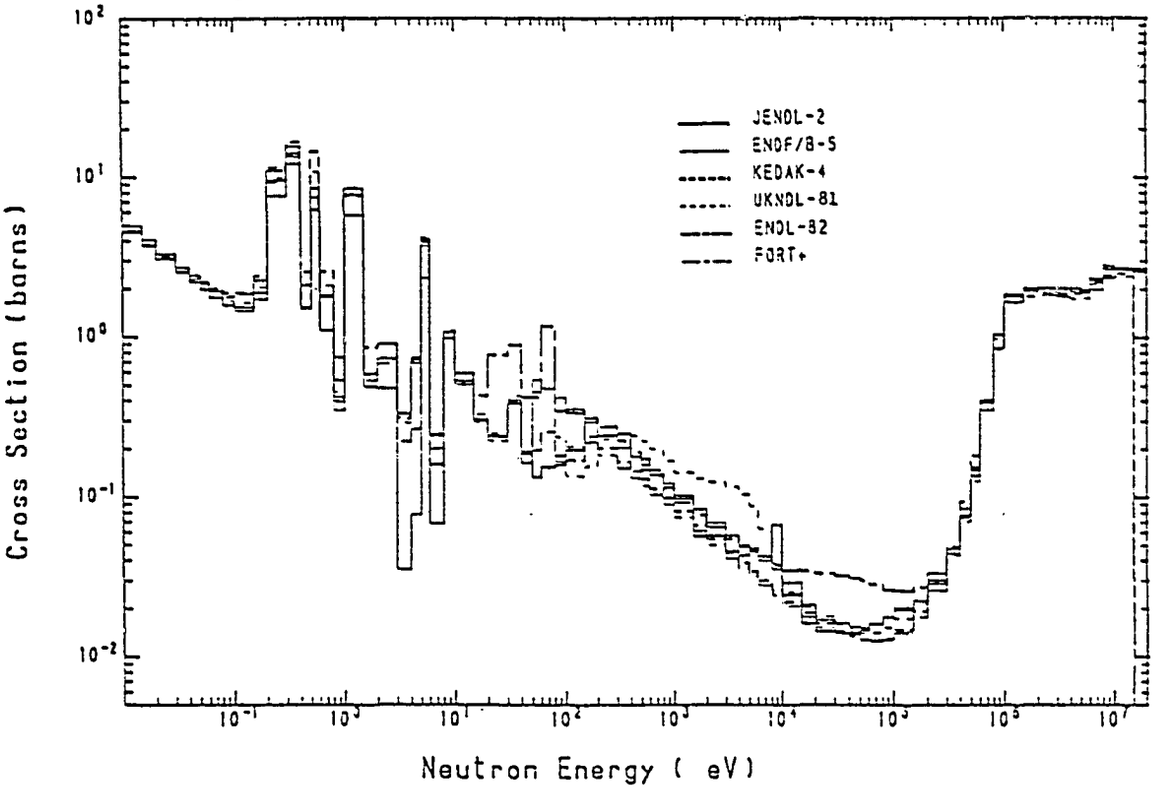

^{243}Am (Figure 11): The measurements have been made up to 30 MeV. Recent measurements[19] cover the energy range from 5 keV to 200 keV where no experimental data had been obtained before the JENDL-2 evaluation was finished. The experimental error at 0.0253 eV is 50%.[20] JENDL-2 adopted the data by Asghar et al.[21], while ENDF/B-V does not give the data below 200 eV. Except the plateau region, the evaluation is very discrepant with each other. Although the data in the plateau region seem to satisfy the requirement, further evaluation should be performed in the whole energy region. Since there are many experimental data, endeavors should be made on the evaluation work rather than on the experiments. Only JENDL-2 seems reasonable.

Figure 11 Fission Cross Section of Am-243

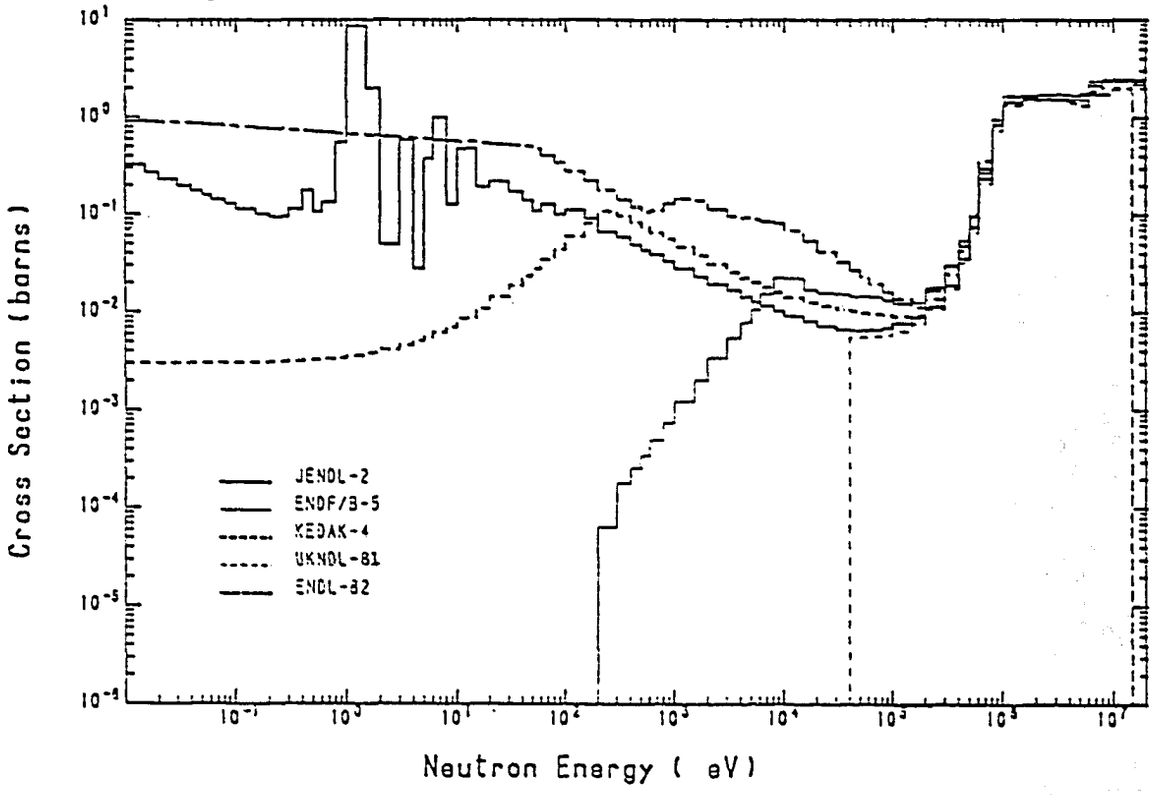

^{244}Cm (Figure 12): The experimental data are not necessarily enough, but cover the whole energy region below 15 MeV. The error of the experimental data at 0.0253 eV is 10% at most[13], but the difference between the JENDL-2 and ENDF/B-V data is 65%. Table 2, Table 3 and Fig.12 show that the two evaluated data files disagree with each other below 10 keV. Even in the plateau region, the difference between the two files is over 10% in average. More measurements and evaluations may be needed in order to satisfy the required accuracy.

^{245}Cm (Figure 13): The experimental data have been obtained up to 20 MeV. At the time when the JENDL-2 evaluation was performed, available experimental data existed below only 300 keV. The error of the experimental data at 0.0253 eV is 2% at most[13]. A recent measurement by White and Browne[22] shows 0.7% for statistical error. The difference between the JENDL-2 and ENDF/B-V data is 10%. Hence, the requirement

Figure 12 Fission Cross Section of Cm-244

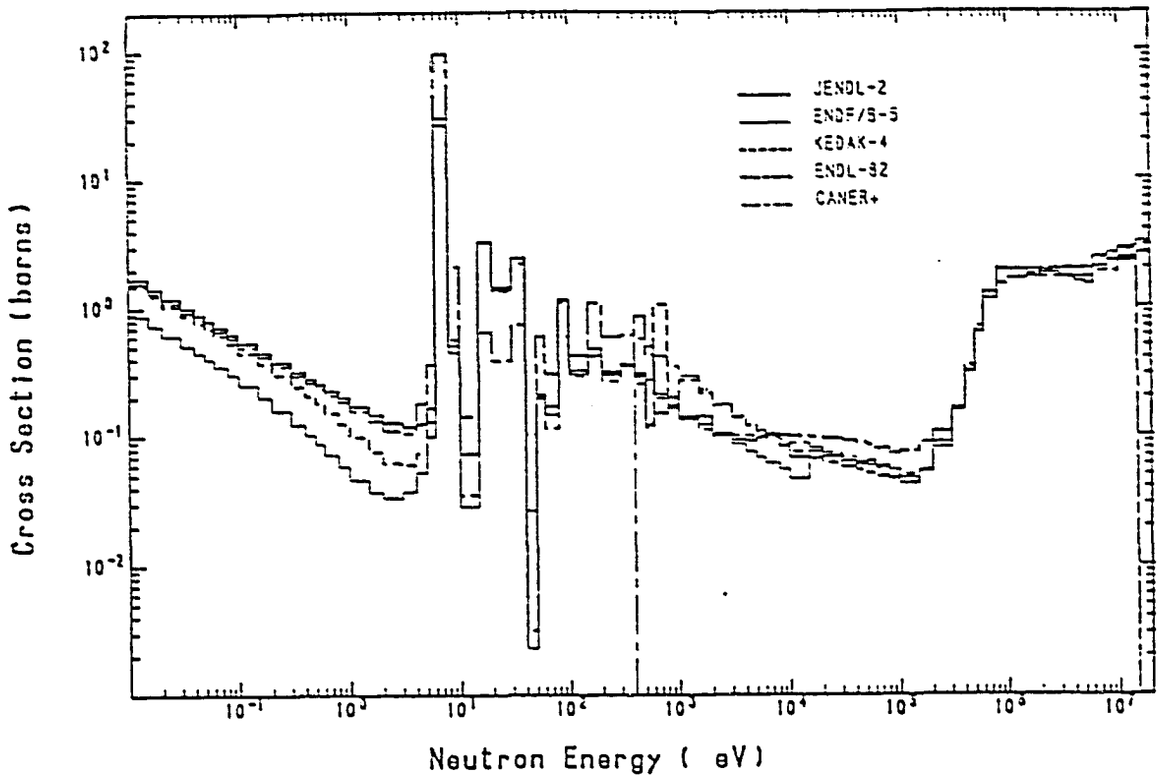

Figure 13 Fission Cross Section of Cm-245

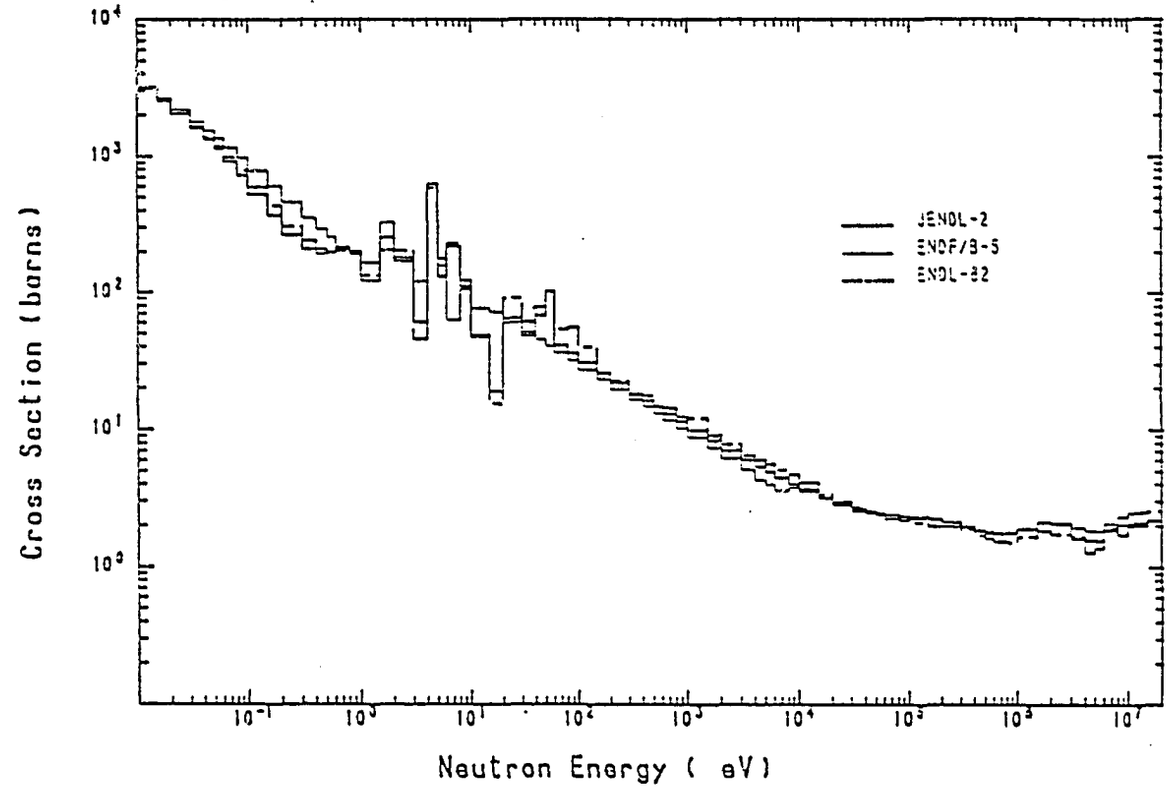

for the thermal value seems to be fulfilled. Table 2, Table 3 and Fig.13 show that there are large differences between the two files below 1 eV. This may be due to the different selectior of the resonance parameters. In fact, some large differences are found in the resonance region. Above 1 keV, the difference is not large in average, and the status of the data seems to satisfy the requirement. Table 2 reveals, however, that there are partly large differences above 3 MeV. More evaluation using the new experimental data should be suggested.

The (n,2n) cross section and $\bar{\nu}$ -value:

^{238}U(n,2n) (Figure 14): The JENDL-2 data were obtained by the evaporation model of Segev and Caner[23], and were normalized to the experimental data by Frehaut and Mosinski[24]. The discrepancy between the experimental data is about 30% around 10 MeV. The difference between the JENDL-2 and ENDF/B-IV is 10% at 10 MeV. Average difference between the two files is 3.6%, and the largest difference is 16%. Above 15 MeV, the evaluated data deviate from the experimental data. The requirement is not always met. As many measurements have been made recently, more evaluation using these new data should be recommended.

Figure.14 (n,2n) Cross Section of U-238

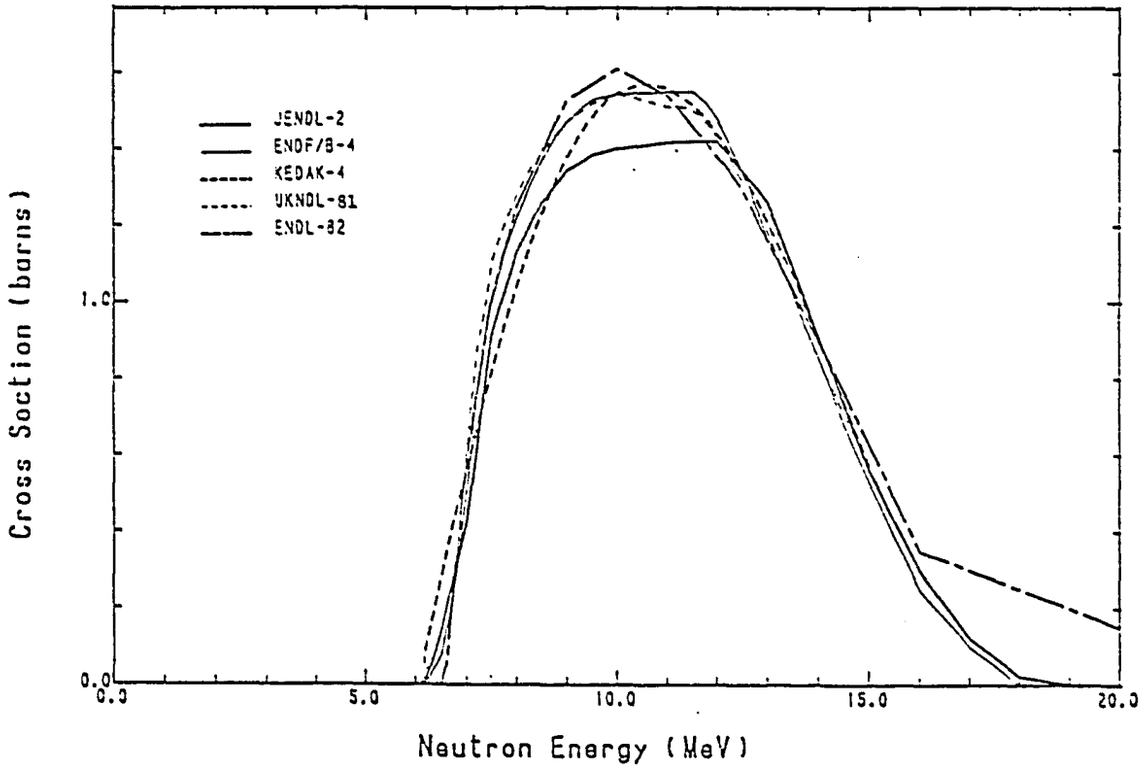

^{237}Np $\bar{\nu}$ (Figure 15): Recent measurement by Frehaut et al.[25] gave the data with error of 1% at most. JENDL-2 adopted this result. The differences between the JENDL-2 and ENDF/B-V data are 5%, 2.6%, 4% and more than 5% respectively at 5, 10, 15 and 20 MeV. Hence the requirement is absolutely satisfied. As many experimental data exist, the difference between the evaluated data may be reduced more.

Figure 15 $\bar{\nu}$ of Np-237

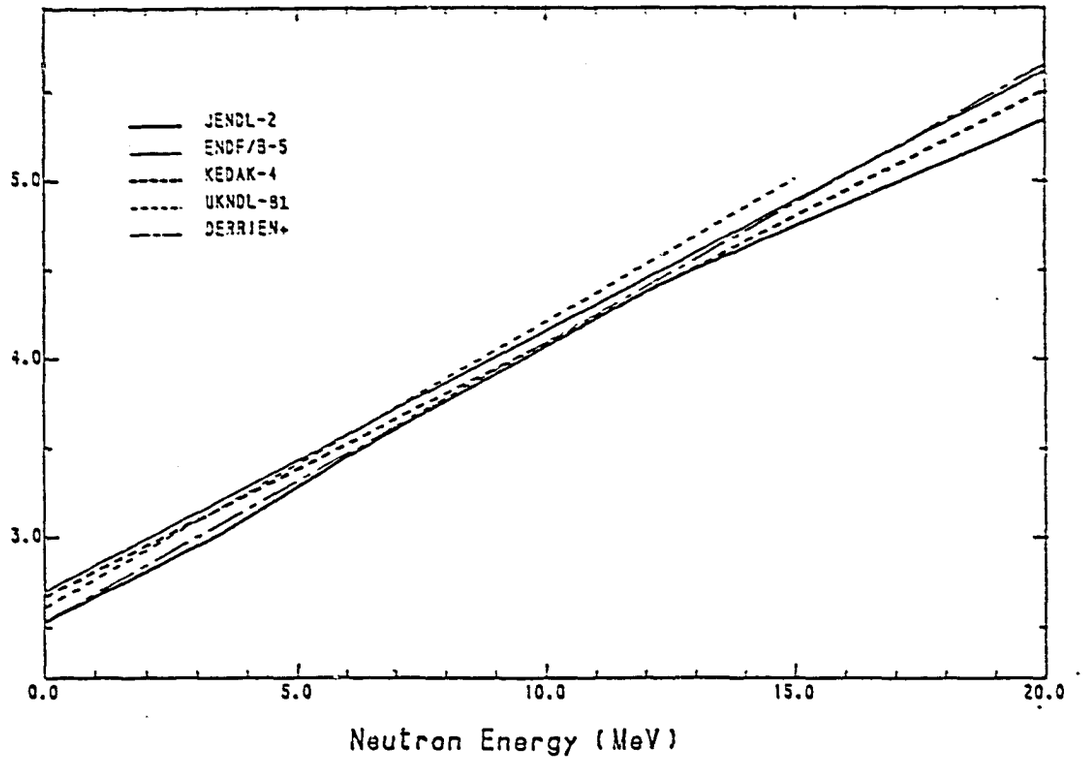

^{241}Pu $\bar{\nu}$ (Figure 16): There are many works of measurements and evaluations for this quantity. JENDL-2 adopted the thermal value by Boldeman and Frehaut[26], and obtained $\bar{\nu}_p$=2.913 (subtracting delayed neutron) by assuming $\bar{\nu}_p$=3.753 for ^{252}Cf. The energy dependence was assumed to be linear by observing the data by Frehaut et al.[27] and D'yachenko et al.[28] The error of the thermal value is about 0.35%. The difference among the evaluated data is very small. The JENDL-2 and ENDF/B-IV data are in good agreement. The data by Konshin et al.[29] deviate only about 2% at 15 MeV from the majority. Hence, the requirement is satisfied.

Figure 16 $\bar{\nu}$ of Pu-241

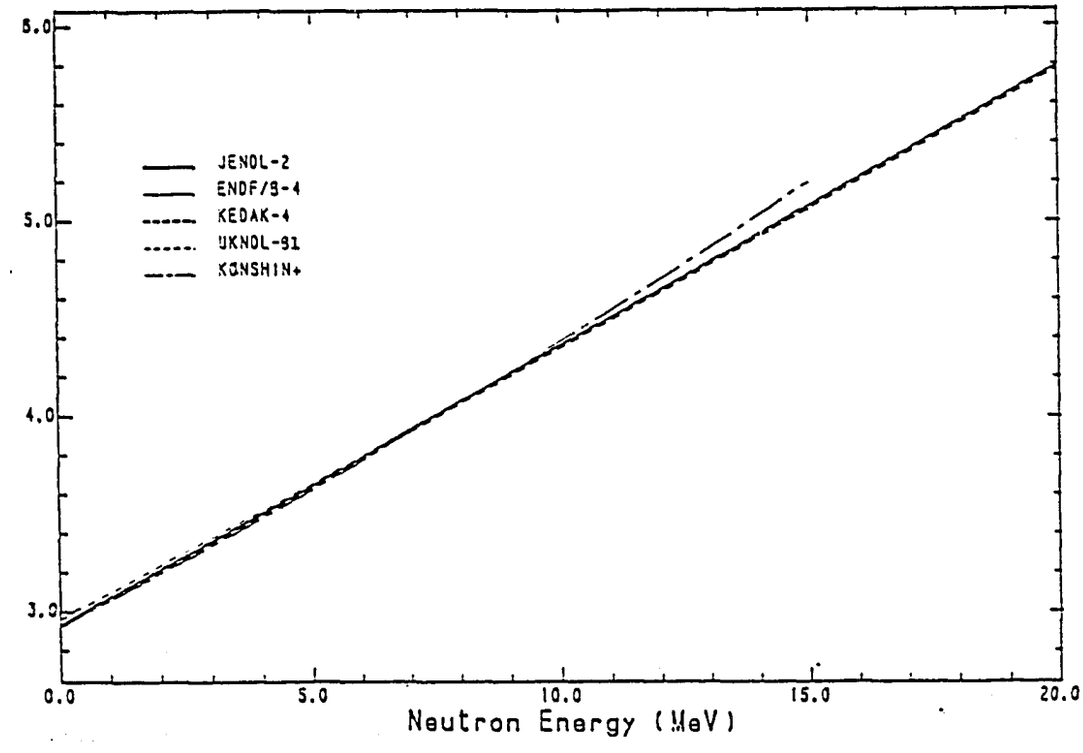

From the above-mentioned review, it may be concluded that as far as these data are concerned, many requirements are satisfied in some energy regions. Still insufficient quantities are as follows,

(i) Insufficient data for whole energy region:
$^{243}Am(n,f)$ evaluation,
$^{244}Cm(n,f)$ measurement and evaluation.

(ii) Insufficient thermal data:
$^{236}U(n,\gamma)$ measurement.

(iii) Insufficient resonance data:
Measurement:
$^{241}Am(n,\gamma)$, $^{243}Am(n,\gamma)$, $^{241}Am(n,f)$.
Evaluation:
$^{236}U(n,\gamma)$, $^{237}Np(n,\gamma)$, $^{240}Pu(n,\gamma)$, $^{241}Am(n,\gamma)$, $^{243}Am(n,\gamma)$, $^{238}Pu(n,f)$, $^{241}Am(n,f)$, $^{245}Cm(n,f)$.

(iv) Partly insufficient data from 1 keV to 1 MeV:
Measurement and evaluation:
$^{240}Pu(n,\gamma)$.
Evaluation:
$^{242}Pu(n,\gamma)$, $^{241}Am(n,\gamma)$, $^{243}Am(n,\gamma)$, $^{237}Np(n,f)$, $^{238}Pu(n,f)$, $^{241}Am(n,f)$.

(v) Partly insufficient MeV data:
Measurement and evaluation:
$^{236}U(n,\gamma)$, $^{237}Np(n,\gamma)$, $^{240}Pu(n,\gamma)$, $^{242}Pu(n,\gamma)$, $^{241}Am(n,\gamma)$, $^{243}Am(n,\gamma)$, $^{245}Cm(n,f)$.
Evaluation:
$^{238}U(n,2n)$,

IV. Conclusion

The status of the required transactinium isotope nuclear data has been reviewed on the basis of the recent experimental and evaluated data. The required data are those submitted to the previous AGM on TND, WRENDA 81/82, and the Working Group on Nuclear Data for Fuel Cycle in JNDC. The required data and reasons of the requirements are listed in Appendix together with the related document lists for measurements and evaluations.

Generally speaking, the status of most data does not meet the requirements. Insufficient or poor data have been sorted out in Chapter II, and the data which seemed to meet the requirements partly or completely have been checked numerically in Chapter III.

It is not easy to proclaim the data completeness because no one knows their true values. In our review in Chapter III, we tried to compare the required accuracy with the difference between the data of JENDL-2 and ENDF/B-V or -IV, and showed that some data are sufficient or almost sufficient to meet the requirements at least. They are $^{241}Pu(\bar{\nu})$, $^{241}Pu(n,f)$, $^{237}Np(\bar{\nu})$ and many data in some parts of the energy range, for example the evaluated thermal cross section of $^{238}Pu(n,f)$. As concluded in the previous chapter, there are still many quantities insufficient partly. Further study like sensitivity test using some simple integral data may be useful to advance improvement of these data.

References:

1) IAEA-186, Proc. of an Advisory Group Meeting on Transactinium Isotope Nuclear Data, held at KFK, (1975).
2) IAEA-TECDOC-232, Proc. of the Second Advisory Group Meeting on Transactinium Isotope Nuclear Data, held at Cadarache, (1979).
3) Rowlands, J.L. : Nuclear Physics and Nuclear Data, p.7, Proc. of an International Conf., held at Harwell, (1978).
4) Küsters, H., Lalovic, M., and Wiese, H.W. : Nuclear Physics and Nuclear Data, p.518, Proc. of an International Conf., held at Harwell, (1978).
5) Hammer, Ph. : Nuclear Physics and Nuclear Data, p.551, Proc. of an International Conf., held at Harwell, (1978).
6) Fuketa, T. : Nuclear physics and Nuclear Data, p.922, Proc. of an International Conf., held at Harwell, (1978).
7) DayDay, N. : WRENDA 81/82, INDC(SEC)-78/URSF (1981).
8) Umezawa, H., and Hisatake, K. : JAERI-M 9993, NEANDC(J)79/U, INDC(JAP)66/L, (1982).
9) Umezawa, H. : Nuclear Data for Science and Technology, Proc. of the International Conf., held at Antwerp, (1982).
10) Carlson, C.W. : GA-9057 (1968).
11) Stupegia, D.C., Heinrich, R.R., and McClaud, G.H. : Reactor Sci. Tech. 15, 200 (1961).
12) Barry, J.F., Bunce, J.L., and Perkin, J.K. : Proc. Phys. Soc. 78, 801 (1961).
13) Mughabghab, S.F., and Garber, D.I. : Neutron Cross Sections, Vol.1 Resonance Parameters, BNL 325 3rd Edition Vol.1 (1973).
14) Lindner, M., Nagle, R.J., and Landrum, J.H. : Nucl. Sci. Eng. 59, 381 (1976).
15) Weston, L.W., and Todd, J.H. : Nucl. Sci. Eng. 79, 184 (1981).
16) Plattard, S., Blons, J., and Paya, D. : Nucl. Sci. Eng. 61, 477 (1976).
17) Auchampaugh, G.F., Moore, M.S., Moses, J.D., Nelson, R.O., Olsen, C.E., Extermann, R.C., Hill, N.W., and Harvey, J.A. : LA-9756-MS (1983).
18) Lynn, J.E., Patrick, B.H., Sowerby, M.G., and Bowey, E.M. : AERE-R 8528 (1979).
19) Wisshak, K., and Käppeler, F. : Nucl. Sci. Eng. 85, 251 (1983).
20) Gavrilov, V.D., Goncharov, V.A., Ivanenko, V.V., Kustov, V.N., and Smirnov, V.P. : Sov. At. Energy 41, 808 (1976).
21) Asghar, M., Caitucoli, F., Perrin, P., Barreau, G., and Leroux, B. : Ann. Nucl. Energy 6, 561 (1979).
22) White, R.M., and Browne, J.C. : Nuclear Data for Science and Technology, p.218, Proc. of International Conf. held at Antwerp (1982).
23) Segev, M., and Caner, M. : Ann. Nucl. Energy 5, 239 (1978).
24) Frehaut, J., and Mosinski, G. : Nucl. Cross Sections and Technology, p.855, Proc. of International Conf. held at Washington, (1975).
25) Frehaut, J., Robert, B., and Bertin, A. : CEA-N-2196, NEANDC(E) 219/L, INDC(FR) 46/L (1981).
26) Boldeman, J.W., and Frehaut, J. : Nucl. Sci. Eng. 76, 49 (1980).
27) Frehaut, J., Mosinski, G., Bois, R., and Soleilhac, M. : CEA-R-4626 (1974).
28) D'yachenko, N.P., Kolosov, N.P., Kuz'minov, B.D., Sergachev, A.I., and Surin, V.M. : Sov. At. Energy 36, 406 (1974).
29) Konshin, V.A., Antsipov, G.V., Sukhovitskij, E.Sh., Bakhanovich, L.A., Klepatskij, A.B., Morogovskij, G.B., and Porodzinskij, Yu.V. : INDC(CCP)-142/GJ (1979).

Appendix

^{230}Th(n,γ) cross section

AGM req. : (1) Estimation of ^{232}U buildup in thermal reactor.
WER.req. : (1) Production of ^{232}U.

Experiment				
Ivanov+	AE	42 505	('77)	0.025 eV
Evaluations				
Jary	CEA-N-2084		('79)	Maxwell
Ohsawa+	NEANDC(J)75U	41	('81)	0.01 meV to 20 MeV
Abagyan+	YK-1(40)	39	('81)	Maxwell
Libraries				
ENDF/B-V				
JENDL-2				

^{232}Th(n,2n) cross section

AGM req. : (1) Fresh fuel fabrication for thermal reactor, (2) Fuel handling.
WRE.req. : (1) Neutron multiplier, (2) Hybrid system design, (3) Calculation of fuel activity in ^{232}Th cycle reactors.

Experiments				
Karius+	JP/G	5 715	('79)	13 MeV to 18 MeV
Chawla+	NIM	174 179	('80)	Fast
Chatani	NIM	205 501	('83)	Fission
Evaluations				
Jary	CEA-N-1971		('77)	1 MeV to 20 MeV
Zijp+	IAEA-208	2 327	('78)	Fission
Fu+	ORNL-TM-6316		('78)	6.2 MeV to 20 MeV
Vasiliu+	INDC(RUM)-10		('80)	6.5 MeV to 20 MeV
Bychkov+	YF	34 684	('81)	6.5 MeV to 20 MeV
Ohsawa+	NST	18 408	('81)	6.5 MeV to 20 MeV
Anand+	INDC(IND)-30		('81)	6.5 MeV to 20 MeV
Libraries				
ENDF/B-V	(Not available)			
JENDL-2				
KEDAK-4				
UKNDL-81				
ENDL-82				
INDL/A-83	(Three evaluations by Vasiliu+, Bychkov+ and KEDAK-4)			

^{232}Th(n,3n) cross section

AGM req. : (1) Fuel handling.
WRE.req. : (1) As neutron multiplier, (2) Hybrid system design.

Evaluations				
Jary	CEA-N-1971		('77)	1 MeV to 20 MeV
Fu+	ORNL-TM-6316		('78)	12 MeV to 20 MeV
Vasiliu+	INDC(RUM)-10		('80)	12 MeV to 20 MeV
Bychkov+	YF	34 684	('81)	12 MeV to 20 MeV
Ohsawa+	NST	18 408	('81)	12 MeV to 20 MeV
Anand+	INDC(IND)-30		('81)	11 MeV to 20 MeV
Libraries				
ENDF/B-V	(Not available)			

JENDL-2
KEDAK-4
UKNDL-81
ENDL-82
INDL/A-83 (Three evaluations by Vasiliu+, Bychkov+ and KEDAK-4)

^{231}Pa(n,γ) cross section

AGM req. : (1) Prediction of ^{232}U content of fresh fuel in thermal reactor core design.
WRE.req. : (1) Control of ^{232}U production, (2) Calculation of fuel activity in ^{232}Th cycle reactors.

Evaluations

Garg	INDC(SEC)-61	('77)	100 keV to 20 MeV
Jary	CEA-N-2084	('79)	Maxwell
Vasiliu+	INDC(RUM)-11	('79)	0.0 eV to 19 MeV
Abagyan+	YK-1(40) 39	('81)	Maxwell

Library
ENDF/B-V

^{233}Pa(n,γ) cross section

AGM req. : (1) U-Th fuel cycle thermal reactor core design.
WRE.req. : (1) Analysis of ^{232}Th cycle thermal reactors, (2) Burn up calculation of Th fueled thermal reactors, (3) Fast reactor project.

Evaluations

Garg	INDC(SEC)-61	('77)	100 keV to 20 MeV
Abagyan+	YK-1(40) 39	('81)	Maxwell

Libraries
ENDF/B-V
JENDL-2
UKNDL-81
ENDL-82
INDL/A-83 (Two evaluations by Vasiliu+ and Bychkov+)

^{232}U(n,γ) cross section

AGM req. : (1) Recycle U or U-Th fuel fabrication and handling.
WRE.req. : (1) Calculation of fuel activity in ^{232}Th cycle reactors.

Evaluations

Garg	INDC(SEC)-61	('77)	100 keV to 20 MeV
Abagyan+	YK-1(40) 39	('81)	Maxwell

Library
ENDF/B-V

^{232}U(n,f) cross section

AGM req. : (1) Recycle U or U-Th fuel fabrication and handling.

Evaluation

Abagyan+	YK-1(40) 39	('81)	Maxwell

Library
ENDF/B-V

$^{233}U(n,2n)$ cross section

AGM req. : (1) U-Th fuel fabrication, (2) Fuel handling.
WRE.req. : (1) In and out of core cycle, (2) Estimation for contamination of ^{233}U by ^{232}U.

Experiment			
Gryntakis	JRC 46 159	('78)	Fission
Evaluations			
Bychkov+	YK-3(42) 26	('81)	6.2 MeV to 20 MeV
Asano+	NST 19 1034	('82)	5.8 MeV to 20 MeV
Libraries			
ENDF/B-V	(Not available)		
JENDL-2			
KEDAK-4			
UKNDL-81			
ENDL-82			
INDL/A-83	(Two evaluations by Bychkov+ and KEDAK-4)		

$^{234}U(n,\gamma)$ cross section

AGM req. : (1) Thermal reactor core design.
WRE.req. : (1) Evaluation of isotope buildup in thermal reactors.

Evaluations			
Mann+	HEDL-TME-77-54	('77)	1 keV to 20 MeV
Voropaev+	YK- 34(3) 35	('79)	Fast
Jary	CEA-N-2084	('79)	Maxwell
Abagyan+	Yk- 1(40) 39	('81)	Maxwell
Libraries			
ENDF/B-V			
JENDL-2			
UKNDL-81			
ENDL-82			

$^{236}U(n,\gamma)$ cross section

AGM req. : (1) Thermal reactor core design.
WRE.req. : (1) For fast reactor calcultions, (2) Burn up calculation of Pu loaded thermal reactors.
JNDC/WG : (1) Fuel faciiity, (2) Safeguards.

Experiment			
Cricchio+	82Antwerp 29	('82)	Fast
Bergman+	AE 52 406	('82)	100 eV to 50 keV
Evaluations			
Mann+	HEDL-TME-77-54	('77)	1 keV to 20 MeV
Jary	CEA-N-2084	('79)	Maxwell
Abagyan+	YK- 1(40) 39	('81)	Maxwell
Libraries			
ENDF/B-V			
JENDL-2			
UKNDL-81			
ENDL-82			

$^{237}U(n,\gamma)$ cross section

AGM req. : (1) Thermal reactor application.
Evaluations

Voropaev+	YK- 34(3) 35	('79)	Fast
Jary	CEA-N-2084	('79)	Maxwell
Abagyan+	YK- 1(40) 39	('81)	Maxwell

Libraries

ENDF/B-V (Not available)
KEDAK-4
UKNDL-81
ENDL-82
INDL/A-83 (Same as KEDAK-4)

$^{238}U(n,2n)$ cross section

AGM req. : (1) Fuel fabrication and handling.
WRE.req. : (1) Fast reactor design, (2) As neutron multiplier, (3) Fast reactor burn up calculation, (4) Dosimetry for FMIT facility.
JNDC/WG : (1) Fuel facility, (2) Burnup evaluation, (3) Safeguards.

Experiments

Krasin+	77Kiev	('77)	order of 1 MeV
Birjukov+	77Kiev 2 22	('77)	9.1 MeV
Hashimoto+	NST 15 626	('78)	Fission
Veeser+	78Harwell 1054	('78)	15 MeV to 19 MeV
Chou	HSJ-77091	('78)	6.8 MeV to 17 MeV
Karius+	JP/G 5 715	('79)	13 MeV to 18 MeV
Ryves+	NEANDC(E)212 8	('80)	14 MeV
Frehaut+	NSE 74 29	('80)	6.5 MeV to 13 MeV
Frehaut	80BNL 399	('80)	7.9 MeV to 15 MeV
Kornilov+	AE 49 283	('80)	6.5 MeV to 11 MeV
Frehaut+	NEANDC(E)211	('81)	Thresh to 13 MeV

Evaluations

Bychkov+	77Kiev	('77)	order of 10 MeV
Jary+	NEANDC(E)174	('77)	2 MeV to 20 MeV
Goel+	KFK-2386 3 37	('77)	6.1 MeV to 15 MeV
Chou	HSJ-77091	('78)	6.8 MeV to 17 MeV
Bychkov+	YK- 35(4) 21	('79)	14 MeV to 15 MeV
Igarasi+	JAERI-1261	('79)	6 MeV to 20 MeV
Fort+	NEANDC(E)212 4	('80)	Thresh to 16 MeV
Bychkov+	YK- 3(42) 60	('81)	Fission
Kornilov+	82Antwerp 679	('82)	6 MeV to 19 MeV

Libraries

ENDF/B-V (Not available)
JENDL-2
KEDAK-4
UKNDL-81
ENDL-82
INDL/A-83 (Same evaluations as JENDL-2 and KEDAK-4)

$^{237}Np(n,\gamma)$ cross section

AGM req. : (1) Thermal reactor core design and fuel fabrication. (2) In-core cycle, fuel handling and fabrication for fast reactors.
WRE.req. : (1) Burnup calculation of thermal and fast reactors, (2) Neutron dosimetry.
JNDC/WG : (1) Fuel reprocessing, (2) Fuel facility.

Experiments

Mewissen+	NSE 70 155	('79)	8 eV to 200 eV
Weston+	NSE 79 2 184	('81)	0.01 eV to 200 keV
Cricchio+	82Antwerp 175	('82)	Fast

Evaluations

Mann+	HEDL-TME-77-54	('77)	1 keV to 20 MeV
Caner+	IA- 1346	('77)	0.025 eV, 200 eV to 15 MeV
Jary	CEA-N-2084	('79)	Maxwell
Derrien+	INDC(FR)-42	('80)	0.01 meV to 14 MeV
Abagyan+	YK- 1(40) 39	('81)	Maxwell

Libraries

ENDF/B-V
JENDL-2
KEDAK-4
UKNDL-81
ENDL-82
INDL/A-83 (Two evaluations by Derrien+ and KEDAK-4)

^{237}Np(n,f) cross section

AGM req. : (1) Thermal reactor application, (2) In-core cycle, fuel handling and fabrication for fast reactors.

WRE.req. : (1) Monitor reaction and radiation dosimetry in neutronics experiments on blanket system of fusion reactors. (2) Materials dosimetry, (3) FMIT dosimetry, (4) Surveillance of damage in pressure vessels using ^{137}Cs.

JNDC/WG : (1) Dosimetry, (2) Fuel reprocessing, (3) Fuel facility.

Experiments

Cierjacks	77NBS 278	('77)	100 keV to 20 MeV
Gilliam	77NBS 299	('77)	Fission
Adamov+	77NBS 313	('77)	Fission
Wagemans+	NP/A 285 32	('77)	Maxwell
Migneco+	NEANDC(E)192 7	('78)	Spontaneous
Kimura+	IAEA-208 2 265	('78)	Fast
Fabry+	IAEA-208 2 191	('78)	Fast
Fabry+	IAEA-208 2 291	('78)	Fission
Kuprijanov+	AE 45 440	('78)	130 keV to 7 MeV
Garlea+	SCF 31 59	('79)	Fast
Gilliam+	DOE-NDC-15 158	('79)	Fission
Burholt+	INDC(NDS)-103	('79)	Fission
Grady+	79Knoxvill IB5	('79)	770 keV to 960 keV
Carlson+	79Knoxvill IB4	('79)	1 MeV to 20 MeV
Adamov+	79Knoxvill 995	('79)	15 MeV
Arlt+	KE 24 48	('81)	15 MeV
Wagemans+	NP/A 369 1	('81)	Maxwell
Behrens+	NSE 80 3 393	('82)	20 keV to 43 MeV
Varnagy+	NIM 196 465	('82)	13 MeV to 15 MeV
Cance+	82Antwerp 51	('82)	2.5 MeV
D'Hondt+	82Antwerp 147	('82)	Maxwell
Cricchio+	82Antwerp 175	('82)	Fast
Meadows	DOE-NDC-30 9	('83)	100 keV to 9.4 MeV
Mahdavi+	DOE-NDC-30 118	('83)	15 MeV
Auchampaugh+	LA-9756	('83)	1 eV to 600 eV

Evaluations

Fabry	AERE-R-8636	('77)	Fission
Mann+	HEDL-TME-77-54	('77)	1 keV to 20 MeV

Grigorev+	AE 43 279	('77)	Fission
Caner+	IA- 1346	('77)	0.025 eV, 200 eV to 15 MeV
Zijp+	IAEA-208 2 327	('78)	Fission, Maxwell to Pile
Ing+	STI/DOC/10-180	('78)	1 eV to 15 MeV
Jary	CEA-N-2084	('79)	Maxwell
Mannhart	NEANDC(E)212 5	('80)	Fission
Derrien+	INDC(FR)-42	('80)	0.01 meV to 14 MeV
Fort	NEANDC(E)242	('83)	5 MeV to 15 MeV

Libraries

ENDF/B-V
JENDL-2
KEDAK-4
UKNDL-81
ENDL-82
INDL/A-83 (Two evaluations by Derrien+ and KEDAK-4)

^{237}Np(n,2n) cross section

AGM req. : (1) In-core cycle, fuel handling and fabrication for fast reactors, (2) Radioisotope power sources.
WRE.req. : (1) Evaluation of contamination of ^{238}Pu by ^{236}Pu, (2) Evaluation of buildup of Tl-208, (3) Fuel cycle out of core, (4) Fast reactor burnup calculation.
JNDC/WG : (1) Fuel facility, (2) Burnup evaluation, (3) Safeguards.

Evaluations

Caner+	IA- 1346	('77)	7 MeV to 15 MeV
Derrien+	INDC(FR)-42	('80)	Thermal to 14 MeV
Andreev+	80Kiev 3 301	('80)	12 MeV to 15 MeV
Bychkov+	YK- 3(42) 26	('81)	7 MeV to 20 MeV
Wiese+	82Antwerp 202	('82)	Maxwell to Fast
Fort	NEANDC(E)242	('83)	5 MeV to 15 MeV

Libraries

ENDF/B-V
JENDL-2
KEDAK-4
UKNDL-81
ENDL-82
INDL/A-83 (Three evaluations by Derrien+, Bychkov+ and KEDAK-4)

^{237}Np $\bar{\nu}$

AGM req. : (1) In-core cycle, fuel handling, and fabrication for fast reactor.

Experiments

Veeser	PR/C 17 385	('78)	1 MeV to 15 MeV
Thierens+	NP/A 342 2 229	('80)	Maxwell
Vorob'Eva+	AE 50 188	('81)	1 MeV to 4 MeV
Kuzminov+	ZFK-459 72	('81)	1 MeV to 6 MeV
Wagemans+	NP/A 369 1 1	('81)	Maxwell
Mueller+	KFK-3220	('81)	800 keV to 5.5 MeV
Frehaut+	82Antwerp 78	('82)	1 MeV to 15 MeV
Malinovsky+	YK- 1(50) 15	('83)	order of 10 MeV

Evaluation

Caner+	IA- 1346	('77)	Pile

Libraries

ENDF/B-V

JENDL-2
KEDAK-4
UKNDL-81
ENDL-82
INDL/A-83 (Two evaluations by Derrien+ and IKEDAK-4)

^{239}Np(n,γ) cross section

AGF req. : (1) In-core cycle and decay heat for fast reactors.
WRE.req. : (1) Burnup calculation for thermal and fast reactors,
(2) Fast reactor operation.
Library
JENDL-2

^{239}Np(n,f) cross section

AGF req. : (1) In-core cycle and decay heat for fast reactors.
WRE.req. : (1) Fast reactor operation.
Library
JENDL-2

^{239}Np(n,2n) cross section

AGM req. : (1) Fuel fabrication and handling.
WRE.req. : (1) In- and out-of-core cycle.
Library
JENDL-2

^{239}Np $\bar{\nu}$

AGM req. : (1) In-core cycle and decay heat for fast reactors.
WRE.req. : (1) Fast reactor operation.
JNDC/WG : (1) Fuel facility.
Library
JENDL-2

^{236}Pu(n,γ) cross section.

AGM req. : (1) Fuel fabrication, handling and Pu-recycling.
WRE.req. : (1) Out-of-core cycle.
Evaluations

Mann+	HEDL-TME-77-54 ('77)	1 keV to 20 MeV
Voropaev+	YK- 34(3) 35 ('79)	Fast

Libraries
ENDF/B-V
JENDL-2

^{236}Pu(n,f) cross section.

AGM req. : (1) Fuel fabrication, handling and Pu-recycling.
WRE.req. : (1) Out-of-core cycle.
Evaluations

Mann+	HEDL-TME-77-54 ('77)	1 keV to 20 MeV
Voropaev+	YK- 34(3) 35 ('79)	Fast

Libraries
ENDF/B-V

$^{238}Pu(n,\gamma)$ cross section.

AGM req. : (1) Thermal reactor core design, (2) In-core cycle for fast reactors, (3) Fuel fabrication for fast reactors, (4) Fuel control.
WRE.reg. : (1) Fast reactor calculation, (2) Burnup calculation of thermal and fast reactors.
JNDC/WG : (1) Fuel facility.

Evaluations

Mann+	HEDL-TME-77-54	('77)	1 keV to 20 MeV
Jary	CEA-N-2084	('79)	Maxwell
Abagyan+	YK- 1(40) 39	('81)	Maxwell
Derrien	INDC(FR)-57	('82)	0.01 meV to 14 MeV

Libraries

ENDF/B-V
JENDL-2
KEDAK-4
UKNDL-81
ENDL-82
INDL/A-83 (Evaluations by Derrien, and KEDAK-4)

$^{238}Pu(n,f)$ cross section.

AGM req. : (1) Actinide recycle.
WRE.req. : (1) Fast reactor calculations.

Experiments

Knitter+	INDC(EUR)15 8	('82)	150 keV to 10 MeV
Budtz-Jorgensen	82Antwerp 206	('82)	5 eV to 10 MeV
Aleksandrov+	YK- 1(50) 43	('83)	2.9 MeV

Evaluations

Mann+	HEDL-TME-77-54	('77)	1 keV to 20 MeV
Jary	CEA-N-2084	('79)	Maxwell
Abagyan+	YK- 1(40) 39	('81)	Maxwell
Derrien	INDC(FR)-57	('82)	0.01 meV to 14 MeV
Knitter+	INDC(EUR)17 35	('83)	5 MeV to 8 MeV
Derrien+	NEANDC(E) 242	('83)	300 keV to 14 MeV

Libraries

ENDF/B-V
JENDL-2
KEDAK-4
UKNDL-81
ENDL-82
INDL/A-83 (Evaluations by Derrien, and KEDAK-4)

$^{238}Pu(n,3n)$ cross section.

AGM req. : (1) Fuel handling.
JNDC/WG : (1) Fuel facility, (2) Safeguards.

Evaluation

Derrien	INDC(FR)-57	('82)	Thresh to 14 MeV

Libraries

ENDF/B-V
JENDL-2
KEDAK-4

UKNDL-81
ENDL-82
INDL/A-83 (Evaluations by Derrien, and KEDAK-4)

$^{238}Pu\ \bar{\nu}$

AGM req. : (1) In-core cycle for fast reactors, (2) Fuel fabrication for fast reactors, (3) Fuel control.
WRE.req. : (1) Fast reactor calculations.
Libraries
ENDF/B-V
JENDL-2
KEDAK-4
UKNDL-81
ENDL-82
INDL/A-83 (Evaluations by Derrien, and KEDAK-4)

$^{239}Pu(n,2n)$ cross section.

AGM req. : (1) Fuel fabrication for fast reactors, (2) Fuel handling.
WRE.req. : (1) Predict buildup of ^{238}Pu, (2) Fuel cycle in core.
Experiment

Frehaut+	CEA-N-2080	('79)	Thermal to 13 MeV

Evaluations

Goel+	KFK-2386 3 11	('77)	5.8 MeV to 15 MeV
Igarasi+	JAERI-1261	('79)	5.8 MeV to 15 MeV
Andreev+	80Kiev 3 301	('80)	13 MeV to 15 MeV
Gupta+	INDC(IND)-30	('81)	5.7 MeV to 20 MeV
Bychkov+	YF 34 684	('81)	6 MeV to 20 MeV

Libraries
ENDF/B-V (Not available)
JENDL-2
KEDAK-4
UKNDL-81
ENDL-82
INDL/A-83 (Four evaluations by Ancipov+, Bychkov+, JENDL-2 and KEDAK-4)

$^{240}Pu(n,\gamma)$ cross section.

AGM req. : (1) Thermal reactor core design.
WRE.req. : (1) Improved precision needed for thermal reactors, (2) Fast reactor calculations, (3) Fast reactor burnup calculations.
JNDC/WG : (1) Fuel facility.
Experiments

Andrijakhina+	YK- 24 48	('77)	Pile
Weston+	NSE 63 143	('77)	200 eV to 350 keV
Wisshak+	NSE 69 39	('79)	48 keV to 210 keV
Ivanov+	YK- 36(1) 26	('80)	Fast
Chrien+	DOE-NDC-24 13	('81)	0.3 meV to 0.025 eV
Kaeppeler	KAEPPELER	('82)	12 keV to 89 keV
Darrouzet+	82Antwerp 181	('82)	Pile
Cricchio+	82Antwerp 29	('82)	Fast

Evaluations

Goel+	KFK-2386 3 17	('77)	4 keV to 1 MeV

Porodzinskij+	77Kiev 4 42	('77)	100 eV to 11 MeV
Goel	78BNL-2 165	('78)	10 keV to 350 keV
Voropaev+	YK- 34(3) 35	('79)	Fast
Igarasi+	JAERI-1261	('79)	0.01 meV to 15 MeV
Jary+	CEA-N-2084	('79)	Maxwell, 10 keV to 3 MeV
Weston+	79Knoxvill EB1	('79)	0.01 meV to 20 MeV
Mughabghab+	INDC(NDS)-129	('81)	0.025 eV
Nakagawa+	INDC(NDS)-129	('81)	0.025 eV, 100 eV to 400 eV
Abagyan+	YK- 1(40) 39	('81)	Maxwell
Reffo+	NSE 83 401	('83)	1 keV to 200 keV

Libraries

ENDF/B-V	(Not available)
JENDL-2	
KEDAK-4	
UKNDL-81	(Two sets of evaluations)
ENDL-82	
INDL/A-83	(Three evaluations by Ancipov+, JENDL-2 and KEDAK-4)

^{241}Pu(n,γ) cross section.

AGM req. : (1) Therman reactor core design.
WRE.req. : (1) Improved precision needed for thermal reactors, (2) Fast reactor calculations, (3) Thermal reactor calculations, (4) Fast reactor burnup calculation.
JNDC/WG : (1) Fuel facility.

Experiments

Andrijakhina+	YK- 24 48	('77)	Pile
Weston+	NSE 65 454	('78)	0.01 eV to 250 keV
Weston+	NSE 68 125	('78)	0.01 eV to 100 eV
Darrouzet+	82Antwerp 181	('82)	Pile
Cricchio+	82Antwerp 29	('82)	Fast

Evaluations

Lemmel	77NBS 170	('77)	0.025 eV
Goel	NEANDC(E)182 5	('77)	10 keV to 250 keV
Kikuchi	NST 14 467	('77)	0.01 meV to 15 MeV
Konshin+	INDC(CCP)-113	('77)	0.1 meV to 15 MeV
Gur+	LS- 276 24	('78)	Pile
Voropaev+	YK- 34(3) 35	('79)	Fast
Konshin+	TMO-2 to TMO-7	('79)	0.1 meV to 15 MeV
Holden+	EPRI-NP-1088	('79)	0.025 eV
Jary	CEA-N-2084	('79)	Maxwell
Weston+	79KNOX EB 1	('79)	0.01 meV to 20 MeV
Kikuchi+	INDC(NDS)-129	('81)	10 eV to 100 eV
Abagyan+	YK- 1(40) 39	('81)	Maxwell

Libraries

ENDF/B-V	(Not available)
JENDL-2	
KEDAK-4	
UKNDL-81	
ENDL-82	
INDL/A-83	(Three evaluations by Konshin+, JENDL-2 and KEDAK-4)

^{241}Pu(n,f) cross section.

AGM req. : (1) Thermal reactor core design.
WRE.req. : (1) Reactor calculations, (2) Fast reactor calculations,

(3) Fast reactor burnup calculations.
JNDC/WG : (1) Disimetry, (2) Fuel facility.
Experiments

Sweet	AEEW-R-1090	('77)	Fast
Van Gils+	NEANDC(E)182 3	('77)	2 meV to 0.08 eV
Carlson+	NSE 63 149	('77)	0.025 eV to 70 keV
Fabry+	IAEA-208 2 291	('78)	Fast
Fursov+	AE 44 236	('78)	24 keV to 7.4 MeV
Weston+	NSE 65 454	('78)	0.01 eV to 250 keV
Czirr	DOE-NDC-12 109	('78)	0.025 eV to 8 eV
Crouch+	NEANDC(E)192 8	('78)	Spontaneous
Vaninbroukx	78Harwell 235	('78)	Spontaneous
Carlson+	NSE 68 128	('78)	1 keV to 30 MeV
Weston+	NSE 68 125	('78)	0.01 eV to 100 eV
Garlea+	SCF 31 59	('79)	Fast
Khan+	NIM 173 137	('80)	15 MeV
Cricchio+	82Antwerp 29	('82)	Fast
Wagemans+	INDC(EUR)17 3	('83)	0.01 eV to 100 keV
Aleksandrov+	YK- 1(50) 43	('83)	1.2 MeV
Grundl+	ANS 44 533	('83)	Fission

Evaluations

Lemmel	77NBS 170	('77)	0.025 eV
Goel	NEANDC(E)182 5	('77)	100 eV to 30 keV
Kikuchi	NST 14 467	('77)	0.01 meV to 15 MeV
Konshin+	INDC(CCP)-113	('77)	0.1 meV to 15 MeV
Goel	78BNL-2 165	('78)	200 eV to 30 keV
Konshin+	TMO-2 to TMO-7	('79)	0.1 meV to 15 MeV
Holden+	EPRI-NP-1098	('79)	0.025 eV
Jary	CEA-N-2084	('79)	Maxwell
Weston+	79Knoxvill EBI	('79)	0.01 meV to 20 MeV
Kikuchi+	INDC(NDS)-129	('81)	10 eV to 100 eV
Abagyan+	YK- 1(40) 39	('81)	Maxwell
Knitter+	INDC(EUR)17 35	('83)	5 MeV to 8 MeV

Libraries

ENDF/B-V	(Not available)
JENDL-2	
KEDAK-4	
UKNDL-81	
ENDL-82	
INDL/A-83	(Three evaluations by Konshin+, JENDL-2 and KEDAK-4)

^{241}Pu $\bar{\nu}$

AGM req. : (1) Thermal reactor core design.
WRE.req. : (1) Fast reactor calculations.
Experiments

Boldeman+	NSE 76 1 49	('80)	0.025 eV
Caitucoli+	NP/A 369 1 15	('81)	Maxwell

Evaluations

Boldeman+	77NBS 182	('77)	0.025 eV
Lemmel	77NBS 170	('77)	0.025 eV
Konshin+	TMO-7	('79)	10 keV to 15 MeV
Holden+	EPRI-NP-1098	('79)	0.025 eV
Sher+	EPRI-NP-1771	('81)	Maxwell

Libraries

ENDF/B-V	(Not available)

JENDL-2
KEDAK-4
UKNDL-81
ENDL-82
INDL/A-83 (Three evaluations by Konshin+, JENDL-2 and KEDAK-4)

$^{242}Pu(n,\gamma)$ cross section.

AGM req. : (1) Thermal reactor core design, (2) Thermal reactor fuel cycle, (3) Actinide recycle.
WRE.req. : (1) Fast reactor calculations, (2) Cm and Cf production calculation, (3) Burnup calculation of a Pu loaded thermal reactors, (4) Thermal reactor applications at high burnup.
JNDC/WG : (1) Fuel facility, (2) Burnup evaluation, (3) Safeguards.

Experiments

Druzhinin+	AE	42	314 ('77)	Fast
Wisshak+	NSE	66	363 ('78)	10 keV to 89 keV
Wisshak+	NSE	69	39 ('79)	50 keV to 250 keV
Bendt+	LA-	7853	('79)	0.025 eV
Darrouzet+	82Antwerp	181	('82)	Pile
Cricchio+	82Antwerp	29	('82)	Fast
Wisshak+	ANL-83-4	336	('82)	10 keV to 200 keV

Evaluations

Jary+	78Harwell	1151	('78)	10 keV to 20 MeV
Mann+	78BNL-2	275	('78)	10 keV to 10 MeV
Goel	78BNL-2	165	('78)	10 keV to 200 keV
Voropaev+	YK- 34(3)	35	('79)	Fast
Jary	CEA-N-2084		('79)	Maxwell
Nakagawa+	INDC(NDS)-129		('81)	0.025 eV
Abagyan+	YK- 1(40)	39	('81)	Maxwell
Reffo+	NSE 83	401	('83)	1 keV to 200 keV

Libraries
ENDF/B-V
JENDL-2
KEDAK-4
UKNDL-81
ENDL-82
INDL/A-83 (Three evaluations by Ancipov+, Bruyeres-le-Chatel/ Bologna and KEDAK-4)

$^{241}Am(n,\gamma)$ cross section

AGM req. : (1) Pu-recycle calculation in thermal reactors, (2) Fuel fabrication, (3) Fuel control, (4) ^{242}Cm production, (5) Production of isomeric state.
WRE.req. : (1) ^{238}Pu program and ^{244}Cm production, (2) Spent fuel shielding, (3) Burnup calculation, (4) Transuranium nuclides buildup, (5) Transport cask shielding, (6) Fuel cycle in-and out-of-core, (7) Actinide production calculations.
JNDC/WG : (1) Fuel reprocessing, (2) Fuel facility, (3) Burnup evaluation, (4) Safeguards.

Experiments

Gayther+	77Kiev	3	3 ('77)	100 eV to 500 keV
Glover+	NEANDC(E)202	8	('79)	Fast
Sanders+	79Aix	1	567 ('79)	Fast
Wisshak+	KFK-3068	21	('80)	15 eV to 30 eV

Wisshak	WISSHAK	('80)	10 keV to 230 keV
Wisshak+	KFK-2180 2 27	('82)	30 keV
Wisshak+	KFK-3290 2 27	('82)	0.015 eV
Darrouzet+	82Antwerp 181	('82)	Pile
Stevenson+	82Antwerp 178	('82)	Fast
Cricchio+	82Antwerp 175	('82)	Fast
Wisshak+	ANL-83-4 336	('83)	10 keV to 200 keV

Evaluations

Mann+	78BNL-2 275	('78)	10 keV to 10 MeV
Lynn+	NEANDC(E)202 8	('79)	0.01 meV to 15 MeV
Jary	CEA-N-2084	('79)	Maxwell
Goel	NEANDC(E)202 5	('79)	0.025 eV to 100 eV
Fort	NEANDC-150	('81)	10 keV to 1 MeV
Goel+	NEANDC(E)222 5	('81)	2 keV to 400 keV
Abagyan+	YK- 1(40) 39	('81)	Maxwell
Wisshak+	NSE 81 3 396	('82)	1 keV to 1 MeV
Kikuchi	JAERI-M-82 096	('82)	0.01 meV to 20 MeV
Reffo	ANL-83-4 133	('82)	10 keV 10 MeV
Derrien	ANL-83-4 379	('82)	1 keV to 40 keV
Froehner+	ANL-83-4 116	('82)	2 keV to 500 keV

Libraries

ENDF/B-V
JENDL-2
KEDAK-4
UKNDL-81
ENDL-82
INDL/A-83 (Two evaluations by Fort+ and KEDAK-4)

^{241}Am(n,f) cross section

AGM req. : (1) In-core cycle in fast reactors, (2) Fuel fabrication, (3) Fuel control, (4) ^{242}Cm production.

WRE.req. : (1) Critical assemblies.

Experiments

Sweet	AEEW-R-1090	('77)	Fast
Gayther+	77Kiev 3 3	('77)	50 eV to 10 keV
Cance+	CEA-N-1969 57	('77)	5 keV to 3 MeV
Kuprijanov+	AE 45 440	('78)	130 keV to 7 MeV
Knitter+	AKE 33 3 205	('79)	100 eV to 5.3 MeV
Aleksandrov+	AE 46 416	('79)	2.5 MeV
Prindle+	PR/C 20 1824	('79)	15 MeV
Liskien+	ZFK-410 7	('80)	150 keV to 5.3 MeV
Khan+	INDC(PAK)-2 1	('80)	15 MeV
Wisshak	WISSHAK	('80)	22 keV to 1 MeV
Wisshak+	NSE 76 148	('80)	10 keV to 250 keV
Cance+	CEA-N-2194	('81)	15 MeV
Behrens+	NSE 77 4 444	('81)	200 keV to 30 MeV
Hage+	NSE 78 3 248	('81)	10 keV to 1 MeV
Cricchio+	82Antwerp 175	('82)	Fast
Aleksandrov+	YK- 1(50) 43	('83)	2.9 MeV
Dabbs+	NSE 83 22	('83)	0.02 eV to 20 MeV

Evaluations

Zijp+	IAEA-208 2 327	('78)	Fission, Maxwell to Pile
Mann+	78BNL-2 275	('78)	1 keV to 10 MeV
Goel	78BNL-2 177	('78)	0.025 eV
Igarasi+	JAERI-1261	('79)	1 keV to 15 MeV

Lynn+	NEANDC(E)202 8	('79)	0.01 meV to 15 MeV
Jary	CEA-N-2084	('79)	Maxwell
Fort	NEANDC-150	('81)	10 keV to 100 keV
Goel+	NEANDC(E)222 5	('81)	2 keV to 400 keV
Abagyan+	YK- 1(40) 39	('81)	Maxwell
Kikuchi	JAERI-M-82 096	('82)	0.01 meV to 20 MeV
Cullen+	NSE 83 497	('83)	Fission

Libraries

ENDF/B-V
JENDL-2
KEDAK-4
UKNDL-81
ENDL-82
INDL/A-83 (Three evaluations by Fort+, Lynn+ and KEDAK-4)

^{241}Am $\bar{\nu}$

AGM req. : (1) In-core cycle in fast reactors, (2) Fuel fabrication,
(3) Fuel control, (4) ^{242}Cm production.
WRE.req. : (1) Fast reactor design, (2) Fuel cycle calculation.

Evaluations

Lynn+	NEANDC(E)202 8	('79)	0.01 meV to 15 MeV
Abagyan+	YK- 4(43) 24	('81)	Maxwell
Kikuchi	JAERI-M-82 096	('82)	0.01 meV to 20 MeV

Libraries

ENDF/B-V
JENDL-2
UKNDL-81
ENDL-82
INDL/A-83 (Evaluation by Fort+)

^{242g}Am total cross section

AGM req. : (1) Actinide recycle,
WRE.req. : (1) Consistent evaluation of partial cross section.

Evaluation

Nakagawa+	JAERI-M-8903	('80)	0.01 meV to 20 MeV

Libraries

ENDF/B-V
JENDL-2
INDL/A-83 (Same as JENDL-2)

$^{242g}Am(n,\gamma)$ cross section

AGM req. : (1) Actinide recycle.
WRE.req. : (1) ^{238}Pu production, (2) Fuel cycle calculation,
(3) Burnup calculation, (4) Transuranium nuclides buildup,
(5) Transport cask shielding.
JNDC/WG : (1) Fuel reprocessing.

Evaluation

Nakagawa+	JAERI-M-8903	('80)	0.01 meV to 20 MeV

Libraries

ENDF/B-V
JENDL-2
INDL/A-83 (Same as JENDL-2)

^{242g}Am(n,f) cross section

AGM req. : (1) Actinide recycle.
WRE.req. : (1) Fuel cycle calculation, (2) Fast reactors,
(3) Pu-recycling, (4) Fuel reprocessing and storage,
(5) Fast reactor burnup calculation.
JNDC/WG : (1) Fuel facility.
Evaluation

Nakagawa+	JAERI-M-8903	('80)	0.01 meV to 20 MeV

Libraries
ENDF/B-V
JENDL-2
INDL/A-83 (Same as JENDL-2)

^{242m}Am total cross section

AGM req. : (1) Actinide recycle.
WRE.req. : (1) Consistent evaluation of partial cross section.
Evaluations

Nakagawa+	JAERI-M-8903	('80)	0.01 meV to 20 MeV
Tellier	CEA-N-2286	('82)	0.025 eV to 3 MeV

Libraries
ENDF/B-V
JENDL-2
INDL/A-83 (Same as JENDL-2)

^{242m}Am(n,γ) cross section

AGM req. : (1) Pu-recycling calculation in thermal reactors,
(2) In-core cycle in fast reactors, (3) Actinide recycle.
WRE.req. : (1) ^{238}Pu production, (2) Fuel cycle calculation,
(3) Burnup calculation, (4) Transuranium nuclides buildup,
(5) Transport cask shielding.
Evaluations

Mann+	78BNL-2	275	('78)	10 keV to 10 MeV
Voropaev+	YK- 34(3)	35	('79)	Fast
Jary	CEA-N-2084		('79)	Maxwell
Nakagawa+	JAERI-M-8903		('80)	0.01 meV to 20 MeV
Tellier	CEA-N-2286		('82)	0.025 eV to 3 MeV
Abagyan+	YK- 4(43)	24	('81)	Maxwell
Froehner+	ANL-83-4	116	('82)	1 keV to 10 MeV

Libraries
ENDF/B-V
JENDL-2
INDL/A-83 (Same as JENDL-2)

^{242m}Am(n,f) cross section

AGM req. : (1) Pu-recycling calculation in thermal reactors,
(2) In-core cycle in fast reactors, (3) Actinide recycle.
WRE.req. : (1) Fuel cycle calculation, (2) Fast reactor,
(3) Pu-recycling, (4) Fuel reprocessing and storage,
(5) Fast reactor burnup calculation.
Experiments

Browne+	78Harwel	887	('78)	0.01 eV to 20 MeV
Formushkin+	YF 33	620	('81)	40 keV to 4.5 MeV, 15 MeV

White+	82Antwerp 218	('82)	1 meV to 20 MeV
Dabbs+	NSE 84 1	('83)	5 meV to 20 MeV
Evaluations			
Mann+	78BNL-2 275	('78)	10 keV to 10 MeV
Voropaev+	YK- 34(3) 35	('79)	Fast
Jary	CEA-N-2084	('79)	Maxwell
Nakagawa+	JAERI-M-8903	('80)	0.01 meV to 20 MeV
Tellier	CEA-N-2286	('82)	0.025 eV to 3 MeV
Abagyan+	YK- 4(43) 24	('81)	Maxwell
Libraries			
ENDF/B-V			
JENDL-2			
INDL/A-83	(Same as JENDL-2)		

^{242m}Am $\bar{\nu}$

AGM req. : (1) In-core cycle in fast reactors.
WRE.req. : (1) Fuel cycle calculation, (2) Fast reactors.

Experiment			
Howe+	NSE 77 4 454	('81)	37 keV to 30 MeV
Evaluations			
Nakagawa+	JAERI-M-8903	('80)	0.01 meV to 20 MeV
Abagyan+	YK- 4(43) 24	('81)	Maxwell
Tellier	CEA-N-2286	('82)	0.025 eV to 3 MeV
Libraries			
ENDF/B-V			
JENDL-2			
INDL/A-83	(Same as JENDL-2)		

$^{243}Am(n,\gamma)$ cross section

AGM req. : (1) Pu-recycling calculation in thermal reactors, (2) In-core cycle in fast reactors, (3) ^{244}Cm production, (4) Actinide recycle, (5) Radioisotope power sources.
WRE.req. : (1) ^{244}Cm production, (2) Long term reactivity calculations, (3) Spent fuel shielding, (4) Fuel cycle calculation, (5) Neutron dose for cycle out-of-core, (6) Fast reactor burnup calculation, (7) Fuel reprocessing and storage, (8) Transuranium nuclides buildup in spent fuel, (9) Transport cask shielding.
JNDC/WG : (1) Fuel reprocessing, (2) Fuel facility, (3) Burnup evaluation, (4) Safeguards.

Experiments			
Glover+	NEANDC(E)202 8	('79)	Fast
Sanders+	79Aix 1 567	('79)	Fast
Darrouzet+	82Antwerp 181	('82)	Pile
Stevenson+	82Antwerp 178	('82)	Fast
Cricchio+	82Antwerp 175	('82)	Fast
Wisshak+	KFK-3503	('83)	5 keV to 250 keV
Evaluations			
Mann+	78BNL-2 275	('78)	10 keV to 10 MeV
Jary	CEA-N-2084	('79)	Maxwell
Abagyan+	YK- 1(40) 39	('81)	Maxwell
Kikuchi	JAERI-M-82 096	('82)	0.01 meV to 20 MeV
Libraries			
ENDF/B-V			

JENDL-2
KEDAK-4
UKNDL-81
ENDL-82
INDL/A-83 (Same evaluations as UKNDL-81, JENDL-2 and KEDAK-4)

^{243}Am(n,f) cross section

AGM req. : (1) In-core cycle in fast reactors, (2) ^{244}Cm production.
WRE.req. : (1) Fuel cycle calculation. (2) Fuel reprocessing and storage.
JNDC/WG : (1) Fuel reprocessing, (2) Fuel facility.

Experiments

Sweet	AEEW-R-1090	('77)	Fast
Asghar+	ANE 6 561	('79)	2.1 meV
Behrens+	NSE 77 4 444	('81)	200 keV to 30 MeV
Cricchio+	82Antwerp 175	('82)	Fast
Wisshak+	KFK-3503	('83)	5 keV to 250 keV
Froehner+	NEANDC(E)242U	('83)	3 keV to 500 keV

Evaluations

Mann+	78BNL-2 275	('78)	10 keV to 10 MeV
Jary	CEA-N-2084	('79)	Maxwell
Lynn+	NEANDC(E)212 8	('80)	0.01 meV to 15 MeV
Abagyan+	YK- 1(40) 39	('81)	Maxwell
Kikuchi	JAERI-M-82 096	('82)	0.01 meV to 20 MeV

Libraries
ENDF/B-V
JENDL-2
KEDAK-4
UKNDL-81
ENDL-82
INDL/A-83 (Same evaluations as UKNDL-81, JENDL-2 and KEDAK-4)

^{243}Am(n,2n) cross section

AGM req. : (1) Actinide recycle, (2) Radioisotope power sources.

Evaluation

Kikuchi	JAERI-M-82 096	('82)	above 6.6 MeV

Libraries
ENDF/B-V
JENDL-2
KEDAK-4
UKNDL-81
ENDL-82
INDL/A-83 (Same evaluations as UKNDL-81, JENDL-2 and KEDAK-4)

^{243}Am $\bar{\nu}$

AGM req. : (1) in-core cycle in fast reactors.
WRE.req. : (1) fuel cycle calculation, (2) fast reactors, (3) fuel reprocessing and storage.

Evaluation

Kikuchi	JAERI-M-82 096	('82)	0.01 meV to 20 MeV

Libraries
ENDF/B-V
JENDL-2

ENDL-82
INDL/A-83 (Same evaluation as JENDL-2)

^{242}Cm total cross section

AGM req. : (1) Pu-recycling calculation in thermal reactors.
Experiment
Artamonov+ 77Kiev 2 257 ('77) 1 eV to 260 eV
Libraries
ENDF/B-V
JENDL-2
ENDL-82
INDL/A-83 (Two evaluations by Maino+ and JENDL-2)

^{242}Cm(n,γ) cross section

AGM req. : (1) Pu-recycling calculation in thermal reactors, (2) Fuel handling, storage, transport and control.
WRE.req. : (1) ^{238}Pu production, (2) Burnup calculation, (3) Transuranium nuclide buildup in spent fuel, (4) Transport cask shielding, (5) Fuel processing and handling.
JNDC/WG : (1) Fuel facility.
Experiment
Darrouzet+ 82Antwerp 25 ('82) Pile
Evaluations
Belanova+ 80Kiev 3 256 ('80) 0.025 eV
Abagyan+ YK- 1(40) 39 ('81) Maxwell
Libraries
ENDF/B-V
JENDL-2
ENDL-82
INDL/A-83 (Two evaluations by Maino+ and JENDL-2)

^{242}Cm(n,f) cross section

AGM req. : (1) Fuel handling, storage, transport and control.
WRE.req. : (1) Fuel cycle calculation, (2) Burnup calculation, (3) Transuranium nuclide buildup in spent fuel, (4) Transport cask shielding, (5) Fuel reprocessing and storage.
JNDC/WG : (1) Fuel reprocessing, (2) Fuel facility.
Evaluations
Belanova+ 80Kiev 3 256 ('80) 0.025 eV
Abagyan+ YK- 1(40) 39 ('81) Maxwell
Libraries
ENDF/B-V
JENDL-2
ENDL-82
INDL/A-83 (Two evaluations by Maino+ and JENDL-2)

^{242}Cm $\bar{\nu}$

AGM req. : (1) Fuel handling, storage, transport and control.
WRE.req. : (1) Fuel cycle calculation, (2) Fuel reprocessing and storage.

Experiments

Popeko+	JINR-P3-11779	('78)	Spontaneous
Halperin+	NSE 75 1 56	('80)	Spontaneous
Zhang+	CNP 3 149	('81)	Spontaneous

Evaluation

Abagyan+	YK- 4(43) 24	('81)	Maxwell

Libraries

- ENDF/B-V
- JENDL-2
- ENDL-82
- INDL/A-83 (Two evaluations by Maino+ and JENDL-2)

$^{243}Cm(n,\gamma)$ cross section

AGM req. : (1) Pu-recycling calculation in thermal reactors,
(2) Actinide recycle.
WRE.req. : (1) Burnup calculations, (2) Transactinium nuclide buildup in spent fuel, (3) Transport cask shielding, (4) Fuel cycle
JNDC/WG : (1) Fuel reprocessing.

Experiments

Bemis+	NSE 63 413	('77)	Maxwell to 0.025 eV
Darrouzet+	82Antwerp 25	('82)	Pile

Evaluations

Voropaev+	YK- 34(3) 35	('79)	Fast
Jary	CEA-N-2084	('79)	Maxwell
Belanova+	80Kiev 3 256	('80)	0.025 eV
Nakagawa+	JAERI-M-9601	('81)	0.01 meV to 20 MeV
Abagyan+	YK- 1(40) 39	('81)	Maxwell

Libraries

- ENDF/B-V
- JENDL-2
- ENDL-82
- INDL/A-83 (Two evaluations by Maino+ and JENDL-2)

$^{243}Cm(n,f)$ cross section

AGM req. : (1) Pu-recycling calculation in thermal reactors,
(2) Actinide recycle.
WRE.req. : (1) Burnup calculation, (2) Transuranium nuclide buildup in spent fuel, (3) Transport cask shielding, (4) Fuel cycle.

Experiments

Bemis+	NSE 63 413	('77)	0.025 eV
Dabbs+	78BNL-2 313	('78)	0.1 eV to 100 keV
Zhuravlev+	AE 47 55	('79)	Maxwell

Evaluations

Voropaev+	YK- 34(3) 35	('79)	Fast
Jary	CEA-N-2084	('79)	Maxwell
Belanova+	80Kiev 3 256	('80)	0.025 eV
Nakagawa+	JAERI-M-9601	('81)	0.01 meV to 20 MeV
Abagyan+	YK- 1(40) 39	('81)	Maxwell

Libraries

- ENDF/B-V
- JENDL-2
- ENDL-82
- INDL/A-83 (Two evaluations by Maino+ and JENDL-2)

$^{244}Cm(n,\gamma)$ cross section

AGM req. : (1) Pu-recycling calculation in thermal reactors, (2) Fuel handling, storage, transport and control, (3) Actinide recycle.
WRE.req. : (1) Burnup physies, (2) Spent fuel shielding, (3) Fuel cycle, (4) Transactinium buildup, (5) Fuel reprocessing.
JNDC/WG : (1) Fuel facility.

Experiments

Gavrilov+	AE 44 246	('78)	Maxwell
Darrouzet+	82Antwerp 181	('82)	Pile

Evaluations

Caner+	IA- 1353	('79)	400 eV to 15 MeV
Jary	CEA-N-2084	('79)	Maxwell
Belanova+	80Kiev 3 256	('80)	0.025 eV
Abagyan+	YK- 1(40) 39	('81)	Maxwell

Libraries

ENDF/B-V
JENDL-2
KEDAK-4
ENDL-82
INDL/A-83 (Three evaluations by Caner+, JENDL-2 and KEDAK-4)

$^{244}Cm(n,f)$ cross section

AGM req. : (1) Fuel handing, storage, transport and control, (2) Actinide recycle.
WRE.req. : (1) Fast reactor calculation, (2) Fuel reprocessing.
JNDC/WG : (1) Fuel reprocessing.

Experiments

Sweet	AEEW-R-1090	('77)	Fast
Fomushkin+	YF 31 39	('80)	300 keV to 4.5 MeV
Vorotnikov+	YK- 1(40) 44	('81)	390 keV to 1.3 MeV
Stopa+	82Kiamesha 1090	('82)	0.14 eV to 80 keV

Evaluations

Gianotti	NSE 65 164	('78)	1 keV to 3.5 MeV
Caner+	IA- 1353	('79)	0.025 eV, 400 eV to 15 MeV
Jary	CEA-N-2084	('79)	Maxwell
Belanova+	80Kiev 3 256	('80)	0.025 eV
Abagyan+	YK- 1(40) 39	('81)	Maxwell

Libraries

ENDF/B-V
JENDL-2
KEDAK-4
ENDL-82
INDL/A-83 (Three evaluations by Caner+, JENDL-2 and KEDAK-4)

$^{245}Cm(n,\gamma)$ cross section

AGM req. : (1) Actinide recycle, (2) Future requirement,
WRE.req. : (1) Fast breeder application, (2) Fuel cycle, (3) Transactinium buildup.

Experiments

Gavrilov+	AE 44 246	('78)	Maxwell
Darrouzet+	82Antwerp 25	('82)	Pile

Evaluations

Voropaev+	YK- 34(3) 35	('79)	Fast
Belanova+	80Kiev 3 256	('80)	0.025 eV
Abagyan+	YK- 1(40) 39	('81)	Maxwell

Libraries
- ENDF/B-V
- JENDL-2
- ENDL-82
- INDL/A-83 (Two evaluations by Maino+ and JENDL-2)

$^{245}Cm(n,f)$ cross section

AGM req. : (1) Future requirement.
WRE.req. : (1) Fast breeder application, (2) Fuel cycle, (3) Transactinium buildup.

Experiments

Browne+	NSE 65 166	('78)	0.01 eV to 35 eV
Nakagome+	DOE-NDC-15 200	('79)	1 eV to 100 keV
White+	79knoxvill 496	('79)	1 meV to 10 keV
White+	82Antwerp 218	('82)	1 meV to 20 MeV

Evaluations

Voropaev+	YK- 34(3) 35	('79)	Fast
Belanova+	80Kiev 3 256	('80)	0.025 eV
Abagyan+	YK- 1(40) 39	('81)	Maxwell

Libraries
- ENDF/B-V
- JENDL-2
- ENDL-82
- INDL/A-83 (Two evaluations by Maino+ and JENDL-2)

$^{246}Cm(n,\gamma)$ cross section

AGM req. : (1) Future requirement, (2) Actinide recycle.
WRE.req. : (1) Cf production, (2) Out-of-core cycle.

Experiments

Gavrilov+	AE 44 246	('78)	Maxwell
Darrouzet+	82Antwerp 25	('82)	Pile

Evaluations

Voropaev+	YK- 34(3) 35	('79)	Fast
Jary	CEA-N-2084	('79)	Maxwell
Belanova+	80Kiev 3 256	('80)	0.025 eV
Abagyan+	YK- 1(40) 39	('81)	Maxwell

Libraries
- ENDF/B-V
- JENDL-3 (Preliminary)
- KEDAK-4
- ENDL-82
- INDL/A-83 (Two evaluations by Maino+ and Caner+)

$^{246}Cm(n,f)$ cross section

AGM req. : (1) Future requirement.
WRE.req. : (1) Out-of-core cycle.

Experiments

Fomushkin+	YF 31 39	('80)	300 keV to 4.5 MeV
Stopa+	82Kiamesha 1090	('82)	0.14 eV to 80 keV

Evaluations

Voropaev+	YK- 34(3) 35	('79)	Fast
Jary	CEA-N-2084	('79)	Maxwell
Belanova+	80Kiev 3 256	('80)	0.025 eV
Abagyan+	YK- 1(40) 39	('81)	Maxwell

Libraries

ENDF/B-V	
JENDL-3	(Preliminary)
KEDAK-4	
ENDL-82	
INDL/A-83	(Two evaluations by Maino+ and Caner+)

^{247}Cm(n,γ) cross section

Experiments

Gavrilov+	AE 44 246	('78)	Maxwell
Darrouzet+	82Antwerp 25	('82)	Pile

Evaluations

Konshin	INDC(CCP)-111	('78)	0.025 eV
Voropaev+	YK- 34(3) 35	('79)	Fast
Jary	CEA-N-2084	('79)	Maxwell
Belanova+	80Kiev 3 256	('80)	0.025 eV
Abagyan+	YK- 1(40) 39	('81)	Maxwell

Libraries

ENDF/B-V	
JENDL-3	(Preliminary)
ENDL-82	
INDL/A-83	(Evaluation by Maino+)

^{247}Cm(n,f) cross section

Evaluations

Konshin	INDC(CCP)-111	('78)	0.025 eV
Voropaev+	YK- 34(3) 35	('79)	Fast
Jary	CEA-N-2084	('79)	Maxwell
Belanova+	80Kiev 3 256	('80)	0.025 eV
Abagyan+	YK- 1(40) 39	('81)	Maxwell

Libraries

ENDF/B-V	
JENDL-3	(Preliminary)
ENDL-82	
INDL/A-83	(Evaluation by Maino+)

^{248}Cm(n,γ) cross section

AGM req. : (1) future requirement.
WRE.req. : (1) out-of-core cycle.

Experiments

Gavrilov+	AE 44 246	('78)	Maxwell
Darrouzet+	82Antwerp 25	('82)	Pile

Evaluations

Mann+	HEDL-TME-77-54	('77)	1 keV to 20 MeV
Voropaev+	YK- 34(3) 35	('79)	Fast
Jary	CEA-N-2084	('79)	Maxwell
Belanova+	80Kiev 3 256	('80)	0.025 eV
Abagyan+	YK- 1(40) 39	('81)	Maxwell

Libraries

ENDF/B-V
JENDL-3 (Preliminary)
ENDL-82
INDL/A-83 (Evaluation by Caner+)

^{249}Bk(n,γ) cross section

AGM req. : (1) Future requirement.
WRE.req. : (1) Out-of-core cycle.
Evaluations

Voropaev+	YK- 34(3) 35	('79)	Fast
Abagyan+	Yk- 1(40) 39	('81)	Maxwell

Libraries
ENDF/B-V
ENDL-82

^{249}Bk resonance integral.

AGM req. : (1) Future requirement, (2) Actinide recycle.
Evaluation

Abagyan+	Yk- 1(40) 39	('81)	Maxwell

^{249}Cf(n,γ) cross section

AGM req. : (1) Future requirement.
WRE.req. : (1) Out-of-core cycle.
Evaluations

Konshin	INDC(CCP)-111	('78)	0.025 eV
Voropaev+	YK- 34(3) 35	('79)	Fast
Abagyan+	YK- 1(40) 39	('81)	Maxwell

Libraries
ENDF/B-V
ENDL-82

^{249}Cf(n,f) cross section

AGM req. : (1) Future requirement.
Evaluations

Konshin	INDC(CCP)-111	('78)	0.025 eV
Voropaev+	YK- 34(3) 35	('79)	Fast
Abagyan+	YK- 1(40) 39	('81)	Maxwell

Libraries
ENDF/B-V
ENDL-82

^{250}Cf(n,γ) cross section

AGM req. : (1) Future requirement, (2) Actinide recycle.
WRE.req. : (1) Cf production.
Experiment

Gavrilov+	YFI-25 49	('77)	order of 1 MeV

Evaluations

Voropaev+	YK- 34(3) 35	('79)	Fast
Abagyan+	YK- 1(40) 39	('81)	Maxwell

Libraries
ENDF/B-V

ENDL-82

^{250}Cf(n,f) cross section

AGM req. : (1) Future requirement. (2) Actinide recycle.
WRE.req. : (1) Cf production.
Evaluations

Voropaev+	YK- 34(3) 35	('79)	Fast
Abagyan+	YK- 1(40) 39	('81)	Maxwell

Libraries
ENDF/B-V
ENDL-82

^{251}Cf(n,γ) cross section

AGM req. : (1) Future requirement.
WRE.req. : (1) Cf production.
Evaluations

Konshin	INDC(CCP)-111	('78)	0.025 eV
Voropaev+	YK- 34(3) 35	('79)	Fast
Abagyan+	YK- 1(40) 39	('81)	Maxwell

Libraries
ENDF/B-V
ENDL-82

^{251}Cf(n,f) cross section

AGM req. : (1) Future requirement, (2) Actinide recycle.
WRE.req. : (1) Cf production.
Evaluations

Konshin	INDC(CCP)-111	('78)	0.025 eV
Voropaev+	YK- 34(3) 35	('79)	Fast
Abagyan+	YK- 1(40) 39	('81)	Maxwell

Libraries
ENDF/B-V
ENDL-82

^{252}Cf(n,γ) cross section

AGM req. : (1) Future requirement.
Evaluations

Voropaev+	YK- 34(3) 35	('79)	Fast
Abagyan+	YK- 1(40) 39	('81)	Maxwell

Libraries
ENDF/B-V
ENDL-82

^{252}Cf(n,f) cross section

AGM req. : (1) Future requirement.
WRE.req. : (1) Cf production.
Experiments

Adams+	NSE 63 41	('77)	Spontaneous
Bicknell+	DOE-NDC-15 197	('79)	1 eV to 100 keV
Cumpstey+	NP/A 359 2 377	('81)	Spontaneous

Evaluations

Voropaev+ YK- 34(3) 35 ('79) Fast
Abagyan+ YK- 1(40) 39 ('81) Maxwell

Libraries
ENDF/B-V
ENDL-82

^{253}Cf(n,γ) cross section

AGM req. : (1) Future requirement.

Evaluation
Abagyan+ YK- 1(40) 39 ('81) Maxwell

Library
ENDF/B-V

^{253}Cf(n,f) cross section

AGM req. : (1) Future requirement.

Evaluation
Abagyan+ YK- 1(40) 39 ('81) Maxwell

Library
ENDF/B-V

^{253}Es(n,γ) cross section

AGM req. : (1) Future requirement.

Library
ENDF/B-V

Review Paper 3

PROGRESS IN TRANSACTINIUM ISOTOPE NEUTRON DATA MEASUREMENTS

J. FREHAUT
Centre d'études de Bruyères-le-Châtel,
Commissariat à l'énergie atomique,
Bruyères-le-Châtel, France

Abstract

This paper reviews the present state of the techniques used in different laboratories for neutron data measurements on transactinium isotopes, with emphasis on recent developments and possible improvements. The different domains investigated are : fission cross sections, prompt neutrons from fission, delayed neutrons from fission, prompt fission neutron spectrum, prompt fission gamma-rays, (n,xn) reactions, capture cross sections and neutron scattering.

I - INTRODUCTION

Transactinium isotope neutron data measurements represent an immense field. The experimental techniques involved depend strongly on the neutron energy range investigated as well as the quantity which is measured. A reviewer has generally a limited domain of expertise out of which he is more or less obliged to rely upon the judgment of other experts. In the present case, the domain of fast fission will be more thoroughly investigated.

In recent years, a number of Specialists' Meetings on subjects of present interest have been held (neutron scattering, capture, delayed neutrons), and therefore only the new developments since these meetings will be reviewed. This paper discusses the present state of techniques and recent developments and emphasizes possible improvements. The different domains are presented in completely independent chapters. The literature cited is rather an illustration of the techniques used in different laboratories and is certainly non complete under the aspect of nuclear data quotation.

II - FISSION CROSS SECTIONS

The use of the ^{235}U fission cross section as a primary standard in the energy region above 100 keV is now generalized. Therefore the fission cross section measurements can be divided in two categories which will be reviewed successively :

1 - Absolute and shape measurements on ^{235}U.
2 - Measurements relative to ^{235}U.

In the energy range below 100 keV the fission cross section of ^{235}U shows strong fluctuations and therefore is not very useful as a standard. The ^{6}Li (n,α) reaction is then often used as a secundary standard for shape measurements, with a normalisation to the ^{235}U fission cross section [1].

II-1-Absolute and shape fission cross section measurements on ^{235}U.

This subject has been reviewed in a recent IAEA Consultant's Meeting [2] and only some brief comments will be given here.

Shape measurements are very similar in nature to some of the relative measurements discussed in the next paragraph. In particular it is obvious that in both cases such defects as sample inhomogeneities or the presence of grains at the surface of the deposits will result in an unpredectible energy dependence of the fission fragment detection efficiency, correlated with the energy dependence of the fission fragment angular distributions. Therefore a high quality sample is essential in achieving unbiased shape measurements.

Special attention has been paid in last years to absolute measurements around 14 MeV. All recent measurements agree within 1%, but they all use the same technique and a larger systematic error cannot be ruled out. A detailed description of the technique involved (the time correlated associated particle method) and a discussion of the results is given in ref.[3].

The derivation of the "best fission cross section set" from the existing data has been a standing problem up to recently.The concern was the choice rather arbitrary of the energy point and of the corresponding cross section value to which renormalise the existing shape measurements. And since shape measurements contained far more data points than absolute measurements they defined in fact the accuracy of the evaluated cross sections.

Surprisingly, the correct evaluation method, using the Bayesian procedure, has only been used recently [4]. Its main advantages compared to the older approximate methods are :

- It is not necessary to choose a normalisation point for the shape measurements.

- The correlations are taken into account. Since shape measurements are highly correlated, they have less relative weight in the final result.

- The method provides a unique fission cross section set for a given data base.

The preliminary results show errors ranging from 0.5 to 2% in the energy range between 100 keV and 20 MeV, which is about 2 times lower than can been estimated from the spread in experimental data. Therefore, the present knowledge of the ^{235}U fission cross section might be more accurate than generally admitted on the basis of rather crude evaluations.

II-2-Relative fission cross section measurements

By "relative measurements" it is generally understood that deposits of the materials to be investigated are placed back to back in fission chambers irradiated in a given neutron flux, so that it is not necessary to measure absolutely this incident neutron flux. Relative fission cross sections are obtained from the ratio of the number of fission events detected for the different deposits.

However in many cases [12, 14-21, 23-25, 27] it is necessary to determine accurately the mass of the deposits and the efficiency of the fission detectors. In fact, these measurements are relative as far as the incident neutron flux is concerned, but are absolute as far as fission detection is concerned.

In another class of experiments, the fission fragment detection efficiencies and the mass of the deposits do not need to be known accurately : only the ratios of theses quantities for the investigated materials are necessary and are obtained directly from experiment. This method, known under the name of threshold cross section method, has been extensively used by BEHRENS et al. [5-11] and occasionnally in others laboratories [13,22,26,28]. It is potentially the most accurate method, and I would like to present it in more details.

Three different chambers are necessary in the most general case. The first contains N_A atoms of the reference isotope A (generally ^{235}U) and its efficiency is ε_A. The second contains N_B atoms of the investigated isotope and its efficiency is ε_B. The third one contains N_M atoms of a mixture of the two isotopes of interest, with an atom ratio η of the isotope A to the isotope B, and its efficiency is ε_M. When placed in a same neutron flux $\phi(E)$, the counting rate for the 3 fission chambers will be, respectively:

$$C_A(E) = \phi(E)\ \varepsilon_A\ N_A\ \sigma_A(E)$$

$$C_B(E) = \phi(E)\ \varepsilon_B\ N_B\ \sigma_B(E)$$

$$C_M(E) = \phi(E)\ \frac{\varepsilon_M\ N_M}{\eta + 1}\left(\eta\ \sigma_A(E) + \sigma_B(E)\right)$$

where $\sigma_A(E)$ and $\sigma_B(E)$ are the fission cross sections for the isotopes A and B, respectively.

The ratio $R(E) = \sigma_B(E)/\sigma_A(E)$ for the fission cross sections of isotopes B and A is then obtained from the counting rates by the relations :

$$R(E) = \frac{\varepsilon_A\ N_A}{\varepsilon_B\ N_B}\ \frac{C_B(E)}{C_A(E)} = \frac{\varepsilon_A\ N_A}{\varepsilon_M\ N_M}\ (1 + \eta)\ \frac{C_M(E)}{C_A(E)} - \eta \qquad (1)$$

One obtains 2 n equations, if the measurements have been done at n different energies. Thus the system is overdimensioned and can be solved using the BAYESIAN method described for exemple in [29,30] to obtain the n R(E) ratios and the 3 constant terms $\frac{\varepsilon_A\ N_A}{\varepsilon_B\ N_B}$, $\frac{\varepsilon_A\ N_A}{\varepsilon_M\ N_M}$ and η.

This method is particularly accurate when B is a threshold isotope, because R(E) varies on a wider range from 0 to a maximum value, provided that some measurements are made below the fission threshold, thus leading to a very good determination of the 3 constant terms in the above equation (1). Moreover, the BAYESIAN fit provides the possibility to use prior information, for example an experimental value of η. In fact nobody has used correctly the method.

In all cases η was measured carefully and advantage was then taken of the linear relation between :

$\frac{C_B(E)}{C_A(E)}$ and $\frac{C_M(E)}{C_A(E)}$ in (1) to derive the best values for $\frac{\varepsilon_A N_A}{\varepsilon_B N_B}$ and $\frac{\varepsilon_A N_A}{\varepsilon_M N_M}$ by a least square fitting to the data. What relation has been used in (1) to determine the final R(E) values is not clear from the publications. However, it is clear that a lot of information has not been used, and moreover the correlations are not correctly accounted for.

In some cases [6,8] the threshold method was combined with a normalisation at thermal energy when ^{235}U and another fissile isotope were involved in a measurement. Unfortunately, the two normalisations were considered as independent and moreover the corresponding errors were increased to obtain consistency, when necessary. Here again, a global BAYESIAN fit including the thermal cross section ratio as a prior datum would have been far more valuable.

It appears that for the threshold cross section method the data reduction procedure is rather an evaluation procedure, so that the appropriate tool, i.e. the BAYESIAN procedure, should be used. It is my feeling that the measurements contain more information than released in the corresponding publications, and a complete treatment of the data, at least for the most important isotopes, would be highly valuable.

II-3-Fissile deposits

When the measurement relies on an absolute determination of the fission rate, a careful determination of the deposit properties is essential. For accurate measurements of the absolute fission cross section of ^{235}U, for example, the total mass and the relative areal density have to be measured. Useful details can be found in ref. [3]. Nevertheless, uncertainties on the deposit characteristics account for a major part of the final uncertainty. This is largely due to the determination of the fraction of fission fragments absorbed in the deposit. Fragment ranges are not very well known and sometimes the chemical nature of the deposit is uncertain. In relative measurements, the areal density is rarely measured ; inhomogeneities or the possible existence of grains of different sizes are not considered.

It is clear that a substantial improvement of accuracy can been achieved by a careful investigation of the deposit characteristics. A large step in the right direction has been taken by BUDTZ-JORGENSEN and KNITTER at GEEL [31]. They used an ionization chamber with FRISCH grid to determine the energy of the fission fragments as a function of the emission angle θ relative to the normal of the deposit. Studying the thermal neutron induced fission of ^{235}U, their data clearly show that energy degradation of the fragments occurs for cos θ approaching zero. Furthermore, they were able to obtain information on the quality of the deposit as shown in fig. II-1, taken from their paper, where events in the low energy tail between 10 and 35 MeV are plotted versus cos θ. For the evaporated UF_4 deposit of 75 μg/cm^2 thickness, the tail is decreasing rapidly with cos θ, whereras for the 100 μg/cm^2 thick eletrosprayed U_3O_8 deposit the tail remains important. This

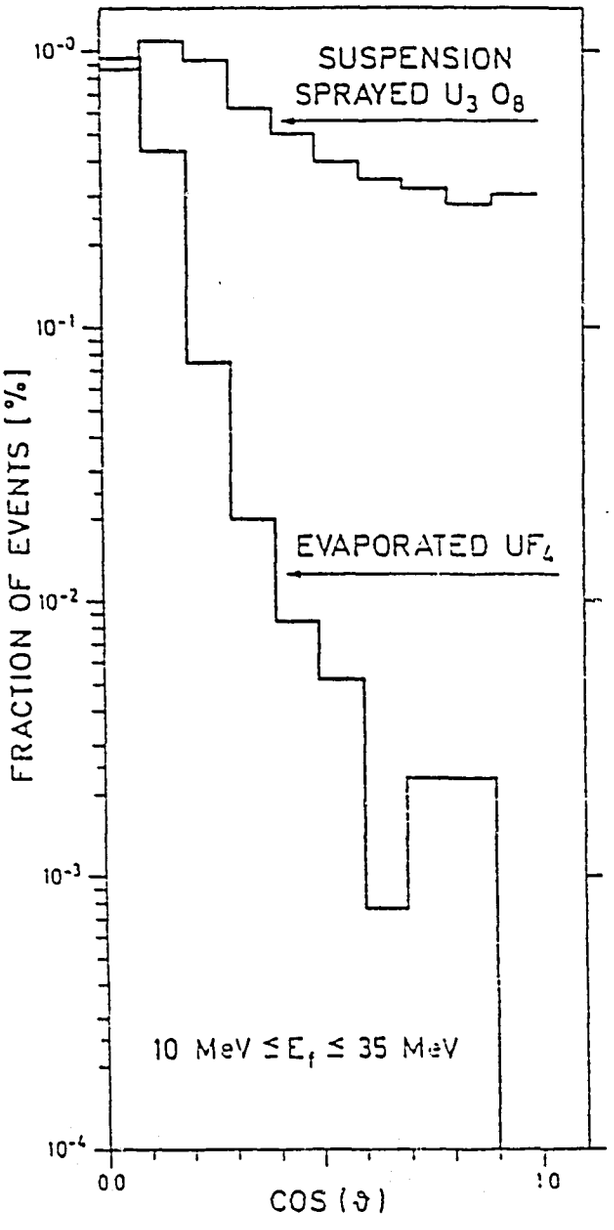

Fig.II-1

The fraction of fission events in percent of the total which were found in cos θ intervals of 0.1 in the fission fragment energy range between 10 MeV and 35 MeV are plotted versus cos θ for the 75 μg/cm^2 vacuum evaporated UF_4 sample and for the 100 μg/cm^2 U_3O_8 suspension sprayed sample with a thick and thin histogram line, respectively. Taken from ref. [31].

latter deposit certainly contains grains with sizes which can be of the order of the fission fragment ranges. It is quite impossible to correct analytically for self-absorption in such a sample. Therefore fission cross section shape measurements using sprayed or painted samples might be distorded when variations in self-absorption due to the energy dependence of the fission fragment angular distributions cannot be correctly accounted for because of the presence of large size grains.

Fig. II-2, also taken from ref. [31], shows the influence of sample thickness on self-absorption. Such data, obtained for isotropic angular distributions, provide the information necessary to determine the fission detection efficiency for any given fission fragment angular distribution.

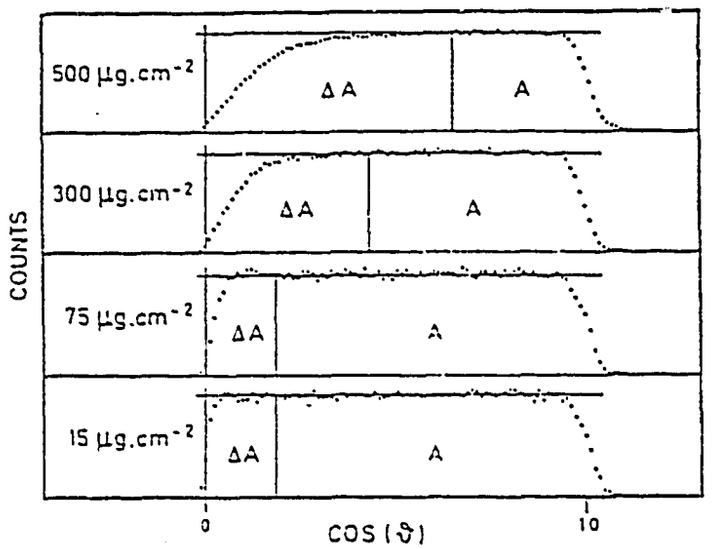

Fig.II-2

The cos θ distributions of the fission fragments for four UF_4 vacuum evaporated samples. Taken from Ref.[31]

Similar investigations have also been made using alpha particles from the samples. The authors of ref. [31] conclude that their method permits a determination of the alpha source strength with an accuracy of less than 0.3% and of the absolute number of fission events with an accuracy better than 0.5%.

Comparable accuracy has been achieved for the absolute determination of the spontaneous fission rate of a ^{252}Cf fission chamber [32] using the fission-neutron coincidence technique. The same technique has already been used 20 years ago [33] for the thermal neutron induced fission of ^{235}U and could constitute an alternative independent method in assessing the fission chamber efficiency for absolute measurements.

Schematically the principle of the method is as follows : a neutron detector of efficiency ε_n registers the fission neutrons from an isotropic source of strength S placed in a fission chamber of average efficiency $\bar{\varepsilon}_f$. The angle between the normal to the fission deposit and the detector axis is θ. To simplify, ε_n incorporates the solid angle factor and must be small. Thus the fission counting rate is :

$$N_f = \bar{\varepsilon}_f \, S$$

the neutron counting rate is :

$$N_N = \varepsilon_n \, \bar{\nu} \, S$$

where $\bar{\nu}$ is the average number of neutrons emitted per fission, and the coincidence rate between the 2 detectors is :

$$N_c = \varepsilon_f(\theta) \, \varepsilon_n \, \bar{\nu} \, S$$

ε_f is a function of θ in this latter case because the direction of the emitted neutrons is correlated to the direction of the fragments. Averaged over all space, $\varepsilon_f(\theta)$ gives $\bar{\varepsilon}_f$. ($\varepsilon_f(\theta)$ is not the angular dependence of the fragment detection efficiency in the chamber but is related to it through the neutron angular distribution). From these relations one can deduce :

$$N_f \, N_n / N_c = \frac{\bar{\varepsilon}_f}{\varepsilon_f(\theta)} \, S$$

$$N_c / N_n = \varepsilon_f(\theta)$$

Thus, from relative measurements at several angles, it is possible to determine the absolute fission rate (S) and the fragment detection efficiency. Fig. II-3 taken from ref. [32] gives an idea of $\varepsilon_f(\theta)$ for a high quality ^{252}Cf source. The effect should be higher for the much thicker deposits used in fission chambers designed to study the neutron induced fission.

II-4-Fission chamber design.

The most common fission chambers are made of parallel electrodes with spacing small compared to the range of a fission fragment in the

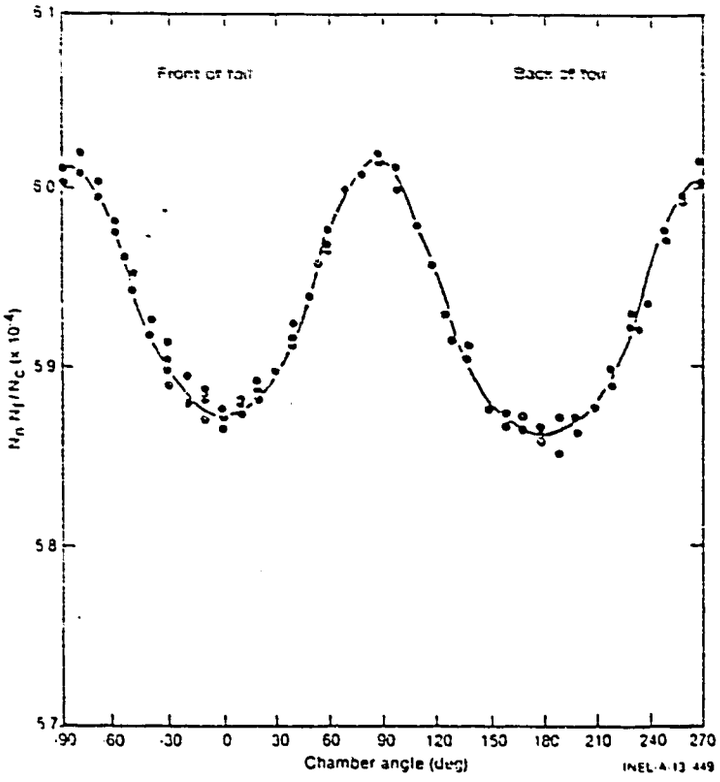

Fig.II-3 - Neutron fission angular correlation function for a fission chamber. Taken from Ref. [32].

counting gas. This arrangement improves the discrimination between fission fragments and alpha particles and can be used for alpha activities up to about 10^6 $\alpha.s^{-1}$. The limitation comes from the larger path for alpha particles emitted at large angles relative to the normal of the deposit.
To reduce the transverse path of alpha particles special fission chambers have been designed at ORNL with hemispherical plates [15] or with parallel plates separated by a honeycomb [14]. A good separation between alpha particles and fission fragments was observed with alpha activities higher than 10^7 $\alpha.s^{-1}$.

Comparable results were obtained at GEEL with different arrangements. A fission chamber [18] used a plate spacing larger than the fragment ranges in the gas. By differentiating the current pulse, a very fast linear pulse was obtained, thus leading to a better discrimination betweeen fission fragments and alpha particles. In another chamber [19], fission fragments were stopped in an intermediate thin electrode, whereas alpha particles passed through it to be collected on the outer electrodes. The spacing of the 3 electrodes was such that no pulse was created by alpha particles on the middle electrode. However it was necessary to collimate using a grid placed above the sample.

Although these special chambers worked properly, their absolute dectection efficiency was quite difficult to determine accurately, especially with the honeycomb structure or the compensated chamber which make use of collimation.

In a sense, these chambers seem to be more appropriate to the threshold cross section method. But in turn this method does not require a perfect separation of fission fragments and alpha particles, and therefore classical chambers with alpha activities up to 10^7 $\alpha.s^{-1}$ were used [5-11]. In the future, the association of the two techniques should allow accurate measurements with alpha activities of the order of 10^8 $\alpha.s^{-1}$.

II-5-Neutron sources

Two kinds of neutron sources have essentially been used : monoenergetic neutron sources and white neutron sources.

Monoenergetic sources are produced with elestrostatic accelerators using the $^7Li(p,n)^7Be$, $^3H(p,n)^3He$, $^2H(d,n)^3He$ and $^3H(d,n)^4He$ reactions.Their main advantage is to produce a neutron beam well defined in energy and with a good resolution, especially at high energies, in the MeV region. But to obtain a good statistics, it is necessary to place the fission chamber close to the source, i.e. in an uncollimated neutron beam. Therefore the correction for fission induced by neutrons scattered from the chamber structure materials can be large (several percent) and limits the accuracy of the measurements. The beam is generally pulsed in order to discriminate between fast neutron induced fission and fission induced by low energy background neutrons or in some cases spontaneous fission. But the short flight path does not give the possibility to distinguish the fast spurious neutrons from the monoenergetic ones ((d,n) reactions on target materials, for example, in the $D(d,n)^3He$ reaction). The corresponding correction has to be estimated from auxiliary experiments or calculations, which further reduces the accuracy [12, 18-20].

With white neutron sources, the fission chamber is placed at several meters from the target. The beam can be well collimated so that fission induced by the neutrons scattered from the chamber structure materials become quite negligible. The time-of-flight technique is used to determine the energy of the neutrons inducing fission. The timing reference

is generally obtained from photofission induced by the γ-ray flash. The neutron energy scale can also be verified or established using well known absorption resonances, particularly those of carbon in the MeV region. A wide energy range from thermal up to about 30 MeV can be covered without changing the experimental conditions with linear electron accelerators, thus providing excellent conditions for shape measurements of fission cross sections. The shortcomings of the method are perhaps the relative low energy resolution in the high energy region and the determination of the beam dependent background using the black resonance technique.

II-6-Conclusion

From the present analysis it can be concluded that the most accurate relative measurements over large energy ranges will be obtained using the threshold cross section method and a white neutron source. Consideration of covariances is essential in data reduction procedures.

For all measurements, including shape measurements on the ^{235}U standard, a careful determination of the sample characteristics, using presently available techniques, would considerably reduce the possibility of systematic errors related to changes in the fragment angular distributions with the incident neutron energy.

With such improvements for relative and shape measurements, the required accuracies between thermal and 20 MeV could probably be obtained using only the accurate absolute measurements available at thermal and 14 MeV as renormalisation points. Here again, consideration of covariances is essential.

A large data basis is now available, which probably is sufficient to guarantee an evaluation meeting the required accuracies for a large number of isotopes in the region from Th to Am. More accurate data are needed only for a limited number of particularly important isotopes. Future needs concern more exotic nuclei in order to extend the data basis. Fission chambers with alpha activities higher than 10^7 $\alpha.s^{-1}$ are now commonly used, and activities of the order of 10^8 $\alpha.s^{-1}$ can be considered with the present techniques. In that domain, and even for higher activities, track detectors [34], already currently used in russian laboratories [21,23-25], have high potentialities.

REFERENCES

[1] - C. WAGEMANS, A.J. DERUYTTER, INDC (NDS) 146, July 1983, p.79.

[2] - IAEA Consultants' Meeting on the U-235 fast fission cross section, SMOLENICE, March 1983, INDC(NDS) 146.

[3] - O.A. WASSON, A.D. CARLSON, K.C. DUVALL, Nucl. Sci. Eng. 80 (1982) 282.

[4] - M.R. BHAT, INDC (NDS)-146, July 1983, p.119.

[5] - J.W. BEHRENS and G.W. CARLSON, Nucl. Sci. Eng., 63 (1977) 250.

[6] - G.W. CARLSON and J.W. BEHRENS, Nucl. Sci. Eng., 66 (1978) 205.

[7] - J.W. BEHRENS, R.S. NEWBURY and J.W. MAGANA, Nucl. Sci. Eng., 66 (1978) 433.

[8] - G.W. CARLSON and J.W. BEHRENS, Nucl. Sci. Eng., 68 (1978) 128.

[9] - J.W. BEHRENS and J.C. BROWNE, Nucl. Sci. Eng., 77 (1981) 444.

[10] - J.W. BEHRENS, J.C. BROWNE, J.C. WALDEN, Nucl. Sci. Eng., 80 (1982) 393.

[11] - J.W. BEHRENS, J.C. BROWNE, E. ABLES, Nucl. Sci. Eng., 81 (1982) 512.

[12] - J.W. MEADOWS, "The fission cross sections of some Thorium, Uranium, Neptunium and Plutonium Isotopes relative to ^{235}U", report ANL/NDM 83 (1983).

[13] - L.W. WESTON and J.H. TODD, Nucl. Sci. Eng., 84 (1983) 248.

[14] - J.W.T. DABBS, C.H. JOHNSON, C.E. BEMIS, Nucl. Sci. Eng., 83 (1983) 22.

[15] - J.W.T. DABBS, C.E. BEMIS, S. RAMAN, R.J. DOUGAN, R.W. HOFF, Nucl. Sci. Eng., 84 (1983) 1.

[16] - R.M. WHITE and J.C. BROWNE, Proc. Int. Conf. Nuclear Data for Science and Technology, Antwerp, Belgium, September 6-10, 1982, p.218.

[17] - C. BUDTZ-JORGENSEN, H.H. KNITTER, D.L. SMITH, Proc. Int. Conf. Nuclear Data for Science and Technology, Antwerp, Belgium, September 6-10,1982, p.206.

[18] - C. BUDTZ-JORGENSEN and H. KNITTER, Nucl. Sci. Eng., 79 (1981) 380.

[19] - H.H. KNITTER and C. BUDTZ-JORGENSEN, Atom-Kernenergie, 33 (1979) 205.

[20] - M.S. MOORE, J.A. WARTENA, H. WEIGMANN, C. BUDTZ-JORGENSEN, H.H. KNITTER, Nucl. Phys. A393 (1983) 1.

[21] - E.F. FOMUSHKIN, G.F. NOVASELOV, Yu. I. VINOGRADOV, V.V. GAVRILOV, V.I. INKOV, B.K. MASLENNIKOV, V.N. POLYNOV, V.M. SURIN, A.M. SHVETSOV, Sov. J. Nucl. Phys. 33 (1981) 324.

[22] - B.I. FURSOV, V.M. KUPRIYANOV, B.K. MASLENNIKOV, G.N. SMIRENKIN, Sov. J. At. Energy 43 (1978) 808.

[23] - B.I. FURSOV, V.M. KUPRIYANOV, V.I. IVANOV, G.N. SMIRENKIN, Sov. J. At. Energy 43 (1978) 894.

[24] - B.I. FURSOV, V.M. KUPRIYANOV, G.N. SMIRENKIN, Sov. J. At. Energy 44 (1978) 262.

[25] - V.M. KUPRIYANOV, B.I. FURSOV, V.I. IVANOV, G.N. SMIRENKIN, Sov. J. At. Energy 45 (1979) 1176.

[26] - V.M. KUPRIYANOV, B.I. FURSOV, B.K. MASLENNIKOV, V.M. SURIN, G.N. SMIRENKIN, Sov. J. At. Energy 46 (1979) 35.

[27] - V.M. KUPRIYANOV, G.N. SMIRENKIN, B.I. FURSOV, Sov. J. At. Energy 55 (1984) 472.

[28] - F.C. DIFILIPPO, R.B. PEREZ, G. de SAUSSURE, D.K. OLSEN, R.W. INGLE, Nucl. Sci. Eng. 68 (1978) 43.

[29] - F.G. PEREY, Proc. Conf. on Neutron Physics and Nuclear Data, HARWELL, U.K. Sept. 1978, p.104.

[30] - D.L. SMITH, "Covariance Matrices and Applications to the field of Nuclear Data", Report ANL/NDM 62 (1981).

[31] - C. BUDZ-JORGENSEN, H.H. KNITTER, INDC (NDS) 146, July 1983, p. 131.

[32] - J.R. SMITH, "Status on the quest for ^{252}Cf $\bar{\nu}$", report EPRI NP-1258 (1979).

[33] - K.G. PORGES, A. De VOLPI, Proc. Conf. Nuclear Data for Reactors.

[34] - H.A. KHAN, S.A. DURRANI, Nucl. Inst. Meth. 98 (1972) 229.

III - Prompt neutrons from fission

The last compilation of $\bar{\nu}_p$, the average number of prompt neutrons emitted per fission, was established by KONSHIN and MANERO in 1972 [1] and is always largerly used. However a number of important results have since been published and therefore a brief status of the data will be presented. The aim of this status is not to provide recommended values, but rather to compare the most accurate sets of data obtained on broad energy ranges, in order to have a good basis to discuss the present state of the techniques.

$\bar{\nu}_p$ values are generally measured relative to $\bar{\nu}_p$ for the spontaneous fission of ^{252}Cf used as a standard. The review of absolute $\bar{\nu}_p$ measurements for ^{252}Cf is beyond the scope of the present investigation. An overview of the present situation can be found in one the last papers published on that subject [20].

III-1- $\bar{\nu}_p$ for ^{235}U.

Two sets of data have been published for ^{235}U : a measurement by GWIN et al. on ORELA [2] from thermal up to 10 MeV incident neutron energy, and our measurement between 1 and 15 MeV [3].

The most accurate data published to date for $E_n < 1$ MeV are compared in Fig. III-1. In this energy range, the BRC data and those of BOLDEMAN et al. have been corrected [4] and are in good agreement. They agree also with the data of GWIN et al. although these latter are about 0.5% higher.

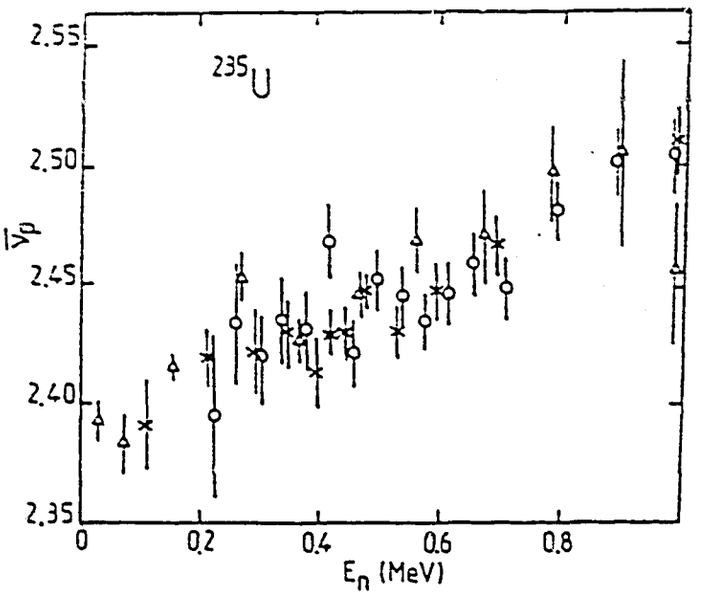

FIGURE III-1

$\bar{\nu}_p$ for ^{235}U for E_n < 1 MeV.

Δ : ref. [2] X : ref. [4] (Boldeman) 0 : Ref. [4] (BRC)

The data of ORELA [2] and BRC [3] for E_n > 1 MeV are compared in Fig. III-2. They agree fairly well. The present BRC data confirm earlier measurements made in the same laboratory [5].

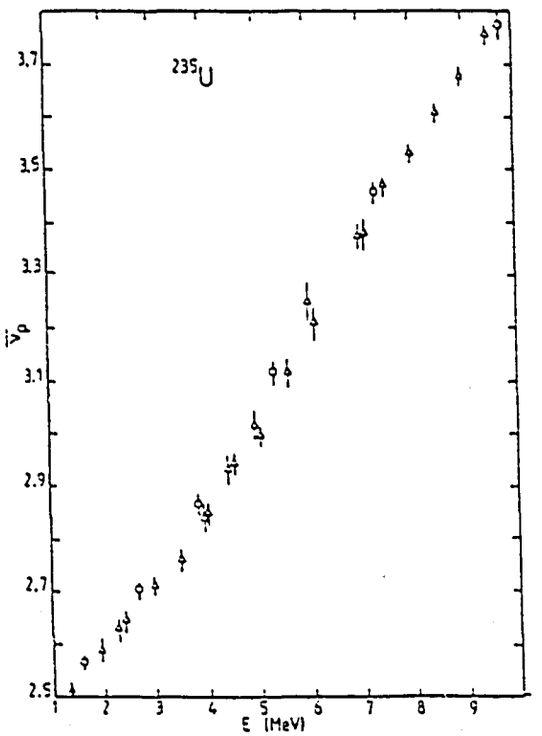

FIGURE III-2

$\bar{\nu}_p$ for ^{235}U for E_n > 1 MeV.

Δ : Ref. [3] 0 : Ref. [2]

III-2- $\bar{\nu}_p$ for ^{238}U

Two series of measurements have been made in USSR for this nucleus [6,7]. These data are compared with BRC data [5] in Fig. III-3. The agreement is fairly good, excepted around 3 MeV incident neutron energy, where the change in slope observed for the BRC data is not reproduced by russian data. However the agreement should be better if the russian data were lowered by about 1%.

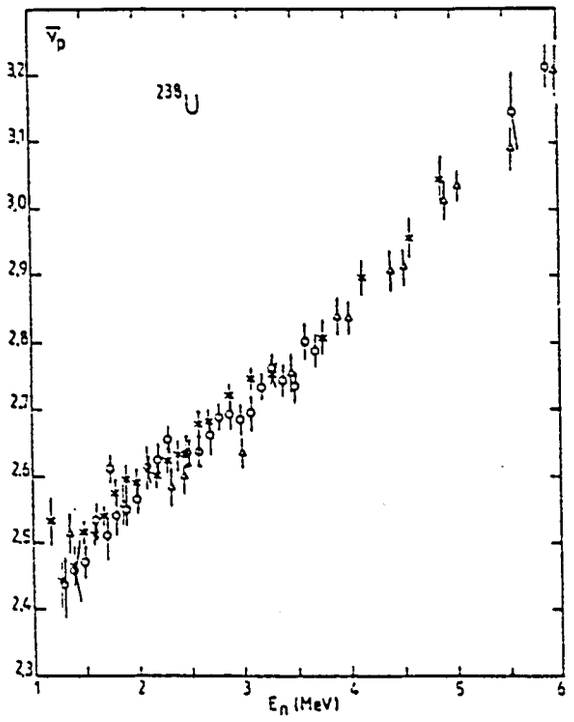

FIGURE III-3

$\bar{\nu}_p$ for ^{238}U.

Δ : Ref. [5] X : Ref. [6]
O : Ref. [7]

III-3- $\bar{\nu}_p$ for ^{239}Pu

Four sets of data, the most accurate published to date, have been compared : the measurements of BRC [5,8], of BOLDEMAN et al. [9], of NURPEISOV et al. [6] and of GWIN et al. [2]. The data below 1.5 MeV incident neutron energy are compared in fig. III-4. An overall good agreement is observed, with however the data of GWIN et al. higher by about 0.5% than others, such as in the case of ^{235}U.

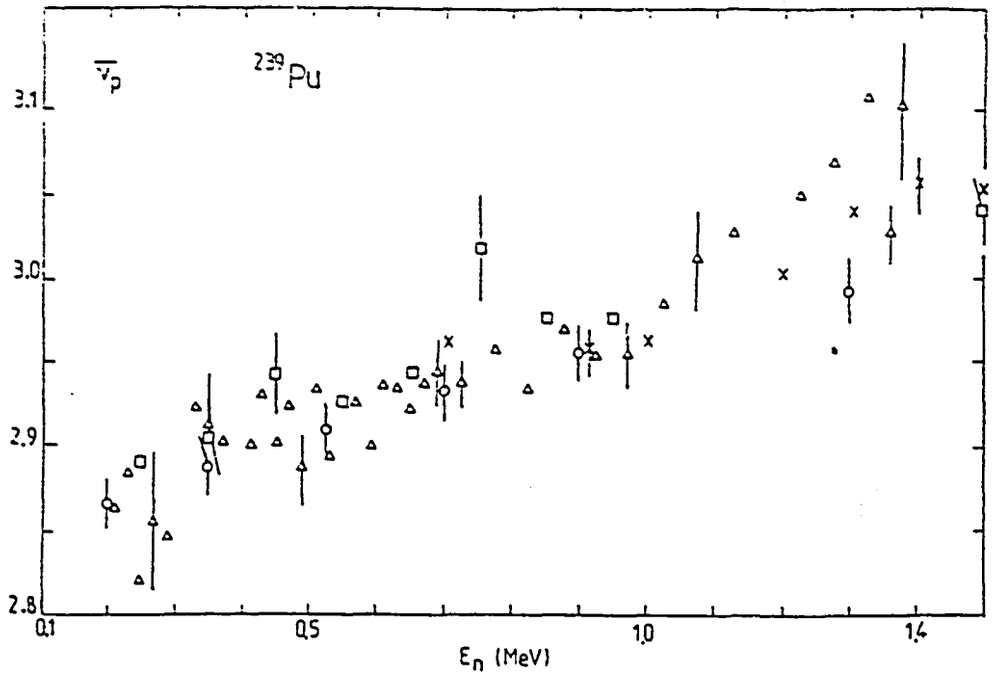

FIGURE III-4

$\bar{\nu}_p$ for ^{239}Pu for E_n < 1.5 MeV

Δ : Ref. [8] □ : Ref. [2] 0 : Ref. [9] X : Ref. [6]

The data for E_n > 1.5 MeV are compared in Fig. III-5. The data of NURPEISOV et al. [6] are about 1% higher than the BRC data [5]. In this energy range the data of GWIN et al. are not accurate enough to permit a fine comparison with other data.

III-4- $\bar{\nu}_p$ for ^{237}Np

The three published measurements of BRC [3], VEESER [10] and VOROBEVA et al. [11] are compared in Fig. III-6. The BRC data are about 3% lower than those of VEESER and about 2% lower than those of VOROBEVA et al. It should be noted however that ^{235}U and ^{237}Np were measured simultaneously in a single experiment at BRC. Since the BRC ^{235}U data, as discussed previously, are consistent with the other published data for this nucleus, we suspect the two other sets to be in error. This point will be discussed later on.

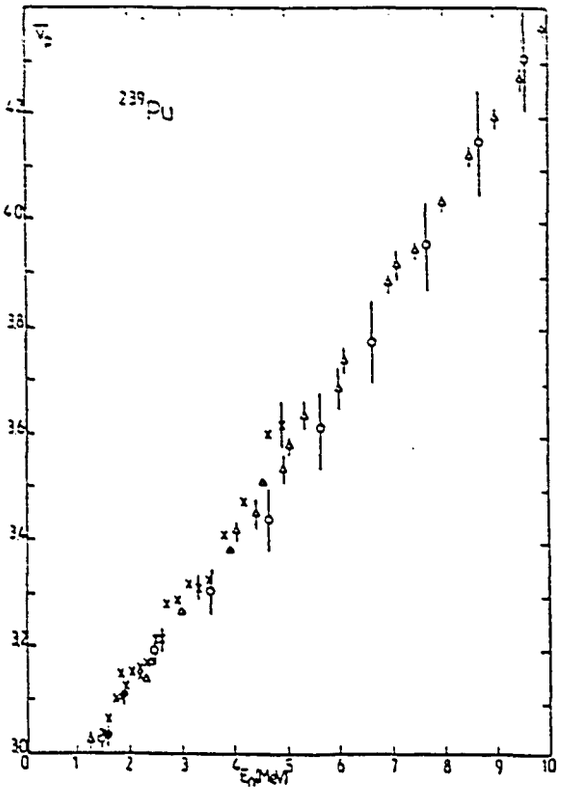

FIGURE III-5

$\bar{\nu}_p$ for ^{239}Pu for E_n > 1.5 MeV.

Δ : Ref. [5] X : Ref. [6]

O : Ref. [2] ● : Ref. [9]

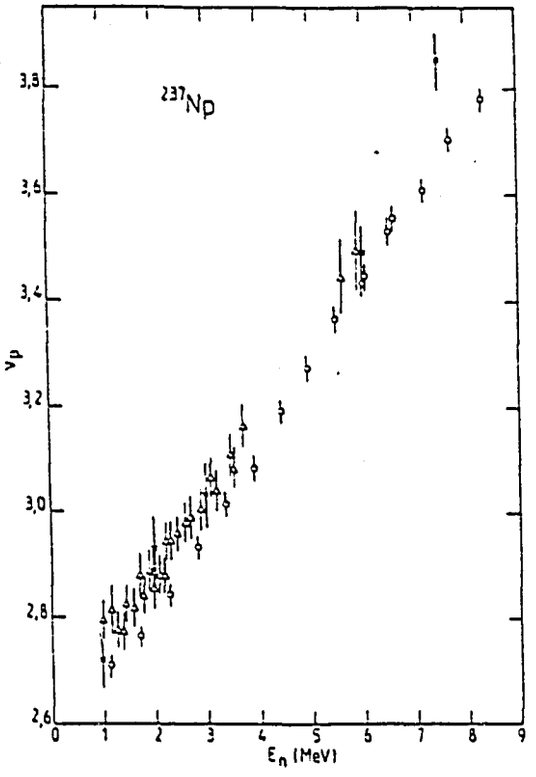

FIGURE III-6

$\bar{\nu}_p$ for ^{237}Np

O : Ref. [3] X : Ref. [10]

Δ : Ref. [11]

III-5- $\bar{\nu}_p$ for ^{232}Th

Three measurements have been made for ^{232}Th, by BRC [3,17], by VOROBEVA et al. [12] and by HOWE et al. [13]. The accuracy of this latter measurement is quite poor, but the data agree on the average with the BRC measurements.

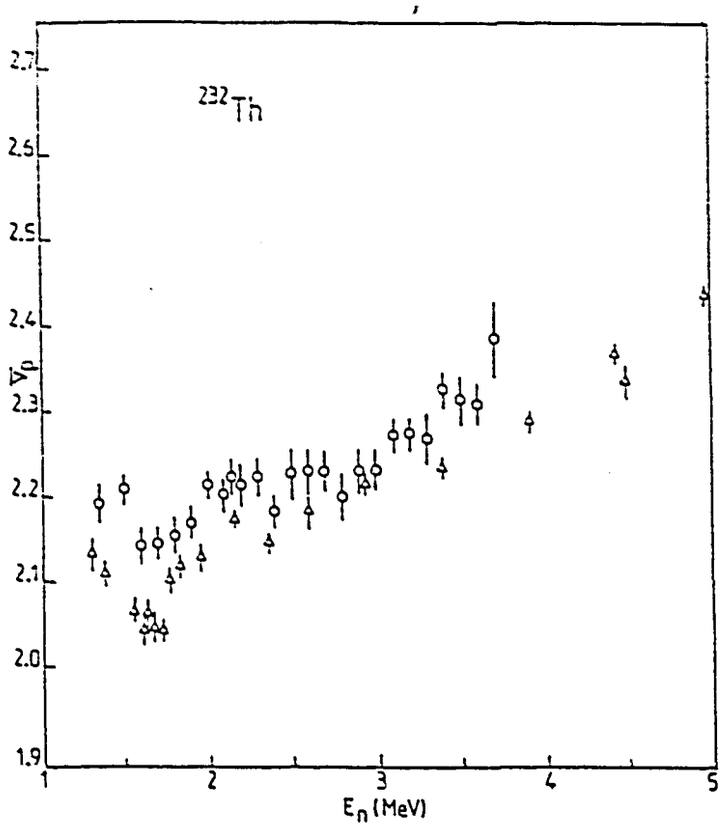

FIGURE III-7

$\bar{\nu}_p$ for ^{232}Th

Δ : Ref. [3] and [17]

o : Réf. [12].

Fig. III-7 compares the data of VOROBEVA et al. and those of BRC. Russian data are higher by about 4% than the BRC data below 2 MeV incident neutron energy. At higher energies the difference is about 2%.

III-6-Other isotopes

Besides ^{238}U and ^{239}Pu, NURPEISOV et al. [6] have also investigated ^{233}U in the energy range from thermal to 5 MeV. A measurement on ^{236}U between 0.8 and 6 MeV has also been performed by MALINOVSKY et al. [18].

For the first time the isotopes ^{242m}Am and ^{245}Cm have been investigated at LIVERMORE in the energy range below 14 MeV [19]. Although the statistical accuracy is quite poor, the data for ^{245}Cm show clearly that the slope $d\bar{\nu}_p/dE_n$ is significantly smaller than estimated from systematic trends.

^{243}Am has been investigated very recently in our laboratory between 6 and 15 MeV with a statistical accuracy of ~ 1%. The preliminary data, unpublished, are well represented by a straight line of equation :

$$\bar{\nu}_p = 0.139\ E_n + 3.28$$

III-7-Discussion and comments

The data which have been compared in the previous sections have been obtained using essentially two experimental techniques :

- ^{3}He counters embedded in a polyethylen block used as a neutron moderator. This technique was used by the two russian groups.

- Large Gd-loaded liquid scintillator ; this technique was used by the other groups.

With the exception of ^{237}Np, the results obtained with the liquid scintillator technique are particularly coherent since the observed systematic differences are of the order of 0.5%. This kind of detector has a large neutron efficiency (~ 80%), is quite isotropic, its main characteristics have been carefully studied ; accurate Monte Carlo simulations of its operation have been made for the absolute $\bar{\nu}_p$ measurements on ^{252}Cf. Therefore the corrections to be applied are quite small and can be determined accurately.

On the contrary, the ^{3}He counter detector technique has not been investigated as carefully. Furthermore, its neutron detection efficiency is of the order of 30%, and this efficiency is more sensitive to the detected neutron energy spectrum than in the case of the liquid scintillator. Also, this detector is less isotropic, and therefore more sensitive to the angular distribution of the neutrons to be detected ; the variation of the detector efficiency as a function of the source position along the detector axis is quite large. The correlation between these two latter effects has not been considered in corrections, but should not be negligible when long fission chambers are used [6,11].

NURPEISOV et al. [6] have improved significantly the angular response of their detector. The systematic difference of about 1% existing between their data and the results obtained using the scintillator technique can be considered as reasonable taking into account the present state of the techniques.

An incorrect estimation of the correction for the fragment emission anisotropy could explain the large difference observed in the case of ^{232}Th around the fission threshold between the data of BRC and those of VOROBEVA et al. (Fig. III-7). In this case, the fission fragments are emitted

preferentially at large angles relative to the direction of incident neutrons inducing fission. Since the angular distribution of the fission neutrons is correlated to the fragment direction, these neutrons are detected with a better efficiency than in the case of an isotropic emission. The correction is quite negligible in the case of the liquid scintillator, but not for the ^{3}He counter detector.

An opposite effect can be predicted in the threshold region for ^{238}U. In fact, russian data appear to be quite low in that region (Fig. III-3).

The identification of the fission events is quite different for the two types of detectors.

For the liquid scintillator technique, the identification results from a coincidence between the detection signal of a fission fragment in a fission chamber placed at the center of the detector and the scintillator signal corresponding to the detection of the prompt fission γ-rays. This procedure vitually eliminates the alpha piling-up problem for active materials such as ^{239}Pu or ^{237}Np and allows using relatively low thresholds on the fission chambers. Typically, 80% of the fission fragments are detected in our chambers.

The ^{3}He counters are quite insensitive to γ-rays, and thus alpha piling-up rejection is obtained by using relatively high thresholds on the fission chambers : only 55% of the fragments were detected above threshold for ^{237}Np in the measurement of VOROBEVA et al. [11].

The correlation between the fission threshold and the neutron detection efficiency has been investigated by BOLDEMAN et al. [14] and by GWIN et al. [2] in the case of the scintillator technique. The efficiency remained almost constant, even when 80% of the fission events were lost. This is because they used fast fission chambers specially designed to obtain a good discrimination between fragment and alpha pulses, for which the height of the delivered pulses was not correlated to the fission fragment energy. Since we use very similar fission chambers at BRC, we have no correction to apply for this effect. We only correct for the lost of fragments in the deposit thickness using the data from our recent investigation [15].

On the contrary, russian groups do observe a correlation between the neutron dectection efficiency and the fission threshold : the height of the pulses delivered by their chambers remains certainly more or less correlated to the fragment energy. We have plotted in Fig. III-8 the $\bar{\nu}_p$ corrective factors given in ref. [6] and [11] as a function of the fragment detection efficiency. For comparison we have also plotted data obtained in our laboratory with the liquid scintillator using a ^{252}Cf source placed in front of a solid state detector. The curve from NURPEISOV et al. is similar to the one we measured, which tends to confirm a linear response for their fission chamber.

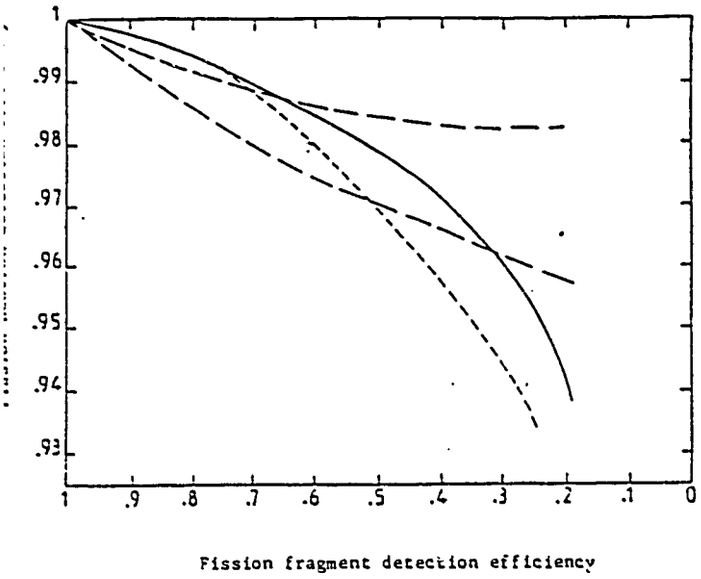

FIGURE III-8

Fission neutron detection efficiency (relative scale) as a function of fission fragment detection efficiency

——— BRC measurement

– – – – – NURPEISOV et al. [6]

- - - - - VOROBEVA et al. [11]

- upper curve : deposit on grounded electrode
- lower curve : deposit on biased electrode.

VOROBEVA et al. [11] find a more important effet. But surprisingly and difficult to understand, the observed effect is different according to whether the fissile deposit is on the grounded or the biased electrode. Moreover, these authors do not use their curves, but only the point they measured for 55% efficiency with their N_p fission chamber, to deduce a correction of 3.7% for their data, which is larger by about 0.8% than the correction deduced from the curve for biased electrodes. And still, although this information is not given explicitely in the paper, it seems that half of the material was deposited on grounded electrodes. On the other hand their curves were obtained from relative data measured between 55% and 80% fission detection efficiency. The shape of the curves and thus the absolute scale are rather arbitrary. Under these conditions the correction could be of the order of 2% for ^{237}Np, in agreement with the curve of NURPEISOV (Fig. III-8), and thus their data would be in agreement with the BRC measurement. It should be

mentioned also that this fission threshold effect on neutron efficiency is correlated to the deposit thickness and to the detector anisotropy and thus the 3 corresponding corrections are not independent. This correlation could be at the origin of the difference between the curves of NURPEISOV et al. and BRC on Fig. III-8.

For the measurements on ^{232}Th, the systematic difference of ~ 2% observed above 2 MeV between the data of VOROBEVA et al. [12] and the data of BRC [3] is larger than the 1.1% correction applied for the fragment detection efficiency by VOROBEVA et al. (to be compared with a correction of 0.2% for ^{238}U [7]). However their publication is not documented enough to draw any valuable conclusion.

We brought attention in 1972 [16] on background problems connected with induced fission measurements. Briefly, the neutron detector background rate and the induced fission rate are proportionnal to be incident neutron flux. Thus, for the background to be measured correctly, the corresponding counting gates must be opened either systematically after each fission event, or randomly by using as a trigger pulses from a neutron detector placed in the incident beam. If the counting gates were opened using an external generator as a trigger - i.e. without reference to the incident neutron flux - any fluctuation in the incident beam intensity would necessarily result in an underestimation of the real background rate, and subsequantly to an overestimation of $\bar{\nu}_p$. Such an effet has been also clearly seen by GWIN et al. [2] for measurements on ORELA, where deviations as large as 3% were observed on $\bar{\nu}_p$. Such an effect is certainly at the origin of the high values of $\bar{\nu}_p$ obtained by VEESER [10] for ^{237}Np.

In fact, all $\bar{\nu}_p$ measurements where an external generator was used to trigger the background measurement are likely to be overestimated and should not be used in an evaluation.

Incidentally, we questioned in the above mentioned 1972 publication [16] our data published in 1969 [5] and provisional corrected values were given ($\bar{\nu}_p$ was increased by 1 to 3% for incident neutron energies below 8 MeV) for ^{235}U, ^{238}U and ^{239}Pu. Such a correction was not confirmed by subsequent control measurements, and thus the data of ref. [5] are always valid.

However use was made of our provisional corrected values in the compilation of KONSHIN and MANERO [1] which is often used as a reference. Therefore this compilation overestimates $\bar{\nu}_p$ below 8 MeV for ^{235}U, ^{238}U and ^{239}Pu.

The foil thickness effect presented in details in ref. [21] might have been underestimated up to now. Fragments emitted at large angles relative to the normal of the deposits are not detected. Since the direction of the fission neutrons is correlated to the direction of the fragments, the measured $\bar{\nu}_p$ value is correlated to the deposit thickness when the neutron detector has not a perfect 4π geometry. This effect has been investigated at BRC [15] for the Gd-loaded liquid scintillator. Corrections of the order of 0.25% have been found for deposits of oxides 1 mg/cm^2 thick. However the amplitude of the correction should depend dramatically of the deposit homogeneity. The presence of grains at the surface, for example, should increase considerably the effet. Thus the quality of the deposit seems to be essential for accurate measurements. The investigation of that effect was originally motivated to explain a discrepancy observed in thermal $\bar{\nu}_p$ measurements by GWIN [2] and by BOLDEMAN [14]. While their ^{239}Pu data are in agreement, their ^{235}U data differ by 0.8%. The deposit thickness was of 0.1 mg/cm^2 for both the ^{239}Pu measurements and for the ^{235}U measurement of GWIN, but of 0.8 mg/cm^2 for the ^{235}U measurement of BOLDEMAN. Only one third of the difference was attributed to the deposit thickness effect [15], but the influence of the possible inhomogeneities remains an open question.

In all $\bar{\nu}_p$ measurements a correction must be applied to account for the difference between the fission neutron energy spectrum of the investigated isotope and that of ^{252}Cf. The energy dependence of the neutron detector efficiency is generally well established, but the fission neutron energy spectrum is rather uncertain. Most of the measurements rely on the TERRELL law [22] which correlates the average maxwellian spectrum energy with $\bar{\nu}_p$. This relation is certainly not valid above the second chance fission threshold. A better approach would be now to use the formalism developed by MADLAND and NIX [23].

III-8- REFERENCES

[1] - F. MANERO, V.A. KONSHIN
At. Energy Rev. 10 (1972) 637.

[2] - R. GWIN, R.R. SPENCER, R.W. INGLE, J.H. TODD
- Report ORNL/TM 6346 (May 1978)
- Report ORNL/TM 7148 (January 1980).

[3] - J. FREHAUT, A. BERTIN, R. BOIS
Proc. Conf. on "Nuclear Data for Science and Technology", Antwerp (1982) p. 78.

[4] - J.W. BOLDEMAN, J. FREHAUT, R.L. WALSH
Nucl. Sci. Eng. 63 (1977) 430.

[5] - M. SOLEILHAC, J. FREHAUT, J. GAURIAU
J. Nucl. Energy 33 (1969) 257.

[6] - B. NURPEISOV, K.E. VOLODIN, V.G. NESTEROV, L.I. PROKHOROVA, G.N. SMIRENKIN, Yu. M. TURCHIN
Soviet J. Atomic Energy 39 (807) 1976.

[7] - V.G. VOROBEVA, B.D. KUZMINOV, V.V. MALINOVSKY, V.M. PIKSAYKIN, N.N. SEMENOVA
INDC (CCP) 177/L (1982) p. 43.

[8] - M. SOLEILHAC, J. FREHAUT, J. GAURIAU, G. MOSINSKI
Proc. Conf. on "Nuclear Data for Reactors", Helsinki (1970) Vol. 2 p. 145.

[9] - R.L. WALSH, J.W. BOLDEMAN
Annals of Nucl. Sci. and Eng. Vol. 1 (1974) 353.

[10] - L. VEESER
Phys. Rev. C17 (1978) 385.

[11] - V.G. VOROBEVA, B.D. KUZMINOV, V.V. MALINOVSKY, N.N. SEMENOVA
- Yad. Konstanty 3, 38 (1980) 44 (in russian).
- INDC (CCP) 177/L (1982) 39.
- Soviet J. Atomic Energy 54 (1983) 226.

[12] - V.V. MALINOVSKY, V.G. VOROBEVA, B.D. KUZMINOV, V.N. PIKSAYKIN, N.N. SEMENOVA, V.S. VALYAVKIN, S.M. SOLOVIEV
Soviet J. Atomic Energy 54 (1983) 229.

[13] - R.E. HOWE
Nucl. Sci. Eng. 86 (1984) 157.

[14] - J.W. BOLDEMAN, A.W. DALTON
AAEC/E 172, March 1967.

[15] - J.W. BOLDEMAN, J. FREHAUT
Nucl. Sci. Eng. 76 (1980) 49.

[16] - J. FREHAUT, G. MOSINSKI, M. SOLEILHAC
EANDC (E) 154 U (1973) 67.

[17] - J. TROCHON, J. FREHAUT, Y. PRANAL, G. SIMON, J. W. BOLDEMAN
Proc. Conf. on "Nuclear Data for Science and Technology", Antwerp (1982), p. 733.

[18] - V.V. MALINOVSKY, V.G. VOROBEVA, B.D. KUZMINOV, V.M. PIKSAJKIN, N.N. SOMENOVA
INDC/P (81) - 47.

[19] - R.E. HOWE, R.M. WHITE, J.C. BROWNE, J.H. LANDRUM, R.J. DOUGHAN, R.W. LOUGHEED, R.J. DUPZYK
Nucl. Phys. A407 (1983) 193.

[20] - R.R. SPENCER, R. GWIN, R. INGLE,
Nucl. Sci. Eng. 80 (1982) 603.

[21] - J.R. SMITH
"Status on the quest for $^{252}Cf\ \bar{\nu}$"
Report EPRI NP-1258, dec. 1979.

[22] - J. TERRELL,
Phys. Rev. 127 (1962) 880.

[23] - D.G. MADLAND, J.R. NIX,
Nucl. Sci. Eng. 81 (1982) 213.

IV - DELAYED NEUTRONS FROM FISSION.

The whole field of delayed neutron properties has been covered in an IAEA consultants' meeting held in Vienna in 1979 [1]. Few new results have been published since that date. The delayed neutron yields from fission of ^{233}U, ^{237}Np, ^{238}Pu, ^{240}Pu, ^{241}Pu and ^{241}Am have been measured using a fast reactor incident neutron spectrum [2]. Using available nuclear data and fission yields of the individual precursors, RUDSTAM [3] has derived the energy spectra for the six delayed neutron groups and for the most common Th, U, Np and Pu isotopes and for ^{252}Cf.

The delayed neutron spectrum of ^{235}U and ^{239}Pu, integrated for the whole collection of precursors, has been measured at different incident neutron energies from 0.5 to 7.5 MeV [4]. A particular attention has been paid to error derivation [5]. The systematic generation of covariance matrices is a major improvement in determining our best knowledge of delayed neutron spectra using data from different laboratories.

At the University of Lowell (USA), the delayed neutron spectra following thermal neutron induced fission of ^{235}U have been measured over eight successive delay time intervals ranging from 0.17 to 85 seconds. Fission fragments were transferred to a low background environment using a helium jet fast transfert system. The time-of-flight technique with ^{6}Li and plastic scintillators was used to measure the delayed neutron energies over the range 10 keV-2 MeV. Delayed events were identified by β counting.

Details are given in ref. [6] and [7]. A typical energy spectrum [8] in shown in fig.IV-1.

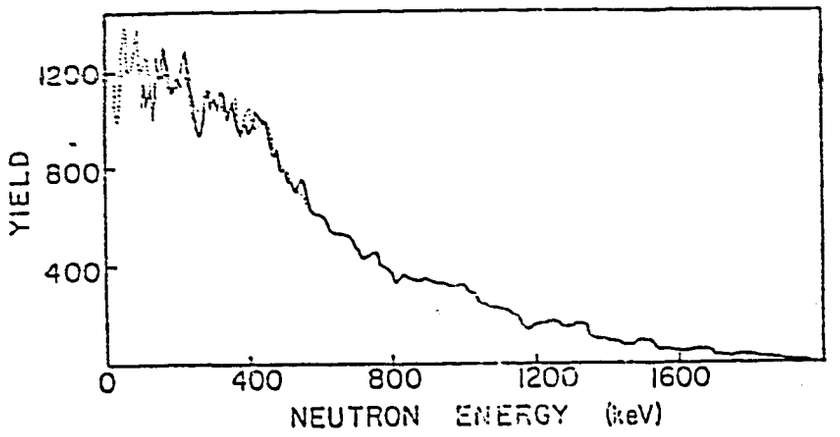

Fig.IV-1 - A delayed neutron energy spectrum from the fission of ^{235}U in the delay-time interval 2.1 to 3.9s. The solid curve is derived from a TOF measurement with Pilot U scintillators at a 50 cm flight path. The dotted curve is from a TOF measurement with ^{6}Li-glass scintillators at a 15 cm flight path. Taken from Ref. [8].

REFERENCES

[1] - Proceedings of the Consultants' Meeting on Delayed Neutron Properties, Vienna, 26-30 March 1979, INDC(NDS)-107/G + special.

[2] - G. BENEDETTI, A. CESANA, V. SANGIUST, M. TERRANI, Nucl. Sci. Eng. 80 (1982) 379.

[3] - G. RUDSTAM, Nucl. Sci. Eng. 80 (1982) 238.

[4] - J. WALKER, D.R. WEAVER, J.G. OWEN, IEEE Transactions on Nuclear Science Vol. NS-28, April 1981, p.1650, and Proc. Int. Conf. on Nucl. Data for Sci. and Technol., Antwerp (1982) 265.

[5] - D.R. WEAVER, J.G.OWEN, J. WALKER, Contribution to A specialists' Meeting on Fission product Yields and Decay Data Sponsored by DOE and NEA, Brookhaven, USA, October 1983.

[6] - G.P. COUCHELL, W.A. SCHIER, D.J. PULLEN, M.N. HAGHIGHI, N.M. SAMPAS, Q. SHARFUDDIN, R.S. TANCZYN, to be published in Proc. Int. Symp. on the Use and Development of low and Medium Flux Research Reactors, MIT, Cambridge, MA, USA, Oct. 1983.

[7] - G.P. COUCHELL et al., in INDC (USA) 91/L (1983).

[8] - G.P. COUCHELL et al., to appear in 1984 Report to the DOE Nuclear Data Comittee.

V - PROMPT FISSION NEUTRON SPECTRUM

The neutron energy spectrum of ^{252}Cf spontaneous fission which is recommended as a standard has now been measured in the energy range from 1 keV to 28 MeV. The subject has been discussed in a recent IAEA consultants' Meeting [1].

Recent investigations, including differential and integral data as well as theoretical approaches, appear to be in fairly good agreement and a new evaluation has been strongly recommended.

For the fast neutron induced fission, recent data are very scarce. Accurate experiments are quite difficult to perform. Generally, a massive sample is placed next to a pulsed monoenergetic neutron source, and fission neutrons are detected using a suitably shielded detector placed at a certain distance in order to use the time-of-flight technique. The quality of the measurement rely heavily on an accurate determination of the energy dependence of the neutron detector efficiency and on the energy calibration.

The discrimination against γ-rays, multiple scattering in the sample, background determination and counting statistics are also important parameters.

Johansson and Holmqvist have made measurements on ^{235}U and ^{239}Pu at 0.53 MeV incident neutron energy [2,3]. Their measurement on ^{235}U [2] represents one of the best investigations to date. Smith et al. [4] adopted a somewhat different approach. They measured the prompt fission neutron spectra of ^{233}U, ^{235}U, ^{239}Pu and ^{240}Pu relative to that of ^{252}Cf. Within uncertainties the measured spectra were Maxwellian. Therefore the logarithms of the spectral ratios were simply linear functions of energy with slopes corresponding to incremental average energies, relative to ^{252}Cf.

Elastic and inelastic scattering on the sample limits the present technique to the part of the energy spectrum higher than the incident

neutron energy. This is the main reason why most of the measurements have been limited to incident energies below 1 MeV. However the high energy part of the 14.5 MeV neutron induced fission of ^{238}U has been recently investigated by the DRESDEN Group [5]. An excess of neutrons, relative to evaporation model calculations, is found above 20 MeV. The same behaviour is also observed for the ^{252}Cf spontaneous fission [6]. These results for ^{238}U and ^{252}Cf are shown in fig.V-1.

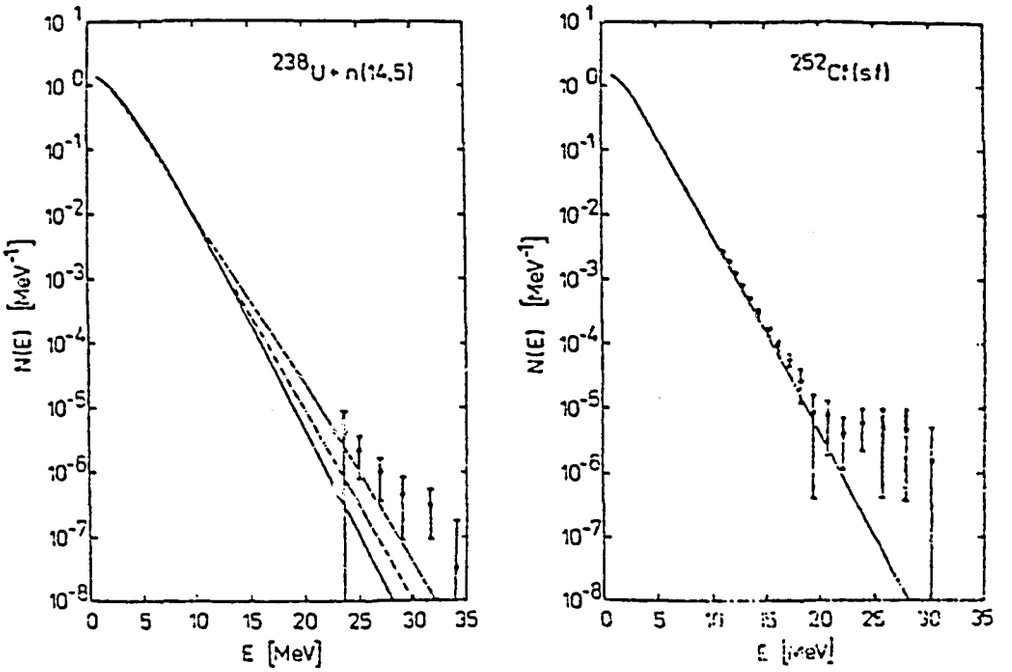

Fig.V.1 - Fission neutron spectrum from 14.5 MeV neutron induced fission of ^{238}U and spontaneous fission of ^{252}Cf. The dashed-dotted line for ^{238}U and the solid line for ^{252}Cf are evaporation model calculations. The solid and the dashed lines for ^{238}U are respectively the Watt and Maxwell distributions fitting the measured data in the MeV range. Taken from [5].

A method combining the use of a fission chamber in addition to an incident pulsed neutron beam has been investigated several years ago in our laboratory [7]. Neutron elastic and inelastic scattering as well as spurious events can be virtually eliminated. The neutron spectra in the energy range from 0.4 to 12 MeV have been obtained for the fission of ^{235}U induced by 0.6 and 7 MeV neutrons and the fission of ^{238}U induced by 7 MeV neutrons [7]. However the statistical accuracy was severely affected by the limited quantity of material available in the fission chamber. Distorsion of the

spectrum due to interaction of the neutrons with the fission chamber frame was also a major concern. As a result, the accuracy was not sufficient enough to show clearly a dependence of the spectrum on excitation energy.

In that domain, theoretical calculations appear to be more reliable. Calculations based on nuclear evaporation theory [6,8] are now reproducing fairly well the existing data. In particular, the formulation developed by MADLAND and NIX [8] requires a limited number of parameters and has already been extended for the multiple chance fission. It is presently the best available tool to derive fission neutron spectra in regions and for nuclei where no experimental data exist.

REFERENCES

[1] - Proc. of IAEA Consultants' Meeting on the ^{252}Cf Fission Neutron Spectrum, Smolenice, 1983, INDC(NDS)-146/L.

[2] - P.I. JOHANSSON, B. HOLMQVIST Nucl. Sci. Eng., 62 (1977) 695.

[3] - P.I. JOHANSSON, B. HOLMQVIST, T. WIELDING, L. JEKY, Proc. Conf. on Nuclear Cross Sections and Technology, Washington, March 1975, Vol.II, p.572, N.B.S. Special Publication 425 (1975).

[4] - A. SMITH, P. GUENTHER, G. WINKLER, R. Mc KNIGHT, Nucl. Sci. Eng. 76 (1980) 357.

[5] - M. MÄRTEN, D. SEELIGER, B. STOBINSKI, Proc. of the Europhysics Topical Conference, Smolenice, June 1982, Neutron Induced Reactions, Physics and Applications, Vol.10, p.287 (1982).

[6] - M. MÄRTEN, D. SEELIGER, Nucl. Phys. 10 (1984) 349.

[7] - A. BERTIN, R. BOIS, J. FREHAUT, Report CEA-R-4913 (1978).

[8] - D.G. MADLAND, J.R. NIX, Nucl. Sci. Eng. 81 (1982) 213.

VI - PROMPT γ-RAYS FROM FISSION

The average prompt γ-ray total energy $\bar{E}_\gamma$ has been measured as a function of excitation energy for the neutron induced fission of ^{235}U, ^{237}Np and ^{232}Th [1]. Results for ^{235}U are given in fig.VI-1. Below the second chance fission threshold $\bar{E}_\gamma$ is a linear function of $\bar{\nu}_p$ with for ^{235}U :

$$\bar{E}_\gamma = 0{,}98\ \bar{\nu}_p + 4.37 \quad \text{(MeV)}$$

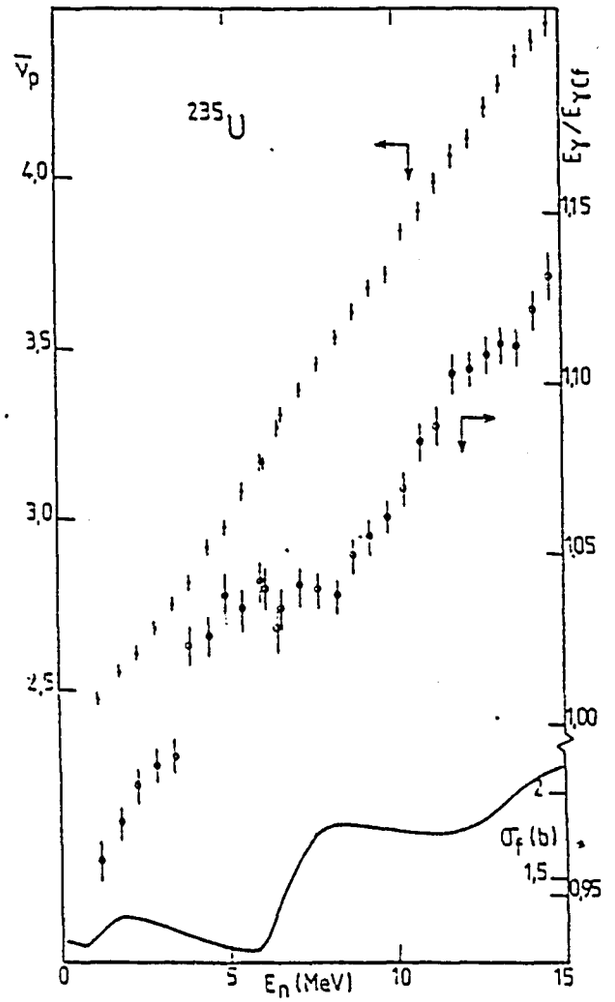

Fig.VI-1

$\bar{\nu}_p$, $\bar{E}_\gamma$ and σ_F as a function of incident neutron energy for the neutron induced fission of ^{235}U. Data taken from [1].

The constant term corresponds to statistical model predictions, whereas the linear relation between $\bar{E}_\gamma$ and $\bar{\nu}_p$ can be interpreted in terms of competition between γ-ray and neutron emission during the desexcitation process of the fission fragments [1].

The plateau in the region where the second chance fission is taking place results from the energy removed from the fissioning system by the neutron evaporated before fission.

These data contain information on the shape of the first chance fission cross section above the second chance fission threshold. Using the definitions given in Table I and assuming that the linear relation $\bar{E}_{\gamma 1} = a\,\bar{\nu}_1 + b$ also holds for second chance fission ($\bar{E}_{\gamma 2} = a\,\bar{\nu}_2 + b$), the proportion α of second chance fission can be deduced straightforwardly from experimental data :

$$\alpha = \bar{\nu}_m - \frac{\bar{E}_{\gamma m} - b}{a}$$

TABLE I - Neutrons and γ-rays from multiple chance fission.

Fission fraction	Proportion	Pre-fission neutrons	fission neutrons	observed neutrons	Fission γ-ray energy
First chance	$1-\alpha$	0	$\bar{\nu}_1$	$(\bar{\nu}_1)$	$\bar{E}_{\gamma 1}$
Second chance	α	1	$\bar{\nu}_2$	$(1+\bar{\nu}_2)$	$\bar{E}_{\gamma 2}$
Total	1	α	$(1-\alpha)\,\bar{\nu}_1+\alpha\bar{\nu}_2$	$\bar{\nu}_m=(1-\alpha)\bar{\nu}_1 + \alpha(1+\bar{\nu}_2)$	$\bar{E}_{\gamma m} = (1-\alpha)\bar{E}_{\gamma 1}+ \alpha\,\bar{E}_{\gamma 2}$

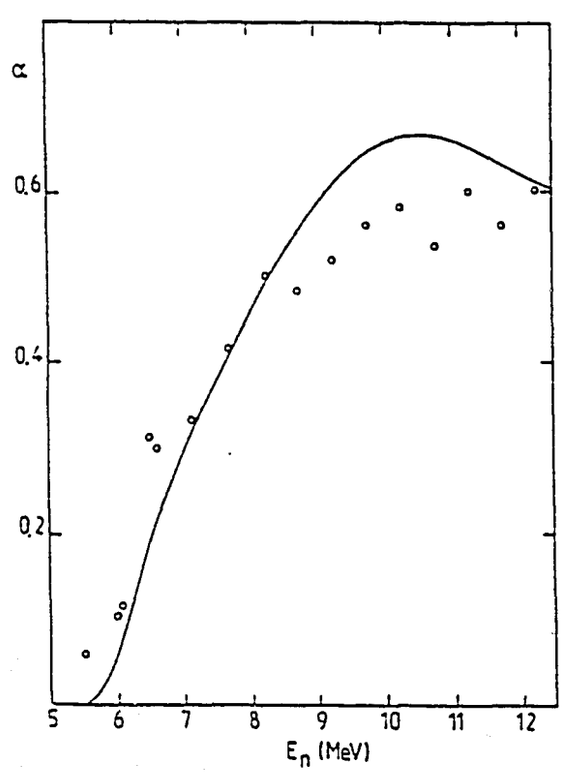

Fig.VI-2

Proportion α of second chance fission as a function of incident neutron energy for ^{235}U.
Curve : calculation [2].
+ : derived from $\bar{\nu}_p$ and $\bar{E}_\gamma$ experimental data from [1].

To what extend such a simple derivation is valid is shown in fig.VI-2 where the values derived for ^{235}U [1] are compared to calculations by MADLAND and NIX [2].

REFERENCES

[1] - J. FREHAUT, A. BERTIN, R. BOIS, Proc. Conf. on Nuclear Data for Science and Technology, Antwerp, Sept. 1982, p.78.

[2] - D.G. MADLAND, J.R. NIX, Nucl. Sci. Eng. 81 (1982) 213.

VII - (n,xn) CROSS SECTIONS

Two independent techniques are available for (n,xn) cross section measurements. The activation technique is based on the determination of the activity produced in a sample bombarded by neutrons. It is therefore limited to nuclides which leave a suitably active residual isotope, originally absent in the sample. In the case of actinides, measurements are complicated by the activity of fission fragments. A good knowledge of decay schemes and branching ratios is also necessary. Up to now, this method has been only used for (n,2n) cross section measurements on ^{232}Th, ^{237}Np and ^{238}U.

The alternative method is based on the direct detection of the emitted neutrons using the large Gd-loaded liquid scintillator technique [1]. A precise knowledge of the fission neutron multiplicity distributions is then necessary in order to discriminate between (n,xn) reactions and fissions where x neutrons have been emitted. The (n,xn) cross sections are obtained directly relative to the fission cross section. Although the method is applicable in principle to a large variety of nuclides in the actinide region, it has only been used for ^{235}U and ^{238}U up to now [2,3,4]. Thermal fission, in the case of fissile nuclei, and the background induced in the neutron detector by the natural γ-activity of the samples (10 to 20g in weight) are introducing severe limitations in practice [1].

The (n,2n) cross section for ^{238}U has been recently reviewed by KORNILOV et al. [5]. Unfortunately, use was made of a preliminary set of data from our laboratory [6] in this evaluation. In that set, it was assumed that the detection efficiency was the same for (n,xn) neutrons and neutrons

from the ^{252}Cf spontaneous fission used as a standard. Fully corrected [1] data, together with additional results, have been published elsewhere [4]. These corrected values are about 10 % lower than the preliminary ones. Therefore, our direct measurement is no longer in agreement with the existing activation data below 10 MeV. However our data in the energy range between 13 and 15 MeV are consistent with activation data. Unfortunately, activation data below and above 10 MeV are from different laboratories so that clear conclusion cannot be drawn without further investigations.

(n,3n) and (n,4n) cross sections have also been published in the energy range up to 22 MeV for ^{238}U [2,4].

One set of (n,2n) data in the energy range between threshold and 13 MeV has been published for ^{235}U [3]. (n,3n) and (n,4n) cross sections have been measured between 15 and 21 MeV [2].

The (n,2n) cross section data for ^{232}Th have been reviewed by ANAND et al. [7]. Below 12 MeV, the evaluated cross section is mainly defined by the only existing data set of BUTLER et al.[8]. More recent measurements between threshold and 10.5 MeV [9] are lower below 7.5 MeV and about 7.5 % higher above 8.5 MeV.

The $^{237}Np(n,2n)^{236}Np$ reaction is of great interest because the penetrating γ-rays emitted by the decay products of ^{236}Pu play an important role in the shielding requirements for fuel reprocessing. The ^{236}Pu results from the β decay(48 % branching ratio) of the short lived ^{236s}Np isomer. The long-lived $^{236\ell}Np$ isomer has little practical importance. ^{236s}Np decays also by electron capture (52 %).

The partial (n,2n) cross section for the formation of ^{236s}Np can be obtained by activation measurements of the decay products ^{236}U or ^{236}Pu.

The previously existing data [10-14] have been recently completed by measurements between threshold and 10 MeV [15]. The corresponding data are plotted in fig.VII-1. The curve appearing in fig.VII-1 is an unpublished calculation by J. JARY of the total (n,2n) cross section, based on a formalism desbribed in [16], to which a scaling factor of 0.75 has been applied. The overall good agreement with experimental data gives some confidence in the interpolation between 10 and 13.5 MeV. Furthermore, the

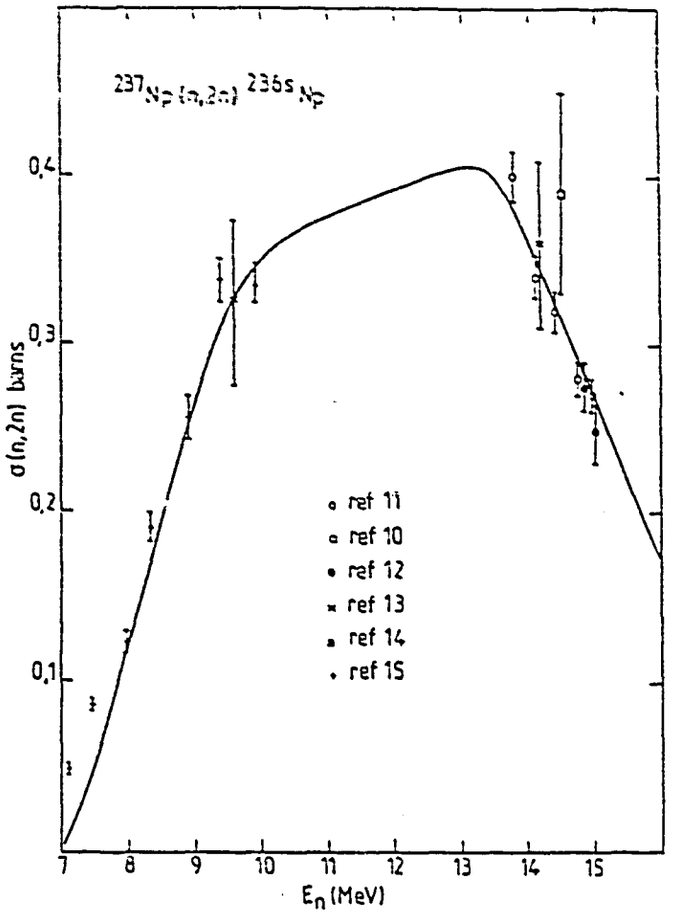

Fig.VII-1 - The ^{237}Np (n,2n) cross section leading to the short-lived ^{236}Np isomer.

applied scaling factor corresponds to assume an energy-independent formation isomeric ratio $^{236\ell}$Np/ ^{236s}Np of 0.33, to be compared with the experimental value of 0.365 at 14 MeV [11].

A measurement on ^{239}Pu using the direct neutron detection method has been reported [17]. However it is likely that the time correlated background pulses due to the spontaneous fission from the ^{240}Pu present in the sample have not been correctly accounted for. Therefore these results are highly questionable. The recent unpublished data around 14 MeV quoted in Ref.[18] are more consistent with the theoretical calculations presented in the same paper.

REFERENCES

[1] - J. FREHAUT, Nucl. Inst. Meth.135 (1976) 511.

[2] - L.R. VEESER, E.D. ARTHUR, Proc. Conf. on Neutron Physics and Nuclear data, Harwell, Sept. 1978, p.1054.

[3] - J. FREHAUT, A. BERTIN, R. BOIS, Nucl. Sci. Eng. 74 (1980) 29.

[4] - J. FREHAUT, A. BERTIN, R. BOIS, J. JARY, Proc. Symp. on Neutron Cross sections from 10-50 MeV, Upton, USA, May 1980, INDC(USA)-84/L, Vol.I, p.399.

[5] - N.V. KORNILOV, V.N. VINOGRADOV, E.B. GAY, N.S. RABOTNOV, O.A. SALNIKOV, P. RAICS, S. DAROCZY, S. NAGY, J. CSIKAI, Proc. Int. Conf. on Nuclear Data for Science and Technology, Antwerpen, Sept. 1982, p.679, and Voprosy Atomnoy Nauky i Techniki, ser. Yadernye Konstanty 45 (1982)33.

[6] - J. FREHAUT, G. MOSINSKI, Proc. Conf. Nuclear Cross Sections and Technology, Washington, March 1975, Conf.750303, Vol.2 p.897.

[7] - R.P. ANAND, M.L. JINGHAN, S.K. GUPTA, M.K. MEHTA, INDC(IND)30 Aug.1981

[8] - J. BUTLER, D. SANTRY, Can. J. Chem.39 (1961) 689.

[9] - P. RAICS, S. DAROCZY, J. CSIKAI, K. ERDEI, N.V. KORNILOV, V. Ya BARYBA, O.A. SALNIKOV, Contribution to the KieV Conf. on Neutron Physics, Oct. 1983 and to be published.

[10] - J.L. PERKIN, R.F. COLEMAN, J. Nucl. Energy 14 (1961) 69.

[11] - J. LANDRUM, R. NAGLE, M. LINDNER, Phys. Rev. C8 (1973) 1938.

[12] - K. LINDEKE, S. SPECHT, H.J. BORN, Phys. Rev. C12 (1975) 1507.

[13] - T. NISHI, I. FUJIWARA, N. IMANISHI, NEANDC(J) 42/L (1975)

[14] - E.A. GROMOVA, S.S. KOVALENKO , Yu. A. NEMILOV, Atomnaya Energiya 54 (1983) 108.

[15] - N.V. KORNILOV, V. Ya. BARYBA, A.V. BALITSKY, A.P. RUDENKO, B.D. KUZMINOV, O.A. SALNIKOV, E.A. GROMOVA, S.S. KOVALENKO, Yu. A. NEMILOV, L.D. PREOBRASHENSKAYA, A.V. STEPANOV, Yu. A. SELITZKI, B.I. TARLER, V.B. FUNSTEIN, S. DAROCZY, P. RAICS, J. CSIKAI, to be published in Atomnaya Energiya.

[16] - J. JARY, Report CEA-R-4647 (1975).
J. JARY, Ch. LAGRANGE, P. THOMET, INDC(FR) 9/L (1977).

[17] - D.S. MATHER, P.F. BAMPTON, R.E. COLES, G. JAMES, P.J. NIND, Report AWRE 072/72 (1972), EANDC (UK) 142-AL.

[18] - E.D. ARTHUR, Progress report LA-9841-PR, Los Alamos Scientific Laboratory, Aug. 1983, p.15.

VIII - CAPTURE CROSS SECTIONS

Neutron capture is a domain where the present accuracy goals are far from being reached. Techniques available up to now, despite their successive refinements, remain in the region of 5 - 8 % accuracy in the best cases.

The subject under all its aspects was discussed in a recent NEANDC/NEACRP specialists' meeting [1]. At this meeting CORVI et al. [2] presented a new measurement of α, the ratio of capture to fission cross sections, in the unresolved resonance region for ^{235}U. Their data were about 10 % lower than the ORNL data [3] generally considered as the best measurement in that energy range. These new results supported accurate values published by MURADYAN et al. [4], which were about 16 % lower than ORNL data. The 3 sets of data are compared in fig.VIII-1, taken from [2]. The most interesting point is that MURADYAN used a completely new technique, largely uncorrelated to previous one. This technique, described in the review paper of GAYTHER and THOM in [1], is based on the multiplicity measurement of the emitted radiation : With a detection efficiency of nearly 100 %, fission can be clearly separated from capture through its greater radiation multiplicity. The same authors have since measured absolutely alpha in the resonances of ^{235}U with an accuracy of about 2 % [5]. Here again, their data are largely below the values obtained previously with other techniques and cast some doubt on the validity of alpha values for other nuclei, and in particular for ^{239}Pu.

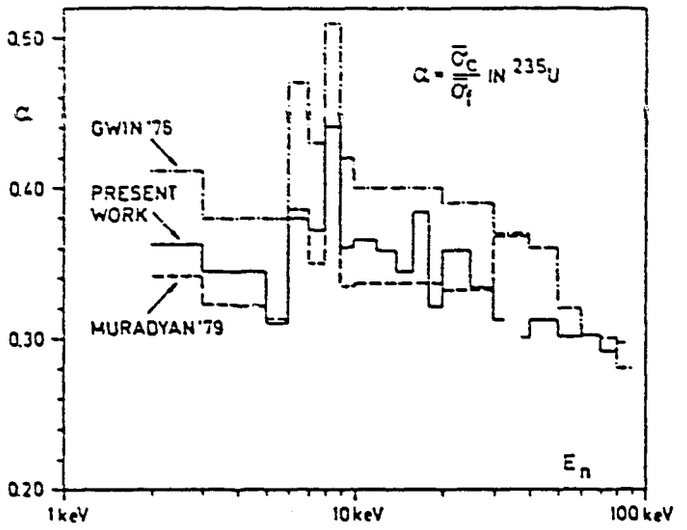

Fig.VIII-1 - Comparison of α-values for different experiments. Taken from Ref. [2].

The multiplicity method constitutes certainly a major breakthrough in the domain of alpha and capture cross section measurements. Present accuracy goals seem now to be within the reach of experiments.

REFERENCES

[1] - Proc. of the NEANDC/NEACRP Specialists' Meeting on the Fast Neutron Capture Cross Sections, Argonne National Laboratory, Apr. 1982, NEANDC(US)-214/L.

[2] - F. CORVI, L. CALABRETTA, M. MERLA, T. VAN DER VEEN, M.S. MOORE, p.347 in Ref.[1].

[3] - R. GWIN, E.G. SILVER, R.W. INGLE, H. WEAVER, Nucl. Sci. Eng.59 (1976)79.

[4] - G.V. MURADYAN, Ya G. SHCHEPKIN, Yu. V. ADAMCHUK, M.A. VOSKANYAN, Proc. Int. Conf. on Nuclear Cross Sections for Technology, Knoxville, 1979, NBS SP 594, p.488.

[5] - Yu. V. ADAMCHUK, M.A. VOSKANYAN, G.V. MURADYAN, P. Yu. SIMONOV, Yu. G. SHCHEPKIN, Proc. Conf. on Nuclear Data for Science and Technology, Antwerp, Sept. 1982, p.730.

IX - NEUTRON TOTAL AND SCATTERING CROSS SECTIONS.

Inelastic scattering on actinide nuclei plays an important role in the fast neutron moderation process in reactors. Accurate cross sections are needed, particularly for ^{238}U. The direct detection of scattered neutrons provides the best source of data, but the use of high-resolution semiconductor photon detectors has allowed the extension of inelastic scattering studies to more closely spaced levels.

The whole domain of fast neutron total and scattering cross sections has been reviewed carefully in a recent NEANDC specialists' meeting [1]. Most of the scattering measurements have been carried out using the time-of-flight technique to study the ground state rotational band. Neutron scattering from higher energy levels has been also studied by the Lowell group. This latter domain has been more commonly investigated with semiconductor photon detectors.

The general trend is to achieve the best possible neutron energy resolution in order to improve the basic physics knowledge. Data for well resolved levels are very important to settle optical model parameters and nuclear deformations.

But for applied purposes, needs are rather for total inelastic scattering cross sections with broad energy resolution, in the domain of excitation energy of 0.5 - 2 MeV. In this energy range, inelastic scattering appears as a continuum surimposed on the fission spectrum in the time-of-flight spectra. Extraction of accurate cross sections appears as an experimental challenge.

[1] - Proc. of a Specialists' Meeting on Fast Neutron Scattering on Actinide Nuclei, OECD, PARIS, Nov. 1981, NEANDC-158"U".

X - CONCLUSION

Most of the experimental techniques presently available in the domain of neutron data measurements have been developed some thirty years ago. Although these techniques have largely evolved in connexion with the tremendous development of electronics and computers, the basic assumptions on

which they rely remained almost the same without questioning. In many cases, these techniques have already given the maximum of their possibilities, and adding up a new measurement is of minor interest, as pointed out in the proceedings of the most recent specialists' meetings.

Nowadays, two main different approaches to achieve more accurate data can be identified. The first one is the development of entirely new techniques in domains where the existing ones are far from reaching the requested accuracies . Perhaps the best example is given by capture cross section measurements based on the radiation multiplicity determination. But even the most accurate data need also to be confirmed by alternative techniques, in order to become sure that the measurements are free from possible systematic errors previously unsuspected. Requests for new techniques to measure absolutely the fission cross section of ^{235}U around 14 MeV is a good illustration of such a concern.

The second approach to increase accuracy is in a thorough investigation of the basic experimental grounds for well established techniques. The ultimate goal is to remove all of the basic assumptions and rough estimates and to replace them by precise measurements of the involved effects. This is a long and exacting task, but important improvements are certainly possible. The experimental study of fission fragment absorption in deposits, for example, is of major importance in improving fission cross section measurements.

Beyond the experimental aspects, the domain of data handling and processing has not held so much the attention of experimentators. The common feeling is that this domain is rather within the competence of evaluators, particularly when covariances are concerned. But this is not true.

In many cases, there is really no difference between data reduction and evaluation, and therefore the appropriate techniques, including covariance matrices and Bayesian procedures, should be used. The threshold cross section method is a typical example. Without these modern evaluation techniques, all experimental progress is illusive.

PROGRESS IN THEORETICAL CALCULATION OF TRANSACTINIUM ISOTOPE NUCLEAR DATA

J.R. SALVY
Centre d'études de Bruyères-le-Châtel,
Commissariat à l'énergie atomique,
Bruyères-le-Châtel, France

Abstract

This paper reviews recent developments in the theoretical calculational methods used in the evaluation of actinide nuclear data in the incident neutron energy range from 10 keV to 20 MeV.

1 - INTRODUCTION

Over the past decade and more precisely since the review by LYNN at the first Advisory Group Meeting (AGM) on Transactinium Nuclear Data in Karlsruhe [1,2], considerable progress has been made in effective use of nuclear theory for evaluation purposes. This was reported on in a number of courses held for example at TRIESTE [3-5] and many meetings, symposia and conferences (an incomplete list is given in refs [6] to [18]). Particularly for the actinide region, and especially for an extended number of secondary actinides, such efforts have been urged partially because of the alarmingly poor condition of the cross sections needed for reactor programs. Needs for new or more accurate data have been confirmed at the second AGM in Cadarache only five years ago [19].

During the past few years a number of basic improvements, including some results from microscopic calculations, have developed in nuclear models commonly used for data evaluation, i.e. essentially spherical and deformed optical models, Hauser-Feshbach-statistical and preequilibrium models, and direct reaction models. Nevertheless up to now only a few of these have been effectively introduced into data evaluation programs. Some of these recent developments have been discussed, without consideration of fission, in extensive reviews on applications of nuclear models, for example by ARTHUR [20] above 3 MeV, GARDNER [21] above 10 MeV, and more recently at the Antwerp Conference by YOUNG [22] in the extended energy range 0.1 to 50 MeV. Actinide data evaluation can also utilize such improvements, but in the actinide region a further complication arises from the presence of fission competition. Generally nuclear codes which account for this require adjustments of calculated fission cross sections to fit experimental data, if any exists.

Partly due to adjustments to explain accumulated experimental values using a conveniently chosen theoretical framework and partly from other studies contributing more or less directly to an improved knowledge of the fundamental fission process, we now have available systematic prescriptions for calculating and even predicting neutron cross sections within an extended actinide region. In the recent past such detailed prescriptions have been suggested by LYNN (see for example refs [23, 24], and the review paper with BJORNHOLM [25]. These works explain clearly the complications the evaluators have to face because of the presence of multiple-humped-type fission barriers. There is also the contribution [26] in a recent very comprehensive book). Excellent lectures on applications of nuclear theory to the computations of neutron cross sections for actinide isotopes were delivered recently by KONSHIN [27]. Many efforts in several laboratories are currently devoted to improving nuclear codes to be used for evaluation purposes. However at the present time most of these codes are based on very conventional phenomenological methods. Numerous basic parameters associated with the neutron-induced fission process as well as neutron and gamma-ray competitions have to be predetermined as input, and the main present difficulty in performing practical calculations consists of choosing correct estimates for these. Thanks to accumulation of experimental data, theoretical calculations, and evaluation works, systematic studies of the behaviour of these parameters (for example, from one actinide to another or as a function of excitation energy) have been initiated with the aim of finding general trends hopefully useful for extrapolation in cases where direct information is lacking. Such trends can emerge from suitable examination of a large number of coherent experimental data, coherent theoretical results, or a combination of these. This seems at the present time to be the most promising means for improving the actinide data evaluation in the near future. Findings from more fundamental methods will certainly be integrated into nuclear codes as soon as the needed modifications are implemented in a practical way.

Obviously the present review neither pretends to be complete nor details recent developments already reviewed previously. The aim of this paper is only to review briefly some of the main improvements either achieved or under way. The concern will be theoretical aspects useful for evaluating actinide data in the restricted incident neutron energy range from 10 keV to 20 MeV. It is intended to focus on examples of systematics as defined above and on some improvements expected from microscopic methods under development. A large part of this work is based on the contributions sent to me for the purposes of this third AGM.

2 - NEED FOR THEORETICAL CALCULATIONS

Table I gives a summary of some recent evaluations or calculations concerning an extensive set of curium isotopes (A = 241 to 248). This isotopic chain has been chosen because neutron data for curium isotopes are both particularly sparse and often affected by large uncertainties. Sometimes data are completely lacking because of the short half-lives involved and the difficulty in producing high purity samples. With this deficiency of experimental information, recent evaluation works for such actinides are largely based on model calculations. They try to account for systematics of data, including cross sections as well as other basis parameters, and microscopic calculations are extensively applied. For example, use was made of systematic behaviour in neutron-induced fission cross sections from 3 to 5 MeV in the actinide region, as outlined by BEHRENS and HOWERTON [55] from extensive measurements of fission cross sections performed in the energy range corresponding to the first fission plateau. Another reliable source of indirect experimental information, which has been used in the curium isotope theoretical evaluation, lies in the fission probability measurements performed by BRITT and co-workers [45] at LOS ALAMOS. As an example of use of microscopic calculations, the BOLOGNA group applied results from BARDEEN - COOPER-SCHRIEFFER (BCS)-type calculations [29,35] for determining a number of needed parameters such as i) the excitation-energy dependence of the nuclear temperature. This is useful to predict or confirm average radiative widths (Γ_γ) calculated from a simple "black-body" formula [42], or neutron spectra from evaporation models ; ii) the level-density parameters at the ground state deformation as well as at the first saddle-point deformation. As a final example, a simple model based on the evaporation formalism, with inclusion of a systematic behaviour of the ratio Γ_n/Γ_f and with allowance of preequilibrium effects and fission competition, has been extensively applied by BYCHKOV et al. [32]. This has been used for predicting (n,2n) and (n,3n) cross sections in the actinide region, including all Cm isotopes of interest.

TABLE I - Summary of recent calculations of curium isotope cross sections

(•) Abbreviations used in Table I :
URR = unresolved resonance region ; c.s. = cross sections ; ARP = average resonance parameters ; RRP = resolved resonance parameters ; CR = continuum region ; DOM = deformed optical model ; HF = Hauser-Feshbach ; SOM = spherical optical model ; σ_{CN} = compound nucleus formation cross section ; P_f = fission probability.

Target	Cross section	En. range	Ref.	Comments
^{248}Cm	Comp. eval. (with neutron spectra) INDL-A	10^{-5}eV-15 MeV	[28]	URR• (1.3 - 10 keV) : c.s.• calculated by means of ARP• deduced from RRP• ($\bar{\Gamma}_f$ for $J\pi = \frac{1}{2}^+$ and $\frac{1}{2}^-,\frac{3}{2}^-$ change slowly with energy so as to smoothly join URR to CR• above 10 keV). CR (10 keV - 15 MeV) : DOM• and HF• models - DOM with coupling base $0^+,2^+,4^+$ but adiabatic approximation above 6 MeV - Level densities are described by a back-shifted Fermi gas formula- Heights and curvatures of two-humped fission barriers are consistent with experimental fission probabilities, and 2^d chance fission-channel densities have been checked by reproducing expl ^{247}Cm $\sigma_{n,f}$. (n,2nf),(n,3n) c.s. and preequilibrium effects have been neglected. The energy spectra for neutrons emitted in the reactions (n,n'γ) continuum, (n,2n) and (n,n'f) have been represented by evaporation formulae ∿ E'exp(-E'/θ(E)) where θ(E) has been calculated for the residual nuclei ^{248}Cm and ^{247}Cm from a finite-temperature Nilsson-Bardeen-Cooper-Schrieffer formalism (see NUDENS code [29]).

TABLE I - continuation

Target	Cross section	En. range	Ref.	Comments
^{248}Cm	Comp.eval. INDL-A	10^{-3}eV-15 MeV	[30]	SOM• (ABACUS code) and HF (NEARREX code up to 1.32 MeV) calculations above 2 keV - Fission penetrability of the form $17/\{1 + \exp[(0.980-E)/0.0876]\}$ adjusted on expl $\sigma_{n,f}$. Extrapolations above 1.32 MeV using shape of ^{238}U $\sigma_{n,\gamma}$, expl $\sigma_{n,f}$ up to 5.5 MeV and (n,n'f) from ENDF/BV above 6 MeV. (n,2n) and (n,3n) c.s. calculated with a statistical model [31] similar to that of Pearlstein but with an improved treatment of (n,3n) competition.
	n,2n n,3n $(\sigma_{n,f})$ INDL-A	threshold-20 MeV	[32]	Evaporation formalism with allowance of preequilibrium effects and fission competition ((n,f),(n,n'f) and (n,2nf)). Only 3 ingredients needed : $\sigma_{CN}(E_n)$• , level density parameter a, and Γ_n/Γ_f for the nuclei A + 1, A, A-1 (only systematized sets used here).
^{247}Cm	Compl.eval. (with neutron spectra) INDL-A	10^{-5}eV-15MeV	[33]	URR (61 eV - 10 keV) : calculations by means of the strength function formalism. CR (10 keV - 15 MeV) : DOM and HF models DOM with coupling base $9/2^-$, $11/2^-$, $13/2^-$ but adiabatic approximation above 8 MeV - CN• contributions calculated with a modified version of the Hauser-4 code [34] - See comments under ^{248}Cm [28] - 2^d chance fission - channels densities have been checked here by reproducing expl ^{246}Cm σ_{nf}. θ(E) associated to neutron spectra from (n,n'γ) , (n,2n) and (n,n'f) reactions has been evaluated for residual nuclei ^{247}Cm and ^{246}Cm through the microscopic procedure of ref. [35].

TABLE I - continuation

Target	Cross section	En. range	Ref.	Comments
^{247}Cm	Comp.eval. (with neutron spectra) JENDL-3	≤20 MeV	[36]	ARP determined so as to reproduce measured σ_{nf}. Fission transition states were assumed from a systematic survey of other fissile nuclei. Above 1.9 MeV (no measurements) : σ_{nf} estimated from trends of other Cm-isotopes, and other c.s. calculated from SOM, statistical and evaporation models. SOM parameterization from adjustment on expl ^{241}Am total cross section. Level density parameters from Gilbert and Cameron tabulation.
	n,2n/n,3n (σ_{nf}) INDL-A	threshold-20 MeV	[32]	See comments under ^{248}Cm
^{246}Cm	Compl.eval. (with neutron spectra) INDL-A	10^{-5}eV-15MeV	[37]	URR (390 eV - 10 keV) : Statistical calculations by means of strength function formalism. Linearly energy-dependent partial fission widths adjusted so as to reproduce recent fission measurements (H.T.Maguire et al., nov-dec 1981). CR (10keV - 15 MeV) : DOM and HF models - See comments under ^{247}Cm [33]. Coupling base : $0^+,2^+,4^+$ - Deformations estimated in coherence with radius parameter from equilibrium shape calculations based on a Saxon-Woods type potential - Fission barrier parameters in agreement with informations from P_f* measurements, and 2d chance-fission channels densities have been checked by reproducing expl ^{245}Cm σ_{nf}. Microscopic procedure of ref. [35] has been used to evaluate energy dependence of neutron spectra temperatures.

TABLE I - continuation

Target	Cross section	En. range	Ref.	Comments
^{246}Cm	Comp.eval.	10^{-3}eV-15 MeV	[40]	ARP deduced from resonance analysis with Fröhner's code STARA. CR (200 eV - 15 MeV) : SOM (ABACUS code) and HF (NEARREX) calculations. Fission penetrability of the form $9/\{1 + \exp[(0.980 - E)/0.0846]\}$ adjusted on expl σ_{nf}. From 3 MeV to 15 MeV the ^{244}Cm σ_{nf} has been renormalized. (n,2n) and (n,3n) cross sections calculated from formalism of ref. [31].
	Comp.eval. (with neutron spectra) JENDL-3	≤20 MeV	[36]	URR (330 eV - 30 keV) : energy-dependent fission widths were searched so as to reproduce recent expl σ_{nf}, by assuming S_0, S_1, S_2 and R' from SOM calculations. CR (30 KeV - 15 MeV) : SOM and statistical model calculations (see comments under ^{247}Cm).
	n,2n/n,3n (σ_{nf}) INDL-A	threshold -20 MeV	[32]	See comments under ^{248}Cm

TABLE I - continuation

Target	Cross section	En. range	Ref.	Comments
^{245}Cm	Compl.eval.	10^{-5}eV-15MeV	[41]	URR (61 eV - 10 keV) : c.s. obtained from statistical calculations with the strength function model, with D_{obs} and Γ_γ chosen after microscopic evaluations [35,42], and S_1 and R' from DOM calculations. CR (10 keV - 15 MeV) : DOM and HF calculations (with statistical fluctuation corrections in neutron and fission channels up to 1 MeV). See comments under ^{248}Cm [28]. The adopted statistical parameters were checked by reproducing the fission probability of ^{245}Cm. The level density parameters (a,Δ,σ^2) were chosen so as to reproduce the cumulative number of levels at low energies and, at higher energies, the total level density calculated in the BCS microscopic approach of ref. [35]. For the $\sigma_{n,\gamma}$ calculation, radiation widths were estimated by means of the Brink-Axel formula where the adopted parameters were checked by reproducing Γ_γ in the keV region.
	Compl.eval. (JAERI)	10^{-5}eV-20 MeV	[43]	CR (60 eV, 20 MeV) : SOM and HF calculations. σ_{CN} from SOM and a 6 parameters empirical formula were used in a least squares fitting onto exp^{l} σ_{nf} - calculations of (n,2n) and (n,3n) c.s. based on the Pearlstein method with σ_{CN} = 2.75 b - Level density parameters from Gilbert and Cameron.

TABLE I - continuation

Target	Cross section	En. range	Ref.	Comments
^{245}Cm	(n,2n),(n,3n) (σ_{nf}) INDL-A	threshold--20 MeV	[32]	See comments under ^{248}Cm.
	σ_{nf}	10^{-3}eV-20MeV (measured) 0.1 - 5 MeV (calculated)	[44]	Test of σ_{nf} calculations for reproducing experimental data in the energy region of the fission neutron spectrum ($\sim$ 100 keV to $\sim$ 5 MeV). Parameters given in ref. [25] have been used with a barrier level density function modified so as to ensure continuous first derivatives (condition needed for reproducing in a first stage ^{235}U σ_{nf}). Calculations could only fit the ^{245}Cm σ_{nf} data by allowing some structure in the level density of the residual ^{245}Cm nucleus at an excitation energy of $\sim$ 1 to 2 MeV.
^{244}Cm	Compl. eval. (JAERI)	$\leq$ 20 MeV	[46]	CR (1 keV - 20 MeV) : SOM and HF calculations - Same procedures as under ^{245}Cm [43] - Use of Pearlstein method with σ_{CN} = 2.7 b for evaluating (n,2n) and (n,3n) reactions.
	Compl. eval. INDL/A	10^{-3}eV-15MeV	[47]	CR (400 eV - 15 MeV) : SOM (ABACUS code) and HF (NEARREX code) calculations- Fission penetrability of the form $24/\{1 + \exp[2\pi(0.9 - E)/0.583]\}$ results from adjustment on exp^{l} σ_{nf}. (n,2n) and (n,3n) cross sections have been calculated by means of the improved evaporation model [31] with σ_{CN} = 3.37b deduced from the following law adjusted on a set of actinides : $\sigma_{CN} = -14.87 + 0.19\,Z^2$ ($Z \geq 90$).

TABLE I - continuation

Target	Cross section	En. range	Ref.	Comments
^{244}Cm	Compl. eval. KEDAK	10^{-3}eV-15MeV	[48]	URR : SOM and HF calculations with a modified version of the code HAUSER-4 [34]. Below ~ 100 - 200 keV level-statistical parameters for ℓ=1,2, 3,4 are adjusted by a simultaneous fit to all angle-integrated average cross section data available, ensuring compatibility with s-wave average parameters deduced from resolved resonance analysis. Above this region conventional HF calculations are performed.
	(n,2n),(n,3n) (σ_{nf}) INDL-A	threshold-20 MeV	[32]	See comments under ^{248}Cm
^{243}Cm	Compl. eval. INDL-A	10^{-5}eV-15MeV	[50]	URR (26 eV - 10 keV) : information mainly derived from the resolved resonances. CR (10 keV - 15 MeV) : DOM (JUPITOR and ADAPE codes) and HF (HAUSER-4 code) calculations. Adiabatic approximation is used above 8 MeV. Level density parameters in n and γ channels are chosen so as to reproduce the cumulative number of discrete levels together with the average level spacing at neutron binding energy. Fission barrier densities are adjusted so as to reproduce the expl σ_{nf} without taking account of axial asymmetry at the first saddle point. Choice of different level schemes seems to induce discrepancies up to 50% in total inelastic cross sections as compared to ENDF/BV evaluation.

TABLE I - continuation

Target	cross section	En. range	Ref.	Comments
^{243}Cm	Compl. eval. (JAERI)	10^{-5}eV-20MeV	[51]	URR (E_n > 27 eV) : simplified HF calculations with adjustments on energy averaged σ_{nf} data (Γ_f and Γ_γ assumed to be constant) CR : SOM and HF calculations - Real well depth has been reduced below 1 keV so as to reproduce a correct value for S_o - σ_{CN} from SCM and a 6 parameter empirical formula were used in a least squares fitting onto experimental σ_{nf} - level density parameters from Gilbert and Cameron - Rather large discrepancies have been found in comparisons with ENDF/BV and ENDL-73 evaluations.
	(n,2n),(n,3n) (σ_{nf}) INDL-A	threshold-20 MeV	[32]	See comments under ^{248}Cm
^{242}Cm	Compl. Eval. with neutron spectra INDL-A	10^{-5}eV-15MeV	[52]	URR (280 eV -10 keV) : c.s. were evaluated by means of the strength function model based on average parameters with smooth energy variation. Poor information from resolved resonances - Use of local systematics in Cm region has been made for average parameters a, Γ_γ, Γ_f, S_o, S_1, R' (see refs [53,23]). CR (10 keV - 15 MeV) : DOM and HF calculations. As a check of adopted parameters the experimental ^{242}Cm fission probability has been reproduced. The BCS microscopic approach [35] helped determine level density parameters of ^{242}Cm and ^{243}Cm at the ground state and first saddle point deformations -

TABLE I - continuation

Target	Cross section	En. range	Ref.	Comments
^{242}Cm	Compl. eval. (JAERI)	10^{-5}eV-15 MeV	[54]	CR : SCM and HF calculations. SCM adjusted onto ^{241}Am total cross sections and strength functions - From 3 to 5 MeV ^{242}Cm σ_{nf} has been taken to be proportional to ^{244}Cm σ_{nf} with a ratio from the systematics proposed by BEHRENS and HOWERTON [55].
^{242}Cm ^{241}Cm	(n,2n),(n,3n) (σ_{nf}) INDL-A	threshold-20 MeV	[32]	See comments under ^{248}Cm

Tables II to V gather the various parameters generally required for theoretical evaluation purposes and resulting from the works summarized in Table I. They include i) average resonance parameters (Table II) which determine the behaviour of cross sections in the unresolved resonance region ; ii) optical model parameters (Table II) for spherical or deformed potential versions ; iii) spectroscopic information concerning discrete levels with their energy-spin-parity characteristics, and the continuum spectra described by level density formula (Table IV) ; and iv) fission barrier parameters with associated level densities (Table V) which are needed for the calculation of the fission competition. Some recent aspects associated with the determination or use of these parameters in the framework of nuclear models are briefly reviewed in the following chapters. This survey is not restricted to the Cm isotopes because further theoretical progress is also needed, but perhaps to a lesser extent, for the other actinide isotope chains. Nuclear models discussed in this paper deal only with energy-averaged cross section, and they do not apply below about 1 keV neutron energy. This is the approximate upper limit of the resolved resonance region for actinides.

TABLE II - Some average resonance parameters used in Cm isotope evaluations

S_0, S_1, S_2 = s-, p-, and d-wave neutron strength functions
R' = potential scattering radius ($\sigma_{pot} = 4\pi R'^2$)
D_{obs} = observable level spacing
Γ_γ = average radiation width
(a) = assumed / (c) = calculated from the optical model
( ) = very uncertain value

Target	Ref.	S_0 (10^{-4})	S_1 (10^{-4})	S_2 (10^{-4})	R' (fm)	D_{obs} eV	Γ_γ (meV)	Comments
^{248}Cm	[28]	1.2	3			24.5	27 ($J\pi=\frac{1}{2}^+$)	
	[30]	$1.17^{+0.34}_{-0.22}$	1.9±0.3		σ_{pot} = 10.4b	32 ± 3	28 ± 3 ($J\pi=\frac{1}{2}^+$)	S_1 = average of ^{235,238}U and ^{239}Pu values.
^{247}Cm	[33]	1.0	1.8(a)			1.2	40(a)	
	[36]				9.1521 (SOM)	1.75	40(a)	
^{246}Cm	[37]	0.77	(2.6)			21.3	33	
	[40]	0.55±0.21	1.9±0.3		σ_{pot} = 10.5b	32 ± 9	32 ± 3	S_1 = average of ^{235,238}U and ^{239}Pu values.
	[36]	0.94(c)	3.17(c)	0.88c	9.15(c)	31.7	31	SOM calculations.

TABLE II - continuation

Target	Ref.	S_0 (10^{-4})	S_1 (10^{-4})	S_2 (10^{-4})	R' (fm)	D_{obs} (eV)	Γ_γ (meV)	Comments
^{245}Cm	[41]	1.19	2.1(c)		9.5(c)	1.24	35	Γ_γ chosen with consideration of a calculated value from a simple "black-body" formula [42] with a temperature derived from BCS microscopic calculations [35].
	[43]	1.0(c)				1.8	40	SOM calculations for S_0.
^{244}Cm	[46]	1.03(c)				14	37	SOM calculations for S_0
	[47]	1.32±0.27	1.9±0.3		σ_{pot}= 10.5b	10.8±0.5	35.0± 1.4	S_1 = average of ^{235}U, ^{238}U and ^{239}Pu
	[48]	1.14	2.30(c)	1.17(c)		11.9	36.2	
^{243}Cm	[50]	1.15±0.30	2.36(c)			0.80	35	S_1 results from DOM calculations - Black-body formula [42] with thermodynamic temperature from BCS level density calculations gives Γ_γ=36meV.
	[51]	2.2±0.2			9.81(c)	2.2	40	
^{242}Cm	[52]	0.71	2.53(c)		8.9(c)	10.8±1.6	38 ± 11	
	[54]	0.64±0.32				17.6±3.3	40(a)	

TABLE III - Optical model parameters used in Cm isotope evaluations (energies are in MeV and lengths in fm)

General reference form :

$$U(r,\beta') = -V f(r,R_0,a_0) - iW_V f(r,R_V,a_V) + 4\,iW_D \frac{d}{dr} f(r,R_D,a_D) + 2\,V_S \lambda^2 \cdot \frac{1}{r}\frac{d}{dr} f(r,R_S,a_S)\vec{l}\cdot\vec{s}$$

$$R_i = r_i A^{1/3}\,[1 + \beta_2 Y_{20}(\beta') + \beta_4 Y_{40}(\beta')] \quad \text{with } i \neq s \qquad (\beta' \text{ refers to the body-fixed system})$$

$$f(r,R,a) = \left\{1 + \exp[(r-R)/a]\right\}^{-1}$$

other imaginary term used : $-iW.\exp[-(r-R)^2/b^2]$

Target	Ref.	V	W_D	V_S	r_0	r_D	r_S	a_0	a_D	a_S	β_2	β_4	Comments
^{248}Cm	[28]	$47.01-0.267E_n$ $-0.00118E_n^2$	$3.195 (E_n \leq 2.25$ MeV) $2.25 + 0.42\,E_n$	7.2	1.259	1.237	1.259	0.66	0.48	0.66	0.246	0.02	
^{247}Cm	[33]	"	"	"	"	"	"	"	"	"	0.25	0.0	See ^{248}Cm
	[36]	$43.4 - 0.107E_n$	$6.95 - 0.339E_n$ $+ 0.0531E_n^2$	7.0	1.282	1.29	1.282	0.60	0.5	0.60			SOM for ^{241}Am
^{246}Cm	[37]										0.245	0.03	See ^{248}Cm
^{245}Cm	[41]										0.24	0.	See ^{248}Cm
	[43]	$40.5 + 0.5E_n$	$8.2 + 0.5\sqrt{E_n}$	7.0	1.32	1.32	1.32	0.47	0.47	0.47			SOM for ^{241}Am

TABLE III - continuation

Target	Ref.	V	W_D	V_S	r_0	r_D	r_S	a_0	a_D	a_S	β_2	β_4	Comments
^{244}Cm	[46]												See ^{245}Cm [43]
	[47]	42	W = 8	7.5	1.3	1.3	1.3	0.47	b=1.5	0.47			SOM for ^{237}Np
	[48]	$47.01-0.267E_n$ $-0.00118E_n^2$	$9.0 - 0.53\,E$		1.21	1.30		0.66	0.48				SOM from ref. [49]
^{243}Cm	[50]										0.235	0.0	See ^{248}Cm
	[51]	$42.0-0.107E_n$	$9.0 - 0.339\,E_n$ $+ 0.0531\,E_n^2$	7.0	1.282	1.290	1.282	0.6	0.5	0.6			SOM adjusted to $\sigma_{CN} \simeq 1.1\,\sigma_{nf}$ ($E_n \gtrsim 1$ keV)
		$40.5-0.107E_n$	"	"	"	"	"	"	"	"			Readjusted to reproduce $S_0 \simeq 2.2 10^{-4}$ (used at low energy)
^{242}Cm	[52]										0.23	0.0	See ^{248}Cm
	[54]												See ^{247}Cm [36]

TABLE IV - Some statistical model parameters (ground-state deformation) used in Cm isotope evaluations

$N^{\bullet}$: number of discrete excited levels with spin-parity characteristics
$E^{\bullet}_{max}$ = energy of the last discrete excited level
(a,Δ,σ) = level density, pairing energy, and spin-cut-off parameters
U = excitation energy corrected for shell and pairing effects
E_X = joining energy between the constant temperature and Fermi gas models
T_n = nuclear temperature in the constant temperature model
(a) = composite Gilbert and Cameron type level density
(b) = back-shifted Fermi gas level density
Energies are in MeV

Nucleus	Ref.	$N^{\bullet}$	$E^{\bullet}_{max}$	a	$\sigma^2/\sqrt{U}$	$\|\Delta\|$	E_X	T_n	Comments
^{249}Cm	[28]	10	0.289	$25.2^{(b)}$		$1.0^{(b)}$			$\sigma^2 = 100$ T
^{248}Cm	[28]	4	0.510	$24.5^{(b)}$		$1.0^{(b)}$			$\sigma^2 = 100$ T
	[36]			$21.46^{(a)}$	$18.03^{(a)}$	$1.623^{(a)}$	4.73	0.411	
	[30]	14	1.302						
^{247}Cm	[36]	10	0.449	$26.20^{(a)}$	$17.89^{(a)}$	$0.72^{(a)}$	3.83	$0.413^{(a)}$	
	[28]	7	0.309	$25.2^{(b)}$		$0.69^{(b)}$			$\sigma^2 = 100$ T
^{246}Cm	[36]	29	1.509	$25.98^{(a)}$	$17.77^{(a)}$	$1.11^{(a)}$	4.22	0.415	
	[33]	4	0.500	$24.0^{(b)}$		$0.37^{(b)}$			$\sigma^2 = 100$ T
	[40]	33	1.671						

TABLE IV - continuation

Nucleus	Ref.	$N^{\bullet}$	$E^{\bullet}_{max}$	a	$\sigma^2/\sqrt{U}$	$\|\Delta\|$	E_X	T_N	Comments
^{245}Cm	[36]	16	0.532	$26.03^{(a)}$	$17.74^{(a)}$	$0.72^{(a)}$	3.83	0.415	
	[37]	17	0.555	$24.5^{(b)}$		0.10			$\sigma^2 = 100$ T
^{244}Cm	[41]			$24.0^{(b)}$		0.01			$\sigma^2 = 100$ T
	[46]	8	1.187	$25.97^{(a)}$	17.67	1.22	4.335		
	[47]	24	1.2	23.94	σ=4	0.72			Spectroscopy supplemented by levels of ^{238}U - Fermi gas model
	[50]	4	0.500	24.0		0.0			$\sigma^2 = 104$ T
	[51]			25.97	17.67	1.22	4.335		
^{243}Cm	[50]	12	0.260	23.0		0.63			$\sigma^2 = 100$ T ; 2 levels were added from a fit to collective $K^{\pi}=1/2^+$ band of the form $E(J,K)-E_0(J_0,K) = AJ(J+1)-BJ^2(J+1)^2$
	[51]	14	0.798	25.59	17.49	0.72	3.837	0.419	

TABLE IV - continuation

Nucleus	Ref.	N°	E^*_{max}	a	$\sigma^2/\mathcal{J}$	$\|\Delta\|$	E_X	T_N	Comments
^{242}Cm	[50]	3	0.285	24.0		0.54			σ^2 = 100 T
	[51]	3	0.284	25.13		1.15	4.27	0.424	See also ref. [54]
^{241}Cm	[51]			24.74		0.72	3.342	0.428	

TABLE V - Some fission barrier parameters (FBP) and associated level densities used in Cm isotope evaluations

$E_{A(B)}$ = height of inner (outer) barrier
$\hbar\omega_{A(B)}$ = associated curvature parameters
B_n = neutron separation energy
Energies are in MeV

Fissioning nucleus	Ref.	B_n	E_A	$\hbar\omega_A$	E_B	$\hbar\omega_B$	a (MeV^{-1})	σ^2/T	$\|\Delta\|$	Comments
^{249}Cm	[28]	4.71	5.7	0.65	4.2	0.55	26.5(b)	98	2.05(b)	FBP consistent with results of analysis of P_f measurements [38]
^{248}Cm	[28]	6.21	6.1	0.90	4.2	0.55	28.0(b)	98	1(b)	FBP in agreement with results from P_γ measurements [39], and level densities checked by reproducing ^{247}Cm σ_{nf}
^{247}Cm	[33]	5.16	6.0	0.63	4.2	0.55	26.5(b)	98	1.7(b)	FBP consistent with results from analysis of P_γ measurements [38], and level densities checked by reproducing ^{246}Cm σ_{nf}
^{246}Cm	[37]	6.45	6.0	0.9	4.2	0.55	26.5(b)	100	0.45(b)	FBP close to those of ^{244}Cm and ^{248}Cm deduced from P_γ measurements [39] and level densities checked by reproducing ^{245}Cm σ_{nf}
^{245}Cm	[41]	5.52	6.0	0.80	4.2	0.55	25.5(b)	98	2.10	As a check of these parameters the ^{245}Cm expl P_γ [45] has been reproduced

TABLE V - Continuation

Fissioning nucleus	Ref.	B_n	E_A	$\hbar\omega_A$	E_B	$\hbar\omega_B$	a (MeV^{-1})	σ^2/T	$\|\Delta\|$	Comments
^{244}Cm	[50]	6.8	6.0	0.78	4.2	0.55	26.0(b)	98	0.63	Level densities adjusted so as to reproduce experimental σ_{nf}
^{243}Cm	[50]	5.6	5.87	0.45	5.0	0.55	27.2(b)	98	1.35	Level densities are adjusted so as to reproduce experimental σ_{nf}
^{242}Cm	[52]	6.9	6.04	0.75	4.2	0.55	25.2	98	0.25	Parameters checked on experimental ^{242}Cm p_f

TABLE VI - Deformed optical potentials for a set of actinides (from ref. [100])

General form is given at the top of Table III (energies in MeV and lengths in fermi)
Neutron strength functions (S_0,S_1) and potential scattering radii (R') are calculated at E_n = 10 keV

$V = V_o - 0.3\,E_n$ $\qquad r_o = 1.26 \qquad a_o = 0.63$

$W_D = \begin{cases} W_{Do} - 0.4\,E_n & E_n \leq 10\ MeV \\ W_{Do} + 4.0 & E_n \geq 10\ MeV \end{cases} \qquad r_D = 1.26 \qquad a_D = 0.52$

$V_S = 6.2 \qquad r_S = 1.12 \qquad a_S = 0.47$

	^{230}Th	^{232}Th	^{234}U	^{238}U	^{242}Pu	^{246}Cm	^{252}Cf
V_o	46.600	46.600	46.42	46.20	46.02	45.4	44.6
W_{D_o}	3.600	3.600	3.720	3.600	3.51	3.200	3.2
S_2	0.180	0.190	0.194	0.198	0.204	0.220	0.230
S_4	0.085	0.071	0.071	0.057	0.051	0.033	0.00
$S_o \times 10^4$	0.969	0.937	1.036	1.003	0.995	1.093	1.338
$S_1^{\bullet} \times 10^4$	1.563	1.586	1.875	2.222	2.633	2.927	3.474
R'	9.332	9.397	9.270	9.240	9.190	9.379	9.643

• calculated by assuming a nucleus radius $R = 1.26\ A^{1/3}$

3 - USE OF R-MATRIX FORMALISM IN THE UNRESOLVED RESONANCE REGION

Resolved-resonance-parameter analyses provide us essentially with s-wave average parameters. Over the unresolved resonance region (URR), considered here up to about 100-200 keV for actinide nuclei, higher angular momenta up to $\ell = 4$ become non-negligible. Figure (1) taken from ref. [56] illustrates the increasing importance of the successive $\ell = 1,2,3,..$ components in the compound nucleus formation cross section (σ_{CN}), as obtained from an optical model calculation for ^{238}U versus increasing incident energy E_n. In this low-energy part of the URR, where the number of different channels to be dealt with is not too large, a physical parametrization of the available energy-averaged cross sections can be accomplished within the theoretical framework of the R-matrix formalism (level-statistical or strength-function model). Of the average parameters entering this formalism, part of them are to be inferred from resolved resonance analyses ; others are either estimated (at least as initial values) from optical-model calculations or adjusted so as to ensure good fits to specific average cross sections. For example, average fission widths are often parametrized as functions of energy in order to reproduce average fission cross sections determined from experimental data.

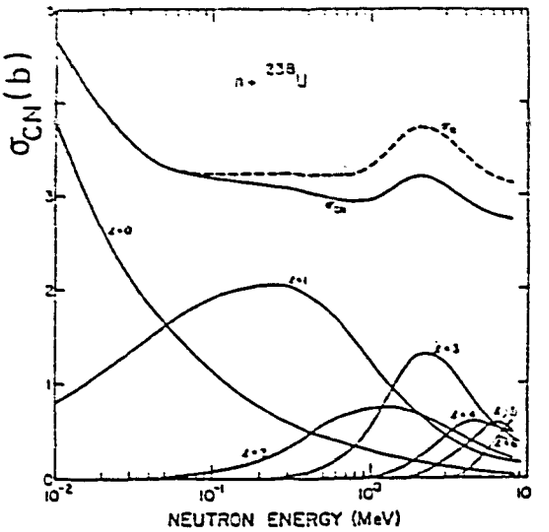

Fig. 1

The calculated compound nucleus formation cross section is shown for n + ^{238}U along with its ℓ constituents. Figure taken from reference [56].

When close comparison is sought with results from the so-called "global" conventional models - namely the optical model or the Hauser-Feshbach (HF) statistical model with width-fluctuation corrections - used preferably in the higher-energy, care has to be taken to use experimental data averaged over energy intervals of appropriate size. An illustration of this problem is given for example in reference [57] where the presence of marked residual fluctuations in the ^{238}U (n, γ) cross section, averaged over 400-eV intervals in the energy region from 5 keV to 100 keV, has been shown to imply the existence of intermediate structure. These fluctuations are wider than the sharp resonances associated with the compound nucleus levels and narrower than the broad structure arising from the energy dependence of the neutron transmission coefficients. Only this latter structure can be reproduced by predictions from the compound nucleus theory. The ^{238}U(n,γ) cross sections averaged over neutron energy intervals 10-keV wide can be compared, for example, to results from the "global" ^{238}U theoretical evaluation by the Bruyères-le-Châtel group [58].

The R-matrix formalism applied in the low-energy resonance region was recently reviewed in a Trieste Course by MOORE [59] for mathematical foundations and by FRÖHNER [60] for the practical formulations. This formalism takes advantage of the properties of the S-matrix, deduced from time reversal invariance (symmetry) or probability conservation (unitarity), to introduce physical constraints in its parametrization. Hence this produces a useful coherence in simultaneous interpretations of several kinds of cross sections.

More or less sophisticated approximations of this reaction theory were used in the past for evaluation purposes. Thanks to increasing quality of new measurements, recently more sophisticated codes have been developed to apply this formalism more widely. An example is the code FITACS (Fit Average Cross Sections) used by the Karlsruhe group [48,61] in recent actinide evaluations. Let me briefly describe its calculational procedure using conventional notation [62].

The average total cross section for each entrance channel $c \equiv \{J\ell s\}$ ($\ell = 0,1,2,3$) is a linear function of the average S-matrix element $\langle S_{cc} \rangle$ which also is the S-matrix element of the optical model. Then :

$$\langle \sigma_c \rangle = 2\pi\lambda_c^2 \cdot g_c \, (1 - \mathrm{Re} \langle S_{cc} \rangle) \qquad (1)$$

with the R-matrix expressions

$$\begin{cases} \langle S_{cc} \rangle = e^{-2i\varphi_c} \dfrac{1 - \bar{R}_{cc} L_c^{o*}}{1 - \bar{R}_{cc} L_c^{o}} \\ \\ \bar{R}_{cc} = R_c^{\infty} + i\pi s_c, \end{cases}$$

where the distant-level parameters R_ℓ^∞ and the strength functions $S_\ell = 2k_c a_c s_c \sqrt{1eV/E}$ are the only average parameters of the model when applied to total cross sections. As an illustrative example, a fitting procedure has been described in reference [63] for the case of ^{240}Pu total cross section. For $\ell = 2,3$ S_ℓ and R_ℓ were taken from a spherical optical model [49] adjusted to fit $\langle \sigma_T \rangle$ and three scattering cross sections between 50 keV and 10 MeV for ^{238}U. For $\ell = 0,1$ the average parameters S_ℓ and R_ℓ were fitted with the code FITACS to measured total cross sections. Values deduced from resolved resonance analysis (S_0 and $R_0^\infty \equiv 1 - R'/a_c$) and calculated from the optical model [49] (S_1 and R_1^∞) were introduced into the fit as a priori information via BAYES'theorem [64] (the prior probabilities for these parameters are taken as normally distributed around the starting values with standard deviations equal to the input uncertainties, a procedure which constrains parameter variations to reasonable ranges). Figure 2 compares the resulting curve (KEDAK 4) to other evaluations by the BRC group [65,66] (using optical model above 10 keV), the JAERI group [67], and the ENDF/B curve (obtained as the sum of all partial cross sections). The experimental data of POENITZ et al. [68] are quite well reproduced but, as a consequence of comparison with the present coherent calculation, one sees that there are probably systematic errors in the KfK measurements [69] below 100 keV.

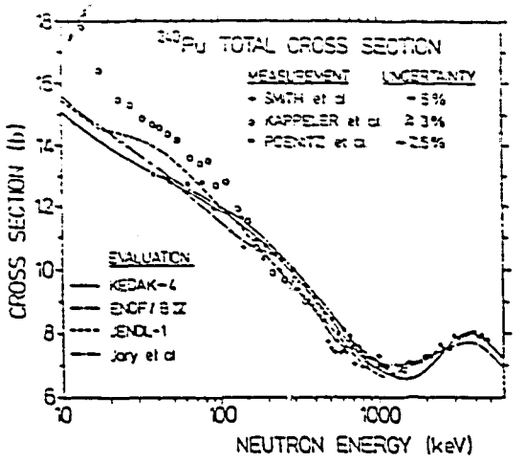

Fig. 2

Figure taken from reference [61] : evaluations of the ^{240}Pu total cross section in the unresolved resonance region in comparison with experimental data. See text for other references.

When the procedure is generalized to require a simultaneous fit to several partial cross sections, including possibly angle-integrated scattering, capture and fission cross sections, some corresponding transmission coefficients are needed, namely :

$$T_c \equiv 1 - |\langle S_{cc} \rangle|^2 = \frac{4\pi\, s_c\, P_c}{|1-\bar{R}_{cc}\, L_c^o|^2} \quad , \quad \text{(neutron channel in absence of direct reactions)} \tag{2}$$

$$T_\gamma = 2\pi \frac{\langle \Gamma_\gamma \rangle}{D_c} \quad , \quad \text{(photon channels)} \tag{3}$$

$$T_f = 2\pi \frac{\langle \Gamma_f \rangle}{D_c} \quad , \quad \text{(fission channels).} \tag{4}$$

The s-wave average parameters entering these expressions can be determined from resolved-resonance analysis. The energy-dependence of strength functions and distant-level parameters can be neglected up to 200-300 keV, whereas the energy-and spin-dependences of the level spacings D_c can be inferred from the use of a level density formula. The determination of the transmission coefficients in global analyses using the optical and Hauser-Feshbach statistical models are briefly considered in Chapter 4 (for T_c) and in Chapter 5 (for T_γ and T_f). These global analyses are the required theoretical methods above 200-300 keV.

4- USE OF OPTICAL MODEL

Many general aspects concerning practical use of the optical model for evaluation purposes, including the actinide region, have been reviewed in the

last few years (for example see ref. [22] and [70] to [75]). This model is important because it is able to provide us with several nuclear data over an extended energy range (typically here 10 keV - 20 MeV) : total, direct elastic and inelastic scattering differential cross-sections, but also quantities of great interest for statistical model calculations, namely the compound nucleus formation cross section (σ_{CN}) and the associated transmission coefficients T_c proportional to the strength functions S_ℓ (ℓ = 0,1,2..). Only some newly developed aspects will be reviewed below.

4-1- Spherical optical model (SOM) calculations

A number of actinide evaluations or calculations are making use of spherical optical potentials. There are generally practical reasons for this, for example :

- saving of computational time,

- search for simplicity in the analysis of an extensive set of actinides for evaluation purposes [67] or to interprete total cross section measurements [68] and compare with deformed optical model calculations,

- utilization in a very limited mass or energy range where only poor quality data are available for parametrization [49],

- studies about the applicability of DWBA type calculations, instead of too complicated coupled channel calculations, for evaluating neutron inelastic scattering cross sections [76,77] by using the first-iteration optical potential obtained by the Los Alamos Group [78],...

Most of the spherical optical potentials used for extrapolating into mass-regions where no measurements exist have been found from satisfactory adjustments on total cross sections and sometimes low energy data (essentially strength functions) measured for neighbouring deformed nuclei (see Tables I and III concerning curium isotopes).

4-2- Deformed optical model (DOM) calculations

4-2-1- Why DOM calculations ?

Use of DOM calculations in order to constitute complete evaluated data file for a given nucleus is to be recommended for the following reasons :

a) It is well known from spectroscopy considerations that actinides belong to a strong deformation region, and it has been recognized that total cross sections for example are non negligibly sensitive to quadrupole defor-

mation with a marked energy-dependence [79], particularly at low energy. As a consequence SOM parametrization cannot be used by translation to deformed potentials without a serious alteration.

b) Nuclear deformation induces a coupling between the neutron channels associated with the ground-state and the low-lying rotational excited states. Due to the strength of this coupling, only coupled-channel calculations have been proved to be able to correctly reproduce the observed energy dependence [58,13] and angular distribution [13,80] of the direct components of the corresponding inelastic cross sections.

c) Complete evaluation over a wide energy range (10 keV - 20 MeV) implies a consistent treatment of all cross section types which are to be evaluated in parallel. For example several partial cross sections calculated by means of the statistical model are proportional to $\sigma_{CN}(E_n)$. Due partially to the presence of direct effects as indicated above, SOM and DOM calculations reproducing the same total cross sections predict σ_{CN} values which are different in magnitude as well as energy-dependence. Figure 3, taken from the work of ref. [81] detailed in the report [82], shows such differences for ^{240}Pu and ^{232}Th between coherent DOM calculations by Lagrange and results from the spherical potential deduced by MATSUNOBU et al. [67].

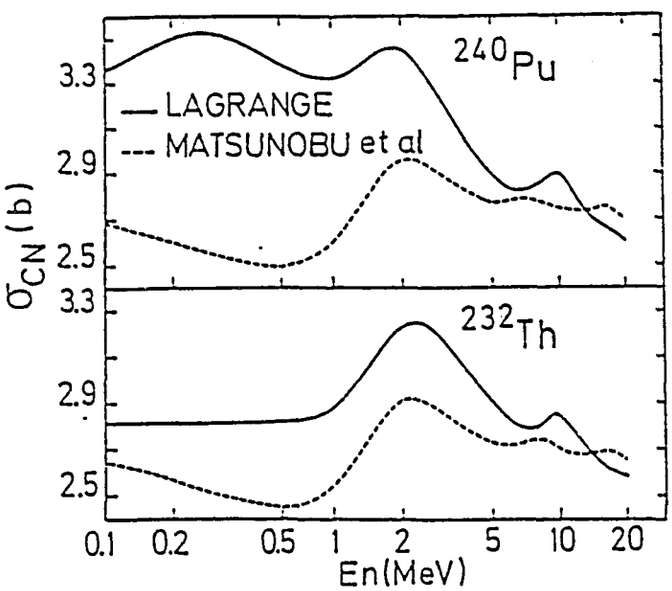

Fig. 3

Figure taken from ref. [81] : comparisons of compound nucleus formation cross sections calculated from deformed optical potential [81] (full lines) and spherical optical potential (dashed lines) [67].

d) Utilization of an assumed more physical model allows information from other different sources to be integrated in the calculational procedure in a coherent manner which gives more confidence when extrapolations are needed in regions where no data exist. Examples will be given below concerning deformation parameters or deformed nuclear density distributions calculated from microscopic methods.

4-2-2- How to parametrize ?

In a number of references quoted above efficient methods were proposed for parametrizing deformed optical potentials for even actinides as well as odd ones [83]. Following numerous tests made for nuclei like ^{238}U[84,58] or ^{232}Th [85] for which many experimental results are available, the importance of some basic data has been recognized, namely : strength functions and scattering radii determined at low energy, total cross sections over the full energy range, and scattering angular distributions above a few MeV. In parallel to progress associated with the determination of these basic data, improvements of the DOM parametrization requiring generally slight readjustments have been achieved. Then, extrapolations to less known nuclei imply mainly, apart from differences in radii, a smooth variation of the real potential strength mostly due to the (N-Z)/A symmetry dependence and a choice for convenient deformation parameters. A number of recent actinide evaluations are based on the use of such a procedure. As examples : concerning the Cm isotopes, see Tables I and III reporting on works by the Bologna group, and for other actinides : works by the Cadarache group for ^{237}Np [86] and ^{238}Pu [87], by the Minsk group [88] for ^{242}Pu, the Romanian group for ^{233}Pa [89], the Los Alamos group for ^{242}Pu [90] and ^{239}Pu [91,92], and the Bruyères-le-Châtel group for ^{242}Pu [66]. Many of these evaluations were made possible thanks to the availability of efficient coupled channel optical model codes such as ECIS by Raynal [70], or locally improved versions of JUPITOR by TAMURA. Only some comments will be given below concerning basic data for DOM parametrizations.

- Low energy data (S_0, S_1, R')

A status of resolved and unresolved resonance parameters with associated discrepancies and error estimates has just been given [16] for the major isotopes of uranium and plutonium (^{235}U, ^{238}U, ^{239}Pu, ^{240}Pu, ^{241}Pu, ^{242}Pu). Concerning the curium region an extensive discussion on the systematic trend of experimental and theoretical values for neutron strength functions (S_0, S_1) and scattering radius (R') has already been published in ref. [53,23].

A discussion on the determination of the strength functions with consideration of capture cross sections in the keV region has been given by Derrien [93] for ^{237}Np, ^{238}Pu and ^{241}Am. More studies on how to improve our knowledge of these low energy data are called for. At the present time strength functions are rather badly known. When they are estimated from resolved resonances large statistical errors are caused by the large variance of the Porter-Thomas distribution. Even if samples of several hundred resonances are available, the uncertainty is not better than 10%. A global estimation of S_0, S_1 and R' in the whole actinide region can be taken as [94] :

$$S_0 = (1.2 \pm 0.3) \times 10^{-4} \quad , \quad S_1 = (2.0 \pm 0.4) \times 10^{-4} \quad , \quad R' = (9.4 \pm 0.5) \text{ fm.}$$

These values may serve as a guide in absence of better local estimations because a reasonable adjustment on the three quantities is already selective for the optical potential. Nevertheless systematic variations within the actinide region would have to be taken into account.

- Total cross sections

Accurate measurements of the average total cross-section are required not only because such data, which can be measured absolutely, constrain all partial cross sections, but also because it is the only observable data type that can be directly compared to optical model calculations (following (1) $\langle\sigma_c\rangle$ is a linear function of the optical model S-matrix). The optical model parametrization is particularly sensitive to total cross sections below 1 MeV, but data at higher energies contribute to the definition of the energy-dependence of the potential strengths.

Recent measurements of total cross sections were performed by the Argonne group [68,95,96] for a set of actinides (^{232}Th, ^{233}U, ^{235}U, ^{238}U, ^{239}Pu, ^{240}Pu) with particular attention to measurement accuracy (typically 2% above 100 keV and 3% below 100 keV), consistency of measured values and, not the least, corrections due to the resonance self-shielding which caused a non negligible shift at low energies. These new measurements have already been taken into account, particularly around 1 MeV, in revised evaluations, which induced slight changes in previously adopted DOM parametrization, for example for ^{239}Pu [91].

- Neutron scattering cross sections

Experimental as well as theoretical aspects concerning elastic and inelastic differential actinide cross sections and their excitation functions were reviewed in November 1981 at the Paris' Meeting [13]. Many angular

distributions measured above a few MeV for neutron scattering from low-lying rotational states of a set of even-and odd-mass actinides, as gathered for example in reference [80], served to usefully test and further optimize optical parameters firstly determined by means of the so-called SPRT procedure [84,72]. In particular, better determinations of the deformation parameters, which influence inelastic scattering from successive excited states of the ground-state rotational band, have been achieved. Extensions of such measurements with higher resolution which are planned at Bruyères-le-Châtel above 5 MeV, will permit to further improve DOM parameters. Elastic and inelastic differential cross sections have just been measured by the Livermore group [97] for ^{232}Th, ^{238}U and ^{239}Pu at 14.1 MeV. The analysis of the data by using DOM calculations will allow parametrization for these actinides to be tested at high energy, with particular consideration of the imaginary central and spin-orbit terms, hence a test for σ_{CN}.

- Information from proton measurements

It is well known that the Lane model has been - and is currently - successfully applied in light- and medium-mass nuclei for determining the neutron optical potential from measurements of proton scattering (p,p) and charge exchange $(p,n)_{IAS}$ reactions to the isobaric analog state (IAS) of the target ground state. Apart from some coulomb correction terms, the real and imaginary potential depths for protons of energy E_p and for neutrons of energy $E_n = E_p - \Delta_c$ are given by the model as follows :

$$V_p\ (E_p) = U_o - \xi\ U_1$$

$$V_n\ (E_n = E_p - \Delta_c) = U_o + \xi\ U_1$$

where Δ_c is the coulomb displacement energy and $\xi \equiv (N - Z)/A$ is the symmetry parameter.

The usefulness of such an information for actinide nuclei depends on the validity of the Lane model in this very heavy-mass region where large isospin mixing is expected and where deformation effects must be considered in the $(p,n)_{IAS}$ reaction. The neutron elastic differential cross sections calculated with the optical potential deduced from distorded-wave Born approximation (DWBA) analyses for $(p,n)_{IAS}$ differential cross sections were in poor agreement with actinide measurements. Recently the Livermore group has measured (p,p) and $(p,n)_{IAS}$ cross sections at the energy E_p = 26 MeV and analysed the results simultaneously by solving the Lane coupled equations generalized so as to explicitly include couplings to the low excited rotatio-

nal states of the target and their analogs [98,99]. Starting from a global optical potential giving the best fit to proton scattering data at 26 MeV, the analysis allowed neutron optical potential parameters to be deduced which gave a good agreement with measurements of ($0^+ + 2^+ + 4^+$) differential cross sections for ^{232}Th and ^{238}U at the neutron energy E_n = 7.0 MeV ($\Delta_c \simeq$ 19 MeV in the actinide region). This study has demonstrated that proton measurements are capable of giving informations on neutron scattering as well as the calculations with neutron potential optimized for actinides [78] on condition that channel couplings be explicitly taken into account.

- Deformation parameters

In conventional DOM parametrization (see at the top of Table III) the deformation parameters β_2, β_4,.. appear in the Legendre polynomial expansion of the nuclear radius $R(\theta)$. In view to compare such deformation parameters as obtained from different optical model analyses as well as from inelastic measurements with various charged projectiles (electron, proton, alpha particles,..) and from coulomb excitation, it has been realized that the multipole moments q_2, q_4,.. of the DOM potentials are the best quantities to be compared because they are less sensitive to the detailed values of the optical parameters used in the calculations. These multipole moments as given by the expression :

$$q_\lambda = \frac{Z.\int V(\vec{r})\ r^\lambda\ Y_{\lambda o}\ (\hat{r})\ d^3r}{\int V(\vec{r})\ d^3r} \qquad (5)$$

have to be calculated numerically using the real part $V(\vec{r})$ of the DOM potential which is assumed to correspond approximately to a folded potential (in this case Satchler's theorem, stating that the normalized moments of the mass distribution of the nucleus are equal to the normalized multipole moments of the folded potential, can be applied). The normalization constant (the atomic number Z) in front of the expression (5) is needed to make comparisons between charge moments. In a number of recent analyses a good agreement was achieved in such comparisons [80,98]. We recommend that the values of q_λ (λ = 2,4) be given after any DOM analysis. Comparing different deformation lengths βR is judged to be unsufficient when coupled channel calculations are performed in a mass-region of strong collectivity, as it is the case for actinides.

4-2-3- Systematics from a limited number of coherent DOM calculations ?

When the DOM parametrization is to be optimized for each nucleus to be studied, for example to take advantage of newly measured data, they are very time consuming, particularly for odd-mass actinides. Concerning these latter an efficient method - the so-called "fictitious even-even nucleus" method - was recently carried out [83] but the problem remains for even nuclei where coupling bases (0^+, 2^+, 4^+) are needed. The less expensive adiabatic approximation also is used generally above about 8 MeV (see Table I). In order to constitute a basis in view to extrapolating, a limited number of coherent (time-consuming and based on all relevant available data) DOM calculations were performed by Lagrange [100] for a set of actinides covering the whole mass region (^{230,232}Th, ^{234,238}U, ^{242}Pu, ^{246}Cm, ^{252}Cf). The adopted parametrization along with calculated low energy data are shown in Table VI. The adequacy of extrapolations between the results, including transmission coefficients, has been tested for ^{238}U, which has been "evaluated" from the results for ^{234}U and ^{242}Pu [81]. The results given in reference [100] for $\sigma_{CN}(E_n)$ are plotted on Figure 4, showing some energy and mass-dependence particularly in the MeV region. The existence of an adequate representation for describing smoothly such variations is an open problem...

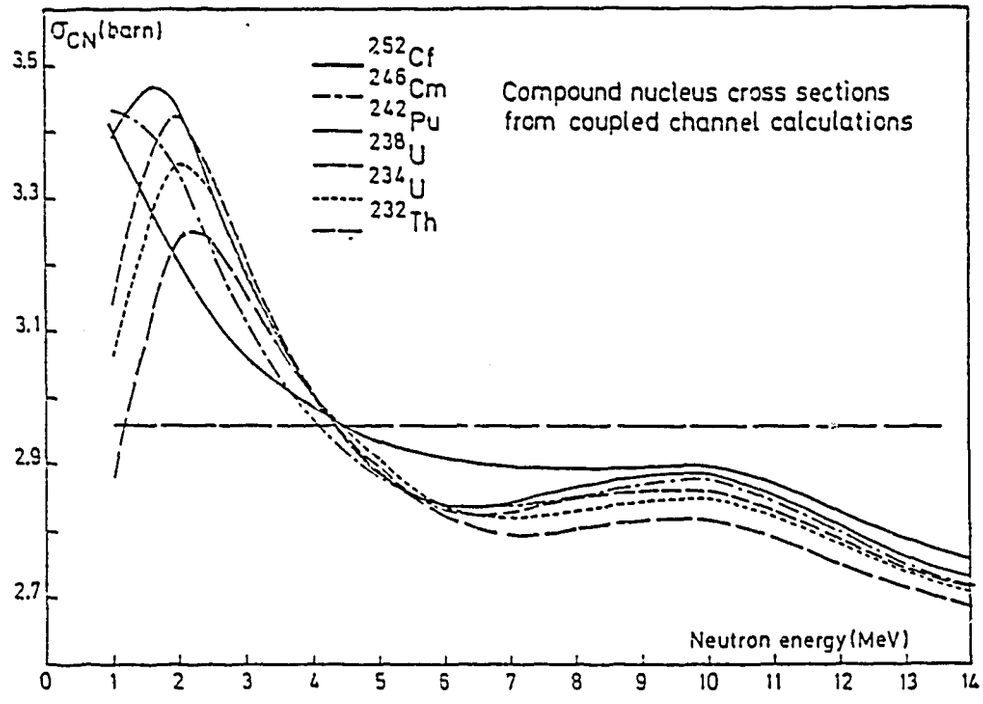

Fig. 4

Calculated compound nucleus formation cross sections obtained from DOM calculation results obtained in reference [100] for a set of actinides. The dashed horizontal line corresponds to the constant value approximation used by LYNN [26].

The neutron transmission coefficients used by LYNN [26] are based on the following values of S_0 and S_1 as suggested by measurements of s-and p-wave resonances in the actinide region (^{238}U and ^{232}Th) :

$$S_0 \simeq 1 \times 10^{-4} \text{ , or (see (2))} \qquad s_0 \simeq T_0/4\pi P_0 \simeq 0.025$$

$$S_1 = 1.8 \times 10^{-4} \text{ , or} \qquad s_1 \simeq T_{\ell=1}/4\pi P_1 \simeq 0.045$$

For $\ell > 1$, these values are used as follows :

$$T_\ell \simeq 1 - \exp(-4\pi P_\ell s_0) \text{ , even } \ell$$

$$T_\ell \simeq 1 - \exp(-4\pi P_\ell s_1) \text{ , odd } \ell$$

This procedure leads for σ_{CN} to a value of the order of 2.96 barn at $E_n \gtrsim 100$ keV. This constant value is reported on figure 4 for sake of comparison.

4-3- Contribution from microscopic calculations

4-3-1- Deformation parameters

Over the past decade the Hartree-Fock-Bogoliubov (HFB) type microscopic methods have considerably progressed. Realistic calculations using effective two-body forces of finite range and density dependent have been made possible even for deformed heavy-mass nuclei thanks to the development of separable methods for calculating the numerous matrix elements involved [101]. In particular the high quality of the charge and nuclear matter distributions calculated from such methods was tested from high energy electron inelastic scattering experiments, even for deformed targets [102,103]. Thus calculations of nuclear density multipole moments q_λ in actinide regions where experimental data are lacking or very uncertain may be helpful for DOM applications. This has been discussed for example in references [104,105].

4-3-2- Contribution from semi-microscopic optical potentials in view to decreasing the phenomenology

Many efforts were devoted to the development of microscopic methods aiming at the construction of optical potentials free of parameters. For a recent approach using the Skyrme forces, see for example the reference [106]. Concerning applied purposes in the actinide region, recent coupled channel calculations have been performed by LAGRANGE and GIROD [107] for ^{232}Th and ^{238}U by using the folding of the complex effective two-body force

derived by JEUKENNE, LEJEUNE and MAHAUX [108] from nuclear matter calculations onto deformed nuclear density distributions obtained from HFB calculations. Only four free parameters remain, two of which have been determined from analogous calculations for ^{208}Pb [109]. The other two parameters - strengths of the real and imaginary central potential - were obtained by adjustment on ^{238}U scattering cross sections measured at 3.4 MeV [80]. Thus a parameter free calculation of the same data has been performed for ^{232}Th which is in good agreement with the experimental results, as shown in figure 5. Further work remains to be done in order to test more generally the predictive power of such calculations where the parametrization problems are largely reduced.

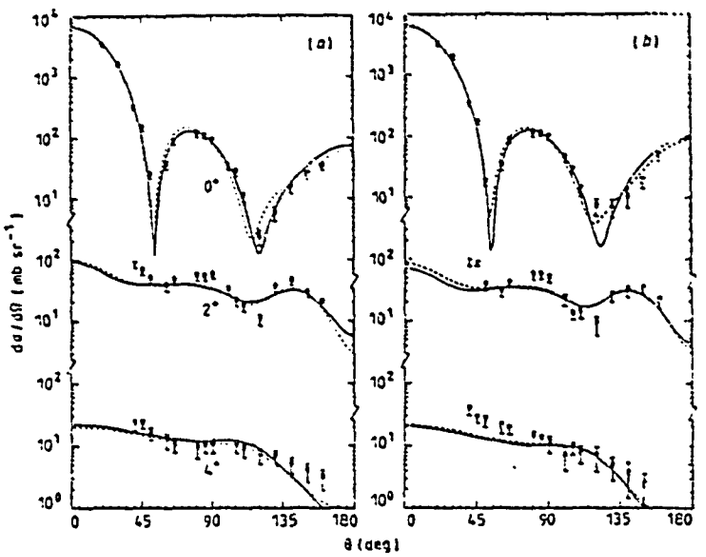

Fig. 5

Figure taken from ref. [107] : scattering cross sections for 3.4 MeV neutrons from 0⁺ ground state, 2⁺ and 4⁺ levels of ^{238}U (a) and ^{232}Th (b). The curves correspond to semi-microscopic (full) or phenomenological (broken) coupled-channel calculations.

5 - USE OF STATISTICAL MODEL AND SYSTEMATICS

For sake of maximum coherence the conventional Hauser-Feshbach statistical model has generally been used in conjonction with the optical model in order to evaluate all the partial cross sections required over a very wide energy range. Apart from the optical model parameters discussed above, a set of other data is needed, namely : i) low-energy average parameters such as D_{obs} and Γ_γ (see Table II for examples) which are useful for normalizing level densities and radiative transmission coefficients at the neutron separation energy, ii) spectroscopic parameters : discrete levels in the low excitation energy region with well defined energy-spin-parity characteristics, supplemented at higher energies by a "continuum" described by means of phenomenologically

optimized level-density formulas (see Table IV), iii) double-humped fission barrier parameters and associated level-densities at the saddle point deformations (see Table V for examples of such data used by the Bologna group in a set of curium isotopes evaluations).

Considerable efforts have been devoted in the last few years to the improvement of our knowledge of these basis data by means of experimental and theoretical studies as well as different systematics made possible thanks to the accumulation of results of all types. Let me comment here on an example concerning low-energy average parameters. A recent benchmark intercomparison study of methods used to determine average parameters from the resolved resonance region has recently been initiated by RIBON [110]. First results showed important systematic discrepancies between different sets of solutions obtained using the same approach for calculating average level spacings, strength functions and radiation widths in the two cases proposed. In particular it has been realized that all best methods, which are based on the distribution of observed neutron widths, systematically overestimated the level spacing by several percent in the actinide region. FRÖHNER [111] has recently pointed out that a possible reason for such a difference seems to be that none of the width-distribution-based estimators so far can account for unrecognised mutiplets. A new prescription derived by him has been applied to resonance parameter data on a set of U and Pu isotopes with the following result : differences relative to the conventional estimation without regard to the multiplet losses were found to be quite small for ^{235}U and ^{238}U whereas for the Pu isotopes effects ranging from 4% (^{239}Pu) to 23% (^{241}Pu) were calculated. Such effects, to be studied more extensively in the actinide region, should be taken into account in statistical calculations where adjustments to level spacings at the neutron separation energy are needed and especially in capture cross-section Hauser-Feshbach calculations. In cases where different experimental estimations give too discrepant values for D_{obs}, results from microscopic calculations may be helpful to adopt a final value. Recent theoretical evaluations of this quantity have been made possible by means of a microscopic method based on shell model potential with pairing interaction treated in the BCS approximations, including collective (rotational) contributions. For example the adopted value for the ^{245}Cm target has been inferred from such considerations by the Bologna group [35]. Systematics concerning the level density parametrization within the whole actinide region have been carried out by the Minsk group [112].

Concerning the parametrization needed for taking account of the fission competition (fission barrier parameters and associated level densities),

extensive reviews have just been published [25,26]. A number of practical aspects associated with the use of statistical model methods for applied purposes in the actinide region have been studied by KONSHIN [27]. Moreover the main problems arising from the need for correct level density formulas at the ground state deformation as well as at the fission barrier saddle point deformations were discussed in a Meeting very recently held at the Brookhaven National Laboratory [113,114]. In the following I will only report on some other ponctual recent developments of interest for evaluation purposes.

5-1- An example of systematics from an extensive set of coherent measurements

During the past decade an extensive set of accurately measured neutron-induced fission cross sections was obtained by Behrens and collaborators. From studies of systematic trends within these basis data, fission cross sections can be hopefully inferred, particularly for the many short-lived actinides that are currently difficult, or impossible, to measure. From first studies done at constant incident neutron energy, reliable correlations were found only within the 3 to 5 MeV neutron energy range corresponding to the fission plateaus [55]. More recently it has been found that comparisons of the basis data made in terms of constant nuclear excitation energy allowed fission cross sections to be inferred over the entire energy range from 0.6

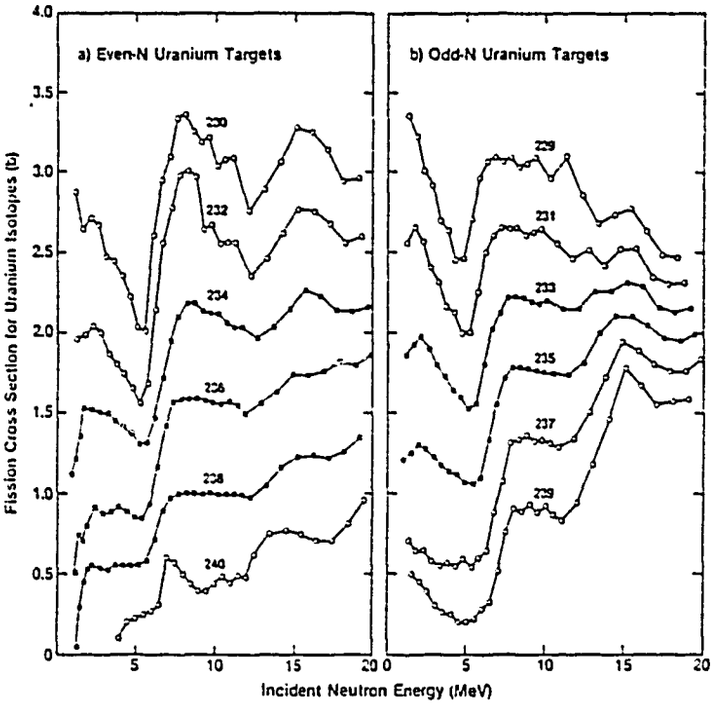

Fig. 6

Fission cross sections of uranium isotopes inferred from systematic trends studied by Behrens [116] in a basis set of measured data considered at given nuclear excitation energies. Only the black points represent the measured data.

to 20 MeV. An example of such an inference obtained with the same accuracy as measurement, i.e. $\lesssim$ 10%, is given for the case of the ^{238}Pu(n,f) cross section in reference [115]. Figure 6 shows a part of results to be published by Behrens concerning an extensive set of uranium, neptunium and plutonium isotopes [116] : even-N uranium targets are treated separately from odd-N uranium targets because of the shift between the corresponding neutron separation energies. The basis data concern only the mass-number sets A = 234, 236,238 and A = 233,235. For the other isotopes the fission cross sections are inferred from the systematics. Such a work is planned to be extended in the near future for the lower-mass elements (thorium, protactinium) and for the higher-mass elements (americium and curium).

5-2- Capture cross sections

The status of fast neutron capture cross sections, with inclusion of the actinide region, was reviewed in a recent Meeting at Argonne [17]. One of the remaining difficulties encountered in their evaluation has been described by WESTON [117] for the target ^{240}Pu : the high measured values of the capture cross sections at around 30 keV are difficult to reproduce with the evaluated average resonance parameters from the resonance region and with the current assumption that $\langle\Gamma_\gamma/D\rangle$ is the same for s-wave and p-wave neutrons. In figure 7 a good fit to the experimental data has been achieved (see dotted line) only on condition that $\langle\Gamma_\gamma/D\rangle$ was $\sim$ 20% higher for p-wave neutrons than for s-wave.

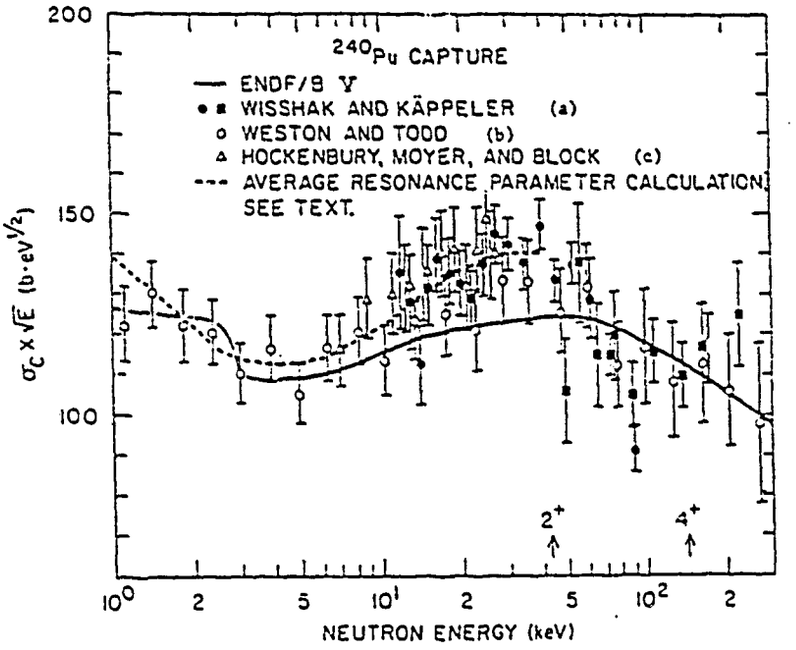

Fig. 7

Figure taken from ref. [117]. Neutron capture cross section of ^{240}Pu mutiplied by the square root of the neutron energy in the neutron energy range from 1 to 300 keV. The experimental data as well as the ENDF/B-V evaluation are illustrated. References : (a) Nucl. Sci. Eng. 66, 363 (1978), also Nucl. Sci. Eng. 69, 39 (1979) ; (b) Nucl. Sci. Eng. 63, 143 (1977) ; (c) Nucl. Sci. Eng. 49, 153 (1972).

A recent experimental data-based systematics of average total radiation widths describes both the s- and p-wave components by means of two different empirical formulas, which are dependent on the atomic number Z, the mass-number A and the neutron separation energy B_n [118].

From a theoretical point of view, statistical evaluations of Γ_γ in the actinide region have been performed by MOORE [119] using a combinatorial level density calculation. This latter suggested that the enhanced density of positive-parity states observed at low excitation energy persists far enough into the continuum to explain a significant difference in s- and p-wave radiation widths for even-even targets.

5-3- Inelastic scattering to vibrational states of the actinides

In the past DOM calculations were applied essentially for interpreting neutron inelastic scattering from the lower-lying rotational states of the actinides. Recently the Lowell group concentrated its efforts upon studies of the higher-lying quadrupole and octupole vibrational states, including level excitation functions up to a few MeV but also, more recently, angular distributions. At the present time the investigations were developed for ^{232}Th, ^{238}U, ^{240}Pu and ^{242}Pu. Careful and critical examination of the band structures is needed in view to applying the coupled-channel approach. As the DOM parametrization studied by the Bruyères-le-Châtel group has been adopted, the only variable parameter in the calculations is the relative band coupling strength, a single adjustable constant which is kept unchanged for all the members of any given band. For sake of comparisons and in order to study the influence of the correlations induced between the coupled-channel neutron widths by the presence of direct interactions, the two following approaches were considered : i) "standard" calculations, in which an incoherent sum of conventional compound nucleus (CN) and direct interaction (DI) cross sections is used, ii) calculations based on the "unified" statistical S-matrix formalism due to TEPEL, WEIDENMULLER et al. [120] for taking account of the above correlations. Many details on the procedure adopted and results obtained are given in references [121] to [124]. Figure 8, taken from reference [121], compares some calculated total inelastic cross sections with experimental results. On figure 9 angular distributions are shown [125] with a comparison between calculations by the Lowell group (curves labelled "S") and calculations by HODGSON [77] (curves labelled "H") based on the less complicated DWBA method but which requires a renormalisation of the calculated direct cross section by comparison with the data in the energy region above about 2 MeV beyond the threshold energy.

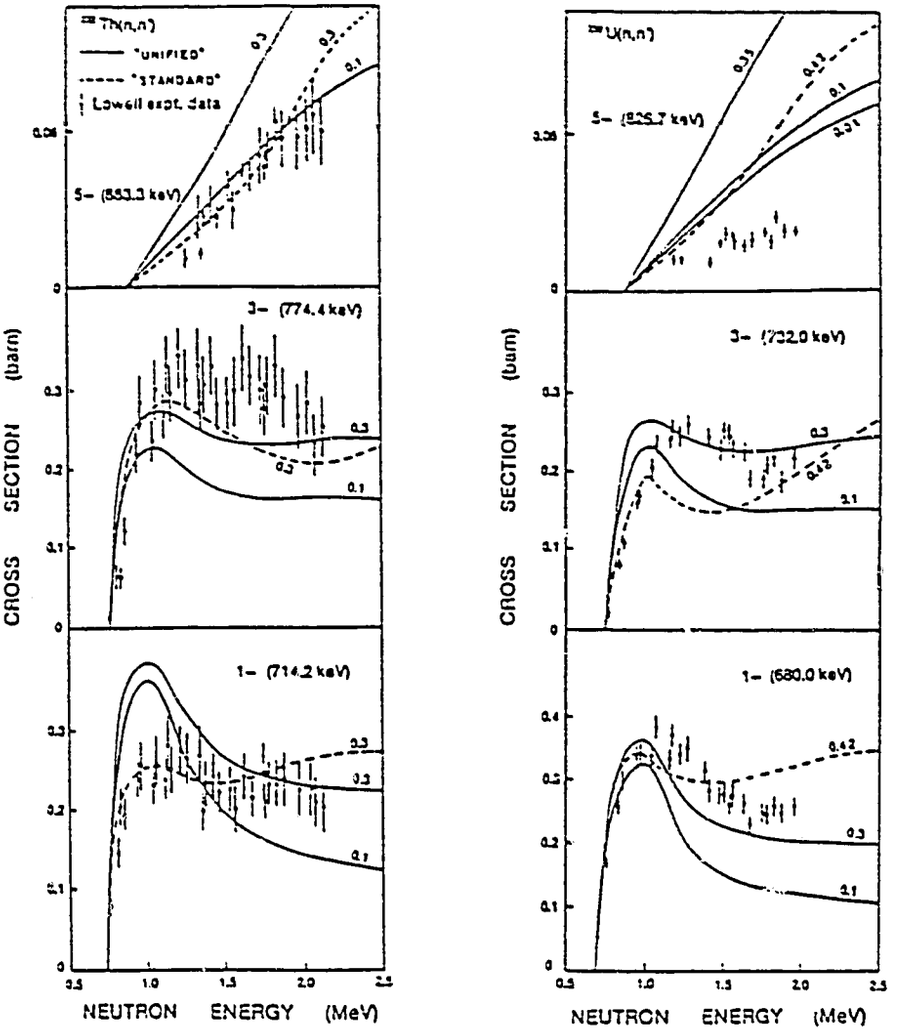

Fig. 8

Figure taken from ref. [121] : comparisons, for $^{232}Th(n,n')$ and $^{238}U(n,n')$ excitation-function data, of the predictions of "unified" S-matrix theory (solid curves, for various values of the coupling strength as indicated beside the respective curves) and of the "standard" (CN + DI) theory (broken curves, with "best-fit" values of the coupling strength as indicated), with the experimental results from $(n,n'\gamma)$ measurements by the Lowell group (points with error bars) for inelastic neutron scattering to states which are members of the K=0- octupole vibrational bands in the respective nuclei. In several instances, the "unified" approach provides a perceptibly better fit to the experimental data than that furnished by the "standard" formalism. Thus, in the case of the ^{232}Th 774.4 keV (3-) level, the "unified" (solid) curves fit the 774-keV data appreciably better than the "standard" calculation, since the broken curve here constitutes a composite of the "standard" results for 774.1 keV (2+) and 774.4 keV (3-) states that are experimentally indistinguishable.

5-4- A test of Lynn's prescriptions for calculating fission cross sections

Lynn's prescriptions for calculating fission cross sections are extensively described for example in reference [26] (see also reference [25]). They result from systematic theoretical interpretations of experimental informations issuing from a number of sources : fission probabilities, inter-

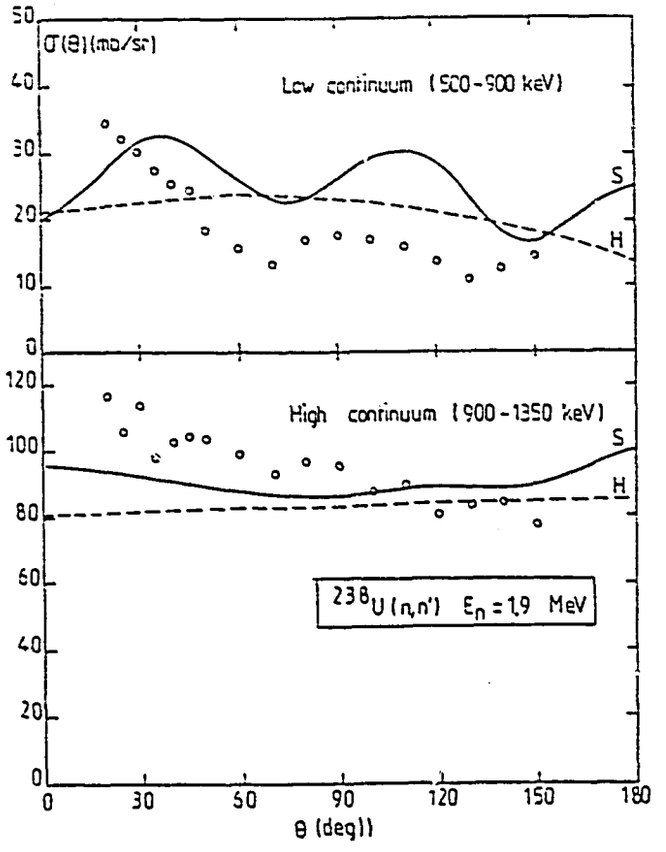

Fig. 9

Neutron inelastic scattering from ^{238}U at the incident neutron energy E_n = 1.9 MeV. This figure [125] represents angular distributions associated with scattering from low and high continuum regions as indicated. Curves "S" are recent calculations by the Lowell group and curves "H" result from calculations including renormalization (see text) by Hodgson. Experimental results are from Knitter, Coppola, Ahmed and Jay, Z. Phys. 244, 358 (1971).

mediate structure in low energy fission cross sections, as well as available fission cross sections measured at higher energies. Comparison of calculations performed along these lines with newly measured fission cross sections allows us to test the proposed methodology and to judge of the progress to be further accomplished. An example of this is commented in reference [44] where calculated and measured fission cross sections are compared in the energy range from 1 to 5 MeV for ^{235}U and ^{245}Cm (see also Table I). Results concerning the $^{245}Cm(n,f)$ reaction are presented on figure 10. The calculation, performed with allowance for readjustments of fission barrier and level density parameters initially chosen in reference [25], failed to reproduce the detailed shape of the fission cross section. A correct fit has been made possible only by requiring level density functions which have continuous first derivatives and which contain some structure for the residual ^{245}Cm nucleus at an excitation energy of $\sim$ 1 to 2 MeV. This "experiment" only confirms that further progress remain to be made at least for evaluating correct energy-dependent level densities [113].

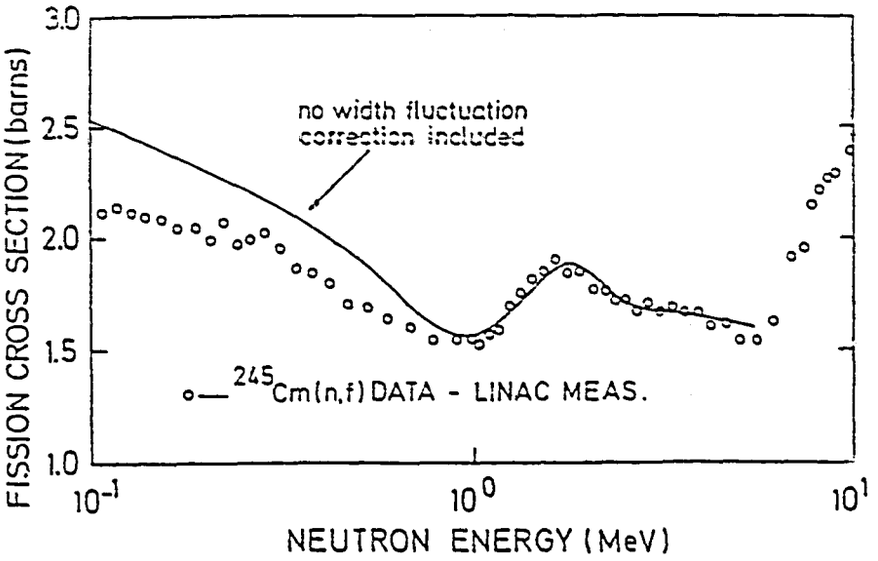

Fig. 10

Figure taken from ref. [44] : Hauser-Feshbach calculation of the ^{245}Cm (n,f) cross section compared to 1979 Linac measurement.

5-5- Role of fission probabilities

Utilization of fission probability (P_f) data, measured from charged particle-induced direct reactions [38,39], to determine fission cross sections was generally made assuming the following expression :

$$\sigma_{nf}(E_n) \simeq \sigma_{CN}(E_n) \times P_f\ (E_n + B_n) \qquad (5)$$

where the compound nucleus formation cross section $\sigma_{CN}(E_n)$ is to be determined from optical model calculations (preferably of the DOM type).

Recently the use of P_f for determining correct fission cross sections below 2 to 3 MeV was based on the more realistic expression [39] :

$$P_f(E) = \sum_{J\pi} \alpha\ (EJ\pi).\ P_f(EJ\pi)$$

in which the spin distributions $\alpha(EJ\pi)$ for charged particle-induced reactions (to be determined from DWBA type calculations for particle stripping or pick-up) are different from those for neutron-induced reactions (to be determined from optical model calculations).

An example of fit obtained in this manner by the Los Alamos group is shown on figure 11.

5-6- (n,xn) and isomer ratio calculations

- An example of possibly useful systematics found in evaluations of (n,2n), (n,n'f).. processes by taking account very carefully of all the bran-

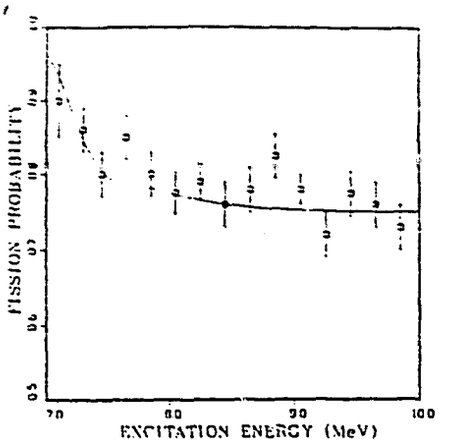

Fig. 11

Figure taken from ref. [130] : comparison of Los Alamos group's fits with fission probabilities measured in the $^{237}Np(^{3}He,d)\ ^{238}Pu(f)$ reaction. In these fits, which were used to determine ^{238}Pu barrier parameters, explicit account was taken of the compound-nucleus spin populations produced in this direct reaction.

ching ratios (for capture as well as neutron and fission channels) associated with the successive residual nuclei is the following. FORT [126] found that the quantity $[a/(B_n-\Delta)]$ containing the three conventional level density parameters is a quasi linear function of the mass-number when plotted separately for even- and odd-mass nuclei. These findings seem to apply to the uranium and plutonium families.

- Another point of interest concerns the necessity found by the Livermore group [127] to take account of many discrete levels in order to converge in calculating isomer ratios for (n,2n) reactions, hence the parallel development of theoretical means for evaluating spectroscopic properties up to high excitation energies. Figure 12 gives an example of this problem concerning the $^{237}Np(n,2n)$ reaction.

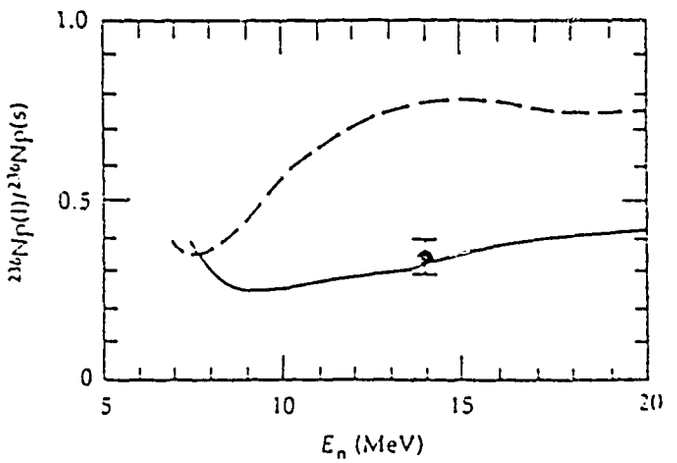

Fig. 12

Figure taken from ref. [127] : $^{237}Np(n,2n)^{236}Np$ isomer ratio as a function of incident neutron energy. The solid curve shows the Livermore group's calculation, which uses 714 levels for ^{236}Np up to 1.2 MeV of energy. The dashed curve shows a calculation made by Mann in 1977. The data point is from the work of Myers et al. (J. Inorg. Nucl. Chem. 37, 637 (1975)).

5-7- An other example of possible contribution from microscopic calculations

Possible contributions from microscopic Hartree-Fock-Bogoliubov (HFB) type calculations have already been reviewed six years ago by GOGNY et al. [128]. In the last few years considerable efforts have been spent in order to extend the application of such methods (see chapter 4-3-1) towards large nuclear deformations. In particular realistic estimations of double-humped fission barriers have been made possible by the extension of calculational methods previously developed for one-centre type basis states to two-centre type basis states. For the first time a realistic interpretation of the nuclear scission has been obtained for the nucleus ^{240}Pu from purely selfconsistent calculations based on the use of the realistic effective two-body interaction D1 [101].

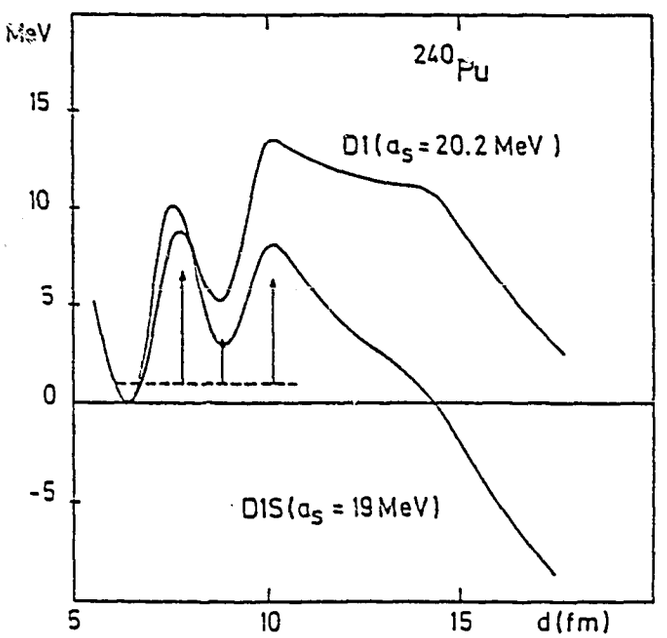

Fig. 13

Figure taken from reference [129] : fission barrier obtained for ^{240}Pu from entirely self-consistent Hartree-Fock-Bogoliubov calculations with two values of the surface coefficient (a_S) of the D1 nucleon-nucleon effective interaction. The barrier is shown as a function of the "distance" between prefragments. Axial asymmetry is included at the inner barrier as well as the left-right asymmetry beyond the isomeric well. Vertical arrows represent model-dependent values deduced from experimental data and referred to the ground state arbitrarily placed at 1 MeV.

This interaction has just been slightly readjusted so as to better reproduce nuclear surface properties. The most recent results obtained by GOGNY's group [129] at Bruyères-le-Châtel are given on figure 13 concerning the double-humped fission barrier of the ^{240}Pu nucleus. It is shown that the calculated results are very close to the experimental (model-dependent) fission barrier,

contrary to all previous tentatives. It is worthwhile to note that dynamical effects are taken into account by the intermediate of deformation-dependent mass coefficients. Moreover such calculations are able to provide a realistic behaviour of the pairing effects as a function of possibly large deformations without any superfluous assumptions. Finally these constrained HFB calculations may easily include the constraint of a given nuclear temperature, hence studies made possible versus the excitation energy. Such calculations are planned to be systematically extended through the actinide region.

6 - CONCLUSION

Considerable efforts - very badly reflected in this paper - have been devoted in the last few years toward accumulating experimental as well as theoretical results in the actinide region. Further progress for applied purposes will be achieved in the near future mainly from the development of systematics using as basis data this accumulated information. In this way future actinide evaluations will be significantly improved. Moreover parallel development of our fundamental knowledge of nuclear structure and neutron interactions, particularly with regard for the fission process, will be helpful in determining the numerous basis parameters needed in the conventional - phenomenological - nuclear models. Finally, if necessary, microscopic methods will help decrease the phenomenology ; hence further progress can be expected.

Only very few examples of trends in evaluating actinide cross sections were given in the present paper. These result from only a small part of the material sent to me prior to this Meeting. I would like to thank the many investigators who have willingly supplied their recent results, in particular those from evaluation groups at Los Alamos, Livermore, Vienna (NDS), Karlsruhe, Lowell, Cadarache, Soreq, Jaeri, Bologna and Bruyères-le-Châtel.

REFERENCES

[1] Transactinide Nuclear Data, Proceedings of an IAEA Advisory Group Meeting (Karlsruhe, 3-7 Nov. 1975) Vienna, IAEA (1976) Vol. I, II and III.

[2] J.E. LYNN, "Theoretical Calculation of Transactinium Isotope Nuclear Data for Evaluation Purposes", Proc. of the Meeting of ref. 1 .

[3] Proceedings of the Course on Nuclear Theory for Applications, Trieste (1978), "Nuclear Theory for Applications", IAEA-SMR-43, ICTP Trieste (1980).

[4] Proceedings of the Inter-Regional Advanced Training Course on Applications of Nuclear Theory, Trieste (1980), "Nuclear Theory for Applications - 1980", IAEA-SMR-68/1, ICTP, Trieste (1981).

[5] Workshop on Nuclear Model Computer Codes, 16 Jan. - 3 Feb. 1984, ICTP Trieste.

[6] Use of Nuclear Theory for Nuclear Data Evaluation (Meeting IAEA, Trieste, Dec. 1975) Vienna, IAEA-150, 1976, Vol. I and II.

[7] Proceedings of an Int. Conf. on Neutron Physics and Nuclear Data for Reactors and Other Applied Purposes", Harwell Sep. 1978, OECD (1978).

[8] Proceedings of the Specialist's Meeting on Nuclear Data of Plutonium and Americium Isotopes for Reactor Applications, Brookhaven National Laboratory, Nov. 20-21, 1978, BNL-50991, NEANDC-L-116 (1979).

[9] Proceedings of the Int. Conf. on "Nuclear Cross Sections for Technology", KNOXVILLE, Oct. 22-26, 1979, NBS special publication 594 (1980).

[10] Proceedings of a Symposium "Physics and Chemistry of Fission 1979", Jülich, 14-18 May 1979, IAEA, Vienna (1980), Vol. I and II.

[11] Proceedings of the Symposium on Neutron Cross Sections from 10 to 50 MeV, Brookhaven, UPTON, May 12-14, 1980, BNL NCS 51245, Vol. I and II.

[12] Translation of Selected Papers, Fifth All-Union Conference on Neutron Physics, 15-19 Sept. 1980, KIEV, INDC (CCP)-161/L, IAEA (1981).

[13] Proceedings of the Specialist's Meeting on Fast-Neutron Scattering on Actinide Nuclei, OECD Paris (1981), NEANDC-158"U".

[14] Proceedings of the International Symposium on Neutron Capture Gamma-Ray Spectroscopy and Related Topics, Grenoble, Sept. 7-11, 1981.

[15] Proceedings of the Conference on Nuclear Data Evaluation Methods and Procedures, Brookhaven National Laboratory, Upton, N.Y. Sept. 22-25, 1980, BNL-NCS-51363, Vol. I and II (1981).

[16] Proceedings of the Meeting on Uranium and Plutonium Isotope Resonance Parameters, INDC (NDS)-129/GJ, IAEA Vienna (1981).

[17] Proceedings of the NEANDC/NEACRP Specialist's Meeting on Fast Neutron Capture Cross Sections, Argonne National Laboratory, April 20-23, 1982, ANL-83-4, NEANDC(US)-214/L.

[18] Proceedings of the International Conference on Nuclear Data for Science and Technology, Antwerp, Sept. 6-10, 1982, Ed. K.H. Böckhoff, CBNM (1983).

[19] Proceedings of the IAEA Advisory Group Meeting on Transactinium Nuclear Data at Cadarache, May 1979.

[20] E.D. ARTHUR, "Calculational Methods Used to Obtain Evaluated Data Above 3 MeV", Proc. of the Conf. of ref. 15, Vol. II, p. 655.

[21] D.G. GARDNER, "Recent Developments in Nuclear Reaction Theories and Calculations", Proc. of the Symposium of ref. 11, Vol. II, p. 641.

[22] P.G. YOUNG, "Application of Nuclear Models to Neutron Cross Section Calculations", Proc. of the Int. Conf. of ref. 18.

[23] J.E. LYNN, AERE-R-7468, UKAEA Harwell (Nov. 1974) "Systematics for Neutron Reactions of the Actinide Nuclei".

[24] J.E. LYNN, "Cross Section Theory for Actinide Nuclei", Proc. of the Int. Conf. of ref. 7, p. 941.

[25] S. BJORNHOLM, J.E. LYNN, "The Double-Humped Fission Barrier", Rev. of Mod. Phys. 52, 725 (1980).

[26] J.E. LYNN, "Theoretical Methods for Calculating the Cross Sections of Fissionable Nuclei" in "Nuclear Fission and Neutron-Induced Fission Cross Sections", A. MICHAUDON (Ed.), Pergamon Press (1981).

[27] V.A. KONSHIN, "Applications of the Nuclear Theory to the Computation of Neutron Cross Sections for Actinide Isotopes", Course of ref. 4, p. 139.

[28] G. MAINO, M. ROSETTI, M. VACCARI, A. VENTURA, "Evaluation of ^{248}Cm Neutron Cross Sections from 10^{-5} eV to 15 MeV", TIB/FICS(83) 4, INDC(ITY)-10 (Nov. 1983).

[29] G. MAINO, M. VACCARI, A. VENTURA, "NUDENS : a Nilsson-Bardeen-Cooper-Schrieffer Code at Finite Nuclear Temperature", Comp. Phys. Com. 29, (1983) 375.

[30] M. CANER and S. YIFTAH, "Curium-248 Neutron Data Evaluation", IA-1383 (Feb. 1983).

[31] M. SEGEV and M. CANER, "A New Formalism for (n,2n) and (n,3n) Cross Sections of Heavy Mass Nuclei", Ann. Nucl. Energy 5, 239 (1978).

[32] V.M. BYCHKOV, V.I. PLYASKIN, Eh.F. TOSHINSKAYA, "Evaluation of the (n,2n) and (n,3n) Cross Sections for Heavy Nuclei with Allowance for Non-Equilibrium Processes", Nuclear Constants 3 (42), 26 (1981), INDC(CCP)-184/L, IAEA (August 1982).

[33] G. MAINO, E. MANAPACE, M. VACCARI, A. VENTURA, "Evaluation of ^{247}Cm Neutron Cross Sections from 10^{-5} eV to 15 MeV, INDC (ITY)-9, ENEA-RT/FIMA (82) 7, (1982).

[34] F.M. MANN, "HAUSER 4 : a Computer Code to Calculate Nuclear Cross Sections", Report HEDL-TME-76-80 (1976).

[35] V. BENZI, G. MAINO, E. MENAPACE, "Nuclear Level Densities with Blocking Effect", Il Nuovo Cimento A66, 1 (1981).

[36] Y. KIKUCHI, "Evaluation of Neutron Nuclear Data for ^{246}Cm and ^{247}Cm", JAERI-M-83-236, NEANDC(J)96/U (January 1984).

[37] G. MAINO, E. MENAPACE, M. VACCARI, A. VENTURA, "Evaluation of ^{246}Cm Neutron Cross Sections from 10^{-5} eV to 15 MeV", INDC(ITY)-8, ENEA-RT/FIMA (82) 5, (1982).

[38] B.B. BACK, H.C. BRITT, O. HANSEN, B. LEROUX, Phys. Rev. C10, 1948 (1974).

[39] B.B. BACK, O. HANSEN, H.C. BRITT, J.D. GARRETT, "Fission of doubly Even Actinide Nuclei Induced by Direct Reactions", Phys. Rev. C9, 1924 (1974).

[40] M. CANER, Y. BARTAL, and S. YIFTAH, "Curium-246 Neutron Data Evaluation", IA-1358 (June 1980).

[41] G. MAINO, T. MARTINELLI, E. MENAPACE, M. MOTTA, M. VACCARI, "Evaluation of ^{245}Cm Neutron Cross Sections from 10^{-5} eV to 15 MeV", CNEN-RT/FI (81) 24 (1981).

[42] V. BENZI, "Neutron Radiative Capture Cross Section Calculations", Proc. of the Int. Conf. of ref. 7, p. 288.

[43] S. IGARASI, T. NAKAGAWA, "^{245}Cm Evaluation", in report IAEA-NDS-12/3 (June 1978).

[44] R.M. WHITE, J.C. BROWNE, "Neutron-Induced Fission Cross Section Measurements and Calculations of Selected Transplutonic Isotopes", Proc. of the Int. Conf. of ref. 18, p. 218.

[45] A. GAVRON, H.C. BRITT, E. KONECNY, J. WEBER, and J.B. WILHELMY; "Γ_n/Γ_f for Actinide Nuclei Using (^{3}He, df) and (^{3}He, tf) Reactions", Phys. Rev. C13, 2374 (1976).

[46] S. IGARASI, T. NAKAGAWA, "Curium-244", in report IAEA-NDS-12/1 (Feb. 1979), revised evaluation.

[47] M. CANER and S. YIFTAH, "Curium-244 Neutron Data Evaluation", IA-1353 (March 1979).

[48] F.H. FRÖHNER, B. GOEL, U. FISHER, H. JAHN, "Neutron Cross Section Evaluation for ^{241}Am, ^{242m}Am, ^{243}Am and ^{244}Cm", Proc. of the Int. Conf. of ref. 18, p. 211.

[49] U. FISHER, report KfK 2907, Karlsruhe (1980).

[50] G. MAINO, T. MARTINELLI, E. MENAPACE, M. MOTTA, M. VACCARI, A. VENTURA, "Evaluation of ^{243}Cm Neutron Cross Sections from 10^{-5} eV to 15 MeV", CNEN-RT/FI (81) 23 (1981).

[51] T. NAKAGAWA, S. IGARASI, "Curium 243", in report IAEA-NDS-12/5 (July 1981).

[52] G. MAINO, E. MENAPACE, M. MOTTA, M. VACCARI,"Evaluation of ^{242}Cm Neutron Cross Sections from 10^{-5} eV to 15 MeV", INDC (ITY)-7, ENEA-RT/FIMA (82) 6, (1982).

[53] E. MENAPACE, A. MONTAGUTI, M. MOTTA and A. VENTURA, "Evaluation of ^{242}Cm in the Resonance Region", CNEN Report RT/FI(79) 2 (1979).

[54] S. IGARASI, T. NAKAGAWA, "Curium 242", in report IAEA-NDS-12/2 (June 1979).

[55] J.W. BEHRENS, "Systematics of Neutron-Induced-Fission Cross Sections in the MeV Range", Phys. Rev. Lett. 39, 68 (1977) ;

J.W. BEHRENS and R.J. HOWERTON, "Predictions of Fission Cross Sections in the 3 to 5 MeV Neutron Energy Range", Nucl. Sc. and Eng. 65, 464 (1978)

[56] E.D. ARTHUR, "Use of the Statistical Model for the Calculation of Compound Nucleus Contributions to Inelastic Scattering on Actinide Nuclei", Proc. of the Meeting of ref. 13, p. 145.

[57] R.B. PEREZ, G. de SAUSSURE, R.L. MACKLIN, J. HALPERIN, "Statistical Tests for the Detection of Intermediate Structure : Application to the Structure of the ^{238}U Neutron Capture Cross Section between 5 keV and 0.1 MeV", Phys. Rev. C20, 523 (1979).

[58] J. JARY, Ch. LAGRANGE, P. THOMET, "Coherent Optical and Statistical Model Calculations of Neutron Cross Sections for ^{238}U between 1 keV and 20 MeV", Report NEANDC(E)174"L", INDC(FR)9/L (1977).

[59] M.S. MOORE, "Fundamentals and Approximations of Multi-level Resonance Theory for Reactor Physics Applications", Proc. of the Course of ref. 3, p. 31.

[60] F. FRÖHNER, "Applied Neutron Resonance Theory", Proc. of the Course of ref. 3, p. 59.

[61] F.H. FRÖHNER, B. GOEL, and U. FISCHER, "Calculation of Average Capture Cross Sections for Actinides - Level-statistical vs. Global Approach", Proc. of the Meeting of ref. 17, p. 116.

[62] A.M. LANE and R.G. THOMAS, Rev. of Mod. Phys. 30 (1958) 257.

[63] K. WISSHAK, F. KÄPPELER, F.H. FRÖHNER, "Review of the ^{240}Pu and ^{242}Pu Unresolved Resonance Region", Proc. of the Meeting of ref. 16, p. 165.

[64] F.H. FRÖHNER, "New Techniques for Multi-level Cross Section Calculation and Fitting", Proc. of the Conf. of ref. 15, vol. I p. 375.

[65] Ch. LAGRANGE, J. JARY, "Coherent Optical and Statistical Model Calculations of Neutron Cross Sections for ^{240}Pu and ^{242}Pu between 10 keV and 20 MeV", report NEANDC(E)198L, INDC(FR)30L (1978).

[66] J. JARY, Ch. LAGRANGE, C. PHILIS, "^{242}Pu : Preliminary Evaluation with Consideration of ^{240}Pu and some Sensitivity Results", Proc. of the Meeting of ref. 8, p. 83.

[67] H. MATSUNOBU, Y. KANDA, M. KAWAI, T. MURATA, and Y. KIKUCHI", "Simultaneous Evaluation of the Nuclear Data for Heavy Nuclides", Proc. of the Int. Conf. of ref. 9, p. 715.

[68] W.P. POENITZ, J.F. WHALEN, and A.B. SMITH, "Total Neutron Cross Sections of Heavy Nuclei", Proc. of the Int. Conf. of ref. 9, p. 698.

[69] F. KÄPPELER, L.D. HONG, H. BEER, Proc. of the Meeting of Ref. 8, p.49 .

[70] J. RAYNAL, "Optical Model and Coupled-Channel Calculations in Nuclear Physics", International Atomic Energy Agency, Vienna, Austria, IAEA-SMR-9/8 (1972) ; see also ref. 5 .

[71] P.G. YOUNG, E.D. ARTHUR, and D.G. MADLAND, "Application of Nuclear Models", Proc. of the Int. Conf. of ref. 9, p.639 .

[72] J.P. DELAROCHE, Ch. LAGRANGE, J. SALVY, "The Optical Model with Particular Consideration of the Coupled-Channel Optical Model", Proc. of the Meeting of ref. 6, Vol. II, p. 251 .

[73] A. PRINCE, "Phenomenological optical potentials and optical model computer codes", Nuclear Theory for applications, IAEA, Vienna, IAEA-SMR-43 (1980), pp 149-164

[74] Ch. LAGRANGE, "Applications of the coupled-channel optical model for the prediction of fast neutron scattering cross sections with emphasis on odd actinides", Proc. of the Meeting of ref. 13, p. 96 .

[75] G.R SATCHLER, Direct Nuclear Reactions (Oxford University Press, New York, 1983) .

[76] P.E. HODGSON, "The Neutron Optical Model in the Actinide Region", Proc. of the Meeting of ref. 13, p.69 .

[77] P.E. HODGSON, "The inelastic scattering of neutrons by Uranium 238", Oxford University report 85/82, and private communication .

[78] D.G. MADLAND and P.G. YOUNG, "Neutron-nucleus optical potential for the actinide region", Proc. of the Int. Conf. of ref. 7, p. 349 .

[79] Ch. LAGRANGE, "Effets systématiques des déformations nucléaires sur la section efficace totale neutron-noyau", J. de Physique Lettres 35 (1974) p. L-111 .

[80] G. HAOUAT, J. LACHKAR, Ch. LAGRANGE, J. JARY, J. SIGAUD and Y. PATIN, "Neutron Scattering Cross Sections for ^{232}Th, ^{233}U, ^{235}U, ^{238}U, ^{239}Pu and ^{242}Pu between 0.6 and 3.4 MeV", Nucl. Sci. and Eng. 81, 491 (1982) .

[81] Ch. LAGRANGE, "On the Usefulness of coupled channel calculations for actinide nuclei", in Report of ref. 82, p. 78 .

[82] "Progress Report of recent works on actinide nuclear data at Bruyères-le-Châtel", Report NEANDC (E) 211 L, INDC (FR) 41/L (march 1981) .

[83] Ch. LAGRANGE, O. BERSILLON, D.G. MADLAND, "Coupled-Channel Optical Model Calculations for evaluating neutron cross sections of odd-mass actinides", Nucl. Sci. and Eng. 83, 396 (1983) .

[84] Ch. LAGRANGE, "Determination of a coherent parameter set for coupled channel calculations of ^{238}U neutron cross sections from 10 keV to 20 MeV", Acta Phys. Slov. 26, 32 (1976) .

[85] H. ABOU YEHIA, J. JARY, J. TROCHON, "Calculation of ^{232}Th neutron cross sections from 0.3 MeV to 2.4 MeV including a fission channel analysis", Report NEANDC (E) 204 "L", INDC (FR) 34/L (1979) .

[86] H. DERRIEN, J.P. DOAT, E. FORT, D. LAFOND, "Evaluation of ^{237}Np neutron cross sections in the energy range from 10^{-5} eV to 14 MeV", Report INDC (FR) 42/L (Sept. 1980) .

[87] H. DERRIEN, "Evaluation of ^{238}Pu neutron cross-sections in the energy range 10^{-5} eV to 14 MeV", Report INDC (FR)-57/L (Sept. 1982) .

[88] "Evaluation of Nuclear Data for ^{242}Pu in the 10^{-5} eV - 15 MeV Neutron Energy Region", Ed. A.K. KRASIN, INDC (CCP)-150/LJH, IAEA (July 1980) .

[89] G. VASILIU, S. MATEESCU, S. RAPEANU, V. AVRIGEANU, M. CIODARU, N. DRAGAN, T. STADNICOV, O. BUJOREANU, "Nuclear Data Evaluation for ^{233}Pa", INDC (ROM) 12, IAEA (May 1980) .

[90] D.G. MADLAND and P.G. YOUNG, "Evaluation of n + ^{242}Pu Reactions from 10 keV to 20 MeV", Proc. of the Meeting of ref. 8 . .

[91] E.D. ARTHUR, "Calculation of ^{239}Pu Neutron Inelastic Cross sections", Proc. of the Int. Conf. of ref. 18, p. 556 .

[92] E.D. ARTHUR, P.G. YOUNG, D.G. MADLAND, R.E. McFARLANE, "Evaluation of n + ^{239}Pu nuclear data for revision 2 of ENDF/B.V", LA-9873-MS (Oct. 1983) .

[93] H. DERRIEN, "Some aspects of the evaluation of ^{237}Np, ^{238}Pu and ^{241}Am capture cross sections in the unresolved region", Proc. of the Meeting of ref. 17, p. 379 .

[94] H. DERRIEN, Cadarache, private communication.

[95] A. SMITH, W. POENITZ, and R. HOWERTON, "Evaluation of the ^{238}U neutron total cross section", ANL/NDM-74 (dec. 1982) .

[96] W.P. POENITZ and J.F. WHALEN, "Neutron Total Cross Section Measurements in the Energy Region from 47 keV to 20 MeV", ANL/NDM-80 (may 1983)

[97] L.F. HANSEN, Ch. LAGRANGE, R.C. HAIGHT, B.A. POHL, C. WONG, "Measurements and calculations of Neutron Scattering in the Actinide Region", Washington DC Meeting of the APS 23-26 April 1984 .

[98] L.F. HANSEN, I.D. PROCTOR, D.W. HEIKKINEN, V.A. MADSEN, "Nuclear deformation in the actinide region by proton inelastic scattering", Phys. Rev. C25, 189 (1982) .

[99] L.F. HANSEN, S.M. GRIMES, C.H. POPPE, C. WONG, "Charge exchange (p,n) reactions to the isobaric analog states of high Z nuclei : $73 \leq Z \leq 92$", Phys. Rev. C28, 1934 (1983) .

[100] Ch. LAGRANGE, "Results of Coupled-Channel Calculations of the Neutron Cross Sections of a Set of Actinide Nuclei", Report NEANDC(E)228"L", INDC(FR)56/L (1982).

[101] D. GOGNY, Proc. Int. Conf. on Nuclear Self-consistent fields, Trieste 1975, ed. G. RIPKA and M. PORNEUF (North Holland, Amsterdam 1975), p.333 .

[102] M. GIROD, B. GRAMMATICOS, "Interpretation microscopique de la densité de transition du ^{58}Ni et du ^{152}Sm", Comptes-rendus de la 6ème Session d'Etudes Biennale de Physique Nucléaire,Aussois (France), 1981 .

[103] B. FROIS, S. TURCK-CHIEZE, J.B. BELLICARD, M. HUET, P. LECONTE, X.H. PHAN, I. SICK, J. HEISENBERG, M. GIROD, K. KUMAR, B. GRAMMATICOS, "The effects of triaxial deformations in the structure of the $2^+_{(1)}$ transition charge density in ^{58}Ni, "Phys. Lett. 122B, 347 (1983) .

[104] M. GIROD, D. GOGNY, "Microscopic calculation of deformation properties in the actinide region", in Report of ref. 82, p.87, and Report of ref. 104, p. 50 .

[105] "Status of activities on actinide Nuclear Data at Bruyères-le-Châtel", Report NEANDC (E) 227/L, INDC (FR) 54/L (march 1982) .

[106] SHEN QINGBIAO, TIAN YE, ZHANG JINGSHANG and ZHUO YIZHONG, "Microscopic Optical potential calculation with Skyrme forces", Proc. of the Int. Conf. of ref. 18, p. 565 .

[107] Ch. LAGRANGE and M. GIROD, "Semi-microscopic calculations of inelastic neutron scattering from heavy deformed nuclei", J. Phys. G : Nucl. Phys. 9, (1983) L 97 - L 102 .

[108] J.P. JEUKENNE, A. LEJEUNE, C. MAHAUX, "Optical Model Potential in finite nuclei from Reid's hard core interaction", Phys. Rev. C16, 80 (1977) .

[109] Ch. LAGRANGE, J. C. BRIENT, "Interprétation semi-microscopique de la diffusion élastique et inélastique de nucléons par ^{208}Pb", J. Physique 44 (1983) 27 .

[110] P. RIBON, A. THOMPSON, "A Benchmark test of computer codes for calculating average resonance parameters", Proc. of the Int. Conf. of ref. 18, p.628 . See also Proc. of the Meeting of ref. 16, p. 249 .

[111] F.H. FRÖHNER, "Level density estimation with account of unrecognised multiplets applied to Uranium and Plutonium resonance data", Proc. of the Meeting of ref. 16, p. 103.

[112] G.V. ANTSIPOV, V.A. KONSHIN, V.M. MASLOV, "Level Density of Transactinium Isotopes", INDC (CCP)- 182, IAEA (february 1982) .

[113] Proc. of the "IAEA Advisory Group Meeting on Basic and Applied Problems of Nuclear Level Densities", Brookhaven National Laboratory, April 11-15 1983, BNL-NCS-51694 (June 1983) .

[114] J.E. LYNN, "Fission Cross Sections and the Nuclear Level Density", Proc. of the Meeting of ref. 112, p. 345 .

[115] J.W. BEHRENS, "Inferred ^{238}Pu (n,f) cross section in the MeV Range", Trans. Am. nucl. Soc. 43, 722 (1982) .

[116] J.W. BEHRENS, N.B.S Washington, private communication , and to be published.

[117] L.W. WESTON, "Review of fast-neutron capture cross section of the higher plutonium isotopes and ^{241}Am", Proc. of the Meeting of ref. 17, p. 355 .

[118] ZHUANG YOUXIANG, WANG SHUNUAN, ZHOU DELIN, JIA ZHIZE, "Systematics of Average Total Radiative Widths for s- and p-Wave Resonances", Proc. of the Int. Conf. of ref. 18, p. 632.

[119] M.S. MOORE, "Systematics of s-and p-wave Radiative Capture Widths for Transactinium Isotopes" , Proc. of the Int. Conf. of ref.7, p.313 .

[120] C.A. ENGELBRECHT and H.A. WEIDENMÜLLER, Phys. Rev. C8, 859 (1973) ; J.W. TEPEL, H.M. HOFMANN and H.A. WEIDENMÜLLER, Phys. Letters 49B, 1 (1974); H.M. HOFMANN, J. RICHERT, J.W. TEPEL and H.A. WEIDENMÜLLER, Ann. of Physics 90, 391 and 403 (1975) ; H.M. HOFMANN, T. MARTELMEIER, M. HERMAN and J.W. TEPEL, Z.Phys. A297,153 (1980) .

[121] E. SHELDON, D.W.S. CHAN, "Evaluation of (n,n') scattering cross sections from 0.8 to 2.5 MeV for higher collective bands of ^{232}Th and ^{238}U in "Standard" (CN+DI) and "Unified" (Weidenmüller S-matrix) formalisms", Proc. of the Meeting of ref. 13, p. 169 .

[122] D.W.S CHAN, J.J. EGAN, A. MITTLER and E. SHELDON, "Analyses of fast neutron inelastic scattering cross sections to higher (vibrational) states of ^{232}Th and ^{238}U . I. Standard formalism", Phys. Rev. C26, 841 (1982) .

[123] D.W.S CHAN and E. SHELDON, "Analyses of fast neutron inelastic scattering cross sections to higher (vibrational) states of ^{232}Th and ^{238}U .II-Intrinsic unified formalism", Phys. Rev. C26, 861 (1982) .

[124] E. SHELDON, "Level excitation function data for fast neutron scattering on Actinide Nuclei calculated with the unified statistical S-matrix formalism" , Proc. of the Int. Conf. of ref. 18, p. 518.

[125] E. SHELDON, University of Lowell, private communication .

[126] E. FORT, Cadarache, private communication, and to be published.

[127] D.G. GARDNER, M.A. GARDNER, and R.W. HOFF, "Isomer-ratio calculations for neutron-induced reactions on deformed nuclei : the effect of recent discrete-level modeling studies", Annual Report FY 83, UCAR-10062-83/1 (LLNL), p.51 .

[128] D. GOGNY, J. DECHARGE, M. GIROD, "Apport des calculs microscopiques self-consistants dans le domaine de l'évaluation", Proc. of the Int. Conf. of ref.7, p. 396 .

[129] J.F. BERGER, M. GIROD, D. GOGNY, "Microscopic analysis of collective dynamics in low energy fission", invited paper at the Int. Conf. on Theoretical approaches to heavy ion reaction mechanisms, Paris 14-18 may 1984 ; and private communication .

[130] E.D. ARTHUR, Los alamos, private communication.

Review Paper 5

PROGRESS IN TRANSACTINIUM ISOTOPE NEUTRON DATA EVALUATION

V.A. KONSHIN
Institute of Nuclear Power Engineering
of the BSSR Academy of Sciences,
Minsk, Sosny, Union of Soviet Socialist Republics

Abstract

A further development of methods for evaluating neutron cross-sections has been discussed, in particular, an optical-statistical approach for calculating and predicting neutron cross-sections, generalization of the coupled-channel method, systematics of nuclear level density, a method for fission cross-section calculation. Some conclusions concerning the possibility of theoretical prediction of neutron cross-sections have been made.

I. INTRODUCTION

For the last years in many laboratories a number of methods for evaluating neutron cross-sections have been elaborated, based on new and often complicated ideas. New mathematical programs using these methods have been developed. As a result, the evaluations of neutron cross-sections have been raised to a new and higher level. It does not mean, however, that all the problems are solved and we can predict neutron cross-sections with a satisfactory accuracy. Let us consider some problems associated with evaluation methods.

2. DETERMINATION OF AVERAGE PARAMETERS FROM THE REGION OF RESOLVED RESONANCES

For evaluating average parameters, methods are used which often yield different values even for the same set of resonance parameters [I] . The reason for a discrepancy lies mainly in the omission of weak resonances and of multiplet ones.

The methods applied at present for evaluating average parameters from the data on resolved resonances fall into four groups: simulation of a set of resonance parameters by the Monte-Carlo method, an evaluation method according to the position of energy levels (the Δ_3 -statistics method) [2] ; methods based on the properties of neutron width distribution [3, 4] ; a method using the properties of neutron width and resonance spacing distributions [5]. Methods [4] and [5] are better than methods [2] , [3] from the point of view of taking into account the experimental data directly used for evaluation (consideration of energy dependence of the resonance detecting threshold, consideration of the threshold diffusivity), and the bulk of evidence on statistical properties of resonance parameters used. A method elaborated by Fröhner [5] seems to be the most reliable in determining average parameters since it allows one to make corrections for the omission of resonances due to small neutron widths and multiplicity of peaks.

The use of methods [2] - [5] for processing the ^{235}U [3] experimental data in which the identification of resonance spins had been made yielded the following results on $\langle D \rangle$ in the range from 0.3 to 70 eV: method [2] - 0.491 ± 0.035 eV; method [3] - 0.447 ± 0.036 eV; method [4] - 0.448 ± 0.011 eV; method [5] - 0.445 ± 0.016 eV.

The values of $\langle D \rangle$ obtained by methods [5] and [4] almost coincide, which demonstrates an insignificant omission of resonances on multiplicity. A further study associated with the generalization of method [5] for the case of a mixed set of the s- and p-resonances is being carried out in our laboratory.

The parametrization and representation of a resonance structure of neutron cross-sections are of great importance in calculating the self-shielding factors for different temperatures and fuel compositions. An accuracy of 1% in calculation of the self-shielding factors depending on dilution and 5% for temperature effects is required for the development and designing of fast reactors [6, 7] .

The method for obtaining average parameters used almost in all evaluations including ours is not deprived of certain disadvantages, in particular for odd nuclei which were discussed in Ref. [8]. From the theoretical point of view, there are no reasons to suppose that the fluctuations in an average cross-section are specified by the fluctuations of the given specific width (we assume rather arbitrarily that the given width, e.g., $<\Gamma_f>^{4-}$ for ^{235}U fluctuates in order to explain fluctuations in the cross-section). There are no reasons either to assume that the neutron widths Γ_n^0 averaged over small energy intervals obey the Porter-Tomas distribution for their local values. In view of rigorous theoretical substantiations being unavailable for this model, it may be considered as some parametrization of average values. It can accurately enough reproduce average cross-sections, however, there are no reasons to expect that it would give sufficiently accurate values for the self-shielding factors since the parametrization is ambiguous and besides, no information on self-shielding was involved when obtaining these parameters.

Therefore, it is necessary that evaluation of average parameters in the range of unresolved resonances rest upon not only average cross-sections but also on the experimental data on transmission functions and fission self-indication, though, at present, the experimental data are very sparse and mainly concern ^{238}U. Application of the experimental data on transmission in the energy range of unresolved resonances for ^{238}U is exemplified by Ref. [9]. The authors of this study have shown that, in order to describe the experimental data on transmission functions in the neutron energy range of I - 46 keV with an accuracy approximating the experimental errors, one can choose a set of parameters not depending on neutron energies and not contradicting the evaluations available in the region of resolved resonances. The initial values of average parameters for ^{238}U are: $S_0 = 1.10 \cdot 10^{-4}$; $S_1 = 2.3 \cdot 10^{-4}$; $R' = 9.28$ fm; $<D> = 22.9$ eV; $\overline{\Gamma_\gamma} = 21.6$ meV, those obtained

by processing the experimental data on transmission functions are:

$S_0 = 1.14 \cdot 10^{-4}$; $S_1 = 2.07 \cdot 10^{-4}$; $R' = 9.13$ fm (groups 10, 11) and 9.28 fm (groups 12, 13); $\langle D \rangle = 21.6$ eV; $\overline{\Gamma}_\gamma = 21.6$ meV. Unfortunately, for all the rest transactinides (except ^{239}Pu and partially ^{235}U), no experimental data on transmission functions required for an unambiguous choice of average resonance parameters seem to be available.

3. CONSIDERATION OF THE ($n, \gamma f$) PROCESS IN CALCULATION OF RADIATIVE-CAPTURE WIDTHS AND AVERAGE CROSS-SECTIONS OF FISSIONABLE NUCLEI

In calculation of the radiative capture cross-section for fissionable nuclei with a negative fission threshold, the consideration of the ($n, \gamma f$) process is of importance. After emitting the first γ-ray there is a possibility of deexcitating the nucleus through neutron emission and by fission. The neutron emission is possible in the case when after emission of the first gamma-ray the excitation energy is higher than the neutron separation energy. Therefore, when calculating the transmission coefficient for radiative capture by use of the cascade theory of gamma-ray emission, it is necessary to consider the competition of the ($n, \gamma n'$) and ($n, \gamma f$) reactions with radiative capture [10].

The consideration of the ($n, \gamma n'$) process when calculating the transmission coefficient for radiative capture turned out to be appreciable only at neutron energies higher than the average energy of the first cascade gamma-rays ($\varepsilon_\gamma \sim 1$ MeV). Thus, the calculation has shown that for ^{242}Pu the consideration of this process at neutron energy of 0.5 MeV reduces $\overline{\Gamma}_\gamma$ only by 0.5%.

The consideration of the ($n, \gamma f$) process is more significant for the fissionable nuclei when the fission of the excited compound nucleus is energetically possible after emitting the primary gamma ray.

The weak energy dependence of radiative capture width for both types of spectral factors at incident neutron energies up to I MeV where there is an experimental information on cross-section for radiative capture, makes none of the two preferable to the other. But the type of spectral factor affects considerably the calculated values of widths $\langle \Gamma_{\gamma f} \rangle$.

The following values were obtained experimentally for ^{239}Pu : $|\Gamma_{\gamma f}^{0+} - \Gamma_{\gamma f}^{1+}| < 4$ meV [II], $\Gamma_{\gamma f}^{1+} = 4.1 \pm 0.9$ meV [I2] and $\Gamma_{\gamma f}^{1+} = 6.1 \pm 2.9$ meV [I3] . Results of calculations by use of different models of level density and different types of spectral factor are given in Table I. The calculation using the spectral factor with the Lorentz dependence generalized for deformed nuclei yields the values of $\Gamma_{\gamma f}$ which agree with the experimental values within their errors.

Table I Theoretical and experimental values of $\Gamma_{\gamma f}$ widths for ^{239}Pu

Level density model and type of spectral factor	$\langle \Gamma_{\gamma f} \rangle^{0+} - \langle \Gamma_{\gamma f} \rangle^{1+}$, meV	$\langle \Gamma_{\gamma f} \rangle^{1+}$, meV
Fermi-gas model; Lorentz factor	5.94	5.46
Fermi-gas model; Weisskopf factor	I0.59	II.55
Fermi-gas model with collective modes included; Lorentz factor	3.62	3.II
Fermi-gas model with collective modes included; Weisskopf factor	7.25	7.28
Superfluid model with collective modes included; Lorentz factor	5.80	5.24
Superfluid model; Weisskopf factor	II.42	I3.37
Experiment /II/	< 4 meV	-
/I2/	-	4.1 ±0.9
/I3/	-	6.1 ±2.9

Thus, the stronger dependence of the calculated widths $\langle \Gamma_{\gamma f} \rangle^{JT}$ on type of the spectral factor in comparison with $\langle \Gamma_\gamma \rangle$ makes it possible to conclude that, within the accuracy of the available experimental data on $\Gamma_{\gamma f}$, the Weisskopf representation of the spectral factor on the whole leads to the worse agreement with the experimental data on the $\Gamma_{\gamma f}$ widths than the Lorenz dependence does, while the latter ensures a satisfactory agreement with the experimental values of $\Gamma_{\gamma f}$. It should be noted that this conclusion depends on values of the parameters (B_n, Δ, $\langle D \rangle$ and especially T_f) used in the calculations. Therefore, in calculating the cross-sections it is of great importance to use the parameters optimized over the whole set of experimental data. That is why the spectral factor in the Lorentz form was used below in calculating the transmission coefficients for radiative capture for the purpose of nuclear data evaluation.

The consideration of the ($n, \gamma f$) and ($n, \gamma n'$) processes leads, as could be expected, to a change in energy dependence of radiative widths $\langle \Gamma_\gamma \rangle$ (Fig. I). This change becomes rather abrupt at energies above I MeV (at I MeV the consideration of these processes leads to a decrease of $\langle \Gamma_\gamma \rangle$ by a factor of I.5). Naturally, such a change of $\langle \Gamma_\gamma \rangle$ also affects the cross-section of radiative capture.

The analysis made by us has shown that in the case of nuclei with a negative fission threshold, the allowance for the competition of fission and inelastic scattering with the gamma-deexcitation only after emitting the primary gamma-rays holds true only at low energies of incident neutrons ($E_n \leq 0.5$ MeV). It is associated with the fact that at higher energies of incident neutrons there is also a certain probability of nuclear fission after emitting two successive gamma-rays. So, in calculating the radiative capture width the competition of fission and inelastic scattering with gamma-deexcitation was considered for one more cascade [I4]. It allowed the radiative capture widths for the ($n, \gamma f$) and ($n, \gamma n'$) processes to be

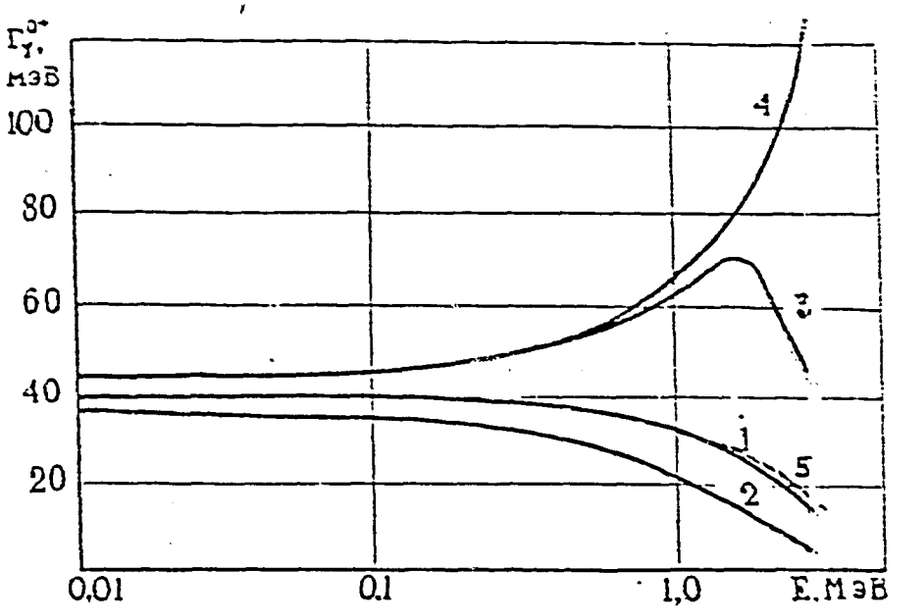

Fig. I. Calculated energy dependence of Γ_γ^{0+} for ^{239}Pu: 5 - with the $(n,\gamma f)$ and $(n,\gamma n')$ processes included, Lorentz spectral factor; 2 - with the $(n,\gamma f)$ and $(n,\gamma n')$ processes included, Weisskopf spectral factor; 3 - with the $(n,\gamma n')$ process alone included, Lorentz spectral factor; 4 - without including $(n,\gamma f)$ and $(n,\gamma n')$ processes, Lorentz spectral factor; 1 - the same conditions as for curve 5 and with the $(n,2\gamma f)$ process additionally included.

calculated with considerable accuracy. The majority of the second cascade gamma-rays is emitted at a nucleus excitation energy below B_n + 0.5 MeV as at higher excitation energies the fission and inelastic scattering processes become predominant. As the average gamma-ray energy $E_\gamma \geqslant 1$ MeV, the nucleus excitation energy becomes lower than the fission threshold after two subsequent cascades of deexcitation and the processes other than gamma-deexcitation are impossible. A comparison of the radiative capture widths obtained for the nuclei ^{238}U and ^{239}Pu with the results of calculations including the competition of fission and inelastic scattering only after the first cascade of gamma-deexcitation shows that at low energies of incident neutrons the widths practically agree (see Fig. 2).

At higher energies the behaviour of Γ_γ is different. For ^{238}U which has a positive fission threshold, the allowance for the competition of the fission and inelastic scattering processes in the second cascade of gamma-deexcitation leads to a slight de-

crease in the radiative capture width, whereas in the case of ^{239}Pu the reduction of Γ_γ is more essential (by about 5%).

The correct consideration of the competition of fission and inelastic scattering at nucleus excitation energies higher than B_n is also of importance. It can be seen in Fig. 2, where the results of calculations made with and without allowance for a contribution from the ~~second cascade~~ gamma-rays emitted at nucleus excitation energies higher than B_n into Γ_γ are compared.

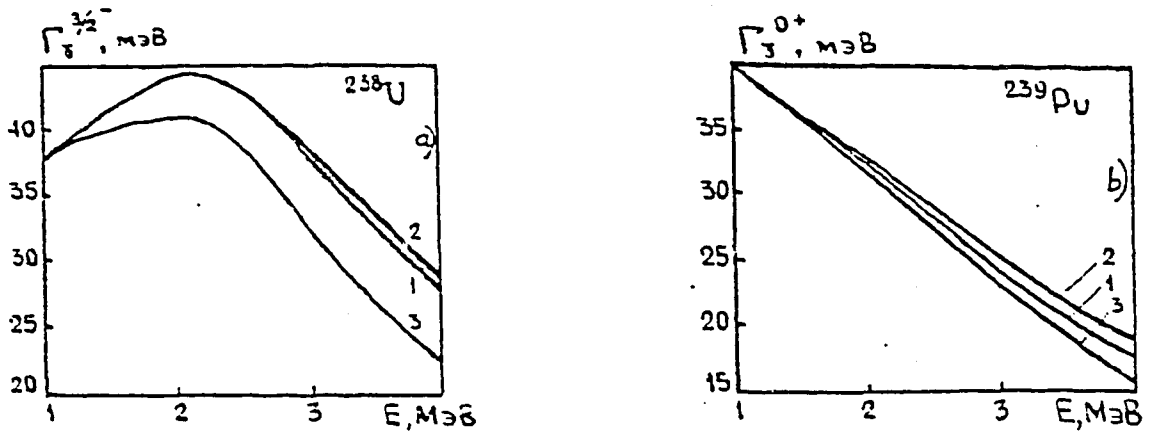

Fig. 2. Comparison between various approaches to calculating the radiative capture widths: (a) $\Gamma_\gamma^{3/2^-}$ - for the target nucleus ^{238}U ; (b) $\Gamma_\gamma^{0^+}$ for the target nucleus ^{239}Pu; curve 1 - - calculations with allowance for the competitions of fission and inelastic scattering after two cascades of gamma-rays; curve 2 - the same but only after the first cascade of gamma-rays; curve 3 - according to [20].

4. APPLICATION OF THE COUPLED-CHANNEL METHOD TO EVALUATION OF NEUTRON CROSS-SECTIONS FOR FISSIONABLE NUCLEI

The heavy fissionable nuclei are strongly deformed and so the neutron scattering cannot be adequately described by the convenient optical model which does not consider the direct connection between the orbital motion of an incident neutron and the nuclear rotation, which leads to a direct excitation of nuclear rotational levels in inelastic scattering.

For the heavy nuclei the coupling between the different channels is rather strong and the coupled-channel method is efficient.

The coupled-channel method [I5] considering this connection describes more correctly the neutron interaction with the deformed nuclei.

Born's distorted wave method [I6] is a success in cases when the nuclear deformation β is small ($\beta = 0.I$). At higher β the differential cross-sections of the elastically and inelastically scattered neutrons are described inadequately by the distorted wave method, as the low-lying collective states affect not only the inelastic scattering processes but also the elastic channel. Therefore, in this case it is more preferable to use the coupled channel method, i.e. to seek a precise solution of the quantum-mechanical problem on scattering by the deformed nonspherical potential with an intrinsic structure.

The spherical optical model does not take into account the intrinsic nuclear structure (i.e. the structure of a potential by which the scattering takes place). Therefore, the elastic scattering by the potential is a single direct process which can be calculated in this model. At the same time the experimental data on angular distribution of inelastically-scattered neutrons (their preferable emission along the direction of incident neutron motion is borne in mind) show that a substantional fraction of inelastic scattering results from the direct mechanism, pointing to a necessity of including an intrinsic structure in the optical model potential.

The application of the coupled-channel method results in the necessity of developing complicated mathematical programs. Such programs have been worked out abroad [I5, I7, I8] and in our country [I9, 20, 2I] . The measures taken for the reduction of the numerical calculation time made it possible to join the coupled-channel method with the optimization problem of searching potential parameters using the χ^2-criterion. The calculation time of neutron cross-sections and angular distributions for ^{238}U on a BESM-6 computer

was ~ 3 min and 20 min at energies of 0.1 MeV and 10 MeV, respectively. The potential parameters were optimized by the searching program which uses the conjugate-gradient method, parameters being fitted by the experimental data simultaneously over the whole energy range from 1 keV to 15 MeV rather than in individual points. An automatic search for parameters of the nonspherical potential was carried out for eight parameters: V_R, W_D, z_R, z_D, a_R, a_D, β_2, β_4 [21].

The procedure of searching for a potential common for the actinide group consisted in the following. At the first stage an optimal set of potential parameters was determined for the nucleus of ^{238}U the experimental information for which is most extensive. Moreover, the zero spin of the ^{238}U ground state makes the search less time-consuming. The estimated values for S_c, S_1 and σ_p within the energy range of a few keV [22] and for σ_t at energies ranging from 1 keV to 15 MeV were used as experimental data which were a basis for obtaining the potential parameters. The most reliable experimental data on angular distribution of elastically -and inelastically-scattered neutrons at 2.5 and 3.4 MeV [23, 24] where the contribution from the lower levels is distinguished and where it is possible to neglect the contribution from the compound mechanism were also used in addition to the above data.

It was assumed when fitting that parameters V_R, W_D, a_R and a_D depend linearly on the energy, but there happened to be no necessity of introducing the energy dependence of the diffuseness of the potential real part to describe the experimental data. However, the introduction of the energy dependence for the diffuseness of the potential imaginary part a_D markedly improves the description.

As a result of the careful optimization over the above experimental data the following values of the nonspherical optical poten-

tial parameters for ^{238}U have been obtained:

$$V_R = (45.87-0.3\,E)\ \text{MeV}, \quad r_R = 1.256\ \text{fm}, \quad r_D = 1.260\ \text{fm},$$

$$W_D = \begin{cases} (2.95 + 0.4\,E)\ \text{MeV} & (E \leq 10\ \text{MeV}), \\ 6.95\ \text{MeV} & (E > 10\ \text{MeV}) \end{cases} \qquad a_R = 0.626\ \text{fm}$$

$$a_D = (0.555 + 0.0045\,E)\ \text{fm}$$

$$V_{so} = 7.5\ \text{MeV}, \qquad \beta_2 = 0.216, \qquad \beta_4 = 0.080 \qquad (1)$$

The calculations by use of these parameters make it possible to describe the available experimental data for ^{238}U at energies ranging from 1 to 15 MeV practically within the experimental errors. The comparison between the calculated and experimental data on σ_t (^{238}U) in the range of 0.1-15 MeV is given in Fig. 3.

Fig. 3. Comparison between experimental and calculated data on σ_t for ^{238}U at energies of 0.1 - 15 MeV.

Figs. 4 - 6 show the differential cross-sections for elastic and inelastic scattering of neutrons at 3.4, 8.56 and 15.2 MeV.

The value of the deformation parameter β_2 for ^{238}U obtained

Fig. 4 Differential cross-sections for 3.4 - MeV neutron scattering by ^{238}U nuclear levels: 1 - ground 0^+ state; 2 - the first excited level (2^+, 44 keV); 3 - the second excited level ($^+4$, 148keV) 4 - elastic scattering by spherical potential with parameters taken from [35].

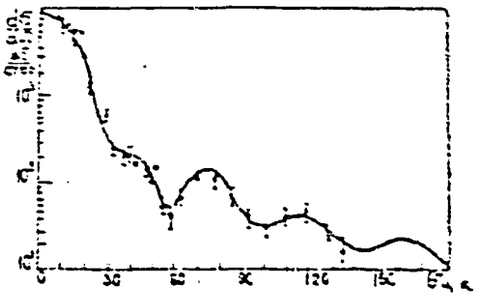

Fig. 5 Differential cross-sections for I5.2 - MeV neutron scattering by the nucleus ^{238}U (sum of the 0^+, 2^+ and 4^+ levels).

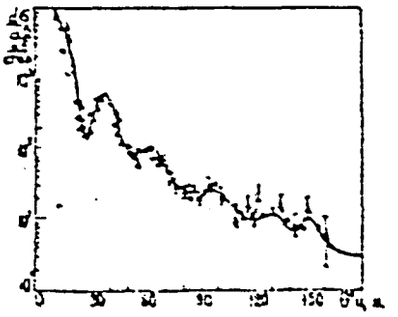

Fig. 6. Differential cross-sections for I5.2 - MeV neutron scattering by the nucleus ^{238}U (sum of the 0^+, 2^+ and 4^+ levels).

by Lagrange [I7] is 0.I98, differing by about 8% from the value of β_2 obtained in this work. This difference results from somewhat different experimental values of S_0, S_1 and σ_p used to determine the potential parameters in the both works and characterizes essentially the error in determining the parameter β_2 due to uncertainties in the starting experimental data. The error in determining the real and imaginary parts of the potential does not exceed 0.2 MeV.

At the second stage of obtaining the common potential for heavy nuclei, an attempt was made to describe the available experimental data for the nuclei ^{235}U, ^{239}Pu and ^{240}Pu with the geometric parameters obtained for ^{232}U. The following data were used: our estimated values of σ_t (at energies to I5 MeV), S_0, S_1, R' and the experimental data on angular distributions in the case of ^{239}Pu and ^{235}U, only the estimated values of S_0, S_1, R' and σ_t (at energies to 3.5 MeV) in the case of ^{240}Pu.

To describe these experimental data it turned out to be quite enough to include in the potential the isotopic dependence obtained in the case of ^{238}U for depths of the potential real and imaginary parts and to fit the deformation parameters β_2 and β_4. It happened to be possible to write the depths of the potential real and imaginary parts taking into account the isotopic dependence by the following way:

$$V_R = 49.72 - 17\,\frac{N-Z}{A} - 0.3\,E; \quad W_D = 5.22 - 10\,\frac{N-Z}{A} + 0.4\,E \qquad (2)$$

The deformation parameters for the potential with the above values of V_R and W_R are

$\beta_2 = 0.201$, $\beta_2 = 0.217$, $\beta_2 = 0.191$ and 0.195

$\beta_4 = 0.072$, 0.082, 0.094 and 0.078

for the nuclei ^{235}U, ^{239}Pu, ^{240}Pu and ^{232}Th, respectively.

The obtained values of the deformation parameters agree well with the values theoretically predicted [25] from the microscopic model by use of the Yukawa single-particle potential and the modified liquid-drop model ($\beta_2 = 0.216$, $\beta_4 = 0.084$).

The set of the above parameters permits the available experimental information for the above nuclei to be described practically within the experimental errors. The example of the experimental data description for ^{239}Pu is given in Figs. 7 and 8. In the case of ^{240}Pu there are no experimental data on angular distributions of the elastically-scattered neutrons, the angular distributions of the 5 MeV neutrons scattered by the nucleus of ^{240}Pu as theoretically predicted by use of the coupled-channel method are presented in Fig. 9.

Thus, the neutron data for the actinides for which there is no experimental information can be obtained by the coupled-channel method with parameters V_R and W_D in the form (2) and with the geometric parameters in the form (I). To do this it is necessary only to fit the values of the deformation parameters β_2 and β_4

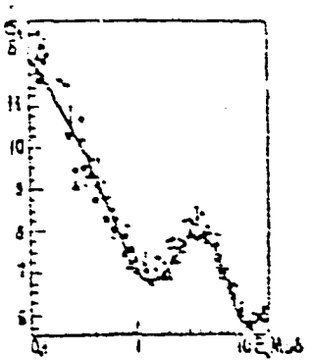

Fig. 7. Comparison between experimental and calculated data on σ_t for ^{239}Pu at energies of 0.1 - 15 MeV.

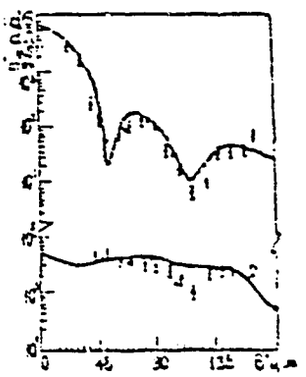

Fig. 8 Differential cross-sections for 3.4 - MeV neutron scattering by the nucleus ^{239}Pu: 1 - sum of the $1/2^+$ and 8 keV $3/2^+$ levels; 2 - sum of the 57 keV $5/2^+$ and 76 keV $7/2^+$ levels.

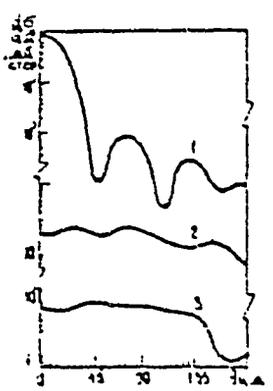

Fig. 9 Differential cross-sections for 5 MeV neutron scattering by the nucleus ^{240}Pu: 1 - ground 0^+ state; 2 - 43 keV 2^+; 3 - 142 keV 4^+ level.

for every nucleus basing on the experimentally estimated values of S_0, S_1 and R', which does not require a long computer time. If there are no experimental data on S_0, S_1 and R', parameters β_2 and β_4 could be taken from the migroscopic calculations [25].

The potential obtained by us differs considerably from other ones by that it includes the energy dependence of the geometric parameter a_t, which permits the competition between the surface and volume absorption to be taken into account in an "efficient" way (it is of especial importance in the range of energies above IO MeV).

The use of the volume absorption at high energies would lead to necessity of fitting, as a minimum, three more potential parameters (depth, radius and diffuseness of the imaginary part describing the volume absorption), whereas the use of the surface absorption diffuseness increasing with energy, $a_p = a_o + a_1 E$ makes it possible to take into account the volume absorption and to describe the experimental data at high energies by one parameter.

The coupled-channel method as considered here makes it possible in the case of fissionable nuclei to describe the experimental data on angular distributions of the elastically-scattered neutrons, to calculate the cross-sections for the direct excitation of levels and to picture the shape of the inelastically-scattered neutron angular distribution on the 4^+ level within the experimental errors. A satisfactory description of angular distributions on the 4^+ level may mean that the sign of the deformation parameter is chosen correctly as the data on the 4^+ level excitation are more sensitive to the choice of the deformation sign as compared to the data on the 2^+ level [58]. The detailed structure of the inelastically-scattered neutron angular distribution on the 2^+ level is reproduced somewhat worse, the structure obtained in the calculations being less noticeable than that from the experiment. The same difficulties arise when describing the behaviour of the angular distribution for the $5/2^+$ and $7/2^+$ levels of ^{239}Pu. It should be noted, however, that the measurement reliability for the first excited level is low (it must be taken into account that the energy of the recoil nucleus is comparable with the first level energy).

For the heavy deformed nuclei the most correct approach to the calculation and evaluation of the neutron cross-sections is the generalized optical model. But this method is too complex and time consuming, so the spherical optical model is still widely used to calculate and to estimate the neutron cross-sections of nuclei including the deformed ones. As the model contains a good many of parameters, to attain a good agreement with experiment within some limited energy ranges is comparatively simple. However, the potential parameters obtained in such a way turn out to be different for the neighbouring nuclei. Moreover, these parameters presented by different authors are rather unlike.

One of the most important advantages of using the coupled-channel method for the purpose of estimation is a possibility of obtaining and using the common, for a group of nuclei, parameters of the optical potential, which appears to be impossible for the spherical optical model. The spherical optical model calculations can not reproduce the general tendency in the strength function variation for the heavy nuclei. However, the calculations by using the generalized optical model with a common set of potential parameters reproduce well this tendency in the change of S_0 and S_1 .

The comparison between the cross-sections for the total interaction σ_t in the case of ^{239}Pu which we have calculated by use of the spherical and generalized optical models shows that the calculated cross-sections most considerably differ at low energies. If the use of the deformed potential allows one to describe σ_t for ^{239}Pu with an accuracy better than 2% over the whole energy range, while using the spherical potential the difference between the calculated and experimental values of σ_t amounts to about 8% in some energy ranges.

The comparison of the elastic scattering cross-sections calculated by using the spherical and deformed potentials with the experimental data shows that the spherical optical model describes worse the cross-section for elastic scattering especially at large angles.

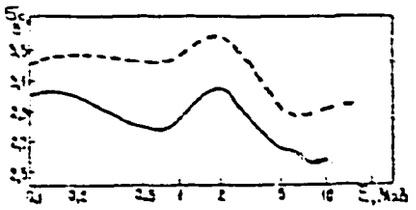

Fig. IO. Comparison between cross-sections for compound nucleus formation σ_c (^{238}U) calculated by use of the spherical optical model (solid line) and by the coupled-channel method (dashed line).

The cross-sections for the compound nucleus formation σ_c is most sensitive to the choice of the model (spherical or nonspherical). In the spherical optical model calculations $\sigma_c^{sp} = \sigma_t - \sigma_n^{dir}$ whereas in the coupled-channel method $\sigma_c^{nonsp} = \sigma_t - \sigma_n^{dir} - \sigma_{nn'}^{dir}$. As $\sigma_{nn'}^{dir}$ depends strongly on energy, the calculation of σ_c by using the spherical optical model through fitting the model parameters to σ_t proves to be rather doubtful. It can be seen from Fig. IO where σ_c for ^{238}U calculated by the coupled-channel method with the potential parameters obtained by us and by use of the spherical optical model with the parameters from [26] are compared. The difference between σ_c^{sp} and σ_c^{nonsp} is rather significant and depends upon energy, which does not permit one to renormalize the results of the calculations with the spherical potential to the results of the calculations obtained by using the generalized optical model. The difference between the neutron transmission coefficients calculated on the basis of the spheriacl and nonspherical models turns out to be of the same order of magnitude as the difference between the values of σ_c.

The influence of the deformation effects on the calculated cross-sections cannot be substituted by the equivalent set of the spherical optical potential parameters. As observed in [I7], the effect of the parameters of both the quadrupole, β_2, and hexadecapole, β_4, deformations is of significance. This effect is illustrated in Fig. II where the comparison is given for the values of σ_t in the case of ^{239}Pu calculated with allowance for parameter β_2 alone

and parameters β_2 and β_4. It is seen from Fig. II, that the difference between the values of σ_t amounts to $\pm 10\%$; and the conclusion can be drawn that for the accurate evaluation of the actinide cross-sections, the deformation parameters β_2 and β_4 should be taken into account.

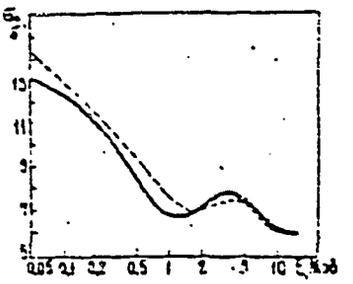

Fig. II. Comparison between σ_t (^{239}Pu) calculated with allowance for the quadrupole deformation β_2 alone (dashed line) and for both the quadrupole and hexadecapole β_4 deformations (solid line).

It is clear from the above cited results that the generalized optical model should be used as a means to evaluate reliably the neutron cross-sections of the heavy deformed nuclei. The parameters obtained by the coupled-channel method fluctuate substantially less from one nucleus to the other compared to the sets of parameters obtained for individual nuclei by the spherical optical model. The use of the spherical optical model is permissible only in the cases when the required accuracy in the calculations of cross-sections is low (less than 20-30%).

The coupled-channel method described above is developed for the nuclei with rotational or vibrational bands of levels. There is still no mathematical program which would allow the coupling of these bands to be taken into account.

A theory of nonaxial even-even deformed nucleus was developed by Davydov and Chaban in [27]. In the framework of this approach the Hamiltonian of intrinsic motion takes into account both rotation and vibration of the nucleus. This theoretical approach makes it possible to describe the lower band levels with a high accuracy. This theory, in principle, can be extended to dynamics of neutron inter-

action with a nucleus, i.e. can be used to calculate the neutron scattering by nuclei. The task consolidates essentially to solving two problems: (I) determination of the intrinsic Hamiltonian parameters (deformation parameter, softness parameter and parameter of nuclear nonaxiality, then the three parameters are fixed), (2) calculation of the neutron scattering process with determination of the corresponding parameters of nuclear potential.

This program is being developed in our laboratory. The interaction cross-sections and other characteristics of the excited nucleus has happened to depend strongly on degree of its twisting. The elements of channel coupling have been calculated for this model. The allowance for nuclear vibrations has been shown to lead to an increase in these coefficients, i.e. to an increase in the calculated contributions from direct reactions.

5. INFLUENCE OF VARIOUS NUCLEAR LEVEL DENSITY CONCEPTS ON THE CALCULATION OF ACTINIDE NEUTRON CROSS-SECTIONS

The level density from the Fermi-gas model is widely used at present in the calculations based on the statistical theory. The model relationships are founded on an idea of the total agitation of collective degrees of freedom in the excited nucleus, and so they do not take into account the collective effects. A semimicroscopic method of level density calculation developed recently by Soloviev et al. [28-29] makes it possible to take into account the contribution from vibrational and rotational motions. When calculating the level density the methods of statistical averaging [30-32] are too widely used, although a number of problems concerning difference between the collective motions of the nuclei at different excitation energies, agitation of collective modes with single-particle ones, etc. remains unsolved in the framework of the adiabatic assessment of collective effects.

These problems can be solved on the basis of the microscopic methods for direct modelling of the structure of highly-excited

nuclear states [33]. But these methods of calculating the level density prove to be rather time-consuming especially at high energies, limiting the possibility of their application to nuclear data assessment.

That is why to learn the influence of the collective effects in the level density upon the calculation of average neutron cross-sections of heavy nuclei we have employed the statistical method of describing the averaged characteristics of the excited nuclei as developed by Ignatyuk et al. [30, 31, 34]. This method takes into account the existance of shell inhomogeneities in the single-particle level spectrum, the correlation effects of the superconducting type and the coherent effects of collective nature. We have prepared a special computer program allowing one to calculate the level density and to extract the parameter a for the following models: the conventional Fermi-gas model, the Fermi-gas model with reverse shift in pairing energy, the Fermi-gas model with an energy dependence a (E) for taking into account the shell effects [35], the Fermi-gas model with collective modes (both rotational and vibrational) of motion included, the superfluid nucleus model which makes it possible to include the residual interactions of the correlation type and the simple version of which has been suggested in [31], the same model but with collective motion modes included.

The allowance for shell effects in the Fermi-gas model is made [35] by including both the dependence of the parameter a upon excitation energy and the shell correction δW . The energy dependence of parameter a is most essential for the nuclei with the nearly completed shell. For the nuclei investigated in our work the values of shell corrections are comparatively small and this effect can be neglected.

The considered models of level density lead to different dependences of level density upon energy, which affects the values of cross-sections calculated by using the statistical model. The allowance for collective effects drastically decreases the value of a

and when calculating by means of the Fermi-gas and the superfluid nucleus models the values of a become comparable to each other and to the quasiclassical assessment ($\overline{a}$ = 0.075A and for ^{243}Pu: $\overline{a}$ = I8.22 MeV^{-I}).

The above models of level density do not allow the growing sum of levels in the discrete spectral range to be described adequately. The requirement to describe the discrete spectrum of levels would evidently be too rigid for any model of level density the main parameter of which is determined from the density of neutron resonance. So, it looks natural when the constant temperature model is used at low energies whose parameters are determined from the condition of describing the discrete spectrum and which ensures the joining with the model accepted at energies close to the neutron binding energy.

The constant temperature model is usually subjected to criticism from the angle of its physical substantiations. Its success becomes clear from the calculations basing on the superfluid nucleus model which gives a weaker drop of ρ (u) to the zeroth excitation energy than the Fermi-gas model. At low energies ρ (u) in accordance with the superfluid nucleus model gives practically a straight line in the semilogarithmic scale.

The joining of the level density models (the constant temperature model and the superfluid nucleus model) was determined from the conditions of description of a growing sum of the discrete spectrum and of equality of level densities calculated with the both models and their logarithmic derivatives at the joining point.

The analysis of the actinide discrete spectrum shows that the identification of levels according to spin is not, as a rule, sufficiently reliable, except for lower bands. However, such information may be also useful. Using the maximum likelihood method, the parameter of spin dependence can be evaluated as follows:

$$\sigma^2_{I\,exp} = \frac{1}{2N} \sum_i J_i \left(J_i + 1\right), \qquad (3)$$

where N is the number of levels identified according to spin. In

spite of the fact that evaluation (3) is slightly sensitive to the omission of levels, in determining $\sigma^2_{I\,exp}$ we have used only the data from the energy regions where the omission of levels was relatively small. In this case the growing sums of levels were described by the constant temperature model.

In the framework of the constant temperature model the parameters of spin dependence of σ_I^2 for 41 nuclei with sufficiently studied discrete spectra have been determined by means of maximum likelihood method. The values of σ_I^2 for even-even and odd nuclei proved not to differ and on an average, they can be described by a linear dependence on mass number A

$$\sigma_I^2 = 0,15624\,A - 20,76 \qquad (4)$$

The use of these values of σ_I^2 makes it possible to describe adequately in terms of the constant temperature law the growing sums of levels $N(U,J)$ for the nuclei ^{234}U, ^{235}U, ^{239}Pu, ^{240}Pu ^{245}Cm, ^{246}Cm for which a relatively great number of levels with a given J is identified. This shows a possibility of substitutiong if necessary the discrete spectrum by the continuous one by use of the constant temperature model and the law:

$$f(U,J) = \frac{(2J+1)\exp\left[-\frac{J(J+1)}{2\sigma_I^2}\right]}{2\sigma_I^2} \qquad (5)$$

with the parameter σ_I^2 given by (4).

The value of σ_I^2 in the form of equation (4) should be used up to an energy where the discrete spectrum can be considered to be identified quite reliably (we shall denote this boundary as E_{bound}). From E_{bound} to E_x (the point of joining the superfluid nucleus model and the constant temperature model) σ_I^2 would be determined by linear interpolation between σ_I^2 given by (4) and $\sigma_I^2(E_x)$ calculated by the superfluid nucleus model. At higher energies the calculation by the superfluid nucleus model is to be used.

For nuclei whose discrete spectra are identified poorly it is possible to use dependence (4) and the following values:

E_{bound} = I.2 MeV for even-even nuclei,

E_{bound} = 0.6 MeV for odd nuclei,

E_{bound} = 0.3 MeV for odd-odd nuclei.

The results of the determination of parameter T in the constant temperature model show that the temperature T for even-even nuclei has very small fluctuations about the mean value $\overline{T}$ =0.385MeV. For odd nuclei the fluctuations of T are markedly higher and moreover, the value of T on an average is somewhat lower than for even-even nuclei, which is a consequence of missing the levels in the spectra of odd nuclei. For odd nuclei having the most studied discrete spectra (for example, ^{235}U) the temperature T is close to the mean value for the even-even nuclei.

The values of parameter E_0 in the constant temperature model for even-even nuclei are grouped very compactly in the vicinity of zero; for odd nuclei $E_0 = -\Delta_0$ and for odd-odd nuclei $E_0 = -2\Delta_0$, where Δ_0 is the correlation function in the ground state (E_0 = = 0.0397 MeV for ^{235}U ; E_0 = -0.I665 MeV for ^{239}Pu). The use of the superfluid nucleus model taking into account the contribution from collective modes in the level density ensures the joining of the models at sufficiently low temperatures and at the points of joining E_x equal to 4, 3.2 and 2.4 MeV for even-even, odd and odd-odd nuclei, respectively (E_x= 3.2, 4.I and 2.6 MeV for ^{235}U, ^{238}U and ^{239}Pu, respectively).

The calculation of the average density of neutron resonances $\langle D \rangle_{theor.}$ with the above parameters shows that a great bulk of experimental data for actinides agrees with the theoretical predictions within ±50%.

Calculated from systematics, the relationship of the main parameter of the level density to the mass number at binding energy $a(B_n)$

appeared to be equal to:

$$\frac{a(Bn)}{A} = 1.487\ 10^{-3}\ A + 0.4529 \qquad (6)$$

which differgs from the systematics of [34] by a faster decrease in $\frac{a(Bn)}{A}$ with increasing A. This decrease can be caused by closing the shell as in the case of double magic nuclei.

The parameters for the transactinide level densities in the range of $^{225}Th - ^{254}Cf$ $(T, E_0, E_B, \delta W, a(Bn), \langle D \rangle)$ are given in Ref. [36].

As the calculated cross-sections for fission at energies above I MeV are usually fitted to experimental data, the cross-section for radiative capture $\sigma_{n\gamma}$ in the calculations by use of the statistical theory proves to be most sensitive to the choice of the level density model. The problem associated with the choice of the level density model can be unambiguously settled only for the nuclei for which there are the experimental data on $\sigma_{n\gamma}$ in a wide energy range. The nucleus ^{238}U whose cross-section for radiative capture was measured in a number of works is most suitable from this point of view. Let us investigate, taking this nucleus as an example, the influence of different level density concepts on the energy dependence of $\sigma_{n\gamma}$, analyze also the influence of uncertainties in $\langle D \rangle_{obs}$ and $\langle \Gamma_\gamma \rangle$ on calculation of $\sigma_{n\gamma}$ and consider the problem of choosing the spectral factor.

The neutron transmission coefficients required for the statistical calculations were calculated by using the coupled-channel method with the non-spherical optical potential parameters which have been obtained by us and carefully optimized over the experimental data.

The conclusion was drawn in a number of works (see, e.g. [37]) that the Weisskopf factor makes it possible in many cases to attain the adequate description of $\sigma_{n\gamma}$, but it does not ensure an agreement as to the energy dependence of radiative strength functions [38]. The use of the Lorentz dependence is physically more substantiated, but in this case the description of the energy dependence

of $\sigma_{n\gamma}$ becomes worse and the calculated values of $\sigma_{n\gamma}$ happen to be essentially higher than the experimental ones.

As the transmission coefficient for radiative capture depends on the level density of the compound nucleus, the above discrepancy with experiment can be assumed to result from incorrectness of the used level density model (the Fermi-gas model). Such a conclusion was drawn in [39], but in this work the calculation for ^{238}U was conducted only to an energy of I MeV ignoring the competition of fission and, moreover, without the use of neutron transmission coefficients calculated by the nonspherical optical model.

The calculation of neutron cross-sections of ^{238}U was made on the basis of the formalism described above, the Teppel formalism etc. being used in the calculations at energies above I.3 MeV. The level diagram of the nucleus ^{238}U was taken from [26].
The calculated cross-sections for excitation of discrete levels of the target nucleus at incident neutron energies lower than I.5 MeV where the cross-sections practically do not depend on the choice of the level density model agree well with the experimental data.

Thus, the chosen parameters of the statistical model describe all the neutron cross-sections, except for $\sigma_{n\gamma}$. The calculated cross-sections for radiative capture depend strongly on the level density model in use, making it possible on the basis of comparison between the calculated and experimental values to choose a level density model permitting one to attain the best agreement with experiment in a wide energy range.

The cross-sections for radiative capture of neutrons by the nucleus ^{238}U calculated by using the spectral factors of both types and the level densities from different models are compared in Fig. I2 with the experimental data on $\sigma_{n\gamma}$ in the energy range from 0.I to 3.0 MeV (where noncompound mechanisms of radiative capture can be neglected). The comparison shows that the best fit to the experiment over the whole range is obtained by use of the level density from the Fermi-gas model with collective motion modes included. The use

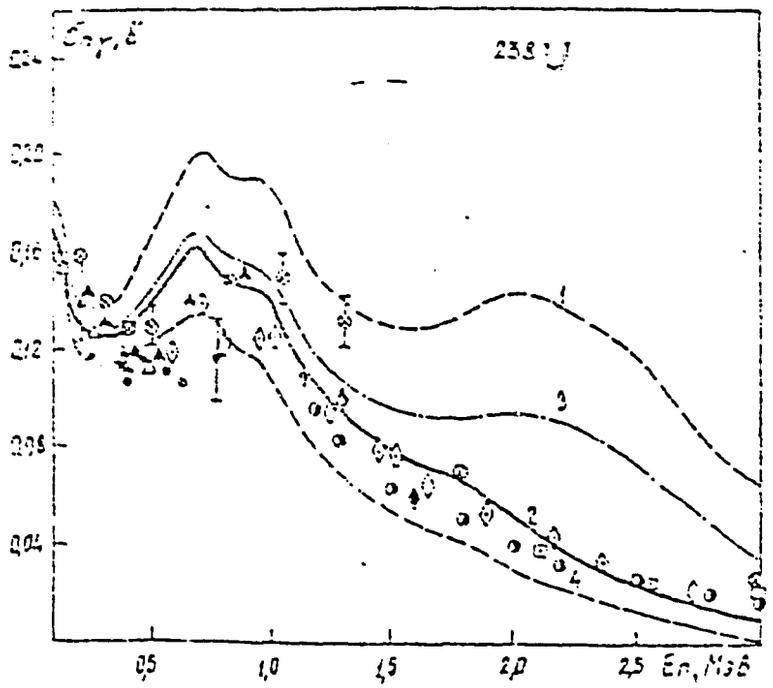

Fig. I2. Comparison between experimental data on $\sigma_{n\gamma}$ (^{238}U) and theoretical data obtained by use of different level density models: I - Fermi-gas model, Lorentz spectral factor; 2 - Fermi-gas model with collective effects included, Lorentz spectral factor; 3 - superfluid nucleus model with collective effects included, Lorentz spectral factor; 4 - Fermi-gas model with collective effects included, Weisskopf spectral factor ($< D >_{obs}$ =24.8 eV [22], $< \Gamma_\gamma >_{obs}$ = 23.5 meV, T_n determined by the coupled channel method).

of the level density from the superfluid nucleus model leads to the discrepancy with the experiment in the enrgy range from I.2 to 3.0MeV, whereas at energies up to I.2 MeV the agreement is the same as when using the level density from the Fermi-gas model with collective motion modes included.

The greatest discrepancy between calculation and experiment occurs for the level density from the conventional Fermi-gas model. The introduction of the energy dependence of the parameter a in the Fermi-gas model for level density results in no essential change of the calculated values of $\sigma_{n\gamma}$. Thus, at 3 MeV this effect attains less than 4%. It is attributed to comparatively small values of the shell corrections δW for ^{238}U and ^{239}U, allowing the dependence a (z) in the level density from the superfluid nucleus model to be neglected.

The use of the Weisskopf spectral factor in the calculations does not yield the better fit to the experimental data on $\sigma_{n\gamma}$ than the fit obtained with the Lorentz spectral factor and the level density from the Fermi-gas model with collective modes included (curve 4 in Fig. I2). Therefore, taking into account the better physical validity of the Lorentz factor, as evidenced by the results of describing the radiative strength functions [38] and the experimenal data on the $(n, \gamma f)$ process widths, we consider it reasonable to use just this spectral factor in the calculations by the statistical theory.

It should be noted that uncertainties in such quantities as $\langle D \rangle_{obs}$ and $\langle \Gamma_\gamma \rangle_{obs}$ and the used values of neutron transmission coefficient can considerably affect the choice of the best model of level density for the description of $\sigma_{n\gamma}$ (Fig. I3)

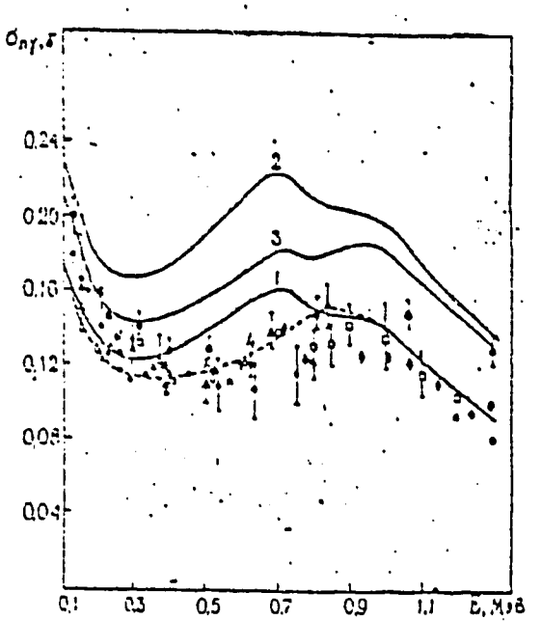

Fig. I3. Comparison between the experimental and calculated data on $\sigma_{n\gamma}$ (^{238}U). The calculation was made for the Fermi-gas model with collective effects included, with the Lorentz spectral factor and $\langle \Gamma_\gamma \rangle_{obs}$ = 23.5 meV. Curve I - $\langle D \rangle_{obs}$ =24.8 eV [22], T_n were determined by the coupled-channel method for a ground nuclear state alone; curve 2 - $\langle D \rangle_{obs}$ = I7.7 eV [4I], nonspherical potential; curve 3 - $\langle D \rangle_{obs}$ = I7.7 eV, spherical potential; curve 4 - $\langle D \rangle_{obs}$ = 24.8 eV, T_n were determined by the coupled-channel method for both ground and excited nuclear states.

The width of the radiative capture of ^{238}U was normalized to the estimated value of $\langle \Gamma_\gamma \rangle_{obs} = 23.5$ meV [42] that agrees with the value of 23.43 meV $\pm$ 0.11 meV $_{stat}$ $\pm$0.70 meV $_{syst}$ obtained by Poortmans et al. [44] . The 4% error in $\langle \Gamma_\gamma \rangle$ leads to the same error in the calculated $\sigma_{n\gamma}$.

In the case of $\langle D \rangle_{obs}$ there are far great uncertainties due to difficulties in identifying S- and p-levels. Thus, according to the recent assessment of De Saussure et al [22] $\langle D \rangle_{obs}$ = = 24.78 $\pm$ 2.0 eV being consistently higher than $\langle D \rangle_{obs}$ = 20.8$\pm$ $\pm$ 0.3 eV [40] . This discrepancy results from that the weak levels considered in [43] as S-levels are actually, as determined by Corvi et al [45] , p-levels. The difference in $\sigma_{n\gamma}$ due to the use of two extreme values of $\langle D \rangle_{obs}$ is about 15%.

The exciting uncertainties in $\langle \Gamma_\gamma \rangle$ and $\langle D \rangle$ do not allow one to explain such a considerable discrepancy between the experiment and calculation based on the conventional Fermi-gas model for level density.

It is seen from Fig. 13 that the neutron transmission coefficients obtained by using the spherical and nonspherical optical models affect the calculation of $\sigma_{n\gamma}$. The difference between the values of $\sigma_{n\gamma}$ for these two cases depends on energy and ranges from 5 to 20%.

The neutron transmission coefficients applied when calculating the processes of the compound nucleus disintegration by the statistical model, strictly speaking, should represent the transmission coefficient for the excited states of the nuclei as they characterize the probability of capture in the inverse reaction of the particle emitted by the excited nucleus. It is required by the detailed balancing principle. When using the spherical optical model the dependence of the neutron transmission coefficients on excitation energy is neglected, as pointed in [46]. In practice, these coefficients are identified with the neutron transmission coefficients for the ground states of nuclei. The coupled-channel method can be used

to calculate the neutron transmission coefficients for the excited states. We have studied the effect of using such coefficients for the first two excited states of the ground rotational band of ^{238}U. The influence of these states is determinative when taking into account the competition of inelastic scattering.

Table 2 lists the values of the neutron strength functions S_0 and S_1 for the ground state and the excited ones which were calculated by use of the coupled-channel method. As it seen from the table, the values of strength functions and, hence, the transmission coefficients for different states differ essentially, especially at low energies of incident neutrons. These differences decrease with increasing energy. The difference between the transmission coefficients manifests itself more strongly in the reaction of radiative capture of neutrons. The performed calculations of $\sigma_{n\gamma}(^{238}U)$ show (Fig. 13) that the use of the neutron transmission coefficients for the excited nuclear states obtained by the coupled-channel method permits the experimental data at energies to 1 MeV to be described significantly better.

Table 2 Strength functions of S - and P - neutrons for the ground state and excited ones of ^{238}U nucleus

Neutron energy, MeV	$S_0 \cdot 10^4$, $eV^{-1/2}$			$S_1 \cdot 10^4$, $eV^{-1/2}$		
	ground state	2^+ state	4^+ state	ground state	2^+ state	4^+ state
$0.5\ 10^{-3}$	1.163	1.032	0.790	1.947	1.893	3.745
0.005	1.133	1.016	0.780	1.941	1.717	2.997
0.01	1.121	1.006	0.774	1.944	1.721	3.003
0.03	1.091	0.981	0.757	1.952	1.731	3.010
0.1	1.034	1.003	0.756	1.916	1.731	3.407
0.2	0.990	0.920	0.717	2.109	1.823	3.068
0.4	0.945	0.912	0.712	1.801	1.462	2.463
1.0	0.820	0.790	0.695	1.428	1.151	1.183

However the experimental data are very poor to make an unambiguous conclusion concerning a change of the optical potential in strongly excited nuclei though the experiments [59] do show that there is a marked difference in neutron absorption in the case of excited and unexcited nuclei.

The performed analysis shows that the use of the conventional Fermi-gas model for level density leads to an appreciable discrepancy between the experimental data and $\sigma_{n\gamma}$ for even-even nuclei calculated with the both types of spectral factor. This discrepancy cannot be explained by uncertainties in the parameters used.

The comparison between the experimental data for $\sigma_{n\gamma}$ (^{239}Pu) and the theoretical ones obtained by use of the different level density models is given in Fig. 14.

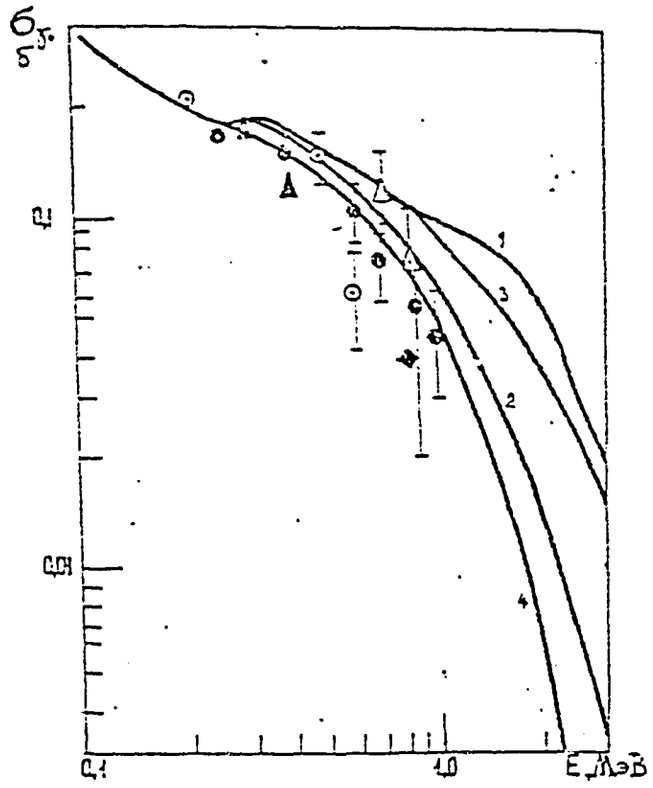

Fig. I4. Calculated data on $\sigma_{n\gamma}$ (^{239}Pu) obtained by use of different level density models and the Lorentz spectral factor: I - conventional Fermi-gas model; 2 - Fermi-gas model with collective modes included; 3 - superfluid model with collective mode included; 4 - conventional Fermi-gas model with the Weisskopf spectral factor ($\langle D \rangle_{obs}$ = 2.58 eV; $\langle \Gamma_\gamma \rangle_{obs}$ = 43.3 meV).

The use of the neutron transmission coefficients from the generalized optical model and the allowance for the direct excitation of the lower levels make it possible to provide a satisfactory fit of the experimental and theoretical cross-sections for excitation of the lower levels, as well as of the levels whose cross-sections are completely determined by compound nucleus disintegration.

The choice of the level density model does not practically affect the value of the total cross-section for the inelastic scattering. The discrepancies between the level densities of the target nucleus taken from different models cause changes in the relation between the cross-sections for scattering by the discrete and continuous spectra of levels as well as in the cross-sections for discrete level excitation.

As is seen from Figs. I5 and I6, the best fit between the calculated and experimental cross-sections data for excitation of the ^{239}Pu levels is provided by use of the level density from the Fermi-gas model with collective modes included and with the neutron transmission coefficients calculated by the coupled-channel method.

Using the nonspherical optical potential, the Lorentz spectral factor and the level density from the Fermi-gas model with collective modes included it is possible to attain the self-consistent description of cross-sections of all the types, including $\sigma_{n\gamma}$, for the even-even target nuclei of the ^{238}U type in a wide energy range. For the odd target nuclei the main problem is the correct allowance for the competition of fission and therefore the choice of different models for the level density affects to a lesser extent the values of the calculated cross-sections in the energy range under consideration ($\sigma_{nn'}$, σ_f and σ_t -up to 5 MeV, $\sigma_{n\gamma}$- up to 0.8 MeV).

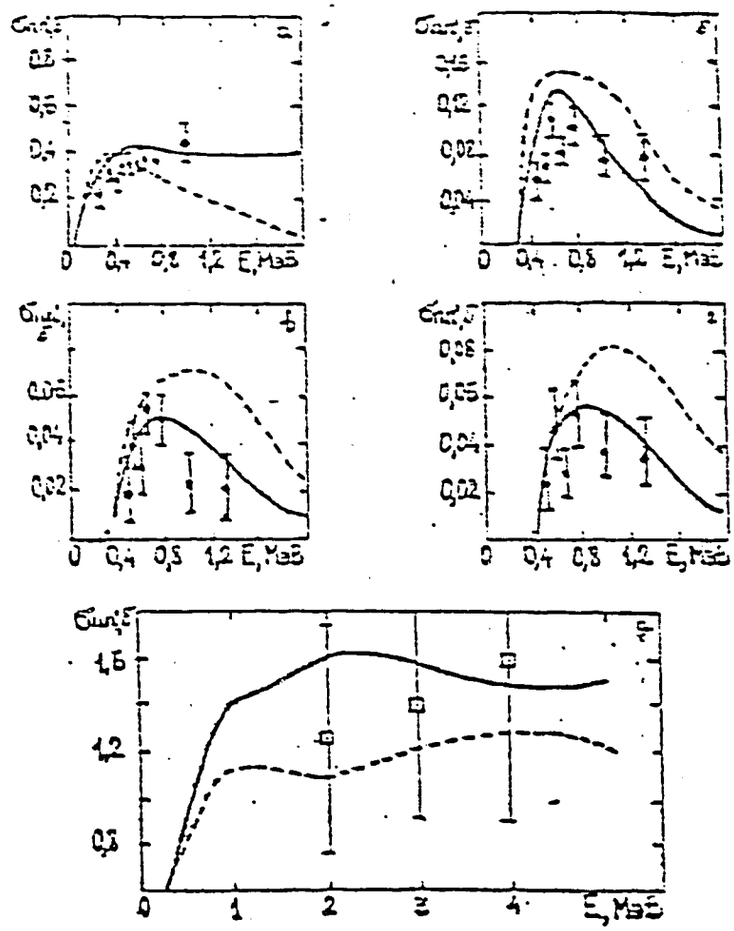

Fig. I5. Comparison between experimental and calculated data on cross-sections for ^{239}Pu nuclear level excitation. The calculations were made with transmission coefficient from the coupled-channel method (solid line) and from the spherical optical model (dashed line): a - sum of 57 - keV and 76 - keV levels; b - 285 keV level; c - 330 - keV level; d - 387 keV and 392 keV levels; 1 - total cross-section for inelastic scattering.

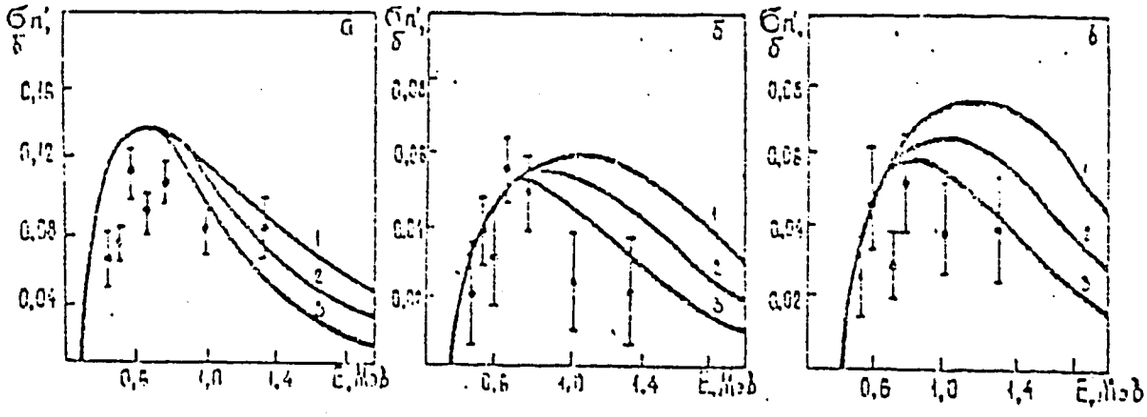

Fig. I6. Cross-sections for ^{239}Pu nuclear level excitation for different level density models: I - Fermi-gas model; 2 - superfluid model; 3 - Fermi-gas model with collective modes included.

The use of conventional Fermi-gas model for level density causes a substantial discrepancy between the experimental and calculated data obtained for even-even nuclei for both types of spectral factors, which cannot be explained by the uncertainty of the parameters applied.

6. CALCULATION OF FISSION CROSS-SECTION FOR TRANSACTINIDES

So far, the fission theory has not attained the stage when σ_f can be predicted quantitatively. When evaluating cross-sections we carried out the parametrization of σ_f determined fission transmissions to take into account the competition of fission with other processes. The fission process is a complicated and, for the time being, insufficiently studied phenomenon. One of the substantial uncertainties in the calculation of σ_f lies in the transition state pattern of the fissionable nucleus and in the form of level density in the continuous energy range. This uncertainty is especially great for the even target-nuclei since for these nuclei, a high centrifugal barrier should be taken into account.

The available systematics for fission probability [47, 48] are inadequate for obtaining σ_f and $\sigma_{nn'}$ since they are made upon the assumption that the compound nucleus cross-section, the fission cross-section, and, as a consequence, the relation of Γ_n/Γ_f are independent of energy.

A satisfactory description of σ_f can be obtained [49] with allowance for evolu tion of shell effects resulting in a double-hump fission barrier, for asymmetry specific to the saddle shape of a fissionable nucleus and allowance for correlated interactions of nucleons, and collective properties of a nucleus.

The discussion below is based on the results obtained in our laboratory in cooperation with the Obninsk Institute [49] . An essential condition for describing the cross-sections of reactions proceeding through the stage of formation of a compound nucleus consists in a correct calculation of the compound nucleus cross-section, σ_c .

The use of the spherical potentials discussed in Refs. [26, 50, 51] in the neutron energy ranges of 0.1 - 6 MeV results in obtaining substantially different σ_c with practically similar description of the total cross-section. It is known that for heavy deformed nuclei, the cross-section of direct excitation of rotational levels of the ground state amounts to a marked value. As a consequence, energy dependences of the compound nucleus cross-section calculated using the spherical [26, 50, 51] and nonspherical models [21] drastically differ (Fig.17).

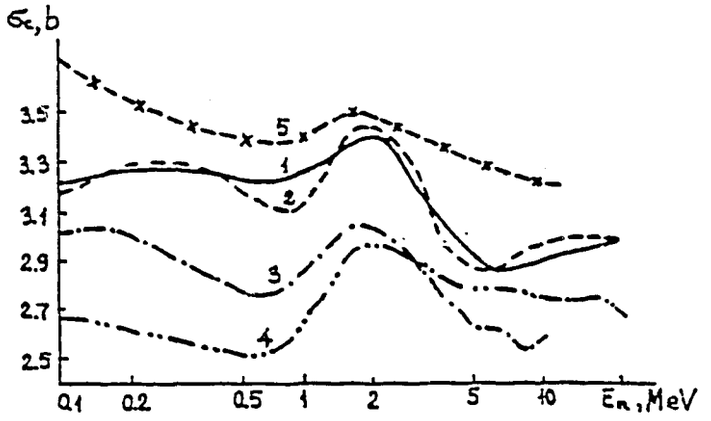

Fig. 17. Compound nucleus cross-section, σ_c (^{238}U) calculated by use of the nonspherical potential [21] - curve 1, and of the spherical potential [49] - curve 2; curve 3 [26]; curve 4 - [50]; curve 5 [51].

In calculation of the level density of fissionable, compound and residual nuclei, the model successfully considering pair correlations, shell inhomogeneities of a single-particle spectrum and coherent effects [34, 35] has been used.

A structural analysis of lower rotational actinide bands shows [52] that in the ground state they have an axial and mirror symmetrical shape. Similar results are obtained in calculation of the potential nucleus energy for equilibrium deformations. These calculations performed for strongly deformed nuclei indicated a drastic dependence of the single-particle spectrum structure on deformation and the possibility of exciting the saddle-shapes with axial [53] and mirror asymmetry [54]. An oscilating shell correction depending on deformation in the region of saddle deformations is positive, which corresponds to a

greater number of levels for the single-particle spectrum. As a result, the two-particle correlated interaction in a nucleus should be intensified. The description of energy dependence σ_f is rather sensitive to increasing constants that determine pair interaction (in the described model it is the correlation function Δ_f).

The investigation of a potential energy structure as a function of deformation [55] showed that in the region of the first maximum of the shell correction for nuclei with $Z \geq 92$, the potential energy has a maximum for axial and a mirror-asymmetrical shapes, while in the region of the second maximum the minimum is for mirror-asymmetrical but axial-symmetric shapes. The asymmetry of a mass distribution of fission fragments may serve as an experimental confirmation of the latter.

It is a consequence of the above effects that the density of the transition states of a fissionable nucleus will change. The mirror asymmetry results in doubling the level density, which is associated with the removal of degradation on parity; in the case of axial asymmetry, the level density increases by a factor of $\sqrt{2\pi}\sigma_{\parallel}$, where $\sigma_{\parallel} = \sqrt{F_{\parallel}^{A(B)} t}$, t is thermodynamic temperature, $F_{\parallel}^{A(B)}$ is inertia momentum of a fissionable nucleus relative to the nucleus symmetry axis.

It follows from the σ_f description of uranium and plutonium isotopes [49] that in order to reproduce the energy dependence of the fission cross-sections up to the $(n, n'f)$ reaction threshold along with the allowance for axial asymmetry of hump A and mirror asymmetry of hump B , it is necessary that the correlation function Δ_f of the nucleus in a transition state be increased by 10% (Fig.18). The difference between correlation functions at equilibrium deformation and at the barrier is a direct consequence of shell effects.

Upon assumption of axial symmetry of saddle shapes of a fissionable nucleus at any σ_c , we failed to reproduce the energy dependence σ_f by variation of fission barriers and correlation func-

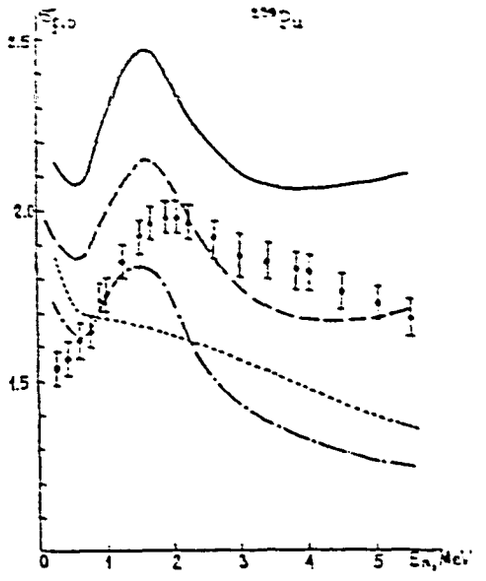

Fig. 18a

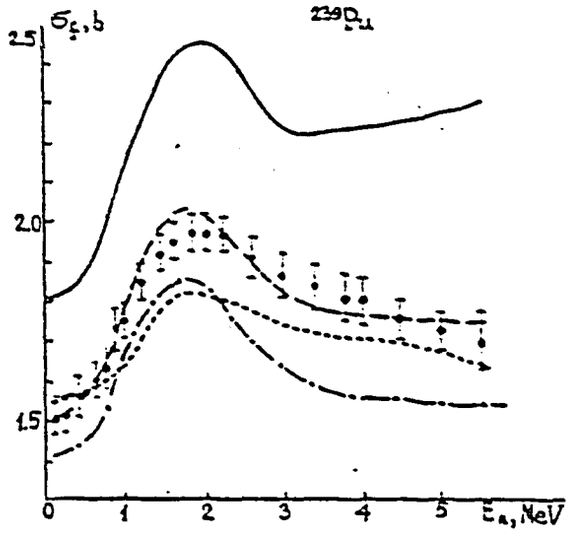

Fig 18b.

Fig. I8. Comparison of the experimental and calculated fission cross-section (^{239}Pu). Calculations for a) - axial-symmetric shapes; b) - asymmetric shapes. Curves: solid line - $\Delta_f = \Delta_c + \frac{12}{\sqrt{A}}$; dashed line - $\Delta_f = \Delta_c + 0.05$ MeV (a); $\Delta_f = \Delta_o + 0.07$ MeV (b); dot and dash line - $\Delta_f = \Delta_b + 0.1$ MeV; dotted line - - optical potential [5I], $\Delta_f = \Delta_c + 0.1$ MeV.

tion: a change in E_B practically results in the parallel shift of curve σ_f ($\Delta E_B = 0.2$ MeV corresponds to $\Delta \sigma_f = 0.05_{barn}$), while the sensitivity to E_A is 4 times as high. (Fig. I9)

The allowance for the total asymmetry of a saddle shape in the region of hump A and the mirror asymmetry of that in the region of hump B without changing the level density parameters in a fission channel does not allow one to describe the energy dependence of σ_f. To describe the energy dependence, σ_f, an increase of the correlation function Δ_f for the transition state of a fissionable nucleus is of great importance. The absolute value of this increase substantially depends on the optical potential used.

So, in the case of the spherical optical potential [5I], $\delta\Delta_f$ = = 0.1 MeV, while with the efficient optical potential $\delta\Delta_f = 0.07$ MeV. Such an excess of Δ_f over $\Delta_o = \frac{12}{\sqrt{A}}$ was obtained in work [56] as a result of analysis of the angular anisotropy of fission fragments for nuclei lighter than thorium.

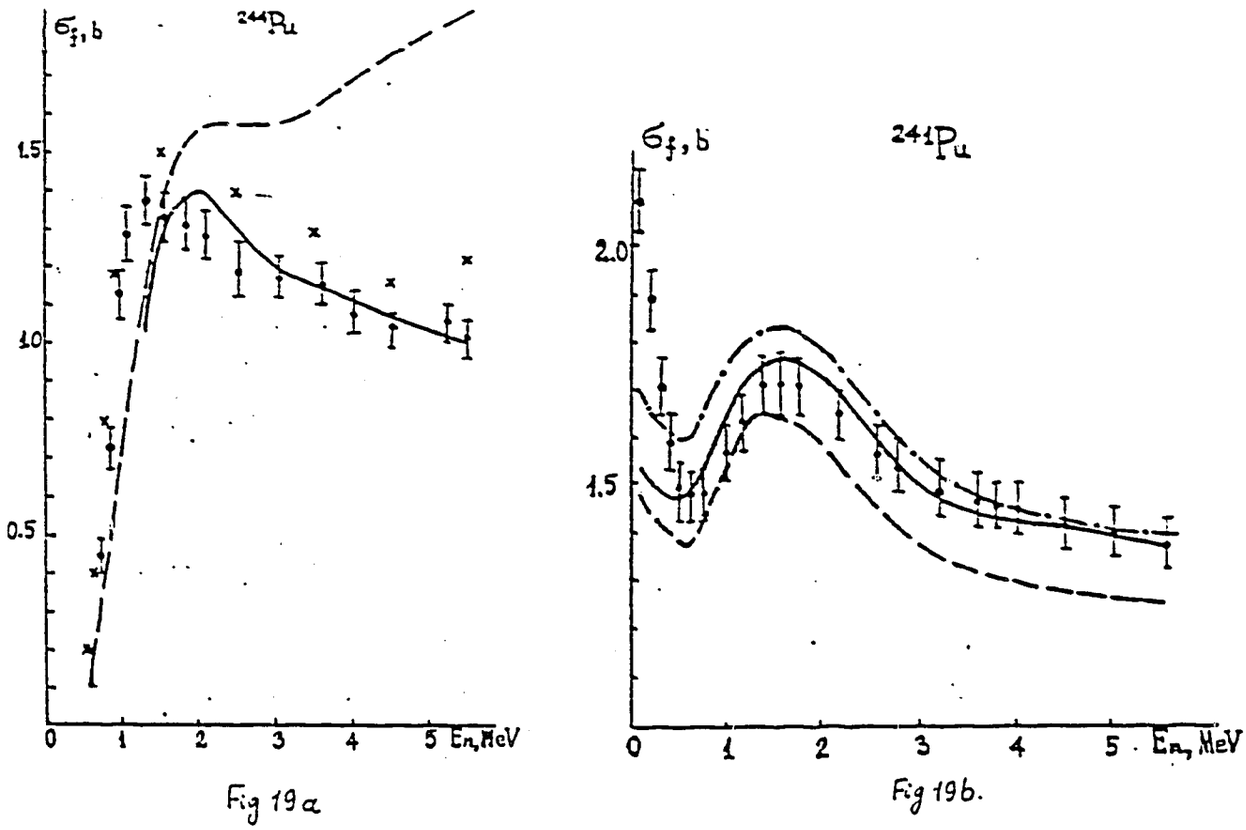

Fig 19a

Fig 19b.

Fig. I9. Comparison of the experimental and calculated fission cross-sections for ^{241}Pu (b) and ^{244}Pu (a).
(b) solid, dot and dash lines - ΔE_B = 0.2 MeV;
solid and dashed line - ΔE_A = 0.I MeV.

Sensitivity of σ_f to the changes of Δ_f shows that for the N-odd targets it is I.5 times higher than for the N-even targets. It results from the difference in efficient condensation energies for nuclei with even and odd N: $E_{N\,even} - E_{N\,odd} = \Delta_f$. Dependence of σ_f on Δ_f is due mainly to a temperature change of a nucleus in the transition state since in the case of N-even targets, Δ_f is a part of both the condensation energy and the efficient excitation energy as an even-odd shift.

It may be assumed that the agreement between energy dependence of the calculated and experimental σ_f can be attained by changing the shell correction for $\delta W^{A(B)}$ at the saddle point, however, the sensitivity of σ_f to $\delta W^{A(B)}$ is much weaker than to Δ_f.

In other words, for σ_f (E_n = 5.5 MeV) to be changed equivalently at $\delta\Delta_f$ = 0.025 MeV, it is necessary that the sign of δW_f^B be changed.

Figs. I8, I9 give the description of σ_f for ^{239}Pu, ^{241}Pu, ^{244}Pu obtained by the authors of [49] . The same description was also obtained for the other isotopes of U and Pu.

Fig. I9a gives σ_f for ^{244}Pu. A dashed line denotes the curve obtained using $\tilde{a}$ (^{245}Pu) fitted to the neutron resonance density which has been shown to be exceeded three fold. If $\tilde{a}$ is calculated in accordance with the level density formula taking into account collective effects, the anomaly disappears (Fig. I9a, solid line).

The resulting parameters of humps A and B are characterized by the following uncertainties: $\delta E_A \leq 0.15$ MeV, $\delta E_B \leq 0.1$ MeV, $\delta\Delta_f \approx 0.05$ MeV. Fig. 20 presents barriers E_A and E_B for uranium isotopes obtained in Refs. [49, 57] from the description of

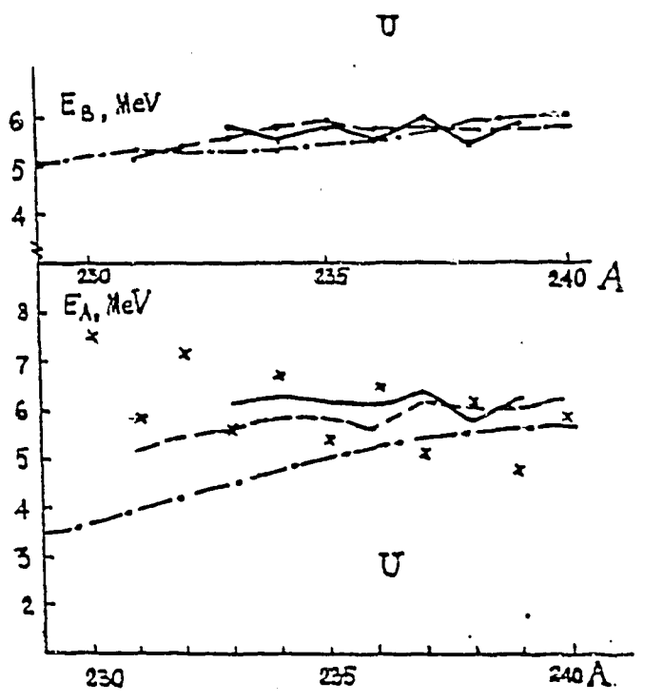

Fig. 20. Comparison of the microscopic fission barriers [55] (dot and dash line) with the experimental data [49] (solid line) and (dashed line) [57] for uranium isotopes, × - neutron removal energy.

fission in direct reactions and microscopic calculations [55] with allowance for the axial asymmetry of a nucleus in the region of hump A. As seen from the figures, the values of E_A and E_B obtained from [49] quite satisfactory agree with the data from Ref. [57] ($\Delta E_A \leq 0.3$ MeV). The differences between the parameters of fission barriers E_A and E_B [49] and the data of [57] may result from the fact that in calculation of the level density for all the nuclei a pattern of single-particle levels has been used in [57] for ^{240}Pu. This assumption justified mainly by the computational problems is equivalent to giving up the consideration of individual properties of nuclei which become apparent in the observed density of neutron resonances.

7. CONCLUSIONS

Thus, using a single set of parameters within the statistical approach and neutron transmissions obtained from the optical model it becomes possible to calculate the reaction cross-sections for fissionable nuclei proceeding through the stage of the compound nucleus formation with an accuracy for σ_t and σ_{nx} about 5%, $\sigma_{n\gamma} \sim$ 15%, $\sigma_{nn'} \sim$ 20-30%, as well as to parametrize σ_f with an accuracy of $\sim$ 10%. In the case of no experimental data on $\sigma_{n\gamma}$ and $\sigma_{nn'}$, for fissionable nuclei are available, they can be calculated by the method described with the above accuracies. The experimental data on σ_f, average parameters, $\langle \Gamma_\gamma \rangle$ and $\langle D \rangle$, and the pattern of nucleus levels may serve as the minimum information required for calculating $\sigma_{nn'}$ and $\sigma_{n\gamma}$.

REFERENCES

1. Ribon P. - Report NEANDC (E) 213- AL, Saclay, 1980, p. I-6 and Report NEANDC (E) 213AL, 1981.
2. Dyson F.J. and Mehta M.L. - J. of Math. Phys., 1963, V.4, p. 701.
3. Moore M.S., Moses J.D., Keyworth G.A. et al - Phys. Rev., 1978, v. C18, p. 1328.
4. Coceva C. and Stefanon M. - Nucl. Phys., 1979, v. A 315, p.1.
5. Fröhner F.H. - Proc. of the IAEA Consultants Meeting on Uranium and Plutonium Isotope Resonance Parameters. IAEA, Vienna, 1982, p.103.
6. Rowlands J.L. - Proc. of the IAEA Consultants Meeting on Uranium and Plutonium Isotope Resonance Parameters IAEA, Vienna, 1982, INDC (NDS)-129/GJ, p. 8.
7. Salvatores M. et al - Proc. of the IAEA Consultants Meeting on Uranium and Plutonium Isotope Resonance Parameters IAEA, Vienna, 1982, p.31.
8. De Saussure G. and Perez R.B. - Proc. of the IAEA Consultants Meeting on Uranium and Plutonium Isotope Resonance Parameters. IAEA, Vienna, 1982, p. 218.
9. Van'kov A.A., Gosteva L.S., Ukraintsev V.F.- Voprosyi atomnoj nauki i tekhniki, serija: "Jadernyie konstantyi", 1983, vyip. 3(52), s.27
10. Zenevich V.A., Klepatskij A.B., Kon'shin V.A. i dr. - V kn. "Nejtronnaja fizika" (Materialyi 5-j Vsesojuznoj konferenzii po nejtronnoj fizike, Kiev, 1980) .M. TsNIIatominform, 1980, ch.3, s.245.
11. Zen Chan Bom, Pantelejev Ts.,Tjan San Khak. - Izv. AN SSSR, ser. fiz. 1973, t.37. s.82.
12. Ryabov Yu., Trochon J., Shackleton D., Frehaut J. - Nucl. Phys. 1973, v. A216, p. 395.
13. Borukhovich G.Z., Zvezdkina T.K., Ivanov K.N. i dr. - Preprint LIJaF, Leningrad, 1978, No 452.

14. Sukhovitskij E.Sh., Klepatskij A.B., Kon'shin V.A.,Antsipov GV.. V kn. "Nejtronnaja fizika " (Materialyi 4-j Vsesojuznoj konferetsii po nejtronnoj fizike, Kiev, 1977).M.,1977,ch.4,s.68.

I5. Tamura T. - Rev. of Modern Physics, I965, v. 37, p. 679.

I6. Chase D.M., Wilets L. and Edmonds A.R. - Phys. Rev., I958, v. II0, p. I080.

I7. Lagrange Ch. - Proc. of the EANDC Topical Discussion on "Critique of Nuclear Models and Their Validity in the Evaluation of Nuclear Data", Tokyo, I974. JAERI, I975, p. 58.

I8. Kikuchi Y. - Proc. of a Panel on Neutron Nuclear Data Evaluation, Vienna, I97I. IAEA, Vienna, I973, IAEA-I53, p. 305.

19.Ignatjuk A.V., Lunev V.P. , Shorin V.S.- Voprosyi atomnoj nauki i tekhniki, serija "Jadernyie Konstantyi", M., TsNiiatominform, 1974, byip.13, c .59.

20. Dzjuba B.M., Marshalkin V.E., Povyishev V.M. i dr. - Voprosyi atomnoj nauki i tekhniki serija "Jadernyie konstantyi".M., Atomizdat, 1978, byp. 23., c.147

2I. Klepatskij A.B., Konshin V.A., Sukhovitskiy E.S. - Report INDC (ccp)-I6I/L, IAEA, Vienna, I98I, p. 9.

22. De Saussure G., Olsen D.K. Perez R.B. et al - Progress in Nuclear Energy, I979, v. 3, p. 87.

23. Haouat G., Sigaud J., Lachkar J., Lagrange Ch. et al - Report NEANDC (E) I80 "L", Commissariat a l'Energie Atomique, I977.

24. Haouat G., Lachkar J., Lagrange Ch. et al - Report NEANDS(E)- - I96 „L" , I978.

25. Möller P., Nilsson S.G., Nix J.R. - Nucl. Phys., I974, v. A229, p. 292.

26. Lambropoulos P. - Nucl. Sci. Eng., I97I, v. 46, p. 356.

27. Davidov A.S., Chaban A.A. - Nucl. Phys., I960, v. 20, p. 499.

28. Soloviev V.G., Stoyanov Ch., Vdovin A.I. - Nucl. Phys., I974, v. A224, p. 4II.

29. Voronov V.V., Komov A.L., Malov A.A., Solovjev V.G. - Jadernaja fisika, 1976, t.24, s.5o4.

30. Ignatyuk A.V. - Proc. of the Meeting on the Use of Nuclear Theory in Neutron Data Evaluation, Triest, I975. IAEA, Vienna, I976, v. I, p. 2II.
31. Ignatjuk A.V., Shubin Y.N. - Izv. AN SSSR, Ser, fis., 1973, t. 37, s. 1947.
32. Dossing T., Jensen A.S. - Nucl. Phys., I974, v. A222, p. 493.
33. Malov L.A., Soloviev V.G. and Voronov V.V. - Nucl. Phys., I974, v. A224, p. 396.
34. Ignatjuk A.V., Istekov K.K., Smirenkin G.N. - Jadernaya fisika, 1979, t. 29, s. 875
35. Ignatjuk A.V., Smirenkin G.N., Tishin A.S. - Jadernaya fisika, 1975, t. 21, s. 485
36. Antsipov G.V., Konshin V.A., Maslov V.M. - IAEA Report INDC(ccp)-I82/G, IAEA, Vienna, I982, p. I-82.
37. Fricke M.P., Lopez W.M., Friesenhahn S.J. et al - Proc. of the Intern. Conf. on Nuclear Data for Reactors, Helsinki, I970. IAEA, Vienna, I970, v. 2, p. 28I.
38. Bartholomew G.A. - Advanced Nuclear Physics, I974, v. 7, p.232.
39. Blohin A.I., Ignatjuk A.V., Platonov V.P., Tolstikov V.A. - Voprosy atomnoi nauki i tehniki, Ser." Jadernye konstanty". M., Atomizdat, 1976, Vyp. 21, s. 3.
40. Rahn F., Camarda H.S., Hacken G. et al - Phys. Rev., I972, v. 6, p. I854.
41. Mughabghab S.F. and Garber D.I. - BNL - 325, 3d Ed., v. I, I973.
42. Abagjan L.P., Korchagina G.A., Nikolaev M.N, Nesterova K.I. - Sb. : " Jader nye konstanty ", M. Tsniiatominform, 1972, Vyp. 8, ch. I, s. 121.
43. Rahn F., Havens W.W., Jr - Report EANDC (us) - I79/U, Columbia University, I977.
44. Poortmans F., Cornelis E., Mewissen L. et al - Proc. of the Intern Conf. on the Interaction of Neutrons and Nuclei. Lowell, I976.

45. Corvi F., Rohr G., Weigman H. - Proc of the Conference on Nuclear Cross Sections and Technology, Washington, I975. NBS Spec. Publ., I975, v. 2, p. 733.

46. Ignatjuk A.V., Lunev V.P. - V kn. "Neitronnaya fisika" (Materialy 5-j Vsesojusnoi konferentsii po neitronnoi fisike, Kiev, 1980). M., Tsniiatom inform, 1980, ch.I, s. 77

47. Istekov K.K., Kuprianov V.M. , Fursov B.I. i dr. Jadernaya fisika, 1979, t. 29, s. 1156

48. Sikkeland T., Giorso A., Nurmia M.J. - Phys. Rev., I968, v. I72, p. I232.

49. Sistematika sechenij i barjerov delenia isotopov urana i plutonia. Ignatjuk A.V., Klepatskij A.B., Maslov V.M i dr. - Trudy 6-j Vsesojusnoj konferentsii po neitronnoi fisike.Kiev, oktyabr 1983.

50. Matsunobu H., Kanda Y., Kawai M. et al - Proc. of the Intern. Conf. on Nuclear Cross Sections and Techn., Knoxville, USA, I979, p. 7I5.

51. Antsypov G.V.,Zenevich V.A., Klepatskij A.B., Konshin V.A. i dr. Izvestia AN BSSR, ser. fis. - energ. nauk, 1979, 4, s. 13

52. Bor O., Mottelson b. Struktura atomnogo jadra, t.2, "Mir",1977

53. Möller P., Nix J.R. - Proc. of the IAEA Symposium on Physics and Chemistry of Fission, I973. IAEA, Vienna, I974, v. I, p. I03

54. Pashkevich V.V. - Nucl. Phys., I97I, v. AI69, p. 275.

55. Möller P. - Nucl. Phys., I972, v. AI92, p. 529.

56. Ignatjuk A.V., Istekov K.K., SmirenKIn G.N. - Jadernaya fisika, 1982, t. 36, s. 54

57. Britt H.C. - Proc. of the IAEA Symp. on Physics and Chemistry of Fission, I979. IAEA, Vienna, I980, v. I, p. 3.

58. Bychkov V.M., Ignatyuk A.V.i dr. Fisika elementarnyh chastits atomnogo jadra, 1983, t. 14, s.2

59. Rao G.R. et al - Phys. Rev., I973, v. C7, p. 733.

Review Paper 6

THE IAEA NUCLEAR DATA LIBRARY FOR ACTINIDES (INDL/A) AND THE RELATED CO-ORDINATED RESEARCH PROGRAMMES (CRP)

H.D. LEMMEL
Nuclear Data Section,
International Atomic Energy Agency,
Vienna

Abstract

This paper reviews the achievements of the IAEA Coordinated Research Programme on the Intercomparison of Evaluations of Actinide Neutron Nuclear Data, presents a survey of the current status of the INDL/A evaluated data file, and describes the proposed objectives of a new IAEA Coordinated Research Programme on the Validation and Benchmark Testing of Actinide Neutron Nuclear Data.

1. The CRP* on the Intercomparison of Evaluations of Actinide Neutron Nuclear Data

Around 1975 there was strong interest in several countries to perform new evaluations of the neutron nuclear data of the actinides, based on new experimental data and improved nuclear models that were either available or in progress. It became obvious that an international co-ordination of actinide evaluation activities was highly desirable.

In the US, neutron data evaluation activities were since long co-ordinated by the Cross-Section Evaluation Working Group (CSEWG). Obviously, the IAEA Nuclear Data Section (NDS) could not play a role that might look similar to an international CSEWG, and the question was:

- to what degree could the actinide evaluation activities in the different countries be co-ordinated?
- in what form could such a co-ordination be organized?

The matter was discussed at the

- IAEA Advisory Group Meeting on Transactinium Isotope Nuclear Data ("TND" Meeting), Karlsruhe, November 1975 [1],
- IAEA Consultants' Meeting on the Evaluation of Actinide Neutron Cross-Sections, Vienna, December 1976 [2], and the
- 9th INDC Meeting, Vienna, May 1977 [2].

---

* CRP = Co-ordinated research programme
[1] Report IAEA-186
[2] Report INDC(NDS)-89

Participants

of the CRP on Intercomparison of Evaluations
of Actinide Neutron Nuclear Data

country	primary interest
France, Bruyères-le-Châtel	Pu-242, et al.
France, Cadarache	Np-237, Pu-238, Am-241
German Dem. Rep.	precision measurements of MeV fission cross-sections
Germany, F.R., Karlsruhe	KEDAK evaluations
Germany, F.R. Stuttgart	intercomparisons
India	Th-232, U-233
Israel	Cm-244, 246, 248, Pu-242 and some earlier KEDAK evaluations
Italy	Pu-241, Am-241, 243, Cm-242, 243, 245-248
Japan	Am-242, 242m, 243, Cm-242-245 and other JENDL evaluations
Romania	Th-232, Pa-233
Sweden	compilations and intercomparisons
UK	Am-241, 243
USSR, Leningrad	precision measurements of MeV cross-sections; Cf-spectrum averaged cross-sections
USSR, Minsk	(U-235), Pu-239, 240, 241, 242
USSR, Obninsk	($\bar{\nu}$); (n,2n), (n,3n)

The result was the creation of the CRP on the intercomparison of evaluations of actinide neutron nuclear data in the years 1977 to 1983. Initially, the CRP had nine participating institutes from nine countries; finally, with a slightly widened scope, 15 participating institutes from 11 countries (including Sweden which regularly participated in the CRP meetings) plus occasional participants, e.g. from Geel, NEA Data Bank, USA.

Considering that the USA had two complete actinide data files, ENDF/B and ENDL, with repeated updates, the geographical scope of the CRP did not include the USA. It should however be acknowledged that the success of the CRP would not have been possible without the US contributions of experimental data and computer codes.

The core of the CRP consisted of evaluators performing comprehensive new evaluations. Additional participants concentrated on specific tasks such as evaluation of specific data types, development of nuclear models, intercomparison of evaluations, or precision measurements of MeV fission cross-sections to be used as standards. Some scientists (e.g. from Sweden and Obninsk) participated without a formal agreement with the IAEA.

What were the goals of the CRP, and what has been achieved?

To anticipate the conclusion: The goals of the CRP have been fulfilled to a high degree, but in some aspects the practice of the CRP deviated somewhat from the original ideas.

It is essential to realize that it was never the intention to create an internationally recommended, comprehensive and internally consistent data file. This might have been desirable but was certainly not possible by means of the CRP.

The primary goal was, to stimulate intercomparisons between the new evaluations and to have a free international exchange of the evaluated actinide data, and this has been achieved by the creation of the IAEA Nuclear Data Library for Actinides, INDL/A, containing now more than 70 evaluations for 26 actinide isotopes.

The CRP was a useful forum to bring new evaluators (e.g. India, Romania) in contact to experienced evaluators.

The CRP agreed on guidelines for performing the evaluations and for documenting the evaluations, and it provided a forum for the discussion of theoretical models, existing discrepancies and various encountered problems. Thus, the CRP contributed to the quality of the evaluations that are now available.

The initial scope of the CRP was restricted to the secondary actinides. However, gradually also the primary actinides were included. Evaluations for U-235 and Pu-239 exist now from USSR (Pu-239 available, for U-235 a new file is expected soon), JENDL-2 and KEDAK-4. As U-235 is a standard, this will rather be a topic of the Advisory Group Meeting on Nuclear Standard Reference Data in Geel, 12-16 Nov. 1984. Research agreements with Dresden, GDR, and Leningrad, USSR, on precision measurements of MeV fission cross-sections for U-235 and other nuclides were included in the CRP.

For the secondary actinides the question of standards was considered as unimportant. The overall accuracy of the data is such that it did not matter very much which standard values were assumed. Most participants used the ENDF/B-5 standards.

In certain aspects the success of the original intentions was limited.

For certain nuclides parallel evaluation work was done. It has been recognized from the beginning that some parallel evaluation work was useful as a cross-check. However, the original recommendation had been to organize more bilateral co-operations where several participants were interested in the same nuclides. A few such co-operations were successful (e.g. Bologna/Bruyères-le-Châtel for Pu-242, or Israel/Karlsruhe). Some more bilateral co-operations would have been useful but were difficult to achieve, partly because the one or other CRP participant could not attend the CRP meetings.

The work distribution within the CRP was according to the national programs, and it seems that the national programs were not always influenced by considerations whether the same work was done in parallel in other countries. As the research agreements or contracts by the Agency involve no or little money, the Agency could hardly take an

influence on a better co-ordination of national programs. Consequently, many actinide isotopes were well covered by three or even four parallel evaluations, whereas other isotopes were not covered at all. Maybe, the isotopes not covered are really of minor importance. However, in 1977 there were 14 nuclei identified as being the most important: Am-241, 242m, 243; Cm-242, 244-248; Bk-249; Cf-249-252. Of these, Bk-249 and the Cf isotopes have not been evaluated by CRP participants, and the US evaluations in ENDF/B-V and ENDL-82 still seem to be the only ones available. Is this satisfactory?

Originally, it had been stressed that the emphasis of the CRP should be towards intercomparisons of evaluations. Indeed, the evaluators intercompared their evaluations, usually with the most recent ENDF/B (IV or V) evaluation. The progress achieved was always obvious due to the more recent experimental data included in the new evaluations. The more interesting intercomparisons of the new evaluations against each other were often not possible because the new evaluations were in progress at the same time, and time elapsed until they became available to the other evaluator in correct ENDF/B format. One participant (Mrs. Mattes, Stuttgart) specialized in intercomparisons by computing group data and spectrum average cross-sections. However, I am not sure whether these intercomparisons are still up-to-date, because some of the evaluations were meanwhile revised. This is a bookkeeping problem and some more thought must be given to this matter.

Little progress has been made with the format for evaluated data. When the CRP started, the USSR (after Japan and some of the West European countries) had adopted the ENDF format, but for some of the CRP participants the UKNDL and KEDAK formats could not yet be abandoned. But also the ENDF-IV and the ENDF-V formats are both being used. The differences between these two versions of the ENDF format are usually not serious, but the conversion from the one to the other which is required for certain computer codes, is an additional workload. Consequently, INDL/A still does not yet have a uniform format, so that its use is still tedious, and intercomparison of evaluations in different formats was difficult if not impossible.

The role of the IAEA Nuclear Data Section within the CRP can be described briefly as follows. NDS convened the CRP meetings, distributed documents and new literature of interest to participants, provided CINDA retrievals in regular intervals and (together with the NEA Data Bank) provided EXFOR retrievals. Then the evaluations produced were collected in the INDL/A library, which was the stimulance for NDS to implement the required ENDF processing and checking routines.

At present, NDS does not touch evaluations received in KEDAK or UKNDL format. Evaluations received in ENDF-IV format (and this is the majority) are converted to ENDF-V format. This conversion is partly trivial but may include pitfalls. For example, in the unresolved resonance region ENDF-IV permits interpolation of parameters (LRF=1), whereas ENDF-V recommends interpolation of the cross-sections derived from the parameters (LRF=2), and the code RECENT does not accept LRF=1. For the evaluator, LRF=1 is convenient, because the parameters need to be given at few energies only with linear interpolation. For LRF=2 and linear interpolation of the cross-sections, parameters must be given at more energy values in order to maintain the same data accuracy of 1 to 5%.

Data received in ENDF-V format and those converted by NDS into ENDF-V format are checked by CHECKER, FIZCON, PSYCHE, and by graphical plotting. Corrections of encountered errors frequently required consultation back with the authors. In this respect special care had to be given to evaluators who were not yet experienced with the rules and procedures of the ENDF format, because the format manual is not ideal for a do-it-yourself training.

This thorough checking could be performed with a good fraction of the ENDF formatted data but, due to manpower limitations, not yet with all of them. Consequently, INDL/A(83) contains for many, but not for all evaluations the ENDF-IV version as provided by the evaluator, not checked by NDS, plus the ENDF-V version converted and checked by NDS. Several evaluations still contain deviations from the strict ENDF format so that computer codes may either reject or misinterpret part of the data given.

The checking and correcting of INDL/A data was primarily done by V. Pronyaev, but I wish to give credit also to D.E. Cullen and K. McLaughlin. At NDS we have now perfect expertise on the maintenance of an ENDF formatted data library. However, manpower limitations did not permit us to do all that should have been desirable. To the tasks still to be solved I will come back later.

The CRP formally ended with its fifth CRP Meeting at Geel in September 1982. However, an informal co-operation continued and new evaluations or revisions to earlier evaluations are still being received at NDS.

2 The present status of INDL/A

The 1983 version of INDL/A was distributed in early 1984. It is documented in IAEA-NDS-12 Rev. 7 dated Dec. 1983. Since then some additional evaluations have been received (Pu-242 by Israel, Cm-248 by Bologna) which are being distributed as a supplement to INDL/A(83) together with further improvements.

INDL/A(83) consists of the following 6 files:

A. Complete evaluations

in ENDF-5 format:	File 1	19 evaluations for 16 nuclides
in ENDF-4 format:	File 2	22 evaluations for 18 nuclides
in UKNDL format:	File 3	2 evaluations (plus UKNDL-80)
in KEDAK format:	File 4	4 evaluations (plus 17 from KEDAK-4)

B. Partial evaluations

in ENDF/B-5 format:	File 5	Obninsk (n,2n) and (n,3n) evaluations, and Harwell Am-241 (n,f)
in ENDF/B-4 format:	File 6	Bologna evaluations in resonance region

Some of the evaluations are available in ENDF/B-4 and ENDF/B-5 formats and were, therefore, included in files 1 and 2. One evaluation is available in the three formats ENDF-5, ENDF-4 and UKNDL.

Theoretically, the format conversions should not change the data, and it will be a useful check to see whether graphical plots or group data calculations derived from different formats will produce identical results.

In addition, we have now available:

C. Point data (RECENT output)

of the ENDF-5 format evaluations: File 7
of the ENDF-4 format evaluations: File 8
(except for evaluations with Reich-Moore-parameters)

The following table shows in detail the contents of INDL/A(83) together with other recent evaluations available.

JENDL-2 Rev. 1 has been received only recently. We have not yet analyzed the extent of the differences between the earlier Japanese contributions to INDL/A and the new issue of JENDL-2 Rev. 1.

The ENDL-82 evaluations are available in ENDL Transmittal Format.

A recent revision of the ENDF/B-V Actinides File ("V.2") contains, in addition to several small corrections, significant re-evaluations for Cm-242 and Bk-249.

3. The CRP on Validation and Benchmark Testing of Actinide Nuclear Data

Realizing that INDL/A requires further improvements and that critical intercomparisons of the new version of INDL/A with other available evaluations is required, a new CRP on validation and benchmark testing of actinide nuclear data has been started. This CRP has its first research co-ordination meeting adjacent to the present Advisory Group Meeting (AGM), and I should like to request advice and assistance from the AGM participants to define specific tasks to be solved by the new CRP.

Due to the JEF project by the NEA Data Bank the geographical scope of the new CRP was to include primarily participants from non-OECD countries. However, the success of the CRP will depend also on support from OECD countries, in particular by providing suitable benchmark data.

Contents of INDL/A (83)
and other evaluations available

Note: (...) parentheses indicate an evaluation in progress but not yet available

-84 indicates an evaluation received in 1984 to be distributed as supplement to INDL/A (83)

	INDL/A 1979/83	ENDF/B V= 1979 IV= 1974	ENDL-82 1982	JENDL-2 Rev.1 1983/84	UKNDL 1980
90-Th-228	-	-	-	+	
-230	-	V	-	+	
-231	-	-	+	-	
-232	Romania	IV	+	+	+
	KEDAK-4 (India)				
-233	-	-	+	+	
91-Pa-231	(Romania)	V	-	-	
-233	Romania	V	+	+	+
92-U- 232	(India)	V	-	-	
- 233	KEDAK-4 (India)	IV	+	+	+
- 234	-	V	+	+	+
- 235	JENDL-2 KEDAK-4 (Minsk)	V	+	+	+
- 236	-	V	+	+	+
- 237	KEDAK-4	V	+	-	+
- 238	JENDL-2 KEDAK-4	IV	+	+	+
- 239	-	-	+	-	+
- 240	-	-	+	-	+
93-Np-237	Cadarache KEDAK-4	V	+	+	+
-238	-	V	-	-	
-239	-	-	-	+	

	INDL/A 1979/83	ENDF/B V= 1979 IV= 1974	ENDL-82 1982	JENDL-2 Rev.1 1983/84	UKNDL 1980
94-Pu-236	-	V	-	+	
-237	-	V	-	-	
-238	Cadarache KEDAK-4	V	+	+	+
-239	Minsk JENDL-2 KEDAK-4	IV	+	+	+
-240	Minsk JENDL-2 KEDAK-4	IV	+	+	+
-241	Minsk JENDL-2 KEDAK-4 Bol: Res. only	IV	+	+	+
-242	Minsk Bruy./Bol. Soreq 84	V	+	+	+
-243	-	V	+	-	
-244	-	V	-	-	
95-Am-241	Cadarache Harwell KEDAK-4 Bol: Res. only	V	+	+	
-242	JAERI	V	-	+	
-242m	JAERI KEDAK-4	V	+	+	
-243	Harwell JAERI KEDAK-4 Bol: Res. only	V	+	+	

	INDL/A 1979/83	ENDF/B V= 1979 V.2= 1983	ENDL-82 1982	JENDL-2 Rev.1 1983/84	UKNDL 1980
96-Cm-241	-	V	-	-	
-242	Bologna JAERI	V.2	+	+	
-243	Bologna JAERI	V	+	+	
-244	JAERI Soreq KEDAK-4 *)	V	+	+	+
-245	Bologna JAERI	V	+	+	
-246	Bologna Soreq KEDAK-4 *)	V	+	-	
-247	Bologna	V	+	-	
-248	Soreq Bologna 84	V	+	-	
97-Bk-249	-	V.2	+	-	
98-Cf-249	-	V	+	-	
-250	-	V	+	-	
-251	-	V	+	-	
-252	-	V	+	-	
-253	-	V	-	-	
99-Es-253	-	V	-	-	

*) Note: For Cm-244 and Cm-246 the Soreq evaluation was used in KEDAK-4.

At present the new CRP includes the following participants.

Participants

of the CRP on Validation and Benchmark Testing
of Actinide Nuclear Data

Brazil:	R. Paviotti Corcuera, Centro Técnico Aerosp., Sao José dos Campos
Bulgaria:	N. Janeva, Inst. of Nucl. Res. and Nucl. En., Sofia
China, P.R.:	Gu Fuhua, Inst. of Atomic Energy, Beijing
India:	S. Ganesan, Reactor Res. Centre, Kalpakkam
USSR:	V.A. Konshin, Inst. of Nucl. Engineering, Minsk
Yugoslavia:	A. Trkov, Inst. Josef Stefan, Ljubljana

According to the research proposals submitted to the Agency, of these participants

Brazil, Bulgaria and Yugoslavia will be fully available to data validation work, whereas the other three participants primarily wish to complete or update specific evaluations

China, P.R.: to complete and update a number of Chinese evaluations; these include evaluations for Am and Cm isotopes of which evaluations already exist in INDL/A, but also include Bk-249, Cf-249 and Cf-252 which are still missing in INDL/A. Some Chinese evaluations are available in EXFOR format ("EXFOR-V" series).

India: to produce a joint file from Indian and Romanian evaluations for the thorium cycle.

USSR: to finalize the U-235 evaluation, to update the evaluations for Pu isotopes, and to improve models for evaluating (n,2n) and (n,3n) cross-sections.

The following table gives a draft summary of the program of the CRP.

Draft program of the "Validation CRP"

A. Data Evaluation

- finalize started evaluations — Priorities? Who does what?
- update earlier evaluations — When?

specific data types:

- "best" (n,2n), (n,3n) data?
- "best" $\bar{\nu}$ data?
- decay-data and F.P. yields, to be included or kept as separate files?

B. "Technical" work

Format conversions

- ENDF-4 --> ENDF-5
- Reich-Moore --> Adler-Adler (code POLLA)
- KEDAK
  UKNDL --> ENDF-5 (who does what?)

Checking (CHECKER, FIZCON, PSYCHE) and correcting

Presenting characteristic figures for each evaluation
in standardized format, for easier intercomparison

Multigroup files (FEDGROUP, 4-ACES)
for graphical intercomparisons (640 groups, COMPLOT)
or tabular intercomparisons (25 groups)

C. Benchmarks

- "simple" benchmarks: comparisons with integral cross-section measurements in defined spectra
- more complex benchmarks integral data in critical facilities (as far as feasible)

A. Data evaluation

Compared to the time 5 years ago we have a new situation. Earlier there was a lack of new evalutions. Now we rather have too many evaluations for the same nuclide. Nevertheless, the problem remains how to get new experimental data speedily into the evaluated data files.

Therefore, those CRP participants who continue to do evaluation, should be encouraged to do so. Priorities should be assigned with a view on the evaluations already available (in addition to the priorities determined by national programs).

Specific questions relate to specific data types. For example, nuclear theory for improved estimates of the (n,2n) and (n,3n) reactions seems to be under development. If an agreement could be reached on a best model, all evaluations could eventually be updated with respect to the (n,2n) and (n,3n) reactions.

In principle, the actinide evaluations should include decay data and fission-product yield data. Such data exist in separate libraries in ENDF format. Is this sufficient? Or would it be essential to include in all INDL/A evaluations decay data and fission-product yield data?

B. "Technical" work

Under "technical" work I mean file maintenance operations with available computer codes, including checking and correcting, documentation, format conversions, etc.

As the ENDF processing codes at NDS operate on the ENDF-5 format, the first task is the conversion of ENDF-4 files to ENDF-5 format as far as not yet done. This includes the conversion of Reich-Moore to Adler-Adler parameters, for which a code will hopefully be available.

Whether KEDAK and UKNDL formatted data will be converted to ENDF-5 format, will have to be decided. Another access to the KEDAK and UKNDL evaluations would be through the FEDGROUP or FOURACES codes which accept data from all of these formats to compute multigroup data.

The ENDF-5 formatted evaluations are checked (CHECKER, FIZCON, PSYCHE) etc and, where necessary, corrected. The corrections performed must be well-documented. Care must be taken that the most recent ENDF/B-5 utility programs are used [K. McLaughlin, ENDF/B-5 Utility Programs, IAEA-NDS-29 Rev. 1, March 1984].

For easier intercomparison of evaluations it is planned to issue characteristic numbers for each evaluation in a standardized format. Such characteristic numbers would be

- 2200 m/s cross-sections
- 20°C Maxwellian spectrum averaged cross-sections
- infinite dilute resonance integrals
- a standard fission-spectrum averaged cross-section
- 14 MeV cross sections

Details will have to be discussed.

The problem encountered is, that such characteristic values are usually available in the documentation of the evaluation provided by the author. However, it is tedious to find the figures, and one needs to have a control whether these figures have been changed due to format conversions or corrections applied. If these characteristic figures are presented in a standardized format for each evaluation, the intercomparison of evaluations will be much easier.

Finally, it is intended to issue the entire actinides library, including evaluations from all formats (ENDF, KEDAK, UKNDL) in a standard multigroup form, most likely in the extended SAND-II 640 multigroup form. For this purpose, only such codes should be used which have been tested by the IAEA Cross-Section Processing Code Verification Project [D.E. Cullen et al., paper presented at the Sixth Int. Conf. on Radiation Shielding, Tokyo, 16-20 May 1983, to be published].

This multigroup file can be used as a basis for graphical intercomparison (code COMPLOT by D.E. Cullen) and as a basis for benchmark calculations.

All this "technical" work would certainly not be restricted to evaluations included in INDL/A but would extend also to other available actinide evaluations.

C. Benchmarks

The benchmark calculations to be done should help to decide which of several competing evaluations may be better. The work in detail will depend on the benchmark data that may become available. Initially, it would be "simple" benchmarks, i.e. comparisons with integral

cross-section measurements in well-defined spectra. Subsequently, one would perhaps consider more complex benchmarks, i.e. comparisons with integral data in critical facilities. Advice and assistance from advanced institutes will be required.

In 1979/80 N. Kocherov already started to compile benchmark data, see Appendix. This work was then interrupted when N. Kocherov left the IAEA, and his list, which is given on the following pages, presumably requires updating. Contributions and suggestions will be highly appreciated.

Appendix

Status of NDS Compilation of integral cross-section and benchmark neutron spectrum data as of June 1980

N. Kocherov

According to the recommendation of the meeting of the participants of this CRP in Aix-en-Provence in May 1979 NDS has started a compilation of data on integral cross-section measurements for actinide nuclides of interest to the participants. NDS has also approached several specialists with requests for the information about the neutron spectra of the benchmark facilities in which these measurements were made. The present status of this compilation is summarized in Table 1.

From 11 benchmark neutron spectra listed in the table three were obtained by evaluation and 8 by calculation. The information about the last spectrum is expected soon. Two evaluations of ^{235}U fission neutron spectra are included in the table. The evaluation by NBS (item 6) was based on different types of measurements and has uncertainties quoted. The ENDF/B-V evaluation (item 7) was based only on recent time-of-flight measurements and does not quote uncertainties. There are some differences between the results of these evaluations. According to recent information from C. Eisenhauer the ENDF/B-V version gives a somewhat better agreement with integral measurements but there was no decision yet which of the two would be selected as a standard in the US.

The two spectra for Zebra are also slightly different but this is due to the difference in sample containers used in these two cases.

The formats of spectrum data presentation range from 26 groups to 620 groups which might cause difficulties in practical application. The best way out of this from our point of view is to use a code which reduces or expands the number of groups to the required format.

The references to documentation of data in the Table are presented below:

List of references

1. D.W. Sweet, Report AEEW-R 1090, Winfrith, U.K., 1977
2. R.A.P. Wiltshire et al., Report AERE-R 7363, Harwell, U.K., 1973
3. F. Helm, Private Communication, 1980, sent to the participants in the Memo dated 24.03.80
4. Report KFK 1273/4

5. W. Scholtyssek, Report KFK 2361

6. Compendium of Benchmark and Test Region Neutro Fields for Pressure Vessel Surveillance, NBS Special Publication

7. W. Mannhart, Private Communication

8. C. Eisenhauer, Private Communication

9. R. Chawla et al., Ann. of Nucl. Energy, V. 6, p. 585-589, 1979

10. K. Gmur, Private Communication information promised

Table 1. Benchmark Neutron Spectra and Integral Cross Sections of Actinide Nuclides Measured in them

	Name of the facility and reference to spectrum documentation	Number of groups	Origin of the spectrum	Type of data measured	Nuclides
1.	Zebra (UK) [1]	37	calc.	$\sigma_i^f/\sigma^f{}_{239Pu}$	$^{240,241,242}Pu$ $^{241,243}Am$ ^{244}Cm
2.	Zebra (UK) [2]	37	calc.	$\sigma^{Prod}_{242Cm}/\sigma^f{}_{239Pu}$	^{242}Cm (production from ^{241}Am)
3.	SNEAK 9B (FRG) [3]	26	calc.	$\sigma_i^f/\sigma^f{}_{235U}$	$^{240,241}Pu$, ^{241}Am [4]
4.	SNEAK 9C-2 (FRG) [3]	26	calc.	$\sigma_i^f/\sigma^f{}_{235U}$ $\sigma_i^f/\sigma^f{}_{239Pu}$	$^{240,241}Pu$, ^{240}Am [5]
5.	^{252}Cf Spontaneous Fission *) Neutron Field, NBS	45	eval.	σ^f_{abs} $\sigma^f/\sigma^f{}_{239Pu}$ $\sigma^f/\sigma^f{}_{235U}$	^{240}Np, ^{237}Np } [6] ^{237}Np [7]
6.	^{235}U Spontaneous Fission *) Neutron Spectrum [8]	620	NBS eval.		
7.	^{235}U Spontaneous Fission *) Neutron Spectrum [8]	620	ENDF/B-V eval.		
8.	Sig-10, USA [8] *)	620	calc.	$\sigma_i^f/\sigma^f{}_{239Pu}$	^{233}U, ^{237}Np [6]
9.	CFRMF, USA [8] *)	620	calc.	$\sigma^f/\sigma^f{}_{239Pu}$	^{233}U, ^{232}Th, ^{237}Np, ^{240}Pu } [6]
10.	ISNF, USA [8] *)	620	calc.	$\sigma^f/\sigma^f{}_{239Pu}$	^{237}Np [6]
11.	ΣΣ, USA [8] *)	620	calc.		
12.	PROTEUS, Wuerenlingen, Switzerland [10]	Spectrum information forthcoming		$\sigma^c/\sigma^f{}_{239Pu}$ $\sigma^c/\sigma^f{}_{239Pu}$	^{232}Th, ^{233}U [10] ^{237}Np [9]

*) Spectrum available at the IAEA Nuclear Data Section

Review Paper 7

CURRENT REQUIREMENTS FOR HEAVY ELEMENT AND ACTINIDE NUCLEAR DECAY DATA – MAY 1984

A.L. NICHOLS
Atomic Energy Establishment,
United Kingdom Atomic Energy Agency,
Winfrith, Dorchester, Dorset, United Kingdom

Abstract

The current world requirements for heavy element and actinide decay data are discussed with respect to a variety of reactor-related applications and environmental studies. The important nuclides and their decay parameters are reviewed in terms of the recommendations made at the Second Advisory Group Meeting on Transactinium Isotope Nuclear Data, Cadarache, May 1979. Some of the accuracies requested in this earlier assessment are questionable, and specific requirements will prove extremely difficult to achieve. Nevertheless, certain improvements in the decay data are still required to assist in long-term storage calculations, non-destructive assays and L-x-ray studies.

1. INTRODUCTION

Approximately 120 heavy element and actinide nuclides are used in or produced by nuclear fission reactors. These include the reactor fuel actinides, all the principal actinide reaction products up to Es-253 and the major decay chain nuclides down to Hg-206. Accuracy requirements for the decay data of these nuclides and relevant neutron-deficient tracers are reviewed and expressed in terms of one standard deviation (1 σ): decay data are defined as the normal radioactive decay modes of a nuclide and do not include fission yields and nuclear reaction cross-sections.

World-wide requirements have been specified at previous IAEA Advisory Group Meetings on Transactinium Isotope Nuclear Data (1, 2). The desired accuracies of the data and the justifications for these requests were described in the associated review papers at Karlsruhe (3-7) and Cadarache (8, 9). The majority of these requirements come from the nuclear power industry and were identified with reactor operation, fuel handling, transport and analysis, waste management, environmental monitoring and safeguards. These applications continue to determine the needs for more accurate measurements of decay data, and few new requirements have emerged since Cadarache, 1979. However, some modifications can be made based upon recent measurements satisfying specific requests and the development of new requirements associated with fuel assay, delayed storage and reprocessing of fuel and environmental monitoring. Brief reviews of important fuel-handling applications are given in this report, and the requirements for specific decay data that are still judged to be inadequate are redefined.

Efforts have also been made to define more realistic accuracy requirements for the decay data requests of the previous IAEA Advisory Group Meetings. It is difficult to envisage measurements that will achieve accuracies of better than 0.5% to 2%, and it is not clear that such high accuracies are ever likely to be required for reactor-related calculations. In particular the requirements of the Cadarache meeting (2)

have been reassessed and the desired accuracies adjusted where appropriate. However, balanced against this need for realism is the problem of predicting future requirements. This unpredictability supports the need to maintain laboratories in which decay data can be measured and evaluated with good accuracy, with the flexibility to meet sudden and unforeseen changes in data priorities.

2. FUEL HANDLING

The important fuel-handling procedures involve fabrication, irradiation, storage, irradiated fuel transport, reprocessing and recycling. Radioactive decay and transmutation occur during and after irradiation, and the composition of the fuel is extremely important in determining the nature and timing of various post-irradiation procedures associated with storage, reprocessing and re-irradiation.

At the present time commercial thermal reactors use a once-through uranium cycle. The actinide nuclides of importance are shown in Figure 1. They include the plutonium nuclides Pu-239, Pu-240, Pu-241 and Pu-242, the decay product Am-241, and the capture products U-239 and Np-239. For higher burn-up and fast reactor fuels a wider range of actinides become important; these include U-237, Np-237, Pu-236 (and decay chain that includes Tl-208 (Figure 2)), Pu-238, Cm-242 and Cm-244. Studies have also been made of the Th-232/U-233-based fuel cycle (Figure 3) in which the dominant nuclides are Th-233, Pa-233 and the U-232 decay chain that includes Tl-208 (Figure 2).

2.1 Decay Heat

The contribution of the actinides to the total decay heat depends upon the composition of the irradiated fuel (10), and varies between 5% and 20% during the first day of cooling for U and U/Pu fuels and becomes increasingly dominant for cooling times beyond 30 years (Figure 4). Individual actinide contributions vary as a function of time, and Figure 5 shows this behaviour for a gas-cooled reactor with a fuel rating of 30 GWd tonne^{-1} (U). For cooling times up to 10 days the important actinides are U-239, Np-239 and Cm-242, whilst for cooling times greater than 3 years Pu-238, Pu-240, Am-241 and Cm-244 predominate (11).

The Th-232/U-233 fuel system shows a different form of actinide contribution to the decay heat (Figure 4). Between 5 and 150 days Pa-233 dominates the actinide contribution, but since the half-life of this nuclide is 27 days this effect declines rapidly beyond 50 days to give the same magnitude of actinide contribution as the other thermal reactor systems.

For low burn-up fuel it is generally accepted that accurate decay scheme data are required for U-239 and Np-239 in the uranium cycle, and for Th-233 and Pa-233 in the thorium cycle. Uncertainties in the neutron flux, cross-section and decay data give an overall uncertainty of between 7% and 12% in heavy element decay heat calculations for uranium-fuelled thermal reactors. Some improvements could be made to these calculations if the important beta and gamma-ray emission probabilities were known with an accuracy to 2% (11). Recent studies have been made of the emission probabilities of U-239 (12), Np-239 (13) and Pa-233 (14), but further measurements may be required to improve the accuracy of some of these data. In higher burn-up and fast reactor fuels the major actinide contribution to the decay heat comes from Pu-238, Cm-242 and Cm-244.

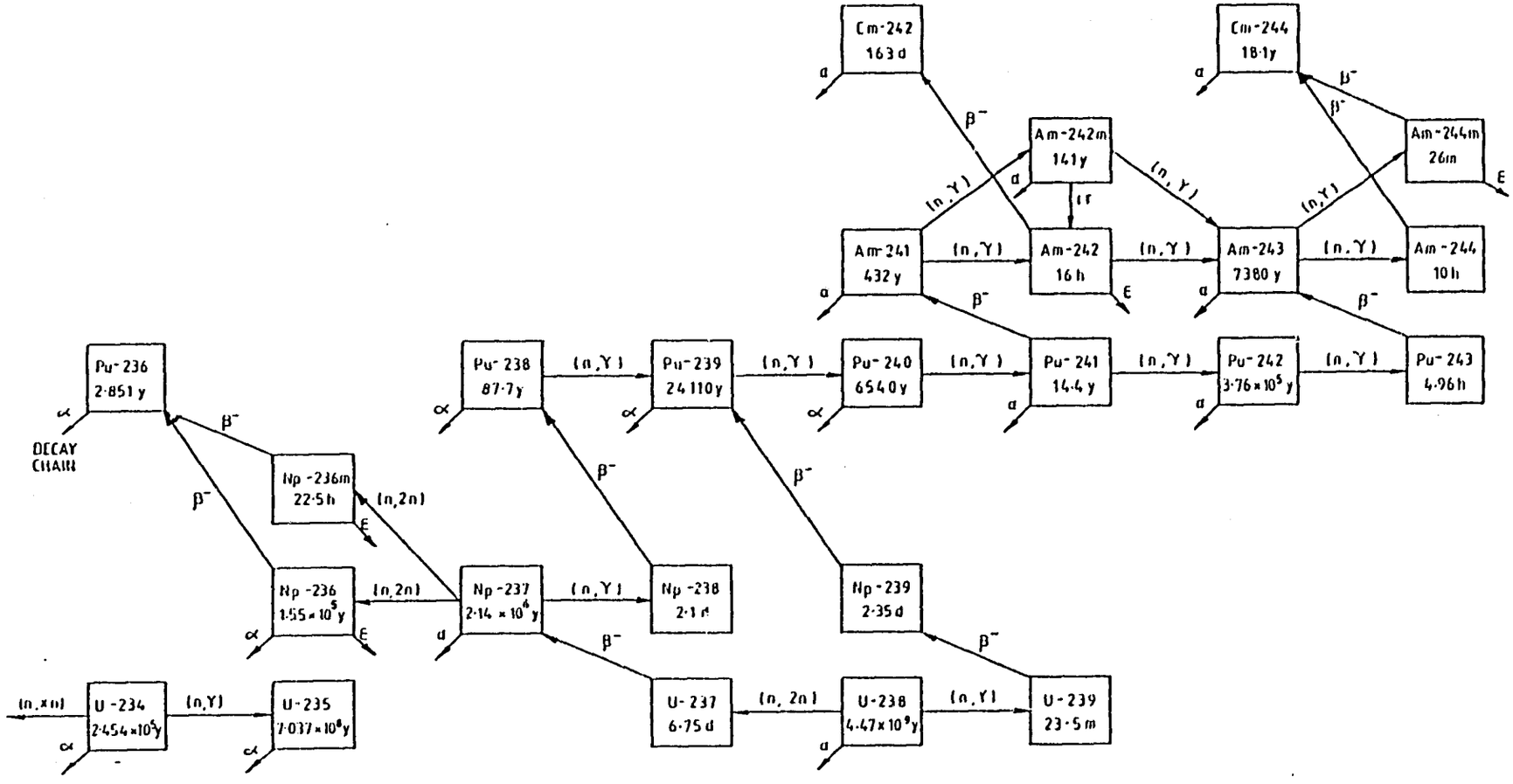

FIG. 1 PRODUCTION CHAIN OF IMPORTANT ACTINIDES IN THE URANIUM-BASED THERMAL REACTOR

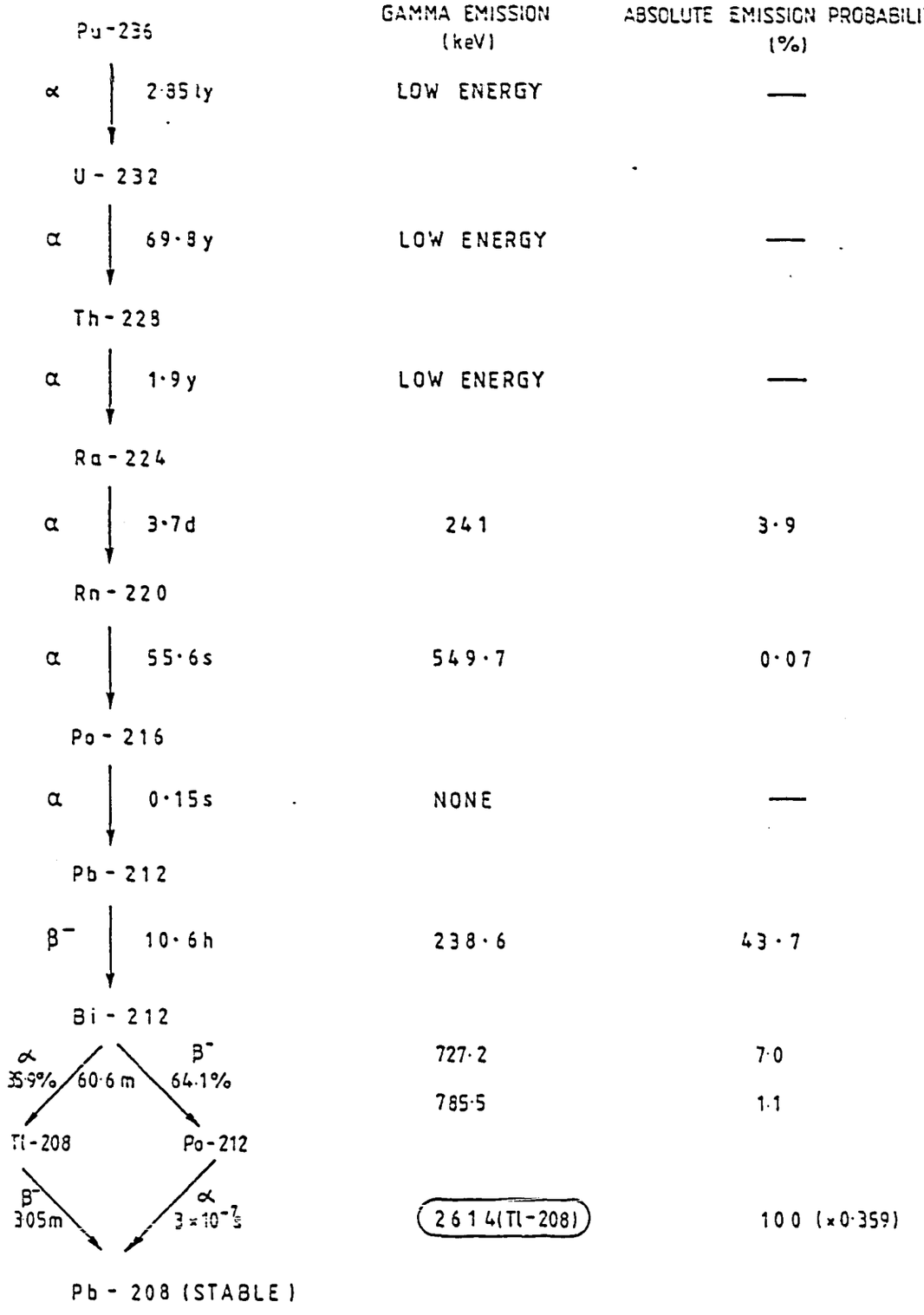

FIG.2 Pu-236 / U-232 DECAY CHAIN

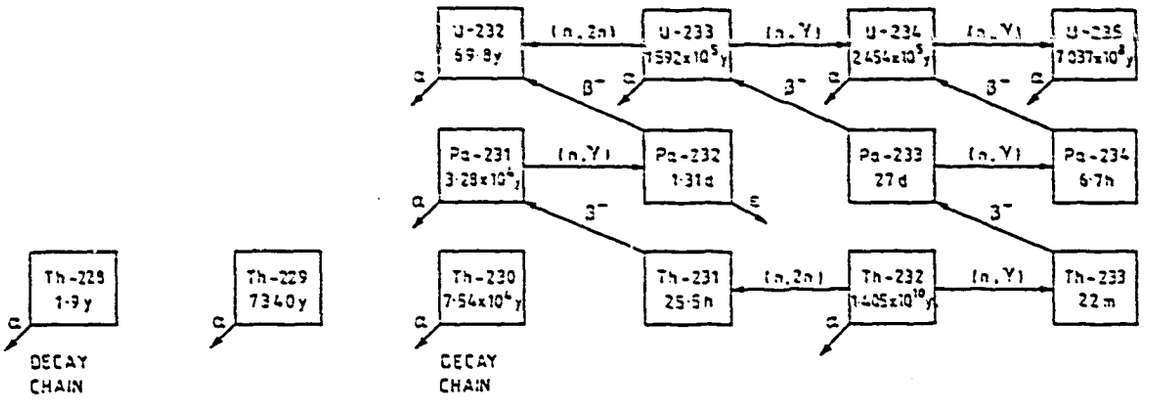

FIG.3 PRODUCTION CHAIN OF IMPORTANT ACTINIDES IN THE U-233/Th-232 THERMAL REACTOR

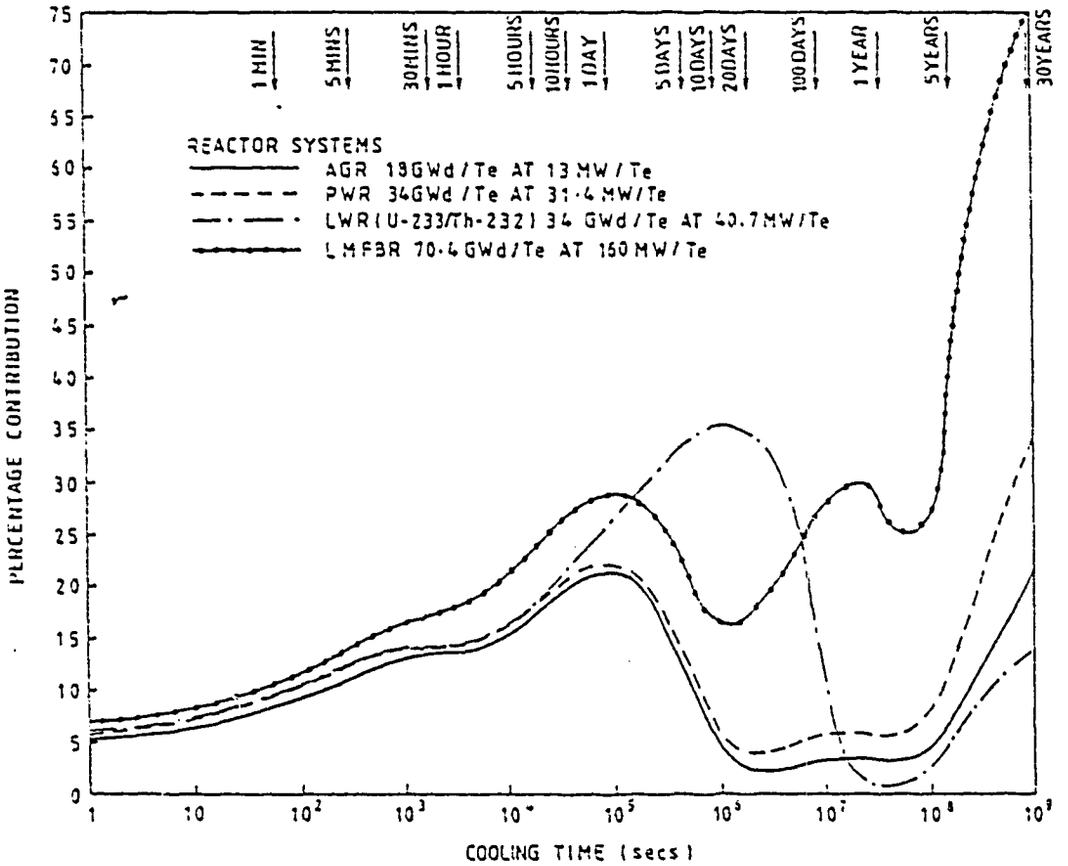

FIG. 4. PERCENTAGE CONTRIBUTION OF ACTINIDES TO TOTAL DECAY HEAT FROM TYPICAL FUEL OF DIFFERENT REACTOR SYSTEMS

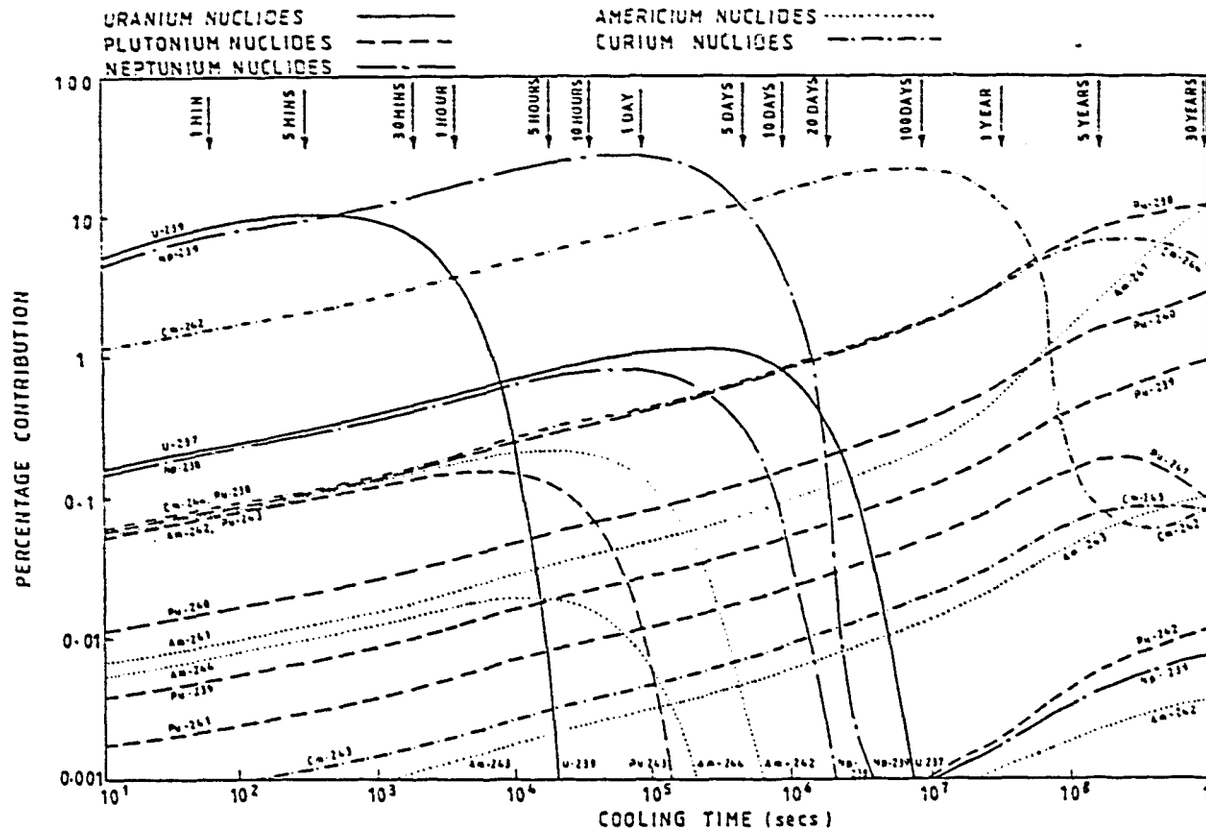

FIG. 5. THE PERCENTAGE CONTRIBUTION FROM INDIVIDUAL ACTINIDES TO TOTAL DECAY ENERGY RELEASE RATES [5MW/Te(U) END OF LIFE RATING 30GWd/Te(U)] FOR GAS-COOLED REACTOR FUEL (AGR)

Cm-242 is produced via

Am-241 (n,γ) Am-242 (β^-) Cm-242,

and this nuclide produces approximately 85% of the actinide decay heat after 30 days cooling (Figure 6). Cm-244 is produced via

Am-242/Am-242m (n,γ) Am-243 (n,γ) Am-244 (β^-) Cm-244,

and contributes almost 50% of the total actinide heating after 3 years cooling (Figure 7). The measured and evaluated accuracies of the decay data for these nuclides are adequate for decay heat calculations, although there are other applications (see Section 2.2) that require some improvements in these data.

2.2 Fuel Assay

Destructive and non-destructive assay techniques are used to monitor the actinide content of fuels and to determine their precise nuclide composition. These measurements require great care and precision to achieve the desired accountancy and safeguards. Various analytical techniques are used including calorimetry and gamma and neutron spectrometry (6, 15). Possible requirements cover a wide range of nuclides and decay parameters, including total, alpha and spontaneous fission half-lives, and alpha, gamma and x-ray energies and emission probabilities for various thorium, protactinium, uranium, neptunium, plutonium, americium and curium nuclides and their daughter products (16, 17). These decay data can be used in non-destructive assays to define the

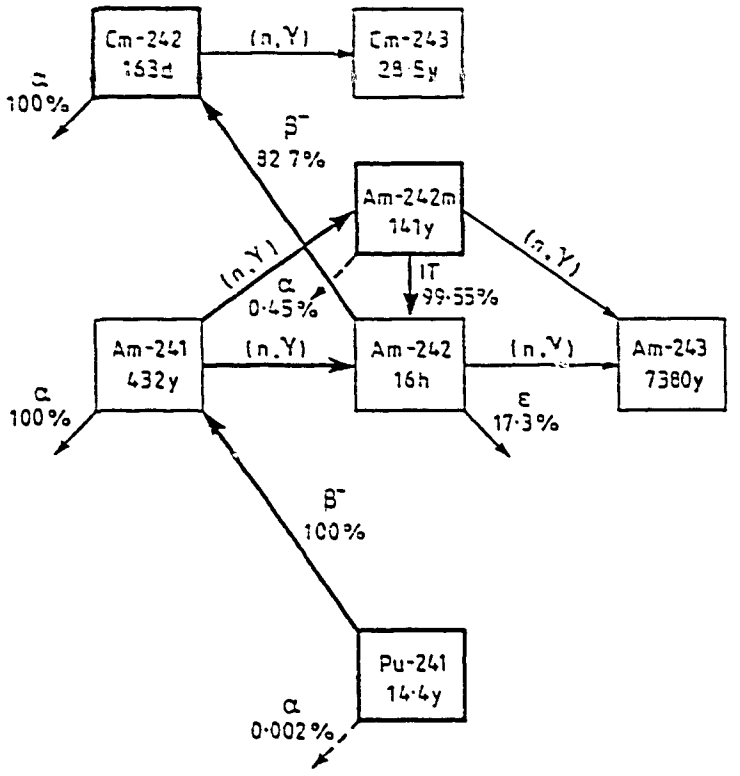

FIG. 6. FORMATION OF 163d Cm-242

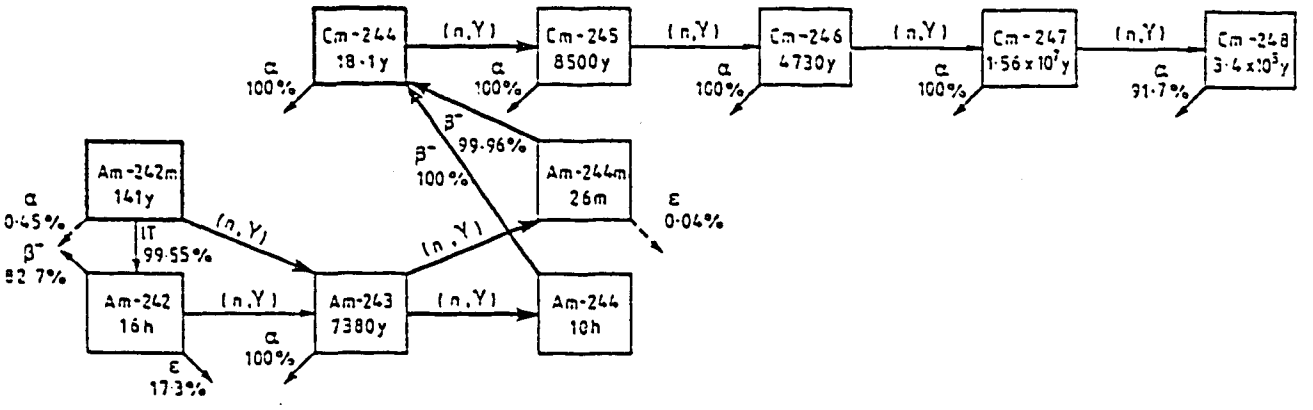

FIG. 7. FORMATION OF 18·1y Cm-244 AND HIGHER Cm NUCLIDES

actinide content of the fuel and hence to predict the reaction products generated by subsequent irradiation in a fast reactor system. Current outstanding accuracy requirements are reasonably weil documented (18, 19, 20) as listed in Table 1, in which P denotes the emission probability. More extensive lists that can be identified with the prolonged storage of fuel have been produced (20), but no accuracy requirements have been specified. Only the nuclide and decay parameters of interest can be listed: Np-236, Pu-236 and Pu-242 half-lives and decay schemes.

Some requests have been made to confirm measurements that already meet the current requirements. A good example of this is the half-life of Np-237 that has been measured to be (2.14 ± 0.01) x 10^6 years by Brauer et al. (21) with a claimed accuracy of 0.5%. Np-237 has been

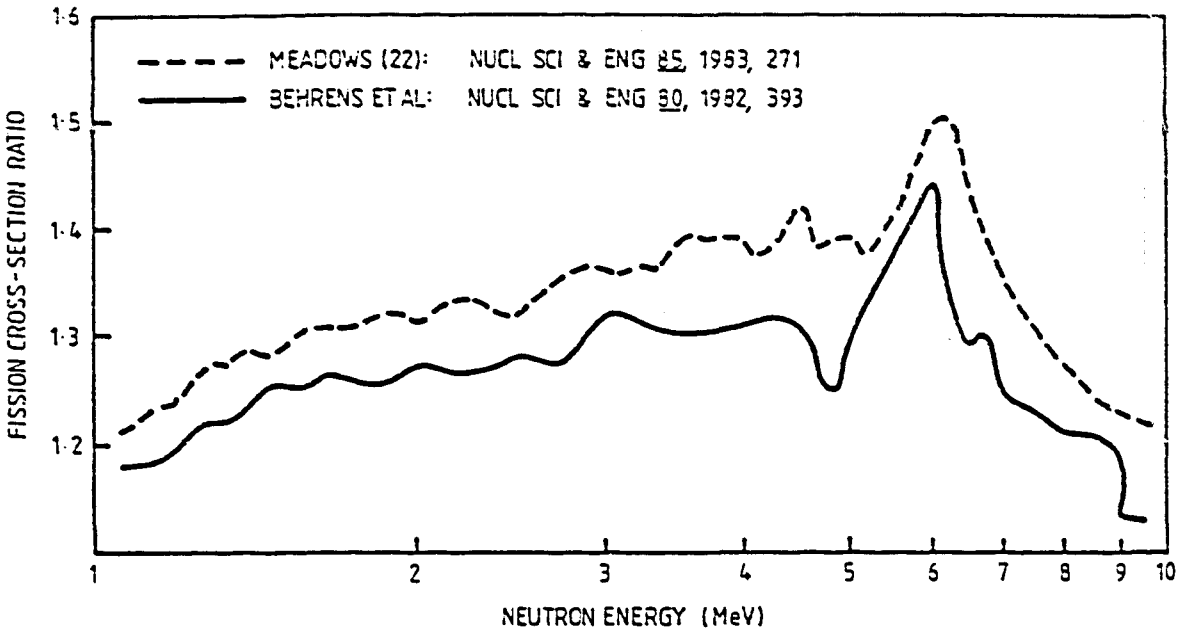

MEADOWS (22): MASS OF Np BASED ON $t_{1/2}$ AND SPECIFIC ACTIVITY MEASUREMENTS OF BRAUER ET AL J.INORG NUCL CHEM 12, 1960, 234

BEHRENS ET AL: CHEMICAL ANALYSES USING CONTROLLED POTENTIAL COULOMETRY (DOES NOT RELY ON $t_{1/2}$)

FIG.8 THE ^{237}Np to ^{235}U FISSION CROSS-SECTION RATIO FROM 1·0 TO 10·0 MeV

proposed as a neutron flux standard in the MeV region to replace U-235 (n, f). However, there is an approximately 4% discrepancy between the Np-237/U-235 fission cross-section ratios measured by means of two different techniques ((22) and Figure 8): one set of measurements involved Np-237 assay using the accepted half-life, whilst controlled potential coulometry was used in other studies. The latter technique does not involve specific activity measurements and does not require a knowledge of the half-life. The single accurate measurement of the half-life requires independent confirmation, since a change in this value might explain the current discrepancy.

The relative concentrations of specific curium nuclides are important because of their significant alpha and neutron emission rates. Neutron production is dominated by the spontaneous fission of Cm-242 and Cm-244, and by the neutrons produced by the (α, n) reactions on oxygen and carbon. The Cm-242 content of the fuel depends on the in-growth of Am-241 by the beta decay of Pu-241 during reactor shutdown and fuel storage (Figure 6), and the subsequent irradiation history. Conflicting data have been produced in measurements of the half-life of Pu-241, and this justifies the continued requests for further studies. An agreed value to an accuracy of at least 1% would also aid in clarifying the materials accountancy figures for plutonium storage (23). Measurements have also been made recently of the spontaneous fission half-life (24) and alpha half-life (25) of Cm-242: the spontaneous fission half-life of (7.15 ± 0.15) x 10^6 years is significantly higher than previous measurements, whilst the alpha half-life of (161.35 ± 0.10) days is lower than the previously accepted value of 162.8 days (Table 2). There are no obvious explanations for these discrepancies, and additional studies are required to assist in resolving the disagreements.

Table 1

Heavy Element and Actinide Decay Data Requirements for Fuel Assay (18,19,20)

Nuclide	Data Type	Required Accuracy (%)	Comments
U-234	$t_{\frac{1}{2}}$ P_α P_γ	0.3 3 3	Superseded by standards requirements (Table 6)
U-235	$t_{\frac{1}{2}}$ P_α P_γ	3 3-5 3	
Np-237	$t_{\frac{1}{2}}$ P_α P_γ	0.5 3 3	Superseded by standards requirements (Table 6)
Np-238	$t_{\frac{1}{2}}$ P_γ (P_β)	2 2 (2)	
Pu-238	P_γ	1	43.48, 99.86 and 152.7 keV emissions
Pu-239	P_γ	1	51.6, 129.3, 375.0 and 646.0 keV emissions
Pu-240	$t_{\frac{1}{2}}$ P_γ	1 1	45.2, 104.2 and 642.5 keV emissions
Pu-241	$t_{\frac{1}{2}}$ P_γ	1 1-5	1% for 103.5 and 148.6 keV emissions 5% for 56.4, 77 and 160 keV emissions
Am-243	$t_{\frac{1}{2}}$ P_α P_γ	1 1 1	
Cm-244	P_α P_γ	5 5	Superseded by environmental monitoring requirements

Table 2

Cm-242 Half-life
S. Usuda, H. Umezawa. J. Inorg. Nucl. Chem. 43, 1981, 3081

Lead Author	Year	Half-Life (Days)	Technique
G. C. Hanna	1950	162.5 ± 2.0	Alpha Counting
W. P. Hutchinson	1954	163.0 ± 1.8	Calorimetry
K. M. Glover	1954	162.46 ± 0.14	Alpha Counting
K. F. Flynn	1965	163.1 ± 0.4	Alpha Counting
W. J. Kerrigan	1975	163.2 ± 0.3	Calorimetry
H. Diamond	1977	162.76 ± 0.04	Alpha Counting
	pre-1981	162.8 ± 0.3	Mean Value
S. Usuda	1981	161.35 ± 0.10	Alpha Counting

The reprocessing of fuel stored for long periods has resulted in detailed assessments of the recycling and production of higher actinides. At present data requirements are uncertain, but there may be a need for improvements in the decay data of Cm-242, Cm-244, Cm-246 and Cm-248 (23). The spontaneous fission branching ratios of Cm-242 and Cm-244 are required with an accuracy to 5% and 3% respectively, and the required accuracy of the average number of prompt neutrons emitted per spontaneous fission ($\bar{\nu}_p$) is 3% for both nuclides. It should also be noted that the decay of Am-242m has a direct effect on the production of Cm-244 (Figure 7), and that a recent half-life measurement of (141 ± 2) years (26) differs significantly from the previously accepted value of 152 years (27): the new value needs to be confirmed with an accuracy to 1%.

Pu-236 and U-232 decay to Tl-208, which is an unwelcome source of high energy gamma emissions (Figure 2). Various routes of U-232 formation have been identified, and the most significant are indicated in Figure 9. If reprocessed fast reactor fuel is prepared and then stored for over 4 years before re-irradiation, significant quantities of Pu-236 will be formed in the reactor via the Np-237 (n, 2n) Np-236m reaction. However, the half-lives of Np-236 and Np-236m are sufficiently well known (28, 29), and the major uncertainties are associated with the fuel-handling procedure and the Np-237 (n, 2n) Np-236m cross-section. The alpha decay of U-234 and U-235 and subsequent (n,γ) reactions and beta decay can also produce U-232. As with the Pu-236 route the relevant decay data for Th-231, Pa-231 and Pa-232 are known to reasonable accuracy, and the problems involve quality control of the fuel constituents. However, the half-life of U-232 has been measured recently (30) and is approximately 4% lower than previous measurements (Table 3): additional studies may be needed to confirm this new value. A relatively large number of measurements of both the U-232 and Th-232 decay chains to Pb-208 have also been made recently (31-36), and a comprehensive re-evaluation of these decay chain data is required (23).

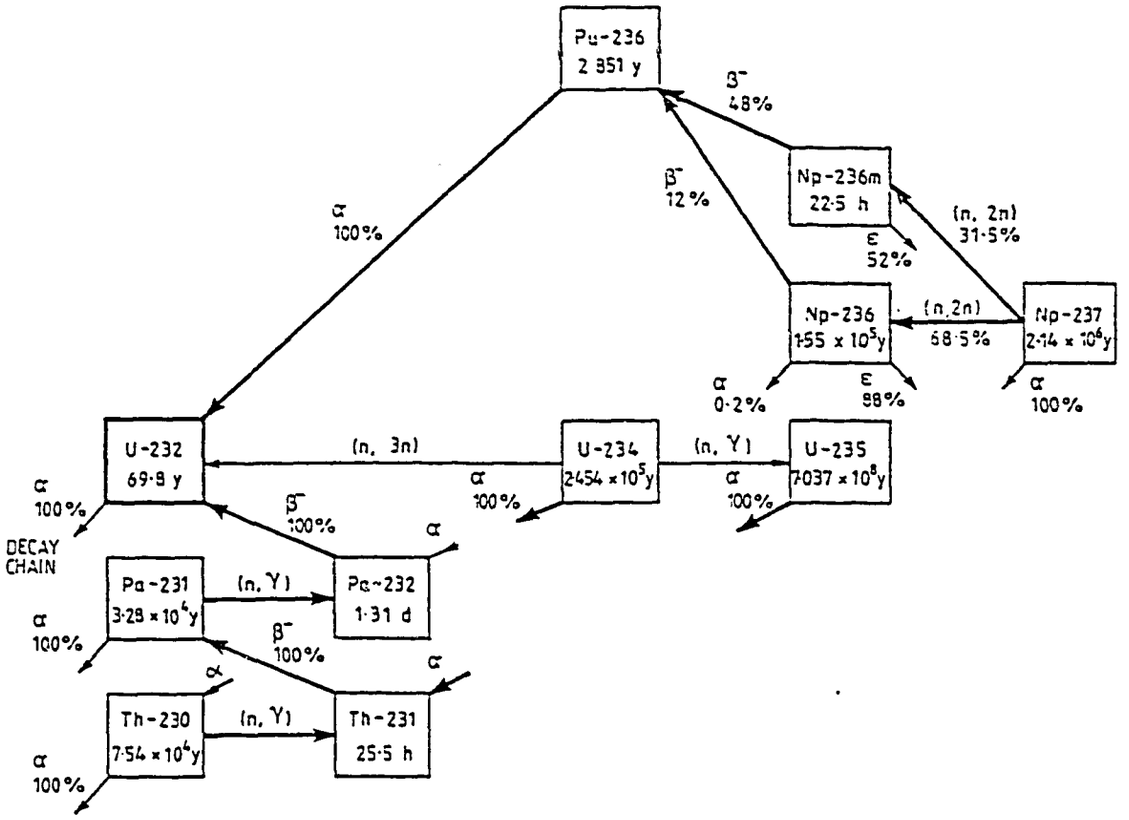

FIG. 9 FORMATION OF U-232 DECAY CHAIN

Table 3

U-232 Half-life
S. K. Aggarwal et al Phys Rev C20, 1979, 1533

Lead Author	Year	Half-Life (Years)	Technique
P. A. Sellers	1954	73.6 ± 1.0	Alpha Counting
J. M. Chilton	1964	71.4 ± 0.6	Calorimetry
		72.1 ± 0.5	Alpha Counting
	pre-1979	72 ± 1	Mean Value
S. K. Aggarwal	1979	69.0 ± 0.4	Alpha Counting
		68.81 ± 0.38	Alpha Counting

Significant improvements have occurred in low-energy photon counting techniques, and inevitably there has been an increasing demand for K- and L-x-ray data for the actinides to assist in fuel assay and plant control. L-x-ray emission probabilities are required for a relatively large number of nuclides, although greater emphasis has been placed on the data for Pu-238, Pu-239, Pu-240, Am-241 and Cm-244 with an accuracy to between 2% and 5%.

Table 4

Spontaneous and Neutron-induced Fission:
Prompt Neutron and Prompt Gamma Spectral Requirements (19)

Nuclide	Required Accuracy (%)			Comment
	$\bar{\nu}_p$	prompt neutron energy spectrum	prompt gamma energy spectrum	
U-233	0.25-2	1-2	-	
U-235	0.2-2	1-5	2	
U-236	1	-	-	
U-238	0.7-1	1-5	-	
Pu-238	4	-	-	
Pu-239	0.2-2	1-10	2	
Pu-240	1-3	3	-	
Pu-241	1-5	2	-	
Pu-242	5	-	-	
Am-241	5-20	-	-	
Am-242m	15	-	-	
Am-243	15-25	-	-	
Cm-242	30	-	-	neutron source requiring even greater accuracy
Cm-244	30	-	-	neutron source requiring even greater accuracy
Cf-252	0.3	1-2	-	prompt neutron energy spectrum for spontaneous fission; neutron standard

Continuous prompt neutron and gamma energy spectra are of particular importance in the context of fast reactor fuel assemblies and associated reactor physics calculations. The required data needs are given in Table 4 (19). A large majority of the requests are associated with neutron-induced fission and are included for completeness. Most of these requirements remain unsatisfied and include spontaneous fission data for Cf-252, which is an important neutron standard (see Section 4). Recent assessments have been made of the spontaneous fission decay data for U-238 and Cf-252 (37) and evaluations have been proposed for the relevant plutonium

nuclides (38). The spontaneous fission data for U-238 can be used for uranium assay, but measurements of the decay constant fall into two distinct groupings that differ by 20% to 25% (Table 5 and Figure 10). The higher values of 10^{16} years have been measured when using the fission track technique, and it has been proposed that partial fading of the fission tracks occurs casting doubt on these specific measurements (37).

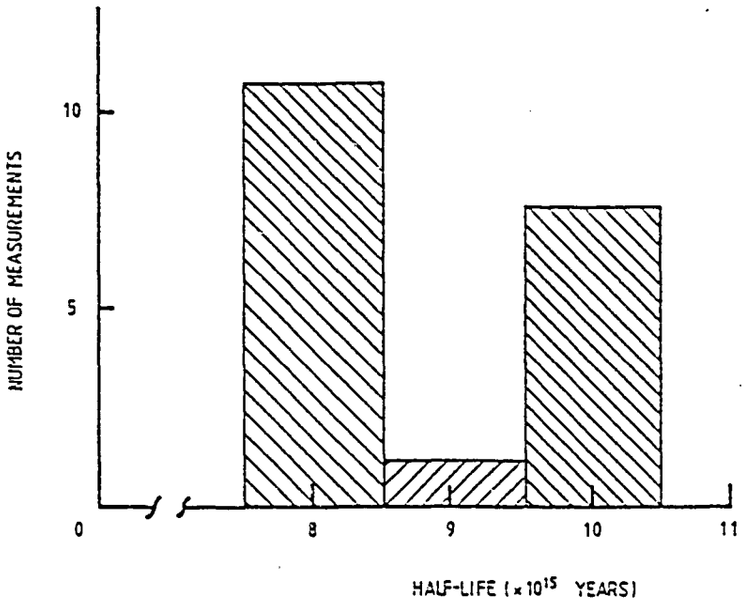

FIG.10 U-238 SPONTANEOUS FISSION HALF-LIFE
N.E. HOLDEN, M.S. ZUCKER. BNL-33965, 1983

All the data described above are required to analyse and resolve complex emission spectra, and so assist in plant control and fuel accountancy. However, in plutonium safeguards studies it has been claimed (39, 40) that the available gamma decay data (41) provide a sufficiently accurate basis for monitoring these nuclides. Such statements need to be treated with caution, and Lammer (15) notes that various assaying techniques are still under development and their accuracy requirements have not been assessed. Support has been given to the construction of a reference handbook of recommended data and uncertainties, and any inadequacies will only be identified when such a well-defined source of data is widely used.

2.3 Nuclear Incineration

In the mid-1970s assessments were made of the process of nuclear incineration in which the long-lived actinides are destroyed by recycling and burn-up. The ultimate aim of repeated recycling is the conversion of actinides to fission products and the reduction in the amount of long-term radioactivity (> 10^3 years). Although the feasibility of this technique has still to be demonstrated, there appear to be no insuperable technical difficulties. Despite this initial enthusiasm, the benefits are only marginal (42), and there has been a decline in data requirements from this source.

Table 5

U-238 Spontaneous Fission Half-life
N. E. Holden, M. S. Zucker. BNL-33965, 1983

Lead Author	Year	Spontaneous Fission Half-Life (10^{15} Years)	Technique
W. J. Whitehouse	1950	8.27	Ionisation Chamber
E. Segre	1952	8.06	Ionisation Chamber
R. L. Fleischer	1964	10.1	Fission Track
A. Spadavecchia	1967	8.23	Bubble Chamber
J. H. Roberts	1968	9.86	Fission Track
H. R. Von Gunten	1969	8.00	Fission Products
D. Galliker	1970	8.19	Bubble Chamber
D. Storzer	1970	8.16	Fission Track
J. D. Kleeman	1971	10.2	Fission Track
W. M. Thury	1971	8.00	Coincidence
M. P. T. Leme	1971	9.50	Fission Track
H. A. Khan	1973	10.2	Fission Track
K. N. Ivanov	1975	9.74	Fission Track
V. Emma	1975	9.63	Fission Track
G. A. Wagner	1975	7.97	Fission Track
K. Thiel	1976	8.09	Fission Track
M. Kase	1978	8.43	Ionisation Chamber
A. G. Popeko	1980	8.77	Neutron Counting
Z. N. R. Baptista	1981	10.5	Fission Track
J. C. Hadler	1981	8.06	Fission Track
H. G. deCarvalho	1982	5.87	Fission Track

3. ENVIRONMENTAL MONITORING

For many years the International Commission on Radiological Protection (ICRP) has studied in depth all the available data on the biological effects of radiation, and has made recommendations regarding permissible levels of exposure. Various laboratories assist in this work by assessing the present and future dose to man that results from the introduction of radionuclides into the environment (43), and there are specific decay data requirements. Most of the actinides present in spent fuel are recovered for re-use, but a small fraction is discharged into coastal waters in large volumes of low-level liquid waste. The movement of these radionuclides is monitored and modelled, and their critical pathways to man are reasonably well understood. The actinides of interest are neptunium, plutonium and americium, and the laboratory studies involve the detection of extremely low levels of radioactivity. The main source of nuclear decay data is a recently published ICRP document (44) which uses the ENSDF data base (45) and is adequate for the assessment of dose from radioactive contamination. However, with the development of gamma spectrometers that have high resolution below 50 keV (as already noted in Section 2.2), a demand has been created for more precise gamma and x-ray emission probability data at these low energies for the long-lived actinides and the more commonly used tracers that undergo electron capture decay, specifically Np-235 and Pu-237 (46). Accurate half-lives are also

requested in this work (including such nuclides as Pb-214 and Po-218 from the natural decay chains (47)), although the major requirement at present is for Pu-241.

Packaged solid waste is dumped in the deep sea, and models have been developed to quantify any radionuclidic movement through the ocean. The possible storage of high level waste on land, on the sea bed and under the sea bed is also being assessed: the heavy element nuclides of concern are identified as Pb-210, Po-210, Ra-225, Ra-226, Th-229, Np-237, Pu-238, Pu-239, Pu-240, Pu-241, Pu-242, Am-241, Am-243 and Cm-245 (47). However, it is important to remember that the important uncertainties involve the chemical behaviour and transport of the actinides in the environment and not their decay data.

4. STANDARDS

Specific heavy elements and actinides are used as calibration standards in alpha, neutron, gamma and x-ray spectrometry (7). Alpha energy and emission probabilities are known to a reasonable degree of accuracy for the purpose of calibration. However, at a recent seminar on alpha-particle spectrometry (48), the alpha-particle emission probabilities of several actinides were regarded as inaccurate for use as standards and in monitoring (Table 6): the required accuracies will be very difficult to achieve for U-235, U-236 and U-238.

Cf-252 is of interest in safeguards because it is the standard for $\bar{\nu}$ p, fission rates and neutron source strengths. It is used as a neutron source for comparison against other nuclides, and to test measurement techniques and equipment. Quite recently a discrepancy has appeared in Cf-252 half-life measurements (37, 49): the accepted value of approximately 2.638 y (and an uncertainty of 0.15%) has been called into

Table 6

Standards Requirements for Alpha-particle Emission Probabilities

Nuclide	Accuracy (%)	
	Required	Achieved
U-234	2	4-5
U-235	3-5	5-10
U-236	3-5	10
U-238	3-5	5-20
Np-237	1	10-25
Pu-238	1	1-2
Pu-239	1	1-2
Pu-240	1	1-4
Pu-242	5	4-6

question by recent measurements of 2.651 y, producing a discrepancy of 0.5% between laboratories (Table 7). Further studies are required to identify the cause of this problem, which may be due to uncertainties in the precise composition of the sources. Decay corrections are required and there may be a need to improve the accuracy of the half-life and $\bar{\nu}_p$ data for other californium nuclides, notably Cf-250.

Table 7

Cf-252 Total Half-life
N. E. Holden, M. S. Zucker. BNL-33965, 1983

Lead Author	Year	Half-Life (Years)	Comments
D. Metta	1965	2.646 ± 0.004	
A. DeVolpi	1969	2.621 ± 0.006	
B. Mijnheer	1973	2.659 ± 0.010	
V. Spiegel	1974	2.638 ± 0.007	Value withdrawn (see below)
V. Shchebolev	1974	2.628 ± 0.010	
V. Mozhaev	1976	2.637 ± 0.005	
W. G. Alberts	1980	2.650 ± 0.002	
V. Spiegel	1980	2.653 ± 0.001	Re-assessment of 1974 measurement
J. R. Smith	1981	2.651 ± 0.003	
F. Lagoutine	1981	2.639 ± 0.007	
	pre-1980	2.638 ± 0.004	Mean Value
	1980/1981	2.651 ± 0.002	Mean Value

Am-241 is used as a standard for low-energy gamma and x-ray studies. The emission probability of the 59.5 keV gamma ray is particularly important since this falls in an energy region in which the efficiencies of solid state detectors change rapidly and there is a lack of suitable data. Previous measurements have varied from 35% to 40% with an uncertainty of approximately 5%. A specially constructed well-type detector was used recently (50) to make an extremely accurate measurement of (35.82 ± 0.12)%. However, there is still disagreement between recent measurements, and further studies are required to confirm the data with an accuracy to at least 0.5% (Table 8). The L-x-ray data of Am-241 are also of interest, and the most intense emission probabilities at 13.9 and 17.8 keV are required with an accuracy to 2%.

Table 8

Am-241, 59.5 keV Gamma-ray Emission Probability
J. M. R. Hutchinson, P. A. Mullen. In J Appl Radiat Isot 34, 1983, 543

Lead Author	Year	$P_{59.5}$ (%)
L. D. MacIsaac	1964	34.6 ± 0.7
W. Michaelis	1965	38.0 ± 6.0
A. Peghaire	1969	35.3 ± 0.6
J. Legrand	1975	36.3 ± 0.4
J. Plch	1976	35.5 ± 0.3
J. M. R. Hutchinson	1983	35.82 ± 0.12
	All Data	35.9 ± 1.2
	Post-1965	35.7 ± 0.4 (1σ of 1.1%)

5. OTHER APPLICATIONS

The current requirements for decay data in non-reactor-related fields are limited, and only a brief discussion is merited. Radioactive dating of the earth is based on the natural decay of U-238 to Pb-206, U-235 to Pb-207, and Th-232 to Pb-208. Decay data are known to sufficient accuracy for this work, and an assay of these heavy element nuclides can be used either to determine the age of the sample in a closed system or to provide useful information on metamorphic heating effects.

Rates of formation of deep-sea sediments can be determined by measuring the Th-230 content that arises from the decay of U-234. The thorium is absorbed preferentially onto marine terraces in excess of the levels expected from the U-234 content, and Th-230 analysis of this material shows a decrease in activity that is commensurate with the half-life of 7.54×10^4 y. This half-life has been requested with an accuracy to 1% for these calculations, and recent studies have satisfied this requirement with a measured accuracy to 0.4% (51).

Nuclear techniques have also become well established in the earth sciences, particularly in the field of oil exploration. The vast majority of data requirements are identified with neutron cross-sections, gamma production data and the need for evaluated listings of these data (52), and there are no specific demands for more accurate decay data.

6. PROVISIONAL ASSESSMENT

Over the previous five years accurate decay data measurements have been made, and many of the outstanding requirements for half-life and emission probability data need to be reassessed. Some of this work has been carried out under the auspices of the IAEA Coordinated Research Programme (53), and specific studies have been discussed in earlier

sections of this report. Accurate alpha and gamma data have been published for most of the important actinides:

U-232/Pu-236	(54, 55, 56)
U-233	(57, 58)
U-234/Pu-238	(59)
U-235	(60, 61)
Np-237	(62, 63)
Pu-237	(56)
Pu-238	(58, 59)
Pu-239	(58, 64, 65)
Pu-240	(58, 66)

Further measurements will be reported before this programme ends in November 1984. Half-life measurements include U-234 (67), Pu-239 (68), Pu-240 (69), Pu-241 (70, 71, 72) and Pu-242 (73), and detailed evaluations have been made of the half-life data for the uranium nuclides (74).

Evaluations are required of the new data in conjunction with earlier measurements, and this exercise poses a number of problems. Achieved accuracies are best obtained from a consistent evaluation of all the available data with their reported uncertainties. Such an exercise will be attempted within the context of the IAEA Coordinated Research Programme (75), and a more up-to-date set of data and associated uncertainties should become available by the end of 1984. However, as might be expected a large number of experimenters tend to have a distinct bias towards the accuracy of their own work, and they fail to appreciate the full extent of the uncertainties and systematic errors in their studies. They rarely present a comprehensive treatment of the uncertainties in terms of error correlations and a covariance matrix. Full reporting is a key factor in such a procedure, and this may present editorial difficulties when lengthy papers are submitted for publication. A full analysis of the data and their uncertainties could be contained in associated laboratory reports. Every effort should be made to address such problems and avoid some of the unbelievably high accuracies claimed for decay data that have to be subsequently evaluated in the context of other measurements for which more realistic uncertainty assessments have been made.

It is expected that many of the decay data requirements formulated at the Karlsruhe (1) and Cadarache (2) Advisory Group Meetings will be satisfied by work completed recently or in progress, although some problems will still remain. These include spontaneous and neutron-induced fission data, the half-lives of Pu-241, Am-242m, Cm-242 and Cf-252, specific alpha decay data, and the low energy gamma and x-ray emission probabilities of Pu-238, Pu-239, Pu-240 and Am-241. Confirmatory measurements are also required to support recent studies that imply significant readjustments of specific decay data.

7. CONCLUSIONS

There have been no major changes in the world requirements for heavy element and actinide decay data since the 1979 Advisory Group Meeting on Transactinium Isotope Nuclear Data (2), and it is satisfying to note that a relatively extensive series of measurements has been undertaken since that meeting (53). Plans have been made by members of the relevant IAEA Coordinated Research Programme (75) to evaluate these data in detail during the latter part of 1984, and a new list of outstanding requirements

cannot be produced with any confidence until this exercise has been completed. Nevertheless, an attempt has been made to summarise the current requirements in Table 9 for the applications discussed earlier. Further experimental studies would appear to be necessary to assist in the assay of U-234, U-235, U-238, Np-237, Np-238, Pu-241, Am-241, Am-243 and Cm-244. Spontaneous and neutron-induced fission data are also required for a wide range of nuclides. Recent specific experimental studies have highlighted discrepancies in the data (half-lives of U-232, Am-242m, Cm-242 and Cf-252), and these anomalies need to be resolved. There are a few new requirements, including more extensive curium decay data for long-term storage calculations and L-x-ray emission probability data for long-lived actinides and specific tracers (Np-235 and Pu-237).

Some of the required accuracies specified in 1979 (2) have been modified, and it is generally accepted that most requests for thermal and fast reactor applications are satisfied apart from spontaneous and neutron-induced fission data ($\bar{\nu}$p, prompt neutron and gamma spectra) and the half-lives of Pu-241, Cm-242 and Cf-252. It is difficult to achieve accuracies of better than 0.5% to 1% for the half-lives and 2% for the alpha and gamma emission probabilities of some actinides, nor is it apparent that such high accuracies are required since there are significant uncertainties in the associated cross-section data (8) that need more urgent attention.

ACKNOWLEDGEMENTS

Discussions and contributions from the following people are gratefully acknowledged

V. Barnes
M. R. Bhat
C. G. Clayton
J. W. Dawson
B. R. Harvey
M. Lammer
J. L. Rowlands
J. R. Smith
M. G. Sowerby
A. Tobias
H. Umezawa
E. V. Weinstock
I. F. White
A. Whittaker

This paper has also been produced with the co-operation of C. McCann and the editorial assistance of R. A. Nichols.

Table 9

Summary of Heavy Element and Actinide Decay Data Requirements

Required accuracies may be already satisfied: these numbers need to be compared with uncertainties in evaluated data files

Nuclide	Accuracy (%)									Comments
	Half-life	Spontaneous fission branching ratio	P_α	P_β	P_γ	$P_{(L\text{-x-rays})}$	$\bar{\nu}_p$	Prompt neutron energy spectrum	Prompt gamma energy spectrum	
Th-230	1									Recent measurements have satisfied this request (see Section 5)
Th-233	1			(2)	2					Thorium cycle decay heat
Pa-231	1		2		2					Non-destructive assay; see also recent measurement (61)
Pa-233	1			(2)	2					Decay heat and mass determination; see also recent measurement (14)
U-232	1		2		2*					Shielding calculations involve most prominent gamma-ray emission probabilities of the decay chain; half-life measurement (30) is lower than previously accepted and confirmatory studies are required. Decay chain is important (Tl-208 formation) and recent studies merit re-evaluation (31-36)
U-233	0.5		2		2	5	0.25-2*	1-2		Thorium cycle; see also recent measurements (57, 58)
U-234	0.3		2		2*					Mass determination and non-destructive assay; see also recent measurement (59)
U-235	1		3-5		3*		0.2-2*	1-5	2	Mass determination and non-destructive assay; see also recent measurements (60, 61)
U-236	1		3-5		3		1			Mass determination and non-destructive assay
U-238	1	2*	3-5		3	3	0.7-1*	1-5		Mass determination and non-destructive assay
U-239	1			(2)	2					Decay heat; see also recent measurement (12)
Np-235						2				Used as tracer in environmental studies (56)
Np-236/	5			(2)	2					U-232 production
Np-236m/	5									
Np-237	0.5*		1*		1*	2				Neutron flux standard and environmental studies; half-life requires confirmation (21, 22)
Np-238	2			(2)	2					Np-237 (n, γ) reaction and Am-242m determination
Np-239	1			(2)	1					Decay heat and detector calibration standard (76)

*Principal requirements

/Branching ratios of Np-236 and Np-236m requested to an accuracy of 5

Table 9 (Continued)

Nuclide	Accuracy (%)									Comments
	Half-life	Spontaneous fission branching ratio	P_α	P_β	P_γ	$P_{(L\text{-x-rays})}$	$\bar{\nu}_p$	Prompt neutron energy spectrum	Prompt gamma energy spectrum	
Pu-236	1		2		3					U-232 production; see also recent measurements (54, 55, 56)
Pu-237						2				Used as tracer in environmental studies (56)
Pu-238	0.5	2	1		1	2	4			Mass determination, non-destructive assay and environmental studies; see also recent measurements (58, 59)
Pu-239	0.5		1		1	3	0.2-2*	1-10*	2	Mass determination, non-destructive assay and environmental studies; see also recent measurements (58, 64, 65)
Pu-240	0.5	2	1		1	3	1-3*	3		Mass determination, non-destructive assay and environmental studies; see also recent measurements (58, 66, 69)
Pu-241	1*				1-5		1-5	2		Mass determination, non-destructive assay and Am-241 production (70, 71, 72)
Pu-242	1	5	5		5	3	5			Mass determination, non-destructive assay and environmental studies; see also recent half-life measurement (73)
Am-241	0.5				0.5-2*	2*	5-20			Low energy gamma emission standard and environmental studies; 59.5 keV gamma-ray emission probability required to an accuracy of 0.5% (50)
Am-242	1									Cm-244 production; Am-242m half-life requires confirmatory measurements (76)
Am-242m	1*					3	15			
Am-243	1		1		1	2	15-25			Long-term storage and environmental studies; neutron capture
Cm-242	0.2*	5*			5		3*			Non-destructive assay; half-life requires confirmation (74, 75)
Cm-243	1		5		5	5				Non-destructive assay and environmental studies
Cm-244	1	3	3		3	3	3*			Neutron source/long-term storage and environmental studies
Cm-245	1		5		5	5				Long-term storage and environmental studies
Cm-246	1		3		3	3				Long-term storage and environmental studies
Cm-248	?		3		3	3				Long-term storage and environmental studies
Cf-250	0.2	2								Impurity in Cf-252 neutron standard (49)
Cf-252	0.2*	1					0.3*	1-2*		Neutron standard; half life discrepancy (47, 49)

*Principal requirements

†Branching ratios of Am-242 and Am-242m requested to an accuracy of 1%

REFERENCES

1. Proceedings of an Advisory Group Meeting on Transactinium Isotope Nuclear Data, IAEA-186, 1, 1976, 1.

2. Second Advisory Group Meeting on Transactinium Isotope Nuclear Data, INDC(NDS)-106/LN, 1979.

3. NUNN, R. M., Proceedings of an Advisory Group Meeting on Transactinium Isotope Nuclear Data, IAEA-186, 1, 1976, 167.

4. BURSTALL, R. F., Proceedings of an Advisory Group Meeting on Transactinium Isotope Nuclear Data, IAEA-186, 1, 1976, 175.

5. KOCH, L., Proceedings of an Advisory Group Meeting on Transactinium Isotope Nuclear Data, IAEA-186, 1, 1976, 191.

6. DIERCKX, R., Proceedings of an Advisory Group Meeting on Transactinium Isotope Nuclear Data, IAEA-186, 1, 1976, 215.

7. ATEN, A. H. W., Proceedings of an Advisory Group Meeting on Transactinium Isotope Nuclear Data, IAEA-186, 1, 1976, 227.

8. BOUCHARD, J., Proceedings of the Second Advisory Group Meeting on Transactinium Isotope Nuclear Data, IAEA-TECDOC-232, 1980, 1.

9. KOUTS, H., Proceedings of the Second Advisory Group Meeting on Transactinium Isotope Nuclear Data, IAEA-TECDOC-232, 1980, 23.

10. TOBIAS, A., Progress in Nuclear Energy 5, 1980, 1.

11. DAWSON J. W., CEGB Barnwood, private communication, April 1984.

12. HOLLOWAY, S. P., OLOMO, J. B., MacMAHON, T. D., HOOTON, B. W., in Nuclear Data for Science and Technology, K. H. Böckhoff (Editor), 1983, 287.

13. MOZHAEV, V. K., DULIN, V. A., KAZANSKII, Y. A., Atomnaya Energiya, 47, 1979, 55.

14. GEHRKE, R. J., HELMER, R. G., REICH, C. W., Nucl Sci and Eng 70, 1979, 298.

15. LAMMER, M., INDC/P(81)-24, 1981.

16. LAMMER, M., IAEA, private communication, April 1984.

17. WEINSTOCK, E. V., Brookhaven National Laboratory, private communication, February 1984.

18. ROWLANDS, J. L., SMITH, R. W., AEEW - M 2015, 1983.

19. PIKSAIKIN, V., INDC(SEC)-88/URSF, 1983.

20. NISHIMURA, K., ASAMI, T., ISHIMA, S., UMEZAWA, H., MATSUURA, S., MATSUNOBA, H., JAERI-memo 58-449, 1983.

21. BRAUER, F. P., STROMATT, R. W., LUDWICK, J. D., ROBERTS, F. P., LYON, W. L., J Inorg Nucl Chem 12, 1960, 234.

22. MEADOWS, J. W., Nucl Sci and Eng 85, 1983, 271.

23. BARNES, V., WHITTAKER, A., BNFL Sellafield, private communication, March 1984.

24. RAGHURAMAN, K., CHAUDHURI, N. K., JADHAV, A. V., SIVARAMAKRISHNAN, C. K., IYER, R. H., Radiochem Radioanal Letters 55, 1982, 1.

25. USUDA, S., UMEZAWA, H., J Inorg Nucl Chem 43, 1981, 3081.

26. ZELENKOV, A. G., PCHELIN, V. A., RODIONOV, Y. F., CHISTYAKOV, L. V., SHUBKO, V. M., Atomnaya Energiya 47, 1979, 404 and INDC(CCCP)-135/LN, 1979.

27. ASARO, F., PERLMAN, I., RASMUSSEN, J. O., THOMPSON, S. G., Phys Rev 120, 1960, 934.

28. LEDERER, C. M., JAKLEVIC, J. M., PRUSSIN, S. G., Nucl Phys A135, 1969, 36.

29. LINDNER, M., DUPZYK, R. J., HOFF, R. W., NAGLE, R. J., J Inorg Nucl Chem 43, 1981, 3071.

30. AGGARWAL, S. K., MANOHAR, S. B., ACHARYA, S, N., PRAKASH, S., JAIN, H. C., Phys Rev C20, 1979, 1533.

31. SADASIVAN, S., RAGHUNATH, V. M., Nucl Inst and Meths 196, 1982, 561.

32. ROY, J. C., BRETON, L., COTE, J. E., TURCOTTE, J., Nucl Inst and Meths 215, 1983, 409.

33. MITSUGASHIRA, T., MAKI, M., SUZUKI, S., SHIOKAWA Y., Radiochem Radioanal Letters 58, 1983, 199.

34. SCHOTZIG, U., DEBERTIN, K., Int J Appl Radiat Isot 34, 1983, 533.

35. VANINBROUKX, R., HANSEN, H. H., Int J Appl Radiat Isot 34, 1983, 1395.
BORTELS, G., REHER, D., VANINBROUKX, R., Int J Appl Radiat Isot 35, 1984, 305.

36. GEHRKE, R. J., NOVICK, V. J., BAKER, J. D., INEL, in press, 1984.

37. HOLDEN, N. E., ZUCKER, M. S., BNL-33965, 1983.

38. HOLDEN, N. E., ZUCKER, M. S., BNL-33992, 1984.

39. OTTMAR, H., EBERLE, H., Proceedings First Annual Symposium on Safeguards and Nuclear Material Management, Brussels, Belgium, ESARDA 10, 1979, 366.

40. LI, T. K., SAMPSON, T. E., JOHNSON, S. S., Proceedings Fifth Annual Symposium on Safeguards and Nuclear Material Management, Versailles, France, ESARDA 16, 1983, 289.

41. GUNNINK, R., EVANS, J. E., PRINDLE, A. L., UCRL-52139, 1976.

42. Proceedings, Second Technical Meeting on the Nuclear Transmutation of Actinides, Ispra, April 1980, EUR 6929 EN/FR.

43. PENTREATH, R. J., J Soc Radiol Prot 3, 1983, 15.

44. International Commission on Radiological Protection, Radionuclide Transformations - Energy and Intensity of Emissions, ICRP Publication 38, Pergamon Press, Oxford, 1983.

45. EWBANK, W. B., SCHMORAK, M. R., ORNL-5054/R1, 1978.

46. HARVEY, B. R., UK Ministry of Agriculture, Fisheries and Food, private communication, February 1984.

47. WHITE, I. F., National Radiological Protection Board, private communication, March 1984.

48. BORTELS, G., HUTCHINSON, J. M. R., Summary Session of the ICRM Seminar on Alpha Particle Spectrometry and Low Level Measurement, Harwell, May 1983.

49. SMITH, J. R., EGG-PBS-6406, 1983.

50. HUTCHINSON, J. M. R., MULLEN, P. A., Int J Appl Radiat Isot 34, 1983, 543.

51. MEADOWS, J. W., ARMANI, R. J., CALLIS, E. L., ESSLING, A. M., Phys Rev C22, 1980, 750.

52. CLAYTON, C. G., INDC(NDS)-151/L, 1984.

53. REICH, C. W., VANINBROUKX, R., Review Paper No 8, Third IAEA Advisory Group Meeting on Transactinium Isotope Nuclear Data, Uppsala, May 1984.

54. RYTZ, A., WILTSHIRE, R. A. P., ICRM Seminar on Alpha Particle Spectrometry and Low Level Measurement, Harwell, May 1983.

55. WELLUM, R., MOLINET, R., ICRM Seminar on Alpha Particle Spectrometry and Low Level Measurement, Harwell, May 1983.

56. WHITTAKER, B., ICRM Seminar on Alpha Particle Spectrometry and Low Level Measurement, Harwell, May 1983.
AHMAD, I., HINES, J., GINDLER, J. E., Phys Rev C27, 1983, 2239.

57. REICH, C. W., HELMER, R. G., BAKER, J. D., GEHRKE, R. J., Int J Appl Radiat Isot 35, 1984, 185

58. AHMAD, I., ICRM Seminar on Alpha Particle Spectrometry and Low Level Measurement, Harwell, May 1983.

59. BORTELS, G., DENECKE, B., VANINBROUKX, R., ICRM Seminar on Alpha Particle Spectrometry and Low Level Measurement, Harwell, May 1983.

60. VANINBROUKX, R., DENECKE, B., Nucl Inst and Meth 193, 1982, 191.

61. BANHAM, M. F., JONES, R., Int J App Radiat Isot 34, 1983, 1225.

62. GONZALEZ, L., GAETA, R., VANO, E., LOS ARCOS, J. M., Nucl Phys A324, 1979, 126.

63. BANHAM, M. F., FUDGE, A. J., J Radioanal Chem 64, 1981, 167.

64. HELMER, R. G., REICH, C. W., GEHRKE, R. J., BARKER, J. D., Int J Appl Radiat Isot 33, 1982, 23.

65. IWATA, Y., YOSHIZAWA, Y., SUZUKI, T., ICHIKAWA, S., OKAZAKI, S., Int J Appl Radiat Isot 35, 1984, 1.

66. HELMER, R. G., REICH, C. W., Int J Appl Radiat Isot 32, 1981, 829.

67. GEIDELMAN, A. M., EGOROV, Y. S., LOVTSYUS, A. V., ORLOV, V. I., PREOBRAZHENSKAYA, L. D., RYZHINSKII, M. V., STEPANOV, A. V., LIPOVSKII, A. A., KHOLNOV, Y. V., BELYAEV, B. N., ADBULLAKHATOV, M. K., AKOPOV, G. A., BELYKH, V. S., GROMOVA, E. A., MISHIN, V. Y., SOLNTSEVA, L. F., Izv Akad Nauk SSSR Ser Fiz 44, 1980, 927.

68. BROWN, D., GLOVER, K. M., KING, M., PHILLIPS, G., ROGERS, F. J. G, WILTSHIRE, R. A. P., J Radioanal Chem 64, 1981, 181.

69. The Half-life of Plutonium-240, Int J Appl Radiat Isot 35, 1984, 153.

70. AGGARWAL, S. K., JAIN, H. C., Phys Rev C21, 1980, 2033.

71. AGGARWAL, S. K., ACHARYA, S. N., PARAB, A. R., JAIN, H. C., Radiochimica Acta 29, 1981, 65.

72. DE BIEVRE, P., GALLET, M., WERZ, R., Int J Mass Spec and Ion Phys 51, 1983, 111.

73. AGGARWAL, S. K., ACHARYA, S. N., PARAB, A. R., JAIN, H. C., Phys Rev C20, 1979, 1135.

74. HOLDEN, N. E., BNL-NCS-51320, 1981.

75. LORENZ, A., INDC(NDS)-147/GE, 1983.

76. AHMAD, I., Nucl Inst and Meths 193, 1982, 9.

CURRENT STATUS OF NUCLEAR DECAY DATA AND REPORT ON THE IAEA COORDINATED RESEARCH PROGRAMME ON THE MEASUREMENT AND EVALUATION OF TRANSACTINIUM ISOTOPE NUCLEAR DECAY DATA

C.W. REICH
Idaho National Engineering Laboratory,
EG&G Idaho, Inc.,
Idaho Falls, Idaho, United States of America

R. VANINBROUKX
Central Bureau for Nuclear Measurements,
Joint Research Centre, Geel Establishment,
Commission of the European Communities,
Geel

Abstract

In 1977, the IAEA organized a Coordinated Research Programme to address the needs for highly accurate actinide-nuclide decay data identified at the first Advisory Group Meeting on Transactinium Isotope Nuclear Data, held in Karlsruhe in 1975. During the years of its existence, this CRP has made significant strides towards achieving the goals outlined at Karslruhe and subsequently refined at a second Advisory Group Meeting, held in Cadarache in 1979. In this paper, the make-up of the CRP and its work in the areas of decay-data measurement and evaluation are presented and its significant accomplishments summarized. We also discuss the contents and philosophy of the final report, containing the results of the measurements and evaluations carried out by the CRP participants, to be published following the planned termination of this Programme in November, 1984.

1. INTRODUCTION

In recent years, as their importance for many areas of science and technology has become more widely recognized, data on the decay properties of radioactive nuclides have come to represent an increasingly visible and significant subset of that body of information referred to as "Nuclear Data". Fission-product nuclides, because of the means by which they are most commonly produced, have always occupied a special position in fission-reactor research and technology. With the expanding emphasis on fast-reactor technology and all aspects of the associated fuel cycle, increasing attention is being focussed on the need for reliable, accurate decay data on a number of isotopes of the actinide elements.

In spite of the wide applicability of decay data in many areas of technology, however, the primary motivation for their measurement has historically

been for the information they provide for basic low-energy nuclear-structure physics. As a consequence of the extensive measurement activity in this area over the past three decades or so, there is at present a large amount of fairly detailed data on the decay properties of unstable nuclei. However, because of the interests and basic orientation of most of the measurers of these data, the existence of this extensive body of information does not necessarily mean that the decay-data needs of any given area are satisfied. To properly assess the adequacy of the existing decay-data base for a given application requires a careful examination of this information in the light of a specific set of user needs, some of which can be rather highly specialized.

In 1975, the IAEA, in cooperation with the OECD Nuclear Energy Agency, convened an Advisory Group Meeting on Transactinium Isotope Nuclear Data [1] at Karlsruhe, F.R.G. This meeting brought together users and measurers of these data to survey the requirements for and status of transactinium isotope nuclear data relevant to fission-reactor research and technology and to formulate recommendations for future work. One of the areas addressed at this meeting was the status of the decay data for these nuclides, especially half lives, $T_{1/2}$, and alpha-particle, P_α, and gamma-ray, P_γ, emission probabilities, and branching ratios, BR. It was found that the accuracy of many of these data was not adequate to satisfy a number of the identified needs. Among the recommendations drawn up at this meeting was one which called for an internationally coordinated programme of decay-data measurement and evaluation to address this situation.

In response to this recommendation, the IAEA Nuclear Data Section in 1977 organized a Coordinated Research Programme (CRP) on the measurement and evaluation of transactinium-isotope nuclear decay data. Five established groups experienced in decay-data measurements agreed to participate in the work of this CRP. The first meeting of the participants was held in April, 1978 in Vienna, and subsequent research-coordination meetings have been held on an approximately annual basis.

Reports describing various aspects of this CRP have been presented previously (see, e.g., Refs.[2,3]). In this paper, we discuss the activities of the CRP, its achievements up to the present time and some of the work that remains to be done.

2. COMPOSITION AND OBJECTIVES OF THE CRP

The five laboratories formally participating in the decay-data CRP are as follows:

Atomic Energy Research Establishment Harwell, Harwell, U.K.,
(represented by A.J. Fudge);

Central Bureau for Nuclear Measurements, Geel, Belgium,
(represented by R. Vaninbroukx);

Idaho National Engineering Laboratory, Idaho Falls, Idaho, U.S.A.,
(represented by C.W. Reich);

Japan Atomic Energy Research Institute, Tokai-Mura, Japan,
(represented by H. Okashita, with previous participation by H. Umezawa);

Laboratoire de Métrologie des Rayonnements Ionisants, Gif-sur-Yvette, France,
(represented by N. Coursol, with previous participation by J. Legrand,
G. Malet and F. Lagoutine).

The programme has been coordinated by A. Lorenz of the IAEA Nuclear Data Section. A.L. Nichols of AEE Winfrith, U.K., has participated as an observer at essentially all the meetings of the CRP and has been actively involved in its work. In addition, K. Debertin of PTB, Braunschweig, F.R.G., W.B. Ewbank of Oak Ridge National Laboratory, U.S.A., and V.M. Kulakov of the Kurchatov Atomic Energy Institute, U.S.S.R., have had helpful input to some of the meetings.

Within the U.S., work at several laboratories is relevant to the objectives of the CRP. In response to specific requests from the CRP, I. Ahmad of Argonne National Laboratory has carried out accurate alpha-emission-probability measurements on several actinide nuclides. Valuable input to the CRP is also being provided by the U.S. Half-Life Evaluation Committee. This committee was set up several years prior to the inception of the IAEA CRP to address the poor status of the half-life data on the important Pu isotopes (primarily ^{239,240,241}Pu). The laboratories (and representatives) making up this committee are: Mound Laboratory (W. Strohm, Chairman); Argonne National Laboratory (A. Jaffey); Los Alamos National Laboratory (J.E. Rein); Lawrence Livermore National Laboratory (A. Prindle); National Bureau of Standards (L. Lucas); and Rocky Flats Laboratory (R. Carpenter).

The main objective of the CRP was to arrive at a consistent set of decay data satisfying the required accuracies. To achieve this objective, it was decided to review regularly the status of the existing data in order to agree on priorities, to coordinate the on-going measurements and the initiation of new ones, to discuss areas of possible cooperation among the participating laboratories and to intercompare the results obtained. The participants

concentrated specifically on the measurement and evaluation of total and partial half lives and alpha-particle and gamma-ray emission probabilities, these being the broad categories of decay data emphasized at the Karlsruhe Advisory Group Meeting.

The initial basis for planning the work of the CRP was provided by the decay-data requirements identified at Karslruhe. From this information, supplemented by additional data needs known to various of the participants, a measurement programme was agreed upon and initiated. At the Second IAEA Advisory Group Meeting on Transactinium Isotope Nuclear Data [4], held at Cadarache in 1979, roughly one year after the initiation of the work of the CRP, this request list was extensively reviewed and several modifications to it were made. In some instances, the required accuracies had been achieved and the related data requests could consequently be regarded as having been satisfied. In others, however, additional data needs were identified or substantially increased accuracy requirements were requested. This upgraded decay-data request list is given in Refs.[4,5] and summarized in Table 1.

TABLE 1.

REQUIREMENTS AND STATUS OF TRANSACTINIUM ISOTOPE DECAY DATA AS IDENTIFIED AT THE CADARACHE ADVISORY GROUP MEETING (1979)

(Adapted from information in Refs. [4] and [5]). The following comment is included in the Table as given in these References:

General comment on uncertainties: for the alpha, gamma and X-ray emission probabilities, the required and achieved accuracies apply to the selected major transitions only. The stated uncertainties are intended to correspond to 1σ confidence levels; the Working Group questions the validity of any presently stated uncertainties of less than 0.1 % for half lives and 0.5 % for other quantities.

NUCLIDE	DATA TYPE	REQUIRED ACCURACY	ACHIEVED ACCURACY	NEEDS AND COMMENTS
^{228}Th	$T_{1/2}$	1 %	0.1 %	Decay Chain Calculations
	P_γ	2 % (a)		
^{229}Th	$T_{1/2}$	1 %	2 %	Mass Determination in ^{233}U Chain
	P_γ	2 % (a)		
^{230}Th	$T_{1/2}$	1 %	4 %	Marine Dating
^{233}Th	$T_{1/2}$	1 %	0.5 %	Decay Heat
	P_β	2 %	UNKNOWN	
	P_γ	2 %	UNKNOWN	
^{231}Pa	$T_{1/2}$	1 %	0.3 %	Non-Destructive Assay (N.D.A.)
	P_α	2 %	2-5 %	
	P_γ	2 %	2-10 %	
^{233}Pa	$T_{1/2}$	0.5 %	0.4 %	Thorium cycle and N.D.A.
	P_γ	0.5 %	1 %	
^{232}U	$T_{1/2}$	1 %	2 %	Shielding Calculations, Mass Determination and N.D.A.
	P_α	2 %	1 %	
	P_γ	2 %	5-10 %	

TABLE 1. (continued)

NUCLIDE	DATA TYPE	REQUIRED ACCURACY	ACHIEVED ACCURACY	NEEDS AND COMMENTS
^{233}U	$T_{1/2}$	0.5 %	0.2 %	Thorium Cycle Studies
	P_α	1 %	1 %	
	P_γ	1 %	10 %	
^{234}U	$T_{1/2}$	0.3 %	0.3 %	Thorium Cycle and N.D.A.
	P_α	1 %	4 %	
	P_γ	2 %	10 %	
^{235}U	$T_{1/2}$	0.5 %	0.1 %	Mass Determination and N.D.A.
	P_α	1 %	5-10 %	
	P_γ	1 %	UNKNOWN	
^{236}U	$T_{1/2}$	0.5 %	0.2 %	Mass Determination and N.D.A.
	P_α	3 %	5-10 %	
	P_γ	1 %	5-10 %	
^{238}U	$T_{1/2}$	0.5 %	0.1 %	Mass Determination and N.D.A.
	$T_{1/2}$(SF)	2 %	1-2 %	Geochronology
	P_α	1 %	5-20 %	Mass Determination and N.D.A.
	P_γ	1 %	15 %	Mass Determination and N.D.A.
^{239}U	$T_{1/2}$	1 %	0.2 %	Decay Heat
	P_β	2 %	(b)	
	P_γ	2 %	10 %	
^{236}Np	$T_{1/2}$	5 %	10 %	^{232}U Production
	Branching ratio(BR)	5 %	2 %	
$^{236}Np^m$	$T_{1/2}$	5 %	2 %	
	BR	5 %	2 %	
^{237}Np	$T_{1/2}$	0.5 %	0.5 %	Mass Determination for Neutron Flux Monitoring
	P_α	1 %	20 %	
	P_γ	0.5 %	10 %	

TABLE 1. (continued)

NUCLIDE	DATA TYPE	REQUIRED ACCURACY	ACHIEVED ACCURACY	NEEDS AND COMMENTS
^{238}Np	$T_{1/2}$	1 %	0.1 %	Activation analysis of ^{237}Np and $^{242}Am^{m}$ Determination
	P_γ	2 %	10 %	
^{239}Np	$T_{1/2}$	1 %	0.3 %	Decay Heat
	P_β	2 %	(b)	
	P_γ	1 %	2 %	
^{236}Pu	$T_{1/2}$	1 %	0.3 %	Fuel Analysis
	P_α	2 %	2 %	
	P_γ	2 %	30 %	
^{238}Pu	$T_{1/2}$	0.5 %	0.1 %	Mass Analysis and N.D.A.
	$T_{1/2}(SF)$	2 %	3 %	
	P_α	1 %	1-2 %	
	P_γ	1 %	2-5 %	
	P_{LX}	2 %	3 %	Standards Calibration and Health Physics
^{239}Pu	$T_{1/2}$	0.5 %	0.1 %	Mass Analysis and N.D.A.
	P_α	1 %	1-2 %	
	P_γ	1 %	2-5 %	
	P_{LX}	5 %	3 %	
^{240}Pu	$T_{1/2}$	0.5 %	0.1 %	Mass Analysis and N.D.A.
	$T_{1/2}(SF)$	2 %	4 %	Health Physics
	P_α	1 %	1-4 %	
	P_γ	1 %	2-5 %	
	P_{LX}	5 %	3 %	
^{241}Pu	$T_{1/2}$ TOTAL	0.5 %	3 %	Mass Analysis and N.D.A.
	$T_{1/2}$ ALPHA	1 %	2 %	
	P_γ	1 %	2-5 %	

TABLE 1. (continued)

NUCLIDE	DATA TYPE	REQUIRED ACCURACY	ACHIEVED ACCURACY	NEEDS AND COMMENTS
^{242}Pu	$T_{1/2}$	1 %	0.6 %	Mass Analysis and N.D.A.
	$T_{1/2}(SF)$	5 %	1 %	
	P_α	5 %	4-6 %	
	P_γ	5 %	UNKNOWN	
^{241}Am	$T_{1/2}$	0.2 %	0.1 %	N.D.A. and Detector Calibration Standard
	P_γ	1 %	2-5 %	
	P_{LX}	2 %	3 %	
^{242}Am	$T_{1/2}$	1 %	0.1 %	Actinide Transmutation Studies
	BR	1 %	1 %	
$^{242}Am^m$	$T_{1/2}$	1 %	5 %	Americium Mass Assay
	BR	2 %	3 %	
^{243}Am	$T_{1/2}$	1 %	0.5 %	Americium Mass Assay and Neutron Capture Studies
	P_α	2 %	UNKNOWN	
	P_γ	1 %	5-10 %	
^{242}Cm	$T_{1/2}$	0.2 %	0.3 %	Safeguards and N.D.A.
	$T_{1/2}(SF)$	3 %	10 %	Fuel Assay
^{243}Cm	$T_{1/2}$	1 %	1 %	Fuel Assay
	P_α	2 %	2-10 %	
	P_γ	2 %	3-10 %	
^{244}Cm	$T_{1/2}$	1 %	0.1 %	Mass Assay
	$T_{1/2}(SF)$	3 %	0.2 %	
	P_γ	1 %	10 %	
	P_{LX}	5 %	3 %	Health Physics
^{245}Cm	$T_{1/2}$	1 %	1 %	
	P_α	2 %	0.5-5 %	Fuel Assay
	P_γ	2 %	UNKNOWN	

TABLE 1. (continued)

NUCLIDE	DATA TYPE	REQUIRED ACCURACY	ACHIEVED ACCURACY	NEEDS AND COMMENTS
^{246}Cm	$T_{1/2}$	1 %	2 %	
	P_α	2 %	1-5 %	Fuel Assay
	P_γ	2 %	UNKNOWN	
^{252}Cf	$T_{1/2}$	0.2 %	0.4 %	N.D.A.
	$T_{1/2}(SF)$	1 %	0.3 %	

(a) The listed requirements represent those for the more prominent (or useful) transitions from all the members of the decay chain of these nuclides. These data at present are of uneven quality, with accuracies of 0.1 % claimed for some transitions and 5-10 % or greater for others. A careful measurement of spectra of the decay chains, in secular equilibrium, headed by these nuclides would be most useful.

(b) The beta-particle emission probabilities, P_β are inferred from the gamma-ray emission probabilities (P_γ) and hence have similar precisions.

3. ACHIEVEMENTS OF THE CRP

3.1 Measurement Activity

The requested accuracies (cf. Table 1 and Refs. [1,4]) for many of the data, especially the emission-probability values, are quite high, and to achieve them has presented a challenging experimental problem. Nonetheless, during the approximately six years of the existence of this CRP this problem has largely been solved and a large amount of data of the required accuracies (at least for the prominent transitions, which are usually the ones of most interest to the user of the information) has been produced.

The present status of the measurement programme being conducted by the participants in the CRP is summarized in Table 2.

3.2 Evaluation Activity

An important part of the work of the CRP, in addition to the measurement activity, has been in the area of decay-data evaluation, directed toward the

preparation of a list of recommended values. During the first two years, and at the first two research-coordination meetings, this evaluation effort was restricted mainly to the preparation of a list of half-life values for 40 nuclides, ranging from ^{228}Th through ^{253}Es. In the following years, this list was updated and expanded to incorporate nuclides with $Z < 90$ that were members of the decay chains of the transactinium nuclides, since it soon became clear that such data had to be included as well.

The most recently issued half-life list [6] contains information on total and partial half lives for 125 nuclides, members of the important actinide-nuclide decay chains. Important input to this list has been obtained from the following existing decay-data files:

(1) ENSDF, the Evaluated Nuclear Structure Data File, resulting from the evaluation effort of the International Nuclear Structure and Decay Data Evaluation Network. The Nuclear Data Sheets are the printed version of this file;

(2) The Actinide Decay-Data File at the Idaho National Engineering Laboratory, which serves as the source file for the decay data incorporated into the Actinide File of ENDF/B; and

(3) The U.K. Chemical Nuclear Data Committee Heavy Element Decay Data File, evaluated at AEE-Winfrith Laboratory.

Where warranted, the data have been supplemented or replaced by recently measured or evaluated values.

More recently, part of this effort has been directed to the preparation of provisional lists of recommended values for α-particle and γ-ray emission probabilities and energies. The values given in the provisional lists (cf., e.g.,Ref. [6]) are based generally on the data published in the Nuclear Data Sheets [7], supplemented where deemed appropriate by values from the Table of Isotopes [8]. They represent the current status of the published evaluated data. These provisional lists contain data, for the more prominent transitions only, on the alpha transitions of 24 radionuclides ranging from ^{228}Th through ^{252}Cf and the gamma transitions of 26 radionuclides from ^{228}Th through ^{246}Cm.

TABLE 2.

NEW DATA MEASUREMENTS REPORTED SINCE 1978

NUCLIDE	DECAY PARAMETER	MEASUREMENTS REPORTED		ACHIEVED ACCURACY (%)
		BY CRP PARTICIPANTS	BY OTHERS (REFERENCES)	
^{228}Th	P_γ*	INEL [10]		1 - 2
	P_γ* (daughters)	CBNM [11]		1 - 5
^{229}Th	P_γ*	INEL (a)	[12 - 14]	2 - 10
^{230}Th	$T_{1/2}$		[15]	0.4
^{231}Th	P_γ*	CBNM [16], AERE [17] INEL [18]		1 - 5
^{232}Th	P_γ (daughters)		[19]	1 - 5
^{233}Th	P_γ	AERE (b)		20
^{231}Pa	P_γ*	AERE (b)		1 - 10
^{233}Pa	P_γ*	INEL [20], AERE [21] CBNM [22]		1 - 10
^{232}U	$T_{1/2}$	AERE (c)	[23]	1.4
	P_γ*	INEL [10], AERE (c)		1 - 2
	P_γ* (daughters)	INEL [10], CBNM [11]	[19, 24]	1 - 5
^{233}U	$T_{1/2}$		[25, 26]	0.1
	$T_{1/2}$ (SF)		[27]	25
	P_α		[28]	1 - 20
	P_γ*	INEL [29], AERE (b)		1 - 2

TABLE 2. (continued)

NUCLIDE	DECAY PARAMETER	MEASUREMENTS REPORTED		ACHIEVED ACCURACY (%)
		BY CRP PARTICIPANTS	BY OTHERS (REFERENCES)	
^{234}U	$T_{1/2}$		[30]	0.2
	$T_{1/2}$ (SF)		[27]	6
	P_{a}*	CBNM [31]		0.1 - 2
	P_{γ}*	CBNM [31], AERE (b) JAERI (b)		1 - 2
^{235}U	$T_{1/2}$ (SF)		[27]	30
	P_{γ}*	CBNM [16], AERE [17] INEL [18]	[32]	1 - 10
^{236}U	$T_{1/2}$ (SF)		[27]	5
^{237}U	P_{γ}*	AERE (b), INEL (b,d)		1 - 3
^{238}U	$T_{1/2}$ (SF)		[33 - 37]	3
	P_{γ}	AERE (e)	[38]	10 - 15
^{239}U	P_{γ}*		[39]	2 - 10
^{236}Np	$T_{1/2}$		[40]	2
^{237}Np	$T_{1/2}$	CBNM (e)		0.5
	P_{a}*	CBNM (e)	[41]	2 - 50
	P_{γ}*	AERE [21], CBNM [22]	[41]	2 - 10
^{239}Np	P_{γ}*	CBNM [31]	[42]	1 - 10
^{237}Pu	$T_{1/2}$		[43]	0.1
^{238}Pu	$T_{1/2}$		[44, 45]	0.1
	P_{a}*	CBNM [46]	[28]	0.1 - 5
	P_{γ}*	CBNM [46], INEL [47] LMRI (c)		1.5 - 2.5

TABLE 2. (continued)

NUCLIDE	DECAY PARAMETER	MEASUREMENTS REPORTED		ACHIEVED ACCURACY (%)
		BY CRP PARTICIPANTS	BY OTHERS (REFERENCES)	
^{239}Pu	$T_{1/2}$	CBNM [48], AERE [49]	[50]	0.1
	P_α*	LMRI (e)	[28]	0.3 - 2
	P_γ*	INEL [51], LMRI [52]	[53]	1 - 10
^{240}Pu	$T_{1/2}$*		[54, 55]	0.1
	$T_{1/2}$ (SF)	CBNM [56]		4
	P_α*		[28]	0.1 - 5
	P_γ*	INEL [57], LMRI (b)		1 - 2
^{241}Pu	$T_{1/2}$*	CBNM [58,59] AERE (c), CBNM (c)	[60 - 65]	1.4
	$T_{1/2(\alpha)}$*	CBNM [58]		1
	P_γ*	AERE (b), INEL (b,d)		1 - 2
^{242}Pu	$T_{1/2}$		[66]	0.5
	P_γ*	CBNM (b)		20
^{241}Am	P_α		[28]	1 - 10
	P_γ*	LMRI [67], CBNM (b)	[68]	0.2 - 10
$^{242}Am^m$	$T_{1/2}$		[69]	1.4
^{243}Am	$T_{1/2}$		[70]	0.5
	P_γ*	CBNM [31]	[71]	2 - 10
^{242}Cm	$T_{1/2}$*	JAERI [72] AERE (b), JAERI (b)	[73, 74]	0.2
	$T_{1/2}$ (SF)	JAERI (b)	[73, 75]	4
^{245}Cm	$T_{1/2}$		[76]	1.2

TABLE 2. (continued)

NUCLIDE	DECAY PARAMETER	MEASUREMENTS REPORTED		ACHIEVED ACCURACY (%)
		BY CRP PARTICIPANTS	BY OTHERS (REFERENCES)	
^{249}Bk	$T_{1/2}$		[77]	2
^{249}Cf	$T_{1/2}$		[78]	1
^{252}Cf	$T_{1/2}$*	LMRI [79]		0.3
^{253}Es	$T_{1/2}$		[80]	0.5

* Indicates detailed evaluation to be carried out by CRP participants.

(a) Measurements carried out in collaboration with I. Ahmad (Argonne National Laboratory).

(b) Measurements in progress and the results are expected before the end of 1984.

(c) Measurements in progress but the results are not expected before 1985-1986.

(d) Complementary measurement being done by H. Willmes and T. Ando (University of Idaho).

(e) Measurements planned.

In order to establish the final lists of recommended data, detailed evaluations for a number of selected nuclides are under way. These will be completed prior to the next (and final) research-coordination meeting of the CRP participants in November, 1984. The list of nuclides and parameters for which such evaluations are being done is given in the Summary Report [9] of the most recent research-coordination meeting of the CRP, held in June, 1983. These cases are also indicated by an asterisk in Table 2.

3.3 Note Regarding the Evaluation Philosophy

In a number of instances, the decay data to be incorporated into the final report of the CRP will differ from those contained in other collections or files of such data. In order for one to assess the significance of such differences, it is important to keep in mind the fact that the data in this final report can be grouped into three general categories, as regards the level of evaluation to which they have been subjected by the participants.

The first of these categories includes new decay data, both those generated through the activities of the CRP and selected results produced independently of it, where several measurements, having roughly comparable accuracies, of a given quantity exist. The second category includes cases where the existence of a new measurement calls for a change in the earlier value or where a reevaluation, either by ourselves or by others, of previous data indicates that changes in the results of earlier evaluations are appropriate. The third category involves data in existing national data files available to us or in other sources (e.g., Refs.[7,8]), which have been taken over with little in the way of additional evaluation on our part.

The emphasis of the CRP's data evaluation effort has been directed primarily toward the data in the first two of the categories mentioned above. Thus, while no particular importance should be attached to differences between listed values in this third category and those available in existing decay-data files or other compilations of evaluated decay data, the CRP participants feel that the values in these first two categories represent significant improvements in our knowledge of these quantities. Consequently, it is hoped that users and evaluators of transactinium-nuclide decay data will regard very seriously any differences, however slight and seemingly unimportant, between these CRP-evaluated values and those previously available and urge that they incorporate these new results into their files and evaluations at the earliest practicable opportunity.

4. CURRENT STATUS OF THE DECAY DATA

Even if all decay-data requirements identified at Karlsruhe and Cadarache (Table 1) are not yet satisfied, for many of them the accuracies have been considerably improved by new measurements in recent years. Table 2 lists the nuclides and parameters for which new measurements have been reported since 1978, the year of the beginning of the CRP activities. All data reported before that time are considered in the evaluation work published in the Nuclear Data Sheets [7] and the Table of Isotopes [8]. The table also gives the estimated accuracies. These accuracies may change somewhat when the ongoing evaluations are finished. The evaluated values and their accuracies will be published in the final report of the CRP. The alpha-particle (P_α)- and gamma-ray (P_γ) emission probabilities given are those for the most prominent lines. Also the measurements in progress or planned by the CRP participants are mentioned in the table.

An example of the considerable improvement of the achieved accuracies is the case of the gamma-ray emission probabilities in the decay of ^{235}U. Before 1982, the recommended data [8,81] were all based on relative measurements and on the value of P_γ = 0.54, without any uncertainty quotation, for the most prominent gamma ray, that at 185.7 keV. The quoted accuracies for the relative values are about 10 %. The results of recent absolute-value measurements for the four most prominent gamma rays are compared to the previously adopted values in Table 3. It should be noted that the given mean values and their uncertainties are to some extent preliminary ones. Again, the final values will be available after finishing the complete evaluation. The achieved accuracies are now 1-2 %, and the value for the 185.7-keV gamma ray is about 6 % higher than the previously adopted one.

The consistency of the P_a and P_γ measurements for even-even nuclei can well be shown by comparing the total internal-conversion coefficients deduced from the measured quantities with the theoretical values. These theoretical values can be calculated with an estimated uncertainty, corresponding to the 68 % confidence level, of about 2 % by interpolations between the values tabulated by Rösel et al. [82]. Table 4, taken from Ref. [31], compares such results for the decay of ^{234}U. In this table, the transition probabilities, P_{tr}, for de-excitation of the two excited levels by emission of gamma rays and conversion electrons (CE) are equal to the sum of transitions populating the respective levels.

TABLE 3.

GAMMA-RAY-EMISSION PROBABILITIES IN THE DECAY OF ^{235}U

E_γ (keV)	EMISSION PROBABILITIES P_γ					
	PREVIOUSLY RECOMMENDED	RECENTLY MEASURED				
		MEASUREMENTS BY CRP PARTICIPANTS			OLSON - 1983	MEAN VALUES FROM THE 1982 - 1983 MEASUREMENTS
	Ref. [81]	CBNM - 1982 Ref. [16]	AERE - 1983 Ref. [17]	INEL - 1983 Ref. [18]	Ref. [32]	
143.8	0.105 ± 0.008	0.109 ± 0.002	0.107 ± 0.002	0.1101 ± 0.0008	0.1093 ± 0.0015	0.1092 ± 0.0010
163.4	0.047 ± 0.004	0.050 ± 0.001	0.0497 ± 0.0010	0.0512 ± 0.0004	0.0507 ± 0.0008	0.0504 ± 0.0007
185.7	0.54	0.575 ± 0.009	0.573 ± 0.006	0.572 ± 0.005	0.561 ± 0.008	0.571 ± 0.006
205.3	0.047 ± 0.004	0.050 ± 0.002	0.0505 ± 0.0005	0.0496 ± 0.0005	0.0503 ± 0.0009	0.0501 ± 0.0005

TABLE 4.

EMISSION AND TRANSITION PROBABILITIES AND RELATED TOTAL INTERNAL-CONVERSION COEFFICIENTS IN THE DECAY OF ^{234}U

LEVELS IN ^{230}Th	CORRESPONDING ENERGIES		EMISSION AND TRANSITION PROBABILITIES			TOTAL INTERNAL CONVERSION COEFFICIENT α	
	E_α (keV)	E_γ (keV)	P_α	P_{trans}(a)	P_γ	$\alpha_{exper.}$(b)	$\alpha_{theor.}$
174 keV	4605	120.88	0.00206 ± 0.00004	0.00206 ± 0.00004	$(3.41 \pm 0.04)10^{-4}$	5.04 ± 0.11	5.0
53 keV	4723	53.20	0.2842 ± 0.0005	0.2862 ± 0.0005	$(1.24 \pm 0.02)10^{-3}$	231 ± 4	233

(a) $P_{trans} = P_\gamma + P_{CE}$ (b) $\alpha_{exper.} = \frac{P_{trans}}{P_\gamma} - 1$

5. DECAY-DATA REQUIREMENTS NOT SATISFIED BY THE CRP MEASUREMENT PROGRAMME

Although the situation has been considerably improved since the Karlsruhe and Cadarache Advisory Group Meetings, several of the identified decay-data needs (Table 1) will remain unsatisfied by the recent measurements. For some of them the required accuracies are questionable or will be difficult, even impossible, to achieve with the present experimental capabilities in the field of decay-data measurements. It would be appropriate for the participants in the present Advisory Group Meeting to reconsider these particular requirements. The most important nuclides and decay parameters for which the required accuracies are not yet satisfied are given in Table 5.

TABLE 5.

PRESENTLY UNSATISFIED DECAY-DATA NEEDS

DECAY PARAMETER	NUCLIDES
Total half life	^{229}Th, ^{232}U, ^{241}Pu, ^{246}Cm
Spontaneous-fission half life	^{238}Pu, ^{240}Pu, $^{242}Am^m$
Alpha-particle emission probabilities	^{235}U, ^{236}U, ^{238}U, ^{237}Np, ^{243}Cm, ^{245}Cm
Gamma-ray emission probabilities	^{233}Th, ^{236}U, ^{238}U, ^{237}Np, ^{238}Np, ^{236}Pu, ^{243}Cm, ^{244}Cm, ^{245}Cm, ^{246}Cm

6. SUMMARY AND CONCLUSIONS

The work of the IAEA CRP on transactinium-nuclide decay data, which formally got underway in April, 1978, is nearing an end. The final meeting of the programme participants is scheduled for November, 1984 and, shortly afterwards, the final report giving the measurement results and recommended values for the various decay data should be issued.

During its existence, the CRP has (or will have) accomplished a number of its goals. Briefly summarized, they include the following:

(1) the evaluation of the accuracy requirements for decay data established by the users at Karlsruhe and Cadarache and the grouping of them into three general categories, viz.: (a) those which are satisfied by presently available data; (b) those which lie beyond the capabilities of present measurement techniques; and (c) those not satisfied but which are achievable with present experimental capabilities;

(2) assessment of the status of the existing data, in the light of these requirements, including keeping abreast of the results of new measurements as they became available;

(3) identification and coordination of existing measurement capabilities in order to acquire the required data; and

(4) preparation of a report which presents critically evaluated, systematically acquired, new information as well as summarizes the current status of knowledge of a large body of transactinium-nuclide decay data.

The CRP participants, through their broad experience in decay-data measurement, have critically evaluated the experimental feasibility of achieving the required data accuracies. Through their access to, and familiarity with, several national decay-data files, they have been able to unify the information from a number of sources and to prepare a list of evaluated data that accurately reflects the status of the relevant data.

One significant aspect of the programme plan of the CRP was to have a number of the quantities measured independently by several of the participating laboratories. The evaluation of the potentially differing results in these cases to produce for each quantity a single recommended value, (as for example, for the P_γ values for ^{235}U given above), will be an especially important task and one which the CRP participants should be uniquely qualified to perform. This reconciliation process, properly carried out using all the

available information, should greatly enhance the credibility of these recommended values and thus increase their acceptance by the international user community.

The required accuracies for many of the decay data were quite high and not normally achieved in many measurements. In this regard, the existence of this Coordinated Research Programme has not only helped focus the existing capabilities of some of the participating laboratories on these measurements but also encouraged the development of such capabilities at other laboratories. This occurrence, together with the systematic production of additional highly accurately measured decay data, may represent one of the more significant long-term effects of this CRP in the area of decay-data measurement.

To help increase the acceptance of the final report of the CRP by the user community and to make the results more readily available to them, several actions are planned. First, prior to its publication and release, the report will be critically reviewed by several experienced evaluators of actinide-nuclide nuclear data not associated with the CRP. Second, upon its release, copies of the report will be made available to those evaluators of nuclear data within the International Nuclear Structure and Decay Data Evaluation Network whose evaluation responsibilities include mass chains to which the new information is relevant. In addition, copies will be made available to those who have the responsibility for the decay-data evaluation for the various national nuclear-data files. In this way, it is hoped that the results of the CRP will expeditiously find their way into the Nuclear Data Sheets and these national nuclear-data files, thereby becoming available to a large body of users.

In spite of the large body of new and highly precise decay data that has been produced by the laboratories involved in the work of the CRP, much remains to be done. A number of the decay-data accuracy requirements established at Karlsruhe and Cadarache have not been, and will not be, met by the time that the activities of the CRP terminate. It is hoped that, by pointing these out, we will be able to encourage other groups or individuals interested in decay-data measurement to become involved in the challenging and important task of producing highly accurate decay data, responsive to internationally identified needs.

ACKNOWLEDGMENTS

The information contained in this report and the accomplishments of the CRP upon which it is based have clearly been the result of the active and competent involvement of all the participants, mentioned above. Special acknowledgment, however, needs to be made of the patient and effective efforts of Alex Lorenz, who has guided and shepherded the Programme throughout all the years of its existence. The work at INEL has been supported by the U.S. Department of Energy under DOE Contract No. DE-AC07-76ID01570.

REFERENCES

1. Proceedings of the IAEA Advisory Group Meeting on Transactinium Isotope Nuclear Data, Karlsruhe, F.R.G., Nov. 3-7, 1975, IAEA-186, Vols. I-III, IAEA, Vienna (1976)

2. Reich C.W., in K.H. Böckhoff (ed.) "Nuclear Data For Science and Technology", D. Reidel Publishing Co., Dordrecht, Holland (1983), p. 277

3. Vaninbroukx R., Int. J. Appl. Radiat. Isot. 34, 1259 (1983)

4. Transactinium Isotope Nuclear Data - 1979, IAEA-TECDOC-232, IAEA, Vienna (1980)

5. Lorenz A., Second IAEA Advisory Group Meeting on Transactinium Isotope Nuclear Data, CEN Cadarache, France, 2-5 May 1979, Summary Report, INDC(NDS)-106/LN, IAEA, Vienna (1979)

6. Lorenz A., Proposed Recommended List of Heavy Element Radionuclide Decay Data, INDC(NDS)-149/NE, IAEA, Vienna (1983)

7. Nuclear Data Sheets, Vol. 17 (1976) through Vol. 33 (1981)

8. Lederer C.M. and Shirley V.S. (eds.), Table of Isotopes, 7th Edition, John Wiley and Sons, New York (1978)

9. Lorenz A., Sixth Research Coordination Meeting on the Measurement and Evaluation of Transactinium Isotope Nuclear Data, INDC(NDS)-147/GE, IAEA, Vienna (1983)

10. Gehrke R.J., Novick V.J. and Baker J.D., Int. J. Appl. Radiat. Isot., in press

11. Vaninbroukx R. and Hansen H.H., Int. J. Appl. Radiat. Isot. 34, 1395 (1983)

12. Dickens J.K. and McConnell J.W., Radiochem. Radioanal. Lett. 47, 331 (1981)

13. Rattan S.S., Reddy A.V.R., Mallapurkar V.S., Singh R.J., Prakash S. and Ramaniah M.V., Phys. Rev. C 27, 327 (1983)

14. Dickens J.K., Phys. Rev. C 28, 1404 (1983)

15. Meadows J.W., Armani R.J., Callis E.L. and Essling A.M., Phys. Rev. C 22, 750 (1980)

16. Vaninbroukx R. and Denecke B., Nucl. Instr. and Meth. 193, 191 (1982)

17. Banham M.F. and Jones R., Int. J. Appl. Radiat. Isot. 34, 1225 (1983)

18. Helmer R.G. and Reich C.W., Int. J. Appl. Radiat. Isot., in press

19. Schötzig U. and Debertin K., Int. J. Appl. Radiat. Isot. 34, 533 (1983)

20. Gehrke R.J., Helmer R.G. and Reich C.W., Nucl. Sci. Eng. 70, 298 (1979)

21. Banhman M.F. and Fudge A.J., J. Radioanal. Chem. 64, 167 (1981)

22. Vaninbroukx R., Bortels G. and Denecke B., Int. J. Appl. Radiat. Isot., in press

23. Aggarwal S.K., Manohar S.B., Acharya S.N., Prakash S. and Jain H.C., Phys. Rev. C 20, 1533 (1979)

24. Sadasivan S. and Raghunath V.M., Nucl. Instr. and Meth. 196, 561 (1982)

25. Geidel'man A.M., Egorov Yu.S., Lipovskii A.A., Lovtsyus A.V., Preobrazhenskaya L.D., Ryzhinskii M.V., Stepanov A.V. and Khol'nov Yu.V., Izv. Akad. Nauk SSSR, Ser. Fiz. 43, 928 (1979)

26. Aggarwal S.K., Acharya S.N. and Jain H.C., Radiochem. Radioanal. Lett. 42, 45 (1980)

27. von Gunten H.R., Grütter A., Reist H.W. and Baggenstos M., Phys. Rev. C 23, 1110 (1981)

28. Ahmad I., Nucl. Instr. and Meth., in press

29. Reich C.W., Helmer R.G., Baker J.D. and Gehrke R.J., Int. J. Appl. Radiat. Isot. 35, 185 (1984)

30. Geidel'man A.M., Egorov Yu.S., Lovtsyus A.V., Orlov V.I., Preobrazhenskaya L.D., Ryzhinskii M.V., Stepanov A.V., Lipovskii A.A., Khol'nov Yu.V., Belyaev B.N., Abdullakhatov M.K., Akopov G.A., Belykh V.S., Gromova E.A., Mishin V.Ya and Solntseva L.F., Izv. Akad. Nauk SSSR, Ser. Fiz. 44, 927 (1980)

31. Vaninbroukx R., Bortels G. and Denecke B., Int. J. Appl. Radiat. Isot., in press

32. Olson D.G., Nucl. Instr. and Meth. 206, 313 (1983)

33. Kase M., Kikuchi J. and Doke T., Nucl. Instr. and Meth. 154, 335 (1978)

34. Popeko A.G. and Ter-Akopian G.M., Nucl. Instr. and Meth. 178, 163 (1980)

35. Hadler J.C., Lattes C.M.G., Marques A., Marques M.D.D., Serra D.A.B. and Bigazzi G., Nucl. Tracks 5, 45 (1981)

36. Baptista Z.N.R., Mantovani M.S.M. and Ribeiro F.B., An. Acad. Brasil. Ciênc. 53, 437 (1981)

37. De Carvalho H.G., Martins J.B., Medeiros E.L. and Tavares O.A.P., Nucl. Instr. and Meth. 197, 417 (1982)

38. Roy J.-C., Breton L., Côté J.-E. and Turcotte J., Int. J. Appl. Radiat. Isot., submitted for publication

39. Holloway S.P., Olomo J.B., Mac Mahon T.D. and Hooton B.W., in K.H. Böckhoff (ed.), "Nuclear Data for Science and Technology", D. Reidel Publishing Co., Dordrecht, Holland (1983), p. 287

40. Lindner M., Dupzyk R.J., Hoff R.W. and Nagle R.J., J. Inorg. Nucl. Chem. 43, 3071 (1981)

41. Gonzalez L., Gaeta R., Vaño E. and Los Arcos J.M., Nucl. Phys. A 324, 126 (1979)

42. Mozhaev V.K., Dulin V.A. and Kazanskii Yu.A., Sov. At. Energy 47, 566 (1979)

43. Baba H., Suzuki T. and Hata K., J. Inorg. Nucl. Chem. 43, 1059 (1981)

44. Aggarwal S.K., Jadjav A.V., Chitambar S.A., Raghuraman K., Acharya S.N., Parab A.R., Sivaramakrishnan C.K. and Jain H.C., Radiochem. Radioanal. Lett. 46, 69 (1981)

45. Sevastianov V.D. and Yanin V.P., Nuclear Constants (USSR) 5 (44), 21 (1981)

46. Bortels G., Denecke B. and Vaninbroukx R., Nucl. Instr. and Meth., in press

47. Helmer R.G. and Reich C.W., Int. J. Appl. Radiat. Isot., in press

48. Vaninbroukx R., Denecke B., Gallet M., Grosse G., Hendrickx F. and Zehner W., in E. Wattecamps and Ch. Berthelot (eds.), "CBNM Progress Report 1978", p. 26, NEANDC(E)-202(U), Vol. III (1978)

49. Brown D., Glover K.M., King M., Philips G., Rogers F.J.G. and Wiltshire R.A.P., Radioanal. Chem. 64, 181 (1981)

50. Strohm W.W., Int. J. Appl. Radiat. Isot. 29, 481 (1978)

51. Helmer R.G., Reich C.W., Gehrke R.J. and Baker J.D., Int. J. Appl. Radiat. Isot. 33, 23 (1982)

52. Despres M., Morel J. and Malet G., Etude du spectre γ du Pu-239, LRMI/78/41 (1978)

53. Iwata Y., Yoshizawa Y., Suzuki T., Ichikawa S. and Okazaki S., Int. J. Appl. Radiat. Isot. 35, 1 (1984)

54. Jaffey A.H., Diamond H., Bentley W.C., Graczik D.G. and Flynn K.F., Phys. Rev. C 18, 969 (1978)

55. Strohm W.W., Int. J. Appl. Radiat. Isot. 35, 155 (1984)

56. Budtz-Jørgensen C. and Knitter H.-H., in R.E. Chrien (ed.), "Proceedings of the Specialists Meeting on Nuclear Data of Pu and Am Isotopes for Reactor Applications", ORNL, Brookhaven (1979)

57. Helmer R.G. and Reich C.W., Int. J. Appl. Radiat. Isot. 32, 829 (1981)

58. Vaninbroukx R., Proc. Int. Conf. on Neutron Physics and Nuclear Data for Reactors and other Applied Purposes, Harwell, Sept. 1978, OCDE Nucl. Energy Agency, Paris (1978), p. 235

59. De Bièvre P., Gallet M. and Werz R., Int. J. Mass Spec. and Ion Phys. 51, 111 (1983)

60. De Regge P. and Boden R., in N. Doly (ed.), Advances in Mass Spectrometry, Vol. 7A, Proc. 7th Int. Mass Spec. Conf., Firenze, August 1976, p. 528, Institute of Petroleum, London (1978)

61. Garner E.L. and Machlan L.A., in T.R. Canada and B.S. Carpenter (eds.), Measurement Technology for Safeguards and Materials Control, NBS Special Publication 582, p. 34, NBS, Washington (1980)

62. Aggarwal S.K. and Jain H.C., Phys. Rev. C 21, 2033 (1980)

63. Marsh S.F., Abernathey R.M., Beckman R.J. and Rein J.E., Int. J. Appl. Radiat. Isot. 31, 629 (1981)

64. Aggarwal S.K., Acharya S.N., Parab A.R. and Jain H.C., Radiochimica Acta 29, 65 (1981)

65. Aggarwal S.K., Chitambar S.A., Parab A.R. and Jain H.C., Radiochem. Radioanal. Lett. 54, 83 (1982)

66. Aggarwal S.K., Acharya S.N., Parab A.R. and Jain H.C., Phys. Rev. C 20, 1135 (1979)

67. Imbert L. and Morel J., Etude du spectre γ de l'Am-241, LMRI/79/61 (1979)

68. Hutchinson J.M.R. and Muller P.A., Int. J. Appl. Radiat. Isot. 34, 543 (1983)

69. Zelenkov A.G., Pchelin V.A., Rodionov Yu.F., Chistyakov L.V. and Shubko V.M., Sov. J. At. En. 47, 1024 (1980)

70. Aggarwal S.K., Parab A.R. and Jain H.C., Phys. Rev. C 22, 767 (1980)

71. Popov Yu.S., Starozhukov D.I., Mishenev V.B., Privalova P.A. and Mishenko A.I. Sov. J. At. En. 46, 123 (1979)

72. Usada S. and Umezawa H., J. Inorg. Nucl. Chem. 43, 3081 (1981)

73. Zhang Huan-Qiao, Xu Jin-Cheng and Wen Tong-Qing, Chin. J. Nucl. Phys. 1, 30 (1979)

74. Aggarwal S.K., Jadhav A.V., Chitambar S.A., Parab A.R., Shah P.M., Almaula A.I., Raghuraman K., Silvaramakrishna C.K. and Jain H.C., Radiochem. Radioanal. Lett. 54, 99 (1982)

75. Raghuzaram K., Chaudhuri N.K., Jadhav A.V., Silvaramakrishna C.K. and Iyer R.H., Radiochem. Radioanal. Lett. 55, 1 (1982)

76. Polyukhov V.G., Timofeev G.A., Kalygin V.V. and Privalova P.A., Radiokhimiya 24, 490 (1982)

77. Polyukhov V.G., Timofeev G.A. and Levakov B.I., Radiokhimiya 23, 884 (1981)

78. Polyukhov V.G., Timofeev G.A. and Levakov B.I., Radiokhimiya 25, 92 (1983)

79. Lagoutine F. and Legrand J., Int. J. Appl. Radiat. Isot. 33, 711 (1982)

80. Polyukhov V.G., Timofeev G.A. and Elesin A.A., Radiokhimiya 24, 494 (1982)

81. Schmorak M.R., Nuclear Data Sheets 21, 91 (1977)

82. Rösel F., Fries H.M., Alder K. and Pauli H.C., Atom Data and Nucl. Data Tables 21, Nrs. 4,5 (1978)

CONTRIBUTED PAPERS

Contributed Paper 1

NUCLEAR DATA REQUIREMENTS FOR PASSIVE NEUTRON ASSAY

R. ARLT
Division of Development and Technical Support,
Department of Safeguards,
International Atomic Energy Agency,
Vienna

Abstract

The paper describes the need for neutron yield data, such as spontaneous fission yields and (alpha,n) neutron yields, for non-destructive analysis of spent fuel assemblies based on the neutron yield from the Cm-244 isotope.

1. Introduction

The basic idea of passive neutron assay (PNA) used for non-destructive analysis for safeguarding light water reactor spent fuel assemblies is as follows:

The neutron emission rate of a spent fuel assembly is determined using a fission chamber (see e.g. /1/). From this measurement the fraction of neutrons originating from the isotope Cm-244 is derived by subtracting from the total neutron number the neutrons from other sources such as spontaneous fission and alpha-n neutrons from isotopes other than Cm-244 and neutron multiplication in the spent fuel assembly. In a second step relationships between the Cm-244 neutron rate (representing Cm-244 concentration in the spent fuel) and the burn-up and plutonium mass are established and used for the verification of the spent fuel parameters.

2. Calculation of the Cm-244 fraction of the neutron rate and the nuclear data required

In Fig. 1 (taken from /2/) the main contributors to the spontaneous fission neutrons emitted by a spent fuel assembly are illustrated. As it can be seen from Fig. 1 Cm-244 is predominant only for high values of burn-up and cooling time while for shorter values of cooling time Cm-242 contributes significantly to neutron emission and for low values of burn-up additional contributions come from even Pu isotopes and Am-241. In Fig. 2 (taken from /3/) the build-up of heavy actinides in a thermal reactor is shown. The build-up of the Cm-241 and Cm-242 isotopes (which for Cm-242 is power history dependent) has to be calculated (the production of all other isotopes which might contribute to the neutron rate at lower values of burn-up are

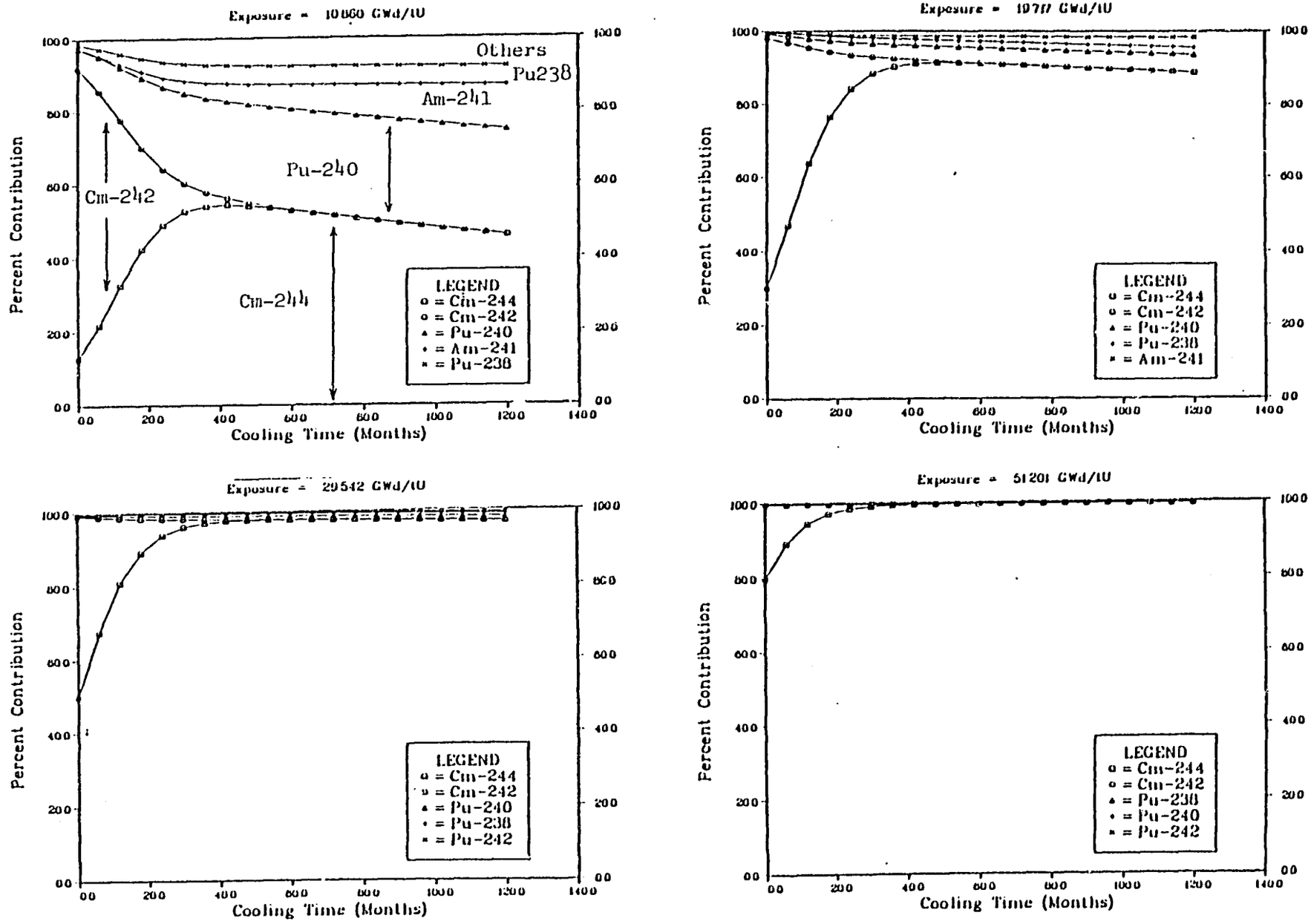

Fig. 1
Per cent contribution of individual isotopes to the total neutron source in an irradiated fuel assembly.

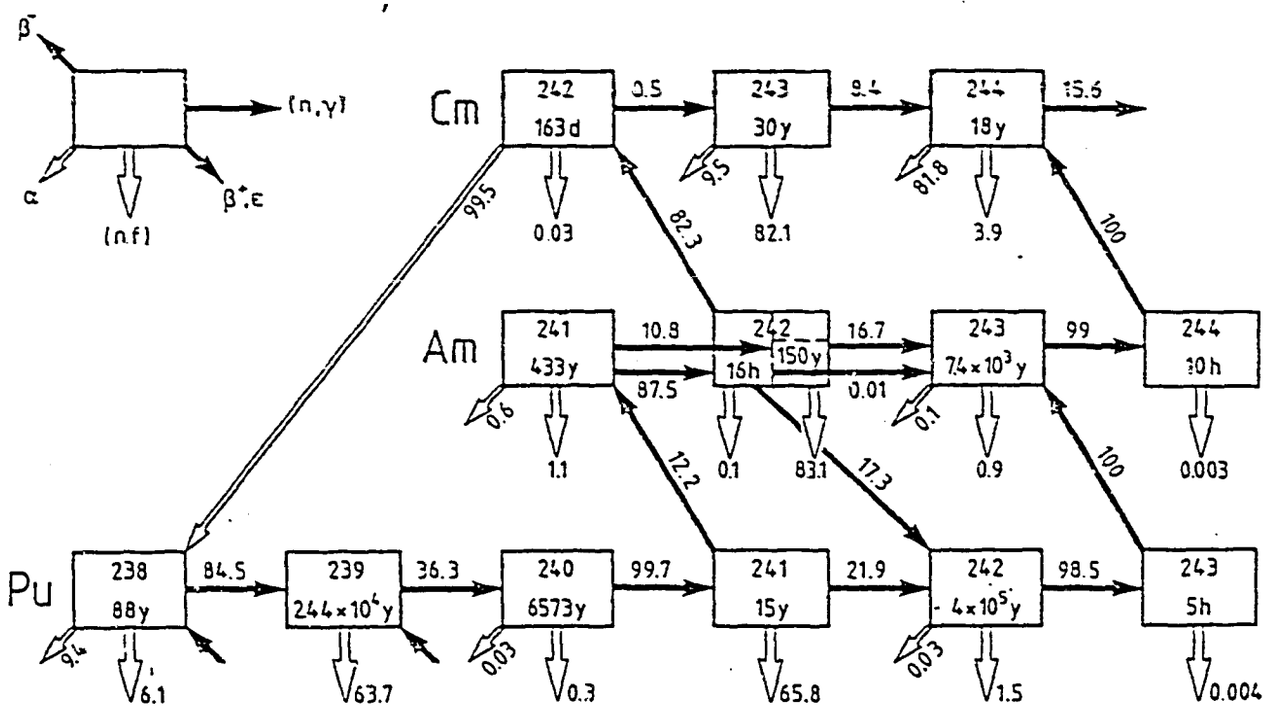

Fig.2 ISOTOPE PRODUCTION IN A THERMAL REACTOR ($\phi_n = 10^{13} n/cm^2 \cdot sec$)

The numbers next to the arrows give the percentage of each isotope undergoing the indicated reaction.

covered by this calculation too). No absolute isotopic concentrations are required but the amount of Cm-242 relative to Cm-244 at different levels of burn-up has to be well described. These two isotopes are mainly obtained in two different production chains (see Fig. 2). Therefore the amount of Cm-242 produced relative to Cm-244 is sensitive to different sets of nuclear data.

From a sensitivity study of the Cm-244 neutron emission /4/ and an analysis of transactinide neutron data /3/ it follows that the Am-243 capture resonance integral seems to be the most critical cross section at present. According to Pinel /4/ an overestimation of the Am-243 neutron capture by 50% leads to an overestimation of the Cm-244 neutron emission by 36%. As shown in /3/ a discrepancy of about 20% exists between the Am-243 capture resonance integral value calculated from differential data and that measured in a reactor!

3. Neutron yields

As the result of the illustrated reactorphysical calculation primarily the isotopic composition of the spent fuel is obtained. Therefore neutron spontaneous fission yields and (alpha, n) neutron yields are necessary to get the relative strength of different neutron sources of a spent fuel assembly.

Lammer /5/ compiled neutron yields used by different authors and concluded that especially for Cm-242 neutron spontaneous fission yields there were considerable discrepancies. If neutron yields used in more recent publications /4, 6/ were compared, an improvement of the consistency of the data is evident. However, there is still a need for the issue of a set of recommended neutron yield data. This is required for the main isotopes contributing to neutron emission directly by spontaneous fission neutrons or indirectly by (alpha, n) neutrons.

4. Summary

The Am-243 capture cross section seems to deliver the most relevant nuclear data related uncertainty in the calculation of Cm-244 built up in light water reactor spent fuel. New experiments measuring directly the capture cross section are recommended. Concerning neutron yields the issue of recommended neutron spontaneous fission yields and (alpha, n) yields for the main isotopes contributing to neutron emission of spent fuel taking into account recent experimental results is very desirable.

Benchmark tests including the measurement of the neutron emission rates, the determination of the Cm-244 fraction of the neutron emission rate (in dependence of burn-up) and its comparison with results of a subsequent destructive analysis of the spent fuel will provide the best overall test of the nuclear data used together with a certain computer code.

References

1. J.R. Phillips, G.E. Bosler, J.K. Halbig, S.F. Klosterbuer, H.O. Menlove, "Non-Destructive Verification with Minimal Movement of Irradiated Light-Water Reactor Fuel Assemblies", Los Alamos Scientific Laboratory report LA-9438-MS (ISPO-172) (October 1982)

2. J.R. Phillips, G.E. Bosler, J.K. Halbig, S.F. Klosterbuer, D.M. Lee, H.O. Menlove, "Neutron Measurement Techniques for the Non-Destructive Analysis of Irradiated Fuel Assemblies", Los Alamos Scientific Laboratory report LA-9002-MS (ISPO-156) (November 1981)

3. B. Goel, U. Fischer, "Validation of KEDAK-4 Data for Thermal Reactors: Resonance Integrals and Postirradiation Fuel Analysis", KfK 3449 (February 1983)

4. J. Pinel, "Determination by Non-Destructive Methods of the Combustion Rate and Fissile Isotope Balance of Irradiated Assemblies in Light-Water Reactors", CEA-N-2336 (March 1983), in French.

5. M. Lammer, "Nuclear Data for Safeguards", INDC/P (81)-24 (October 1981)

6. G.E. Bosler, J.R. Phillips, W.B. Wilson, R.J. LaBauve, T.R. England, "Production of Actinide Isotopes in Simulated PWR Fuel and Their Influence on Inherent Neutron Emission", Los Alamos Scientific Laboratory report LA-9343 (July 1982)

Contributed Paper 2

THE MEASUREMENT OF $^{237}Np(n, 2n)^{236}Np(22.5\ h)$ REACTION CROSS-SECTIONS IN THE NEUTRON ENERGY RANGE 7–10 MeV

N.V. KORNILOV, V.Ja. BARYBA, A.K. BALITSKY,
A.P. RUDENKO, B.D., KUZMINOV, O.A. SALNIKOV
Institute of Physics and Power Engineering (FEI),
Obninsk

E.A. GROMOVA, S.S. KOVALENKO, L.D. PREOBRAZHENSKAYA,
A.V. STEPANOVA, Yu.A. NIMILOV, Yu.A. SELITSKY,
B.I. TARLER, V.B. FUNSHTEIN, V.A.,YAKOVLEV
Khlopin Institute of Radium,
Leningrad

Union of Soviet Socialist Republics

S. DAROCZY, P. RAICS, J. CSIKAI
Institute of Experimental Physics,
Kossuth L. University,
Debrecen, Hungary

Abstract

The paper presents the results of the measurements of $^{237}Np(n, 2n)^{236}Np(s)$ reaction cross-sections in the neutron energy range 7 ÷ 10 MeV. The measurements have been carried out by an activation method. α - radiation of ^{236}Pu has been used for the determination of the amount of $^{236}Np(s)$ nuclei formed under irradiation.

The reactions $^{27}Al(n, \alpha)^{24}Na$, $^{238}U(n, f)$, $^{238}U(n, 2n)^{237}U$ were used for neutron flux measurement.

The total uncertainty is about 5%. The experimental and evaluated data available for $^{237}Np(n, 2n)$ - reaction cross-sections have been analyzed.

A closed fuel cycle with nuclear fuel breeding is a constitutional element of nuclear power engineering with fast reactors.

The fuel cycle includes the processes of storage, transportation reprocessing of irradiated fuel elements and fabrication of new fuel elements. A nuclide composition of irradiated fuel elements determines the economy of these processes. In this respect a ^{232}U is one of unfavairable nuclei. This nuclide cannot be chemically isolated from ^{238}U and accompanies it at all stages of the closed fuel cycle.

The half-life of ^{232}U is about 80 years, and its decay is accompanied by a whole series ($\sim$10) of product nuclei decays with short life-time and hard γ - radiation emission ($E \sim 2.6$ MeV) / 1 /.

Besides there are radioactive gases among products of ^{232}U decays.

One of the main ways of ^{232}U nuclei formation in fast reactors is through (n, 2n) reaction:

$$^{238}U(n, 2n)^{237}U \xrightarrow{-\beta} {}^{237}Np$$

$$^{237}Np(n, 2n)^{236}Np \begin{cases} \xrightarrow{e.c.} {}^{236}U \\ \xrightarrow{-\beta} {}^{236}Pu \end{cases}$$

$$^{236}Pu \xrightarrow{\alpha} {}^{232}U$$

Energy dependence of the first reaction cross-section was studied in detal earlier /2/ , and evaluated cross-section for this reaction are given in /3/ .

With the exception of the measurement of Nishi et all /4/ at E_n = 9.6 MeV, the measurements of $^{237}Np(n, 2n)$ reaction cross-sections were carried out only in the neutron energy range 14 ÷ 15 MeV.

$^{237}Np(n, 2n)$ reaction results in the formation of ^{236}Np nuclides in two states short-lived ($T_{1/2}$= 22.5 ± 0.4 h) and long-lived ($T_{1/2}$ = 1.15 ·10^5 years) with spins 1^- and 6^-, respectively /7/. For the time being the direct experiment determining which of the two states is ground and what is the excitation energy of metastable state has not been carried out. The latest excitation energy value is ~50 keV /4, 5/. Each of the states β - decays into ^{236}Pu , or capturing an electron - into ^{236}U, 48% of S - states and 8.9% of 1 - states go into ^{236}Pu /5/. From the point of view of applied problems, it is most important to know the cross-section of $^{237}Np(n, 2n)^{236}Np(s) \longrightarrow {}^{236}Pu$ reaction. The present work is devoted to the study of this reaction.

The reaction cross-section was measured by the activation method. A neutron flux at the samples was determined relative to reference reactions $^{27}Al(n, \alpha)^{24}Na$, $^{238}U(n, f)^{237}U$, $^{238}U(n, 2n)$. The neutrons with energy 7 ÷ 10 MeV were obtained at the EGP -10M accelerator in D(d, n) reaction using gas deuterium target.

Neptunium in the form of oxide was placed into thin-walled containers 10 mm in diameter and 2 ÷ 3mm in height. The weight of samples was 140 - 400 mg. Neptunium was prepurfied from plutonium isotope impurities by a factor of ~10^5. For all irradiations the background activity of ^{236}Pu was within 0.1% of the induced one.

The neptunium sample with the ones of ^{238}U and ^{27}Al was fixed at the fission ionization chamber with a layer of ^{238}U. The distance between the target edge and sample assembly was 10 mm. Each neptunium sample at a current 2 μa was under irradiation for 80 - 100 hours.

The activity of ^{237}U and ^{24}Na was measured by Ge(Li)-detectors, their efficiency was known with an accuracy (2 - 3)%. Besides, the activitig of ^{24}Na was measured by a $\beta - \gamma$ - coincidence detector. The results of activity measurements with different detectors agree within 2%.

$^{27}Al(n, \alpha)$, $^{238}U(n, f)$ reaction cross-sections are taken from work /6/, for $^{238}U(n, 2n)$ reaction the present results are used /3/. When determining the neutron flux we took into account the neutron flux fluctuation during irradiation time $\lesssim 10\%$ (only for $^{27}Al(n, \alpha)$ reaction), the contributions of background neutron from (d, n) reaction at structural materials of the target and from D(d, np) reaction.

An average neutron flux, mean energy, a flux dependence on the distance to the target and on the energy were calculated taking into account kinematics of D(d, n) reaction, experiment geometry and deutron energy losses in the gas and the entrance window of the target.

To determine amount of nuclei formed under irradiation of $^{237}Np(s)$ we used α - radiation of ^{236}Pu. ^{239}Pu was a carrier in the course of ^{236}Pu chemical release from irradiated target. A more detailed description of the experimental technique is given in work /7/.

The measurement results for $^{237}Np(n, 2n)^{236}Np(s)$ reaction cross-section, and the errors of their measurement are listed in the Table. The error of (n, 2n) - reaction cross-section included the error of determination of neutron flux densities (mean-square error by the data of different reference reactions) ($\lesssim 4\%$), the numbers of ^{237}Np nuclei (0.6%), activities of ^{239}Pu inserted as a carrier ($\sim 1\%$), relations (^{236}Pu)/ ^{239}Pu) ($\lesssim 3\%$), the probability of β -decay($\sim 2\%$).

Table

$^{237}Np(n, 2n) ^{236}Np (s)$ reaction cross-section

$\overline{E}_n \pm \Delta E$ MeV	$\sigma \pm \Delta\sigma$ mb	E_n min MeV	E_n max MeV
7.09 ± 0.10	49 ± 3	6.85	7.31
7.47 ± 0.10	86 ± 4	7.18	7.68
7.90 ± 0.09	123 ± 7	7.60	8.07
8.32 ± 0.11	191 ± 9	7.97	8.52
8.90 ± 0.11	256 ± 13	8.54	9.10
9.37 ± 0.12	338 ± 13	9.00	9.56
9.90 ± 0.10	335 ± 13	9.54	10.08

The Table also lists average values, minimum and maximum neutron energies and mean-square spreads of energies.

In addition to the present data figure I presents experimental cross-sections from other studies. At E_n= 9.6 MeV the cross-section measured by Nishi et al. is represented in the form of two values taken from the figures of papers /4/ and /8/. In the range E_n= 14 ÷ 15 MeV, the most detailed results of the measurements from work /9/ are given, as well as the cross-section measured in work /10/ by two methods: by α -activity of ^{236}Pu and γ - activity of ^{236}U. The four curves in figure I represent different variants of (n, 2n) - reaction cross-sections calculation /4, 11, 12, 13/. All of them are calculated taking into account the total cross-section (n, 2n) in the range E_n= 14 ÷ 15 MeV, where it is known from the experiment at thermonuclear explosion, that the ratio of ^{237}Np(n, 2n)^{236}Np(1) to ^{237}Np(n, 2n)^{236}Np(s) reactions cross-sections is 0.35 ± 0.05 /14/. The difference between the calculated curves increases as E_n decreases.

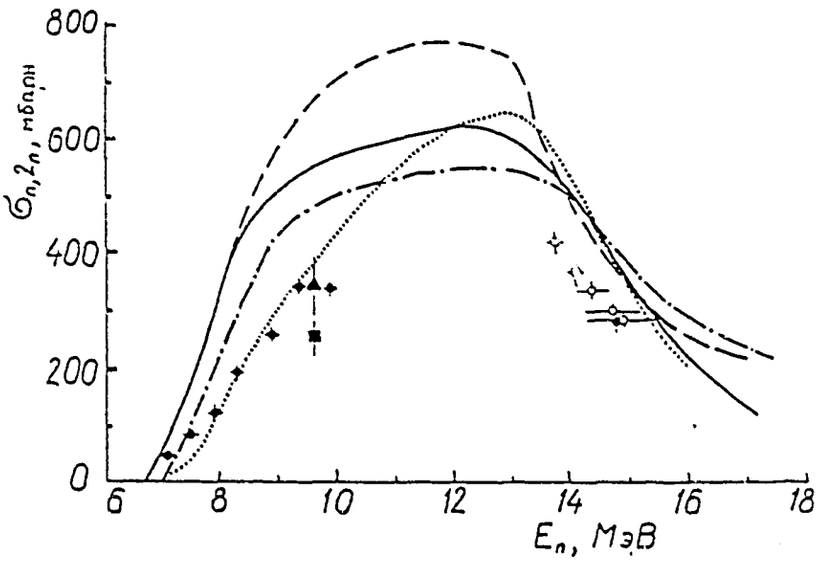

Fig.1. Experimental values of ^{237}Np(n,2n)^{236}Np(s) reaction cross-section (• - the present work and /10/ at E_n =14 MeV , ▲ - /8/ , ■ - /4/ , ○ - /9/) and calculated dependences of ^{237}Np(n, 2n)^{236}Np(s + 1) total reaction cross-section on neutron energy (——— - /11/ , - - - - /12/ , - · - · - /13/ , · · · · - /4/).

The figure shows, that Fort's calculation /4/ does not agree with the measurements of the present work because the total cross-section of short-life - and long-life states being even less than the experimental cross-section of ^{236}Np(s) formation.

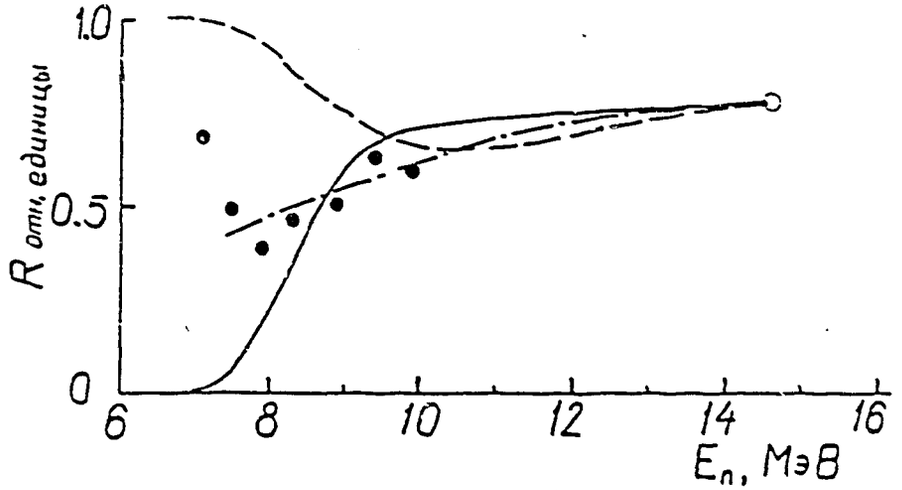

Fig.2 Energy dependence of $R = \sigma^{s}_{n,2n} / \sigma_{n,2n}$ ratio. (• - the values of $\sigma^{s}_{n,2n}$ in the present work related to $\sigma_{n,2n}$ from /11/ . o - the experimental meaning from work /14/ , ___ - and --- - energy dependence R for the cases when the shortlife state is excited or ground assumed in work /4/.

For the discussion of the characteristics of the ground and metastable states of ^{236}Np, a diagram of dependence on neutron energy of the ratio $R = \sigma_{n,2n}(s) / \sigma_{n,2n}(s+1)$ (fig.2) is of interest/4/. Depending on whether the state of ^{236}Np(s) is ground or metastable the curve $R = f(E_n)$ at the threshold goes up to a unity or drops to a zero. The Forts curves (see fig.2) in the vicinity of the thereshold reproduce only qualitative features. An increase of R at $E_n = 7.5$ MeV according to the data of our work and of the total cross-section calculated in indicates that the ^{236}Np(s) is the ground state. Howerer, the accuracy of calculated $\sigma_{n,2n}$ cross-section seems to be insufficient in this area.

The qualitative dependence R(E) resulting from this work and the total cross-section (n, 2n) is shown in fig.2 by a dash-dotted line.

The experimental data presented in this work result from the first detailed investigation of the energy dependence of ^{236}Pu cross-section formation in the reaction ^{237}Np(n, 2n) from the thereshold to 10 MeV. Together with the results for the energy ranges in the vicinity of 14 MeV they give a possibility of describing this cross-section in the whole energy interval essential for fast reactors. However theoretical study of the reaction under consideration taking into account quantum characteristics of low-lying levels is still necessary.

References

1. Zaritskaya T.S., Zaritsky S.M., Kruglov A.N. et al. - Atomnaja Energija, 1980, v.48, No 2, p.67.
2. Kornilov N.V., Zhuravlev B.V., Salnikov O.A. et al. - Atomnaja Energija, 1980, v.49, No 6.
3. Kornilov N.V., Vinogradov V.N., Gay E.V. et al. - Voprosi Atomic Nauki Techniki Jadernye Kostanty, 1983, No 1(45),p.33.
4. Fort E., Derrien H., Doat J.P. Nucl. Data for Sciene and Techn., Antwerp, Sep. 1982, p. 673.
5. Schmorak M.R. Nucl. Data Sheets, 1982, v.36, No 3, p. 367.
6. ENDF/B -V, Dosimetry files.
7. Kornilov N.V., Baryba V.Ya et al. - Atomnaja Energija (in the press).
8. Andreev M.F., Serov V.I. - Neutron Physics, 1980, part 3, p. 301 - Proceedings of the V All-Union Conference on Neutron Physics, Kiev, 1980.
9. Landrum I., Nagle R., Lindner M. - Phys. Rev., 1970, v. C8, p. 1938.
10. Gromova E.A., Kovalenko S.S., Nemilov Yu.A. et al. - Atomnaja Energija, 1983, v.54, No 2, p. 108.
11. Segev M., Caner M. Ann. of Nucl. Energy, 1978, v.5, p.239.
12. ENDL - 76 - Liver. Libr. of Nucl. Data.
13. Bychkov V.M., Plyaskin V.I., Toshinskaya E.F. - Voprosi Atomoi Nauki Techn. ser. Jadernye Konstanty, 1981, No 3(42), p.26.
14. Myers W., Lindner M., Newbery R. J.Inorg. Nucl. Chem., 1975, v.37, p.637.

Contributed Paper 3

^{232}U FISSION CROSS-SECTIONS BY FAST NEUTRONS

B.I. FURSOV, B.F. SAMYLIN, G.N. SMIRENKIN
Institute of Physics and Power Engineering (FEI),
Obninsk, Union of Soviet Socialist Republics

Abstract

This paper presents preliminary results from a recent measurement of the U232 fission cross section in the energy range of 0.1 - 100 MeV. The experimental method is described and the results compared with those of earlier measurements.

Experimental study of ^{232}U fission cross-sections is needed both from a practical and scientific standpoint. The build-up of ^{232}U in fast reactors essentially affects the radioactive environment in the out-of-pile fuel cycle due to its high α-activity. At the same time, the investigation of fission probability of the lightest uranium isotope in the (n,f) reaction provides good information on the fissionability of the compound ^{233}U nucleus, whose neutron binding energy may well be equal to the maximum of the fission barrier humps. In this case there cannot be a threshold in the ^{232}U fission cross-section contrary to the even-even target-nuclei of heavier uranium isotopes (^{234}U, ^{236}U, ^{238}U).

For ^{232}U fission cross-section measurements we employed a technique which was used earlier to study fission cross-sections of a wide range of nuclides [1]. The experiment consisted in the measurement of the ^{232}U to ^{239}Pu fission cross-section ratio. The ^{239}Pu fission cross-section was taken as a standard from the standpoint of convenience of ^{239}Pu utilization when measuring the numbers of fissile nuclei in the layers by comparing their α-activity. The measurements were performed on an electrostatic accelerator. The neutron source reactions were ^{7}Li(p,n), T(p,n) and D(d,n), using solid targets. The energy resolution was 30-200 keV. A ^{232}U layer (100 % enrichment) of mass 12 mkg (8 mm in diameter) was deposited on a platinum backing, and an equally sized ^{239}Pu layer of mass 200 mkg (99,89 % enrichment) were used in the work.

The fissile nuclei numbers ratio in the samples were determined by measuring their α-activity with the use of a semiconductor detector. The following values of half-lives were used: ^{232}U-(72 ± 2) years, ^{239}Pu-(24110 ± 100) years.

Fission fragments were detected by ionization chambers. Owing to the high α-activity of ^{232}U, the measurements were carried out at a high level of discrimination. The efficiency of ^{232}U fission fragments detection was about 80 %, and 97 % for ^{239}Pu spectrum of pulses due to ^{232}U fission could not be correctly extrapolated to the zero level of discrimination, that is why the ionziation fission chambers efficiency ratio was determined in another experiment at E_n = 2,0; 1,3; and 0,40 MeV. A technique with cylindrical glass detectors [1] was employed. In this method the fragment detection efficiency is dependent only on geometrical factors kept equal for the both fissile layers and fragment angular anisotropy which is measured in this experiment. The uncertainty of fissile nuclei number ratio in the ^{232}U and ^{239}Pu layers was 3,5 %, including the uncertainty of the half-lives. An uncertainty of the measurements of the absolute value of ^{232}U and ^{239}Pu fission cross-section ratio in the glass method for E_n = 2 MeV was 4,5 %. This represents an error of the energy dependence normalization measured using the ionization chamber.

The background of neutrons scattered on the accelerator target was measured by the two-fold increase of the effective thickness of the target with the subsequent extrapolation to the zero thickness (0,1-2,7 % correction). The neutron background of the concurrent (p,n) and (d,n) reactions at the target backing was measured by substituting the target by a target model not containing tritium or deuterium. For the (p,n) reaction the correction was as high as 1,5 %, for the (d,n) reaction 1 to 6,4 %. The neutron background of the experimental room was 0,2 - 0,7 %.

In the course of calculation we have taken into account:

- energy dependence of fission chamber efficiency ratio (correction to 4 %);
- ^{240}Pu impurity fission in the ^{239}Pu layer;
- absorption of fission fragments in the layers;
- inelastic scattering of neutrons on backings of the layers;
- difference of the neutron flux through the layers.

The results obtained in the present work are given in the figure. The ^{239}Pu fission cross-section values are used according to ENDF/B-V evaluation. There is a total error of the data (5-6,5 %), which is a mean-square sum of the following components:

- uncertainty due to neutron background measurement (0,5-3,5 %);
- uncertainty of fission chamber efficiency ratio energy dependence calculation (2 %)
- uncertainty as a result of other calculation corrections (0,5-1,5 %);
- normalization accuracy (4,0 %).

The total error does not include the ^{239}Pu reference fission cross-section error.

Comparison of the results obtained in the present work with data from reference [2] shows a two-fold disagreement in the ^{232}U fission cross-section value for E_n = 130 keV. For higher energies the disagreement decreases, but up to E_n = 1,4 MeV it exceeds the summarized experimental uncertainties. The absolute data of the two studies for E_n = 1,5 MeV are in good agreement. It enables us to assume that there is no essential disagreements in the calibration between the two sets, and that the difference is attributed to the energy dependence shape of the ^{232}U fission cross-section. The results in reference [3] in the range 10-20 keV (1,5 barn) substantiate the validity of our data.

The results of this work are preliminary. The final data will be published after additional measurements have been completed; these are necessary for better accuracy and reliability of the results, particularly in the range E_n = 0.1-1 MeV.

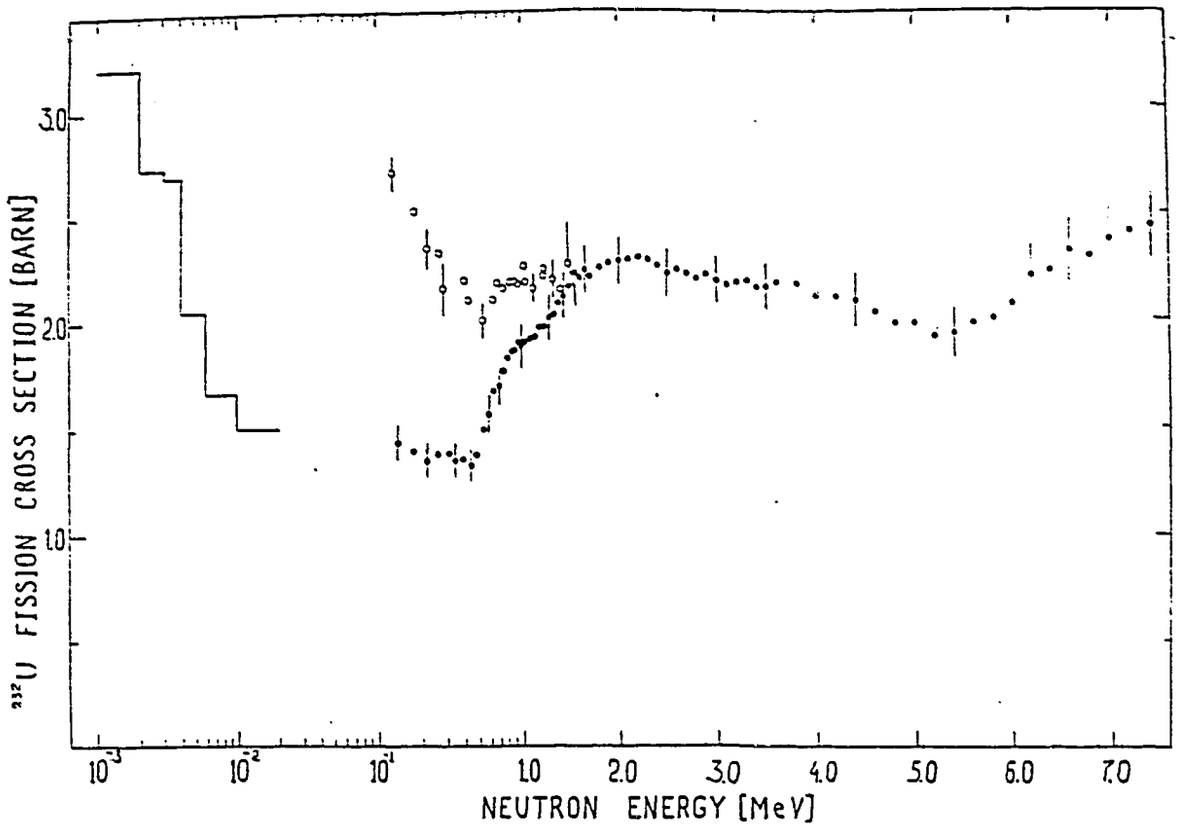

^{232}U Fission Cross-section

○ - [2], ___ _ [3], ◈ - the results of the present work

REFERENCES

1. B.I. Fursov, V.M. Kupriyanov, G.N. Smirenkin, Atomnaja Energia, 1977, v.43, No. 3, p. 181; v.43, No. 4, p. 261; 1978, v.44, No. 3, p. 236; v.45, No. 6, p. 440; 1979, v.46, No. 1, p. 35; 1983, v.55, No. 1, p. 31.

2. P.E. Vorotnikov, S.M. Dubrovina, G.A. Otroshenko, V.A. Shigin, A.V. Davydov, E.S. Palshin. Yadernaya Fisika, 1970, v.12, No. 3, p. 474.

3. J.A. Farrel. Report LA-4420, 1970.

Contributed Paper 4

THE ^{236}U AND ^{238}U TO ^{235}U FISSION CROSS-SECTIONS RATIOS IN THE NEUTRON ENERGY RANGE 5–11 MeV

A.A. GOVERDOVSKY, A.K. GORDJUSHIN, B.D. KUZMINOV,
V.F. MITROFANOV, A.I. SERGACHEV
Institute of Physics and Power Engineering (FEI),
Obninsk, Union of Soviet Socialist Republics

Abstract

This paper presents the results of recent measurements of the fission cross-section ratios of U236 and U238 to U235 in the neutron energy range of 5.0 to 11.0 MeV. The experimental method and error analysis are described, and the results compared with earlier measurements.

The ratios of ^{236}U and ^{235}U fission cross-section in the neutron energy range 4.25 ÷ 10.7 MeV and ^{238}U and ^{235}U in the range 5.4 ÷ 14.7 MeV have been measured at electrostatic accelerators operating in the pulse conditions.

The source of neutrons with energy up to 11 MeV was the reaction D(d, n)^{3}He in the deuterium target representing a thin-walled nickel cylinder 4 cm long and 1 cm in diameter. At the bottom of the target a platinum disk 0.02 mm thick was attached. The inlet window was molybdenum foil 8.2 mg/cm^2 thick. The pressure of gas in the target was 1.2 At. The mean oin current was 1.5 μA.

The neutrons with energy 13.8 ÷ 14.7 MeV have been obtained in the reaction T(d, n)^{4}He in a solid tritium-scandium target 1.5 mg/cm^2 thick. The initial deutron energy was 250 keV. A double ionization chamber filled with methane to the pressure 1.8 At. was used as a fission fragment detector. The distance between the electrodes was 2 mm, the field strength - 2 kV/cm. The detection efficiency was 99.3, 99.2, 98.5% for isotopically pure samples of ^{238}U, ^{236}U, ^{235}U, respectively (without taking into account deceleration of some fragments inside the target).

In the study the targets of U_3O_8 compounds of 200 ÷ 500 μg/cm^2 thinckness on aluminium backings of 0.1 mm thickness were used. The active spot diameter was 50 mm. Non-uniformity over the layer thickness was 10%.

The target characteristics are given in table 1.

The energy dependence σ_f^6 / σ_f^5 was investigated at targets No 1 and No 2. Normalization was carried out at neutron energies 7.34, 8.10, 8.91 MeV with the use of targets No 3 ÷ No 6. For σ_f^8 / σ_f^5 No 1 and No 7 were used, and normalization of the dependence was performed at E_n= 7.34 MeV at targets No 3 and No 9, 10.

Table 1 Target Characteristics

No	Isotopic Composition (at. %)				ρ, мг/см²
	U - 234	U - 235	U - 236	U - 238	
1	0.0020 ± 0.005	99.992 ± 0.001	0.0040 ± 0.0005	0.0020 ± 0.0005	0.41 ± 0.04
2	0.0001	0.047 ± 0.002	99.845 ± 0.005	0.107 ± 0.002	0.49 ± 0.05
3	0.0020 ± 0.0005	99.992 ± 0.001	0.0040 ± 0.0005	0.0020 ± 0.0005	0.258 ±0.026
4		3.002 ± 0.009	96.87 ± 0.10	0.13 ± 0.02	0.198 ±0.020
5		4.973 ± 0.015	94.90 ± 0.09	0.13 ± 0.02	0.198 ±0.020
6		6.943 ± 0.003	92.929 ± 0.003	0.127 ± 0.002	0.198 ±0.020
7				99.99	0.48 ±0.05
8*		7.01		92.99	0.30 ±0.03
9		3.213 ± 0.010	0.001 ± 0.002	96.78 ± 0.01	0.204 ±0.020
10		6.864 ± 0.007	0.020 ± 0.002	93.116 ±0.007	0.204 ±0.020

* Ratio of ^{238}U and ^{235}U nuclei numbers in target No 8 is known with accuracy 1% .

To determine the relation of nuclei numbers in the samples a method of isotope impurities was employed. Isotopic weighting of the samples was carried out in the neutron flux from the reaction $T(p, n)^3He$ decelerated by a polyethelene layer of 20 cm thickness. The initial neutron energy was 500 keV. The targets were examined prior to and after energy dependence measurement. The ratio of ^{238}U and ^{235}U fission cross-sections by neutrons with energy 13.8 ÷ 14.7 MeV was measured at samples No 3, No 8.

When measuring both energy dependences and normalization values of fission cross-sections ratios we had to take into account a number of factors capable of distorting the value of relative counting rate of fission fragments for the standard and isotope under investigation.

They are:

1. Complete deceleration of some fragments in targets

The correction was determined through calculation similar to work /1/ using the data on angular distributions of fragments from /2/. The maximum correction is within (n, n'f) thresholds for ^{235}U, ^{236}U and ^{238}U, and is 0.6% for σ_f^8 / σ_f^5 and 0.4% for σ_f^6 / σ_f^5.

2. Incomplete recording of fission events due to final level of amplitude discrimination

The effect is taken into account when processing amplitude spectra of fission chamber pulses obtained in the control of singnals drriving from the output the time analyzer shaping circuit. The value of the corresponding correction was as high as 0.3 ÷0.7% both for σ_f^6 / σ_f^5 and σ_f^8 / σ_f^5.

3. Scattered neutron background

The influence of background of neutrons scattered at structural materials of the target, ionization chamber and layer backings was calculated by the Monte-Carlo method. The correction is maximum in the neutron energy range 6.5 ÷ 7.2 MeV and is 0.5% for σ_f^8/σ_f^5 and 0.25% for σ_f^6/σ_f^5.

4. The background of secondary particles from reactions (n,p) and (n,d)

at structural materials of the detector and target backings was determined at the irradiation of aluminium foil without a fissile material. The value of the effect observed at the operating level of amplitude discrimination was 0.3% for $E_n \leq 9$ MeV and 0.9% in the range $E_n \sim 14.5$ MeV.

5. Fission of non-basic isotopes was taken into account on the basis of data heavy nuclei fission cross-sections. The corresponding correction was as high as 0.15%.

6. The experimental room background was as high as 1 ÷ 3 % within the whole range of neutron energies under investigation.

7. The neutron background of concurrent reactions in the target consisted of three components:

a) neutron reaction D(d,np)D ;
b) reaction of desintegration of deutons in target structure;
c) reaction $D(D,n)^3He$ on deutons implanted into target materials.

In the neutron energy range 5 ÷ 11 MeV the background was from 0.6 to 65% of ^{235}U fission events due to monoenergetic neutrons. For ^{236}U and ^{238}U the background was within 0.3 ÷ 55%. The distance between the target and fissile samples was chosen so as to obtain adequate separation of the main and background groups of events in the time spectra of pulses in the ionization chamber while maintaining sufficient counting rate. In the pulsed operating conditions of the accelerator with ion current chopping frequency 5 Mg and pulse duration 1 nsec, the time resultion 2 nsec was achieved (FWHM), which enabled us to have path of flight not exceeding 60 cm for $E_n \sim 7$ ÷ 11 MeV. The partial overlap of the main and background groups for $E_n \geq 9.5$ MeV resulted in the necessity of introducing a correction into σ_f^6/σ_f^5 from 0.2 to 6% at $E_n = 10.7$ MeV.

The gaseous target state and the neutron spectrum were permanenly controleed by a neutron time - of - flight spectrometer on the basis of a scintillation detector.

8. The difference of neutron fluxes through the samples due to the final distance between them was eliminated by reversing the chamber relative to the neutron flux direction.

The total error of measuring σ_f^6/σ_f^5 and σ_f^8/σ_f^5 fission cross-sections ratios was 1.0 ÷ 1.7% . A random part of the total error is due to fission fragment counting statisics and to the statistical part of the recording efficiency ratio error . The statistical error is basically due to the energy dependence normalization error.

Table 2 lists the typical values of the total error constituents for determining cross-sections ratios and their reference values.

The results of measuring the ratios of σ_f^8/σ_f^5 and σ_f^6/σ_f^5 fission cross-sections are given in table 3 and 4 .

In fig. 1 and 2 the data of the present work are comparable with the data by other authors /3 ÷ 13/.

Table 2

Source of uncertainty	: σ_f^6/σ_f^5, %	: σ_f^8/σ_f^5, %
Energy dependence :		
Statistics of fission events counting	0.6 -1.0	1.0
Calculated corrections	0.2	0.2
Isolation of neutron backgrounds	0.02-0.6	0.1
Absolutization of energy dependence	0.51	1.01
Reference values:		
Statistical error	0.2	0.2
Extrapolation of amplitude spectrum	0.8	0.6
Uncertainty of isotopic composition of samples	0.3	0.3-1.6

Table 3

E_n, MeV	$\pm \Delta E_n$, keV	σ_2^0 / σ_2^3	δ stat.%	δ total,%
1	2	3	4	5
4.24	190	0.790	1.60	1.86
4.65	180	0.794	0.90	1.22
4.97	130	0.801	0.95	1.25
5.21	123	0.780	1.00	1.30
5.43	120	0.782	1.00	1.30
5.66	116	0.825	0.32	0.81
5.90	108	0.846	0.85	1.16
6.11	102	0.849	1.03	1.30
6.32	97	0.813	0.73	1.09
6.50	93	0.860	0.70	1.03
6.68	89	0.866	0.83	1.14
6.86	86	0.914	0.79	1.09
7.02	83	0.908	0.72	1.04
7.19	80	0.926	1.05	1.29
7.34	78	0.921	0.66	1.00
7.51	76	0.923	0.95	1.21
7.66	74	0.893	0.99	1.25
7.81	72	0.892	1.06	1.29
7.96	70	0.884	0.93	1.28
8.10	68	0.893	0.89	1.20
8.25	67	0.873	1.07	1.31
8.39	65	0.871	0.74	1.05
8.52	64	0.874	0.75	1.06
8.64	63	0.875	0.73	1.05
8.78	62	0.886	0.79	1.08
8.91	61	0.874	0.78	1.11
9.03	60	0.875	1.06	1.30
9.18	59	0.880	0.75	1.05
9.13	58	0.871	0.72	1.05
9.44	57	0.887	0.76	1.10
9.56	56	0.875	0.64	1.02
9.67	55	0.872	0.72	1.07
9.82	54	0.872	0.66	1.05
9.94	53	0.897	1.07	1.46
10.06	53	0.899	0.87	1.21
10.20	52	0.893	1.05	1.32
10.44	51	0.847	0.96	1.36
10.56	50	0.861	0.82	1.45
10.69	50	0.874	1.26	1.66

Table 4

Ratios of ^{238}U and ^{235}U fission cross-sections

E_n, MeV	$\pm\Delta E$, MeV	$\sigma_f^{28}/\sigma_f^{25}$	δ stat., %	δ total, %
5.44	0.15	0.491	0.83	1.56
5.64	0.14	0.521	1.03	1.69
5.89	0.14	0.548	1.00	1.68
6.14	0.13	0.575	0.90	1.59
6.38	0.12	0.597	0.89	1.59
6.50	0.12	0.601	0.80	1.52
6.61	0.11	0.609	1.13	1.72
6.84	0.11	0.620	1.20	1.76
7.07	0.10	0.598	1.20	1.76
7.19	0.10	0.581	0.90	1.57
7.30	0.10	0.584	0.20	0.68
7.52	0.10	0.576	1.21	1.77
7.74	0.09	0.572	0.86	1.55
7.96	0.09	0.570	1.20	1.77
8.17	0.09	0.564	1.16	1.74
8.33	0.08	0.570	0.91	1.58
8.49	0.08	0.562	0.90	1.56
8.65	0.08	0.555	0.80	1.52
8.81	0.08	0.569	0.87	1.56
8.97	0.08	0.565	0.87	1.56
9.12	0.07	0.557	1.30	1.83
9.28	0.07	0.568	0.81	1.53
9.44	0.07	0.556	0.78	1.51
9.59	0.07	0.560	0.80	1.52
9.80	0.07	0.559	1.05	1.67
10.00	0.07	0.578	0.85	1.55
10.41	0.06	0.567	1.05	1.67
13.82	0.15	0.528	1.0	2.3
14.12	0.13	0.554	0.7	2.2
14.47	0.20	0.559	0.7	2.2
14.64	0.23	0.553	0.7	2.2
14.76	0.19	0.543	0.7	2.2

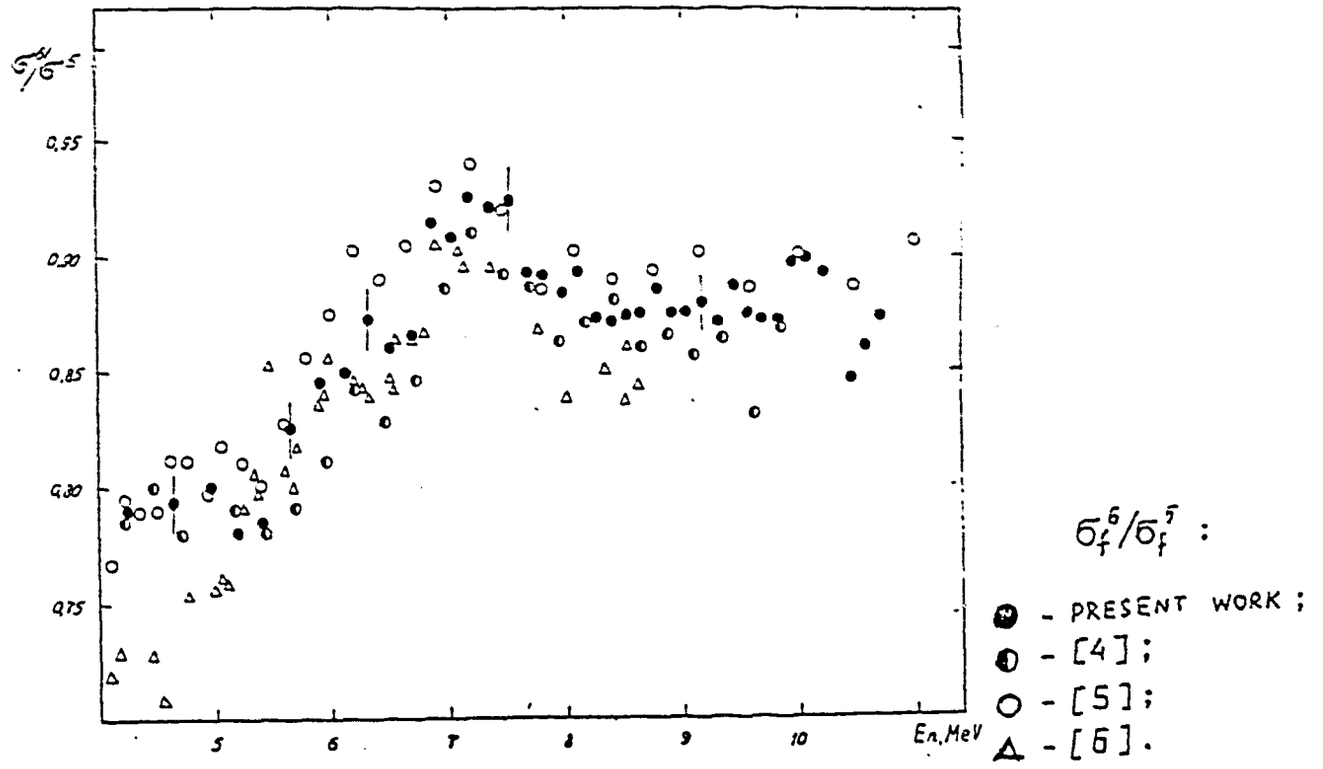
0,55
0,50
0,45
0,40
0,35
5
6
7
8
9
10
E_n, MeV
σ_f^6/σ_f^5 :
● - PRESENT WORK ;
◐ - [4] ;
○ - [5] ;
△ - [6].

FIG. 1.

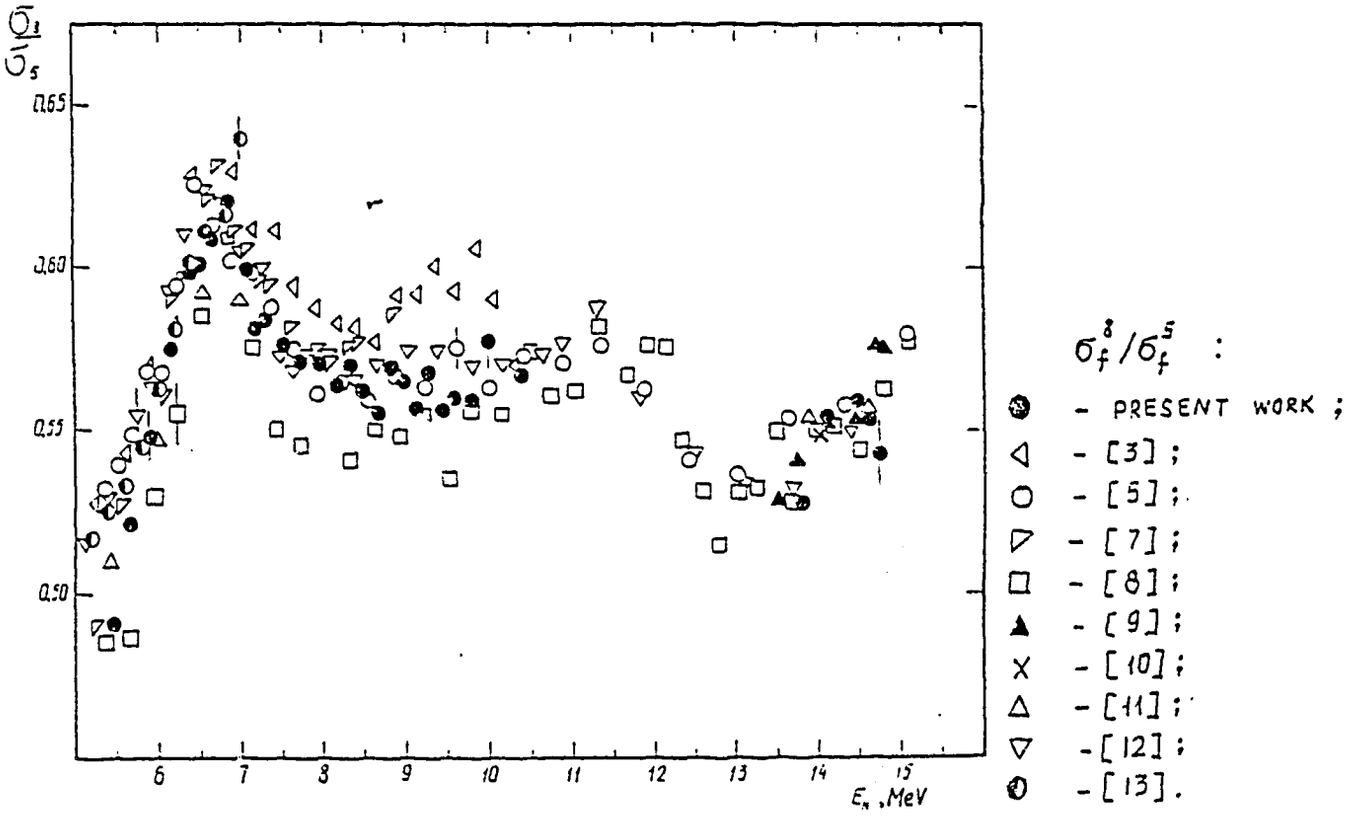
0,65
0,60
0,55
0,50
6
7
8
9
10
11
12
13
14
15
E_n, MeV
σ_f^8/σ_f^5 :
● - PRESENT WORK ;
◁ - [3] ;
○ - [5] ;
▷ - [7] ;
□ - [8] ;
▲ - [9] ;
× - [10] ;
△ - [11] ;
▽ - [12] ;
◐ - [13].

FIG. 2.

REFERENCES

1. Carlson G.W. - Nucl. Instr. Meth., 1974, v.119, p.97.
2. Simmons J.E., Henkel R.L. - Phys. Rev., 1960, v.120, p.198.
3. Meadows J.W. - Nucl. Sci. Eng., 1975, v.52, p.255.
4. Meadows J.W. - Nucl. Sci. Eng., 1978, v.65, p.171.
5. Behrens J.W., Carlson G.W. - Nucl.Sci.Eng., 1977, v.63,p.250.
6. Nordborg C., et al. - In: Proc. Int. Conf.,Harwell, 1978.
7. Nordborg C., et al. - In: Proc. Of the NEANDC/NEACRP SPECIAL. Meeting on fast neutron fission cross-sections of U-233,U-235,U-238 and Pu-239, 1976, ANL-76/90,p.128.
8. Cierjacks S., et al. - IBID, p.94.
9. Varnagy M., Csikai J. - Nucl. Instr. Meth., 1982, v.196, p.465.
10. White P., Warner C. - J.Nucl. Energy, 1976, v.21, p.671.
11. Cance M., Granier G. - Nucl. Sci. Eng., 1978, v.68, p.197.
12. Difilippo F.S., Perez R.B. - Nucl. Sci. Eng., 1978, v.68, p. 43.
13. Fursov B.I., Kuprianov V.M., Smirenkin G.N. -Atomic energy, 1977, v.43, p.181.

Contributed Paper 5

STATUS OF NEUTRON RADIATIVE CAPTURE DATA FOR ^{236}U AND ^{237}Np

V.A. TOLSTIKOV, V.N. MANOKHIN
Institute of Physics and Power Engineering (FEI),
Obninsk, Union of Soviet Socialist Republics

Abstract

This paper describes the requirements for the neutron radiative capture cross section data for U236 and Np237 in fast reactor fuel cycle calculations, reviews the status of these data, and identifies the discrepancies in the available data.

Introduction. An investigation of neutron radiative capture cross sections of ^{236}U and ^{237}Np is of great interest from point of view of understanding fast neutron interaction with actinide nuclei and obtaining the information for nuclear reaction model test and from point of view of technological processes connected with fast reactor fuel cycle.

The chain of main nuclear transformations arising from irradiation of ^{236}U and ^{237}Np in fast reactors is the following:

$$^{235}U(n,\gamma)^{236}U(n,\gamma)^{237}U(\beta^-)^{237}Np(n,\gamma)^{238}Np(\beta^-)^{238}Pu(\alpha, T_{1/2}\ 86{,}4y)$$
$$\downarrow (n,2n)$$
$$^{236}Np(\beta^-, \sim 50\%)^{236}Pu(\alpha, T_{1/2}\ 2{,}85y)$$

The ^{238}Pu obtained as a result of this process can be used as a radioisotope source. The burn-up of ^{238}Pu and ^{236}Pu (which are short lived relative to α-decay) in irradiated fuel makes essentially complicated a fuel treatment in the process of its manyfold reprocessing and regeneration.

The calculation of technological processes connected with the ^{236}Pu and ^{238}Pu burn-up requires knowledge of evaluated capture cross sections with the accuracy $\sim 5\%$ for ^{236}U and $\sim 10\%$ for ^{237}Np. The correspondent requirements are laid on experimental information. However the evaluation of work [13] allows to assume that the present uncertainty of capture cross sections for the isotopes mantioned is hardly better then 40%. This evaluation was made in 1979, when there were little experimental works: the works [1-3] were considered for ^{236}U and the works [10,11] for ^{237}Np. The data of these works are overlapped only partially in energy range, absolute cross section values and energy dependences are quite different.

Lately a number of new experimental works has been issued which enable to reexamine the status of ^{236}U capture cross section. For ^{236}U these are works [4-6,9] , for ^{237}Np - [7,8,12], unpublished works by Gofman [14] and Weston [15] , which data have been given as curves in Derrien's work [16].

^{236}U. A ^{236}U data status has been partially analyzed in the report [17], presented on the INDC Meeting in Rio-de-Janeiro in May 1983. Since then the data of soviet authors were refined and expanded (concerning method of measurement). The numerical data of Carlson's work [3] became also available.

Fig.1 shows the present status of $^{236}U(n,\gamma)$ experimental data in comparison with the ENDF/B-V data in energy range 1kev-15MeV. In the energy region less 200 kev the data from ENDF/B-V averaged by means of GRUCON program are given. Averaging was made by V.Sinitsa and J.Korchagina in energy range 1-10kev over 1 kev intervals, in energy range 10-100kev over 2kev intervals and in energy range 100-200kev over 10kev intervals. Further a smooth curve has been drawn through ENDF/B-V data. It seems that the ENDF/B-V evaluation is based on experimental data of works by Carlson [3], Stupegia [1] and Barry [2].

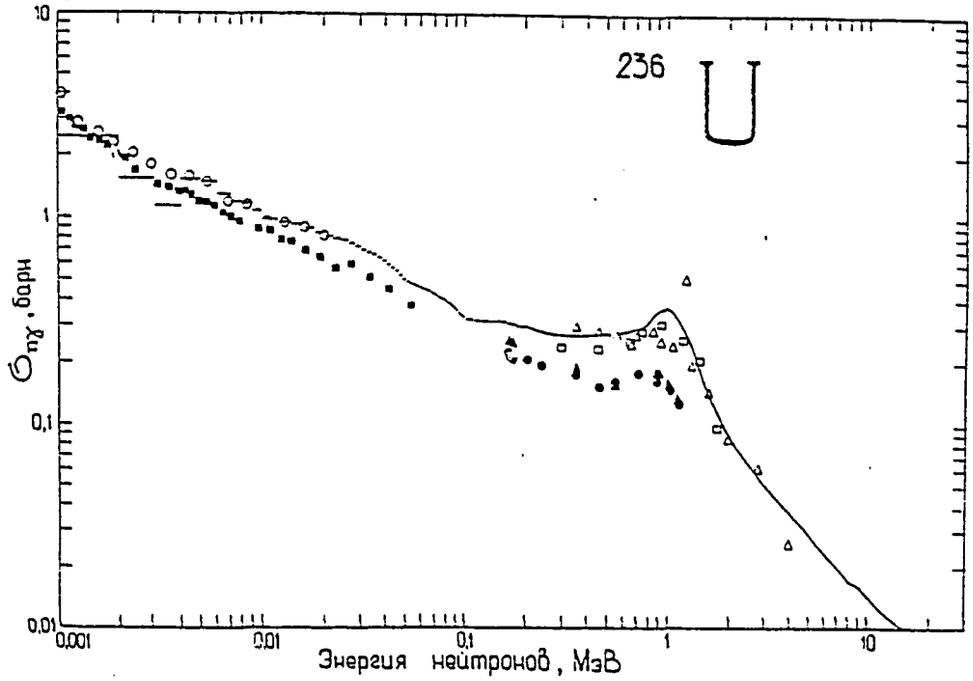

Fig. 1. ^{236}U radiative cross section in the neutron energy range 1 kev - 15 Mev.
● - [5] , relative to $\sigma_{n,\gamma}$ ^{197}Au, ENDF/B-V
▲ - [6] , relative to $\sigma_{n,p}$ of hydrogen
■ - [4] , o - [3] ; □ - [1] ; △ - [2] ;
⌐ - averaged(using GRUCON Program) ENDF/B-V data;
—— - ENDF/B-V data

Some experimental data of authors from the USSR [5,6], which have been obtained by activation method in the energy range 0.15-1.15 MeV, were presented at the All-Union Conference on Neutron Physics (Kiev, 1983). The incident neutron flux was determined relating to ^{197}Au capture cross section by means of recoil proton counters. The measurement technique is described in detail in [9]. Together with the work [4] these works give the qroup of data which are systematically above the ENDF/B-V data over the whole energy region except 1-4 kev where averaged ENDF/B-V data are close (region 1-3 kev) or by ~ 20% below (region 3-4 kev) in comparison with the data of work [4]. For En in the region 4-53 kev the ENDF/B-V data (issentially experimental data of Carlson [3]) are in average by 20-25% above then the data of work [4]. This discrepency is within 1-1.5 summerized root mean square uncertainties of the experiments by Carlson [3] and work [4] (not more 10% in [3] and 5% - in [4]). The energy dependences are also different to some extent. From our point of view one should consider more attentively the problemm connected with cross section self-screening in the low energy region and with cross section absolute normalization.

More essential discrepencies are in the energy region >200kev: about 50%. It is possible that the reason for discrepences is also connected with systematic uncertainties of normalization. It should be noted that in works [5,6] the cross section normalization has been made by the two independent methods however experimental de - pendences are in good agreement within experimental uncertainties.

On the other side the theoretical works [9,10] indicate that lower values are preferable as they are described with $\overline{\Gamma}_\gamma$ and $\overline{D}_{res}$ lying within its uncertainties. At the same time the description of higher data values requires half as much $\overline{D}_{res}$.

The additional experimantal data obtained by different methods activation measurements are needed.

^{237}Np. Fig. 2 gives available information on the reaction ^{237}Np. One can see that the data by Lindner [11] and our data obtained relative to $^{197}Au(n,\gamma)$ cross section [8] and cross section reaction on hydrogen [7] are in good agreement. They naturally agree with ENDF/B-V data which are based on Lindner's data. Tro - fimov's data [12] (except value at 330kev) differ from ENDF/B-V data in energy region 60kev up to 50%. The data by Stupegia [10] should be considered excessively high. Partially it may be connected with normalization. However systematic increase of discrepency as a function of energy one can link with underestimation of influance of ^{236}U(or ^{235}U) fission. The second reason which

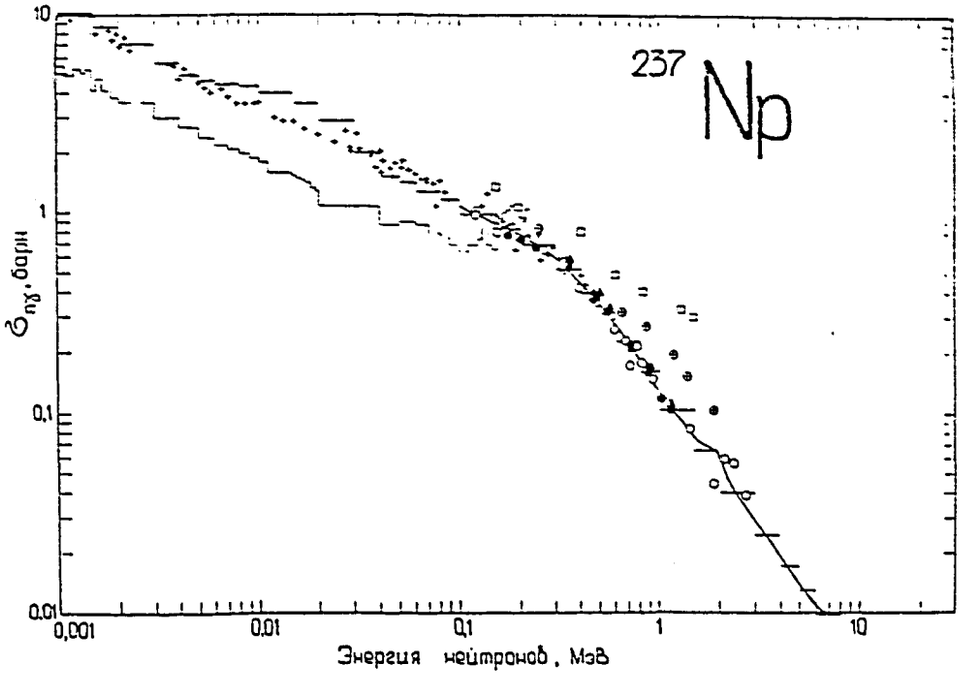

Fig. 2. ^{237}Np radiative capture cross section in the neutron energy region 1 kev - 15 Mev.

● [8], relative $^{197}Au(n,\gamma)$, ENDF/B-V;
▲ [7], relative $\sigma_{n,p}$ of hydrogen;
⊖ [12]; o - [11]; □ - [10]; + - [15];
⌋ - [14]; —— ENDF/B-V;
—— averaged ENDF/B-V data

has general feature for activation method may be influance of scattered low energy neutrons.

The data of the work by Weston [15] and Goffman [14] (the numerical data and method description of which are absent at our disposal) differ qreatly for $E_n < 150$kev. For E_n = 150-200kev they are overlapped but at $E_n > 150$kev Weston's data are close in average to activation data. It seems that for this reason in some evaluation the $\sigma(n,\gamma)$ curves are drawn toking into account Weston's data.

Fig.2 shows also ^{237}Np capture cross sections from ENDF/B-V averaged in 74-qroups. The data in resonance energy region were averaged using RECENT code. The results of averaging coinside with those using GRUCON code and the same data from ENDF/B-V.

It is seen from Fig. 2 that for $E_n > 200$ kev there are strong necessity in new measurements. New measurements in energy range > 1,5 Mev are also needed for determination of more exact form of $\sigma_{n,\gamma}(E)$ curve.

References

1. D.C.Stupegia, R.R.Heinrich, J.N.Maclound, Neutron Capture Cross Sections of ^{236}U. Journ. of Nucl. Energy, parts A/B , vol. 15, N 4, p. 200, 1961.

2. J.F.Barry, J.L.Bunce, J.L.Perkin. The Radiative Capture Cross Section of ^{236}U for Neutrons in the Energy Range 0.3 - 4.0 Mev. Proc. Phys. Soc., v. 78, N 503, p. 801, 1961.

3. A.D. Carlson, S.J.Friesenhahn, W.N. Lopes, M.P.Fricke. The ^{236}U Neutron Capture Cross Section. Nucl. Phys. A141(1970), 577-594.

4. A.A.Bergman, A.N.Medvedev, A.E.Samsonov, V.A.Tolstikov, A.G.Kolosovskij, M.V.Mordovskij, A.Melikzhanov. The Radiative Capture Cross Section Measurement of ^{236}U in the Energy Range 0.1 - 50 kev. Voprosy Atomnoj Nauki i Tekhniki, series "Yadernye Konstanty", 1982, issue 1 (45), p. 3.

5. A.N. Davletshin, A.O.Tipunkov, S.V.Tikhonov, V.A.Tolstikov, V.V.Tuzhilov, L.E.Sherman, O.T.Grudzevich. The results of ^{236}U $\sigma(n,\gamma)$ measurements relative to ^{197}Au (n,γ) in the neutron energy range 0.16 - 1.15 Mev. Report at the 6th All-Union Conference on Neutron Physics, Kiev, 2 - 6 October, 1982.

6. A.N.Davletshin, A.O.Tipunkov, S.V.Tikhonov, V.A.Tolstikov, V.V. Tuzhilov, L.E.Sherman. The results of ^{236}U $\sigma(n,\gamma)$ relative $\sigma_{n,p}$ in the neutron energy range 0.16 - 1.15 Mev. Report at 6 All - Union Conference on Neutron Physics, Kiev, 2 - 6 October, 1982.

7. A.N.Davletshin, A.O.Tipunkov, S.V.Tikhonov, V.A.Tolstikov, V.V. Tuzhilov, S.N.Baikalov, S.N.Korolev. The results of ^{237}Np. Measurements Relative to $\sigma_{n,p}$ in the Neutron Energy Range 0.16 - 1.15 Mev. Report at the All - Union Conference on Neutron Physics, Kiev, 2 - 6 October, 1983.

8. A.N.Davletshin, A.O.Tipunkov, S.V.Tikhonov, V.A.Tolstikov, V.V.Tuzhilov. The Results of Measurements $\sigma_{n,\gamma}$ ^{237}Np Relative to $\sigma_{n,\gamma}$ ^{197}Au in the Neutron Energy Range 0.16 - 1.15 Mev, Report at 6th All-Union Conference on Neutron Physics, Kiev, 2-6 October, 1982.

9. O.T.Grudzevich, A.N.Davletshin, S.V.Tikhonov, V.A.Tolstikov, V.V.Tuzhilov, L.E.Sherman. The Neutron Radiative Capture Cross Sections of ^{236}U in the Energy Range 0.15 - 1.1 Mev. Voprosy Atomnoi Nauki i Tekhniki, Series "Yadernye Konstanty", 1983, issue 2 (51), p. 3.

10. D.C.Stupegia, M.Smidt, C.R.Keedy. The Capture Cross Section of ^{237}Np. Nucl. Sci. Eng., vol. 29, N 2, p. 218, 1967.

11. M.Lindner, R.I.Nagle, J.N.Landrum. Neutron Capture Cross Sec - tions from 0.1 to 3 Mev by Activation Measurements. Nucl. Sci. Eng.
12. Yu.N.Trofimov, Yu.A.Nemilov. The ^{237}Np Radiative Capture Cross Sections at E_n = 0.3 - 1.9 Mev, Report at the 6th All-Union Conference on Neutron Physics, Kiev, 2 - 6 October, 1983.
13. A.I.Voropaev, A.A.Van'kov, V.V.Vozjakov, A.S.Krivtsov, V.N.Manokhin, A.G.Tsykunov. Group Neutron Fission and Radiative Capture Cross Sections of Transactinide Isotopes. Voprosy Atomnoi Nauki i Tekhniki, Series "Yadernye Konstanty", 1979, issue 3(34), p.34.
14. M.M.Hoffman et al., 1971, see [16].
15. L.W.Weston, J.H.Todd. Private Communication, 1979, see [16].
16. H.Derrien, E.Fort. Proc. Intern. Conf. Neutron Cross Sections and Technology, oct. 22-26, 1979, Knoxville, 1980, p. 872, Report at Soviet - French Seminar in Obninsk, 15-22 December, 1980: "Evaluations des sections efficaces neutronique de ^{237}Np de 10^{-5} ev a 14 Mev".
17. A.N.Davletshin, A.O.Tipunkov, V.A.Tolstikov. On Discrepences of the Two Groups of the ^{236}U Fast Neutron Radiative Capture Cross Section Data. Report at INDC Meeting, Rio de Janeiro, May, 1983..

Contributed Paper 6

ON UNCERTAINTIES AND FLUCTUATIONS OF AVERAGED NEUTRON CROSS SECTIONS IN UNRESOLVED RESONANCE ENERGY REGION FOR ^{235}U, ^{238}U, ^{239}Pu

A.A. VAN'KOV, A.I. BLOKHIN, V.N. MANOKHIN,
I.V. KRAVCHENKO
Institute of Physics and Power Engineering (FEI),
Obninsk, Union of Soviet Socialist Republics

Abstract

This paper analyses the reasons for the differences which exist between group-averaged evaluated cross-section data from different evaluated data files for U235, U238 and Pu239 in the unresolved resonance energy region.

Introduction. The specific difficulties resulting from necessity of model representation of irregularities in neutron cross section energy dependence arise in evaluation of neutron cross section in unresolved resonance energy region. By its nature such irregularities ought to be a consequence of interme - diate structure in the neutron cross sections.

However the analysis of experimental data shows that the character of observable irregularities depends on measurement method. One can point out two main reasons which are responsible for irregularities not linked with intermediate structure in cross sections:

1. Presence both statistical and systematic uncertainties in measurements. The example of systematic uncertainties is an effect of neutron resonance scattering in samples of finite thickness at capture cross section measurements.

2. The second physical reason for fluctuations is the fi - nite number of resonances on resolution function width of experimental device. The magnitude of such fluctuations depends on a way of averaging cross sections in experiment. Hence it is necessary to consider all the sources of fluctuations at analysis and evaluation of neutron data in unresolved resonance re - gion.

In present paper we shall consider some aspects connected with fluctuations and uncertainties of average cross sections for ^{235}U, ^{238}U and ^{239}Pu in unresolved resonance region.

The evaluation of group constant uncertainties. The constant system BNAB-78[1] is used in the USSR for reactor design calculation. In this system for the low energy region energy groups are used with the following boundaries:

Number of group	10	11	12	13	14	15	16	17
E^{low}, KeV	21,5	10,0	4,65	2,15	1,00	0,465	0,215	0,100
E^{upper}, KeV	46,5	21,5	10,0	4,65	2,15	1,66	0,465	0,215

We attributed to the unresolved resonance region the following energy groups: 10-14 for ^{238}U, 11-15 for ^{235}U, 11-17 for ^{239}Pu. Neutrons of this energy region contribute considerably to neutron balance in LMFBR. In large cores the contributions into reaction rate energy distributions of energy region $E_n < 21,$% kev are as follows: 55% for $^{238}U(n,\gamma)$, 70% for $^{239}Pu(n,\gamma)$, 30% for $^{239}Pu(n,f)$, while correspondent contribution for neutron spectrum is only about 17%. One should emphasize, that the characteristics of LMFBR are affected by resonance structure of total cross section (through self-shielding factors of cross sections and diffusion coefficients, which influance energy distribution). A Knowledge of total cross section is also of great importance in theoretical analysis of neutron cross section for the estimates of average resonance parameters.

The evaluated averaged cross sections of nuclides mentioned above in the unresolved resonance energy region have approximately the following uncertainties: in $\langle\sigma_t\rangle$ - 4-5%, in $\langle\sigma_\gamma\rangle$ and $\langle\sigma_f\rangle$ - 6-8%. In various design calculations decreasing these uncertainties by factor 1,5-2 is needed.

In Fig.1 the achieved (I) and reguired (II) uncertainty levels for ^{235}U, ^{238}U, ^{239}Pu cross sections are shown by horizontal dashed lines. The uncertainty values of these quantities are studied of recent evaluations using Monte Carlo method and Reich-Moore multilevel formalism.

The estimation of fluctuation errors of group cross sections has been also obtained in the framework of the same approach. These fluctuation errors are shown on the Fig. as hystogram (solid line). One can see, that inspite of wide intervals for averaging the fluctuation errors are comparable or exceed the achieved uncertainties (line I) of the evaluated average cross sections in groups 13 and 14 for ^{238}U, in groups 14 and 15 for ^{235}U. Morover the fluctuation errors exceed the required uncertainties (lines II) on the Fig. in the energy region considered.

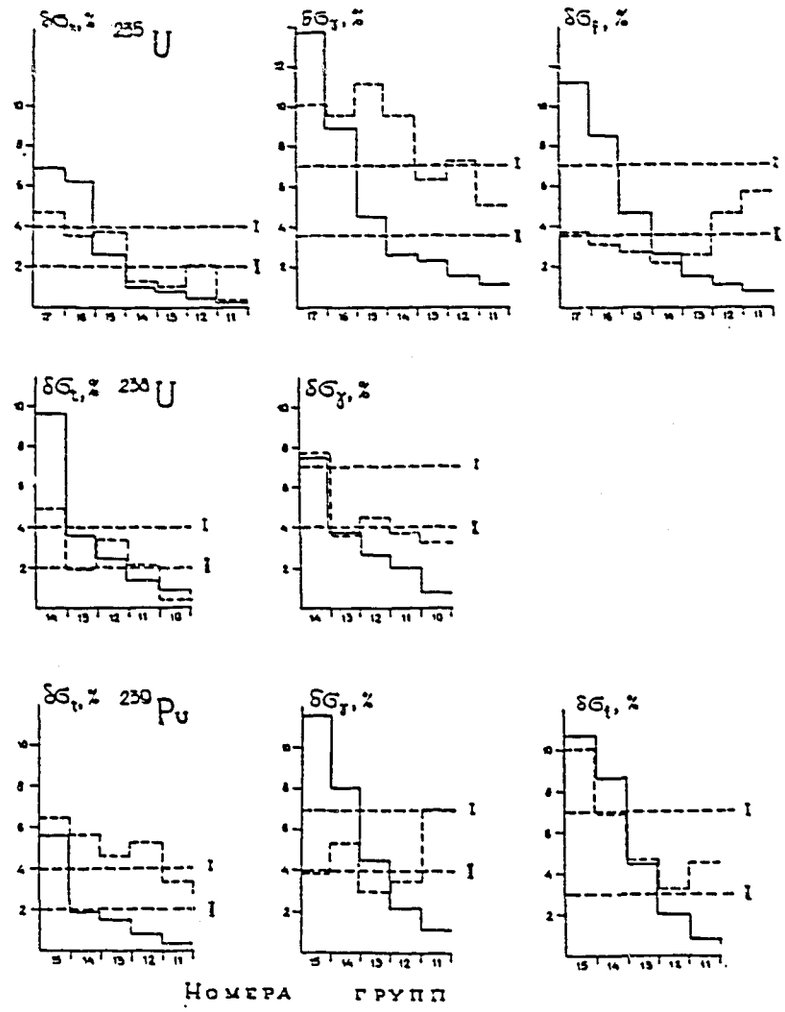

Fig.1. Uncertainties and fluctuations of the ^{235}U, ^{238}U, ^{239}Pu cross sections:

dashed lines (I) and (II) - achieved and required uncertainties respectively

hystogram (solid line) - calculated cross section flucturation using Monte-Carlo method

hystogram (dashed line) - cross section spread on the base of data from BNAB-78, ENDF/B-4, ENDF/B-5, JENDL-1, ENDL-78.

The fluctuation errors increase by about $\sqrt{n}$ at averaging cross sections over smaller intervals. This means that dividing the group considered, for example, into 10 small subgroups the fluctuation errors will increase by about a factor 3, at the same time the achieved uncertainties will not change practically because of strong correlation of evaluations of averaged cross section energy depen - dence. On can conclude from this fact that it makes no physical sanse to use for average resonance parameter evaluation the neutron strength functions S_0 and S_1 adjusted to detailed average cross sec-

tions within its published uncertainties. We can require from these evaluations to give description "in average" within fluctuation errors. That is why the detailed energy evaluation of strength functions (for example in [4]) has no theoretical ground.

Spread of evaluations. It would be interesting to consider the spread of average cross section data of different evaluations. We have analyzed group average cross section data, which have been obtained from the following evaluations available in Nuclear Data Center (Obninsk): ABBN data [1], the data from [2,3], Kon'shin's data on ^{239}Pu [5], the data from libraries ENDL-78, JENDL-1, ENDF/B-IV, ENDF/B-V. As a measure of spread we took a half of the maximum difference of average cross sections in each group. In separate cases the data were ignored if its deviations were extremely high. These cases are the following: ENDL-78 data for $\langle\sigma_t\rangle$ of ^{238}U and ^{239}Pu and for $\langle\sigma_\gamma\rangle$ of ^{239}Pu. The obtained spread values are presented on Fig.1 as hystogram (dashed line). For ^{238}U the spread of $\langle\sigma_\gamma\rangle$ data is on the level of required uncertainty (except group 14). The spread for $\langle\sigma_t\rangle$ at high energies is also small. The spread of $\langle\sigma_f\rangle$ for ^{235}U by 1.5 - 2 times lees then achieved uncertainty. The picture for ^{235}U $\langle\sigma_t\rangle$ is simular to that for ^{238}U $\langle\sigma_t\rangle$. The characher of the spread resembling the energy dependence of fluctuation error. The spread of $\langle\sigma_\gamma\rangle$ data characterizes actually a real uncertainty. The trend of decreasing spread in comparison with real uncertainty is characteristic of $\langle\sigma_\gamma\rangle$ and $\langle\sigma_f\rangle$ for ^{239}Pu. It is evident that this trend can be explained by strong correlation of different evaluation and by shortage of independent new experimental data during last years.

REFERENCES

1. L.P.Abagjan, N.O.Bazazjants, M.N.Nikolaev, A.M.Tsybulja, Group Constants for Calculations of Reactors and Shielding, Moscow, Energoizdat, 1981.
2. A.A.Van'kov, C.Toshkov, V.F.Ukraintsev, N.Yaneva, Group Cons - tants and Resonance Selfshreaning Factors of ^{239}Pu, Voprosy Atomnoj Nauki i Tekhniki, Series "Yadernye Konstanty", 1983, issue 4(53), p.18.
3. A.A.Van'kov, L.S.Gosteva, V.F.Ukraintsev, The Analysis of Transmission Experiments for ^{238}U in Unresolved Resonance Region, Voprosy Atomnoj Nauki i Tekhniki, Series "Yadernye Konstsnty" 1983, issue 3(52), p.27.

4. Munoz Cobos I.L., G.de Saussure, R.B.Perez, Sensitivity of Computed ^{238} Self-shilding factors to the Choise of the Unre - solved Average Resonance Parameters, Nucl.Sci.Eng., 1982,vol 81, port 1, p.55.
5. G.V.Antsipov, V.A.Kon'shin, E.S.Sukhovitskij, Nuclear Constants for Plutonium Isotopes, Minsk, 1982, "Nauka i Tekhnika".

Contributed Paper 7

ACTIVITIES OF TRANSACTINIUM ISOTOPE NUCLEAR DATA AT THE CHINESE NUCLEAR DATA CENTRE (CNDC)

Zhang HUANQIAO
Institute of Atomic Energy,
Beijing, China

Abstract

Activities of the Chinese Nuclear Data Centre in the field of transactinium isotope nuclear data are presented, including lists of current TND evaluations and measurements performed in China.

I am very pleased to be here as the first Chinese representative to the IAEA Advisory Group Meeting on Transactinium Isotope Nuclear Data (TND). The meeting gives us an opportunity to share our experiences with each other and to discuss the further request on TND and to exchange some information of common interest. In order to improve our mutual understanding and further contact, please allow me to briefly introduce the activities on TND in the framework of the Chinese Nuclear Data Centre (CNDC).

CNDC was established at the Institute of Atomic Energy (IAE), Beijing, in 1975. Since then the activities on transactinium isotope nuclear data have been purposively and gradually developed. Up to now, we have evaluated complete sets of neutron data for $^{235,238}U$ and $^{239,240}Pu$ which are collected in "Evaluated Compilation of Neutron Data" (Vols. 1 and 2). In addition, evaluations of ν_p, α, σ_f, $\sigma_{n,\gamma}$, $\sigma_{n,2n}$, $\sigma_{n,3n}$, σ_{el}, σ_{inel}, $\frac{d\sigma s}{d\Omega}$, σ_t, σ_{non}, secondary neutron spectra, fission neutron spectra and related resonance parameters as well as fission product yields have been carried out for some transactinium nuclei. A survey of them is listed in Table 1.

Also the evaluation of nuclear data was fulfilled for some transactinium nuclei in 1981. For details, see "Decay Schemes of Commonly Used Radioactive Nuclides" (1981) in which the data for $^{228,232}Th$, ^{233}Pa, $^{232-240}U$, $^{236-246}Pu$, $^{236-241,236m,240m}Np$, $^{241-245,242m,244m,246m,g}Am$, $^{240-246}Cm$ and ^{252}Cf etc. are included. Parallel to the evaluation of TND, the theoretical studies of nuclear fission have been conducted at the CNDC. Calculations for TND have been performed using spherical and deformed optical model, statistical theory,

TABLE 1

Survey of Some TND Evaluation

Data Type	Nuclide	Neutron Energy
σ_f	$^{233-236,238}U$, ^{237}Np, $^{238-241}Pu$ $^{241,242,242m}Am$, ^{249}Bk, ^{249}Cf	1 keV - 20 MeV
υ_p	$^{233-236,238}U$, $^{239-241}Pu$, ^{252}Cf	10 keV - 15 MeV
$\sigma_{n,\gamma}$	$^{235,236,238}U$, ^{240}Pu	spontaneous fission
α	^{235}U, ^{239}Pu ^{238}U	1 keV - 1 MeV
$\sigma_{n,2n}$	^{238}U	6 - 18 MeV
$\sigma_{n,3n}$	$^{235,238}U$, $^{239,240}Pu$	1 keV - 20 MeV
σ_{el}, σ_{in}, $\frac{d\sigma}{d\Omega}$, N(E)		
$N_{in}(E)$	^{238}U	1 keV - 20 MeV
σ_t	$^{235,238}U$, $^{239,240}Pu$	1 keV - 20 MeV
σ_{non}	^{238}U, ^{239}Pu	1 keV - 20 MeV
Resonance Parameters	^{232}Th, $^{233,235,236,238}U$, $^{239-242}Pu$, $^{241,242m,243}Am$, $^{243-248}Cm$, ^{249}Bk, $^{249,252}Cf$	
Fission neutron spectrum	$^{235,238}U$, ^{239}Pu	
Delayed neutron absolute yields	^{232}Th, $^{233,235,238}U$, ^{239}Pu	
Fission product yields	^{232}Th, ^{233}Pa, $^{233-239}U$, ^{237}Np, $^{239-242}Pu$, $^{241-242m}Am$, ^{245}Cm, $^{249,251}Cf$, ^{254}Es, $^{255,257}Fm$	thermal neutron, fast reactor neutron, fission neutron, 14.8 MeV and 1 KeV - 15 MeV monoenergetic neutron
Decay data	$^{228,232}Th$, ^{233}Pa, $^{232-240}U$, $^{236-241,236m}Np$, ^{240m}Np, $^{236-246}Pu$, $^{241-245,242m,244,246m,g}Am$, $^{240-246}Cm$, ^{252}Cf	

exiton model and coupled channel theory. The investigation of semi-empirical systematics has been made for thermal neutron fission cross sections for transactinium nuclei. CNDC has also begun to collect and evaluate transplutonium nuclear data. We plan to evaluate fission product yields of evaluate fission product yields of transplutonium nuclei at first. For experimental data compilation, after analysing and evaluating, we have published a series of evaluation reports for the data which have been measured in a great number of experiments. CNDC has also carried out preliminary evaluations of data for which only a few experimental measurements are available. We made no formal publications of those preliminary evaluations.

Now I would like to give a brief account of TND measurements at the Institute of Atomic Energy (IAE) in recent years. Firstly, the fission cross section measurement program started in 1970. During the past 14 years the fission cross sections for several actinide nuclides, such as $^{233,235,238}U$, ^{237}Np and ^{239}Pu, have been measured in different neutron energy regions including thermal neutron, 0.03-1.5 MeV, 3-6 MeV and 14-18 MeV neutrons which are available at IAE. The relative measurement and the absolute measurements using the hydrogeneous proportional counter, the recoil telescope and the associated particle with time correlation technique have been developed. An accuracy of 2 % for absolute measurements has been achieved. The properties of the samples of the fissile material are listed in Table 2. The measurement results and the methods used are listed in Table 3.

As an example, the comparison of fission cross section for fast neutron induced fission of ^{239}Pu is shown in Fig. 1.

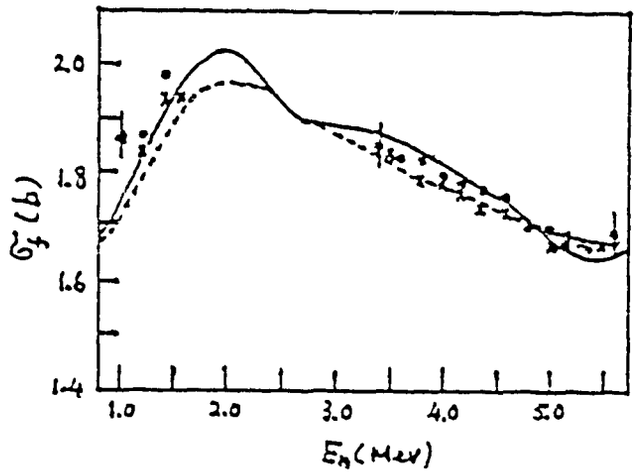

Fig. 1 ^{239}Pu fission cross section

ϕ This work _ _ _ ENDF/B-IV

x Kari _____ Liu's evaluation

TABLE 2

The Properties of the Samples of the Fissile Material

Nuclide	Diameter (Cm)	Weight (mg)	Quantity Error (%)	Error from Nonuniformity of sample (%)
^{233}U	2.60	~ 1.1	1.1	
^{235}U	2.60	~ 1.1	1-1.5	1.1
^{238}U	2.60	~ 1.0	1.0	
^{237}Np	2.60	~ 0.5	1.0	
^{239}Np	2.60	~ 1.0	1.0	1.2

TABLE 3

Some Measurement Results

Nuclide	E_n (MeV)	Measuring Method	Accuracy (%)
^{233}U	thermal neutron	relative to $^{235}U(n,f)$	2.1
	0.02-0.3 eV	relative to $^{6}Li(n,\alpha)^{4}He$	2.5-2.8
	0.5 and 1.0 MeV	hydrogeneous proportional counter	5
	0.03-2.5 MeV 3.5-5.6 MeV 14-18 MeV	relative to $^{235}U(n,f)$	2.4-2.8
^{235}U	0.0253 eV	relative to $^{10}B(n,\alpha)$	1.5
	0.02-0.3 eV	relative to $^{6}Li(n,\alpha)$	1.2-2.0
	0.5 and 1.0 MeV	hydrogeneous proportional counter	5
	14.7 MeV	associated particle with time correlation	2
^{238}U	3.5-5.5 MeV	recoil telescope	2.0-2.6
^{237}Np	3.5-5.5 MeV	recoil telescope	2.9-3.3
^{239}Pu	0.02-0.3 eV	relative to $^{6}Li(n,\alpha)$	2.5-2.8
	0.03-5.6 MeV	relative to $^{235}U(n,f)$	2.0-2.6
	14-18 MeV	relative to $^{235}U(n,f)$	2.0-2.6
	1.0-1.6 MeV 3.5-5.6 MeV	absolute measurement with recoil telescope	2.8
	14.7 MeV	associated particle with time correlation	2

Secondly, on the aspect of the measurements of the average number of prompt fission neutrons, a large Cd-loaded scintillation counter was constructed in 1967. Then we reconstructed the large Gd-loaded liquid scintillation counter in 1978. During the past 17 years, the average number of prompt neutrons and the multiplicity distribution of prompt neutrons emitted by spontaneous fission and fast neutron induced fission have been measured. The efficiency of the large liquid scintillation counter was calibrated on the basis of occurring n-p scattering as the collimated monochromatic fast neutron incident on the stilbene crystal, combined with Monte Carlo simulation method. Therefore, the accuracy achieved was 0.48 % for $\bar{\upsilon}_p$ absolute measurement. The $\bar{\upsilon}_p$-s for spontaneous fission of some transactinium nuclides are listed in Table 4.

TABLE 4

The $\bar{\upsilon}_p$ for Spontaneous Fission of Some Transactinium Nuclides

Nuclide	$\bar{\upsilon}_p \pm \Delta\bar{\upsilon}_p$	Reference	Measuring Method	Year
^{238}U	1.96 ± 0.05	$\bar{\upsilon}_p(^{240}Pu)=2.154$	Loaded-Cd liquid scintillation	1967
^{240}Pu	2.138 ± 0.034	absolute measurement	Loaded-Cd liquid scintillation	1972
^{240}Pu	2.141 ± 0.016	$\bar{\upsilon}_p(^{252}Cf)=3.743$	Loaded-Gd liquid scintillation	1980
^{242}Cm	2.562 ± 0.020	$\bar{\upsilon}_p(^{252}Cf)=3.743$	Loaded-Gd liquid scintillation	1980
^{244}Cm	2.721 ± 0.021	$\bar{\upsilon}_p(^{252}Cf)=3.743$	Loaded-Gd liquid scintillation	1980
^{252}Cf	3.743 ± 0.018	absolute measurement	Loaded-Gd liquid scintillation	1979

The dependence of $\bar{\upsilon}_p$ for $^{235,238}U$ and ^{239}Pu at fast neutron energies has been measured at Van de Graff accelerator. The results are listed in Table 5.

TABLE 5

$\bar{\upsilon}_p(E_n)$ for Fast Neutron Induced Fission of $^{235,238}U$ and ^{239}Pu

Nuclide	Energy Range (MeV)	Error (%)	Reference	Year
^{235}U	0.1-1.6	1.5-2	$\bar{\upsilon}_p(^{240}Pu)=2.151$	1973
^{238}U	1.2-5.5	1.5-2	$\bar{\upsilon}_p(^{240}Pu)=2.151$	1973
^{239}Pu	0.1-1.5	0.8	absolute measurement	1978

For example, the comparison of $\bar{\nu}_p(E_n)$ for fast neutron induced fission of ^{238}U is shown in Fig. 2.

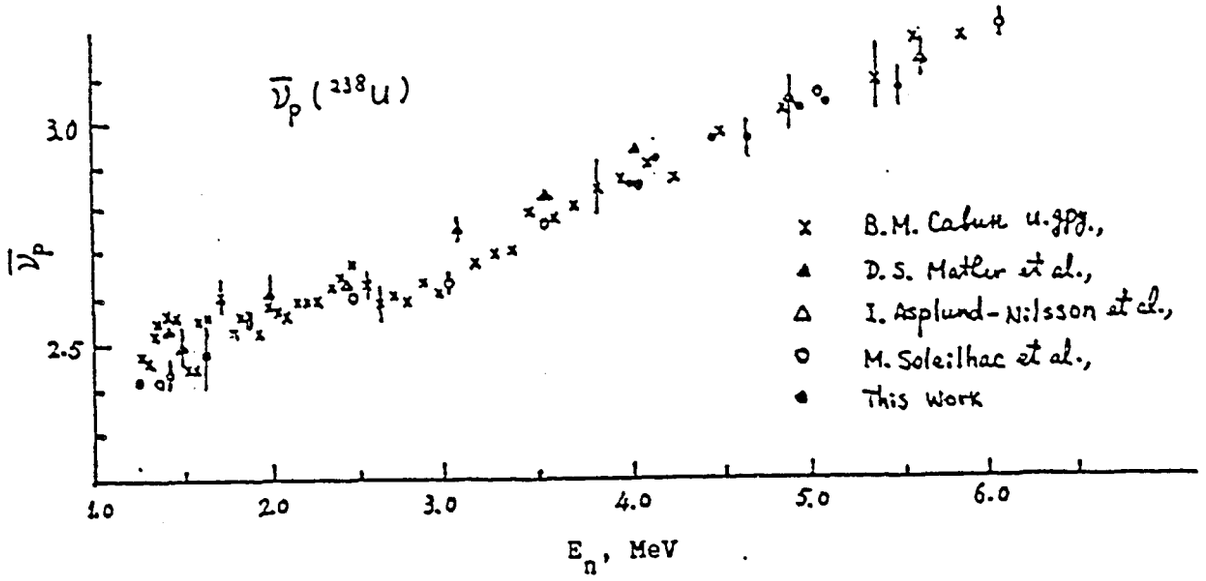

Fig. 2

During late 1950's, neutron energy spectra for thermal neutron induced fission of ^{235}U and ^{239}Pu were measured by means of emulsions. In 1980, the prompt neutron energy spectrum from ^{252}Cf spontaneous fission was measured in the energy range 0.45-15 MeV using the time-of-flight technique.

TABLE 6

The Results of Fission Neutron Spectra

Nuclide	Fission Mode	N(E)	E(MeV)
^{235}U	thermal neutron	const sh. $\sqrt{2.30E}e^{-E/0.96}$	1.867 ± 0.015
^{239}Pu	thermal neutron	const sh. $\sqrt{1.65E}e^{-E/1.10}$	1.989 ± 0.024
^{252}Cf	spontaneous fission	const. $\sqrt{E}\, e^{-E/kT}$	2.124 ± 0.035

In addition, neutron scattering cross sections, angular distributions and secondary neutron spectra for the interaction of 14.7 MeV neutron with ^{238}U have been measured by means of time-of-flight. Those data are still being analyzed. Finally, it should be noted that a set of precise reference data on TND has been obtained at IAE, including $\sigma_f(^{235}U)$, $\bar{\nu}_p(^{252}Cf)$ and ^{252}Cf spontaneous fussion neutron spectrum.

In recent years, half-life measurements have experimentally been carried out for a few transactinium nuclides. The half-life of spontaneous fission of ^{238}U was measured by a large volume multiplated ionization chamber as well as by mica detectors. The masses of the uranium deposits were determined by measuring the alpha activity with a 2π ionization chamber. The accuracy of the deposit mass measurements is about 2 %. The result with the multiplated ionziation chamber is $T_{1/2}(SF)=(8.03 \pm 0.23)10^{15}$ years. But the result from mica detector is $T_{1/2}(SF)=(8.81 \pm 0.33)10^{15}$yr. In view of the importance of the spontaneous fission half-life of ^{238}U and the large divergence of this value obtained by different authors, we compiled the experimental data of $T_{1/2}(SF)(^{238}U)$ which has been published before 1977 and recommended the evaluated value $T_{1/2}(SF)=(8.19 \pm 0.15)10^{15}$ yr.

Alpha activities of ^{242}Cm have been measured by a low geometry device with a silicon surface barrier detector. The α-decay of ^{242}Cm has been followed for 309 days. The α-decay half-life for ^{242}Cm has been obtained $T_\alpha=(163.02 \pm 0.11)$ days. The method of specific activity was used to determine the half-life of the spontaneous fission of ^{242}Cm. The mass of ^{242}Cm deposit was determined by measuring the alpha activity with a low geometry device. The half-life of ^{242}Cm spontaneous fission obtained is $T_{1/2}(SF)=(7.46 \pm 0.06)\times10^{6}$ yr. The comparisons of $T_\alpha(^{242}Cm)$ and $T_{1/2}(SF)(^{242}Cm)$ with that of authors are listed in Tables 7 and 8, respectively.

TABLE 7

The Comparison of α-Decay Half-life of ^{242}Cm

Author	Year	$T_{1/2}$ (days)	Method	Measuring device
Hanna	1950	162.5 ± 2	follow (0.8-2.2)T_α	a low geometry device
Glover et al	1954	162.46 ± 0.14	follow 1.4 T_α	a low geometry device
Treiman	1957	162.7 ± 0.1	calorimetry	calorimeter
Flynn	1965	163.1 ± 0.4	follow 7.3 T_α	2π proportional counter with flowing gas
Kerrigan	1975	163.2. ± 0.2	calorimetry	calorimeter
Diamond	1977	162.76 ± 0.04	follow 1.6 T_α	proportional counter with mid-geometry
Ours	1977	163.02 ± 0.11	follow 1.9 T_α	a low geometry device with Si(Au) detector

TABLE 8

The Comparison of Spontaneous Fission Half-life of ^{242}Cm

Author	Year	$T_{1/2}(SF)(v)$	Measuring method
Hanna	1951	$(7.2 \pm 0.2)10^6$	Ionization chamber detected fragments
Armani	1967	$(6.09 \pm 0.18)10^6$	Detected fission neutrons
Ours	1977	$(7.46 \pm 0.06)10^6$	Mica detected fission fragments

So much for the brief review of the activities on TND in CNDC. We are capable of extensively measuring fission cross section, neutron radiation, capture cross section, secondary neutron spectrum, fission product yield and transactinium isotope nuclear decay data, etc. In nuclear data evaluation, we hope to make systematical evaluations for transactinium isotope nuclear data, e.g., transplutonium nuclear data, TND decay data and fission product yields etc. We would like to develop further contact and international cooperation with the IAEA.

Contributed Paper S

ABSOLUTE MEASUREMENTS OF ^{235}U AND ^{239}Pu FISSION CROSS SECTION INDUCED BY 14.7 MeV NEUTRONS

Li JINGWEN, Li ANLI, Rong CHAOFAN, Ye ZHONGYUAN
Wu JINGXIA, Hao XIUHONG
Institute of Atomic Energy, Academia Sinica,
Beijing, China

The cross section of uranium-235 and plutonium-239 fission induced by 14.7 MeV neutrons were measured using associated particle method with time correlation technique. The results obtained are 2.098±0.040 b and 2.532±0.050 b for U-235 and Pu-239 respectively. Comparison with data of other authors is also given.

[$^{235}U(n,f)$, $^{239}Pu(n,f)$, fission cross sections, E_n=14.7 MeV, nuclear data.]

Introduction

The values of fission cross sections for neutron energies in the vicinity of 14 MeV are of significant importance in nuclear energy application. They are usually used as normalization values in the relative measurement of cross sections, so the accuracy needed is higher than that of other energy region. In fact, though, the results from different laboratories do not agree with each other. For instance, White[1] gave the value 2.17±0.04 b for U-235 fission at 14.1 MeV, but at 14.6 MeV, the data of 2.075±0.040 b and 2.063 ± 0.039 b were provided by Czirr[2] and Cance[3] respectively. The latter two values are about 5 % lower than the former one. The situation for σ_f of Pu-239 is similar. In order to eliminate the discrepancy mentioned above more careful experimental determinations are needed. We have measured the σ_f of U-235 and Pu-239 using associated particle method.

Experimental Arrangement

Fig.1 shows the device and the block diagram of electronic circuits used in our experiment.

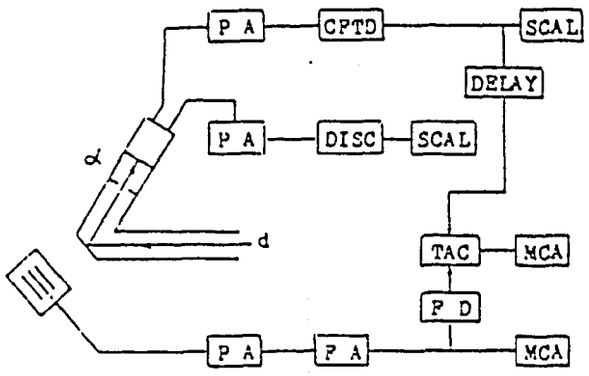

Fig.1. Experimental arrangement

Neutron Source. Neutrons with energy 14.7 MeV were produced by $T(d,n)^4He$ reaction on the 600 kV Kockcroft-Walton accelerator in IAE. The incident energy of deuteron beam was 220 keV. The recoil angle of ^4He particle was selected as 135°. In the direction of 40° with respect to the deuteron beam the corelated neutrons of 14.7 MeV were obtained.

Fission Chamber. The fission ionization chamber was a cylindrical one 100 mm in diameter 50 mm in length, which was composed of two identical halves. The incident direction of correlated neutron beam was along the axis of the chamber. The chamber was filled with methan gas of one atmosphere. The fast current collection was adopted.

Samples. The sample of uranium and plutonium were electrodeposited on platinum backings. The diameter of the deposited fissile material layer was 26 mm. Three methods were used to determine the quantity of uranium contained in the samples by direct weighing, by alpha counting in a low solid angle equipment and by titration. For plutonium the alpha counting technique and the constant current Coulomb method were used. The details of preparation and quantitative analysis determination of samples had been described elsewhere[4,5]. The nonuniformity of the deposited layer was tested in following way: A small diaphragm was placed in front of the sample and the alpha particles were counted using a silicon detector of surface barrier type.

Measurement

The alpha particles produced in reaction $T(d,n)^4He$ were detected by a thin film scintillation counter consisted of a 100 μm thick plastic scintillation film and a fast photomultiplier of 56/DVP/03A type. The resolution time of the output alpha signal was smaller than 2 ns. Alpha detector was placed in the direction 135° with respect to the incident deuteron beam. The fission chamber was located 5 cm away from the T-Ti target at the correlated direction. This ensured that all the associated neutrons were strike on the U or Pu sample. The courting rate of alpha particles was restricted within 10^4 to 10^5/s through whole process of measurement. In order to determine the correct position of the neutron beam correlated with the 135° alpha particles we have used a small plastic scintillator as a neutron detector scanning along the horizontal and verticle directions to measure the coincidence rate with alpha particles.

The fission fragment pulses after discremination was fed to the time-to-amplitude converter (TAC) as its start signal. The duration of the TAC gate was 200 ns. The alpha particle pulses were fed into a constant fraction timing discriminator (CFTD) which gave a narrow output pulse used as stop signal for TAC after a delay of 100 ns. The output signals of the TAC were recorded in a multichannel analyzer directly. In Fig.2 a typical time distribution of fission pulses was shown. It can be seen that by use of TAC the correlated events were separated clearly from the background. As for the background, one may notice that the average counting number per channel in the left side of the coincident peak is higher slightly than that in the right side region from the peak. This effect was caused by two facts, one was that the collecting time of electrons produced by fission fragments in ionization gas reveals a distribution which has rather long tail, the other was that in some cases the TAC, after being started by the fragment pulse, might be erroneously stopped due to a uncorrelated alpha pulse which preceded the right correlated one. So we take the average number of counts per channel in the righthand region with respect to the peak as the background counts per channel.

The main advantage of the associated particle method is that the neutron fluence could be determined directly and precisely. The inter-

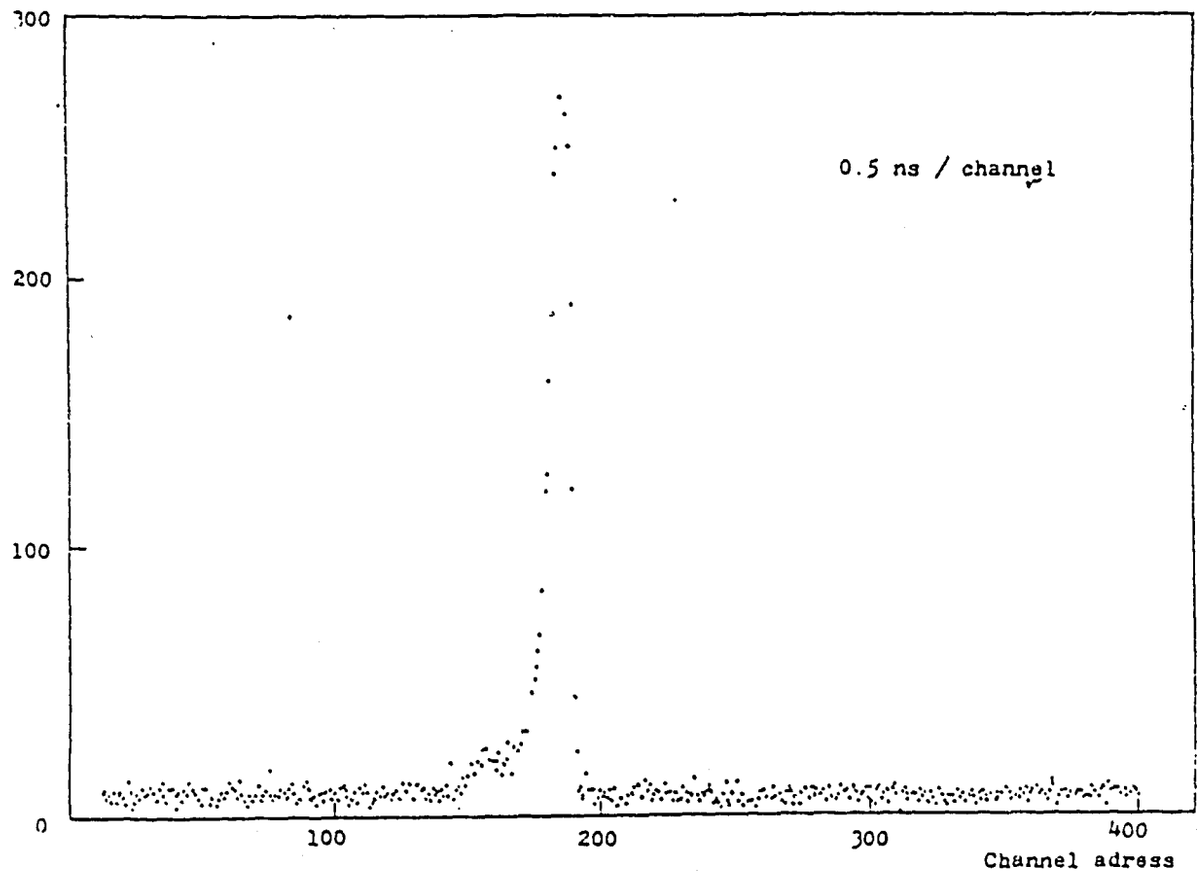

Fig. 2. Typical time distribution of fission pulses.

ference of all background fission events induced by scattered neutrons, by slowing down neutrons and by the neutrons from $D(d,n)^3He$ reaction as well as the false fission events due to alpha pile up were greatly supressed. Backgrounds of different origins could be subtracted directly in the time distribution. In calculating σ_f the detail knowledge of the solid angle and the other geometric factors were no longer needed.

The protons from the parasitic reaction D(d,p)T may produce pulses higher than the alpha's in the plastic scintillator. We used a seperate discriminator with the threshold higher than the endpoint of alpha pulse distribution to record these protons simultaneously and then subtracted from the total alpha counts. In order to reduce the yield of these protons the target used in the experiment was changed with new one every time if the proton yield exceed 1 % of the alpha's.

Corrections and Uncertainties

1. There are two factors which would reduce the efficiency of fission detector. The first effect is that the pulse height of some fragments outgoing from the sample layer would be lower than the setting threshold of the discriminator. The fraction of these events may be obtained by extrapolating the amplitude distribution of fragment pulses to zero threshold. The second effect is the self absorption of fragments in the sample layer. In the mean time it is necessary to take into account the absorption variation due to the momentum brought in by the incident neutrons and due to the anisotropic angular distribution of fission fragments.

2. The attenuation of neutrons

The target backing, water layer for cooling the target, the cadmium cover in front of the fission chamber, the front window of the chamber and the backings of the samples--all these caused some attenuation of neutron beam striking on the fissile layer. This correction was calculated according to transmission consideration. The amount resulted was 2.68 %.

3. Fission events due to the other isotopes contained in the sample such as ^{234}U, ^{238}U, ^{240}Pu, and ^{241}Pu were calculated directly according to the isotope composition shown in Table I. The contribution was 5.92 % and 3.00 % for U-235 and Pu-239 respectively.

Table I. Isotope composition of samples

Uranium	234	235	238
	1.0 0.1	90.5 0.9	8.5 0.8
Plutonium	239	240	241
	96.9 0.8	3.0 0.5	0.1 0.1

Results and Discussion

From our experiment it was obtained that the σ_f of U-235 induced by 14.7 MeV neutrons was equal to 2.098±0.040 b. Our result was in agreement with those of Czirr[2], Cance[3] and Alhazov[6] within standard error. As for the σ_f of Pu-239, the present result was equal to 2.532±0.050 b at 14.7 MeV.

The ratio of the σ_f(Pu-239) to σ_f(U-235) in present work was equal to 1.207 which agrees well with the previous result 1.196 obtained in a relative cross section measurement of our laboratory[5].

As for the compiled data, the ENDF/B-IV gave the values 2.218 b and 2.552 b for U-235 and Pu-239 respectively, but the ENDF/B-V gave the U-235 σ_f value 2.101 b which is in good agreement with present result.

References

1. P.H.White, J.Nucl.Energy A/B, 19,325(1965).
2. J.B.Czirr et al , Nucl. Sci. Eng.,57,18 (1975).
3. M.Cance et al., Nucl. Sci. Eng., 68,197 (1978).
4. Yan Wuguang et al., Keiji,No.2,133 (1975).
5. Den Xinlu et al., Keiji,No.1,12 (1981).
6. I.D Alhazov et al., Atomnaja energia, 47, 416 (1979).

Contributed Paper 9

COMPILATION OF ACTINIDE NEUTRON NUCLEAR DATA

Part A: Experimental and evaluated cross sections

Part B: Evaluated group cross sections

P. ANDERSSON
Department of Nuclear Physics,
Lund Institute of Technology,
Lund

H. CONDÉ
Gustaf Werner Institute,
Uppsala

Sweden

C. NORDBORG
OECD/NEA Data Bank,
Gif-sur-Yvette

B. TROSTELL
The Studsvik Science Research Laboratory,
Nyköping, Sweden

Abstract

This paper describes the content of the Swedish compilation of actinide neutron nuclear data which was initiated by the Swedish Nuclear Data Committee, and sponsored by the Swedish Nuclear Power Inspectorate. The compilation, published in report form, presents available neutron cross section data to allow comparison between evaluated and experimental data.

1. INTRODUCTION

The Swedish Nuclear Data Committee has initiated a compilation of a selected set of neutron cross section data for the most important actinide isotopes. The compilation work has been done by a working group sponsored by the Swedish Nuclear Power Inspectorate. The main part of the data information has been obtained from the OECD/NEA Data Bank at Saclay, France.

The aim of the report is to present available neutron cross section data in a comprehensible way to allow a comparison between different evaluated libraries and to judge about the reliability of these libraries from the experimental data.

The first result of the compilation was reported in 1979 (1). Since that time the compilation has been updated and further isotopes have been added. It now consists of 24 isotopes ranging from ^{232}Th to ^{252}Cf (KDK-75, Part A). Furthermore, in place of the resonance integrals reported in KDK-35 the compilation now includes group cross sections of the main evaluated data files for each of the 24 isotopes (KDK-75, Part B).

Part A of the compilation consists of experimental and evaluated neutron cross section data in the neutron energy regions from 10^{-4} to 1 eV and from 10 keV to 20 MeV. The reported data are the total, capture and fission cross sections for ^{232}Th, ^{233,235,238}U, ^{237}Np, $^{239-242}$Pu, $^{241-243}$Am, $^{242-248}$Cm, ^{249}Bk, $^{249-252}$Cf, furthermore the elastic cross sections for ^{235,238}U and ^{239}Pu, the neutron inelastic and (n,2n) cross sections for ^{238}U and the $\bar{\nu}$-values of ^{232}Th, ^{233,235,238}U and ^{239}Pu. Evaluated data are from the last available versions of the main libraries i.e. versions IV and V of the U.S. Evaluated Neutron Data File part B (ENDF/B), the 1982 version of the Lawrence Livermore Laboratory Evaluated Neutron Data Library (ENDL), the 1981 version of the U.K. Neutron Data Library (UKNDL), the version 4 of Karlsruhe Evaluated Data File (KEDAK) and version 2 of the Japanese Evaluated Data Library (JENDL). Furthermore, recent versions of $^{239-242}$Pu evaluations from A.V.Lykov Institute of Thermal and Mass Exchange Byelorussian SSR Academy of Sciences, Minsk, USSR (ITMO) and a ^{232}Th evaluation from the IAEA/NDS International Neutron Data Library (INDL) are also given.

The experimental data are taken from the "International Library of Nuclear Experimental Information" (EXFOR) and from recent publications. A representative subset of the most recent information is included.

The data information is stored in a computer by which drawings could be made of selected subsets of the information in an interactive manner. In preparing the figures in the report a compromise had often to be done between the magnification necessary to avoid too much overlap between different data sets and the number of pages that could be accepted.

Part B of the compilation gives the total, elastic, capture and fission group cross sections for the same isotopes as in Part A. The CSEWG 239 group structure (2) was chosen which gives a reasonable detailed information for a comparison of different data libraries. The flat weighted cross sections averaged over the group structure from any evaluated file formal

was calculated with the program HENRI (3). A computerized plotting of the group cross sections was made by Studsvik Data, Studsvik Energiteknik AB.

The authors wish to acknowledge L. Björklund, FOA and G. Olsson, Studsvik Data for helping with the computer plottings and Ch. Spolén for typing the manuscript.

References

1. Compilation of Actinide Neutron Nuclear Data, Swedish Nuclear Data Committee Report, KDK-35 (NEANDC(OR) 153/L, INDC(SWD) 13L, SKI B32/78), 1979

2. Specification of a Generally Useful Multigroup Structure for Neutron Transport, Los Alamos Scientific Laboratory Report LA-5277-MS

3. Nordborg C.
HENRI - a computer program for calculation of average cross sections in the resonance region of evaluated files.

2.1 LIST OF EVALUATED AND EXPERIMENTAL DATA LIBRARIES

ENDF/B: Evaluated Nuclear Data File, Version B, National Neutron Cross Section Center, Brookhaven National Laboratory, Upton, New York 11973

UKNDL: United Kingdom Atomic Energy Authority Nuclear Data Library

ENDL: Lawrence Livermore Laboratory Evaluated Nuclear Data Library, Lawrence Livermore Laboratory, University of California, Livermore, California 94550

KEDAK: Karlsruhe Evaluated Nuclear Data Library, Kernforschungs-zentrum Karlsruhe, Karlsruhe, Germany

JENDL: Japanese Evaluated Neutron Data Library, Japan Atomic Energy Research Institute, Tokai, Ibaraki, Japan

ITMO: A.V. Lykov Institute of Thermal and Mass Exchange Byelorussian SSR Academy of Sciences, Minsk, USSR

INDL/A International Nuclear Data Library for the Actinides, Nuclear Data Section, IAEA, Vienna

EXFOR: Computerized system of codes and formats used for the exchange of experimental neutron nuclear data between the Four Neutron Data Centres

BNL 325: Neutron Cross Section Analysis Report, National Neutron Cross Section Center, Brookhaven National Laboratory, Upton New York 11973

Contributed Paper 10

NUCLEAR DATA FOR ^{235}U, ^{238}U AND ^{239}Pu IN THE UNRESOLVED RESONANCE REGION

N. JANEVA
Institute for Nuclear Research and Nuclear Energy,
Sofia, Bulgaria

Abstract

The evaluation of nuclear constants for the heavy isotopes ^{235}U, ^{238}U and ^{239}Pu in the unresolved resonance energy region is described. Experimental data was analyzed using the R-matrix formalism, group constants were obtained using the probability table method.

This presentation has to be considered as a brief review of the activity performed in co-operation between our group from the Institute for Nuclear Research and Nuclear Energy (Sofia, Bulgaria) and Dr. Vankov's group from the Institute of Physics and Power Engineering (Obninsk, USSR). We are developing an approach for creation of nuclear data banks, based on the whole primary set of microscopic experimental information and the advanced nuclear theories for evaluation of the self-consistent nuclear constants.

Our particular case concerns the evaluation of nuclear constants for heavy isotopes in the unresolved resonance region. We have analyzed the data for the major actinides - ^{235}U, ^{238}U and ^{239}Pu. There are some new points distinguishing this work from the similar ones:

a) The transmission T(n) and self-indication in fission $T_f(n)$ were measured by significant variations of the samples' thicknesses n and analyzed simultaneously with the average neutron cross sections in the unresolved resonance region. For the analysis, the R-matrix formalism (in the Reich-Moore approximation) has been applied. The new algorithms for the

use of Monte Carlo technique in such a case have been developed.

b) The evaluation has been done by consistent statistical method with the help of a priori information on the average resonance parameters. The better accuracy in the self-shielding resonance factors was achieved due to the complementary experimental information on transmission functions.

c) In the generation of the group constants, the use of probability table method gives some advantages by our procedure.

d) The new evaluation of the average resonance parameters and the group constants (average neutron cross sections, self-shielding factors, etc.) for ^{238}U, ^{235}U, ^{239}Pu have been obtained.

Experimental part

The measurements were carried out in the unresolved resonance region $E_n < 50$ keV for ^{238}U, $E_n < 20$ keV for ^{235}U and ^{239}Pu by the time-of-flight method on the pulsed neutron source IBR-30 in Dubna. Its repetition rate and pulse widths are 5 Hz, 90 μS and 100 Hz, 4 μS in reactor mode and linear accelerator mode, respectively. In the measurements of the transmission T(n) for ^{238}U, ^{235}U and ^{239}Pu a battery of ^{3}He-proportional counters was used/1/, while high-efficiency fission chambers containing the fission material (2g of ^{235}U and 0.6 g of ^{239}Pu)/2/ were used in the self-indication $T_f(n)$ measurements for ^{235}U and ^{239}Pu. Disc metallic samples having well-known characteristics were placed almost equidistantly from the source and detector, so that good geometry conditions were fulfilled. The samples of ^{238}U had diameters of 160 mm and 200 mm, the fission samples (^{235}U and ^{239}Pu) were of diameters 50 mm.

All possible sources of background have been studied very carefully in our experiment: detector's self-background, scat-

tered neutrons in the experimental area, neutrons from the beam. In these measurements, the background in the neutron beam being significant was controlled by means of resonance filters of Ti, Na, Mn. The measured fraction of the background in the open beam was 6 - 12% and increased with the sample thickness. In applying resonance filter method, a correction was made for neutron spectrum attenuation, due to the final value of the macroscopic cross section of the resonance filters in the region between the resonances.

We measured the transmission of neutron:

$$T(n) = \int_{\Delta E_n} \varphi(E_n)\,\varepsilon(E_n)\exp\left[-\sigma_t(E_n)\cdot n\right] dE_n \Big/ \int_{\Delta E_n} \varphi(E_n)\,\varepsilon(E_n)\,dE_n \qquad (1)$$

and self-indication in fission:

$$T_f(n) = \int_{\Delta E_n} \varphi(E_n)\,\sigma_f(E_n)\exp\left[-\sigma_t(E_n)\cdot n\right] dE_n \Big/ \int_{\Delta E_n} \varphi(E_n)\,\sigma_f(E_n)\,dE_n . \qquad (2)$$

Here $\varphi(E_n)$ is the neutron flux, $\varepsilon(E_n)$ - the detector efficiency, $\sigma_t(E_n)$ and $\sigma_f(E_n)$ - total and fission cross section, n - the sample thickness.

Calculational method

We developed a multilevel method for calculation of the average neutron cross section in the energy region of unresolved resonances. Following /3/ we chose the well known Reich-Moore approximation in which the R-matrix elements for a state with a given momentum and parity are:

$$R_{cc'} = \sum \frac{\gamma_{\lambda c}\,\gamma_{\lambda c'}}{E_\lambda - E - i\,\bar{\Gamma}_\gamma/2}, \qquad (3)$$

where $\gamma_{\lambda c}$ is the reduced width amplitude in a channel with a set of quantum members "c", E_λ is the resonance energy, $\bar{\Gamma}_\gamma$ - the average resonance width.

We used the well known relation between the collision matrix S and the K-matrix

$$S = \Omega(1+iK)(1-iK)^{-1}\Omega \qquad (4)$$

Ω - is a diagonal matrix with elements $\Omega_c = \exp(-i\varphi_c)$, φ_c -

the phase shift. The K-matrix elements are given by:

$$K_{cc'} = \frac{1}{2} \frac{\bar{\Gamma}_c^{1/2} \bar{\Gamma}_{c'}^{1/2}}{\bar{D}} \sum_{\lambda} \frac{\beta_{\lambda c} \beta_{\lambda c'}}{\frac{E_\lambda - E}{\bar{D}} - \frac{i \bar{\Gamma}_\lambda}{2\bar{D}}} \qquad (5)$$

$\Gamma_{\lambda c}$ - are partial widths, $\bar{D}$ is the average level spacing

$\beta_{\lambda c}$ are random numbers obeying normal distribution law (0.1)

$\frac{E_\lambda - E_{\lambda-1}}{\bar{D}}$ are random numbers obeying Vigner distribution law (0.1).

The neutron cross sections are expressed by:

$$\begin{aligned}
\sigma_t &= 2\pi\lambda^2 \sum_{J,\pi} g(J) \sum_{\ell,j} \left(1 - \mathrm{Re}\, S^{J\pi}_{n\ell j, n\ell j}\right), \\
\sigma_f &= \pi\lambda^2 \sum_{J,\pi} g(J) \sum_{\ell,j} \left| S^{J\pi}_{n\ell j, f\ell j} \right|^2, \\
\sigma_{el} &= \pi\lambda^2 \sum_{J,\pi} g(J) \sum_{\ell,j} \left| 1 - S_{n\ell j, n\ell j} \right|^2,
\end{aligned} \qquad (6)$$

J^π denotes the total moment and the parity of the compound nucleons, $j = |\ell + s|$.

In the energy region in question, the contribution of the S and p neutrons is accounted for. The parameters Γ_n and φ_ℓ, which depend on l, are expressed as usual:

$$\begin{aligned}
\varphi_0 &= R_0/\lambda, \\
\varphi_1 &= R_1/\lambda - \mathrm{arc\,tg}\,(R_1/\lambda), \\
\Gamma_n\,(\ell=0) &= \Gamma^0_{n0} \sqrt{E}\, v_0, \\
\Gamma_n\,(\ell=1) &= \Gamma^0_{n1} \sqrt{E}\, v_1.
\end{aligned} \qquad (7)$$

v_0, v_1 are the penetrative coefficients for the S and p neutrons, R_0, R_1 - the scattering radii of the s- and p-neutrons which are supposed to be equal.

We used the presented multilevel formalism for calculating the average functionals of cross sections (transmission, average cross sections, self-shielding factors, etc.) by stochastic modelling of the neutron cross sections resonance structure[4]. The Monte Carlo technique is applied for simulating the multiple "emissions" of neutrons at the points of a uniform lethargic set

with steps of Δu in a wide range ΔU (e.g., Δu = 5 meV, ΔU = 100 eV). The neutron resonance picture of each J^{π} state is generated according to the statistical laws for resonance parameters in the 10-level approximation and the K-matrix of rank 3. The resulting cross section is obtained by summation of the respective cross sections of all states over momentum and parity. The procedure of the cross sections Doppler broadening lies in the sequential multiple neutron emission from points u with a transmission to point u' because of the random Doppler shift. In this way the cross sections $\bar{\sigma}_x(u_i, T_x)$ are evaluated in all the points for a set of temperatures T_x (the mean is taken over the Doppler broadening function).

The transmission functions can be presented as:

$$T_n = \int_0^{\infty} exp(-\sigma_t \cdot n) \cdot p(\sigma_t)\, d\sigma_t ,$$
$$T_f = \int_0^{\infty} \frac{\sigma_f(\sigma_t)}{\langle \sigma_f \rangle} exp(-\sigma_t \cdot n) \cdot p(\sigma_t)\, d\sigma_t . \qquad (8)$$

The cross section distribution functions $p(\sigma_t)$ and $\sigma_f(\sigma_t)$ describe the full information about the structure of neutron cross sections and their correlations. These functions can be calculated on the basis of evaluated average resonance parameters. Having at disposal $p(\sigma_t)$ and $\sigma_f(\sigma_t)$, it is easy to calculate any functional $\langle F(\sigma_t, \sigma_f) \rangle$

$$\langle F(\sigma_t, \sigma_f) \rangle = \int_0^{\infty} F[\sigma_t, \sigma_f(\sigma_t)]\, p(\sigma_t)\, d\sigma_t . \qquad (9)$$

The evaluation of the neutron cross sections model parameters has been performed in the frame of the Gaussian approach (i.e. with the help of a priori information)[5].

Results

Data on ^{238}U.

In the optimization procedure, our averaged experimental data for the transmission T(n) have been used in the 10-13th group (here and after the group boundaries are considered in the sense

of ABBN library[6]). We assumed that all the average resonance parameters have a priori uncertainty of 15%. In Table 1 a posteriori evaluation of the average resonance parameters is presented.

Table 1

Evaluation of the ^{238}U average resonance parameters

Parameter	$S_0 \cdot 10^4$	$S_1 \cdot 10^4$	R' fm	$\bar{D}$ eV
Value	1.14	2.07	9.13(10,11gr) 9.28(12,13gr)	2.16
Uncertainty %	6	10	1.5	12

For better description of the experimental values we had to assume the energy dependence of the scattering radius R'. The groups of averaged cross sections and self-shielding factors are presented on tables 2 and 3 respectively.

Table 2

Group cross sections

Group Number	σ_f barn	σ_t barn	$\delta\sigma_t$ %
10	0.444	13.9	2.3
11	0.630	15.1	2.8
12	0.882	17.0	3.9
13	1.23	19.5	4.4

Table 3

Self-shielding factors of ^{238}U

Group Number	$f_t(10)$	$\delta f_t(10)$ %	$f_t(100)$	$\delta f_t(100)$ %	$f_\delta(10)$	$\delta f_\delta(10)$ %	$f_\delta(100)$	$\delta f_\delta(100)$ %
10	0.873	1.8	0.963	0.5	0.930	0.8	0.963	0.2
11	0.778	2.9	0.912	1.2	0.865	1.5	0.961	0.5
12	0.683	4.7	0.837	2.9	0.715	1.9	0.910	0.7
13	0.575	5.7	0.721	3.7	0.586	2.2	0.803	1.2

^{235}U data[9]

Our experimental data on T(n) and $T_f(n)$ were analyzed together with the ENDF/B-V data on the average ^{235}U cross section in the unresolved resonance region [7,8]. The results are shown in Fig. 1. The data of Czirr[10] are also drawn which agree sufficiently well with our data. The optimization results are presented in tables 4 and 5.

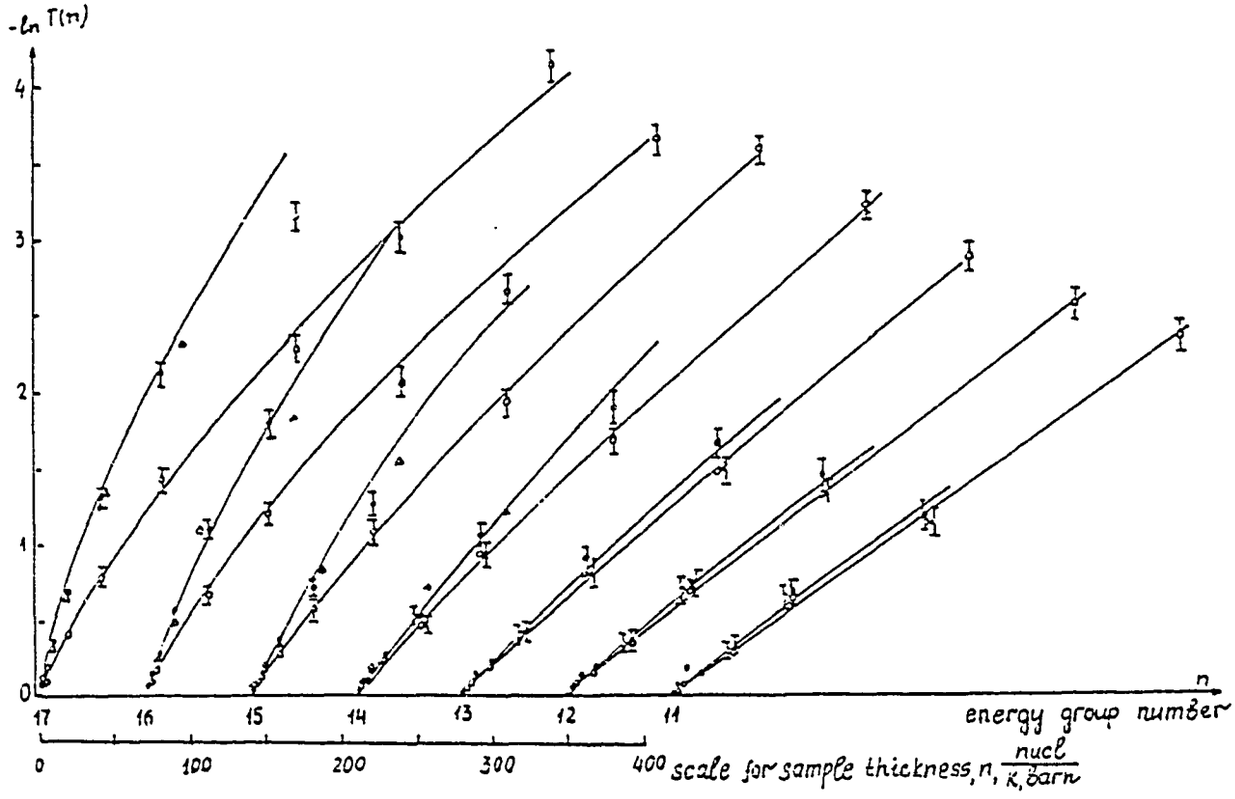

Fig. 1 Transmission T(n) and self-indication $T_f(n)$ for ^{235}U

- ◇ T(n) - experimental data [9]
- ● $T_f(n)$ - experimental data [9]
- △ $T_f(n)$ - averaged data of [10]

Table 4

Evaluation of the average ^{235}U resonance parameters

J^π	$\bar{D}$ eV	$\bar{\Gamma}_\gamma$ meV	$S_n.10^4$	$\bar{\Gamma}_f$ eV	f_1	f_2
3^-	0.967	30	var	var	0.5	0.5
4^-	0.801	30	var	var	0.5	0.5
2^+	1.256	30	1.677	0.486	0.5	0.5
3^+	0.967	30	1.677	0.165	1	0
4^+	0.801	30	1.677	0.322	0.5	0.5
5^+	0.770	30	1.677	0.130	1	0

var - parameters depending on energy

$f_1 f_2$ - relative contributions of both fission channels

Table 5

Evaluation of the ^{235}U average resonance parameters depending on energy

Group Number	R' fm	$S_0.10^4$	$\bar{\Gamma}_f$ (l=0) meV
11	9.1	1.05	153
12	9.2	0.964	170
13	9.2	0.901	293
14	9.2	0.910	170
15	9.2	1.05	176
16	9.2	0.940	144
17	9.5	0.950	120

It has been assumed $\bar{\Gamma}_f^{3^-} = \bar{\Gamma}_f^{4^-}$.

The uncertainty of S_0 is 5-10%, the a posteriori precision of R' is about 1.5%, but in the optimization S' is presized slightly.

Data on ^{239}Pu[11]

The analysis of experimental data on T(n) and $T_f(n)$ has been performed together with the data for the average cross section σ_f and σ_γ [6]. The results are drawn on Fig. 2 (there

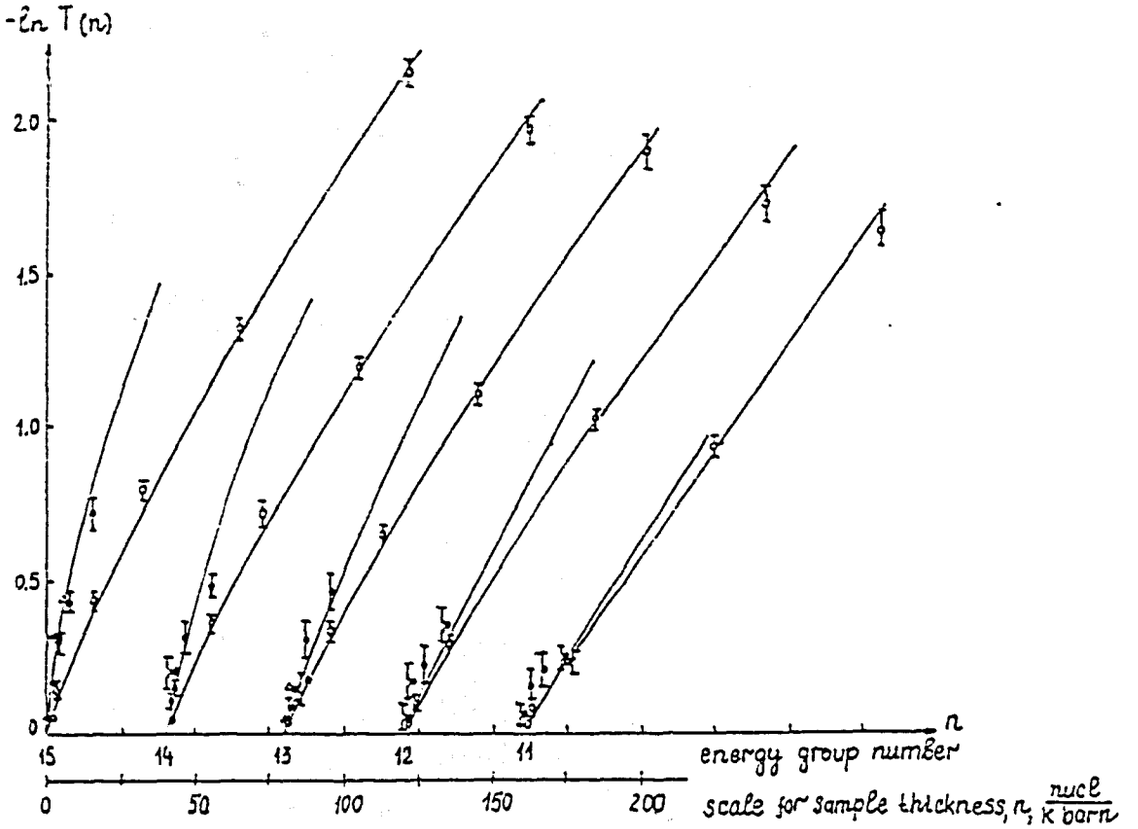

Fig. 2. Transmission T(n) and self-indication $T_f(n)$ for ^{239}Pu

- $\bar{T}(n)$ - experimental data[11]
- $\bar{T}_f(n)$ - experimental data[11]
- $\bar{T}_f(n)$ - experimental data of [12]

are also shown the points from [12]). As in the previous case, the analysis showed the necessity of a slight change in the radius of scattering with the neutron energy. The evaluation of the average resonance parameters is presented on tables 6 and 7.

Table 6

Evaluation of the ^{239}Pu average resonance parameters

J^π	$\bar{D}$ eV	$\bar{\Gamma}_\gamma$ meV	$S_n.10^4$	$\bar{\Gamma}_f$ eV	f_1	f_2
0^+	9.34	39.5	0.982	1.83	0.8	0.2
1^+	3.17	39.5	0.982	var	1	0
0^-	9.34	39.5	2.17	0.01	1	0
1^-	3.17	39.5	2.17	1.021	0.5	0.5
2^-	1.96	39.5	2.17	0.614	0.5	0.5

Table 7

Evaluation of the ^{239}Pu average resonance parameters depending on energy

Group Number	R' fm	$\bar{\Gamma}_\gamma (J^\pi = 1^+)$ meV
11	9.1	35.0
12	9.1	23.3
13	9.1	26.2
14	9.2	30.4
15	9.5	51.0

A posteriori R' error is found to be 1.9% and the S_o error is equal to 4.7%. The remaining parameters uncertainties did not diminish strongly in comparison with their a priori estimate and are of the order of 10%.

REFERENCES

1. Bemer B., Vankova A.A. et al., PTE, 1974, v.6, p.57.
2. Bogdzel A.A., Grigoriev Yu.V. et al., PTE, 1976, v.1, p.36.
3. Lukyanov A.A., The Neutron Cross Sections Structure, M., Atomizdat, 1978.
4. Vankov P.A., in "Problems of Atomic Science and Engineering", Series:"Nuclear Constants", 1983, v.4(53)
5. Vankov A.A., in "Problems of Atomic Science and Engineering", Series:"Nuclear Constants", 1974, v.16.
6. Grouppovye konstanti dlya rascheta reaktorov i zashtiti, M., Energoizdat, 1981, Auth.: Abagjan L.P., Bazazjants N.O., Nikolaev M.N., Tsibulja A.M.
7. Bhat M.R., BNL-NCS-51184, 1980.
8. Garber D., ENDF-102, BNL-NCS-50496, 1979.
9. Vankov A.A., Mateeva A., et al., JINR, P3-84320, 1984.

10. Czirr J.B., NSE, 1970, v.70, No.3.
11. Vankov A.A., Toshkov S., et al., in "Problems of Atomic Science and Engineering", Series "Nuclear Constants", 1983, v.4 (53)
12. Czirr J.B., Bramblet R.L., NCE, 1967, v.28, No.1.

Contributed Paper 11

THE (α, n) NEUTRON YIELD AND ENERGY SPECTRUM IN OXIDE NUCLEAR FUELS

V. BENZI
ENEA, Centro Ricerche Energia "E. Clementel",
Bologna, Italy

Abstract

- The basic formulae and parameters adopted for yield and energy spectrum calculations of the neutrons emitted by (α ,n) sources in nuclear fuel oxides, are reported. Numerical results obtained with the above formulae are compared with experimental data.

1. INTRODUCTION

In many circumstances, the Oxygen (α ,n) reactions in oxide nuclear fuels represent an important component of the spontaneous fast neutron source whose characteristics should be rather accurately known in order to provide adequate shielding during handling, transport, storage and reprocessing of the fuel.

In addition, neutrons from (α,n) reactions in a reactor containing Plutonium oxides can appreaciably contribute to the total start-up source or to the neutron flux after shut-down.

Notwithstanding the technological significance of the above-mentioned topics, the available data on total yield and energy spectrum of neutrons emitted by (α,n) sources in fuel oxides were rather scarce up to a few years ago. More recently, however, several papers and technical reports have been published on the matter, showing a renewed interest in the subject. Thus, it was felt useful to report here on some calculations that were found reasonably accurate in predicting (α ,n) thick target neutron yields and energy spectra of neutrons emitted by oxide mixtures or compounds, like UO_2 or PuO_2.

2. NEUTRON YIELD AND ENERGY SPECTRUM CALCULATIONS

Let us consider an ideal homogeneous mixture containing N_o atoms per unit volume of a single Oxygen isotope and an emitter of monoenergetic α-particles having initial energy E_α.

By definition, the thick target neutron yield $Y(E_\alpha)$ of the mixture, i.e. the number of neutrons produced via Oxygen (α,n) reactions per α-particle emitted, is given by

$$Y(E_\alpha) = N_o \int_0^{R(E_\alpha)} \sigma(E)dx = N_o \int_0^{E_\alpha} [\sigma(E)/(-dE/dx)]\, dE \qquad (1)$$

In the above formula, $\sigma(E)$ is the thin target (α,n) cross section of the considered Oxygen isotope at α-particle energy E in the laboratory system (l.s.), whereas $R(E_\alpha)$ and $(-dE/dx)$ represent, respectively, the total range and rate of energy loss (or "stopping power") at E by an α-particle having initial energy E_α.

Once the thick target yield is known, the neutron source strength $S_{\alpha,n}$ can be easily determined. In fact, if λ_α and N_α represent the α-decay constant and the concentration of the α-emitter, one has

$$S_{\alpha,n} = \lambda_\alpha N_\alpha Y(E_\alpha) \qquad (2)$$

neutrons produced per unit time and volume.

The relationships (1) and (2) can be very easily generalized to the case of homogeneous mixtures (or compounds) containing natural Oxygen and various kinds of α-emitters, simply by assuming that the stopping power of the mixture is given by the so-called "additivity rule" by Bragg and Kleeman (1905).

In many cases, however, in addition to the source strength $S_{\alpha,n}$ or the thick target yield $Y(E_\alpha)$, knowledge of the energy distribution in the l of the emitted neutrons is required, too. To this end, theoretical calculations were carried out, among others, by Rimshaw and Ketchen (1969) and by Lessor and Schenter (1971), whereas measurements and

calculations have been performed, very recently, by Jacobs and Liskien (1983).

Let $\sigma_{i,k}(E;\vartheta)$ represents the differential cross section at α-particle energy E of the i-th Oxygen isotope for an (α,n) reaction which leaves the residual nucleus in its k-th excited state. If the variable ϑ represents the angle between the directions in the center of mass (c.m.) system of the α-particle and the emitted neutron, one has

$$F(E_n)dE_n = (2\pi N_o) \sum_i \sum_k \rho_i \int_{E'_{i,k}}^{E''_{i,k}} \sigma_{i,k}(E;\vartheta)\phi(E)\sin\vartheta d\vartheta dE \qquad (3)$$

where $F(E_n)$ is the required energy distribution function, or the "energy spectrum" of the emitted neutrons.

In the above Equation, N_o represents the number of Oxygen atoms per unit volume and ρ_i the relative abundance of the i-th Oxygen isotope, whereas $\phi(E)dE$ gives the α-particle flux in the energy range $(E,E+dE)$, as will be explained below.

For a given neutron energy E_n, the integration limits $E'_{i,k}$ and $E''_{i,k}$ are obtained by putting $\vartheta=0$ and $\vartheta=\pi$, respectively, in the kinematic relationship

$$E_n = a_{i,k}(E) + b_{i,k}(E)\cos\theta \qquad (4)$$

where, as shown in Appendix, $a_{i,k}(E)$ and $b_{i,k}(E)$ are simple functions of the α-particle energy E, the reaction Q-values, and the masses of interacting particles and nuclei.

Taking the derivative of E_n with respect to angle θ, we obtain

$$\left[(d\theta/dE_n)\sin\theta\right]_{i,k} = -\left[1/b_{i,k}(E)\right] \qquad (5)$$

from which follows

$$F(E_n) = (2\pi N_o) \sum_i \sum_k \rho_i \int_{E''_{i,k}}^{E'_{i,k}} \left[\sigma_{i,k}(E;\vartheta)/b_{i,k}(E)\right]\phi(E)dE \qquad (6)$$

The differential cross sections appearing in Equation (6) can be expanded in terms of Legendre polynomial $P_\ell(\mu)$ up to an integer depending on (i,k); namely,

$$\sigma_{i,k}(E;\theta) = \sum_\ell \left[C_{i,k}(E)\right]_\ell P_\ell(\mu) \tag{7}$$

where $\ell = 0,1,2,\ldots,L_{i,k}$, and $\mu = \cos\theta$. Moreover, one can reasonably represent the energy dependence of the coefficients $\left[C_{i,k}(E)\right]_\ell$ by means of power polynomials, like

$$\left[C_{i,k}(E)\right]_\ell = \sum_n \left[c_{i,k,\ell}\right]_n E^n \tag{8}$$

where $n=0,1,2,\ldots M_{i,k,}$. Then, taking into account that the μ's are functions of E_n and E, as shown by Equation (4), the explicit dependence on θ of the differential cross sections can be removed from Equation (6).

In particular, one has

$$\mu_{i,k}(E_n;E) = \left[(E_n - \beta - \gamma Q_{i,k})/(\eta E^2 + \nu E Q_{i,k})^{1/2}\right] \tag{9}$$

where the parameters represented by the Greek letters depend on the masses of the particles and nuclei involved in the reaction, as shown in Appendix.

3. CROSS SECTIONS

Let m_α and m_i represent the nuclear masses of the α-particle and the initial (target) nucleus, respectively.

The threshold energy in the l.s. of an (α,n) reaction which leaves the residual nucleus (index r) in its k-th excited state, is given by

$$\left[E_{i,k}\right]_{thr} = -\left[(m_\alpha + m_i)/m_i\right] Q_{i,k} \tag{10}$$

The $Q_{i,k}$-value depends on the excitation energy $E_{r,k}$ of the residual nucleus through the relationship

$$Q_{i,k} = \left| \left[(\Delta_\alpha + \Delta_i) - (\Delta_n + \Delta_r) \right] - E_{r,k} \right| = (Q_{i,o} - E_{r,k}) \qquad (11)$$

the Δ's being the mass excesses of the particles and nuclei involved in the reaction. From the above Equations, it is found that the reaction $^{17}O(\alpha,n)^{20}Ne$ is exothermic ($E_{thr} = -0.725$ MeV), whereas the reactions $^{16}O(\alpha,n)^{19}Ne$ and $^{18}O(\alpha,n)^{21}Ne$ are both endothermic, with threshold energy of 14.824 and 0.851 MeV, respectively.

It follows that α-particles having kinetic energy up to about 5.5 MeV, like those usually produced by radioactive decay, can interact via (α,n)channels with isotopes ^{17}O and ^{18}O only, leaving the residual nuclei ^{20}Ne and ^{21}Ne in up to three or seven different excited states, respectively. Thus, in order to evaluate the energy spectrum $F(E_n)$, we need detailed knowledge over the entire range from threshold up to $\sim$ 5.5 MeV of twelve differential cross sections, corresponding to twelve final states(ground states included)accessible to the residual nuclei.

Unfortunately, the experimental data available are rather scarce.

For both isotopes there are thin target measurements on total (α,n) cross sections below 5.2 MeV (1.s.) by Bair and Willard (1962) and Bair and Haas (1973), together with some broad resolution measurements by Hansen et al. (1967) in the energy range 5 to 12 MeV. As far as natural Oxygen is concerned (containing 0.037 and 0.204 percent of ^{17}O and ^{18}O, respectively), thin target yields up to 8 MeV have been obtained from thick target measurements by Bair and Gomez del Campo (1979). A thin target Oxygen cross section was also measured by these authors in order to renormalize the previously quoted measurements by Bair and Haas; a correction factor of 1.35 to the old values was found.

Lacking detailed experimental data, the coefficients $[c_{i,k,L}]_n$ appearing in Equation (8) can be estimated by means of Hauser-Feshbach statistical model calculations. As pointed out by Lessor and Schenter

(1971), the neutron energy spectrum $F(E_n)$ should be rather insensitive to detailed resonance structure. In addition, Hansen et al. (1967) showed that the compound nucleus mechanism should be fully adequate below 8 MeV to represent angular distribution of the emitted neutron in $^{17,18}O(\alpha,n)^{20,21}Ne$ reactions, so that the adoption of the above-mentioned model seems well justified for the purposes of the present work.

Taking statistical fluctuations into account, calculations at various α-particle energies have been performed by means of POLIFEMO, a computer code developed by Fabbri and Reffo (1977) which allows for consistent optical and statistical model cross section calculations.

The optical model potentials adopted for calculation of the entrance and exit channel penetrabilities have been assumed as recommended by Grulhe and Möbius (1977) for the channels $(\alpha + {}^{16}O)$ and $(n + {}^{19}Ne)$, respectively, with the exception of the imaginary part of the entrance channel-potential, which was assumed to be energy-dependent in our calculations.

The values of the optical model parameters are shown in Table 1, according to the notation

$$V_{opt}(r) = [V_c(r) - V_o f(x_o)] - i\,[Wf(x_w) - 4V_D \frac{d}{dx_D} f(x_D)] \qquad (12)$$

Here, $V_c(r)$ is the Coulomb potential of a homogeneous charged sphere with radius $R_c = r_c A^{1/3}$, whereas $f(x_i) = [1+\exp(x_i)]^{-1}$ with $x_i = (r-R_i)/a_i$ and $R_i = r_i A^{1/3}$.

Table 1. OPTICAL MODEL PARAMETERS (E in c.m. units)

Reaction	Potential Parameters (MeV)			Geometrical Parameters (fm)					
Channel	V_o	W	V_D	$r_o;r_c$	r_w	r_D	a_o	a_w	a_D
α-entrance	56.900	4.700-0.367E	-	1.730	1.730	-	0.584	0.464	-
n- exit	47.010-0.270E	-	9.250-0.053E	1.300	-	1.260	0.660	-	0.480

As usual, the potential values given in Table 1 are in MeV, whereas the radial and surface parameters r_i and a_i are in fm.

The energy-dependence up to 6 MeV of the calculated (α,n) cross sections is shown in Figure 1. As one can see, the theoretical total cross sections (full lines) fit the low resolution experimental data (dots) reasonably well. In the same Figure, thin target data up to 5 MeV for natural Oxygen, as obtained by Bair and Gomez del Campo (1979), are compared with the results of our calculations; the overall agreement between experimental and calculated values seems quite satisfactory.

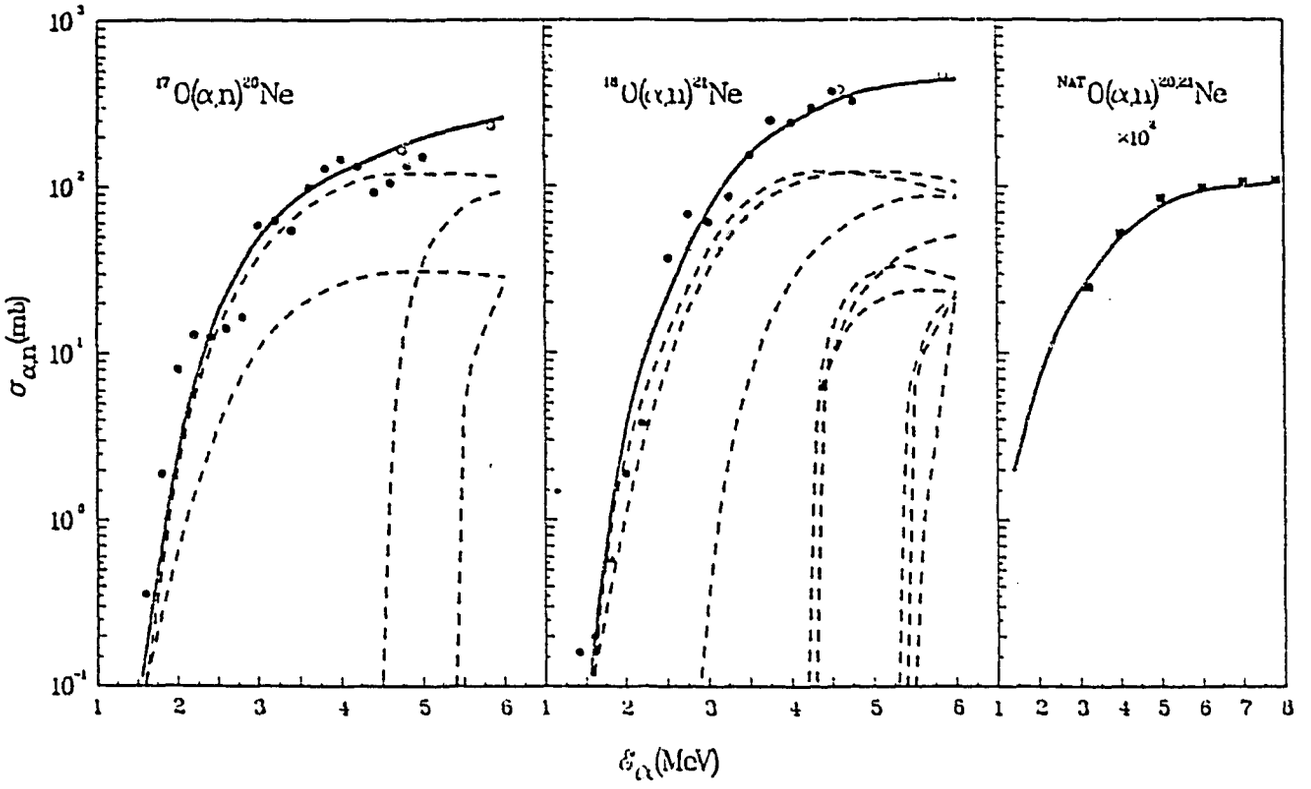

Figure 1. Calculated and measured O(α,n)Ne cross sections. Full points : Bair and Haas (1973). Open points : Hansen et al. (1967). Squares : Bair and Gomez del Campo (1979), from thick target yield measurements (notice the changes in both scales).

As far as the angular distribution of the emitted neutrons is concerned it should be noted that the assumption of isotropy in the c.m., as suggested among others by Taherzadeth (1971), seems to be in general rather incorrect, as shown by the examples in Figure 2.

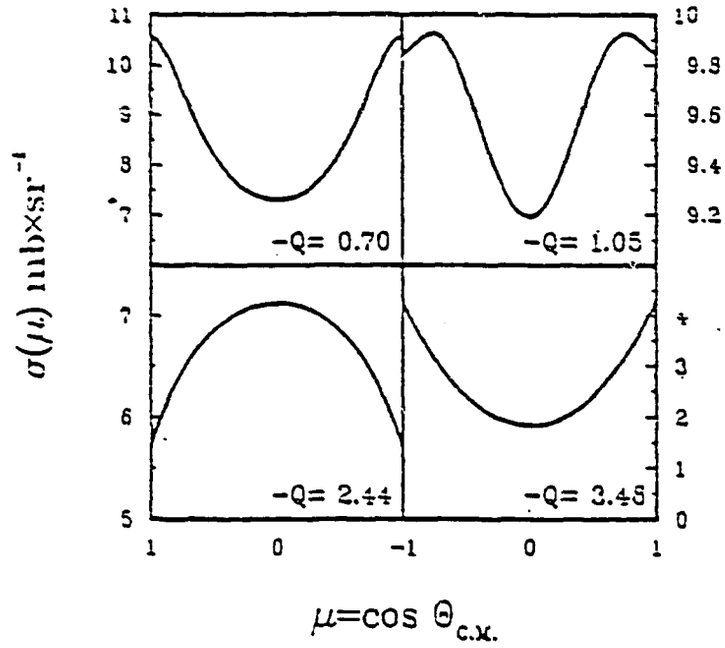

Figure 2. Some calculated differential $^{18}O(\alpha,n)^{21}Ne$ cross sections at E=5.4 MeV. The anisotropy of the angular distribution is quite evident.

4. ENERGY SPECTRUM OF THE α-PARTICLES

As previously mentioned, the differential α-particle energy spectrum $\rho(E)dE$ in a given mixture of α-emitters, Oxygen and other homogeneously mixed elements, can be easily estimated by means of the Bragg-Kleeman rule, which states that the stopping power $(-dE/dx)_{mix}$ of a mixture of N different kinds of atoms, is approximately given by the relationship

$$(-dE/dx)_{mix} = \sum_j n_j(-dE/dx)_j \qquad (13)$$

where, n_j (=1,2,...N) represents the concentration of the j-th chemical element present in the mixture and $(-dE/dx)_j$ the corresponding stopping power.

Then, if N_K represents the concentration of the k-th isotope, emitting α-particles with energies $(E_{k,1};E_{k,2}; \ldots;E_{k,m})$ and corresponding

decay constant ($\lambda_{k,1}; \lambda_{k,2}; \ldots; \lambda_{k,m}$), one has

$$\phi(E) = \sum_k \sum_i N_k [\lambda_{k,i} \delta_{k,i}(E)] / (-dE/dx)_{mix} \qquad (14)$$

with $\delta_{k,i} = 1$ if $E \leq E_{k,i}$; otherwise $\delta_{k,i} = 0$.

In the present work, for all elements other than Plutonium we have adopted the Helium ion stopping powers evaluated by Ziegler (1977). For Plutonium, whose stopping power is not given by Ziegler's evaluation, the estimate given by Perry and Wilson (1981) was adopted above 0.5 MeV; for lower energies we have assumed (E in MeV)

$$(-dE/dx)_{Pu} = 235 (E^{1/2} - 0.01) \qquad (15)$$

where the stopping power is given in units (MeV cm^{-1}).20^{21} atoms.

The decay constants $\lambda_{i,k}$ of the α -emitters have been obtained from total half-lives and relative intensities as reported in the well known "Tables of Isotopes" edited by Lederer and Shirley (1978).

In order to test the validity of the sum rule, the stopping power of UO_2 has been calculated by means of Equation (13) for α -particle energies ranging from 2 to 6 MeV, and the results compared with the experimental data given by Nitzki and Matzke (1973). It was found that the calculated values are systematically higher by a factor of $\sim$1.02 above 3 MeV, increasing to 1.06 at 2 MeV.

5. COMPARISON OF MEASURED AND CALCULATED NEUTRON SOURCE SPECTRA AND YIELDS

In order to estimate neutron source spectra and thick target yields in fuels containing Uranium and/or Plutonium oxides, a FORTRAN computer code was developed along the lines previously reported (Benzi et al., 1982).

Given the atomic and isotopic composition of a mixture, the code provides the strength and energy spectrum of the neutron source (including spontaneous fissions), together with the thick target neutron yield and energy spectrum of the α-particles, as given by Equation (4). Optionally, the spectrum can be obtained in a given group structure suitable for multigroup calculations.

Before performing any comparison between calculated and measured data, it has to be noted that the measured energy spectrum should, in general, be somewhat different from the corresponding calculated one, even though the latter is correct. There are several reasons for this.

First, both elastic and inelastic neutron scattering inside the sample always produce some softening of the spectrum, as was clearly demonstrated by Anderson and Bond (1963). In particular, it was found by these authors that the neutron spectrum produced by Pu-Be sources remained practically the same above $\sim$ 2 MeV in a variety of cases, whereas below $\sim$ 2 MeV there was a rather strong, size-dependent variation in neutron number, mainly due to the above-mentioned neutron reactions within the source. Second, an apparent softening of the measured spectrum may also be produced by fast fissions induced in the medium by source neutrons; here again the relative importance of the process strongly depends on source size.

In addition to the above-mentioned facts, it should be noted that the neutron spectra were frequently measured in the past by means of scintillators used as proton-recoil fast neutron spectrometers. The disadvantage of almost all these instruments was that neutrons with energy below $\sim$ 2 MeV were difficult to detect, because of excessive sensitivity to γ-radiation. Additional uncertainties at low energies were also produced by the rapid variation of counter efficiency, a feature which makes any unfolding procedure rather questionable.

Taking the above considerations into account, we have assumed that the measured and calculated spectra can be reasonably compared at energies above $\sim$ 2 MeV, where the perturbing effects seem to be rather small. As a matter of fact, in all the cases we have considered

it was found that it is possible to obtain good agreement between the measured and calculated spectrum simply by assuming that the position of the measured and calculated maxima should coincide.

In the examples here reported, a shift in the energy scale of the measured spectra by a factor ranging within the limits (1.07±0.02) was found good enough to give both coincidence in the maxima and reasonable agreement in the shape of the measured and calculated spectra above ∿ 2 MeV.

This is shown in Figure 3 where a) refers to a $^{210}Po-H_2O$ source, 24% enriched in ^{18}O (Khabakhpashev, 1959), and b) to a $^{238}PuO_2$ source with Oxygen having 45,61% content of ^{18}O(Anderson, 1966). Figure 3-c) refers to a $^{238}PuO_2$ source corrected for spontaneous fissions (Herold, 1968), whereas figure 3-d) represents the neutron spectrum (corrected for spontaneous and induced fission neutrons) of SNAP 27-1, a PuO_2 power source containing 3.7 Kg of PuO_2, of which 2.6 Kg was $^{238}PuO_2$ (Anderson and Neff, 1969).

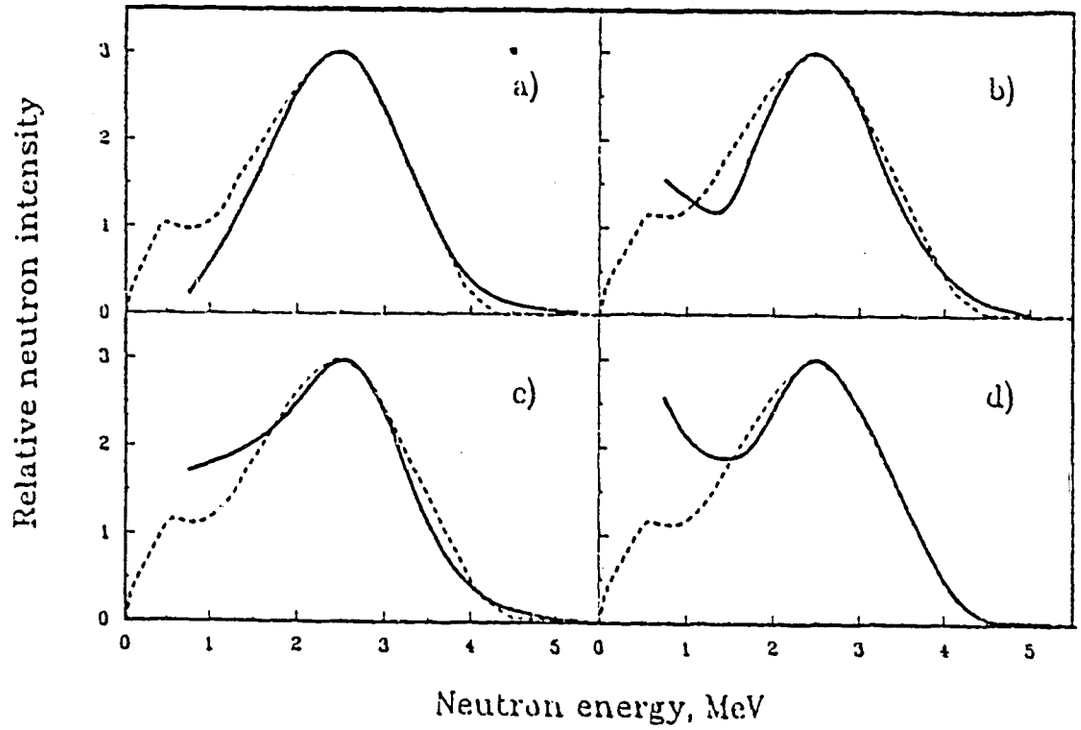

Figure 3. Experimental (full line) and calculated neutron energy spectra produced by different α-sources and compounds. See text for more details.

Rather good agreement between theory and experiment was also found in the case of the UO_2 neutron spectrum produced by 5.5 MeV α-particles as measured by Jacobs and Liskien (1983), who used an NE 213 scintillator as time-of-flight spectrometer.

Here again some difference below ∿ 1 MeV and above ∿ 3.5 MeV was found, probably due to the presence of a small component of neutrons from induced fission in Uranium.

Finally, the code was tested as a tool for estimating thick target yields in compounds. Figure 4 shows the experimental results obtained by Bair and Gomez del Campo (1979), West and Sherwood (1982) and

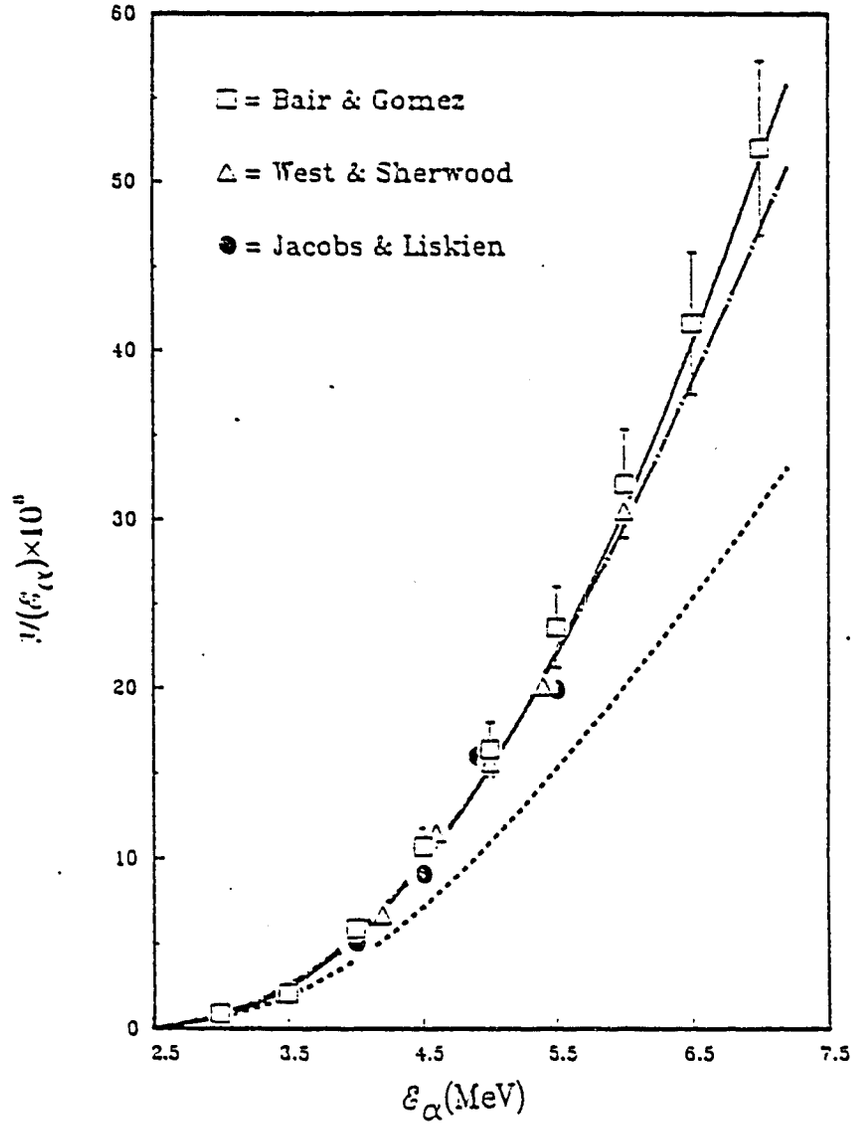

Figure 4. Theoretical and experimental total (α,n) neutron yield by a UO_2 thick target.
Full line : this work. Dashed line : Perry and Wilson (1982). Point line : Liskien and Paulsen (1977)

Jacobs and Liskien (1983) in the case of a UO_2 thick target, together with the theoretical estimates obtained by Liskien and Paulsen (1977), Perry and Wilson (1982) or by using our code. As one can see, the agreement between our theoretical predictions and the available experimental data seems to be very good.

ACKNOWLEDGMENTS

The author's grateful thanks are due to Miss F.Fabbri and Mr. G. Panini for performing the numerical calculations required by the present work and for producing the graphs via DISSPLA Graphic System.

REFERENCES

/1/ ANDERSON M.E. (1966) Trans. Ann. Nucl. Soc.9,2,600.

/2/ ANDERSON M.E. and BOND Jr.W.H. (1963) Nucl. Phys.43,300

/3/ ANDERSON m.E. and NEFF R.A. (1969) Nucl. Appl. Technol. 7,62

/4/ BAIR J.K. and GOMEZ DEL CAMPO J. (1979) Nucl.Sci. Engeen. 71,18

/5/ BAIR J.K. and HAAS F.X. (1973) Phys.Rev. 7,4,1356

/6/ BAIR J.K. and WILLARD H.B. (1962) Phys.Rev. 128,1,299

/7/ BENZI V., FABBRI F. and PANINI G. (1982), unpublished

/8/ BRAGG W.H. and KLEEMAN R. (1905) Phil.Mag. 10, 318

/9/ FABBRI F. and REFFO G. (1977), unpublished

/10/ GRUHLE W. and MOBIUS K.H. (1977) Z. Phys. A283,97

/11/ HANSEN F.L. et al. (1967) Nucl. Phys. A98,25

/12/ HEROLD T.R. (1968) Nucl. Appl. 4,19

/13/ JACOBS G.J. H. and LISKIEN H. (1983) Ann. Nucl. Energy, 10, 541

/14/ KHABAKHPASHEV A.G. (1959) Atom.Energy 7,71

/15/ LEDERER C.M. and SHIRLEY V.S. Eds. (1978) "Table of Isotopes, Seventh Edition", John Wiley and Sons, Inc. New York

/16/ LESSOR D.L. and SCHENTER R.E. (1971) Report BNWL-B-109

/17/ LISKIEN H. and PAULSEN A. (1977) Atomkerenergie 30, 59

/18/ NITZKI V. and MATZKE H. (1973) Phys.Rev. B8, 1984

/19/ PERRY R.T. and WILSON W.B. (1981) Report LA-8869-MS

/20/ RIMSHAW S.J. and KETCHEN E.E. (1969) "Curium Data Sheets", ORNL-4357

/21/ TAHERCADETH M. (1971) Nucl.Sci. Engeen. 44, 190

/22/ WEST D. and SHERWOOD A.C. (1982) Ann.Nucl.Energy, 9, 551

/23/ ZIEGLER J.F. (1977) "Helium Stopping Powers and Ranges in all Elemental Matter", Pergamon Press, Oxford

APPENDIX

Let

$$E^{*}_{i,k} = \left[(m_r m_i)/(m_n+m_i)(m_\alpha+m_i)\right] E + \left[m_r/(m_n+m_i)\right] Q_{i,k} \qquad (A.1)$$

be the kinetic energy in the c.m. system of a neutron emitted in an (α,n) reaction induced by an α-particle having kinetic energy E in the l.s., which impinges on a target nucleus (index i) at rest in its gound state. The index r refers to the residual nucleus, which is assumed to be left in the k-th excited state corresponding to the given $Q_{i.k}$-value.

While the emitted neutron is monoenergetic in the c.m. system, in the l.s. we have

$$E_{i,k} = E^{*}_{i,k} + \left[(m_n m_\alpha)/(m_\alpha+m_i)\right] E$$

$$+ 2\left\{\left[(m_n m_\alpha)/(m_\alpha+m_i)^2\right](E E^{*}_{i,k})\right\}^{1/2}\cos\vartheta$$

$$= a_{i,k}(E) + \left[b_{i,k}(E)\right]\mu \qquad (A.2)$$

where $\mu = \cos\theta$ and

$$a_{i,k}(E) = \left[(m_i m_r + m_n m_\alpha)/(m_\alpha + m_i)\right] E + \left[m_r/(m_n + m_r)\right] Q_{i,k} = (\beta E + \gamma Q_{i,k}) \tag{A.3}$$

$$b_{i,k}(E) = 2\left\{\left[(m_n m_\alpha m_i m_r)/(m_n + m_r)(m_\alpha + m_i)^3\right] E^2 + \left[(m_n m_\alpha m_r)/(m_n + m_r)(m_\alpha + m_i)^2\right] E Q_{i,k}\right\}^{1/2} = (\eta E^2 + \nu E Q_{i,k})^{1/2} \tag{A.4}$$

the meaning of the symbols β, γ, η and ν being obvious.

Equation (9) in the text can be easily obtained by properly combining the last three above-given Equations.

Contributed Paper 12

TOTAL GAMMA RAY SPECTRA AND ISOMERIC RATIO CALCULATIONS IN THERMAL AND FAST NEUTRON CAPTURE FOR ^{238}U, ^{240}Pu, ^{242}Pu AND ^{241}Am

G. REFFO
ENEA, Laboratorio Dati Nucleari e Codici,
Bologna, Italy

Abstract

The model, the code and the methodology developed for the calculation of the isomeric ratio and of the gamma ray spectrum which follows the neutron capture process are illustrated.

Results of detailed calculations in the transactinide region are discussed. The role of optical model, of Brink-Axel and Weisskopf assumptions as well as the impact of the most important parameters is duscussed.

The results of these calculations satisfactorily agree with experimental information in all cases considered.

Spectra calculations were also used in relative neutron capture measurements for correction of systematic uncertainties due to non-linear efficiency of the Moxon-Rae detector.

1. Introduction

Total spectrum of gamma-ray emissions, total cross section for excitation of discrete levels via gamma-decay, isomeric ratios, are expensive information from the experimental as they are complex from the calculation view point.

Renewed interest, in view of the increasing importance of this information in reactor technology has led to recent studies [1-4] how to handle the problem from the various view points from modelling to coding and parameterizing the problem.

In this paper model, methods, codes and results of recent calculations [1-3] (in thermal and fast neutron energy region) are summarized and spectra analyses for different parameter and model assumptions are briefly discussed.

2. The model and the code

The cascade model adopted has been illustrated in detail in ref. 1.2 and will be described here only briefly.

The gamma-decay widths of E1 transitions are estimated according to the Brink-Axel model as used in Ref. 5,6 where

$$\overline{\Gamma_\gamma}(E,J,\pi) = \frac{C}{\rho(E,J,\pi)} \left(\delta_{J_n,|J-1|} + \delta_{J_n,J=0} + \delta_{J_n,J+1}\right) * \\ * \delta_{\pi_n,-\pi} (E-E_n)^2 \sigma_L(E-E_n)$$

gives the width for gamma decay from continuum levels (E,J,π) to discrete level (E_n, J_n, π_n) and

$$\Delta\overline{\Gamma_\gamma}(E,J,\pi) = \frac{C}{\rho(E,J,\pi)} \varepsilon^2 \sigma_L(\varepsilon) \sum_{|J-1|}^{J+1} \rho(E-\varepsilon,J',-\pi)\Delta\varepsilon$$

the width for gamma decay from continuum levels (E,J,π) to continuum levels $(E-\varepsilon, J',-\pi)$ where

$$\sigma_L(\varepsilon) = \sum_{iR}^{2} \sigma_R \frac{\varepsilon^2 \Gamma_R^2}{(\varepsilon^2-E_R^2)^2+\varepsilon^2\Gamma_R^2}$$

is the adopted (Lorentzian) form for the splitted photon-absorption cross section and $C=2/3\,(\pi\hbar c)^2$.

The continuum of levels is split into a high energy and a low energy part as described in Ref. 6,7. At high excitation energies a total level density

$$\rho_2(E) = \frac{\sqrt{\pi}}{12} \frac{\exp\left[2\sqrt{a(E-\Delta)}\right]}{a^{1/4}(E-\Delta)^{5/4}\sqrt{2\pi\sigma^2(E)}}$$

is assumed, Δ being the pairing correction and "a" the level density parameter. The latter can be determined from the fit to either the resonance spacings or to BCS calculations (8).

At low excitation energies the empirical formula

$$\rho_1 = \frac{1}{T} \exp\left[(E-E_o)/T\right]$$

is adopted for the total level density with T and E_o as input parameters. A theoretical spin distribution law of the type

$$f(E,J) = \frac{(2J+1)\exp\left[-(J+1/2)^2/2\sigma^2(E)\right]}{2\,\sigma^2(E)}$$

is assumed with a spin cut-off factor $\sigma^2(E) = 0.146\,\sqrt{a(E-\Delta)}\,A^{2/3}$, according to Ref. 7, which has proven to hold pretty well in the high energy range.

Continuum bands are treated like discrete levels. For each band spin and parity dependent branching ratios are calculated allowing for the competition of E1, M1, E2 transition probabilities which are estimated according to Lorentz curve approximations to the respective giant resonances (GR).

A split GR model is used for E1, M1, E2 photon absorption, the Lorentzian parameters being taken from the systematics of Ref. 6,9,10,11.

The experimental branching ratios are used for discrete levels. Missing ones are estimated assuming single particle state transitions (with E1, M1 transitions dominating) for spherical nuclei and assuming collective transitions (with E2 transitions dominating) for collective nuclei.

A spherical optical model was used for calculating neutron transmission coefficients for U and Pu isotopes, whereas coupled channel calculations were adopted for Am in order to account better for the neutron channel competition.

The fission channel competition, was treated using a double humped fission barrier with two inverted harmonic oscillators. The width fluctuation correction factor was applied to all channels (12),(13),(14).

These calculations were performed with our modular master code the IDA MODULAR SYSTEM[15] of codes. It is capable of calculating integrated and differential cross sections for all reactions possible up to 50 MeV incident energies including most reaction mechanisms, whatever the projectile including gamma-rays. As a particular option gamma-ray cascades may be started at any step of the multiple cascading particle emission.

The main effort of the code is on organization. Cascade events are simultaneously ordered in as many different ways as there are purposes of the code i.e. according to: a) stories with the same number of steps in the cascade (which allows for calculating cross sections of each gamma-ray multiplicity and the corresponding partial spectra; b) cascades feeding levels a priori marked (for calculating excitation cross sections of marked levels, corresponding spectra and isomeric ratios, IR); c) emitted energy bands, where single-step contributions are lumped according to the respective gamma-ray energies (for total gamma-ray spectra calculations); d) initially a),b),c) are given for any J^{π} couple of the initial decaying level (this can be useful in several investigations e.g. either to isolate a), b), c) for given incident angular momentum, l, when the initial level is a compound nucleus one; or to estimate a), b), c), for a given $J\pi$ couple; etc.).

The code includes coupled channel calculations providing for collective direct scattering and for the transmission coefficients describing the inelastic scattering to coupled states via the compound nucleus mechanism.

After the probability for compound nucleus formation has been computed for all possible J and π , the code determines

the gamma-decay probabilities in J and π for each step of each gamma-ray cascade story.

After summation over all J and π and, by considering the electromagnetic selection rules, all single step contributions are lumped together into energy bins according to the energies of the emitted gamma-rays so that partial and total gamma-ray spectra can be obtained on option. The code also traces particular gamma-ray stories which feed some particular levels. In this way, it is possible to calculate the cross sections for the population of isomeric states and the corresponding gamma-ray spectra as well. In the calculations of gamma ray cascade it is assumed that E1, M1, E2 transitions are possible. For the transitions between discrete levels, gamma-ray decay schemes and branching ratios can either be given as input or are internally calculated according to different options admitted. (Further details in the following text).

3. Model Parameterization

Gamma-ray decay stories and consequently gamma-ray spectra and isomeric ratios (through electromagnetic selection rules) also depend on the initial population of compound nucleus states of given J and π i.e. expecially at low incident energies, they depend on the relative magnitude of S_0 and S_1 strength functions. Finally, the correct knowledge of discrete levels characteristics and gamma-decay branchings are of capital importance in order to determine the isomeric ratio.

Therefore much care has to be spent to check the relevant input information like optical model and level density parameters with all available experimental information, e.g., with the average resonance parameters s- and p-wave strength functions, resonance spacings and scattering radius and with measured cross sections for σ_T and $\sigma_{n,\gamma}$ and with total radiative width $\Gamma_\gamma^{J\pi}$ of neutron resonances.

In order to check the level density assumptions and to verify the reliability of the assumptions for calculating the gamma-decay probabilities, the total radiative width at the neutron binding energy has been calculated for -s and p-wave neutron resonances. Such calculations, require the giant resonance parameters, which in turn depends on the deformation parameter β according to the systematics of Ref. 6.

As can be seen, the calculated values for the total radiative widths of s-wave neutrons, as given in Table I, compare quite well (within the quoted uncertainties) to the experimental results, thus offering additional confidence with respect to those parameters that influence on the spectra calculations. The parameters involved in Γ_γ calculation are given in Table I.

Our parameters for the optical model potential (OMP) were determined by fitting s- and p- wave strength functions and the scattering radii (S_0, S_1, and R), respectively.

^{241}Am has been treated as a rotational nucleus with a coupling scheme $5/2^-$, $7/2^-$, $9/2^-$, $11/2^-$, $13/2^-$. Above .15 MeV coupled channel calculations were performed with the parameter set of Madland and Young [16] using a deformation parameter $\beta = .24$.

This parameter set allowed a consistent description of the available total cross sections of Phillips and Howe [17] and it yielded correct values for s- and p-wave strength functions $S_0 = .97 \times 10^{-4}$, $S_1 = 2.66 \times 10^{-4}$ which are in excellent agreement with evaluated results (see table I).

TABLE I

Relevant Neutron

Target Isotope	$S_0 \times 10^{+4}$			$S_1 \times 10^{+4}$			
	Evaluated	Reference	This Work Optical Model	Evaluated	Reference	This Work Optical Model	Evaluated
^{238}U	1.15 ± 0.12	19		~2	19		
	1.0 ± 0.1	20	1.0	1.7 ± 0.3	20	2.25	9.6 ± 0.1
^{240}Pu	$1.04 \pm \begin{matrix}0.14\\0.12\end{matrix}$	21		2.56 ± 0.24	21		8.44
	0.93 ± 0.08	20	0.9			2.7	9.6 ± 0.2
	1.02	22		1.98	22		
^{242}Pu	0.9 ± 0.1	21		~2.6	21		8.46
	0.94	20					9.6
	1.1	23	1.1	2.7	23	2.7	9.6
	1.05	22		2.0	22		
^{241}Am	0.9	this work	0.97	2.4	this work	2.66	
	0.94±0.09	24		2.54	24		

I

Resonance Parameters*

R (fm)		D (eV)			$\Gamma_\gamma^{1/2^+}$ (meV)		
Reference	This Work Optical Model	Evaluated	Reference	Adopted for This Work	Evaluated	Reference	Calculated (This work)
19	9.5	20.3 ± 0.2	19		23.5 ± 1.0	19	
		22.5 ± 1.4	20	20.3	23.2 ± 0.3	20	24.0
		24.8 ± 2.0	21				
20		13.0 ± 0.7	21		30.8 ± 1.0	21	
19	9.3	11.5 ± 1.9	20	13.0	31.0 ± 0.2	20	31.6
		13.1	22		32.5	22	
		13.5 ± 0.5	25				
20		17.5 ± 1	21		24.0 ± 2.0	21	
19							
22	9.3	15.0	23	15.0	25.0	23	23.7
		12.6	22		22.5	22	
		14.3 ± 0.54	24				
		0.53±.05	this work	0.53±.05	43.8±0.7	25	37.5
		0.55	25		41.5±7	this work	

*For each isotope, the parameters S_0, S_1, and R from recent analyses are given with the values adopted in this work. In the last two columns, our calculated radiative widths are compared to evaluated experimental results.

For U-238 and Pu-240,-242 as a first guess for our OMP search, we adopted the parameters given by Madland and Young [16] (iteration zero). Our final OMP sets differ from these only in the real and imaginary part, V and W, of the well depth. These are

$$V = 47.07,\ 47.4,\ \text{and}\ 46.8\ \text{MeV}$$

$$W = 4.8,\ 5\ ,\ \text{and}\ 6\ \text{MeV}$$

for U-238 and Pu-240,-242, respectively. The evaluated experimental values for S_0, S_1 and R were taken from the most recent resonance analyses and are compared in Table I with those derived by our OMP analysis. For U-238 and Pu-240, the total cross sections predicted by our OMP are in good agreement with the measurements by Poenitz et al. [18]. This also indicates consistency among the various sources of experimental information.

The theoretical level density and inherent spin distribution used above E_{cut} is shown (full line) in Fig. 1 and compared with the corresponding experimental quantities.

The level schemes adopted with the respective quantum characteristics and gamma-decay branchings are given in the tables II and III.

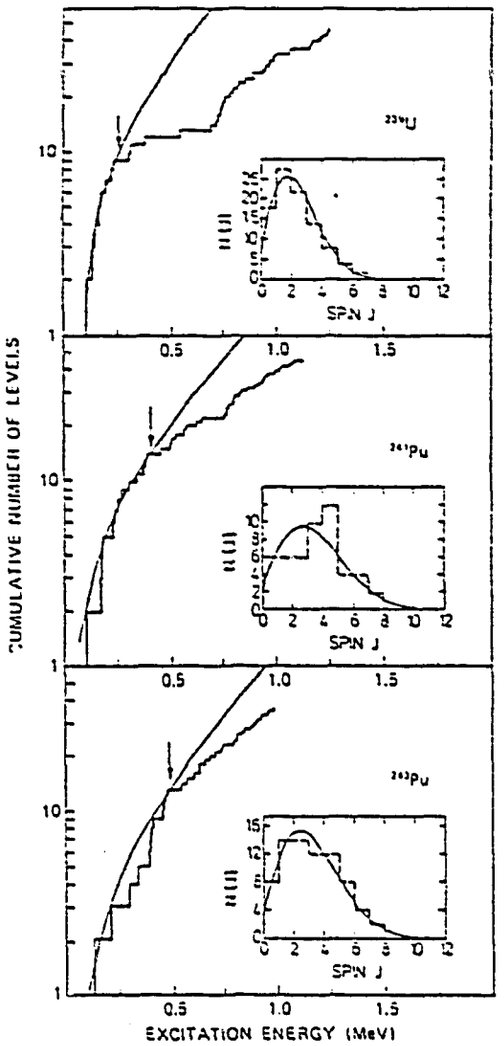

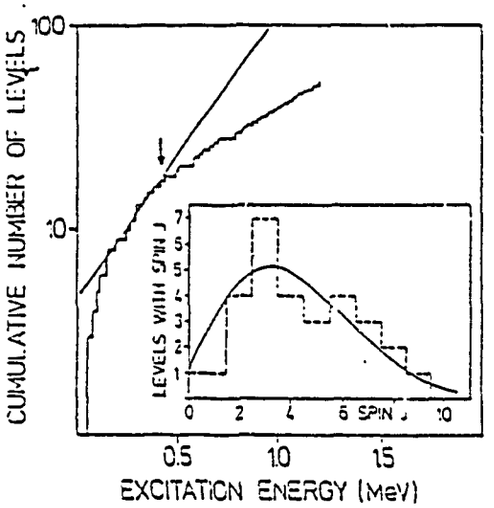

Fig. 1. Comparison between the experimental and calculated cumulative number of levels for all compound nuclei. The energy, E_{cut}, where the level continuum was supposed to start is marked by an arrow. In the respective inserts, the theoretical spin distribution (solid line) and the spin distribution of the known discrete levels (histogram) are given below E_{cut}.

TABLE II Adopted level scheme for ^{242}Am. J, π characteristics between brackets are arbitrarily assigned. Gamma-decay scheme and gamma-decay probabilities are given according to the assumption that E2 collective state transitions dominate (first group) or that M1 single particle state transitions dominate (second group).

Level Number	Energy (MeV)	Spin	Parity	Branching Ratio (Collective Transitions) (Level Number, Probability %)	Branching Ratio (Single Particle Transitions (Level Number, Probability %)
1	0.	1	-		
2	.044	0	-	(1,100)	(1,100)
3	.049	5	Isomeric state		
4	.05	3	-	(1,100)	(1,100)
5	.075	2	-	(1,97) (2,1) (3,1) (4,1)	(1,96) (4, 4)
6	.099	(3)	-	(1,96) (3,2) (4,2)	(4,90) (5,10)
7	.114	6	-	(3,100)	(3,100)
8	.148	4	-	(3,45) (4,45) (5,9) (6,1)	(3,47) (4,47) (6, 6)
9	.149	5	-	(3,49) (4,49) (6,2)	(3,96) (7, 4)
10	.19	7	-	(3,96) (7,4)	(7,100)
11	.244	3	-	(1,96) (3,2) (4,2)	(4,46) (5,30) (6,19) (8,5)
12	.263	6	-	(3,100)	(3,65) (7,22) (9,10) (10,3)
13	.289	2	-	(1,45) (2,20) (4,19) (5,10) (6,5) (8,1)	(1,44) (4,25) (5,18) (6,13)
14	.290	4	-	(3,31) (4,31) (5,10) (6,10) (7,7) (8,2) (9,1)	(3,34) (4,34) (6,17) (8,8) (9,7)
15	.325	3	-	(1,41) (3,10) (4,10) (5,11) (6,7) (8,3) (9,2)	(4,46) (5,30) (6,19) (8,5)
16	.341	3	-	(1,41) (3,10) (4,10) (5,11) (6,7) (8,3) (9,2)	(4,46) (5,30) (6,19) (8,5)
17	.372	4	-	(3,31) (4,31) (5,10) (6,10) (7,7) (8,2) (9,1)	(3,34) (4,34) (6,17) (8,8) (9,7)
18	.409	6	-	(3,53) (7,20) (8,11) (9,11) (10,5)	(3,45) (7,25) (9,17) (10,10) (12,1)
19	.432	5	-	(3,27) (4,27) (6,14) (7,11) (8,11) (9,6) (10,3) (11,1)	(3,41) (7,24) (8,16) (9,16) (12,1)
20	.487	7	-	(3,52) (7,24) (9,14) (10,8) (12,2)	(7,50) (10,30) (12,12)
21	.500	6	-	(3,53) (7,20) (8,11) (9,11) (10,5)	(3,45) (7,25) (9,17) (10,10) (12,1)
22	.580	8	-	(7,64) (10,26) (12,10)	(10,99) (20,1)
23	.581	7	-	(3,52) (7,24) (9,14) (10,8) (12,2)	(7,50) (10,30) (12,12)
24	.608				
25	.626				
26	.650				
27	.678				
28	.697				
29	.790				
30	.794	9	-		
31	.822				
32	.833				
33	.846				
34	.873	2	-		
35	.899	3	-		
36	.915				
37	.936				
38	.951				
39	.975	3	+		
40	.994				
41	1.011	2	+		
42	1.03				
43	1.05	3	+		
44	1.065				
45	1.073				
46	1.088				
47	1.097				
48	1.119				
49	1.14				
50	1.162				
51	1.168				
52	1.187				
53	1.199				

TABLE III

Adopted Level Schemes for the Compound Nuclei ^{239}U, ^{241}Pu, and ^{243}Pu*

Level Number	Energy (MeV)	Spin	Parity	Branching Ratios
		^{239}U		
1	0	2.5	+	
2	0.0425	3.5	+	(1.100%)
3	0.097	4.5	+	(1.95%) (2.05%)
4	0.134	0.5	+	(1.100%)
5	0.146	1.5	+	(1.85%) (2.15%)
6	0.165	5.5	+	(2.95%) (3.05%)
7	0.173	3.5	+	(1.80%) (2.19%) (3.01%)
8	0.194	2.5	+	(1.76%) (2.22%) (3.02%)
9	0.222	3.5	+	(1.71%) (2.25%) (3.04%)
10	0.229	4.5	+	(1.71%) (2.25%) (3.04%)
11	0.300	5.5	+	(2.73%) (3.22%) (6.03%) (7.02%)
12	0.307	4.5	+	(1.61%) (2.29%) (3.09%) (6.01%)
		^{241}Pu		
1	0	2.5	+	
2	0.042	3.5	+	(1.100%)
3	0.094	4.5	+	(1.95%) (2.05%)
4	0.162	0.5	+	(1.100%)
5	0.1708	1.5	+	(1.80%) (2.20%)
6	0.172	3.5	+	(1.51%) (2.49%)
7	0.223	2.5	+	(1.70%) (2.25%) (3.05%)
8	0.229	4.5	+	(1.70%) (2.25%) (3.05%)
9	0.243	3.5	+	(1.68%) (2.26%) (3.06%)
10	0.26	(3.5)	+	(1.66%) (2.27%) (3.07%)
11	0.3	5.5	+	(2.74%) (3.24%) (6.02%)
12	0.335	4.5	+	(1.57%) (2.30%) (3.11%) (6.02%)
13	0.368	6.5	+	(3.97%) (8.03%)
14	0.376	(3.5)	(+)	(1.53%) (2.29%) (3.13%) (5.03%) (6.02%)
15	0.384	(4.5)	(+)	(1.54%) (2.30%) (3.13%) (6.03%)
		^{243}Pu		
1	0	3.5	+	
2	0.056	4.5	+	(1.100%)
3	0.124	5.5	+	(1.96%) (2.04%)
4	0.204	6.5	+	(2.96%) (3.04%)
5	0.287	2.5	+	(1.75%) (2.25%)
6	0.329	3.5	+	(1.68%) (2.26%) (3.06%)
7	0.384	0.5	+	(5.100%)
8	0.388	4.5	+	(1.62%) (2.28%) (3.09%) (4.01%)
9	0.392	1.5	+	(1.100%)
10	0.403	4.5	−	(1.94%) (2.02%) (3.04%)
11	0.447	2.5	+	(1.66%) (2.34%)
12	0.45	3.5	+	(1.58%) (2.30%) (3.12%)
13	0.454	5.5	−	(2.55%) (3.31%) (4.14%)
14	0.467	5.5	+	(1.56%) (2.29%) (3.12%) (4.03%)

*The J,π characteristics between parentheses were arbitrarily assigned close to the most probable observed values. Underlined gamma-decay characteristics were estimated according to the criteria illustrated in the text.

The complete parametrization for the high energy level density is given in Table IV.

Table IV

Parameters Adopted for the Description of the Total Level Density and Its Spin Distribution

Compound Nucleus	E_{cut} (MeV)	a $(MeV)^{-1}$	E_x (MeV)	σ_c^2
^{239}U	0.35	32.9	3.5	5.2
^{241}Pu	0.405	30.8	3.5	8.7
^{243}Pu	0.50	31.7	3.1	10.1
^{241}Am	0.59	29.42	2.015	14.3

For the split giant dipole electric resonance, we used the same parameters for all isotopes:

E_1 =11.6 MeV, E_2=13.8 MeV, Γ_1=2.7 MeV, Γ_2=3.8 MeV, σ_1=0.300b, σ_2=0.410b.

For Am-241 the influence of fission channels is significant and must be taken into account.

The parameters adopted for the double humped fission barrier of Am-242 and for the level density in the fission channels were taken from the systematics of Lynn [26], which gave a good overall agreement with the measured cross sections of Refs. 27, 28.

4. Results

Numerical calculations have been carried out in the energy range from 1 keV to 1000 keV and are presented in Table V and VI and a detailed discussion is given for each quantity separately.

4.1 Isomeric Ratio

The dependence of IR on the parameters described in the previous sections was investigated explicitely. First, the extreme assumptions on the gamma decay and the respective

branching ratios were found to influence the calculations of IR to an almost negligible degree as can be seen by comparing columns 2 and 4 in Table V. Secondly, the continuum level density was modified assuming E_{cut} = 0.29 MeV which means that half of the known levels between .29 and .581 MeV were skipped.

TABLE V

Summary of the present calculations. The isomeric ratio IR = $\sigma^{g}_{n,\gamma}/\sigma_{n,\gamma}$ is given in the 2nd column. Columns 3 to 5 demonstrate the dependence of IR for different assumptions on the discrete level scheme in ^{242}Am skipping all levels above E_{cut} and for the assumption that M1 single particle transitions dominate in the decay of the compound nucleus. In columns 6 to 8 the capture cross section, the fission cross section and the total neutron cross section are listed.

Incident Neutron Energy (keV)	Isomeric Ratio $\sigma^{g}_{n,\gamma}/\sigma_{n,\gamma}$				$\sigma_{n,\gamma}$ (barn)	$\sigma_{n,f}$ (barn)	σ_{tot} (barn)
	Collective Transitions		Single Particle Transitions				
	E_{cut} =.581 MeV	E_{cut} =.29 MeV	E_{cut} =.581 MeV	E_{cut} =.050 MeV			
1	.76	.71			10.5	.065	24.6
10	.76				3.36	.020	15.8
30	.75	.69	.73	.5	2.39	.015	13.9
100	.74				1.50	.015	11.6
200	.74				1.08	.021	11.5
400	.72				.68	.057	8.8
600	.71				.52	.18	8.4
800	.67				.40	.55	7.6
1000	.65				.29	1.15	7.2
THERMAL $J^{\pi}= 2^{-}$	.84		.82				
THERMAL $J^{\pi}= 3^{-}$	.71		.68				

Also in this case (compare columns 2 and 3 in Table VI) there is no significant effect on the results for IR. The same is found for a variation of the spin distribution for the continuum levels in Am-242. By reducing the spin cut-off factor by a factor 2 and by readjusting the residual parameters correspondingly the calculation for 30 keV incident neutron energy agreed to better than 0.5 % with the value in column 2 of Table V. The third possibility, however, appeared to be of great influence

on IR. If we reduce E_{cut} to 0.05 MeV, that means, if we neglect all low lying levels in Am-242 above the isomeric state, then IR is decreased by 35 %. This reflects that the isomeric ratio is mostly determined by the properties of low lying levels. From the above variations of relevant parameters we estimate a 10 % uncertainty for the calculated isomeric ratio.

An estimate of the isomeric ratio at thermal energy (IR_{TH}) has been attempted assuming that s-wave capture dominates at that energy. Accordingly, thermal neutron capture is expected to be a composition of contributions from the tails of several s-wave resonances. Therefore, IR_{TH} can be guessed from values $IR^{J\pi}$ calculated in the keV region with quantum characteristics $J;\pi$ equal to those of the contributing resonances.

It was shown in Ref. 6 that pure s-wave capture only depends (except for a multiplying factor) on the ratios of the total radiative width and the level spacing $\Gamma_f^{J\pi}/D^{J\pi}$. This implies that in calculating $IR^{J\pi} = \sigma_{n,f}^{J\pi} / \sigma_{n,f}^{J\pi}$ for given J, π, the multiplying factors (carrying an incident energy dependence) cancel out. Therefore IR is expected to be determined by the ratio between the probability for gamma-ray stories for each J,π ending at the groundstate and the total radiative width of that J,π. The present Am-241 calculations (which were arbitrarly performed at 1 keV) yielded IR_{TH}^{3-} =.71 and IR_{TH}^{2-} =.84. In view of the experimental value IR_{TH} =.9 this provides some evidence for a 2^- resonance dominating at thermal energies.

In Fig. 2 our experimental and theoretical results for the isomeric ratio IR are displayed together with those calculated by Mann and Schenter [29]. In comparing our calculated isomeric ratio with the thermal value of Ref. 30 we find a significant difference not only in the absolute values but in particular in the relative magnitudes of IR for spin 2 and 3. In our calculations IR($J,\pi = 2^-$) appears to be larger than for

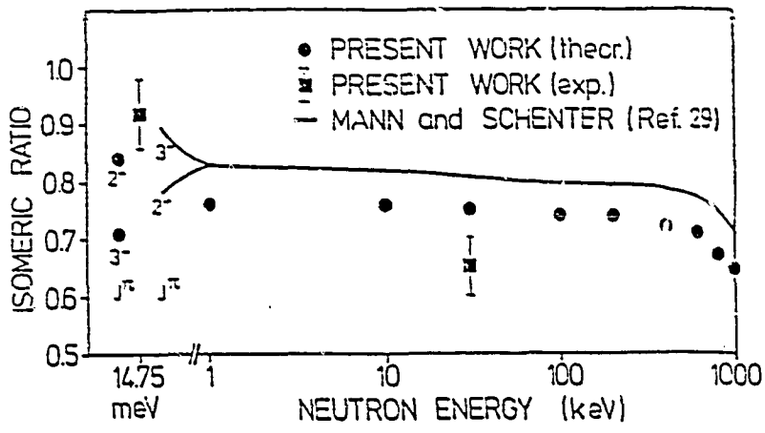

Fig. 2

IR ($J^{\pi}=3^{-}$) which seems to be plausible because the isomeric state has spin 5 and therefore $\sigma^{m}_{(n,\gamma)}$ is likely to be higher for spin 2. In turn, this would explain the larger value of IR for J=2. Another hint in favour of this result comes from the calculated average multiplicity where we find a slightly higher value ($\bar{m}$ =4.9) for spin 2 than for spin 3 ($\bar{m}$ =4.7). The same conclusion may also be drawn by application of the graphical method of Wetzel and Thomas (Ref. 31). Quantitatively, the agreement between measured and calculated values is satisfactory at thermal energy our theoretical value being 7% lower than the experimental results.

At fast neutron energies we find an almost identical energy dependence of IR compared to Ref. 29. However, our results are systematically lower and within the quoted uncertainties they agree with the experimental point at 30 keV. It is interesting to note, that we obtain even smaller isomeric ratios if we use different assumptions on the level scheme or the gamma decay of the compound nucleus.

The calculations of Ref. 29 were carried out with a theoretical level scheme which was derived from the Nilsson model and with the assumption of single particle state transitions for the gamma decay. It should be noted that the resulting sequence of level energies as well as spin and parity assignments

differ considerably from the more recent evaluation in Ref. 32. This might be one reason for the systematic discrepancy between our two calculations. In spite of these differences, apparently both calculations predict a less pronounced decrease of IR between thermal and fast neutron energies as it follows from the experimental results.

This discrepancy is more disturbing as our calculations were found to be remarkably stable against the variation of most significant parameters. Further improvements of the calculation might not be possible until more experimental information on the level scheme and on gamma branching ratios of the compound nucleus Am-242 become available.

4.2 Total Capture Cross Section

The numerical results for the total neutron capture cross section of Am-241 are given in column 6 of Table V.

In Fig. 3 the results for the total capture cross section are compared to experimental and theoretical information from literature. As can be seen the measured capture cross sections [30,33,34] of Am-241 are well described by the present calculations.

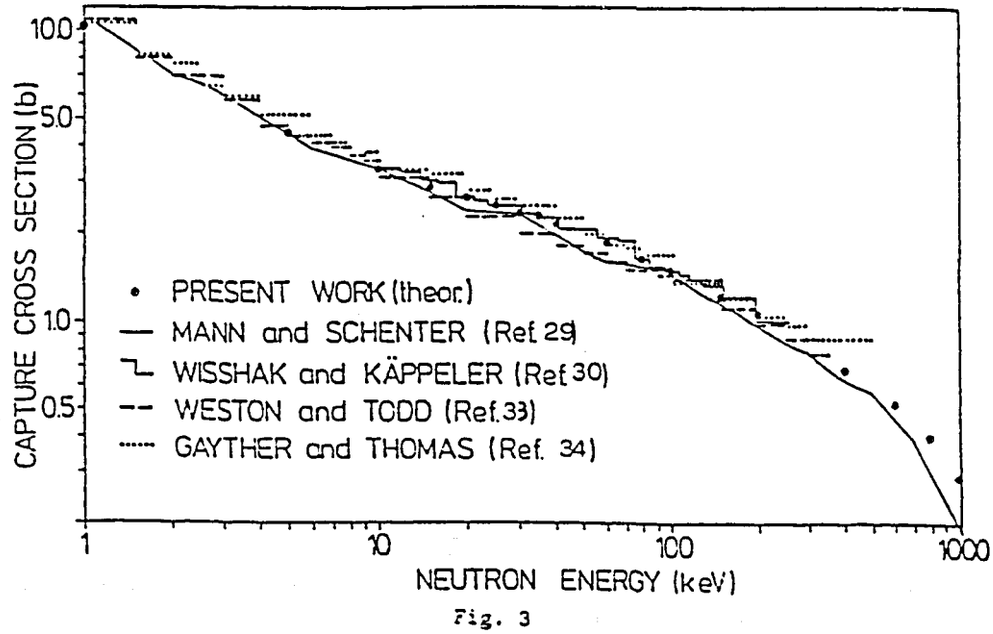

Fig. 3

Only the values of Ref. 33 are lower by 10% between 20 and 80 keV neutron energy. We find also good agreement with the calculations of Mann and Schenter[29] up to .600 MeV neutron energy. At higher neutron energies the cross sections of Ref. 16 start to diverge from our results leading to a 30% discrepancy at 1.0 MeV. A possible reason might be that the target level density was overestimated by Mann and Schenter. We obtain lower cross sections, too, if the low lying collective levels are not excluded in the determination of the level density in Am-241.

The total neutron cross section and the fission cross section of Am-241 are in excellent agreement with recent measurements[17].

The calculated cross sections for U and Pu isotopes are given in Table VI.

Table VI
Calculated Total and Neutron Radiative Capture Cross Sections (b)

Isotope and Quantity	Energy (keV)				
	1	10	50	100	200
^{235}U					
$\sigma_{n,\gamma}$	4.20	0.83	0.37	0.22	0.16
σ_T	24.9	15.77	13.17	12.14	10.76
^{240}Pu					
$\sigma_{n,\gamma}$	4.0	1.18	0.61	0.35	0.25
σ_T	22.93	15.09	13.05	12.22	11.00
^{242}Pu					
$\sigma_{n,\gamma}$	3.60	1.03	0.47	0.26	0.18
σ_T	25.52	15.89	13.31	12.35	11.06

The total cross sections for U-238 and Pu-240 agree well with the measurements by Poenitz et al.[18] For Pu-242 our results lie between the optical model calculations of Poenitz et al.[18] and those of Lagrange and Jary[35], being very close to the latter. The neutron capture cross sections, for U-238 are 4 to 5% higher than the evaluation of Poenitz[18]; however, this discrepancy is not significant in view of the spread of the quoted D_{OBS} values (see Table I). For Pu-240 and Pu-242, no significant discrepancies were found between the present calculations and existing measurements (see Fig. 4).

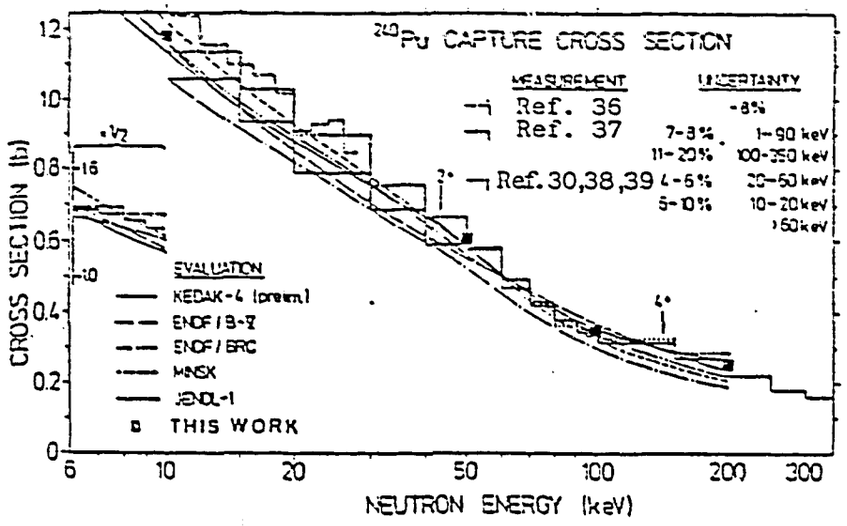

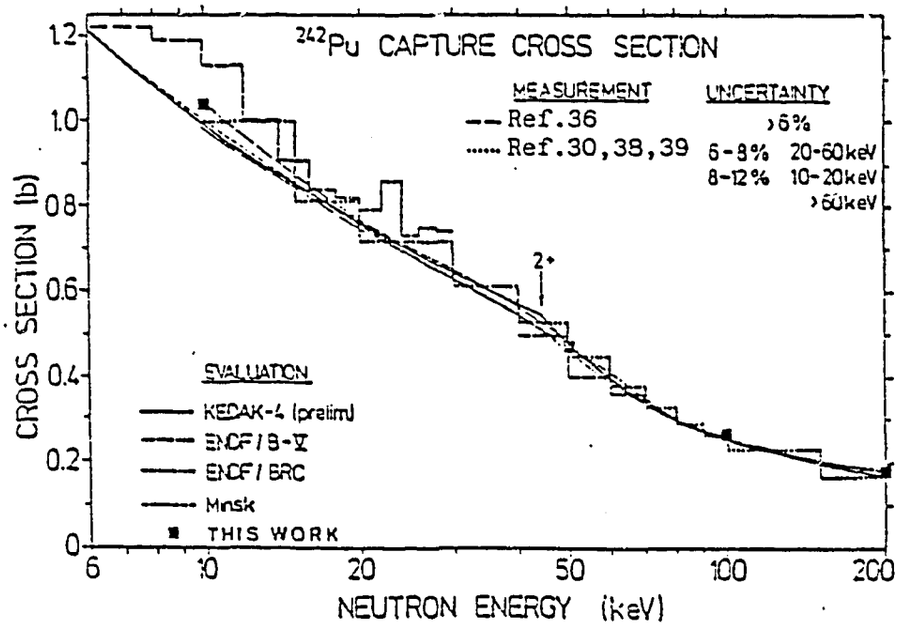

Fig. 4

4.3 Gamma ray cascade multiplicities

The calculation of the capture gamma ray spectra allowed also for the determination of the multiplicity m of the gamma ray cascade. Such an information is a very important one for the design and use of advanced gamma-ray detectors which will allow to improve considerably n-capture cross section measurements. It has been found that a maximum multiplicity m=7 accounted for 98-99% of the total neutron capture cross section at all

energies investigated. Partial capture cross sections $\sigma_{n,m\gamma}$ for multiplicity m were also calculated at all energies and gave for Am-241 an average $\langle m \rangle = \sum_m m \cdot \sigma_{n,m\gamma} / \sigma_{n,\gamma}$ between 4.7 and 4.9 in the energy range considered.

Results of detailed calculation of U-238 and Pu-240,-242 isotope are given in Table VII.

Table VII

Calculated Capture Cross Sections σ_m for Various Multiplicities*

	Calculated Capture Cross Sections, σ_m (b)		
	^{238}U	^{240}Pu	^{242}Pu
Multiplicity	E_n = 100 keV		
1	0.00054	0.0010	0.0
2	0.0111	0.0181	0.0082
3	0.0532	0.0834	0.0489
4	0.0834	0.1317	0.0916
5	0.0519	0.0858	0.0741
6	0.0142	0.0260	0.0299
7	0.0015	0.0037	0.0065
$\sum_1^7 \sigma_m$	0.216	0.350	0.260
$\sigma_{n,\gamma}^{tot}$	0.220	0.350	0.260
$\langle m \rangle$	4.0	4.1	4.4

*Their sum is compared to the total capture cross section determined by Hauser-Feshbach calculations. The average multiplicity $\langle m \rangle$ is given at the bottom of the table.

4.4 Capture gamma ray spectra

The calculation of the capture gamma-ray spectra showed that a large amount of the total neutron capture cross section could be accounted for if only E1 transitions were allowed for the decay from continuum to continuum and from continuum to discrete levels. However, at the low neutron energies considered here, mainly compound states with low spin are populated. In this case the interplay of gamma-ray multiplicities and selection rules for E1 transitions does not allow feeding the large number of discrete high spin levels into the compound

nuclei considered. Therefore some of the cascades are lost because they end in continuum levels from which no E1 transition to a discrete level is possible. This difficulty was overcome after E2 and M1 transitions were included in the model. As for E1 transitions, a giant resonance model for E2 and M1 transitions was assumed that was characterized by empirical estimates-based on the work of Bertrand [10] and Bergqvist [11] for the peak energies

$$E_R(E2)=63\ A^{-1/3}.\mathrm{MeV}$$
$$E_R(M1)=46\ A^{-1/3}.\mathrm{MeV}$$

and the half maximum widths were assumed.

$$\Gamma_R(E2)=0.3E(E2)$$
$$\Gamma_R(M1)=0.2E(M1).$$

Assuming that one type of transition dominates, the peak cross sections, σ_R, cancel out in the calculation of branching ratios. In Fig. 5 the calculated capture gamma-ray spectra at E =100 keV are shown. The dashed curves represent the contribution of E1 transitions to the total spectrum. As one can see, inclusion of E2 and M1 transitions does not change the spectrum shape significantly.

In the spectra for Pu-240 and Pu-242, we find pronounced dips around 1-MeV gamma-ray energy. These structures might be unphysical effects that could not be avoided because only a few known discrete levels were available for these isotopes. It is shown in Section 5. at the example of Au-197 (Ref. 2) that the soft part of the spectrum was considerably modified when the experimental information was replaced by a statistical treatment of the low-lying levels.

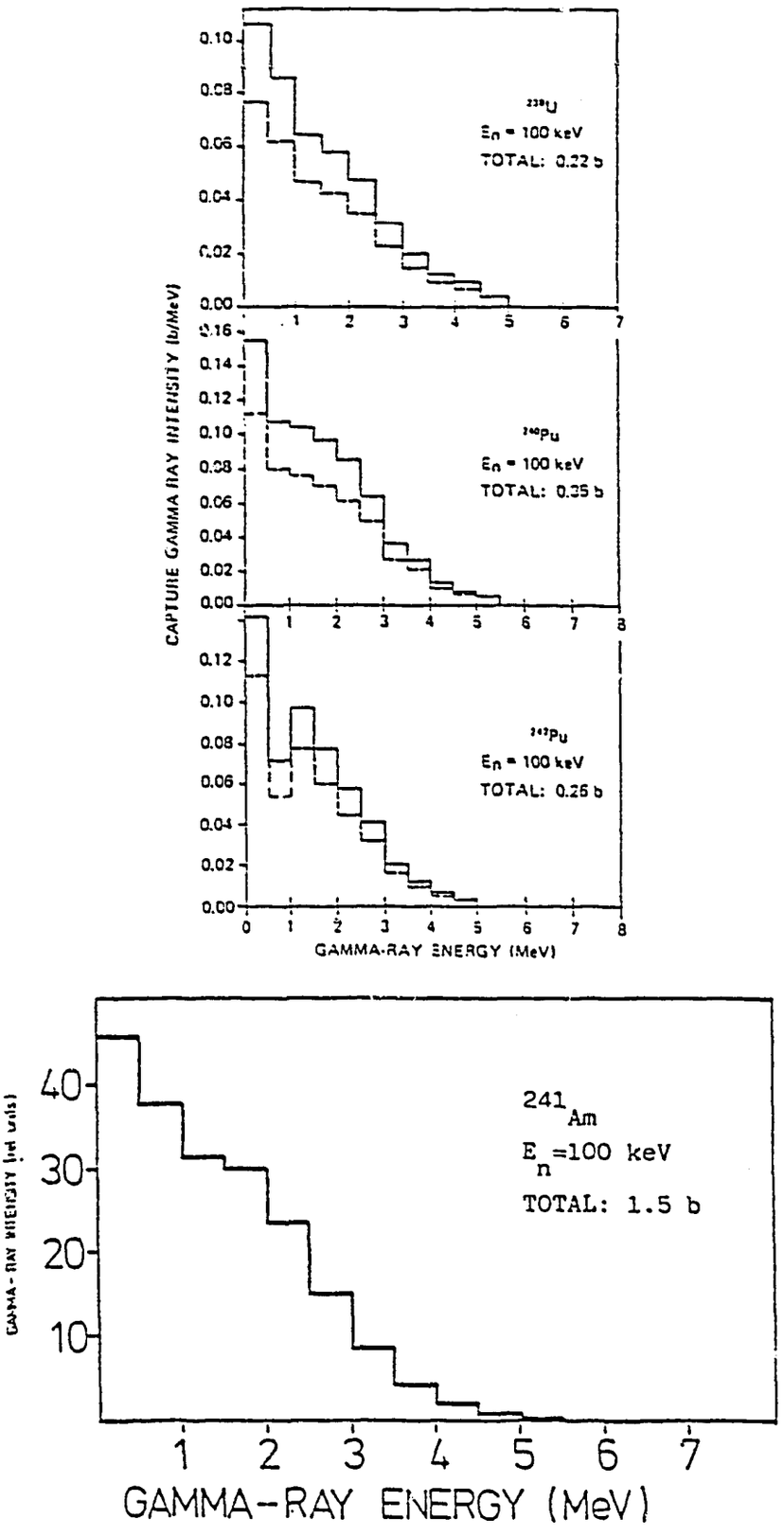

Fig. 5 - Theoretical gamma ray spectra for neutron capture in U-238, Pu-240, -242 and Am-241 at E_n=100 keV. The dashed curves represent the contribution of E1 transitions to the total spectrum.

5. Role of relevant parameters

5.1 Optical model parameters

The optical model affects especially those calculations (like for IR determination) where the population probability of initial levels of given spin plays an important role and may be strongly influenced by the relative magnitude of strength functions.

5.2 Giant resonance parameters (GRP)

GRP are involved only in the decay of continum levels, where in most cases only one type (among E1, M1, E2) of transition dominates in each branching ratio. M1 or E2 transitions play their role when the other two types are forbidden. As a consequence, Lorentzian curve parameters do not greatly influence these calculations because they all tend to cancel out in the gamma-ray branching ratios, whenever gamma-ray energies are smaller than the giant resonance peak energy.

For higher emitted gamma-ray energies only peak energy (which is the best known) is expected to affect calculations.

5.3 Level density parameters

The result of gamma-ray cascade calculations greatly depends on the level density and level schemes adopted.

In spite of the encouraging success of recent investigations (especially BCS), the corresponding model parametrizations do not yet offer the same confidence level as the model and the systematics [7] here adopted. The validity of this approach has been recently discussed in Ref. 40.

The effect of the spin distribution of level density was tested on Am-241 calculations, by reduction of the spin cut off factor of 2. This produced only slight effects with a shift of the spectrum toward the soft part. In addition, an increase in IR of 5% was observed.

As far as the low energy region is concerned large difficulties arise where discrete level information is missing (like energy levels, their quantum characteristics or branching ratios).

In the case of the spectrum for gold which is a very well known one, we have investigated the impact of certain level scheme assumptions: (i) all known levels (28, at all, up to .571 MeV) are neglected, and replaced by the level density treatment; (ii) all discrete levels have been included, but experimental branching ratios are replaced by theoretical estimates according to sec. II.

The resulting spectra, dashed and dotted histograms, respectively, are given in Fig. 6 together with the result of the standard calculation, full line.

As can be observed from the figure, hypothesis i) is much too crude and introduced severe changes in the energy trend of the spectrum. On the contrary hypothesis ii) does not appreciably influence the final result.

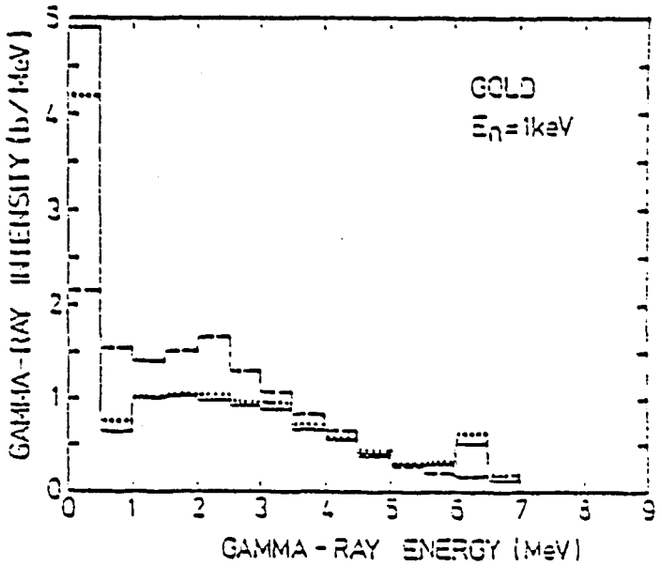

Fig. 6

The influence of the discrete level scheme on isomeric ratio calculations has been investigated in Am-241 at 30 KeV, where a value IR=.75 is obtained from standard calculations.

Skipping half of the discrete levels we got IR=.69, while, by skipping the complete level scheme we obtained IR=.5 (see Table V).

No significant difference was observed through replacing E2 collective transition probabilities by E1, M1 single particle transition probabilities (see Table V).

5.4 Effect of width fluctuations

It was assumed that width fluctuations effects influence only the primary gamma-ray spectrum. An investigation of the width fluctuation correction on the primary gamma-ray spectrum leads to the conclusion that (exception made for very weak transitions, which are strongly enhanced) single transition probabilities are affected by correction factors very close to that of the corresponding integral cross section.

Thus the whole primary spectrum is uniformly shifted by width fluctuation correction factor.

5.5 Energy dependence of gamma-ray intensities

Essentially one has three types of energy dependences for E1 transitions:

i) E^3, according to Blatt-Weisskopf single particle transitions.

ii) E^5, according to Brink-Axel.

iii) E^7, according to Dover et al.[41], Arenhovel et al.[42], Gardner et al.[43].

Recently, McCullagh et al.[44] found experimental evidence for an $E^{5.5}$ energy dependence, while Raman[45] verified that the validity of the Brink-Axel hypothesis has only a few exceptions.

The impact of the above three assumptions has been investigated in the total spectrum calculation of gold where measurements are available from Ref. (46). To this end Fig. 20 of Ref. [43] is here reproduced as Fig. 7, where we have plotted, for comparison, our results (hystograms).

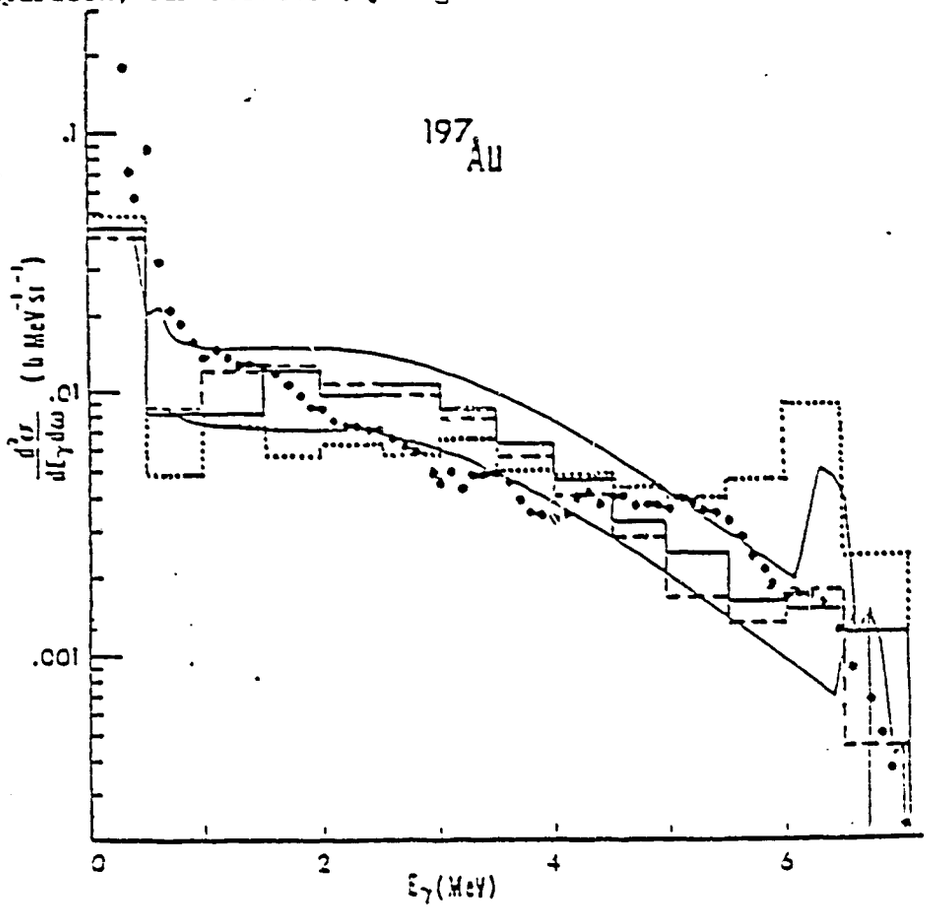

Fig. 7

The data in Fig. 7 correspond to the following incident neutron energies: the experimental ones are measured in the interval .2÷6. MeV, the two full line curves have been calculated[43] at .2 and .6 MeV, respectively while tne hystograms at .4 MeV. (It should be noted that the spread of neutron energies, ΔE=.4 MeV, may affect the comparison of present calculations especially in the last hystogram step).

One observes that the spectrum from our E^{5} -calculation, full line hystogram, well agrees with the Gardner et al.[43] spectrum, except for the hard part. This seems in contradiction with the wrong trend of the E^{7}- calculation (dotted hystogram) which clearly favours the hard tail against the soft one, as expected.

Except for the hard tail of the spectrum, no remarkable difference is observed between E^{5} - and E^{3} - calculations (dashed hystograms).

On the whole, one may conclude on the better results of the E^{5} - law, in agreement with the mentioned experimental investigations of Refs. 44 and 45.

As far as M1 and E2 transitions are concerned, there is not sufficient information for a more than tentative treatment.

Finally, it must be noted that only the Brink-Axel approach allows for absolute calculations of $\Gamma_{\gamma}(B_n, J, \pi)$, as shown in Refs. 5 and 6, provided correct parameterization is adopted for both the level density and Lorentz-curve.

5.6 Effect of gamma branchings of discrete levels in IR calculations

In order to determine the isomeric ratios $\sigma^{g}_{n,\gamma}/\sigma_{n,\gamma}$ the cross section $\sigma^{g}_{n,\gamma}$, $\sigma^{m}_{n,\gamma}$ for excitation of the ground and metastable states were calculated separately. This type of calculations requires spins and parities of the discrete levels as well as the gamma-decay scheme and the branching ratios for the gamma-decay scheme and the branching ratios for the gamma-decay between discrete levels. Unfortunately, in the case of Am-242 all these decay parameters were not always available. In view of this difficulty gamma decay schemes and branching ratios were guessed for all discrete levels up to .580 MeV using the two extreme assumptions of pure collective state transitions, characterized by dominant E2 transitions and pure single particle state transitions which are characterized by dominant M1 transitions. As one can see from Table V, no remarkable difference is observed between the results of the two extreme assumptions adopted.

6. Use of Total capture gamma ray spectra for the correction of Neutron Capture Cross Section Measurements

In recent years, Moxon-Rae detectors in connection with kinematically collimated neutrons from the ^{7}Li(p,n) or the T(p,n) reaction and very short flight paths proved to be a suitable method to measure capture cross sections of highly radioactive actinide samples. Measurements have been performed for Pu-240, ^{242}Pu, and ^{241}Am, using ^{197}Au and ^{238}U as standards.(1,2,3,30,38,39)

As the efficiency of the Moxon-Rae detector deviates slightly from the ideal shape, which linearly increases with gamma-ray energy, these measurements are affected by a systematic uncertainty.

Correction of deviations of the Moxon-Rae efficiency from the ideal shape requires knowledge of two quantities: (i) the shape of the capture gamma-ray spectrum of sample and reference sample and (ii) the shape of the efficiency curve for the particular converter material.

Usually in the relative neutron capture measurements by use of Moxon-Rae detectors, it is supposed that the shape of the neutron capture gamma ray spectrum is the same both for the target and the standard.

In Refs. 1,2,3 as well as here the shape shown for the spectra of Au-197, U-238 standards and of Am-241, Pu-240, Pu-242 indicates that this assumption is correct only for those measurements that were carried out relative to U-238 as a standard, while the shape of the capture gamma ray spectrum of gold differs significantly from those of the actinide isotopes investigated. The gold spectrum shows a strong soft component (below 500 keV) and also a sizable hard component (above 6 MeV). Therefore, in relative measurements with gold as a standard, the correction due to deviations of the detector efficiency from a linear increase with gamma ray energy must be considered explicitly.

The results of Ref. 1,3 show that, for a Moxon-Rae detector with graphite converter and U-238 as a standard, the

correction due to deviations of the detector efficiency from a linear increase with gamma ray energy is < 1%. However, for the isotopes investigated here, a correction factor of ~ 3% has to be applied if a gold standard is used (see Table VIII).which results in a reduction of ~ 50% of the total measurement uncertainty.

Table VIII

Correction Factors K for Our Previous Capture Cross-Section Ratios $^{240,242}Pu$ Versus ^{197}Au and ^{238}U*

Cross-Section Ratio	Correction Factor K
$^{240}Pu/^{197}Au$	0.973
$^{240}Pu/^{238}U$	0.995
$^{242}Pu/^{197}Au$	0.978
$^{242}Pu/^{235}U$	1.000
$^{238}U/^{197}Au$	0.978
$^{241}Am/^{197}Au$	0.973

7. Conclusions

Statistical model calculations using an advanced code and carefully evaluated parameter sets proved to reproduce satisfactorily the experimental data for integral and differential quantities characterizing (n,gamma) capture process.

Spectra and IR calculations are valuable in view of the need for them in a number of applications and of the measurement difficulty in the fast neutron energy region.

Recently, spectra calculations offered appreciable help in correcting systematic errors of relative neutron radiative capture measurements made with Moxon-Rae detectors.

A number of recent experiment proves tha validity of basic assumptions adopted for the energy dependence of gamma ray intensities.

A weak point of these calculations remains however the determination of reliable level schemes and inherent gamma ray branchings when these are not measured. In fact, the considerable theoretical efforts in these directions proved very useful

in understanding nuclear structure, but cannot yet replace all cases where experimental information is missing. A possible improvement of present calculations may be obtained by the introduction of considerations of rotational bands in order to fill the gaps in level schemes and introducing K-selection rules in the gamma ray transitions.

Further improvements in the calculations might be possible as soon as more detailed information on level scheme and gamma branching ratios of the investigated nuclei becomes available.

In view of these difficulties, stress should be laid on the need for experts to provide cross section evaluators with appropriate level schemes, at least for the cases of recognized interest.

References

1) Wisshak K., Wicknehauser J., Kaeppeler F., Reffo G., Fabbri F., Nucl. Sc. Eng. 81 (1982), 396.

2) Reffo G., Fabbri F., Wisshak K., Kaeppeler F., Nucl. Sc. Eng. 80 (1982), 630.

3) Reffo G., Fabbri F., Wisshak K., Kaeppeler F., Nucl. Sc. Eng. 83 (1983), 401.

4) Wisshak K., Kaeppeler F., Reffo G., Fabbri F., Nucl. Sc. Eng. 86 (1983), 168.

5) Benzi V., Reffo G., Vaccari M., IAEA Report 169, 123 (1974).

6) Reffo G., IAEA Report SMR-43(1980) p.205. Lecture held at the "Winter Course on Nuclear Physics and Reactors" at ITCP Trieste, 17 Jan.- 10 Mar. 1978.

7) Reffo G., "Theory and Applications of Moment Methods in Many Fermion Systems", edited by B.J. Dalton, S.M. Grimes, J.P. Varey, S.A. Williams, Plenum Press, New York 1980.

8) G. Maino, E. Menapace, Contributed paper to the Advisory Group Meeting on Basic and Applied Problems of Nuclear Level Densities. Report BNL-NCS 51694 (June 1983, pag. 75).

9) Kopecki J., Proc. of the 4th (n,) Int. Symp., Grenoble 7-11 Sept. 1981, pag. 423. Inst. of Phys. Conf. Series n. 62. Bristol and London.

10) Bertrand F.E., "Giant Multipole Resonance, an Experimental Review", Proc. Conf. Nuclear Structure and Ion Collisions, E.Fermi International School of Physics,July 9-21,1979, Varenna,Italy, p.620,North Holland Publishing Company (1981).

11) Bergqvist I., Proc. IAEA Consultant Mtg. Use of Nuclear Theory in Neutron Data Evaluation, December 8-12, 1975, IAEA-190, Vol.2, p.29, IAEA (1976).

12) Reffo G., Fabbri F., Gruppelaar H., Nuovo Cimento Lett., Vol. 17, n. 1 (1976) pag. 1.

13) Gruppelaar H., Reffo G., Nucl. Sci. Eng. 62 (1977) 756.

14) Reffo G., Fabbri F., Nucl. Sci. Eng. 66 (1978), 251.

15) Reffo G., Fabbri F., IDA Modular System (not to be published).

16) Madland D.G. and Young P.G., Proc. Int. Conf. Neutron Physics and Nuclear Data for Reactors and Other Applied Purposes, Harwell, United Kingdom, Sept. 25-29, 1978, p.349, Organization for Economic Cooperation Development, Nuclear Energy Agency (1978).

17) Phillips T.W. and Howe R.E., Nucl. Sci. Eng. 69, 375 (1979).

18) Poenitz W.P., Whalen J.F. and Smith A.B., Nucl. Sci. Eng., 78, 333 (1981).

19) Froehner F.H., Private Communication (1981).

20) de Saussure G., Private Communication (1981).

21) Weigmann H., Proc. IAEA Consultants' Mtg. U and Pu Resonance Parameters, Vienna, Austria, September 28-October 2, 1981, INDC(NDS)-129/GJ, p.112, IAEA (1982).

22) Wisshak K., Kaeppeler F., Froehner F.H. and B. Goel, Proc.IAEA Consultants'Mtg. U and Pu Resonance Parameters, Vienna, Austria, September 28-October 2, 1981, INDC(NDS)-129/GJ, p.165, IAEA (1982).

23) Menapace E., Motta M., Ventura A., Proc. Specialists' Mtg. Nuclear Data of Plutonium and Americium Isotopes for Reactor Applications, Upton, New York, November 20-21, 1978, BNL-50991, NEANDC-L-116, R.E. Chrien, Ed.,Brookhaven National Lab.,Upton,New York.

24) Fort E., Private Communication (1980).

25) Maslov V.M., Antsipov G.V. and V.A. Konshin, Proc. IAEA Consultants' Mtg. U and Pu Resonance Parameters, Vienna, Austria, September 28-October 2, 1981,INDC(NDS)-129/GJ, p. 329, IAEA (1982).

26) Lynn J.E., "Systematics for Neutron Reactions of the Actined Nuclei", AERE Report R7468 (1974). AERE, Harwell, United Kingdom.

27) Hage W., Wisshak K., Kaeppeler F., accepted for publication in Nucl. Sci. Eng.

28) Knitter H.H., Budtz-Jørgensen C., Conf.on Neutron Physics and Nuclear Data for Reactors and Other Applied Purposes, Harwell, United Kingdom, 25-29 Sept. 1978, p.899.

29) Mann F.M. and Schenter R.E., Nucl. Sci. Eng. 63 (1977) 242.

30) Wisshak K and Kaeppeler F., Nucl. Sci. Eng. 76 (1980) 148.

31) Wetzel K.J. and Thomas G.E., Phys. Rev. C1, 1501 (1970).

32) Lederer C.M. and Shirley V.S., Ed., Table of Isotopes, 7th Edition, John Wiley and Sons, Inc., New York, 1978.

33) Weston L.W. and Todd J.H., Nucl. Sci. Eng., 61, 356 (1976).

34) Gayther D.B. and Thomas B.W., Proc. of the 4th All-Union Conference on Neutron Physics, Kiev, USSR, April 18-22, 1977, Vol. III, p. 3 and private communications (1977).

35) Lagrange C. and Jary J., "Coherent Optical and Statistical Model Calculations", INDC(FR)-30/L, INDC/IAEA (1978).

36) Hockenbury R.W., Moyer W.R., Block R.C., Nucl. Sci. Eng. 49 (1972), 153.

37) Weston L.W. and Todd J.H., Nucl. Sci. Eng. 63 (1977) 143.

38) Wisshak K. and Kaeppeler F., Nucl. Sci. Eng. 66, 363 (1978).

39) Wisshak K. and Kaeppeler F., Nucl. Sci. Eng. 69, 39 (1979).

40) Reffo G., "Limits and Validity of the Phenomenological Gilbert-Cameron Level Density Approach. Invited paper at the IAEA Advisory Group Meeting on "Basic and Applied Problems of Nuclear Level Densities", Brookhaven Nat. Lab. (USA), April 11-15, 1983.

41) Dover C.B., Lemmer R.H., Halme F.J.W., Ann. Phys. (N.Y.) 70 (1972) 458.

42) Arenhovel H., Grainer W., Danos M., Phys. Rev. 157 (1967), 109.

43) Gardner D.G., Gardner M.A., Dietrich F.S., Report UCID-18759, August 7, 1980 and in Nuclear Cross Sections for Technology, edited by J.L. Fowler, C.H. Johnson and C.D. Bowman (NBS Special Publication No. 594), Washington, D.C., 1980.

44) McCullagh C.M., Stelts M.L., Chrien R.E., Phys. Rev. 23, 1394, (1981).

45) Raman S., invited paper at IV Int. Symposium on Neutron Capture Gamma-Ray Spectroscopy and Related Topics, Sept. 7-11, 1981, Grenoble.

46) Morgan G., Newman E., Report ORNL-TM-4973, August 1975.

Contributed Paper 13

INTERCOMPARISON OF DIFFERENT EVALUATIONS IN VARIOUS FORMATS FOR THE SAME MATERIALS

A. TRKOV, M. BUDNAR, A. PERDAN
Institute Jožef Štefan,
E. Kardelj University,
Ljubljana, Yugoslavia

Abstract

The principle of data intercomparison is discussed. As an example group constants are generated for Am-243 and U-235 from all available recent evaluated files that we could process. The discrepancies are summarized and discussed briefly.

Acknowledgement

This work was supported by the International Atomic Energy Agency as part of the Coordinated Research Program on the Validation and Benchmark Testing of the INDL/A Actinides Library under Research Agreement No.3691/RB.

1. INTRODUCTION

Several evaluated nuclear data libraries of various origins are available. A user who is not restricted by format to a particular data library is in great pain to decide which evaluation to use for his purpose. The evaluations do differ from one another. Usually the discrepancies can be traced to the large scattering of experimental data and sometimes to a more rigorous evaluation approach in certain data types and energy ranges, depending on the final purpose of the evaluation. Before one can decide on what evaluation to use it is no doubt useful to know what is the difference between them.

2. THE PRINCIPLE OF DATA INTERCOMPARISON

For the time being let us limit ourselves to the simple energy dependent parameters - usually the cross-sections. The most obvious way of intercomparing the data would be to generate pointwise files from all the data and plot them together with their ratio. However there are a number of serious drawbacks with this approach:

(i) Evaluations in ENDF format could be handled at present but the available software can not handle other formats;

(ii) Due to the resonances a problem of presentation would arise. There is a danger that in the large mass of information the important discrepancies would be overlooked;

(iii) If the discrepancies were small a fine tool for performing the intercomparisons would be necessary, but as it will be seen later the discrepancies remain surprisingly large even after averaging the data over fairly wide energy ranges.

From the above considerations it was decided to perform the intercomparisons of data in group constant form. Monitoring the discrepancies in such a way has a further advantage that the effects on the calculations which use the group constants as input can be stipulated.

3. THE CHOICE OF THE GROUP CONSTANTS ENERGY MESH

The ideal group constants set should have an energy mesh which would have:

a) sufficiently high range in the fast energy region (at least a few groups above 10 MeV),
b) sufficient resolution in the thermal energy region (at least a few groups below 1 eV),
c) reasonably small number of groups so that an inspection by eye is still possible but without too much loss of detail,
d) some practical usefulness which means that an established group constants scheme would be preferable.

Table 1: The 69-group WIMS energy mesh

GROUP	ENERGY		ENERGY WIDTH	LETHARGY WIDTH
	MeV			
1	10.0	- 6.0655	3.9345	0.49997
2	6.0655	- 3.679	2.3865	0.49998
3	3.679	- 2.231	1.448	0.50019
4	2.231	- 1.353	0.878	0.50013
5	1.353	- 0.821	0.532	0.49956
6	0.821	- 0.500	0.321	0.49592
7	0.500	- 0.3025	0.1975	0.50253
8	0.3025	- 0.183	0.1195	0.50260
9	0.183	- 0.1110	0.072	0.49996
10	0.111	- 0.06734	0.04366	0.49978
11	0.06734	- 0.04035	0.02649	0.49585
12	0.04035	- 0.02478	0.01607	0.49987
13	0.02478	- 0.01503	0.00975	0.49999
14	0.01503	- 0.009118	0.005912	0.49980
	eV			
15	9118.0	- 5530.0	3588.0	0.50006
16	5530.0	- 3519.1	2010.9	0.45198
17	3519.1	- 2239.45	1279.65	0.45198
18	2239.45	- 1425.1	814.35	0.45199
19	1425.1	- 906.898	518.202	0.45197
20	906.898	- 367.262	539.636	0.90395
21	367.262	- 148.728	218.534	0.90396
22	148.728	- 75.5014	73.2266	0.67797
23	75.5014	- 48.052	27.4494	0.45187
24	48.052	- 27.700	20.352	0.55085
25	27.700	- 15.968	11.732	0.55085
26	15.968	- 9.877	6.091	0.48038
27	9.877	- 4.00	5.877	0.90391
28	4.00	- 3.30	0.700	0.19237
29	3.30	- 2.60	0.700	0.23841
30	2.60	- 2.10	0.500	0.21357
31	2.10	- 1.50	0.600	0.33647
32	1.50	- 1.30	0.200	0.14310
33	1.30	- 1.15	0.150	0.12260
34	1.15	- 1.123	0.027	0.02376
35	1.123	- 1.097	0.026	0.02342
36	1.097	- 1.071	0.026	0.02399
37	1.071	- 1.045	0.026	0.02458
38	1.045	- 1.020	0.025	0.02421
39	1.020	- 0.996	0.024	0.02381
40	0.996	- 0.972	0.024	0.02439
41	0.972	- 0.950	0.022	0.02289
42	0.950	- 0.910	0.040	0.04302
43	0.910	- 0.850	0.060	0.06821
44	0.850	- 0.780	0.070	0.08594
45	0.780	- 0.625	0.155	0.22154
46	0.625	- 0.500	0.125	0.22314
47	0.500	- 0.400	0.100	0.22314
48	0.400	- 0.350	0.050	0.13353
49	0.350	- 0.320	0.030	0.08961
50	0.320	- 0.300	0.020	0.06454
51	0.300	- 0.280	0.020	0.06899
52	0.280	- 0.250	0.030	0.11333
53	0.250	- 0.220	0.030	0.12783
54	0.220	- 0.180	0.040	0.20067
55	0.180	- 0.140	0.040	0.25131
56	0.140	- 0.100	0.040	0.33647
57	0.100	- 0.080	0.020	0.22314
58	0.080	- 0.067	0.013	0.17733
59	0.067	- 0.058	0.009	0.14425
60	0.058	- 0.050	0.008	0.14842
61	0.050	- 0.042	0.008	0.17435
62	0.042	- 0.035	0.007	0.18232
63	0.035	- 0.030	0.005	0.15415
64	0.030	- 0.025	0.005	0.18232
65	0.025	- 0.020	0.005	0.22314
66	0.020	- 0.015	0.005	0.28768
67	0.015	- 0.010	0.005	0.40547
68	0.010	- 0.005	0.005	0.69315
69	0.005	- 0.	0.005	-

It is unlikely to be able to find a group constants scheme which would satisfy all the above requirements. On Fig.1 the plots of the radiative capture cross-section of Americium-243 [ref.1-5] on the same scale but in different group constants schemes are presented. The schemes built into the FEDGROUP-C84 [ref.6] package were considered. For the intercomparisons which follow the 69-group WIMS scheme was chosen as the one which requires the smallest compromise from the stated basic requirements.

4. GROUP CONSTANTS INTERCOMPARISON

To simplify the references to individual evaluations the following nomenclature has been adopted:

E5/A	The ENDF/B V Actinides evaluated data library [7]
E5/S	The ENDF/B V Standards evaluated data library [8]
UK-80	The UKNDL evaluated data library released in 1980 [9]
IU	The UK evaluation (DFN-1010) contained in the INDL/A 83 evaluated data library [10]
IU/E4	The same evaluation in ENDF IV format contained in the INDL/A 83 library
IU/E5	The same evaluation in ENDF V format contained in the INDL/A 83 library
IJ/E4	The JAERI evaluation originating from JENDL-2 and contained in the INDL/A 83 library
IK	The KEDAK-4 evaluation contained in the INDL/A 83 library

The averaging spectrum for the group constants calculation is not important as long as the same spectrum is used for averaging all the data. For convenience the "Standard spectrum" built into FEDGROUP-C84 [ref.6] was used.

4.1 Intercomparison of various evaluations for Americium-243

4.1.1 The Total Cross-section with reference to IU/E5

(i) E5/A

In group 1 (see Table 1) the ENDF/B V data are 16% higher. In groups 2 to 21 (5 MeV to 250 eV) the cross section follows a different shape as compared to the other evaluations. Due to the difference in shape of the cross-section the discrepancies of up to 5% are observed in groups 5 to 69 (below 250 eV) as well.
Note that this evaluation agrees with the IJ evaluation below 250 eV (the resolved resonance region) to within 1% .

(ii) UK-80

The evaluation differs from the more recent IU/E5 evaluation most. Above 1 eV the discrepancy reaches 47% . Below 1 eV the discrepancy is larger still (up to 240%) due to the different shape of the cross-section [ref.11]

(iii) IU

This evaluation is generally higher by 1 - 2 % and not more than 3% in the entire energy region. The exceptions are groups 33 to 48 (0.4 - 1.3 eV) where the discrepancy reaches 18% and is particularly high in groups 33, 38, 40, and 48.

(iv) IU/E4

Due to missing resonances with respect to the IU/E5 evaluation discrepancies of up to 1.5% are noted.

(v) IJ

In group 1 the discrepancy reaches 21% . Between groups 10 and 21 (0.2 MeV to 250 eV - including the unresolved resonance region) the IJ evaluation is up to 11% higher. Below 250 eV the same comments apply as for the ENDF/B V evaluation.

(vi) IK

The evaluations agree to within 12% in the entire region. The IK evaluation is up to 12% higher in groups 5 to 20 (1 MeV to 300 eV) and up to 9% lower between groups 43 to 66 (0.9 eV to 0.01 eV).

4.1.2 The Fission Cross-section With Reference to IU/E5

(i) E5, IJ, IK

The evaluations are progressively higher from group 1 to 15 (10 MeV - 5.5 KeV). This trend continues for IJ and IK evaluations up to group 25 (16 eV). Below this energy the cross-sections in the IK, IJ and E5 evaluations approach zero rapidly.

(ii) IU, IU/E4

The conclusion are similar as for the respective evaluations of the total cross-sections.

4.1.3 The Radiative Capture Cross-section With Reference to IU/E5

(i) E5, IJ, IK

Important discrepancies are observed in groups 1 to 21 (10 MeV to 250 eV). Below 250 eV the evaluations agree to within 6% .

(ii) IU, IU/E4

The conclusion are similar as for the respective evaluations of the total cross-sections.

4.2 Intercomparison of various evaluations for Uranium-235

Americium-243 is a secondary actinide so it could be expected that experimental data were scarcely requested. Thus it is not surprising that the evaluations for particular reactions deviate considerably from one another. However the situation with an important primary actinide such as Uranium-235 is not unambiguous either.

The ENDF/B V Standards (denoted E5/S) evaluation for the fission cross section of U-235 is a standard so this evaluation was chosen arbitrarily as the reference to which other evaluations are compared.

4.2.1 The Total cross-section with reference to ES/S

(i) IK

This evaluation is higher in groups 8 to 11 (0.3 MeV to 41 KeV) by up to 5% and in groups 16 to 21 (5 KeV to 150 eV) by up to 14% . The most outstanding is the discrepancy around the 1.1 eV resonance in IK which is slightly higher at the peak but much more narrow. This produces a discrepancy of 29% . The IK evaluation generally agrees much better with the ES/S evaluation than the KEDAK-3 (1979) evaluation [12] except around the 1.1 eV resonance where the differences are larger still.

(ii) IJ

This evaluation is slightly higher (up to 8.6%) almost throughout the resonance region and down to thermal energies (groups 7 to 60, 0.5 MeV to 0.05 eV). Like the IK evaluation the largest discrepancies (8.9%) are observed around the 1.1 eV resonance except that the situation is reversed: the resonance is wider and has a lower peak value than in ES/S.

4.2.2 The Elastic cross-section with reference to ES/S

(i) IK

This evaluation is much higher in the resonance region (28%) and consistently lower by about 18% below 75 eV.

(ii) IJ

The predicted cross-section is smaller in the fast region (14% in group 1, from 10 to 5 MeV). The evaluations agree to within 8% in the resonance region but the IJ evaluation is consistently higher by up to 16% in the thermal region.

4.2.3 The Fission Cross-section with Reference to ES/S

(i) IK

The discrepancy in groups 1-5 (form 10 to 1 MeV) of 1-2 % is in agreement with the uncertainty of the experimental data in this region (5%). In groups 6-10 (from 1 to 0.1 MeV) recent experimental data would indicate a 1-2 % decrease in the ES/S cross-section curve as discussed in [ref.13]. The IK cross-section estimate is on the contrary by 1-2 % higher. (It is interesting to note that the same is true for the IJ evaluation). In the resonance region there are discrepancies in individual groups of up to 11% . They probably result from the difficulty of data representation in the unresolved resonance region. Around the 1.1 eV resonance the same comments apply as for the total cross-section.

(ii) IJ

For the fast and the resonance region the same comments apply as for the IK evaluation. For the region around the 1.1 eV resonance the discussion of the total cross-section is applicable.

4.2.4 The Radiative Capture Cross-section With Reference to ES/S

(i) IK

The differences reach 24% and oscillate over the entire energy region. The agreement around the 1.1 eV resonances is better than for the total and the fission cross-sections.

(ii) IJ

In group 1 (from 10 to 5 MeV) the IJ evaluation is lower by a factor 30 and then rises very sharply to exceed the ES/S value by 130% in group 4 (from 2.2 to 1.3 MeV). This large discrepancy screens all the others which remain within the 27% limit over the remaining energy interval.

4.2.5 The Nu-bar with Reference to ES/S

(i) IK

The agreement between the two evaluations is better than 0.6% over the entire region. It is interesting to note that the IK estimate is consistently lower from group 10 (0.1 MeV) onwards. A constant discrepancy of 0.57% is observed from groups 21 to 69 (From 350 eV to thermal).

(ii) IJ

The nu-bar is higher in the fast region (groups 1-6, from 10 to 0.5 MeV) by up to 1.6% in group 2 and consistently lower below 0.5 MeV. A constant discrepancy of 0.33% is observed from group 20 to 69 (from 900 eV to thermal).

5. CONCLUSIONS

Several recent evaluations were intercompared in group constants form. For calculating the group constants the program FEDGROUP-C84 was used because it can process various formats of evaluated files. The WIMS 69-group structure was used for group constants preparation. The discrepancies between various evaluations were presented. It was noted that the differences between UKNDL evaluations for Am-243 do not occur purely due to different format representation. Another interesting point to note is the discrepancy of about 30% in the KEDAK evaluation for U-235 around the 1.1 eV resonance. There are also some other significant differences between various evaluations. It remains to be explored whether they could have a significant impact on reactor calculations.

REFERENCES

[1] ABBN - Abagyan L.P., Bazazyants N.O, Bondarenko I.I., and Nikolaev M.N., Group Constants for Nuclear Reactors, Consultants Bureau, New York (1964)

[2] GRACE - Z.Szatmary, J.Valko, KFKI-70-14 RPT(1970)

[3] WIMS - Taubmann C.J., AEEW-MI324 (1975)

[4] DLC-2D - RSIC Data Library Collection

[5] SAND II - McElroy W.N. et.al., AFWL-TR-67-41 (1967)

[6] A.Trkov, A.Perdan, M.Budnar: FEDGROUP-C84 - An Improved and Modified CDC Version of the Program for the Calculation of Group Constants in KEDAK, UKNDL and ENDF/B Format, IJS DP-2758, to be published.

[7] ENDF/B V Actinides, Am-243 MAT1363, Hann, Benjamin, Howerton et.al., IAEA-NDS-13(1979)

[8] ENDF/B V Standards, U-235 MAT1395, M.R.Bhat, IAEA-NDS-15(1980)

[9] UKNDL-80, IAEA-NDS-30(1980)

[10] INDL/A-83 Library, IAEA-NDS-12(193)

[11] Compilation of Actinides Neutron Nuclear Data, KDK-35, NEANDC(OR)153/L, INDC(SWD)13/L, SKI 832/78

[12] A.Trkov et.al. Calculation of Multigroup constants in WIMS Format with Programs FEDGROUP and FLANGE and Comparison of Results Obtained Using Different Evaluated Libraries, INDC(YUG)-7 (1982)

[13] V.G.Pronyaev,D.E.Cullen,H.D.Lemmel,Current Problems in the Data Base for a Reevaluation of the U-235 Fission Cross Section in the Fast Neutron Energy Region, IAEA Consultants' Meeting on the U-235 Fast Neutron Fission Cross Section and the Cf-252 Fission Neutron Spectrum, Smolenice, 28 March to 1 April, INDC(NDS)-146

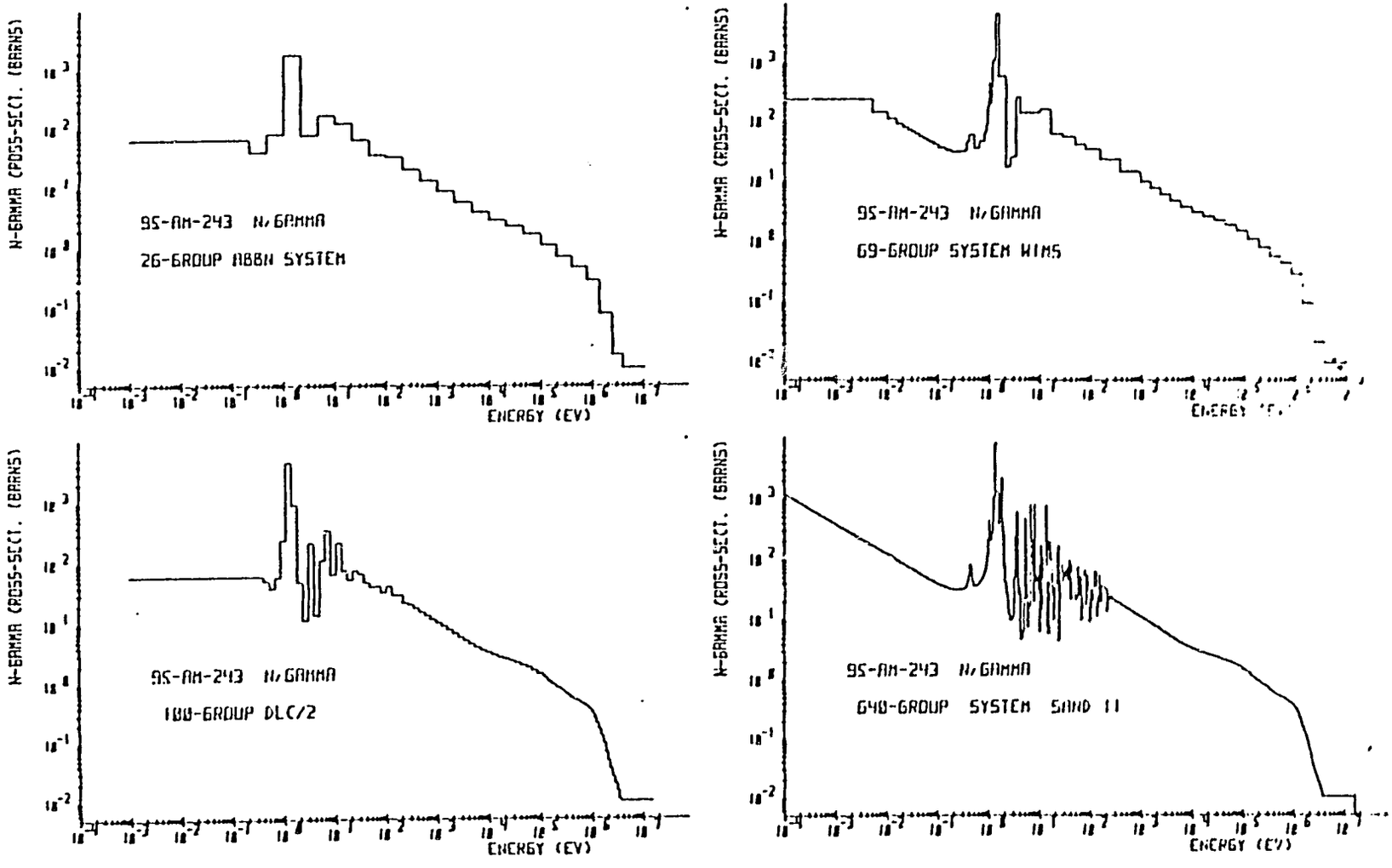

Fig.1 Presentation of Am-243 radiative carture cross-section in various group constants schemes.

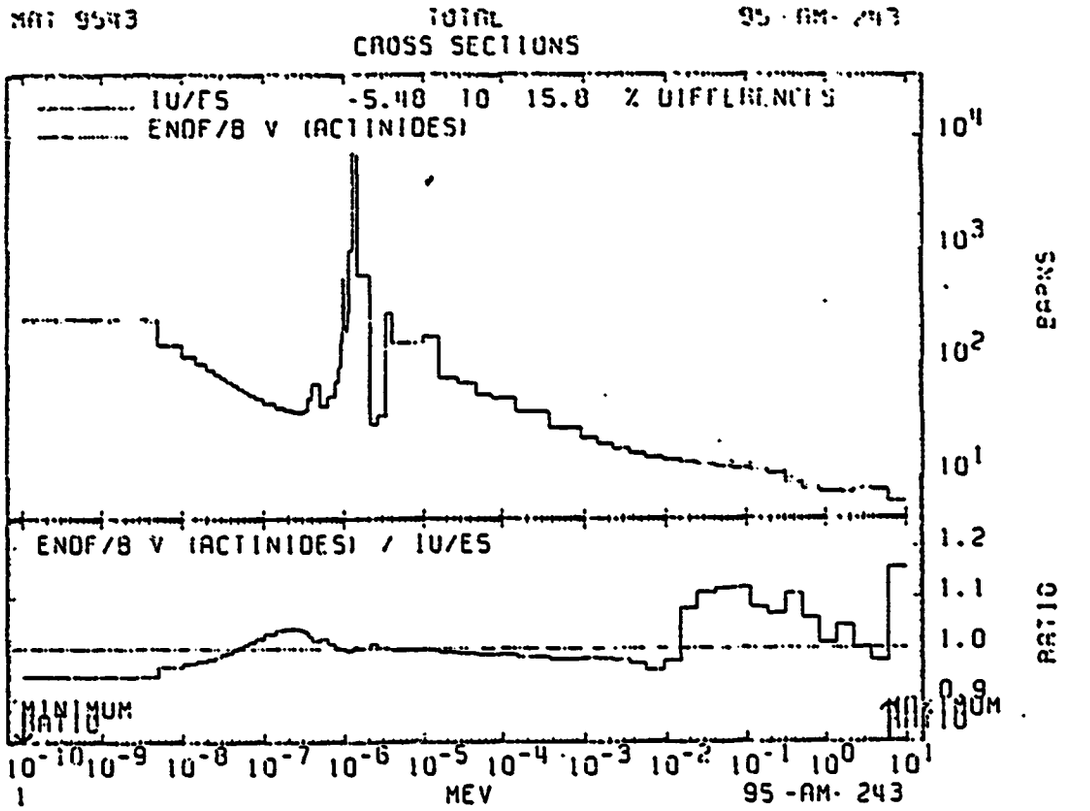

Fig.2 Intercomparison of the total cross-section of Am-243 calculated from UK evaluation in ENDF-5 format contained on the INDL/A file and the ENDF/B V (Actinides) library.

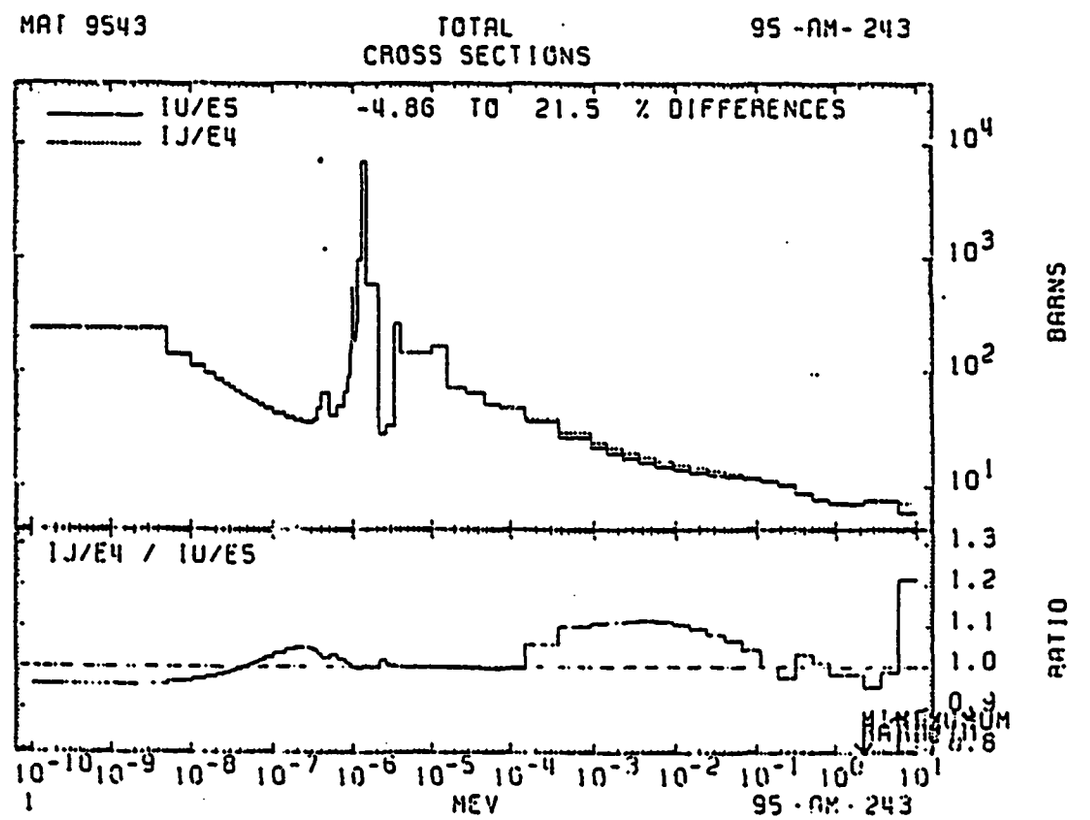

Fig.3 Intercomparison of the total cross-section of Am-243 calculated from UK evaluation in ENDF-5 format and the JENDL-2 evaluation, both contained on the INDL/A file.

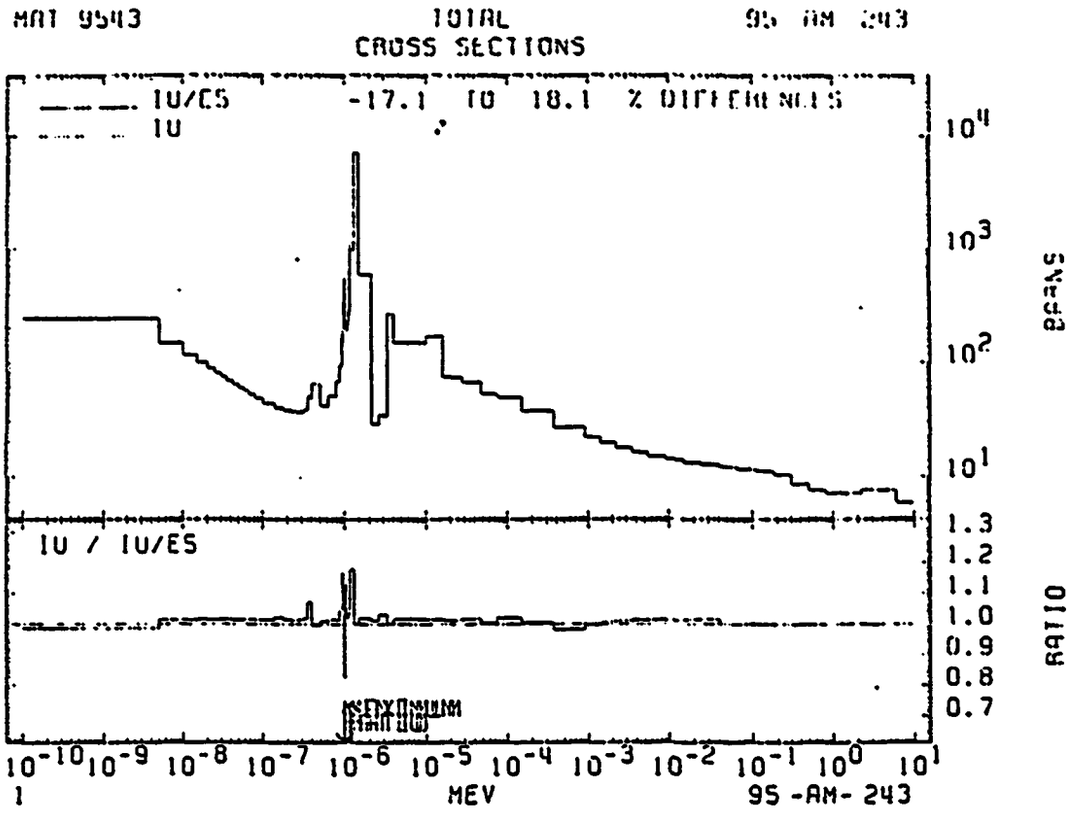

Fig.4 Intercomparison of the total cross-section of Am-243 calculated from UK evaluation in ENDF-5 format and the original UKNDL evaluation (DFN1010), both contained on the INDL/A file.

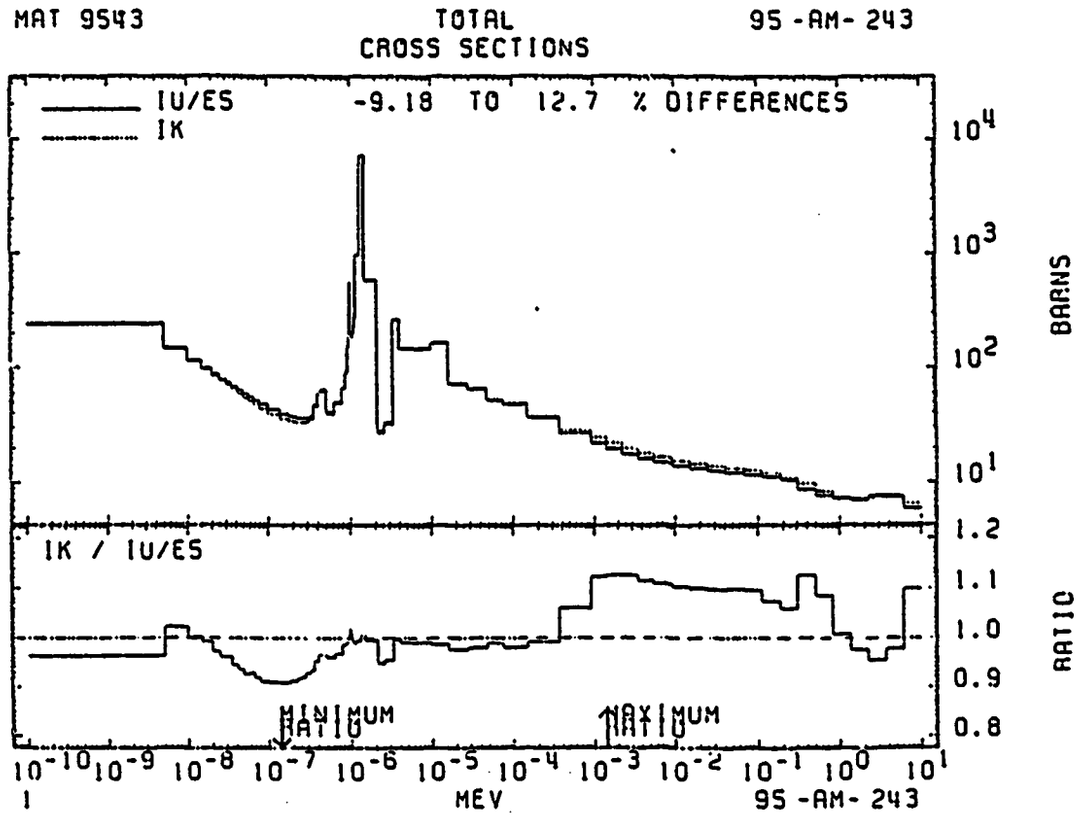

Fig.5 Intercomparison of the total cross-section of Am-243 calculated from UK evaluation in ENDF-5 format and the KEDAK-4 evaluation, both contained on the INDL/A file.

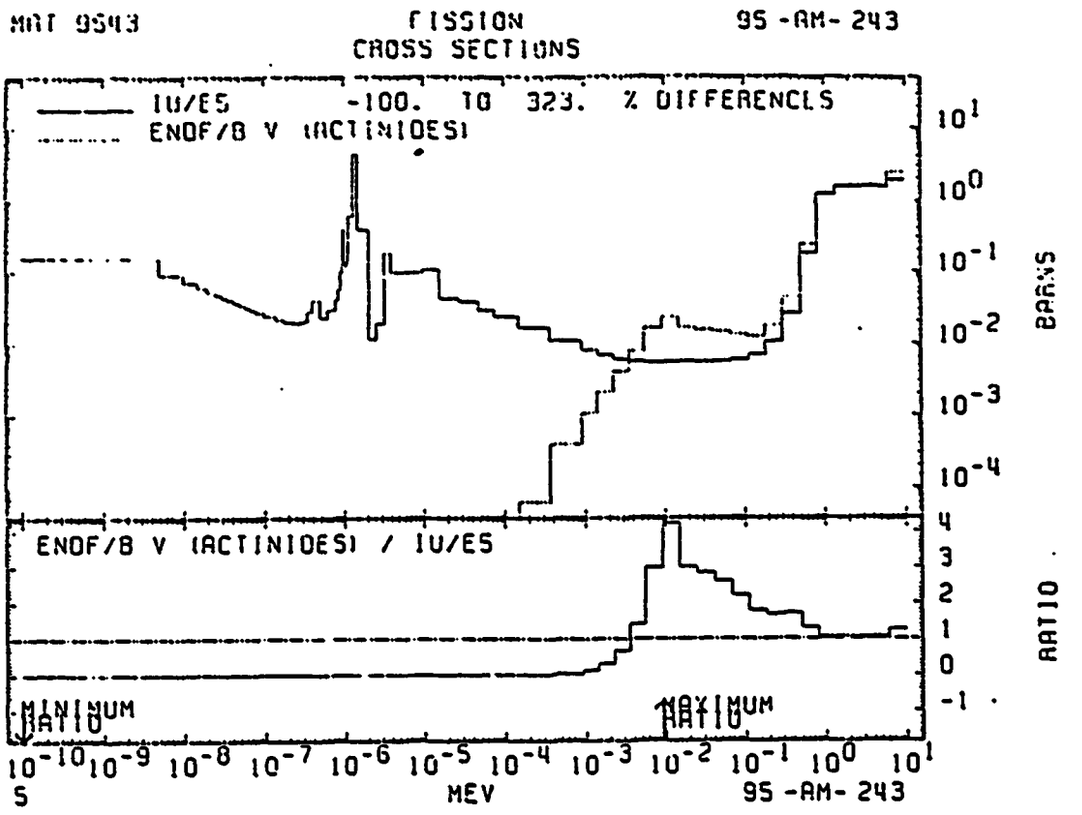

Fig.6 Intercomparison of the fission cross-section of Am-243 calculated from UK evaluation in ENDF-5 format contained on the INDL/A file and the ENDF/B V (Actinides) library.

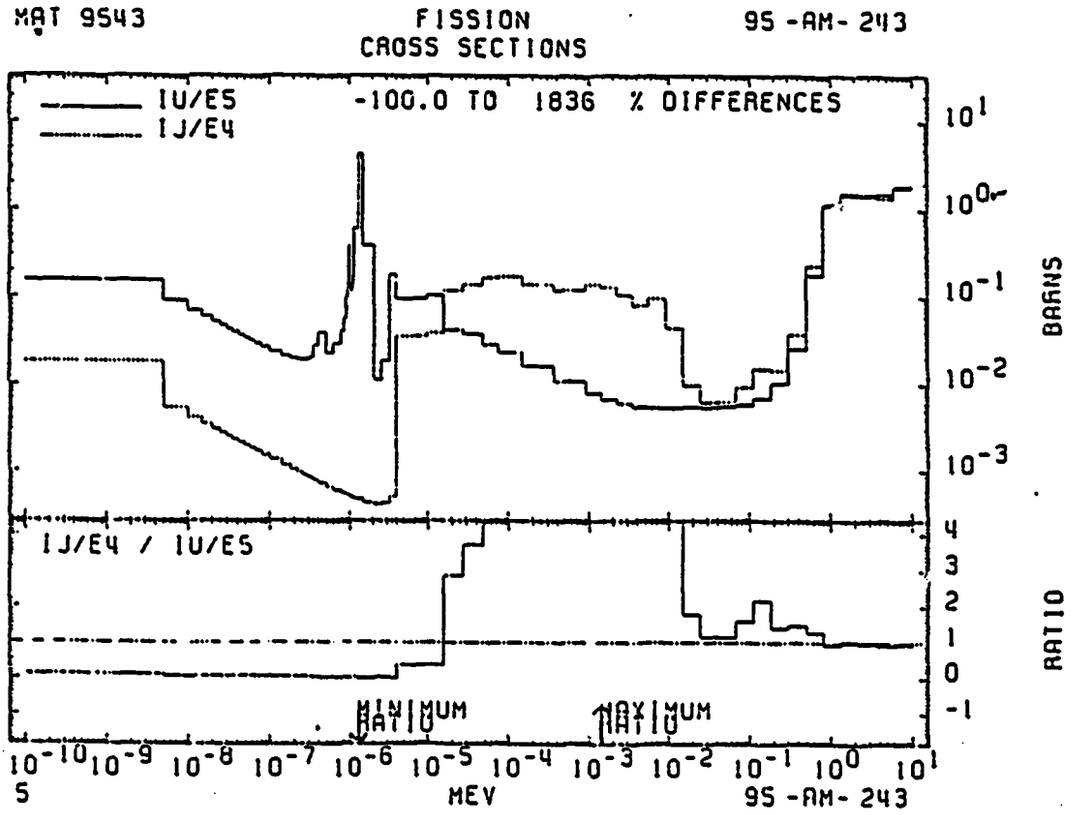

Fig.7 Intercomparison of the fission cross-section of Am-243 calculated from UK evaluation in ENDF-5 format and the JENDL-2 evaluation, both contained on the INDL/A file.

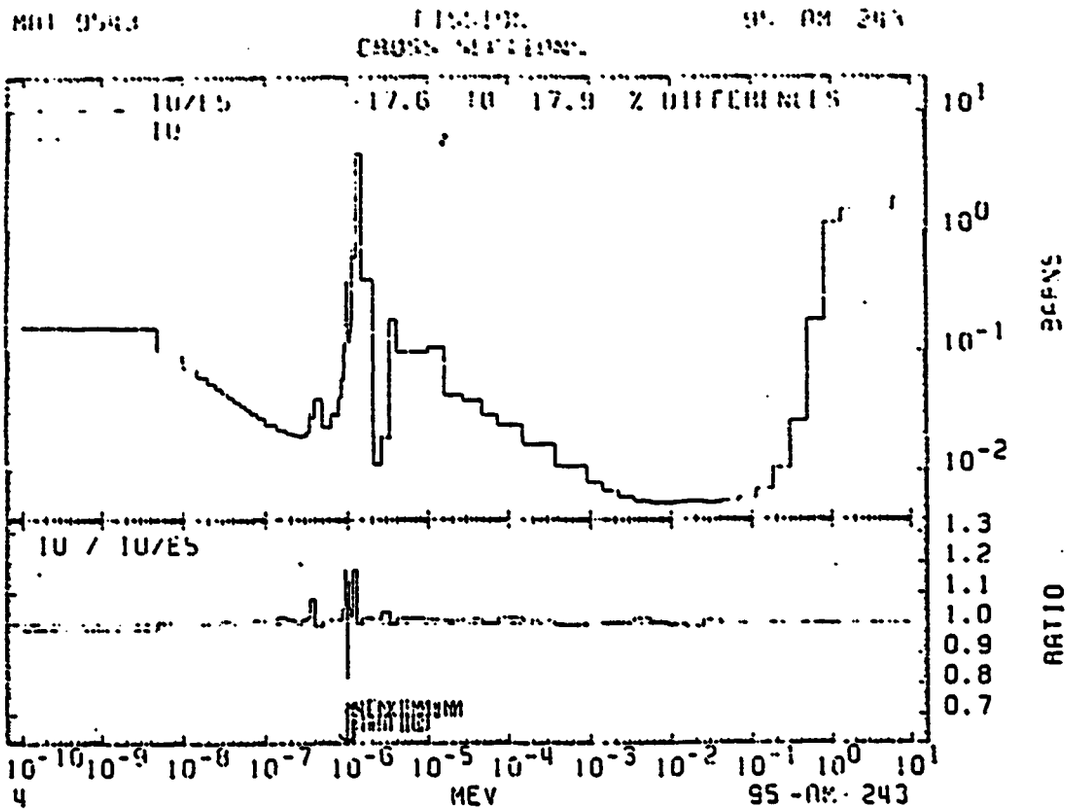

Fig.8 Intercomparison of the fission cross-section of Am-243 calculated from UK evaluation in ENDF-5 format and the orisinal UKNDL evaluation (DFN1010), both contained on the INDL/A file.

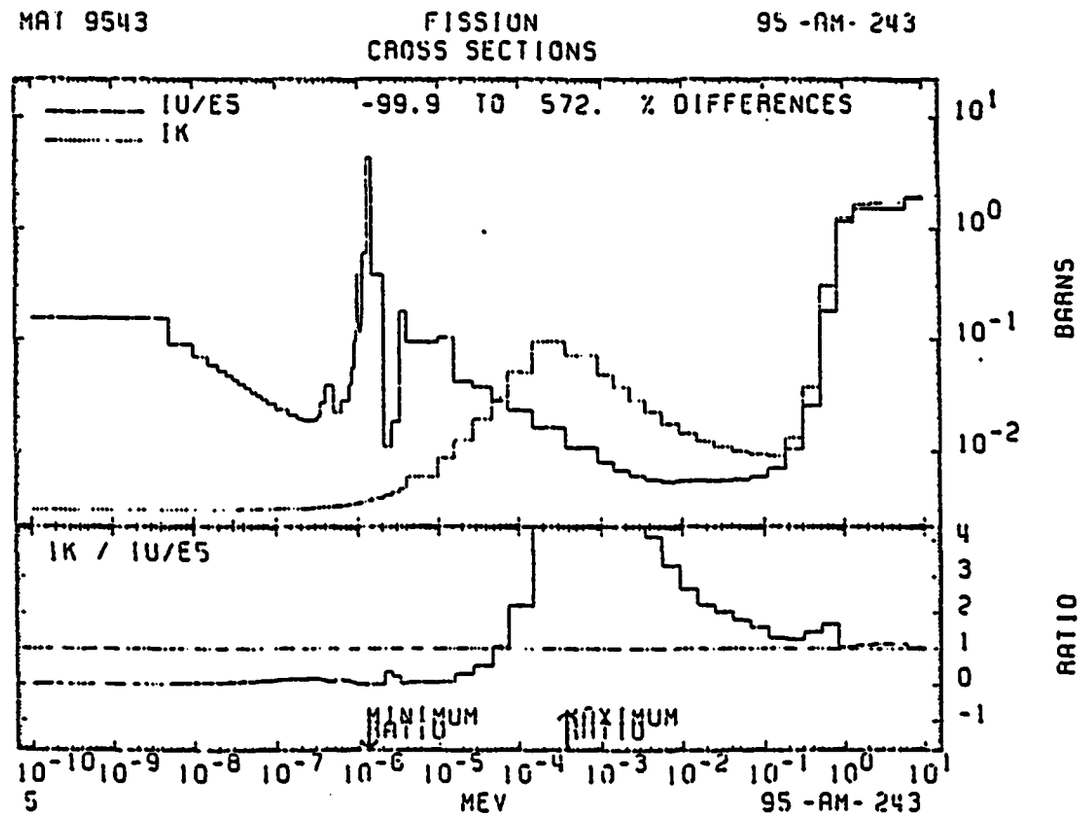

Fig.9 Intercomparison of the fission cross-section of Am-243 calculated from UK evaluation in ENDF-5 format and the KEDAK-4 evaluation, both contained on the INDL/A file.

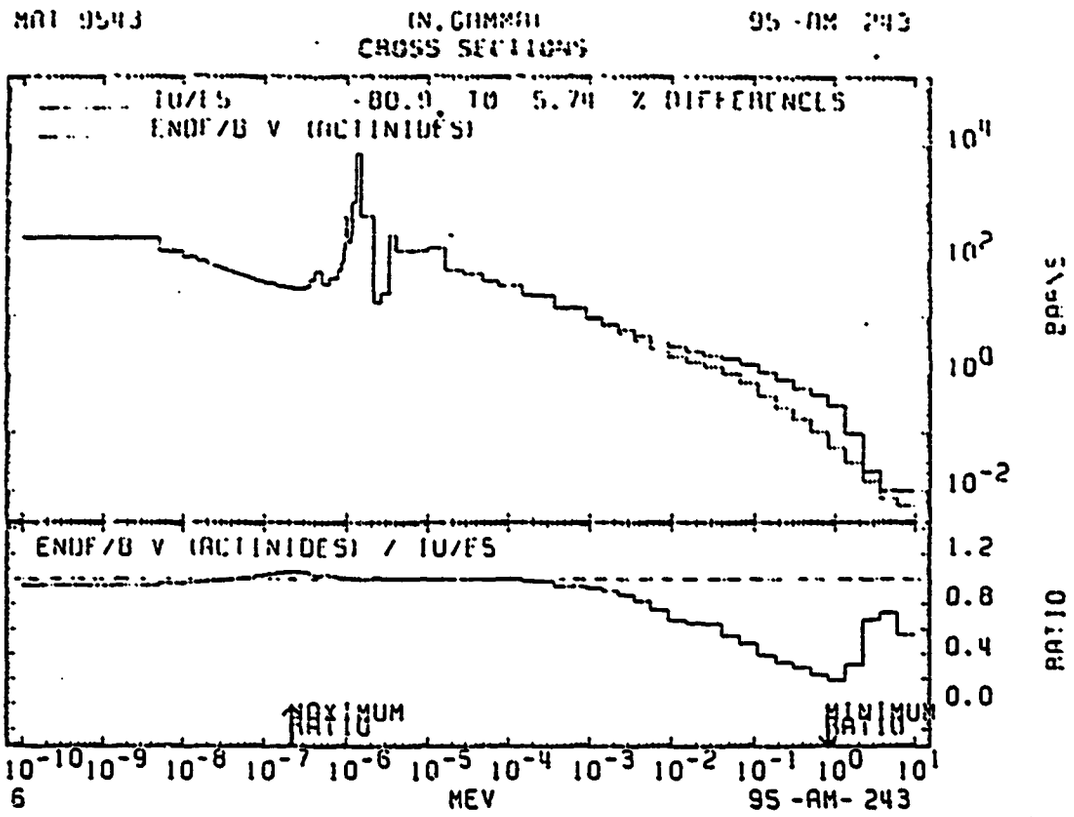

Fig.10 Intercomparison of the (n,gamma) cross-section of Am-243 calculated from UK evaluation in ENDF-5 format contained on the INDL/A file and the ENDF/B V (Actinides) library.

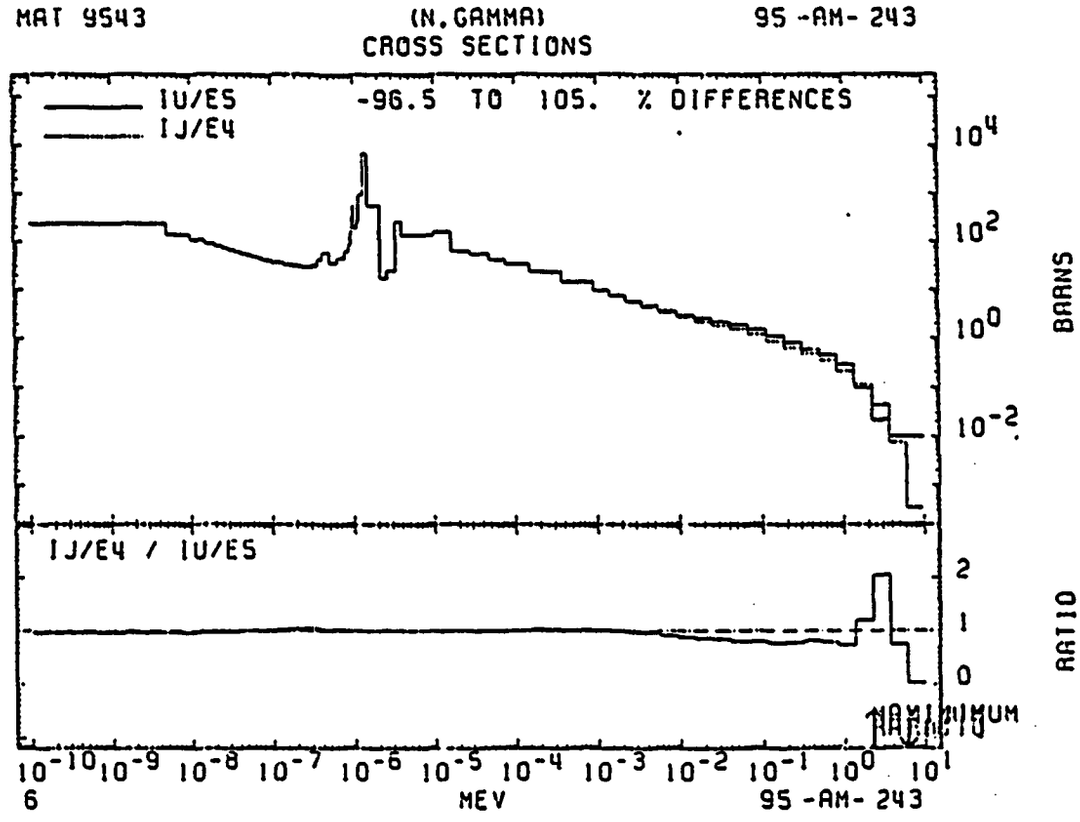

Fig.11 Intercomparison of the (n,gamma) cross-section of Am-243 calculated from UK evaluation in ENDF-5 format and the JENDL-2 evaluation, both contained on the INDL/A file.

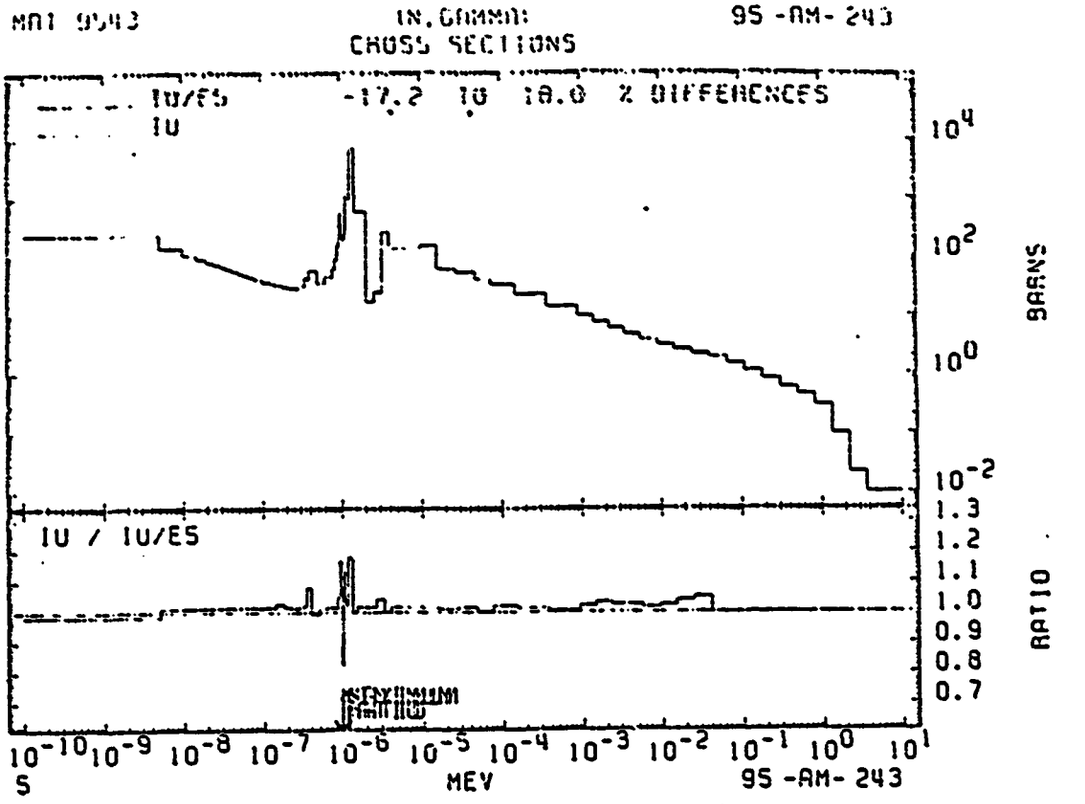

Fig.12 Intercomparison of the (n,gamma) cross-section of Am-243 calculated from UK evaluation in ENDF-5 format and the original UKNDL evaluation (DFN1010), both contained on the INDL/A file.

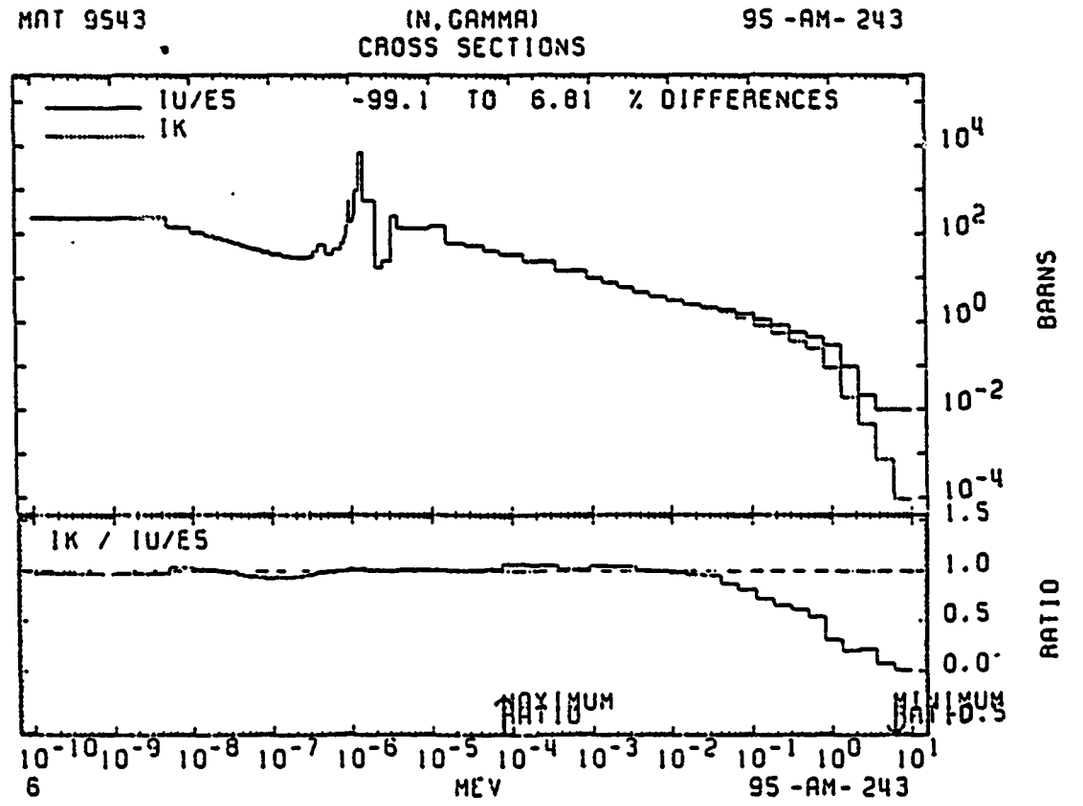

Fig.13 Intercomparison of the (n,gamma) cross-section of Am-243 calculated from UK evaluation in ENDF-5 format and the KEDAK-4 evaluation, both contained on the INDL/A file.

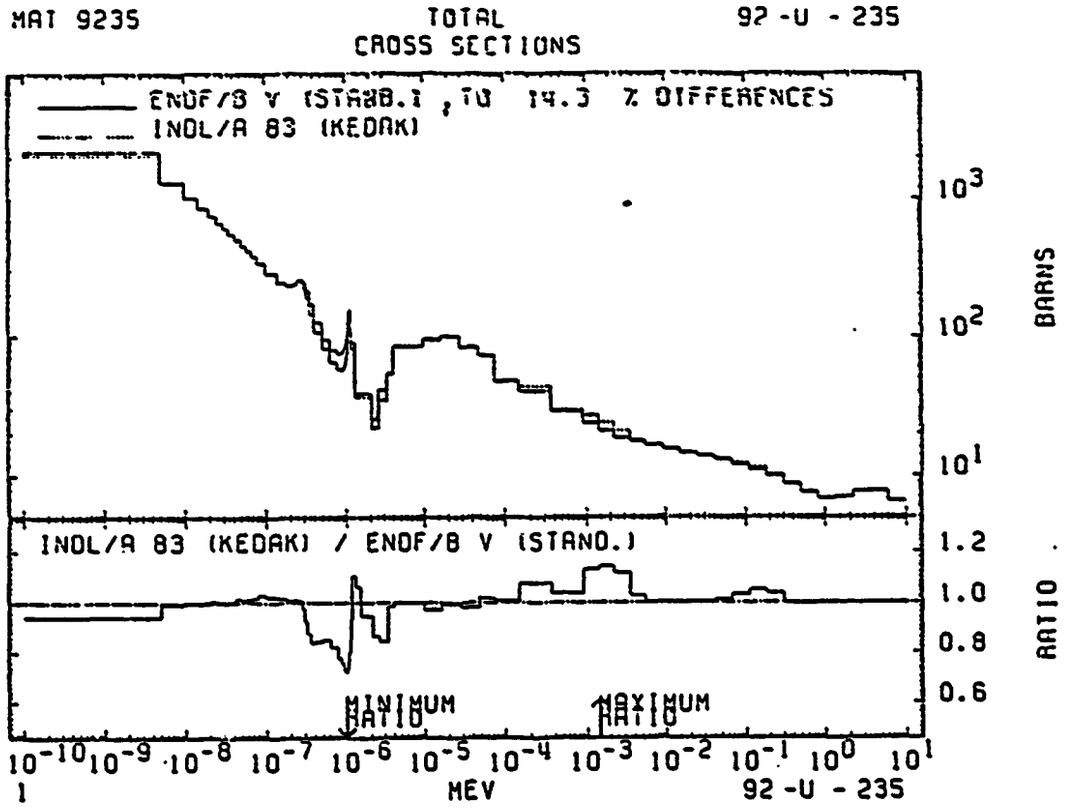

Fig.14 Intercomparison of the total cross-section of U-235 calculated from the ENDF/B V (Actinides) evaluation and the KEDAK-4 evaluation contained on the INDL/A file.

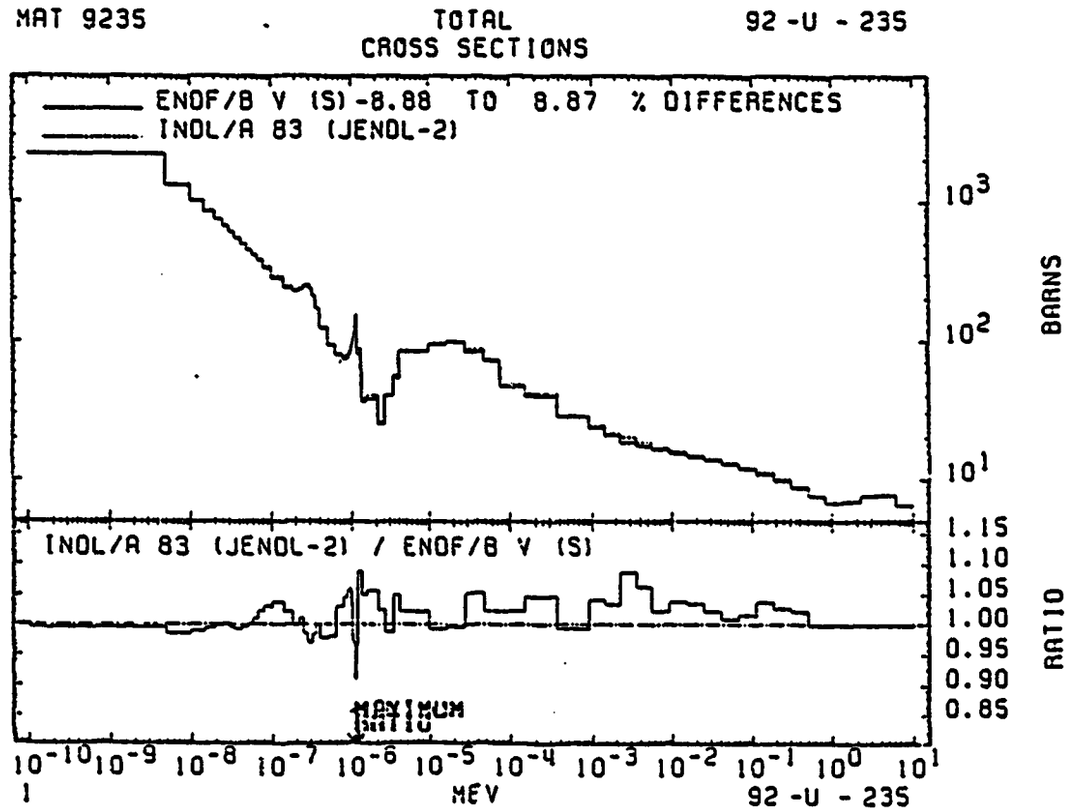

Fig.15 Intercomparison of the total cross-section of U-235 calculated from the ENDF/B V (Actinides) evaluation and the JENDL-2 evaluation contained on the INDL/A file.

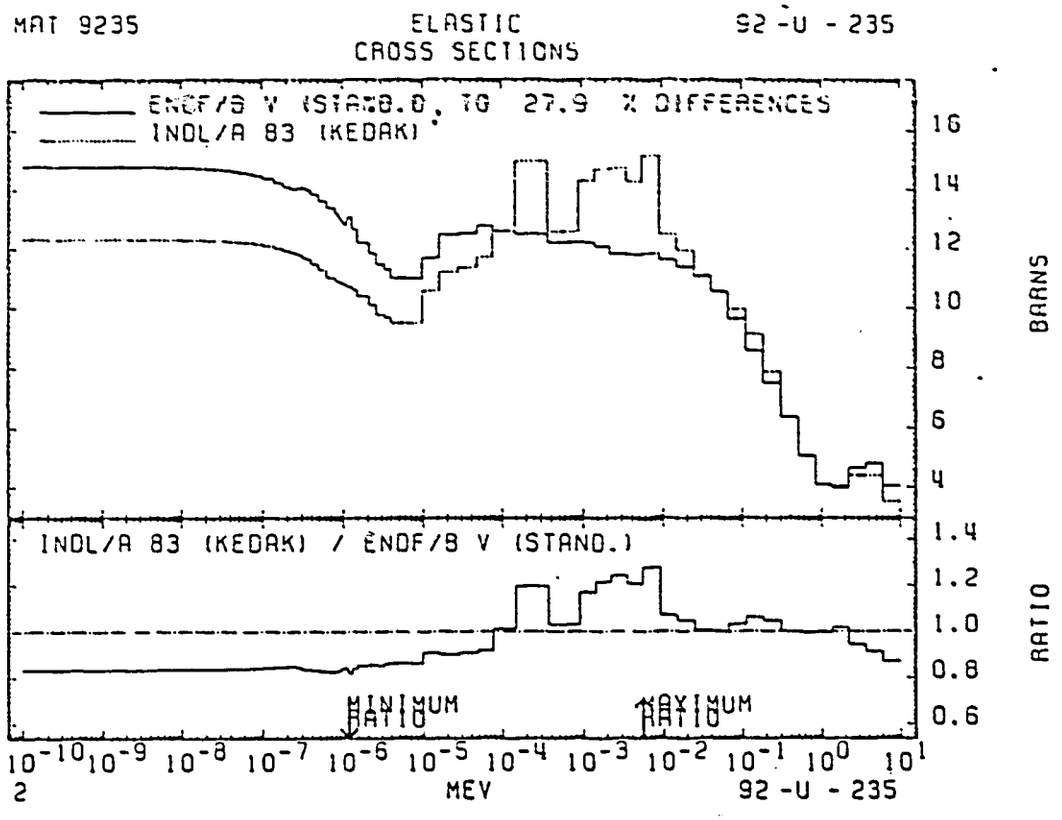

Fig.16 Intercomparison of the elastic cross-section of U-235 calculated from the ENDF/B V (Actinides) evaluation and the KEDAK-4 evaluation contained on the INDL/A file.

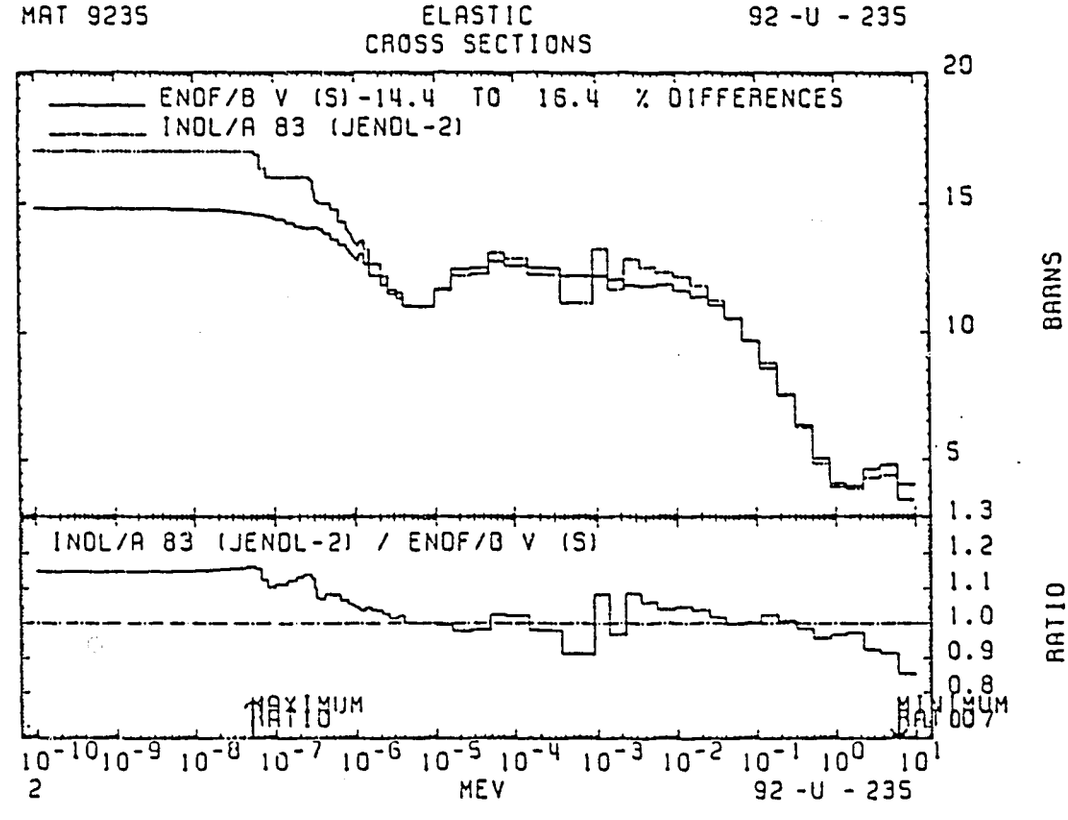

Fig.17 Intercomparison of the elastic cross-section of U-235 calculated from the ENDF/B V (Actinides) evaluation and the JENDL-2 evaluation contained on the INDL/A file.

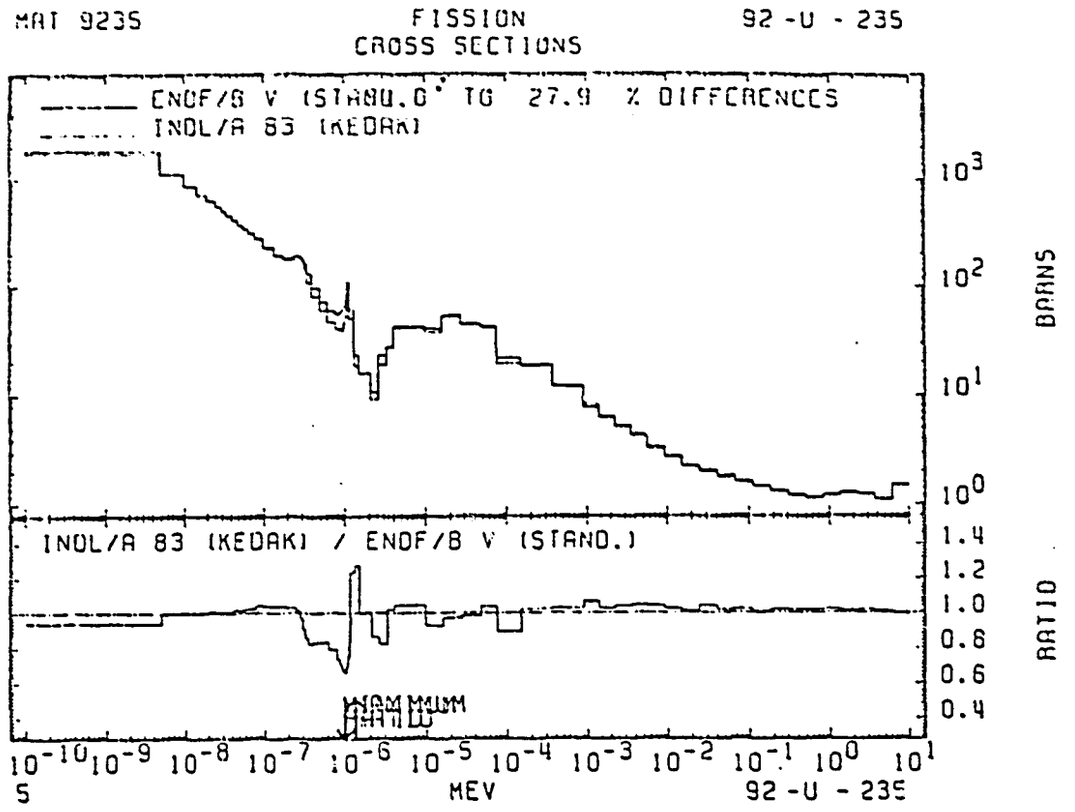

Fig.18 Intercomparison of the fission cross-section of U-235 calculated from the ENDF/B V (Actinides) evaluation and the KEDAK-4 evaluation contained on the INDL/A file.

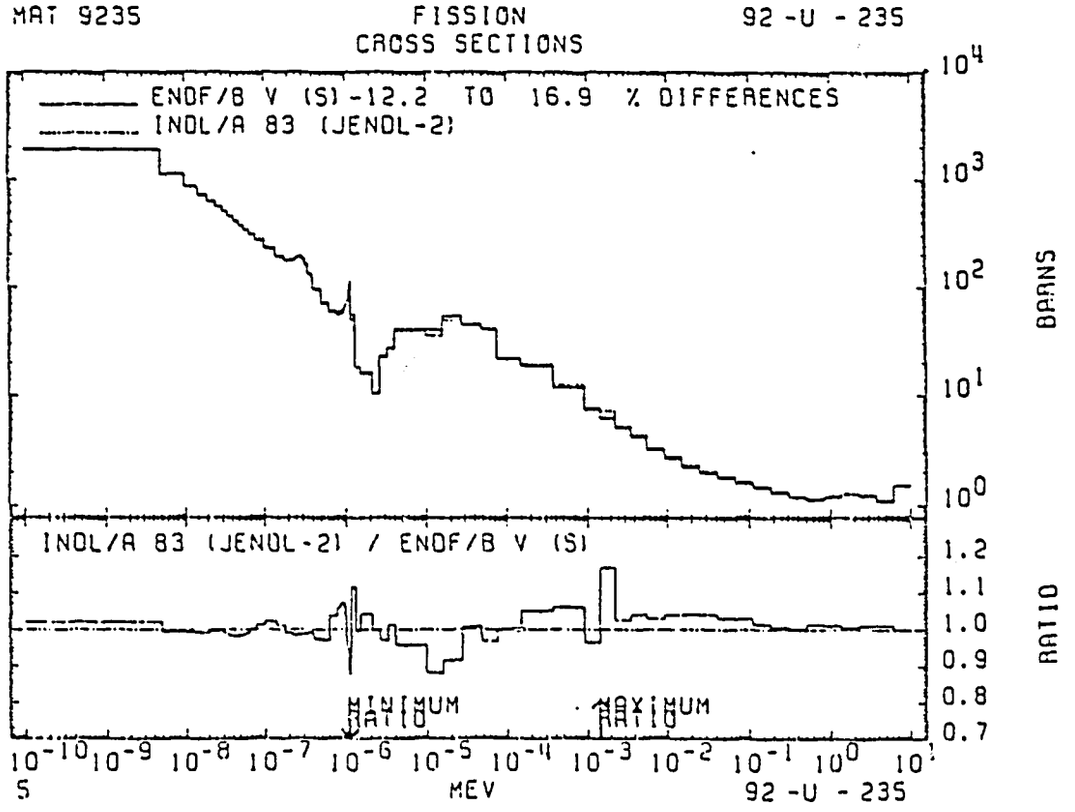

Fig.19 Intercomparison of the fission cross-section of U-235 calculated from the ENDF/B V (Actinides) evaluation and the JENDL-2 evaluation contained on the INDL/A file.

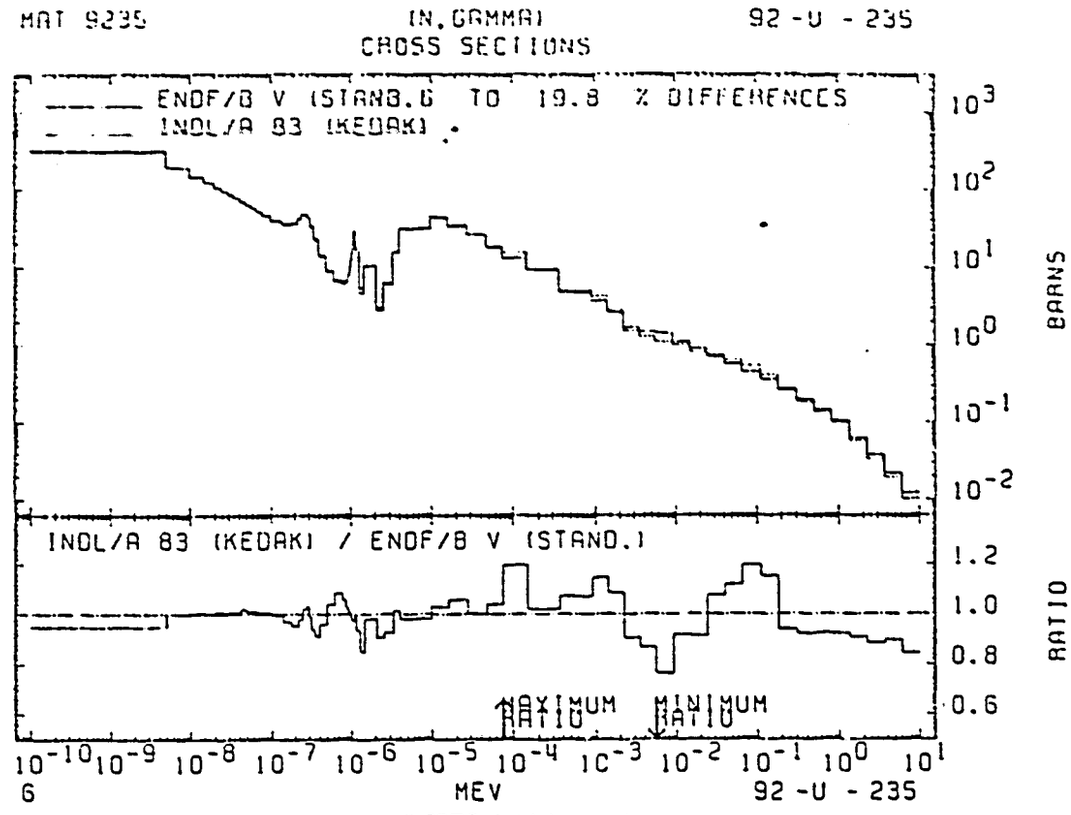

Fig.20 Intercomparison of the (n,gamma) cross-section of U-235 calculated from the ENDF/B V (Actinides) evaluation and the KEDAK-4 evaluation contained on the INDL/A file.

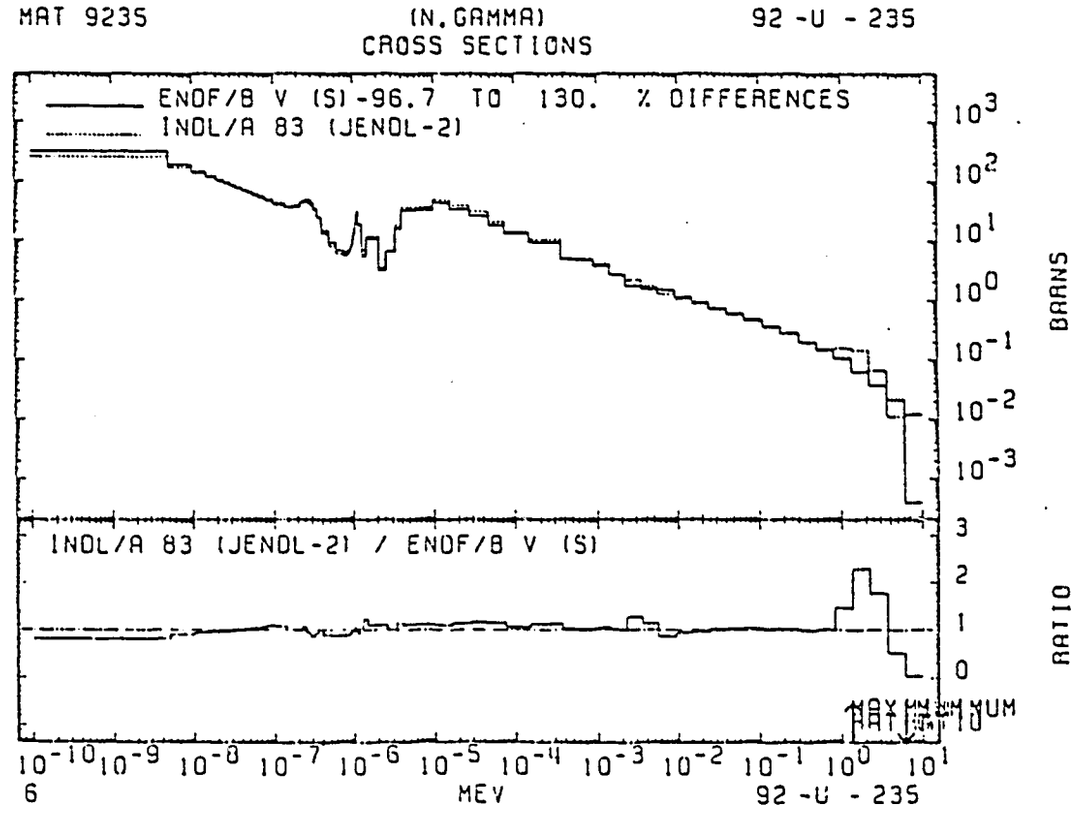

Fig.21 Intercomparison of the (n,gamma) cross-section of U-235 calculated from the ENDF/B V (Actinides) evaluation and the JENDL-2 evaluation contained on the INDL/A file.

Contributed Paper 14

A PROGRAMME OF EVALUATION, PROCESSING AND TESTING OF NUCLEAR DATA FOR Th-232

S. GANESAN, M.M. RAMANADHAN, V. GOPALAKRISHNAN, R.S. KESHAVAMURTHY
Reactor Research Centre,
Kalpakkam, Tamil Nadu, India

Abstract

The initial part of a programme of evaluation and validation of nuclear data for Th-232 is described. A file of evaluated data and a 25-group set of cross section for Th-232 have been generated. The data have been compared with other evaluations and used in calculations of the THOR integral experiment.

1.0 Introduction

Within the framework of a RRC-IAEA research contract[1] on validation and benchmark testing of actinide nuclear data, work has been initiated at Kalpakkam on a programme of evaluation and validation of nuclear data for Th-232 and U-233 for fast reactor applications. The present report gives an account of the progress made thus far for the isotope Th-232. The contents of this report are in the nature of preliminary progress report covering the isotope Th-232 and throw light on developments made thus far and problem areas that have been identified for attention in the immediate future.

2.0 Present status of Indian nuclear data evaluations for fast reactor applications for Th-232

M.K.Mehta and his coworkers[2] in BARC, Bombay have completed evaluations of σ_t, $\sigma_{n,\gamma}$, $\sigma_{n,f}$, $\sigma_{n,2n}$, $\sigma_{n,3n}$, σ_{el} and σ_{inel} in the energy region 150 Kev to 20.0 Mev for Th-232. Discrete level excitation cross sections in 1.0 to 20.0 Mev energy range have also been calculated for the thirteen levels. These cross sections in tabular form were readily supplied to us by R.P.Anand.

A Fortran program[3] 'UPDATE' was written at Kalpakkam to cast these data in ENDF/B format. An output of UPDATE for Th-232 is shown in Appendix A. Further efforts are being made at present to check for any inconsistencies or to remove any defect in the representation of these data in ENDF/B format. It is planned to include in these data also the unresolved resonance parameters in 4 - 50 Kev energy region evaluated at Kalpakkam earlier[4]. Since all these[2] presently available evaluations for Th-232 are based on CINDA and EXFOR information sources upto about 1979, it is necessary to consider updating of all these evaluations by incorporation of recently published data since 1979. Further we need to evaluate the following data which have not been included in the above evaluations performed thus far.

1. $\overline{\nu}$, the total number of neutrons released per fission as a function of incident neutron energy.

2. Angular distributions for outcoming neutrons in elastic as well as inelastic scattering reactions.

3. Evaluations of all neutron induced reactions in resolved and unresolved resonance regions.

By borrowing these data temporarily from JENDL[5] file we have created in ENDF/B format, presently, a JENDL-INDIAN file for Th-232 at Kalpakkam. The JENDL portion in this file will be gradually replaced in a consistent manner in the future as and when our own corresponding evaluations become available.

3.0 Programme of generation of new multigroup cross section sets for Th-232 and comparisons with available French set

The 1969 adjusted French multigroup cross section set[6] is presently being used at RRC for fast reactor design calculations.

Generations of four different new multigroup cross section sets in 25 energy group structure (Table B.2)

using the following basic data files are in progress for Th-232

a. ENDF/B-IV
b. JENDL-1
c. Rumanian file (INDL/A-83) (Ref.7)
d. JENDL-INDIAN file presently created at Kalpakkam

The first three files a, b, c were obtained from IAEA Nuclear Data Section. The processings of all these data files are being done by processing code system RAMBHA[8] developed at Kalpakkam in the last few years.

Different multigroup cross section sets can be compared by utilizing the program COMPLOT[9] developed at Kalpakkam. COMPLOT gives tables of ratios of the two sets in each energy group for σ_t, σ_{tr}, σ_f, $\bar{\nu}\sigma_f$, σ_{nonel}, σ_c, $\sigma_{removal}$, σ_{el} and also for the elements of the non-elastic transfer matrix. The program has also been extended to cover the self shielding factors.

In Fig.1 and Fig.2 we compare for Th-232 the 1969 adjusted French set with ENDF/B-IV based RRC set and also with JENDL-1 based RRC set for multigroup capture and fission reaction cross sections. Both the French and the ENDF/B-IV based RRC set have higher σ_c values as compared to JENDL-1 based set in the Mev energy region. At the time of writing this report the files c and d referred to above were being processed.

The analysis of THOR assembly discussed in next section clearly favours σ_c values lower than French and ENDF/B-IV based set. This trend favours the Indian evaluation for capture for Th-232 by Mehta and Jain[2]. Note that $\sigma_{n,\gamma} = \sigma_c$ for Th-232 for our purposes.

4.0 Analysis of integral experiments for validation of nuclear data

Results of analyses of THOR assembly[10] available at the time of writing this report are given in APPENDIX B. The following remarks are made with regard to results of our calculations presented in APPENDIX B.3.

1. Analysis of THOR assembly using 1969 adjusted French set shows an underprediction of K_{eff} by 3.3%. This deficiency is attributed mainly to incorrect cross sections for Th-232 in French set. The cross sections of other isotopes in THOR assembly are not likely to be responsible for this discrepancy as analyses of other fast critical assemblies by us using French set have shown that French set predicts K_{eff} very well for Pu and U fueled cores not involving thorium blanket (see for example Ref.11).

2. The K_{eff} calculated for THOR assembly by ENDF/B-IV based RRC set is close to the experimental value of unity but differs from the calculated value reported in U.S.A. using ENDF/B-IV data base by Hansen and Paxton[10] by 0.85%. This difference in K_{eff} of 0.85% is large. It is attributed mainly to differences in processing and to some extent in the codes used in the calculation of K_{eff} by us and by the U.S. team, since both calculations use same model and same (ENDF/B-IV) data base. This result particularly once again stresses the importance of IAEA processing Code Verification Project[12,13].

3. The ratio $\sigma_\gamma(^{232}Th)/\sigma_f(^{232}Th)$ derived by us from other spectral indices gives our derived experimental uncertainty of 7%. The C/E values given in Table B.3 for this ratio clearly shows that both the 1969 French set and the ENDF/B-IV data base have higher σ_c values in MeV energy range by about 20 - 25%. This conclusion is reached considering that $\sigma_f(^{232}Th)$ does not show large uncertainty in the fission source energy range (except at threshold where σ_f is any way very small) as revealed in Fig.2, and also that neutron transport in THOR assembly occurs mainly in Mev energy range (See flux distribution in Table B.2)

It is interesting to note that the present Indian evaluation[2] for Th-232 also recommends σ_c values lower than most of the other data files such as ENDF/B-IV, UKNDL, RUMANIAN, ENDL-76. The JENDL 1 also shows, as seen in Fig.1, a lower σ_c value in the higher energy group.

The present results for THOR assembly qualitatively supports the Indian evaluation for σ_c for Th-232 in 1-10 Mev range. This will be confirmed quantitatively by the analyses of THOR assembly using JENDL-1 and JENDL 1 - INDIAN files for Th-232 which is currently in progress.

It is further planned to intercompare, test and validate the various multigroup cross section sets for both Th-232 and U-233 by analysing integral reactor experiments reported in the literature wherever possible. Details of specific integral experiments and measured integral values of parameters including uncertainties for benchmark testing purposes are being compiled from published information.

Acknowledgement

The authors thank Dr. R.P.Anand for his supplying the BARC evaluated data for Th-232, and, Dr. M.K.Mehta and Dr. S.S.Kapoor for their keen interest in this work.

It is a pleasure to acknowledge fruitful correspondence with Dr. Hans D. Lemmel of IAEA Nuclear Data Section during the course of this work.

Thanks are due to Dr. S.Pearlstein, BNL, USA for fruitful correspondence on specifications for various benchmarks.

Our thanks are due to Shri C.V.Sundaram, Director, RRC for his keen interest and encouragement, to Dr. S.R.Paranjpe Director Reactor Engineering and Design Group, RRC for his keen interest, support and encouragement.

Last, but not least, thanks are due to Miss R.Rangamani for patiently typing this Note.

REFERENCES

1. Research within the framework of 'Co-ordinated Programme on Validation and Benchmark Testing of Actinide Nuclear Data' Agency Research Contract No.3690/RB (13 Dec. 1983) Kalpakkam

2. M.K.Mehta et al., Contribution to C.R.P. Meeting (1984). M.K.Mehta and H.M.Jain, IAEA TECDOC-232 p.287 (1980); Amar Sinha and S.B.Garg, Atomkernenergie 38, 282 (1981); M.L.Jhingan et al., Annals of Nucl. Energy 6, 495 (1979); M.L.Jhingan et al., Proc. Int. Conf. on Neutron Physics and Nuclear Data for Reactors and other applied purposes Harwell p.1049 (1978).
R.P.Anand et al., INDC(IND)-30 p.155 (1981);
M.L.Jhingan et al., Nucl. Phys. (India) 21B, 244 (1978);
M.K.Mehta, H.M.Jain, INDC Discrepancy File - 1979, INDC-32/L p.2 to 4 (1980).
H.M.Jain and M.K.Mehta, p.657 in Nuclear Data for Science and Technology, Proc. Antwerp Conference, D.Reidel Publishing Company (1983),

3. M.M.Ramanadhan and S.Ganesan, 'UPDATE, a program for casting the given partial data in ENDF/B format', (1984) unpublished.

4. S.Ganesan, RRC-42; INDC(IND)/26-GJ (1980).

5. N.DayDay, 'JENDL-1, Japanese Evaluated Nuclear Data Library, Version-1, IAEA-NDS-18 Rev.0 (Sep. 1979).

6. J.Y.Barre, 'Lessons Drawn from Integral Experiments on a Set of Multigroup Cross Sections', pp. 165-179 in Proceedings of the Conference on the Physics of Fast Reactor Operation and Design, June 24-26 (1969).

7. V.G.Pronyaev, H.D.Lemmel, K.McLaughlin 'INDL/A-83, IAEA Nuclear Data Library for Evaluated Neutron Reaction Data of Actinides' IAEA-NDS-12 Rev.7 (December 1983).

8. S.Ganesan et al, 'Development of a New Fast Reactor Processing Code RAMBHA at RRC' in Proceedings of the Workshop on Nuclear Data Evaluation, Processing and Testing, August 4-5, 1981, Kalpakkam, Report No. INDC(IND)-30 (1981) IAEA, Vienna; See also V.Gopalakrishnan and S.Ganesan, 'A Note on the program REX1 for Accurate Generation of Infinite Dilution Cross Sections, Elastic and Inelastic Transfer Matrices for Fast Reactor Applications, Internal Note REDG/RP-243 (Sept. 1983) and 'A Note on Program REX2 for Accurate Calculations of Self Shielding Factors in Resolved Resonance Region for Fast Reactor Applications, Internal note REDG/RP-248 (Feb. 1984), Kalpakkam.

9. M.M.Ramanadhan, 'Input Specifications for the Program 'CØMPLØT' for Comparison of Multigroup Constants from Various Evaluated Data Libraries in SETR Format, Internal Note REDG/RP-239 (1983).

10. Fast Reactor Benchmark No.25 in BNL-19302 (ENDF-202) 'Cross Section Evaluation Working Group Benchmark Specifications (1983) Brookhaven National Laboratory, U.S.A. See also G.E.Hansen and H.C.Paxton, Nucl. Sci. Eng. 71, 287 (1979).

11. S.Ganesan, M.M.Ramanadhan and V.Gopalakrishnan, 'Analyses of ZPR-9 Assembly 31 the Advanced Fuels Program Carbide Benchmark Assembly', RRC-61 (1983) Kalpakkam.

12. D.E.Cullen., 'Verification of Nuclear Cross Section Processing Codes' Report INDC(NDS)-134/G (1982) Nuclear Data Section, IAEA, Vienna.

13. S.Ganesan et al 'Problems and Experiences in Nuclear Data Processing in Developing Countries' (Feb. 1984) Unpublished.

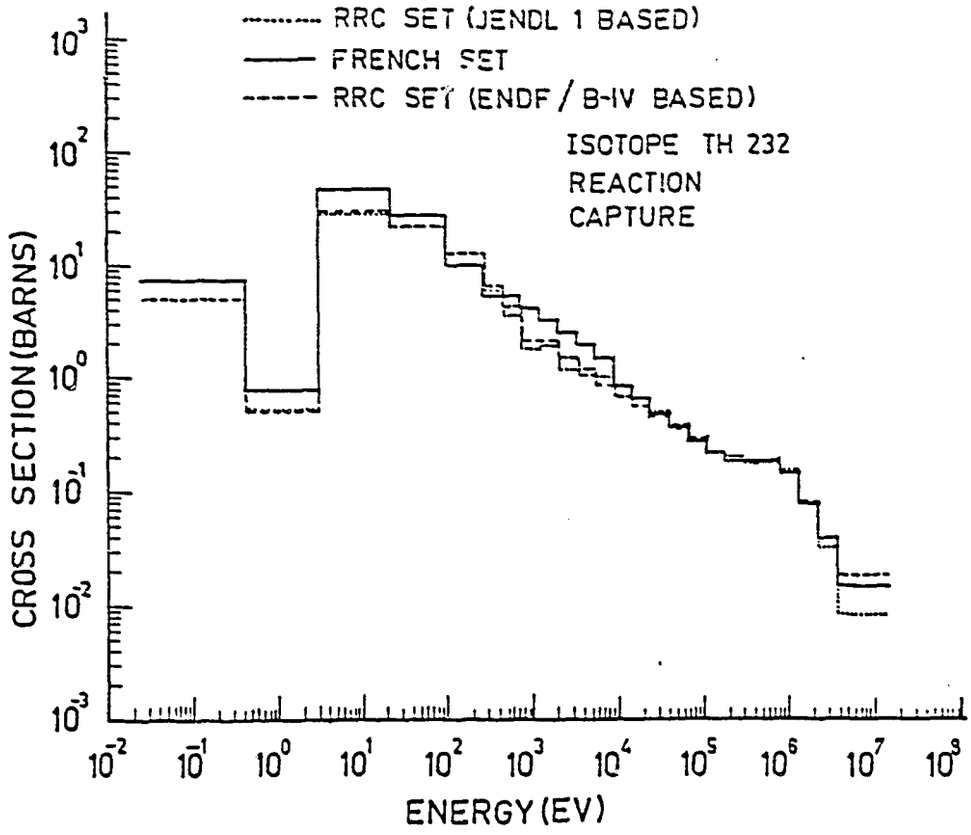

Fig.1 COMPARISON OF THREE MULTIGROUP CAPTURE CROSS SECTION SETS FOR TH-232

Note: CAPTURE CROSS SECTION FOR TH-232:

$\sigma_c = \sigma_{n,\gamma} + \sigma_{n,p} + \sigma_{n,D} + \sigma_{n,\alpha} + \ldots$

$= \sigma_{n,\gamma}$ as other terms are negligible in our energy range.

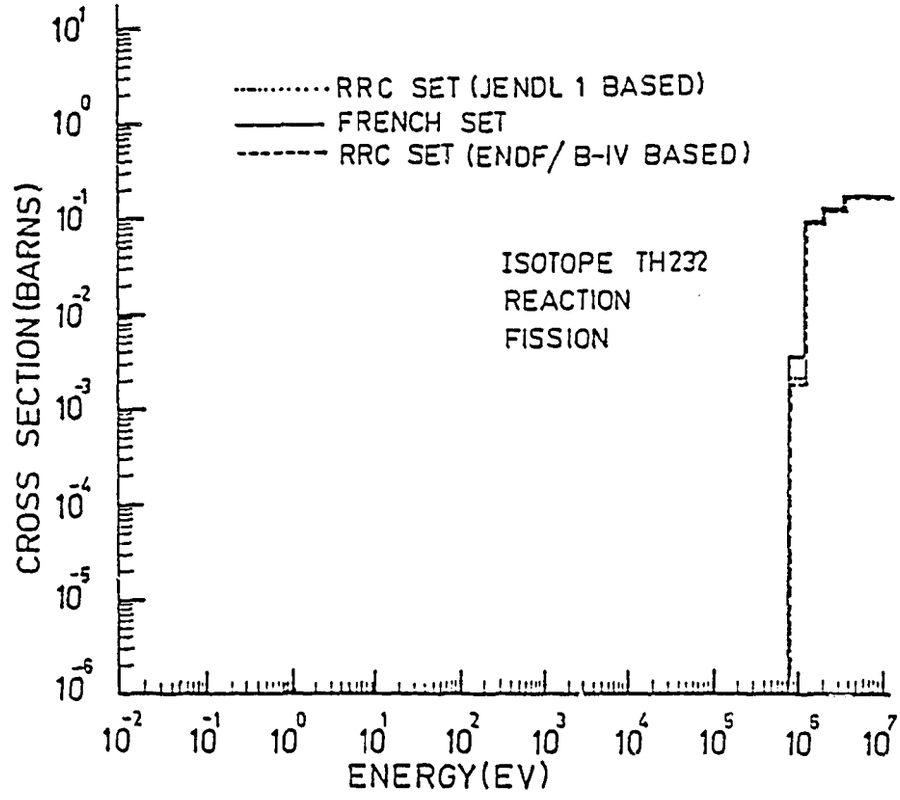

Fig.2 : COMPARISON OF FISSION CROSS SECTIONS IN MULTIGROUP FORM FOR THREE SETS. NOTE THE SPREAD NEAR THRESHOLD.

APPENDIX A

THE NUMERICAL DATA FOR TH-232 EVALUATED IN INDIA IN ENDF/B FORMAT

This data file is currently undergoing further processing including updating. Checks for any errors or inconsistencies are also being made presently at Kalpakkam.

```
9.02320+ 4 2.30045+ 2          1          1          0          201901 1451
0.0     + 0 0.0     + 0        0          0          14          C1901 1451
90-TH-232                                                          1901 1451
                                                                   1901 1451
  THIS FILE CONTAINS PARTIAL DATA IN ENDF/B FORMAT.A JOINT         1901 1451
  JENDL1-INDIA FILE HAS ALSO BEEN CREATED SEPARATELY.              1901 1451
                                                                   1901 1451
  THIS FILE WAS PREPARED AS APPENDIX-A TO THE NOTE VISTRIBUTED     1901 1451
  AT A MEETING OF PARTICIPANTS IN THE CO-ORDINATED RESEARCH        1901 1451
 PROGRAMME(CRP) ON "VALIDATION AND BENCHMARK TESTING OF ACTINIDE   1901 1451
 NUCLEAR DATA" ON 24,25 MAY 1984 AT GUSTAF WERNER INSTITUTE        1901 1451
 UPPSALA,SWEDEN.                                                   1901 1451
                                                                   1901 1451
     EVALUATION PERFORMED IN THE FRAME WORK OF IAEA-NDS            1901 1451
     COORDINATED RESEARCH PROGRAMME ON THE INTERCOMPARISON         1901 1451
     OF EVALUATIONS OF ACTINIDE NEUTRON NUCLEAR DATA               1901 1451
                                BY                                 1901 1451
     M.K.MEHTA,R.P.ANAND,S.K.GUPTA,M.L.JHINGAN,S.B.GARG,           1901 1451
     V.K.SHUKLA,AMAR SINHA AND H.M.JAIN OF BHABHA ATOMIC           1901 1451
     RESEARCH CENTRE, BOMBAY AND S.GANESAN,M.M.RAMANADHAN,         1901 1451
     V.GOPALAKRISHNAN,R.S.KESHAVAMURTHY, REACTOR RESEARCH          1901 1451
     CENTRE, KALPAKKAM, INDIA                                      1901 1451
                                                                   1901 1451
     EVALUATIONS HAVE BEEN PERFORMED FOR THE FAST ENERGY           1901 1451
     REGION OF  50KEV TO 20MEV ONLY.                               1901 1451
     MOST OF THE EXPERIMENTAL DATA WAS SUPPLIED BY                 1901 1451
     NDS-IAEA,VIENNA FROM EXFOR DATA BASE UNTIL DECEMBER           1901 1451
     1977 PLUS THE DATA WAS TAKEN FROM THE REFERENCES              1901 1451
     PUBLISHED IN CINDA OF UP TO JUNE 1979.                        1901 1451
     1. TOTAL CROSS SECTION EVALUATED FROM EXPERIMENTAL            1901 1451
     DATA 150KEV UP TO 15MEV. BEYOND 15MEV DEFORMED OPTICAL        1901 1451
     MODEL WITH ADIABATIC APPROXIMATION HAS BEEN USED.             1901 1451
     2.ELASTIC CROSS SECTION EVALUATED FROM MEASURED DATA          1901 1451
     UPTO 2MEV. BEYOND 2MEV IT HAS BEEN CALCULATED USING           1901 1451
     DEFORMED OPTICAL MODEL PARAMETERS.  THE COMPOUND              1901 1451
     NUCLEAR CONTRIBUTIONS HAVE BEEN DESIRED BY  USING THE         1901 1451
     OPHERICAL OPTICAL MODEL PARAMETERS.                           1901 1451
              REFERENCES                                           1901 1451
       1. T. TAMURA , REV. OF. MOD PHYS.37,679(1965)               1901 1451
       2. C. BARRET, NUCL. PHYS. 51,27(1963)                       1901 1451
       3. U. FASOLI, NUCL PHYS. A151,369(1970)                     1901 1451
       4. P.T.GUENTHER ET AL.,NUCL.SCI.ENGG. 65,174(1978)          1901 1451
       5. F.FABRI AND L.ZUFFI RT/FJ(69) 7 (1969)                   1901 1451
       6. M.K.MEHTA AND H.M.JAIN,IAEA TECDOC-232 P.287 (1980)      1901 1451
       7. AMAR SINHA AND S.B.GARG,ATOMKERNENERGIE 38,282(1981)     1901 1451
       8. M.L.JHINGAN ET AL.,ANNALS OF NUCL.ENERGY 6,495(1979)     1901 1451
       9. M.L.JHINGAN ET AL.,PROC.INT.CONF.ON NEUTRON PHYSICS      1901 1451
          AND NUCLEAR DATA FOR REACTORS & OTHER APPLIED PURPOSES   1901 1451
          HARWELL P.1049 (1973)                                    1901 1451
      10. R.P.ANAND ET AL., INDC(IND)-30 P.155(1981);              1901 1451
      11. M.L.JHINGAN ET AL., NUCL.PHYS.(INDIA) 21B, 244 (1978);   1901 1451
      12. M.K.MEHTA,H.M.JAIN,INDC DISCREPANCY FILE - 1979,         1901 1451
          INDC-32/L,P.2 TO 4 (1980);                               1901 1451
      13. H.M.JAIN AND M.K.MEHTA, P.657 IN NUCLEAR DATA FOR        1901 1451
          SCIENCE AND TECHNOLOGY, PROCEEDINGS OF ANTWERP CONF.     1901 1451
          D.REIDEL PUBLISHING COMPANY (1983);                      1901 1451
      12. S.GANESAN, RRC-42,INDC(IND)/26-GJ (1980).                1901 1451
     3. INELASIIC C.S. HAS BEEN ESTIMATED AS THE                   1901 1451
     DIFFERENCE BETWEEN TOTAL AND ALL THE OTHERS                   1901 1451
     CROSS-SECTIONS.                                               1901 1451
     4. CAPTURE CROSS-SECTIONS EVALUATED FROM EXPERIMENTAL         1901 1451
     DATA UPTO 4MEV                                                1901 1451
     5. (N,2N) AND FISSION CROSS SECTIONS EVALUATED FROM           1901 1451
     EXPERIMENTAL DATA.                                            1901 1451
     6. (N,3N) CROSS-SECTIONS CALCULATED TAKING INTO               1901 1451
     ACCOUNT PRE-EQUILIBRIUM EMISSION.                             1901 1451
     7. UNRESOLVED RESONANCE PARAMETERS ARE TO BE TAKEN FROM       1901 1451
        KALPAKKAM EVALUATION FOR 4 KEV TO 50KEV (RRC-42).THIS      1901 1451
        DATA HAS NOT YET BEEN CODED IN THIS FILE.                  1901 1451
******************************  C O N T E N T S  *****************1901 1451
                         (MF)          (MT)      (CARDS)           1901 1451
                           3             1           53            1901 1451
                           3             2           52            1901 1451
                           3             4           48            1901 1451
                           3            16           29            1901 1451
                           3            17           15            1901 1451
                           3            18           47            1901 1451
                           3            51            6            1901 1451
                           3            52            6            1901 1451
                           3            53            6            1901 1451
                           3            54            6            1901 1451
                           3            55            6            1901 1451
                           3            56            6            1901 1451
                           3            57            6            1901 1451
                           3            58            6            1901 1451
                           3            59            6            1901 1451
                           3            60            6            1901 1451
                           3            61            6            1901 1451
```

```
                                                 3          62          5          1901 1451  900
                                                 3          65          6          1901 1451  910
                                                 3         102         53          1901 1451  920
                                                                                   1901 1    0  930
                                                                                   1901 0    0  940
 .90232+ 5 2.30045+ 2                            0           0          1         01901 2151  950
 .90232+ 5 1.00000+ 0                            0           0          1         01901 2151  960
1.0000-  5 2.00000+ 7                            0           0          0         01901 2151  970
0.0000+  0 9.55000- 1                            0           0          C         01901 2151  980
                                                                                   1901    0  990
 .90232+ 5 2.30045+ 2                            0          99          0          1901 3  1 1000
 .0          .0                                  0           0          1       1581901 3  1 1010
          158          2                                                           1901 3  1 1020
0.15000E 060.11420E 020.20000E 060.10206E 020.25000E 060.10266E 021901 3  1 1030
0.30000E 060.97790E 010.35000E 060.93430E 010.40000E 060.89530E 011901 3  1 1040
0.45000E 060.85030E 010.50000E 060.83040E 010.55000E 060.80390E 011901 3  1 1050
0.60000E 060.73090E 010.65000E 060.76130E 010.70000E 060.74450E 011901 3  1 1060
0.75000E 060.73060E 010.80000E 060.71900E 010.85000E 060.70950E 011901 3  1 1070
0.90000E 060.70190E 010.95000E 060.69580E 010.10000E 070.69100E 011901 3  1 1080
0.11000E 070.68400E 010.12000E 070.68000E 010.13000E 070.67860E 011901 3  1 1090
0.14000E 070.67950E 010.15000E 070.63220E 010.16000E 070.68660E 011901 3  1 1100
0.17000E 070.69210E 010.18000E 070.69840E 010.19000E 070.70520E 011901 3  1 1110
0.20000E 070.71220E 010.21000E 070.71910E 010.22000E 070.72590E 011901 3  1 1120
0.23000E 070.73250E 010.24000E 070.73380E 010.25000E 070.74480E 011901 3  1 1130
0.26000E 070.75040E 010.27000E 070.75560E 010.28000E 070.76030E 011901 3  1 1140
0.29000E 070.76440E 010.30000E 070.76790E 010.31000E 070.77090E 011901 3  1 1150
0.32000E 070.77320E 010.33000E 070.77510E 010.34000E 070.77640E 011901 3  1 1160
0.35000E 070.77720E 010.36000E 070.77750E 010.37000E 070.77730E 011901 3  1 1170
0.38000E 070.77670E 010.39000E 070.77560E 010.40000E 070.77410E 011901 3  1 1180
0.41000E 070.77320E 010.42000E 070.77000E 010.43000E 070.76740E 011901 3  1 1190
0.44000E 070.76450E 010.45000E 070.76130E 010.46000E 070.75780E 011901 3  1 1200
0.47000E 070.75410E 010.48000E 070.75010E 010.49000E 070.74600E 011901 3  1 1210
0.50000E 070.74160E 010.51000E 070.73710E 010.52000E 070.73250E 011901 3  1 1220
0.53000E 070.72770E 010.54000E 070.72280E 010.55000E 070.71790E 011901 3  1 1230
0.56000E 070.71300E 010.57000E 070.70800E 010.58000E 070.70300E 011901 3  1 1240
0.59000E 070.69800E 010.60000E 070.69300E 010.61000E 070.68300E 011901 3  1 1250
0.62000E 070.68310E 010.63000E 070.67820E 010.64000E 070.67330E 011901 3  1 1260
0.65000E 070.66850E 010.66000E 070.66370E 010.67000E 070.65900E 011901 3  1 1270
0.68000E 070.65430E 010.69000E 070.64930E 010.70000E 070.64530E 011901 3  1 1280
0.71000E 070.64090E 010.72000E 070.63670E 010.73000E 070.63250E 011901 3  1 1290
0.74000E 070.62850E 010.75000E 070.62460E 010.76000E 070.62080E 011901 3  1 1300
0.77000E 070.61710E 010.78000E 070.61360E 010.79000E 070.61020E 011901 3  1 1310
0.80000E 070.60700E 010.81000E 070.60380E 010.82000E 070.60080E 011901 3  1 1320
0.83000E 070.59790E 010.84000E 070.59520E 010.85000E 070.59250E 011901 3  1 1330
0.86000E 070.59000E 010.87000E 070.58760E 010.88000E 070.58530E 011901 3  1 1340
0.89000E 070.58310E 010.90000E 070.58100E 010.91000E 070.57910E 011901 3  1 1350
0.92000E 070.57720E 010.93000E 070.57550E 010.94000E 070.57390E 011901 3  1 1360
0.95000E 070.57230E 010.96000E 070.57090E 010.97000E 070.56960E 011901 3  1 1370
0.98000E 070.56830E 010.99000E 070.56720E 010.10000E 080.56610E 011901 3  1 1380
0.10200E 080.56420E 010.10400E 080.56270E 010.10600E 080.56140E 011901 3  1 1390
0.10800E 080.56040E 010.11000E 080.55970E 010.11200E 080.55910E 011901 3  1 1400
0.11400E 080.55880E 010.11600E 080.55870E 010.11800E 080.55870E 011901 3  1 1410
0.12000E 080.55890E 010.12200E 080.55930E 010.12400E 080.55970E 011901 3  1 1420
0.12600E 080.56040E 010.12800E 080.56110E 010.13000E 080.56190E 011901 3  1 1430
0.13200E 080.56230E 010.13400E 080.56390E 010.13600E 080.56500E 011901 3  1 1440
0.13800E 080.56620E 010.14000E 080.56750E 010.14200E 080.56900E 011901 3  1 1450
0.14400E 080.57050E 010.14600E 080.57220E 010.14800E 080.57390E 011901 3  1 1460
0.15000E 080.56730E 010.15200E 080.56810E 010.15400E 080.56840E 011901 3  1 1470
0.15600E 080.56880E 010.15800E 080.56910E 010.16000E 080.56940E 011901 3  1 1480
0.16200E 080.56930E 010.16400E 080.56920E 010.16600E 080.56920E 011901 3  1 1490
0.16800E 080.56910E 010.17000E 080.56900E 010.17200E 080.56840E 011901 3  1 1500
0.17400E 080.56780E 010.17600E 080.56720E 010.17800E 080.56650E 011901 3  1 1510
0.18000E 080.56590E 010.18200E 080.56470E 010.18400E 080.56350E 011901 3  1 1520
0.18600E 080.56240E 010.18800E 080.56120E 010.19000E 080.56000E 011901 3  1 1530
0.19200E 080.55320E 010.19400E 080.55650E 010.19600E 080.55480E 011901 3  1 1540
0.19800E 080.55300E 010.20000E 080.55130E 010.          0.            1901 3  1 1550
                                                                       1901 3  0 1560
 .90232+ 5 2.30045+ 2                            0          99          0          1901 3  2 1570
 .0          .0                                  0           0          1       1551901 3  2 1580
          155          2                         0           0          0         01901 3  2 1590
0.30000E 060.82900E 010.35000E 060.78900E 010.40000E 060.74900E 011901 3  2 1600
0.45000E 060.70900E 010.50000E 060.67200E 010.55000E 060.63200E 011901 3  2 1610
0.60000E 060.59700E 010.65000E 060.56300E 010.70000E 060.53400E 011901 3  2 1620
0.75000E 060.50900E 010.80000E 060.48900E 010.85000E 060.47300E 011901 3  2 1630
0.90000E 060.46000E 010.95000E 060.45000E 010.10000E 070.44500E 011901 3  2 1640
0.11000E 070.43400E 010.12000E 070.42500E 010.13000E 070.41300E 011901 3  2 1650
0.14000E 070.40700E 010.15000E 070.39100E 010.16000E 070.40300E 011901 3  2 1660
0.17000E 070.41500E 010.18000E 070.42700E 010.19000E 070.43900E 011901 3  2 1670
0.20000E 070.45200E 010.21000E 070.44800E 010.22000E 070.44440E 011901 3  2 1680
0.23000E 070.44070E 010.24000E 070.43690E 010.25000E 070.43320E 011901 3  2 1690
0.26000E 070.42740E 010.27000E 070.42570E 010.28000E 070.42170E 011901 3  2 1700
0.29000E 070.41320E 010.30000E 070.41440E 010.31000E 070.41560E 011901 3  2 1710
0.32000E 070.41580E 010.33000E 070.41800E 010.34000E 070.41920E 011901 3  2 1720
0.35000E 070.42040E 010.36000E 070.42150E 010.37000E 070.42270E 011901 3  2 1730
0.38000E 070.42390E 010.39000E 070.42510E 010.40000E 070.42630E 011901 3  2 1740
0.41000E 070.42360E 010.42000E 070.42090E 010.43000E 070.41820E 011901 3  2 1750
0.44000E 070.41550E 010.45000E 070.41290E 010.46000E 070.41020E 011901 3  2 1760
0.47000E 070.40760E 010.48000E 070.40790E 010.49000E 070.40230E 011901 3  2 1770
0.50000E 070.39760E 010.51000E 070.39560E 010.52000E 070.39150E 011901 3  2 1780
```

0.53000E	070.33740E	010.54000E	070.33530E	010.55000E	070.37920E	011901	3	2	1790
0.56000E	070.37510E	010.57000E	070.37100E	010.58000E	070.36690E	011901	3	2	1800
0.59000E	070.36230E	010.60000E	070.35870E	010.61000E	070.35490E	011901	3	2	1810
0.62000E	070.35110E	010.63000E	070.34720E	010.64000E	070.34340E	011901	3	2	1820
0.65000E	070.33960E	010.66000E	070.33570E	010.67000E	070.33190E	011901	3	2	1830
0.68000E	070.32830E	010.69000E	070.32420E	010.70000E	070.32040E	011901	3	2	1840
0.71000E	070.31750E	010.72000E	070.31460E	010.73000E	070.31170E	011901	3	2	1850
0.74000E	070.30350E	010.75000E	070.30590E	010.76000E	070.30300E	011901	3	2	1860
0.77000E	070.30010E	010.78000E	070.29720E	010.79000E	070.29430E	011901	3	2	1870
0.80000E	070.29130E	010.81000E	070.28930E	010.82000E	070.28740E	011901	3	2	1880
0.83000E	070.28550E	010.84000E	070.28370E	010.85000E	070.28130E	011901	3	2	1890
0.86000E	070.28000E	010.87000E	070.27310E	010.88000E	070.27630E	011901	3	2	1900
0.89000E	070.27440E	010.90000E	070.27260E	010.91000E	070.27170E	011901	3	2	1910
0.92000E	070.27030E	010.93000E	070.26990E	010.94000E	070.26900E	011901	3	2	1920
0.95000E	070.26800E	010.96000E	070.26710E	010.97000E	070.26620E	011901	3	2	1930
0.98000E	070.26530E	010.99000E	070.26440E	010.10000E	080.26350E	011901	3	2	1940
0.10200E	080.25330E	010.10400E	080.26310E	010.10600E	080.26230E	011901	3	2	1950
0.10800E	080.26260E	010.11000E	080.26240E	010.11200E	080.26340E	011901	3	2	1960
0.11400E	080.26440E	010.11600E	080.26540E	010.11800E	080.26630E	011901	3	2	1970
0.12000E	080.26720E	010.12200E	080.26920E	010.12400E	080.27130E	011901	3	2	1980
0.12600E	080.27530E	010.12800E	080.27540E	010.13000E	080.27740E	011901	3	2	1990
0.13200E	080.27940E	010.13400E	080.28130E	010.13600E	080.28330E	011901	3	2	2000
0.13800E	080.28520E	010.14000E	080.28720E	010.14200E	080.28960E	011901	3	2	2010
0.14400E	080.29200E	010.14600E	080.29440E	010.14800E	080.29680E	011901	3	2	2020
0.15000E	080.29920E	010.15200E	080.30150E	010.15400E	080.30370E	011901	3	2	2030
0.15600E	080.30600E	010.15800E	080.30820E	010.16000E	080.31050E	011901	3	2	2040
0.16200E	080.31240E	010.16400E	080.31430E	010.16600E	080.31620E	011901	3	2	2050
0.16800E	080.31510E	010.17000E	080.32000E	010.17200E	080.32140E	011901	3	2	2060
0.17400E	080.32230E	010.17600E	080.32420E	010.17800E	080.32560E	011901	3	2	2070
0.18000E	080.32700E	010.18200E	080.32780E	010.18400E	080.32870E	011901	3	2	2080
0.18600E	080.32950E	010.18800E	080.33040E	010.19000E	080.33120E	011901	3	2	2090
0.19200E	080.33140E	010.19400E	080.33160E	010.19600E	080.33190E	011901	3	2	2100
0.19800E	080.33210E	010.20000E	080.33230E	010.	0.	1901	3	2	2110
						1901	3	0	2120
.90232+ 5	2.30045+ 2		0	99	0	1901	3	4	2130
.0	.0		0	0	1	1421901	3	4	2140
	142	2	0	0	0	01901	3	4	2150
0.30000E	060.13480E	010.35000E	060.13110E	010.40000E	060.13170E	011901	3	4	2160
0.45000E	060.13670E	010.50000E	060.14270E	010.55000E	060.15530E	011901	3	4	2170
0.60000E	060.16760E	010.65000E	060.18200E	010.70000E	060.19450E	011901	3	4	2180
0.75000E	060.20530E	010.80000E	060.21470E	010.85000E	060.22170E	011901	3	4	2190
0.90000E	060.22770E	010.95000E	060.23220E	010.10000E	070.23300E	011901	3	4	2200
0.11000E	070.23800E	010.12000E	070.24340E	010.13000E	070.24830E	011901	3	4	2210
0.14000E	070.25690E	010.15000E	070.27530E	010.16000E	070.26250E	011901	3	4	2220
0.17000E	070.25960E	010.18000E	070.25620E	010.19000E	070.24800E	011901	3	4	2230
0.20000E	070.24180E	010.21000E	070.25290E	010.22000E	070.26220E	011901	3	4	2240
0.23000E	070.27530E	010.24000E	070.28650E	010.25000E	070.29570E	011901	3	4	2250
0.26000E	070.30590E	010.27000E	070.31430E	010.28000E	070.32290E	011901	3	4	2260
0.29000E	070.33040E	010.30000E	070.33770E	010.31000E	070.33970E	011901	3	4	2270
0.32000E	070.34060E	010.33000E	070.34170E	010.34000E	070.34170E	011901	3	4	2280
0.35000E	070.34140E	010.36000E	070.34050E	010.37000E	070.33890E	011901	3	4	2290
0.38000E	070.33710E	010.39000E	070.33500E	010.40000E	070.33250E	011901	3	4	2300
0.41000E	070.33320E	010.42000E	070.33360E	010.43000E	070.33370E	011901	3	4	2310
0.44000E	070.33330E	010.45000E	070.33260E	010.46000E	070.33170E	011901	3	4	2320
0.47000E	070.33050E	010.48000E	070.32930E	010.49000E	070.32780E	011901	3	4	2330
0.50000E	070.32620E	010.51000E	070.32530E	010.52000E	070.32540E	011901	3	4	2340
0.53000E	070.32480E	010.54000E	070.32400E	010.55000E	070.32330E	011901	3	4	2350
0.56000E	070.32240E	010.57000E	070.32130E	010.58000E	070.32000E	011901	3	4	2360
0.59000E	070.31860E	010.60000E	070.31710E	010.61000E	070.31440E	011901	3	4	2370
0.62000E	070.31130E	010.63000E	070.30730E	010.64000E	070.30320E	011901	3	4	2380
0.65000E	070.29390E	010.66000E	070.29230E	010.67000E	070.28630E	011901	3	4	2390
0.68000E	070.27800E	010.69000E	070.26840E	010.70000E	070.25830E	011901	3	4	2400
0.71000E	070.24530E	010.72000E	070.23210E	010.73000E	070.21930E	011901	3	4	2410
0.74000E	070.20660E	010.75000E	070.19420E	010.76000E	070.18320E	011901	3	4	2420
0.77000E	070.17240E	010.78000E	070.16300E	010.79000E	070.15470E	011901	3	4	2430
0.80000E	070.14570E	010.81000E	070.13980E	010.82000E	070.13300E	011901	3	4	2440
0.83000E	070.12720E	010.84000E	070.12250E	010.85000E	070.11780E	011901	3	4	2450
0.86000E	070.11400E	010.87000E	070.11040E	010.88000E	070.10700E	011901	3	4	2460
0.89000E	070.10420E	010.90000E	070.10130E	010.91000E	070.97600E	001901	3	4	2470
0.92000E	070.94100E	000.93000E	070.91000E	000.94000E	070.83400E	001901	3	4	2480
0.9.5000E	070.35700E	000.96000E	070.83200E	000.97000E	070.80800E	001901	3	4	2490
0.98000E	070.73700E	000.99000E	070.77000E	000.10000E	080.75400E	001901	3	4	2500
0.10200E	080.71700E	000.10400E	080.63500E	000.10600E	080.67000E	001901	3	4	2510
0.10800E	080.65800E	000.11000E	080.55100E	000.11200E	080.64600E	001901	3	4	2520
0.11400E	080.64600E	000.11600E	080.64900E	000.11800E	080.65300E	001901	3	4	2530
0.12000E	080.67200E	000.12200E	080.67100E	000.12400E	080.63900E	001901	3	4	2540
0.12600E	080.64600E	000.12800E	080.62000E	000.13000E	080.59500E	001901	3	4	2550
0.13200E	080.55700E	000.13400E	080.47400E	000.13600E	080.46500E	001901	3	4	2560
0.13800E	080.41900E	000.14000E	080.37900E	000.14200E	080.34500E	001901	3	4	2570
0.14400E	080.32500E	000.14600E	080.32100E	000.14800E	080.32800E	001901	3	4	2580
0.15000E	080.26600E	000.15200E	080.27000E	000.15400E	080.27800E	001901	3	4	2590
0.15600E	080.23200E	000.15800E	080.29000E	000.16000E	080.27700E	001901	3	4	2600
0.16200E	080.24700E	000.16400E	080.22200E	000.16600E	080.18400E	001901	3	4	2610
0.16800E	080.14200E	000.17000E	080.10100E	000.17200E	080.62000E-	011901	3	4	2620
0.17400E	080.25000E-	010.	0.	0.	0.	1901	3	4	2630
						1901	3	0	2640
.90232+ 5	2.30045+ 2		0	99	0	1901	3	16	2650
.0	.0		0	0	1	871901	3	16	2660
	87	2	0	0	0	01901	3	16	2670

```
0.64300E 070.              0.65000E 070.20000E-020.66000E 070.27000E-011901 3 16 2680
0.67000E 070.52000E-010.68000E 070.10200E 000.69000E 070.17600E 001901 3 16 2690
0.70000E 070.25000E 000.71000E 070.36400E 000.72000E 070.47500E 001901 3 16 2700
0.73000E 070.59400E 000.74000E 070.71200E 000.75000E 070.83000E 001901 3 16 2710
0.76000E 070.93500E 000.77000E 070.10420E 010.78000E 070.11370E 011901 3 16 2720
0.79000E 070.12210E 010.80000E 070.13050E 010.81000E 070.13670E 011901 3 16 2730
0.82000E 070.14290E 010.83000E 070.14510E 010.84000E 070.15230E 011901 3 16 2740
0.85000E 070.15650E 010.86000E 070.15990E 010.87000E 070.16330E 011901 3 16 2750
0.88000E 070.16640E 010.89000E 070.16920E 010.90000E 070.17200E 011901 3 16 2760
0.91000E 070.17480E 010.92000E 070.17760E 010.93000E 070.18010E 011901 3 16 2770
0.94000E 070.18230E 010.95000E 070.18450E 010.96000E 070.18670E 011901 3 16 2780
0.97000E 070.18890E 010.98000E 070.19080E 010.99000E 070.19240E 011901 3 16 2790
0.10000E 080.19400E 010.10200E 080.19640E 010.10400E 080.19860E 011901 3 16 2800
0.10600E 080.19940E 010.10800E 080.20010E 010.11000E 080.20050E 011901 3 16 2810
0.11200E 080.19970E 010.11400E 080.19860E 010.11600E 080.19720E 011901 3 16 2820
0.11800E 080.19540E 010.12000E 080.19300E 010.12200E 080.18980E 011901 3 16 2830
0.12400E 080.18630E 010.12600E 080.18250E 010.12800E 080.17870E 011901 3 16 2840
0.13000E 080.17350E 010.13200E 080.16830E 010.13400E 080.16230E 011901 3 16 2850
0.13600E 080.15720E 010.13800E 080.15130E 010.14000E 080.14450E 011901 3 16 2860
0.14200E 080.13650E 010.14400E 080.12760E 010.14600E 080.11800E 011901 3 16 2870
0.14800E 080.10790E 010.15000E 080.97500E 000.15200E 080.87100E 001901 3 16 2880
0.15400E 080.77000E 000.15600E 080.67200E 000.15800E 080.59700E 001901 3 16 2890
0.16000E 080.52500E 000.16200E 080.48100E 000.16400E 080.44600E 001901 3 16 2900
0.16600E 080.42200E 000.16800E 080.40700E 000.17000E 080.39500E 001901 3 16 2910
0.17200E 080.38300E 000.17400E 080.37100E 000.17600E 080.35700E 001901 3 16 2920
0.17800E 080.33300E 000.18000E 080.32000E 000.18200E 080.30800E 001901 3 16 2930
0.18400E 080.29600E 000.18600E 080.28600E 000.18800E 080.27800E 001901 3 16 2940
0.19000E 080.27000E 000.19200E 080.26200E 000.19400E 080.25400E 001901 3 16 2950
0.19600E 080.24700E 000.19800E 080.24100E 000.20000E 080.23500E 001901 3 16 2960
                                                                  1901 3  0 2970
 .90232+ 5 2.30045+ 2          0         99          0          1901 3 17 2980
 .0         .0                 0          0          1        431901 3 17 2990
         43          2         0          0          0         01901 3 17 3000
0.11600E 080.              0.11800E 080.20000E-020.12000E 080.50000E-021901 3 17 3010
0.12200E 080.18000E-010.12400E 080.45000E-010.12600E 080.80000E-011901 3 17 3020
0.12800E 080.12500E 000.13000E 080.18500E 000.13200E 080.25700E 001901 3 17 3030
0.13400E 080.33100E 000.13600E 080.42900E 000.13800E 080.51800E 001901 3 17 3040
0.14000E 080.61000E 000.14200E 080.70600E 000.14400E 080.79600E 001901 3 17 3050
0.14600E 080.88000E 000.14800E 080.95800E 000.15000E 080.10300E 011901 3 17 3060
0.15200E 080.11020E 010.15400E 080.11630E 010.15600E 080.12300E 011901 3 17 3070
0.15800E 080.12870E 010.16000E 080.13360E 010.16200E 080.13840E 011901 3 17 3080
0.16400E 080.14150E 010.16600E 080.14560E 010.16800E 080.14880E 011901 3 17 3090
0.17000E 080.15160E 010.17200E 080.15430E 010.17400E 080.15680E 011901 3 17 3100
0.17600E 080.15900E 010.17800E 080.16110E 010.18000E 080.16310E 011901 3 17 3110
0.18200E 080.16430E 010.18400E 080.16530E 010.18600E 080.16590E 011901 3 17 3120
0.18800E 080.16630E 010.19000E 080.16650E 010.19200E 080.16650E 011901 3 17 3130
0.19400E 080.16640E 010.19600E 080.16610E 010.19800E 080.16570E 011901 3 17 3140
0.20000E 080.16480E 010.         0.         0.         0.         1901 3 17 3150
                                                                  1901 3  0 3160
 .90232+ 5 2.30045+ 2          0         99          0          1901 3 18 3170
 .0         .0                 0          0          1       1401901 3 18 3180
        140          2         0          0          0         01901 3 18 3190
0.11000E 070.15000E-020.12000E 070.49000E-020.13000E 070.19400E-011901 3 18 3200
0.14000E 070.56500E-010.15000E 070.64900E-010.16000E 070.12220E 001901 3 18 3210
0.17000E 070.93500E-010.18000E 070.73000E-010.19000E 070.10900E 001901 3 18 3220
0.20000E 070.11720E 000.21000E 070.12100E 000.22000E 070.13800E 001901 3 18 3230
0.23000E 070.11600E 000.24000E 070.11000E 000.25000E 070.12000E 001901 3 18 3240
0.26000E 070.11600E 000.27000E 070.12500E 000.28000E 070.12700E 001901 3 18 3250
0.29000E 070.13300E 000.30000E 070.13500E 000.31000E 070.13600E 001901 3 18 3260
0.32000E 070.13900E 000.33000E 070.13700E 000.34000E 070.13900E 001901 3 18 3270
0.35000E 070.13900E 000.36000E 070.14100E 000.37000E 070.14300E 001901 3 18 3280
0.38000E 070.14300E 000.39000E 070.14200E 000.40000E 070.14000E 001901 3 18 3290
0.41000E 070.14100E 000.42000E 070.14200E 000.43000E 070.14300E 001901 3 18 3300
0.44000E 070.14500E 000.45000E 070.14600E 000.46000E 070.14700E 001901 3 18 3310
0.47000E 070.14800E 000.48000E 070.14800E 000.49000E 070.14800E 001901 3 18 3320
0.50000E 070.14700E 000.51000E 070.14600E 000.52000E 070.14500E 001901 3 18 3330
0.53000E 070.14400E 000.54000E 070.14400E 000.55000E 070.14400E 001901 3 18 3340
0.56000E 070.14500E 000.57000E 070.14700E 000.58000E 070.15100E 001901 3 18 3350
0.59000E 070.15600E 000.60000E 070.16200E 000.61000E 070.17700E 001901 3 18 3360
0.62000E 070.19700E 000.63000E 070.22700E 000.64000E 070.25700E 001901 3 18 3370
0.65000E 070.28900E 000.66000E 070.32100E 000.67000E 070.34700E 001901 3 18 3380
0.68000E 070.37200E 000.69000E 070.38700E 000.70000E 070.40200E 001901 3 18 3390
0.71000E 070.40300E 000.72000E 070.41300E 000.73000E 070.41200E 001901 3 18 3400
0.74000E 070.41000E 000.75000E 070.40600E 000.76000E 070.40100E 001901 3 18 3410
0.77000E 070.39500E 000.78000E 070.38900E 000.79000E 070.38300E 001901 3 18 3420
0.80000E 070.37700E 000.81000E 070.37200E 000.82000E 070.36700E 001901 3 18 3430
0.83000E 070.36300E 000.84000E 070.35900E 000.85000E 070.35600E 001901 3 18 3440
0.86000E 070.35300E 000.87000E 070.35000E 000.88000E 070.34600E 001901 3 18 3450
0.89000E 070.34500E 000.90000E 070.34300E 000.91000E 070.34200E 001901 3 18 3460
0.92000E 070.33900E 000.93000E 070.33700E 000.94000E 070.33500E 001901 3 18 3470
0.95000E 070.33400E 000.96000E 070.33200E 000.97000E 070.33000E 001901 3 18 3480
0.98000E 070.32800E 000.99000E 070.32700E 000.10000E 080.32500E 001901 3 18 3490
0.10200E 080.32100E 000.10400E 080.31800E 000.10600E 080.31500E 001901 3 18 3500
0.10800E 080.31200E 000.11000E 080.31000E 000.11200E 080.30800E 001901 3 18 3510
0.11400E 080.30600E 000.11600E 080.30600E 000.11800E 080.30600E 001901 3 18 3520
0.12000E 080.30600E 000.12200E 080.30800E 000.12400E 080.31100E 001901 3 18 3530
0.12600E 080.31400E 000.12800E 080.31900E 000.13000E 080.32400E 001901 3 18 3540
0.13200E 080.33100E 000.13400E 080.33800E 000.13600E 080.34600E 001901 3 18 3550
0.13800E 080.35500E 000.14000E 080.36400E 000.14200E 080.37300E 001901 3 18 3560
```

```
0.14400E 080.38300E 000.14600E 080.39200E 000.14800E 080.40100E 001901 3 18 3570
0.15000E 080.41000E 000.15200E 080.41800E 000.15400E 080.42600E 001901 3 18 3580
0.15600E 080.43300E 000.15800E 080.44000E 000.16000E 080.44700E 001901 3 18 3590
0.16200E 080.45300E 000.16400E 080.45900E 000.16600E 080.46400E 001901 3 18 3600
0.16800E 080.45900E 000.17000E 080.47400E 000.17200E 080.47800E 001901 3 18 3610
0.17400E 080.48200E 000.17600E 080.43600E 000.17800E 080.49000E 001901 3 18 3620
0.18000E 080.49400E 000.18200E 080.49800E 000.18400E 080.50300E 001901 3 18 3630
0.18600E 080.50800E 000.18800E 080.51400E 000.19000E 080.52100E 001901 3 18 3640
0.19200E 080.52800E 000.19400E 080.53600E 000.19600E 080.54500E 001901 3 18 3650
0.19500E 080.55600E 000.20000E 080.56700E 000.              0.          1901 3 18 3660
                                                                        1901 3  0 3670
  .90232+ 5 2.30045+ 2        0          1          0                   1901 3 51 3680
  .0        .0                0          0          1                 181901 3 51 3690
          18         2                                                  1901 3 51 3700
0.10000E 070.10640E 010.20000E 070.47131E 000.30000E 070.49494E 001901 3 51 3710
0.40000E 070.41416E 000.50000E 070.36382E 000.60000E 070.32581E 001901 3 51 3720
0.70000E 070.24660E 000.80000E 070.12866E 000.90000E 070.86558E-011901 3 51 3730
0.10000E 080.61616E-010.11000E 080.50770E-010.12000E 080.53429E-011901 3 51 3740
0.13000E 080.43571E-010.14000E 080.26038E-010.15000E 080.18375E-011901 3 51 3750
0.16000E 080.19873E-010.17000E 080.66532E-020.18000E 080.               1901 3 51 3760
                                                                        1901 3  0 3770
  .90232+ 5 2.30045+ 2        0          2          0                   1901 3 52 3780
  .0        .0                0          0          1                 181901 3 52 3790
          18         2        0          0          0                   1901 3 52 3800
0.10000E 070.30564E 000.20000E 070.32337E 000.30000E 070.46191E 001901 3 52 3810
0.40000E 070.44905E 000.50000E 070.43060E 000.60000E 070.40890E 001901 3 52 3820
0.70000E 070.32359E 000.80000E 070.17337E 000.90000E 070.11953E 001901 3 52 3830
0.10000E 080.36618E-010.11000E 080.72675E-010.12000E 080.77531E-011901 3 52 3840
0.13000E 080.53657E-010.14000E 080.38627E-010.15000E 080.27475E-011901 3 52 3850
0.16000E 080.28523E-010.17000E 080.10072E-010.18000E 080.               1901 3 52 3860
                                                                        1901 3  0 3870
  .90232+ 5 2.30045+ 2        0          3          0                   1901 3 53 3880
  .0        .0                0          0          1                 181901 3 53 3890
          18         2                                                  1901 3 53 3900
0.10000E 070.10338E-010.20000E 070.71171E-010.30000E 070.20728E 001901 3 53 3910
0.40000E 070.26871E 000.50000E 070.29584E 000.60000E 070.31596E 001901 3 53 3920
0.70000E 070.27703E 000.80000E 070.15849E 000.90000E 070.11415E 001901 3 53 3930
0.10000E 080.85869E-010.11000E 080.74415E-010.12000E 080.31554E-011901 3 53 3940
0.13000E 080.63354E-010.14000E 080.42459E-010.15000E 080.30769E-011901 3 53 3950
0.16000E 080.30439E-010.17000E 080.11582E-010.18000E 080.               1901 3 53 3960
                                                                        1901 3  0 3970
  .90232+ 5 2.30045+ 2        0          4          0                   1901 3 54 3980
  .0        .0                0          0          1                 181901 3 54 3990
          18         2                                                  1901 3 54 4000
0.10000E 070.          0.20000E 070.23990E-020.30000E 070.35932E-011901 3 54 4010
0.40000E 070.82373E-010.50000E 070.12224E 000.60000E 070.15673E 001901 3 54 4020
0.70000E 070.15639E 000.80000E 070.99239E-010.90000E 070.76896E-011901 3 54 4030
0.10000E 080.61710E-010.11000E 080.56502E-010.12000E 080.65139E-011901 3 54 4040
0.13000E 080.57361E-010.14000E 080.36672E-010.15000E 080.27389E-011901 3 54 4050
0.16000E 080.29587E-010.17000E 080.10842E-010.18000E 080.               1901 3 54 4060
                                                                        1901 3  0 4070
  .90232+ 5 2.30045+ 2        0          5          0                   1901 3 55 4080
  .0        .0                0          0          1                 181901 3 55 4090
          18         2                                                  1901 3 55 4100
0.10000E 070.19734E 000.20000E 070.11545E 000.30000E 070.12381E 001901 3 55 4110
0.40000E 070.99367E-010.50000E 070.86301E-010.60000E 070.77382E-011901 3 55 4120
0.70000E 070.38570E-010.80000E 070.30816E-010.90000E 070.20718E-011901 3 55 4130
0.10000E 080.14514E-010.11000E 080.11874E-010.12000E 080.12338E-011901 3 55 4140
0.13000E 080.99933E-020.14000E 080.59426E-020.15000E 080.41603E-021901 3 55 4150
0.16000E 080.42572E-020.17000E 080.15093E-020.18000E 080.               1901 3 55 4160
                                                                        1901 3  0 4170
  .90232+ 5 2.30045+ 2        0          6          0                   1901 3 56 4180
  .0        .0                0          0          1                 181901 3 56 4190
          18         2                                                  1901 3 56 4200
0.10000E 070.35959E 000.20000E 070.34486E 000.30000E 070.42478E 001901 3 56 4210
0.40000E 070.37428E 000.50000E 070.33679E 000.60000E 070.30745E 001901 3 56 4220
0.70000E 070.23383E 000.80000E 070.12286E 000.90000E 070.83072E-011901 3 56 4230
0.10000E 080.59650E-010.11000E 080.49337E-010.12000E 080.51965E-011901 3 56 4240
0.13000E 080.42471E-010.14000E 080.30964E-010.15000E 080.17941E-011901 3 56 4250
0.16000E 080.18519E-010.17000E 080.64992E-020.18000E 080.               1901 3 56 4260
                                                                        1901 3  0 4270
  .90232+ 5 2.30045+ 2        0          7          0                   1901 3 57 4280
  .0        .0                0          0          1                 181901 3 57 4290
          18         2                                                  1901 3 57 4300
0.10000E 070.34380E 000.20000E 070.34296E 000.30000E 070.42348E 001901 3 57 4310
0.40000E 070.37358E 000.50000E 070.33629E 000.60000E 070.30714E 001901 3 57 4320
0.70000E 070.23368E 000.80000E 070.12274E 000.90000E 070.33072E-011901 3 57 4330
0.10000E 080.59650E-010.11000E 080.49337E-010.12000E 080.51965E-011901 3 57 4340
0.13000E 080.42471E-010.14000E 080.30964E-010.15000E 080.17941E-011901 3 57 4350
0.16000E 080.18519E-010.17000E 080.64992E-020.18000E 080.               1901 3 57 4360
                                                                        1901 3  0 4370
  .90232+ 5 2.30045+ 2        0          8          0                   1901 3 58 4380
  .0        .0                0          0          1                 181901 3 58 4390
          18         2                                                  1901 3 58 4400
0.10000E 070.          0.20000E 070.          0.30000E 070.30071E-031901 3 58 4410
0.40000E 070.77974E-020.50000E 070.23527E-010.60000E 070.44915E-011901 3 58 4420
0.70000E 070.57969E-010.80000E 070.43316E-010.90000E 070.38249E-011901 3 58 4430
0.10000E 080.33430E 000.11000E 080.36644E-010.12000E 080.39732E-021901 3 58 4440
0.13000E 080.37275E-010.14000E 080.24865E-010.15000E 080.19415E-011901 3 58 4450
```

```
0.160000E 080.21783E-010.170000E 080.92242E-020.180000E 080.                1901  3 58 4460
                                                                             1901  3 58 4470
  .90232+ 5 2.30045+ 2           0           9           0                  1901  3 59 4480
  .0        .0                   0           0           1           181901  3 59 4490
          18          2                                                      1901  3 59 4500
0.100000E 070.29751E-010.200000E 070.20502E 000.300000E 070.37703E 001901  3 59 4510
0.400000E 070.39507E 000.500000E 070.39226E 000.600000E 070.38203E 001901  3 59 4520
0.700000E 070.30507E 000.800000E 070.16540E 000.900000E 070.11485E 001901  3 59 4530
0.100000E 080.83309E-010.110000E 080.70423E-010.120000E 080.75385E-011901  3 59 4540
0.130000E 080.62358E-010.140000E 080.37787E-010.150000E 080.26955E-011901  3 59 4550
0.160000E 080.25111E-010.170000E 080.92875E-020.180000E 080.                1901  3 59 4560
                                                                             1901  3  0 4570
  .90232+ 5 2.30045+ 2           0          10           0                  1901  3 60 4580
  .0        .0                   0           0           1           181901  3 60 4590
          18          2                                                      1901  3 60 4600
 .100000E 070.          0.200000E 070.22088E-010.300000E 070.15013E 001901  3 60 4610
 .400000E 070.21923E 000.500000E 070.26010E 000.600000E 070.28847E 001901  3 60 4620
 .700000E 070.25501E 000.800000E 070.14863E 000.900000E 070.10867E 001901  3 60 4630
 .100000E 080.32498E-010.110000E 080.71753E-010.120000E 080.79045E-011901  3 60 4640
 .130000E 080.66855E-010.140000E 080.42537E-010.150000E 080.29989E-011901  3 60 4650
 .160000E 080.31645E-010.170000E 080.11335E-010.180000E 080.                1901  3 60 4660
 .190000E 080.          0.200000E 080.          0.210000E 080.              1901  3 60 4670
                                                                             1901  3  0 4680
  .90232+ 5 2.30045+ 2           0          11           0                  1901  3 61 4690
  .0        .0                   0           0           1           181901  3 61 4700
          18          2                                                      1901  3 61 4710
 .100000E 070.          0.200000E 070.24780E 000.300000E 070.28365E 001901  3 61 4720
 .400000E 070.24912E 000.500000E 070.22176E 000.600000E 070.20206E 001901  3 61 4730
 .700000E 070.15256E 000.800000E 070.79217E-010.900000E 070.53685E-011901  3 61 4740
 .100000E 080.38487E-010.110000E 080.31833E-010.120000E 080.33458E-011901  3 61 4750
 .130000E 080.27182E-010.140000E 080.16264E-010.150000E 080.11441E-011901  3 61 4760
 .160000E 080.11849E-010.170000E 080.41583E-020.180000E 080.                1901  3 61 4770
                                                                             1901  3  0 4730
  .90232+ 5 2.30045+ 2           0          12           0                  1901  3 62 4790
  .0        .0                   0           0           1           181901  3 62 4800
          18          2                                                      1901  3 62 4810
 .100000E 070.          0.200000E 070.26559E 000.300000E 070.39625E 001901  3 62 4820
 .400000E 070.39177E 000.500000E 070.37243E 000.600000E 070.35424E 001901  3 62 4830
 .700000E 070.27823E 000.800000E 070.14793E 000.900000E 070.10140E 001901  3 62 4840
 .100000E 080.73508E-010.110000E 080.61415E-010.120000E 080.65243E-011901  3 62 4850
 .130000E 080.53664E-010.140000E 080.32215E-010.150000E 080.22882E-011901  3 62 4860
 .160000E 080.23698E-010.170000E 080.83474E-020.180000E 080.                1901  3 62 4870
                                                                             1901  3  0 4880
  .90232+ 5 2.30045+ 2           0          13           0                  1901  3 63 4890
  .0        .0                   0           0           1           181901  3 63 4900
          18          2                                                      1901  3 63 4910
 .100000E 070.          0.200000E 070.          0.300000E 070.              1901  3 63 4920
 .400000E 070.          0.500000E 070.          0.600000E 070.              1901  3 63 4930
 .700000E 070.94113E-020.800000E 070.10504E-010.900000E 070.12152E-011901  3 63 4940
 .100000E 080.12642E-010.110000E 080.14023E-010.120000E 080.18925E-011901  3 63 4950
 .130000E 080.19087E-010.140000E 080.13624E-010.150000E 080.11268E-011901  3 63 4960
 .160000E 080.13197E-010.170000E 080.53904E-020.180000E 080.                1901  3 63 4970
                                                                             1901  3  0 4980
  .90232+ 5 2.30045+ 2           0          99           0                  1901 3102 4990
  .0        .0                   0           0           1          1581901 3102 5000
          158         2                                                      1901 3102 5010
0.150000E 060.18600E 000.200000E 060.15900E 000.250000E 060.14600E 001901 3102 5020
0.300000E 060.14100E 000.350000E 060.14200E 000.400000E 060.14600E 001901 3102 5030
0.450000E 060.15100E 000.500000E 060.15700E 000.550000E 060.16100E 001901 3102 5040
0.600000E 060.16300E 000.650000E 060.16300E 000.700000E 060.16100E 001901 3102 5050
0.750000E 060.15800E 000.800000E 060.15300E 000.850000E 060.14800E 001901 3102 5060
0.900000E 060.14200E 000.950000E 060.13600E 000.100000E 070.13000E 001901 3102 5070
0.110000E 070.11900E 000.120000E 070.11100E 000.130000E 070.10400E 001901 3102 5080
0.140000E 070.99200E-010.150000E 070.94500E-010.160000E 070.89300E-011901 3102 5090
0.170000E 070.84300E-010.180000E 070.73600E-010.190000E 070.72900E-011901 3102 5100
0.200000E 070.67000E-010.210000E 070.61100E-010.220000E 070.55200E-011901 3102 5110
0.230000E 070.49400E-010.240000E 070.44000E-010.250000E 070.39100E-011901 3102 5120
0.260000E 070.34700E-010.270000E 070.30900E-010.280000E 070.27700E-011901 3102 5130
0.290000E 070.24900E-010.300000E 070.22400E-010.310000E 070.20300E-011901 3102 5140
0.320000E 070.18500E-010.330000E 070.17000E-010.340000E 070.15700E-011901 3102 5150
0.350000E 070.14700E-010.360000E 070.14200E-010.370000E 070.13800E-011901 3102 5160
0.380000E 070.13500E-010.390000E 070.13200E-010.400000E 070.13000E-011901 3102 5170
0.410000E 070.12300E-010.420000E 070.12600E-010.430000E 070.12400E-011901 3102 5180
0.440000E 070.12200E-010.450000E 070.11900E-010.460000E 070.11700E-011901 3102 5190
0.470000E 070.11500E-010.480000E 070.11300E-010.490000E 070.11200E-011901 3102 5200
0.500000E 070.11000E-010.510000E 070.10900E-010.520000E 070.10800E-011901 3102 5210
0.530000E 070.10700E-010.540000E 070.10600E-010.550000E 070.10400E-011901 3102 5220
0.560000E 070.10300E-010.570000E 070.10200E-010.580000E 070.10100E-011901 3102 5230
0.590000E 070.10000E-010.600000E 070.99000E-020.610000E 070.98000E-021901 3102 5240
0.620000E 070.97000E-020.630000E 070.96000E-020.640000E 070.95000E-021901 3102 5250
0.650000E 070.94000E-020.660000E 070.93000E-020.670000E 070.92000E-021901 3102 5260
0.680000E 070.92000E-020.690000E 070.91000E-020.700000E 070.90000E-021901 3102 5270
0.710000E 070.89000E-020.720000E 070.88000E-020.730000E 070.88000E-021901 3102 5280
0.740000E 070.87000E-020.750000E 070.86000E-020.760000E 070.86000E-021901 3102 5290
0.770000E 070.85000E-020.780000E 070.84000E-020.790000E 070.83000E-021901 3102 5300
0.800000E 070.83000E-020.810000E 070.82000E-020.820000E 070.81000E-021901 3102 5310
0.830000E 070.81000E-020.840000E 070.80000E-020.850000E 070.80000E-021901 3102 5320
0.860000E 070.79000E-020.870000E 070.78000E-020.880000E 070.78000E-021901 3102 5330
0.890000E 070.77000E-020.900000E 070.76000E-020.910000E 070.76000E-021901 3102 5340
```

```
0.92000E 070.75000E-020.93000E 070.75000E-020.94000E 070.74000E-021901 3102 5350
0.95000E 070.73000E-020.96000E 070.73000E-020.97000E 070.72000E-021901 3102 5360
0.98000E 070.72000E-020.99000E 070.71000E-020.10000E 080.71000E-021901 3102 5370
0.10200E 080.70000E-020.10400E 080.65000E-020.10600E 080.67000E-021901 3102 5380
0.10800E 070.65000E-020.11000E 080.65000E-020.11200E 080.64000E-021901 3102 5390
0.11400E 070.63000E-020.11600E 080.62000E-020.11800E 080.61000E-021901 3102 5400
0.12200E 080.60000E-020.12200E 080.59000E-020.12400E 080.58000E-021901 3102 5410
0.12600E 080.57000E-020.12800E 080.56000E-020.13000E 080.56000E-021901 3102 5420
0.13200E 080.55000E-020.13400E 080.50000E-020.13600E 080.53000E-021901 3102 5430
0.13800E 080.52000E-020.14000E 080.52000E-020.14200E 080.51000E-021901 3102 5440
0.14400E 080.50000E-020.14600E 080.50000E-020.14300E 080.49000E-021901 3102 5450
0.15000E 080.45000E-020.15200E 080.47000E-020.15400E 080.47000E-021901 3102 5460
0.15600E 080.45000E-020.15300E 080.45000E-020.16000E 080.44000E-021901 3102 5470
0.16200E 080.43000E-020.16400E 080.42000E-020.16600E 080.42000E-021901 3102 5480
0.16800E 080.41000E-020.17000E 080.40000E-020.17200E 080.40000E-021901 3102 5490
0.17400E 080.39000E-020.17600E 080.38000E-020.17800E 080.38000E-021901 3102 5500
0.18000E 080.37000E-020.18200E 080.36000E-020.18400E 080.36000E-021901 3102 5510
0.18600E 080.35000E-020.18500E 080.34000E-020.19000E 080.33000E-021901 3102 5520
0.19200E 080.33000E-020.19400E 080.32000E-020.19600E 080.31000E-021901 3102 5530
0.19800E 080.31000E-020.20000E 080.30000E-020.        0.                1901 3102 5540
                                                                        1901 3    0 5550
                                                                          -1 0    0 5560
```

COMPUTER CENTRE KALPAKKAM

APPENDIX B

It is planned to analyze THOR assembly (Ref.B.1) which being a plutonium sphere surrounded by thorium metal throws light on neutron transport in Th-232 in fission source energy range.

In this appendix, details of analyses of THOR assembly whose specifications are given in Table B.1, using the 1969 French set are presented. In our calculations the homogenized region dependent cross sections were first generated using EFFCROSS code (Ref.B.2). The neutronic calculations of K_{eff} and spectral indices at core center were performed using one-dimensional transport code DTF-IV (Ref.B.3). The latter calculations utilized S_{16} with 150 mesh intervals in core, 150 in reflector surface and a 25 energy group structure shown in Table B.2. The results of calculations are given in Table B.3. These results which reveal the need for improving cross sections for Th-232 are interpreted in Section 4.0 of the text.

Table B.1

THOR assembly (Ref.B.1) is a thorium reflected Pu sphere. It consists of a sphere of plutonium within 5.1% ^{240}Pu content centered in a close fitting 53.3 cm equilateral cylinder of thorium metal. It emphasizes neutron transport in Th-232 in fission source energy range. (Ref.B.1)

The equivalent spherical model is a core of radius 5.310 cm centered in a reflector of 5.310 cm inner radius and 29.88 cm outer radius. The compositions are as follows (Ref.B.1)

Isotope	Core	Reflector
(nuclei/barn-cm)		
^{239}Pu	0.03618	-
^{240}Pu	0.00194	-
Ga	0.00133	-
^{232}Th	-	0.03005

Table B.2 Energy Group Structure and flux for THOR assembly

Group	Upper Energy	Lower Energy	Lethargy Width	Speed Cm/S	Flux*
1	14.5 MeV	3.68 MeV	1.37	0.30490E 10	0.68833
2	3.68 MeV	2.23 MeV	0.50	0.23200E 10	1.13819
3	2.23 MeV	1.36 MeV	0.50	0.17990E 10	1.40164
4	1.36 MeV	822 KeV	0.50	0.14010E 10	1.37167
5	822 KeV	499 KeV	0.50	0.10920E 10	1.15538
6	499 KeV	302 KeV	0.50	0.85030E 09	0.86021
7	302 KeV	183 KeV	0.50	0.67290E 09	0.54067
8	183 KeV	111 KeV	0.50	0.52080E 09	0.31835
9	111 KeV	67.5 KeV	0.50	0.40570E 09	0.17000
10	67.5 KeV	40.9 KeV	0.50	0.31610E 09	0.08670
11	40.9 KeV	24.8 KeV	0.50	0.24940E 09	0.04123
12	24.8 KeV	15.1 KeV	0.50	0.19360E 09	0.01676
13	15.1 KeV	9.13 KeV	0.50	0.15030E 09	0.00495
14	9.13 KeV	5.54 KeV	0.50	0.11730 E09	0.00191
15	5.54 KeV	3.36 KeV	0.50	0.92430E 08	0.00075
16	3.36 KeV	2.04 KeV	0.50	0.67460E 08	0.00029
17	2.04 KeV	1.24 KeV	0.50	0.55200E 08	-
18	1.24 KeV	750 eV	0.50	0.43170E 08	-
19	750 eV	455 eV	0.50	0.33650E 08	-
20	455 eV	276 eV	0.50	0.26200E 08	-
21	276 eV	101 eV	1.00	0.18420E 08	-
22	101 eV	22.6 eV	1.50	0.10240E 08	-
23	22.6 eV	3.06 eV	2.00	0.50950E 07	-
24	3.06 eV	0.414 eV	2.00	0.18750E 07	-
25	0.414eV	0.025 eV	2.79	0.21800E 06	-

* Calculated using ENDF/B-IV data based data set. The fluxes calculated by French set and JENDL 1 based set differ from these values by 1 to 5% in various groups.

Table B.3 Analysis of THOR assembly using 1969 adjusted French set and ENDF/B-IV based RRC set

Sr. No.	Quantity	Experimental (E)	Calculated (C) and (C/E)	
			French set	ENDF/B-IV based RRC set
1.	$\sigma_{f(^{238}U)}/\sigma_{f(^{235}U)}$	0.195 ± 0.003	0.156 (0.8)	0.169 (0.867)
2.	$\sigma_{f(^{232}Th)}/\sigma_{f(^{238}U)}$	0.260 ± 0.01	0.259 (0.996)	0.234 (0.900)
3.	$\sigma_{\gamma(^{238}U)}/\sigma_{f(^{235}U)}$	0.083 ± 0.003	0.0707 (0.852)	0.0744 (0.896)
4.	$\sigma_{\gamma(^{232}Th)}/\sigma_{\gamma(^{238}U)}$	1.20 ± 0.06	1.4067 (1.172)	1.387 (1.156)
5.	$\sigma_{\gamma(^{232}Th)}/\sigma_{f(^{232}Th)}$	1.9645 ± 0.146*	2.463 (1.253)	2.615 (1.330)
6.	K_{eff}	1.000 ± 0.001	0.9666	0.9950 0.9865**

* The experimental value and its error are derived by us from the experimental values of the first four ratios reported in Ref.(B.1)

** from Ref.B.1 (Hansen and Paxton) Calculated by using ENDF/B-IV.

REFERENCES TO APPENDIX B

B.1 Fast Reactor Benchmark No.25 in BNL-19302 (ENDF-202) 'Cross Section Evaluation Working Group Benchmark Specifications (1983) Brookhaven National Laboratory, U.S.A. See also G.E.Hansen and H.C. Paxton, Nucl. Sci. Eng., 71, 287 (1979).

B.2 J.Damiens and J.Ravier, 'Programme SETR-512 Exploitation des Constants Multigroups SETR Cadarache' Report DTR SETR No.67/746 (1967). Modified Version at Kalpakkam is called EFFCROSS.

B.3 K.D.Lathrop, 'DTF-IV, a FØRTRAN-IV Program for Solving the Multigroup Transport Equation with Anisotropic Scattering' LA-3373 (1965).

Contributed Paper 15

STATUS OF ^{239}Pu CROSS-SECTION EVALUATION IN THE RESONANCE REGION AT CADARACHE

H. DERRIEN*, P. LONG**

* DRNR/SPCI/LEPh
CEA, Centre d'études nucléaires de Cadarache,
Saint-Paul-lez-Durance

** CISI
Paris
(seconded to DRNR/SPCI/LEPh)

France

Abstract

The evaluation of ^{239}Pu cross sections in the resonance region is described. As set of resonance parameters resulting from a multi-level analysis in the energy range from thermal to 200 eV, and from a single level analysis in the energy range of 200 eV to 660 eV are proposed for the calculation of the cross sections for energies ranging from thermal to 660 eV. In view of some inconsistencies between the calculated and measured total and fission data over the broad resonances it is suggested that new transmission measurements be performed.

At the IAEA consultants Meeting on Uranium and Plutonium Isotope Resonance parameters in 1981 several recommandations were made concerning the evaluation of the ^{239}Pu cross-sections in the resonance region. It was tressed that the use of non smooth background should be avoided in the calculation of the cross-sections. It is well known that accurate ^{239}Pu cross-sections could not be obtained without a multilevel - multi-channel R matrix formalism specially in the broad 0^+ resonances. The purpose of the present evaluation is mainly to use a set of Reich-Moore parameters which was obtained several years ago by a simultaneous fit of the measured total and fission cross-sections of Saclay[20]. A reevaluation of the thermal data is also proposed to take into account the results of recent evaluations of the 2200 m data[6]. Unfortunately there is no multilevel data for the resonances in the energy range above 200 ev. Nevertheless, an up-dated version of the previous RIBON et al.[23] evaluation is proposed in the energy range 200 ev to 600 ev. But we should not expect that this evaluation could be enough accurate in the high energy range of the resolved

region to achieve the 0.5 % accuracy requirement in self-shielding factor calculations.

I - THERMAL AND LOW ENERGY REGION

1) Renormalization of the experimental fission cross-sections - Most of the fission cross-section measurements in the low or intermediate energy range are directly or indirectly normalized to the absolute measurement results obtained in thermal region. The data sets available for 2 200 m/s neutrons has been widely examined by several authors[1, 2, 3] in the past few years. However, the determination of an accurate value of the fission cross-section is strongly dependant on the half-life of ^{239}Pu, since the amount of the fissile material is obtained by alpha counting in the most precise absolute measurements. This half-life was supposed to be equal to (24 290 ± 70) years in the evaluation performed by H.D. LEMMEL[1] in 1975, when the value recommended in the most recent evaluation [4] is (24110 ± 30) years, i.e. a decrease of 0.75 %. Table I, which has been taken from the up-dated INDC/NEANDC standard file[6], compares the results of two evaluations[2, 3] taking into account the change in the ^{239}Pu half-life, to the ENDF/B-V evaluation which obviously refers to the earlier value of the half-life. In the present work, a 2 200 ms cross-section value of 748.1 barns has been used to renormalize all the available experimental fission cross-section data.

2) Reich-Moore multilevel calculation at low energy - The cross-sections in the low energy region can be reproduced by performing a multilevel formalism calculation with one unbound level at - 1.20 ev and the set of resonance parameters obtained by fitting the higher energy region (see next section). The parameters of the first resonances are given in table II. One should note that the energy of the unbound level is the same as the one used by E. VOGT[17] in a multilevel fit of the 0.01 ev to 10 ev region. But the other parameters are quite different for the reason that, in the present evaluation, the resonances at - 1.20 ev and 0.29 ev belong to the same spin family (0^+), which was not the case in E. VOGT calculation.

Table 1 2200 m/s cross sections for ^{233}U, ^{239}Pu, ^{241}Pu

(cross sections in barns)

		ENDF/B-V 1979	Evaluation by NNDC group 1983	Evaluation by Axton 1983
^{233}U	σ_A	574.2	574.7 ± 1.0	574.1 ± 1.8
	σ_f	528.4	529.1 ± 1.2	531.9 ± 2.4
	σ_γ	45.8	45.5 ± 0.7	42.2 ± 1.8
	α	0.0866	0.086 ± 0.002	0.079 ± 0.004
	η	2.296	2.296 ± 0.004	2.305 ± 0.006
	ν_t	2.495	2.493 ± 0.004	2.488 ± 0.006
^{239}Pu	σ_A	1011.9	1017.3 ± 2.9	1017.7 ± 3.8
	σ_f	741.7	748.1 ± 2.0	748.3 ± 2.4
	σ_γ	270.2	269.3 ± 2.2	269.4 ± 3.4
	α	0.3643	0.360 ± 0.003	0.360 ± 0.005
	η	2.119	2.115 ± 0.005	2.115 ± 0.007
	ν_t	2.891	2.877 ± 0.006	2.876 ± 0.007
^{241}Pu	σ_A	1376.4	1369.4 ± 7.7	1378.9 ± 12.7
	σ_f	1015.0	1011.1 ± 6.2	1018.0 ± 10.0
	σ_γ	361.4	358.2 ± 5.1	360.9 ± 5.6
	α	0.356	0.354 ± 0.006	0.355 ± 0.006
	η	2.178	2.169 ± 0.008	2.169 ± 0.008
	ν_t	2.953	2.937 ± 0.007	2.937 ± 0.007

TAKEN FROM INDC/NEANDC STANDARD FILE
(H.D. LEMMEL, Technical Reports Series nº 227, IAEA, page 71)

TABLE II

PARAMETERS OF THE LOW ENERGY RESONANCES

ENERGY (ev)	NEUTRON WIDTHS (mev)	FISSION WIDTHS (mev)		CAPTURE WIDTHS (mev)	G
		CHANNEL 1	CHANNEL 2		
-1.200	2.052	394.3	0.	26.6	0.25
0.296	0.236	3.1	57.9	39.0	0.25
7.800	0.770	-47.0	0.	40.0	0.75
10.910	1.850	-120.0	0.	55.0	0.75
11.250	0.900	-5000.0	0.	42.0	0.25
11.878	0.980	21.0	0.	42.0	0.75
14.307	0.660	61.0	0.	34.0	0.75
14.660	1.920	37.0	0.	38.0	0.75
15.455	1.780	-442.0	99.4	42.0	0.25

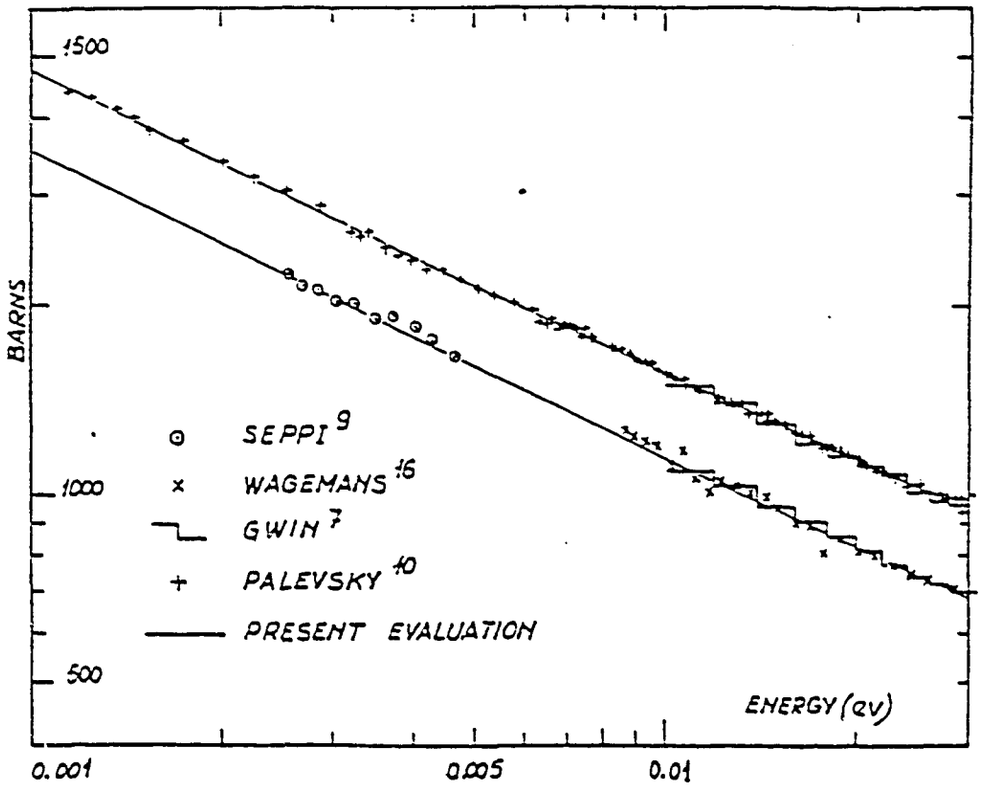

FIGURE 1 : Fission and total cross-sections at low energy

The results of the calculation below 0.03 ev are compared to the available experimental data on figure 1. The shape of the measured total, absorption and fission cross-sections are quite well reproduced. The lowest energy part corresponds to the total cross-section from PALEVSKY[10] down to 0.0012 ev and to the fission data of SEPPI[9] between 0.0025 ev and 0.0048 ev. The later has been renormalized to 478.1 b at 0.10 ev, corresponding to 748.1 b at 0.0253 ev. The reference value for the total cross-section at 0.0253 ev has been obtained from an examination of all the measured values in the energy range 0.02 ev to 0.03 ev by comparing the mean value of $\sigma_T \sqrt{E}$ for each set of data. The comparison between the experimental results is done in table III and figure 2.

The most recent data are from Columbia by SAFFORD et al.[14] (1961) who obtained (1018.0 $\pm$ 10) barns at 0.0253 ev, which superseeds the value of 1077.9 barns obtained in 1951 in the same laboratory[12] (HAVENS being coauthor of both measurements). In the present evaluation, the value (1028.0 $\pm$ 15.0) barns has been choosen ; it is a weighed average value of the experimen-

tal results taking into account the statistical accuracy of the measured data points. The systematic errors, which are not known, could not be considered. This averaged value agrees within 1 % with SAFFORD et al.[14] results and within 0.4 % with PALEVSKY value[10]. One should also note that, independently of any sophisticated calculation, the absorption cross-section could be obtained by subtracting a scattering cross-section of (8 ± 2) barns, leading to a value of (1020.0 ± 16) barns in agreement with the experimental value of (1023 ± 10) barns obtained by DURHAM et al[15] from sample irradiation experiment.

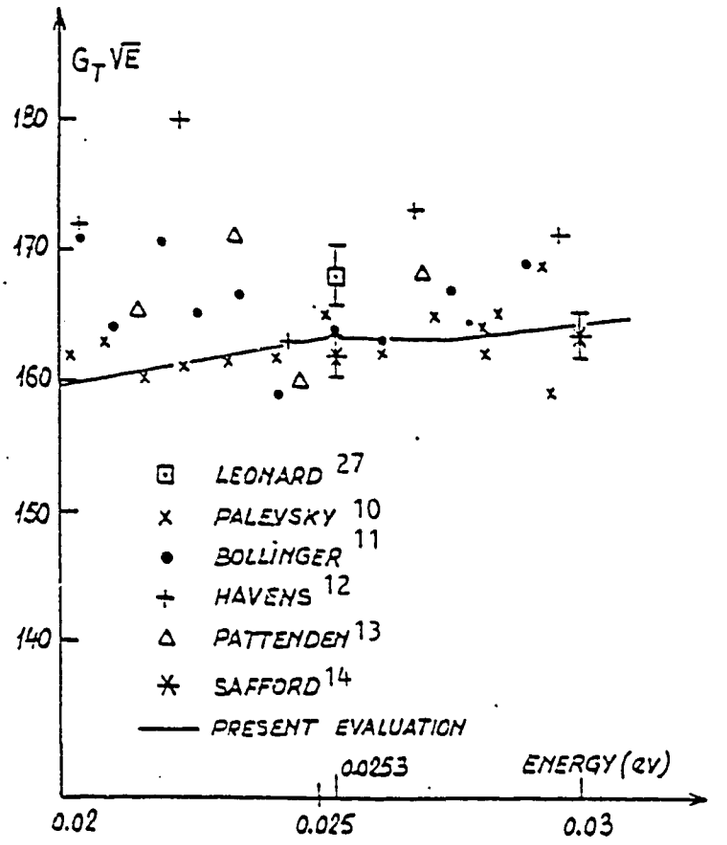

FIGURE 2 : Total cross-sections between 0.02 eV and 0.03 eV

In the energy range from 0.03 eV to 6 ev, the shape of the cross-section is dominated by the resonance at 0.29 ev. It is well known[17] that an exact description of the fission cross-section in this energy range could not be obtained with a single or multilevel Breit-Wigner calculation. Particularly, using the accepted one level parameters should lead to a fission cross-section at 3-4 ev which is too small by a factor of about 2. The results of the present Reich-Moore multilevel calculations are shown on figure 3 and compared

to some experimental data. The agreement is better than 5 % at the low energy wing of the resonance, but a difference of about 15 % still remains in the 3-4 ev region when compared to the lowest experimental data. No attempt has been made to improve the calculated data in this small energy region, since accurate cross-sections could be obtained from the experimental data.

TABLE III

MEASURED TOTAL AND ADSORPORTION CROSS-SECTIONS AT 0.0253 ev

	TOTAL (BARNS)	ABSORPTION (BARNS)
HAVENS (1951)[12]	1078 +-53	
PALEWSKY (1955)[10]	1023.4 +- 5.1	
PATTENDEN (1956)[13]	1044.4 +-16.7	
LEONARD (1956)[27]	1055.0 +-13.7	
BOLLINGER (1958)[11]	1042.8 +-15.6	
SAFFORD (1961)[14]	1018.0 +-10.0	
DURHAM (1966)[15]		1023.0 +-12.0
HANNA (1970)[28]		1025.6

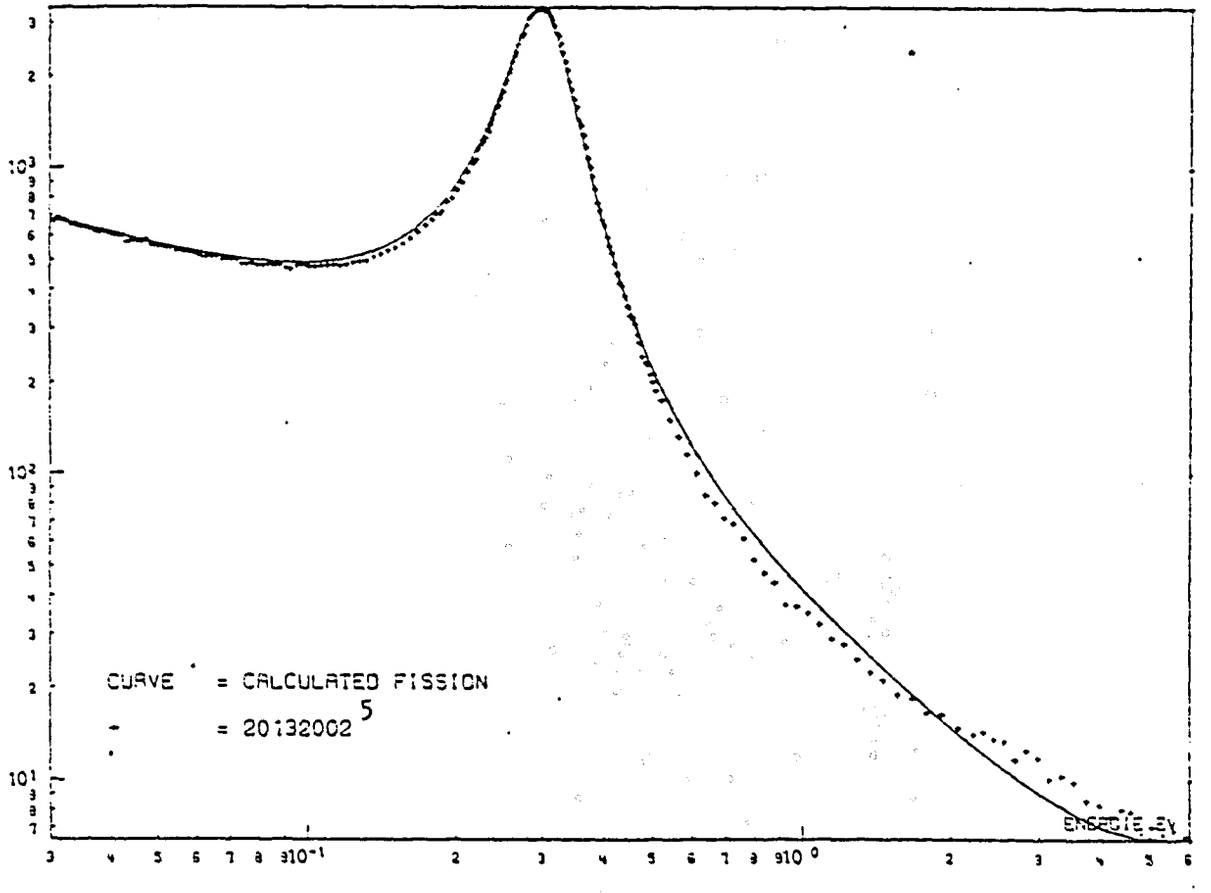

FIGURE 3 : Reich moore multilevel calculations with the parameter of Table II, compared to one set of experimental data

3) Experimental evaluation in the energy range 0.03 ev to 6 ev. Over the 0.29 ev resonance, the most recent experimental data are the fission cross-sections from DERUYTER[5], GWIN[7], WAGEMANS[16] and BERCEANU[8], and the absorption cross-section from GWIN[7]. At such low energy the effect of the experimental resolution on the shape of the resonance is negligible, and averaging the four available fission cross-sections should be feasible provided that the normalization and the energy scale are the same. As a matter of fact, the data from BERCEANU show values which are 10 to 25 % larger that those from WAGEMANS and GWIN in the wings of the resonance, although there is no apparent discrepancy at the top of the resonance. One should also note that there is a small shift of about 0.003 ev in energy between WAGEMANS and DERUYTER at the top of the resonance, WAGEMANS being in agreement with GWIN energy data. Comparing the average fission cross-sections in the energy range 0.03 ev to 0.50 ev, one finds the following values for the fission integral $1/(E_2 - E_1)\int_{E_1}^{E_2} \sigma f \, dE$:

Energy (ev)	0.03 - 0.10	0.10 - 0.50
DERUYTER (1972)	534.1 b	1208.0 b
GWIN (1976)	530.0 b	1179.8 b
WAGEMANS (1979)	537.9 b	1208.0 b
BERCEANU (1979)	534.4 b	1339.1 b

(all cross-sections are renormalized to 748.1 b at 0.0253 ev).

Over the 0.29 ev resonance, there is a difference of 14 % between GWIN and BERCEANU average value. No attempt has been made to explain this difference and the BERCEANU data have not been taken into account in the present evaluation. The other average data are consistent within a few percent. Finally the data from GWIN, DERUYTER and WAGEMANS have been used to obtain the point-wise fission cross-sections at 300°K in the energy range 0.03 ev to 6 ev. The result of this experimental evaluation is shown on figure 4. The absorption cross-sections from GWIN have also been fitted in the same energy range and used as reference in the experimental

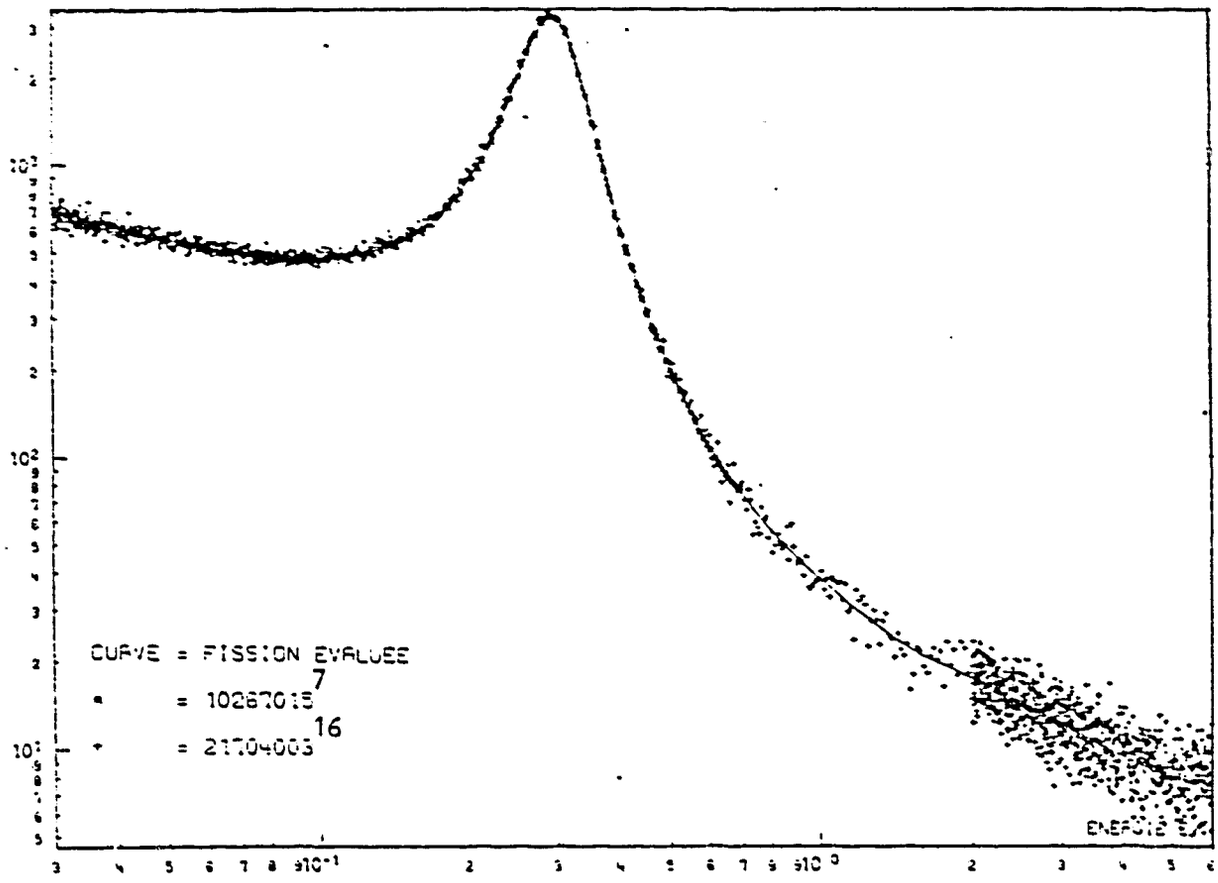

FIGURE 4 : Evaluated fission cross-sections compared to some experimental data

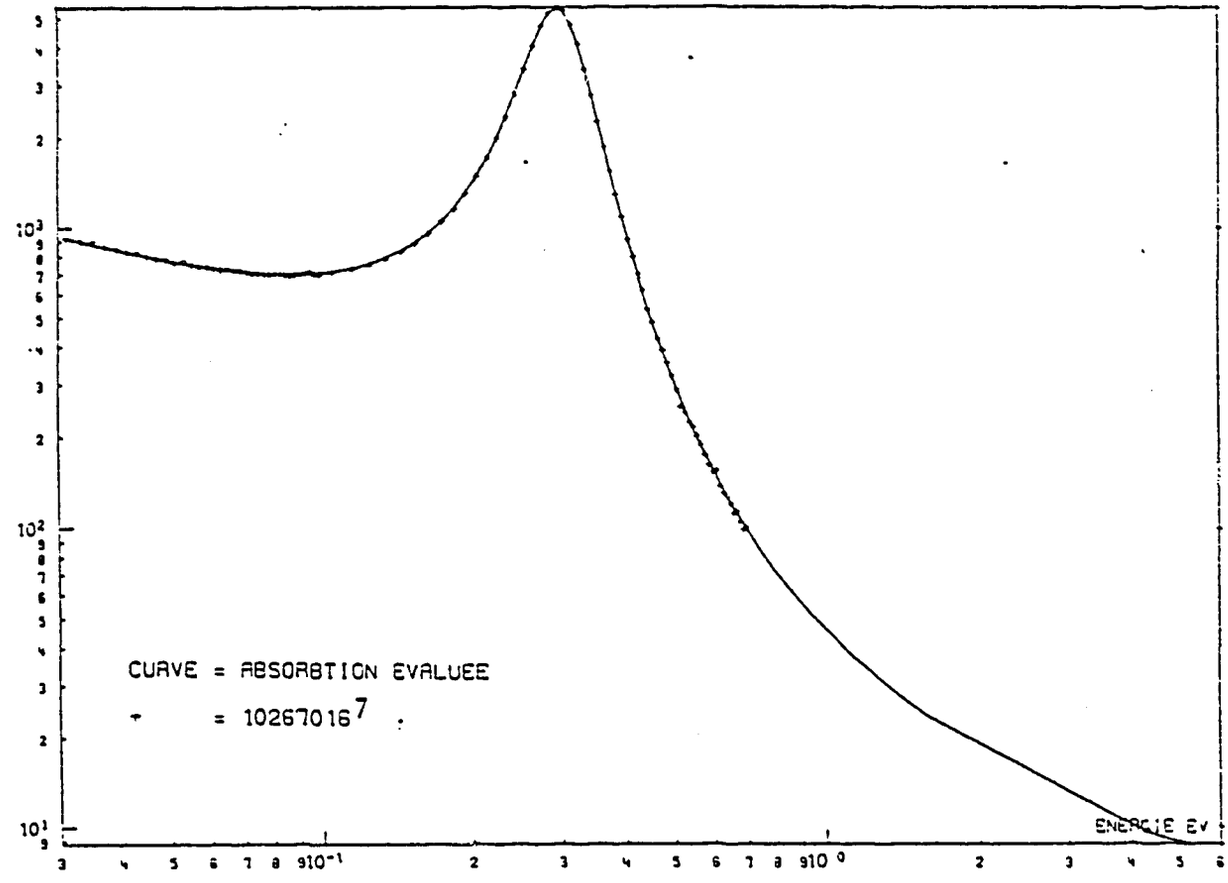

FIGURE 5 : Evaluated absorption cross-sections compared to GWIN experimental data

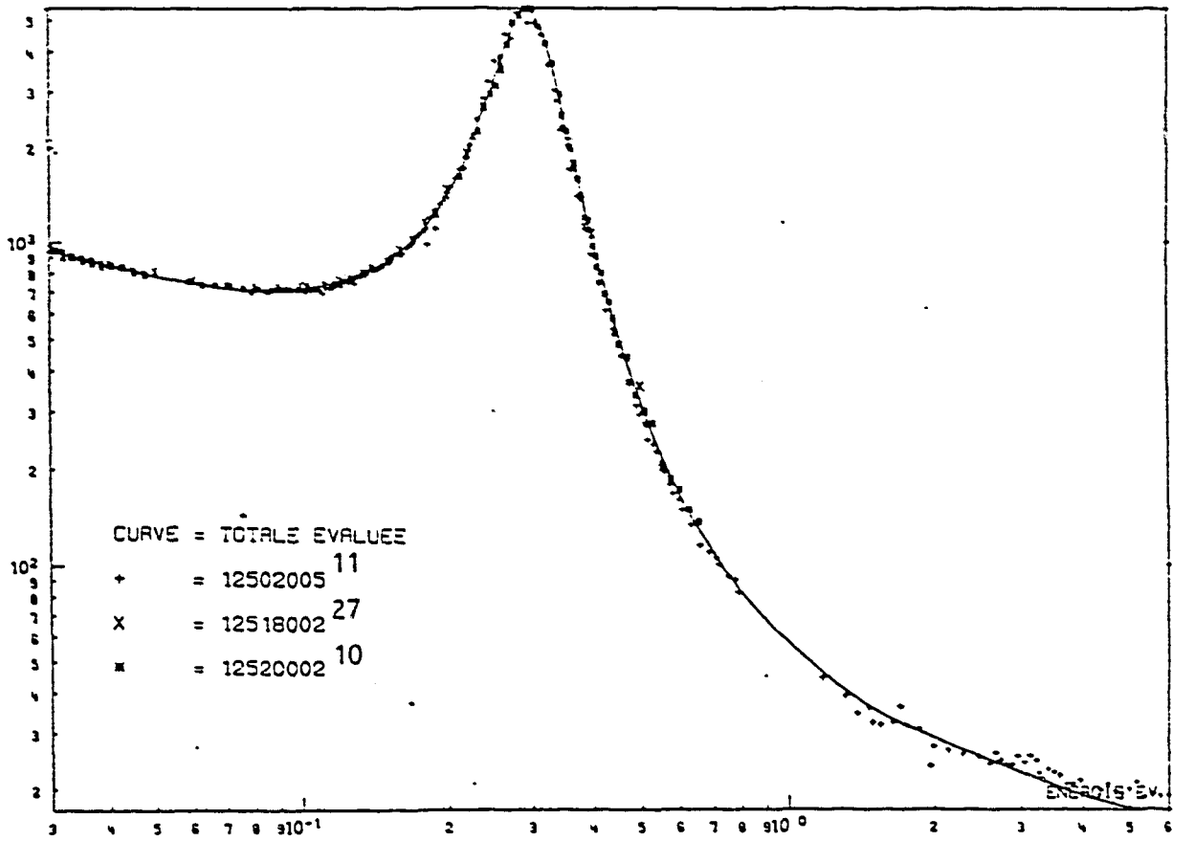

FIGURE 6 : Evaluated total cross-sections compared to some experimental data

evaluation. The results are shown on figure 5. The capture cross-section is then obtained by difference between the absorption and the fission data. As for the scattering cross-section, it can not be obtained by difference between any measured total cross-section and the absorption cross-section, since the accuracy should be very poor ; better accuracy is obtained by using the calculated cross-section. The total cross-section data are shown on figure 6.

The α values can now be calculated from the experimental evaluation cross-section data. They are shown on figure 7 along with some measured values.

4) Final results in the thermal and low energy range.

The evaluated file contains the point-wise cross-sections in the energy range 10^{-5} ev to 6 ev at 0°K. They are obtained from the Reich-Moore multilevel calculation between 10^{-5} ev

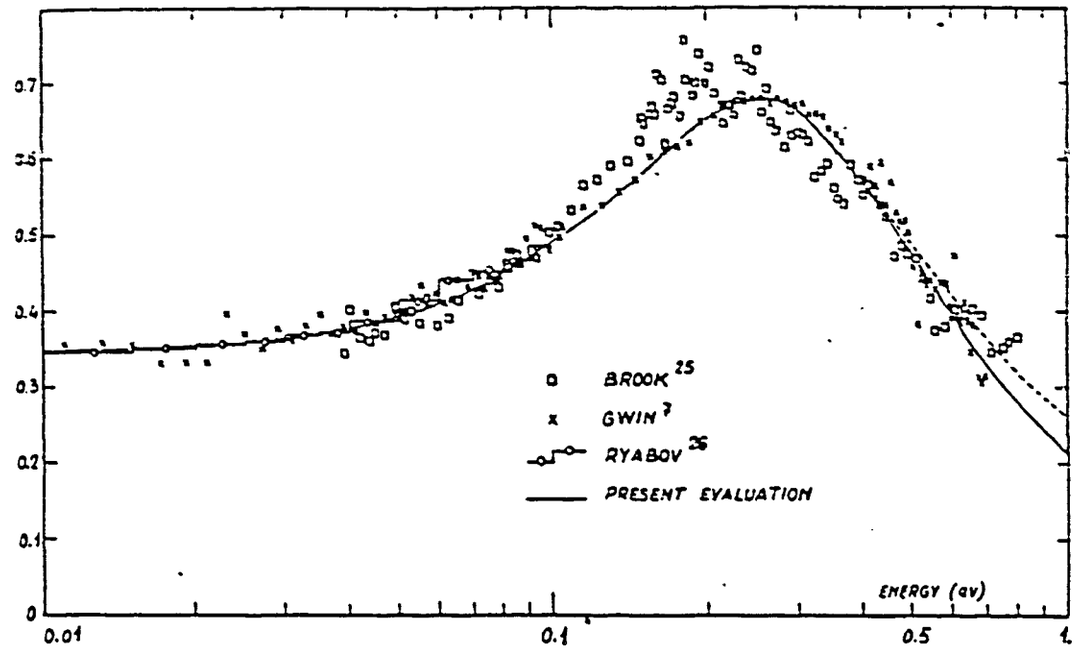

FIGURE 7 : Evaluated alpha values compared to the experimental data

and 0.03 ev, normalized at 0.0253 ev. The reference value at 0.0253 ev are given in table IV. In the region dominated by the resonance at 0.29 ev a correction to the experimental evaluation has been applied to obtain the value at 0°K from the value at 300°K, this correction was equal to the ratio between the Reich-Moore calculated cross-sections at 0°K and 300°K ; a typical value of the correction is about 3 % at the top of the resonance.

TABLE IV

EVALUATED CROSS-SECTIONS AT 0.0253 ev. IN BARNS

	PRESENT EVALUATION	NNDC GROUP (1983)	ENDF/B-V (1979)	JENDL-2 (1982)
TOTAL	1027.0	1025.1 +-3.4		1019.9
ABSORPTION	1019.0	1017.3 +-2.9	1011.9	1011.9
FISSION	748.1	748.1 +-2.0	741.7	741.7
CAPTURE	270.9	269.3 +-2.2	270.2	270.2
SCATTERING	8.0	7.8 +-1.0		6.7
ALPHA	0.362	0.363+-0.003	0.364	0.364

Miscellaneous comparaisons with experimal data are shown on table V.

TABLE V

AVERAGED CROSS-SECTIONS OVER THE 0.29 ev ENERGY RESONANCE (0.1 ev TO 0.5 ev), IN BARNS

	GWIN [7]	DERUYTER [5]	BERGEANU [8]	WAGEMANS [16]	PRESENT EVALUATION
FISSION	1180	1208	1340	1208	1195
ABSORPTION	1980				1954
CAPTURE	748				759

II - MULTILEVEL CROSS-SECTIONS IN THE ENERGY RANGE 6 ev to 200 ev

Two important sets of multilevel resonance parameters are available in the EXFOR experimental data file. The first is the result of a Reich-Moore multilevel shape analysis of the Los-Alamos bomb-shot fission data[21], performed by J.A. FARRELL[19] in 1968 in the energy range 14 ev to 90 ev. The second was obtained at Saclay in 1970[20] from a simultaneous shape analysis of the fission and total cross-sections using also the Reich-Moore formalism, in the energy range 4 ev to 205 ev. The comparison between these two sets of resonance parameters has already been done in reference [20] and it was shown that the FARRELL parameters, which provide a very accurate description of Los-Alamos fission cross-sections, are not suitable for an accurate description of the total and capture cross-sections. Nevertheless, none of these sets of data has been used for the ^{239}Pu cross-section evaluation. The most recent data files are still using the Breit-Wigner formalism in the resolved resonance region ; one remedies the deficiency of the formalism by adding to the calculate cross-sections a background which is supposed to represent the difference between the calculated values and the true values of the cross-sections. For the fissile elements the differences correspond mainly to the interferences between resonances in the fission channels ; they are positive or negative and fluctuate strongly. Usualy, in ENDF/B format, the background should be smooth since it was supposed to reproduce mainly the

contribution of the levels outside the energy range of analysis or in the unresolved region . As a matter of fact, the most sophisticated formalism cannot reproduce exactly a measured cross-section for several reasons : deficiency of the formalism itself, systematical errors on the measured data (efficiency of the detectors, background, normalization etc...), unknown experimental resolution function and other unknown experimental effects. Strong local deviations, incompatible with the statistical fuctuations, are observed between different sets of experimental data, even if an overall agreement of a few % exists between the averaged data. Some exemples are given on table VI where averaged experimental fission data from BLONS[18], GWIN[7] and WAGEMANS[16] are shown ; differences of more than 10 % are seen on the values averaged over 10 ev energy intervals, when the data averaged over the 150 ev energy region are in agreement within 1.5 %. It is then obvious that the shape and the amplitude of the background which could be associated to a calculated cross-section depend strongly on the experimental data set choosen as reference. The only way to obtain an

TABLE VI

AVERAGED FISSION CROSS-SECTIONS(BARNS)

ENERGY RANGE (ev)	SACLAY[22]	GEEL[16]	OAK-RIDGE[7]	AVERAGE *	EVALUATED **
50 _ 60	77.23	74.03	72.66	74.70	73.51 (-1.6)
60 _ 70	57.05	57.21	56.90	57.07	56.25 (-1.4)
70 _ 80	65.61	65.37	63.49	64.82	64.70 (-0.3)
80 _ 90	68.74	68.75	67.63	68.37	69.10 (+1.0)
90 _ 100	31.62	30.87	30.97	31.15	30.99 (-0.5)
100 _ 120	25.91	24.40	23.02	24.44	23.85 (-2.5)
120 _ 140	18.69	19.25	19.03	18.66	20.23 (+9.3)
140 _ 160	17.61	17.74	17.95	17.77	17.50 (-1.5)
160 _ 180	10.72	10.12	10.22	10.35	9.93 (-4.2)
180 _ 200	22.80	21.77	20.51	21.69	21.95 (+1.2)
50 _ 200	32.77	32.19	31.54	32.17	31.79 (-1.2)

AVERAGED ABSORPTION CROSS-SECTIONS (BARNS)

ENERGY RANGE (ev)	OAK-RIDGE[7]	EVALUATED **
50 _ 100	92.84	93.81 (+1.0)
100 _ 200	33.66	33.73 (+0.2)

* AVERAGE OF SACLAY, GEEL AND OAK-RIDGE
** IN BRACKETS : PERCENTAGE DEVIATION BETWEEN AVERAGE AND EVALUATED

accurate background should be to perform a simultaneous shape fit of selected experimental data sets in which a common background value, characteristic of the formalisms used, is separated from the background corresponding to the systematic errors on each experiment. Such analysis should be much time consuming and has never been done for the ^{239}Pu data.

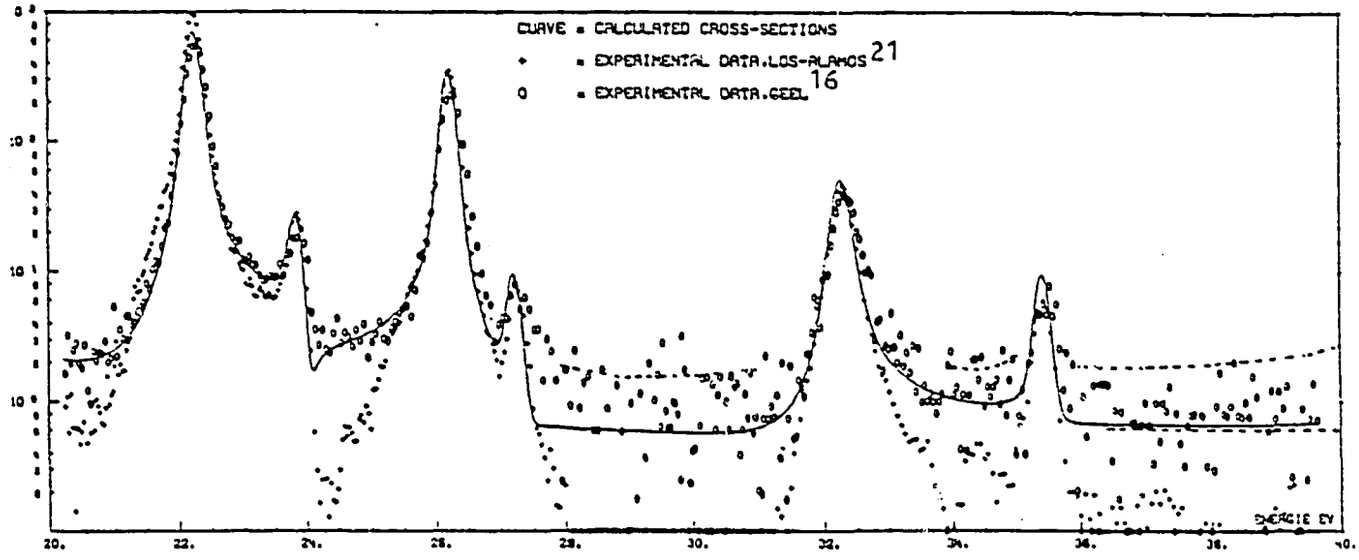

FIGURE 8 : Fission cross-sections in the energy range 20 eV to 40 eV

The present evaluation uses essentially the parameters obtained at Saclay. Then the evaluated total and fission cross-sections are close to those published in reference[20]. Some fission widths of the 0^+ resonances (broad resonances) have been modified to improve the agreement between the calculated and the experimental fission data. Comparisons between the calculated fission and absorption cross-sections and the experimental values from BLONS, GWIN and WAGEMANS are shown in Table VI in the energy range 50 ev to 200 ev. The agreement is rather good for the fission cross-sections ; the absorption values averaged over the energy ranges 50 ev to 100 ev and 100 ev to 200 ev agree perfectly well with those from GWIN although these experimental data were not considered in the multilevel analysis of reference[20]. However, one should note that some inconsistencies remain in the calculated fission and total cross-sections when compared to the Saclay fission and

total experimental data. That was already pointed out in SIMPSON et al.[22] single level evaluation. The study of these inconsistencies are underway by examining all the available data in the corresponding energy ranges. One example is shown on figure 9 and 10 over the broad resonance at 132 ev where the fission cross-section is 2 or 3 barns too large when the total cross-section is well reproduced.

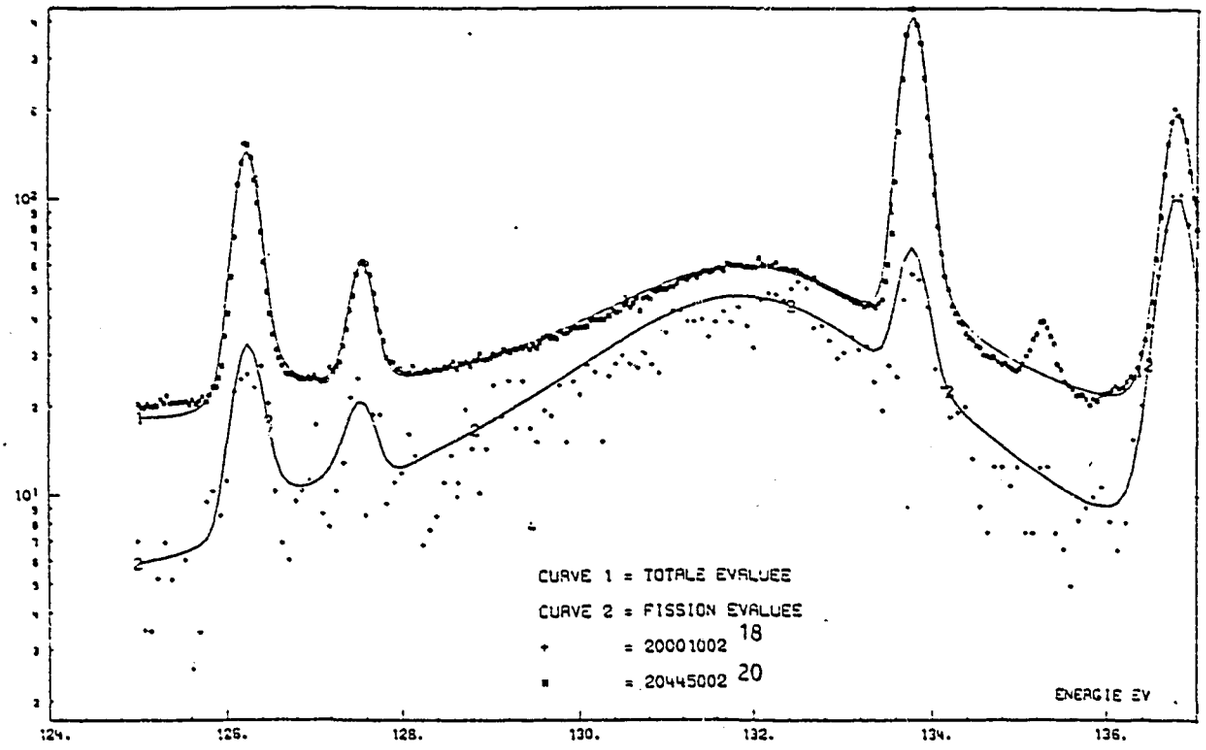

FIGURES 9 and 10 : Total and fission cross-sections over the 132 eV broad resonance, showing the difficulties of fitting simultaneously the experimental total and fission data

Another aspect of the difficulties of the evaluation is shown on figure 8 which compares the fission cross-sections from WAGEMANS to those from the Los-Alamos bomb shot experiment, in the energy range 20 ev to 40 ev. In this example the background problems appear clearly. The value of the cross-section between the resonances is close to 0 in the Los-Alamos data, when in WAGEMANS data one finds about 1 barn. The cross-sections calculated with a resolution width equal to 0 and no background contribution are also shown on the figure. They agree fairly well with WAGEMANS values between the resonances, but are in better agreement with Los-Alamos data at the top of the resonances. Here the situation is not clear and the discrepancy in the background is not understood.

In conclusion, in the 6 ev to 200 ev energy region, the evaluated cross-sections should be calculated by using the set of Reich-Moore multilevel resonance parameters and, for a part of the background contribution, the set of the Breit-Wigner parameters of the resonances in the energy range 200 ev to 660 ev (see next section). Then the smooth background file should be essentially due to the levels outside the energy range - 1.20 ev to 660 ev. Their contribution could be calculated by a picket-fence model of single resonances[24] or of a sample of known resolved resonances. No other kinds of background are considered in the present evaluation.

III - BREIT WIGNER CALCULATIONS IN THE ENERGY RANGE 200 ev TO 600 ev

There are no multilevel resonance parameters available for the calculations in this energy range. The only almost complete set of data is the one from reference[20] obtained by a Breit-Wigner shape analysis of Saclay experimental data, performed separatly on the fission cross-sections and on the transmission of several sample thicknesses. These resonance parameters have already been used in a previous evaluation by RIBON et al.[23]. In the purpose of well understanding the validity and the limit of the present evaluation, it is worth to remind of the method used in reference[20] to obtain the resonance parameters. The method was the following :

1) the total resonance area A_T, proportional to the neutron width 2 $g\Gamma n$, and possibly the total widths Γ were obtained from the shape analysis of the transmission data, and the fission resonance area A_f from the shape analysis of the fission cross-sections ;

2) then, the fission widths were calculated by the relation : $\Gamma_f = \Gamma (A_f/A_T)$ when the total width was known, and by the relation : $\Gamma_f = \sqrt{< \Gamma\gamma > + 2\, g\Gamma n / 2g}\ A_f/(A_T - A_f)$ in the other cases, $< \Gamma\gamma >$ being an averaged value of the capture width ;

3) the spin 0^+ and 1^+ was assigned to 65 % of the resonances by direct or indirect method (scattering area , fission width distribution, capture width values) ; the spin 1^+ was assigned to all the remaining resonances mainly for statistical reasons (see page 96 of reference 20) ;

4) when possible, the capture width was calculated by the relation : $\Gamma_\gamma = \Gamma - \Gamma_f - \Gamma_n$;

5) compared to the energy interval 0 - 300 ev, 16 % of the levels were supposed to be missed in the energy range 300 ev to 660 ev.

Obviously, one should not demand to this set of resonance parameters to reproduce exactly the cross-sections in each energy point, particularly between resonances in the region where some strong interference effects should necessarily exist. Nevertheless, the general aspect of the cross-sections is well reproduced, as it is shown on figures 11 and 12 in the energy range 200 ev to 300 ev. Table VII and VIII show the calculated cross-sections averaged over 50 ev energy

TABLE VII

AVERAGED FISSION CROSS-SECTIONS(BARNS)

ENERGY RANGE (ev)	22 SACLAY	16 GEEL	7 OAK-RIDGE	* AVERAGE	** EVALUATED
200 _ 250	13.94	13.72	13.71	13.79	14.12 (+2.4)
250 _ 300	22.04	22.50	22.20	22.05	22.34 (+0.4)
300 _ 350	10.39	9.91	9.70	10.00	10.76 (+7.6)
350 _ 400	7.48	7.57	7.32	7.46	7.17 (-4.0)
400 _ 450	9.62	9.68	9.63	9.64	9.24 (-4.3)
450 _ 500	10.04	10.16	9.84	10.01	9.91 (-1.0)
500 _ 550	19.00	18.50	19.50	19.00	19.22 (+1.2)
550 _ 600	12.45	12.74	12.51	12.57	12.68 (+0.8)
200 _ 600	13.12	13.11	13.05	13.09	13.31 (+1.7)

* AVERAGE OF SACLAY,GEEL AND OAK-RIDGE
** IN BRACKETS: PERCENTAGE DEVIATION BETWEEN AVERAGE AND EVALUATED

TABLE VIII

AVERAGED TOTAL AND ABSORPION CROSS-SECTIONS(BARNS)

ENERGY RANGE (ev)	TOTAL 20 SACLAY	TOTAL ** EVALUATED	ABSORPTION 7 ORNL	ABSORPTION ** EVALUATED
200 _ 250	43.52	43.73 (+0.4)	33.72	33.80 (+0.2)
250 _ 300	57.63	57.02 (-1.1)		
300 _ 350	39.40	40.37 (+2.5)	17.74	17.68 (-0.3)
350 _ 400	25.26	23.99 (-5.3)		
400 _ 450	26.55	25.80 (-2.9)	13 58	13.67 (+0.7)
450 _ 500	25.68	24.65 (-4.2)		
500 _ 550	46.47	44.16 (-5.2)	25.34	25.58 (+0.9)
550 _ 600	41.30	41.43 (-1.5)		
200 _ 600	38.23	37.64 (-1.5)	22.59	22.68 (+0.4)

** IN BRACKETS: PERCENTAGE DEVIATION BETWEEN EVALUATED AND EXPERIMENTAL DATA

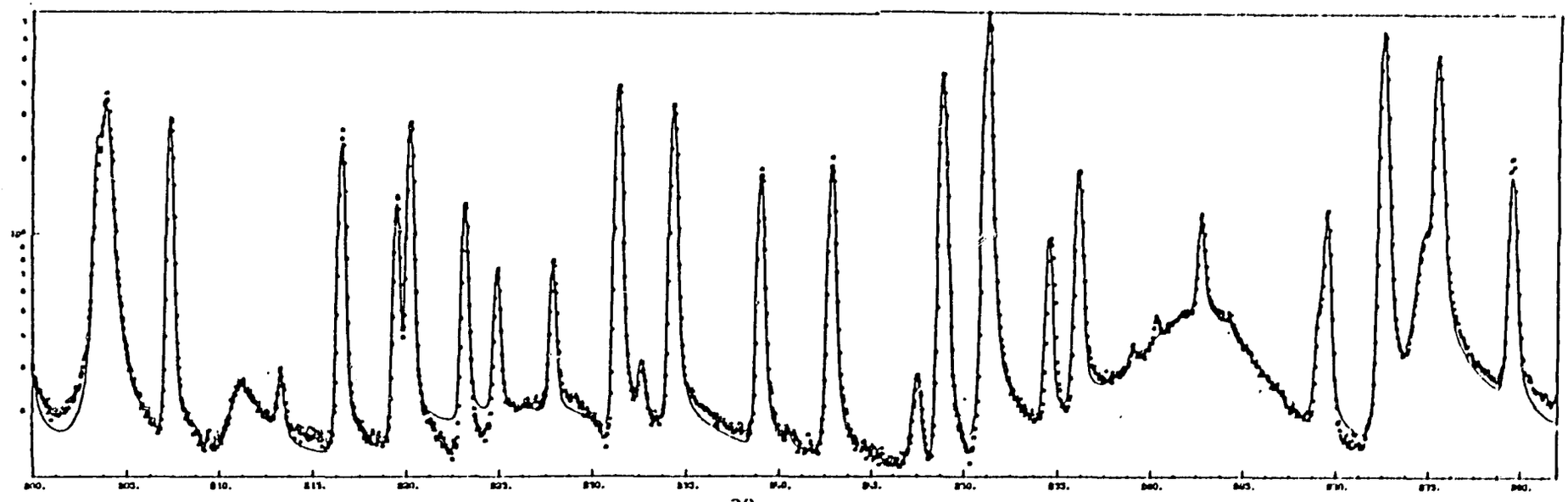

FIGURE 11: Calculated (single level) and experimental ^{20} total cross-sections in the energy range 200 eV to 300 eV

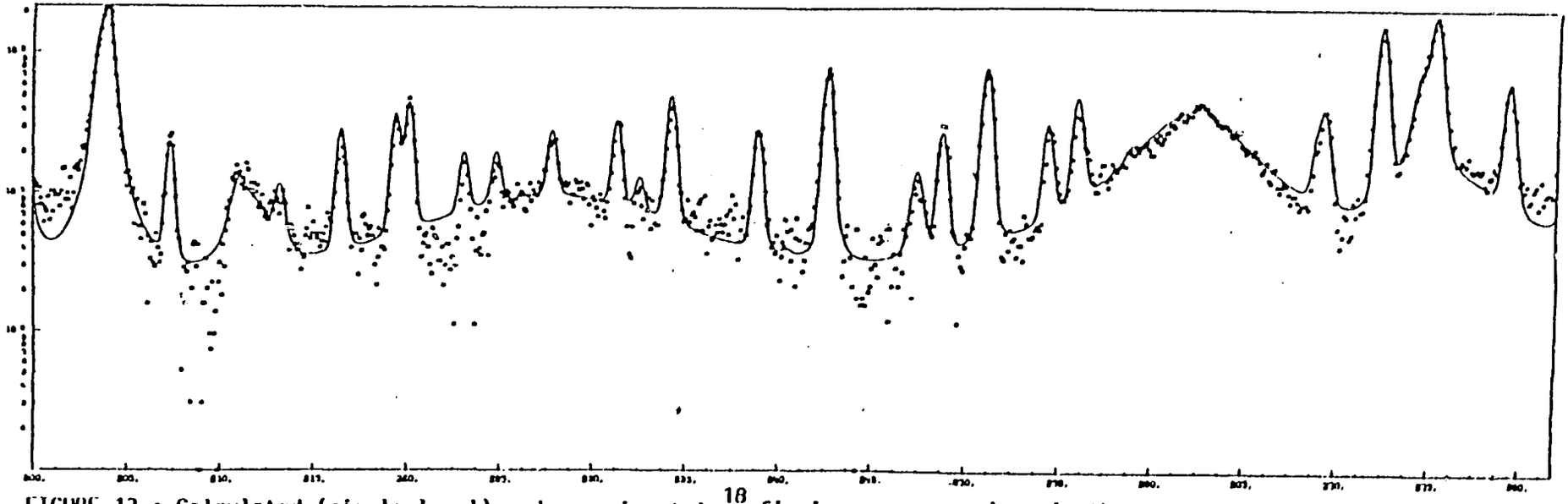

FIGURE 12 : Calculated (single level) and experimental ^{18} fission cross-sections in the energy range 200 eV to 300 eV

interval in the energy range 200 ev to 600 ev, compared to the corresponding value of the experimental data. The agreement is better than 6 % in each energy interval. The agreement between GWIN absorption and the calculated absorption is particularly excellent (better than 1 %). In these calculations the background contribution comes only from the unresolved or non analysed outside resonances. As for the missed resonances in the energy above 300 ev, their contributions are implicitly contained in the parameters A_t and A_f issuing from the shape analysis of the transmissions and fission cross-sections (multiplets considered as single resonances). A capture width of 46 mev, which is 10 % larger than the measured averaged value in the well resolved region, was also assigned to the resonances above 450 ev to take account of the missed resonances in the calculation of the capture cross-section.

CONCLUSIONS

Some aspects of the evaluations of ^{239}Pu cross-sections in the resonnance region have been presented in this report. A set of resonnance parameters assembling the results of a multilevel analysis in the energy range thermal to 200 ev and the result of a single level analysis in the energy range 200 ev to 660 ev is proposed for the calculation of the cross-sections in the energy range thermal to 600 ev. These parameters provide a quite good representation of the most recent measured fission cross-sections. The accuracy on the calculated fission cross-sections averaged over small energy intervals is better than 5 % and is close to 2 % on larger energy interval. The agreement with GWIN averaged absorption cross-sections is excellent. As for the total cross-sections, one should note once more that there are some difficulties to find a consistency between the calculated and measured total and fission data over the broad resonances. Then, it should be most valuable to perform new transmission measurements with a resolution and statistical accuracies at least as good as those achieved in the old Saclay transmission measurements.

REFERENCES

1 - H.D. LEMMEL
Symp. on neutron standard and applications, NBS, Gaithersburg, 28-31 Mars 1982.

2 - J.R. STEHN et al.
Int. Conf. on Nuclear Data for Science and Technology, Antwerp, 6-10 Sept. 1982.

N.E. HOLDEN et al.
EPRI-NP-1098, 1979.

J.R. STHEN et al.
Private communication to H.D. LEMMEL for NEANDC/INDC standard file, 1983.

3 - C.J. AXTON
Private communication to H.D. LEMMEL for NEANDC/INDC standard file, 1983.

4 - A. LORENZ
INDC(NDS)-121 NE, results of a IAEA/NDS CRP (1980).

5 - A.J. DERUYTER
J. Nucl. Energy 26, 293 (1972).

6 - INDC/NEANDC. Standard file, Technical Report serie n° 227, IAEA, Vienne 1983.

7 - R. GWIN
Nucl. Scien. Eng. 61, 116 (1976).
Nucl. Scien. Eng. 59, 79 (1979).

8 - J. BERCEANU et al.
Rev. Roum. Phys. 23, 867 (1978).

9 - E.J. SEPPI et al,
HW-55879 3 (1958),

10 - W. PALEVSKY,
1955, Private communication for EXFOR file (1976).

11 - L.M. BOLLINGER et al.
Conf. on Peaceful use of Atomic Energy, Geneva, 1-13 Sept. 1958.

12 - W.W. HAVENS
CUD-92 (1951).

13 - N.J. PATTENDEN
J. Nucl. Energy 2, 187 (1956).

14 - G.J. SAFFORD et al.
Nucl. Scien. Eng. 11, 65 (1961).

15 - R.W. DURHAM et al.
Conference on Nuclear Data for Reactors Paris, 17-21 Oct. 1966.

16 - W. WAGEMANS
Annals of Nuclear Energy 7, 9, 495 (1980).

17 - E. VOGT
Physical Review 118, 724 (1960).

18 - J. BLONS
Nucl. Scienc. Eng. 51, 130 (1973).

19 - J.A. FARRELL
Physical Review 165, 1371 (1968).

20 - H. DERRIEN
Thèse série A n° 1172, Orsay (1973) and NEANDC (E) - 163U (1975).

21 - E.R. SHUNK et al.
LADC-7620 (1966).

22 - O.D. SIMPSON et al.
ANCR-1045

23 - P. RIBON et al.
Note CEA-N 1484, EANDC (E) 138-AL.

24 - G. DE SAUSSURE et al.
ORNL/TM-6152 (1978).

25 - F.D. BROOKS
AERE-M-1709 (1966).

26 - J.V. RYABOV
AE 41, (1), 45 (1976).

27 - B.R. LEONARD et al.
P. HW-44525, 47 (1956).

28 - W. HANNA (1969), EXFOR FILE 10013004
M. LOUNSBURY et al., 70 HELSINKI, 1, 287 (1970)

Contributed Paper 16

COMPLETE EVALUATIONS OF NEUTRON NUCLEAR DATA FOR Cm ISOTOPES

G. MAINO, E. MENAPACE, M. VACCARI
ENEA, Laboratorio Dati Nucleari e Codici,
Bologna, Italy

Abstract

The complete evaluation of the nuclear data for the Cm-242, Cm-243, Cm-245, Cm-246, Cm-247 and Cm-248 in the energy interval 10^{-5} to 15 MeV is described. The evaluation was compared with the ENDF/B-V, JENDL-2 and Soreq Cm-246 files.

Summary

In connection with the Coordinate Research Project on Intercomparison of Actinide Neutron Nuclear Data cross sections of Pu, Am, Cm isotopes were evaluated and intercompared at ENEA-Bologna, namely for Pu-241 and -242, Am-241 and -243 as partial evaluations (thermal and resonance regions), and for Cm-242,-243,-245,-246,-247 and -248 as complete evaluations in the energy interval 10^{-5} eV to 15 MeV.

The present review concerns the Cm isotopes, among which:

- evaluations of Cm-242,-243,-245 are required for calculations and analyses with regard to irradiated fuel management and formation of nuclides like Pu-238;
- evaluation of Cm-246,-247,-248 are required in order to analyze the production and decay chain to Cf-252.

A critical comparison was performed with available evaluated files from different sources, namely ENDF/B-V, JENDL-2 and Soreq Cm-246 file in order to take advantage by different criteria or considerations both on the experimental information and evaluation methods.

At ENEA, Bologna, in the past years an evaluation of neutron cross sections from 10^{-5} eV to 15 MeV was performed for the $^{242-243-245-246-247-248}$Cm isotopes [1]. In the

following, we shortly summarize the main results obtained and the methodologies adopted in the calculations; particular emphasis is devoted to the approximations and the limits of the utilized nuclear models and computer codes and to the possible improvements for further evaluations.

As far as the resolved resonance region is concerned, the experimental parameters taken from the literature were adopted; the neutron cross sections for capture, fission, elastic and inelastic scattering processes were calculated in the framework of the multilevel Breit-Wigner formalism by means of the CRESO code [2]. For the fission widths, a multilevel Reich-Moore analysis was performed and introduced in the evaluations.

In order to reproduce the thermal values of neutron capture and fission cross sections, a bound level was added to the observed resonances for each isotope. This procedure was preferred since more physically significant than arbitrary "ad hoc" changes in the experimental widths of the neutron resonances. With the resulting set of parameters, the (n,γ) and (n,f) resonance integrals were calculated; for the fission reaction, the contribution arising from the continuum region must be taken into account, because it is not negligible. The agreement with the experimental data is generally reasonable, even if not completely satisfactory. However, more reliable experimental information is needed to draw any definite conclusion because in many cases only few data from old measurements are available and often in disagreement among themselves.

Results of the Bologna evaluations are presented in Tables I - III, and compared with the calculated values from the ENDF/B and JENDL files.

TABLE I

Thermal cross sections

Isotope	Capture (b)			Fission (b)		
	ENEA-Bologna	ENDF/B-V[a]	JENDL-2[b]	ENEA-Bologna	ENDF/B-V[a]	JENDL-2[b]
^{242}Cm	16.5	17.2	15.92	5.0	3.01	5.0
^{243}Cm	131.0	58.0	131.3	599.0	69.1	612.3
^{244}Cm	—	10.4	14.41	—	0.60	1.18
^{245}Cm	345.0	383.0	346.4	2143.	2161.	2001.
^{246}Cm	1.46	1.30	1.33	0.17	0.06	0.142
^{247}Cm	59.7	58.2	59.9	81.6	83.4	97.0
^{248}Cm	9.81	2.44	—	0.39	0.009	—

a) Evaluated Nuclear Data File ENDF/B, Version V, BNL, Brookhaven National Laboratory (1973)

b) Evaluated Nuclear Data File JENDL-2, Japan Evaluated Nuclear Data Library, Version 2 (1983) rev.

TABLE II

Resonance Integrals

Isotope	Capture (b)			Fission (b)		
	ENEA-Bologna	ENDF/B-V	JENDL-2	ENEA-Bologna	ENDF/B-V	JENDL-2
^{242}Cm	117.0	157.0	116.0	11.6	5.51	11.1
^{243}Cm	301.0	248.0	436.0	1855.	1953.	1750.
^{244}Cm	—	596.0	594.0	—	17.8	18.4
^{245}Cm	114.0	118.3	108.0	779.0	835.0	800.0
^{246}Cm	113.0	103.7	102.5	6.94	10.4	9.5
^{247}Cm	494.0	491.0	495.0	662.0	750.0	769.0
^{248}Cm	270.0	254.0	—	9.61	14.9	—

TABLE III

Average parameters for the unresolved region adopted in the Bologna evaluation of Curium isotopes

Isotope	$\bar{D}$ (eV)	$S_o(\times 10^{-4})$	$S_1(\times 10^{-4})$
^{242}Cm	10.8	0.71	2.53
^{243}Cm	0.80	1.15	2.36
^{245}Cm	1.24	1.19	2.10
^{246}Cm	21.3	0.77	2.60
^{247}Cm	1.20	1.00	1.80
^{248}Cm	24.5	1.20	3.10

The unresolved resonance region was assumed to range up to 10 KeV of incident neutron energy; the average parameters adopted for neutron cross section evaluations in this interval were deduced both from a statistical analysis of the resonance data and from extrapolation of deformed optical and statistical model calculations in the continuum region. To connect the experimental capture and fission widths of the observed resonances to the values deduced from the transmission coefficients obtained in the framework of the statistical model above E_n = 10 KeV, a proper dependence on the excitation energy and J^{π} quantum numbers was assumed for the average neutron capture and fission widths in the unresolved resonance region.

The s- and p-wave neutron strength functions and the scattering length R' were derived from the statistical and deformed optical model calculations and are in good agreement with the available experimental information and the local systematics for transactinides.

The average spacing of s-wave resonances, $\bar{D}$, was obtained from the experimental data, with a correction for missed resonances,

estimated by means of the CAVE code [3], based on a likelihood function method. Moreover, realistic nuclear level density calculations, performed with the NUDENS code (4) in the framework of the microscopic Nilsson-BCS model, reproduce these empirical spacings at excitation energies corresponding to the neutron binding energies. Obviously, the phenomenological level density formulae utilized in the statistical model calculations were normalized to these values.

In effect, nuclear structure data, i.e. discrete spectra at low energy (below 1-2 MeV) and level densities in the continuum, play a crucial role in cross section calculations and much more attention than usually made in the evaluations would have to be devoted to them. In our Cm evaluations the discrete levels of the literature ("Nuclear Data Sheets", etc.) were adopted, while the parameters of a phenomenological "back-shifted" level density formula were determined on the basis of the experimental information on the cumulative number of states at low energy and the s-wave spacing $\bar{D}$ at the neutron binding energy. This procedure is quite questionable because it does not necessarily reproduce the correct dependence of level densities on the excitation energy (see ref.(5) and papers quoted therein); moreover it is not applicable where the experimental data are lacking, e.g. at the first saddle of the fission barrier. As a consequence, nuclear structure parameters for the fission channel in neutron cross sections are arbitrarily chosen, to reproduce the fission cross sections as only requirement: generally a simple Fermi gas expression is assumed all over the considered energy range, since no experimental information is available about the discrete transition levels. As far as the low energy spectrum is considered, a convenient and largely practicable approach for medium-heavy mass nuclei may be constituted by calculations in the framework of the IBM [6] (interacting boson model, for even-even nuclei) and the IBFM [7] (interacting boson-fermion model for odd-A nuclei).

Figures 1 and 2 from ref. (8) show the collective spectra of even uranium isotopes in the first and second minimum, respectively, of the potential surface, compared with the experimental level energies. In the description of higher energy states realistic nuclear level densities would be introduced in neutron cross section calculations. To avoid too much computer time consuming, reliable but still closed-form expressions would be desirable. On the basis of the Nilsson-BCS model with inclusion of the blocking effect for odd N and/or Z nuclei [9], and approximate treatment of collective enhancement factors, an empirical formula was proposed [5] that is able to reproduce the microscopic calculations performed with the NUDENS code [4] by introducing an energy dependence of the "a" parameter in the usual Fermi-gas formalism:

$$a = \tilde{a}\,(1 - e^{-\gamma E}) \qquad (1)$$

where $\tilde{a}$ and γ are adjustable parameters obtained for each isotope from fitting the NBCS calculations that agree with the experimental data (average neutron resonance spacings, cumulative number of discrete levels, etc.).

Results of an analysis performed for Curium isotopes are presented in Table IV. As one expects, the values of the level density parameters in (1) for odd A-isotopes are slightly higher than for even ones due to the more rapid increasing of level density for odd nuclei with respect to even-even adjacent isotopes.

In comparison with a previous systematic analysis for nuclei in the mass region $124 \leq A \leq 160$, the $\tilde{a}$ parameter is larger, as it is known to increase with the mass number. The γ-values (0.15 ± 0.02 for the even Curium isotopes and 0.18 ± 0.04 for the odd ones) have to be compared with the average results of ref. (15), 0.20 ± 0.03 and 0.23 ± 0.05, for even-even and odd-A nuclei, respectively.

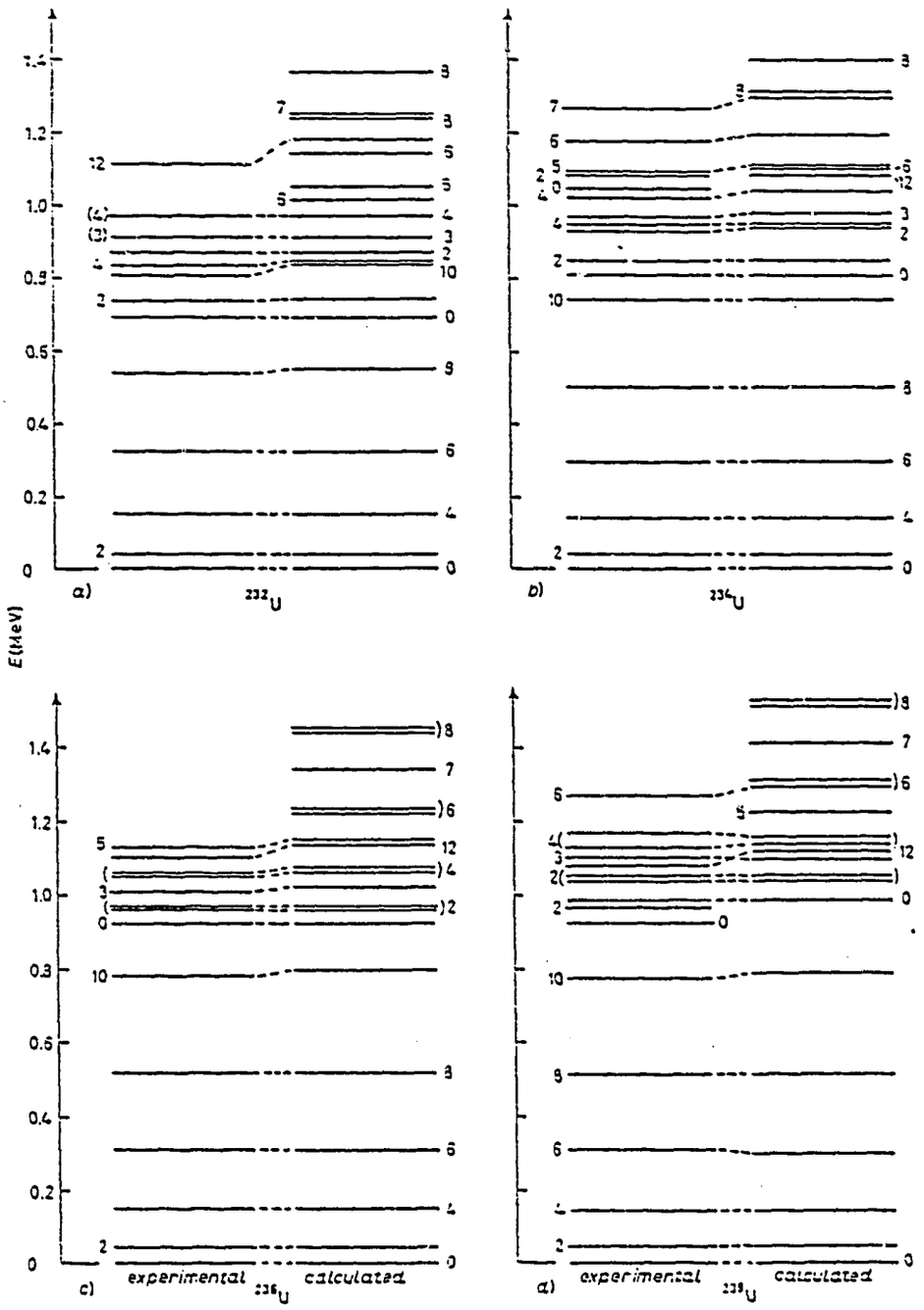

Fig. 1. – Experimental(*) and calculated level schemes for a) ^{232}U, b) ^{234}U, c) ^{236}U, d) ^{238}U.

(*) M. R. Schmorak: *Nucl. Data Sheets*, 20, 165 (1977); Y. A. Ellis: *Nucl. Data Sheets*, 21, 493, 549 (1977); C. M. Lederer and V. S. Shirley (Editors): *Table of Isotopes*, 7th ed. (New York, N. Y., 1978).

Fig. 1 Experimental and calculated (in the framework of the IBA model) level schemes for $^{232-234-236-238}U$ (taken from ref.(8)).

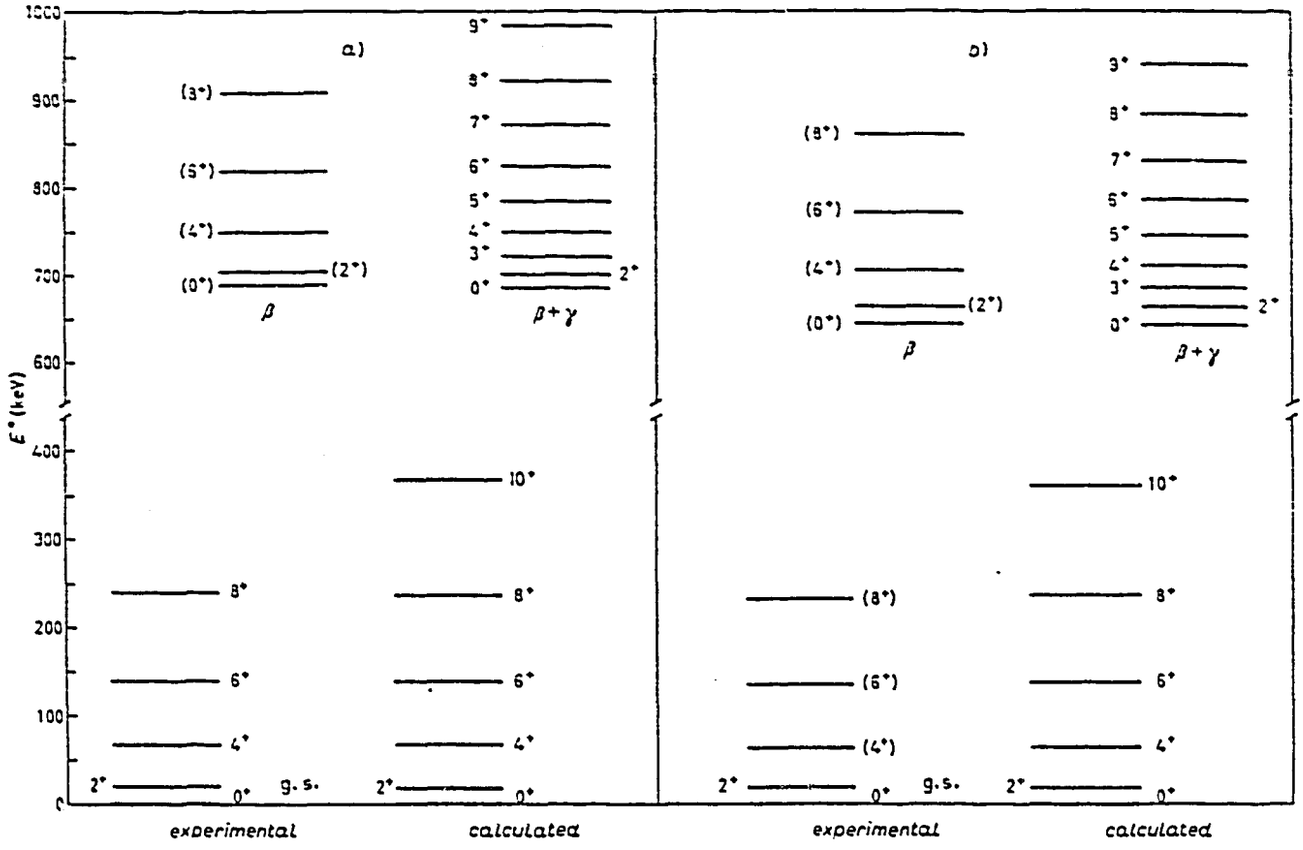

– Experimental (*) and calculated levels in the ground-state, β and γ bands for fission isomers ^{236m}U (a)) and ^{238m}U (b)).

(*) U. Goerlach, D. Habs, V. Metag, B. Schwartz, H. J. Specht and H. Backe: *Phys. Rev. Lett.* 48, 1160 (1982).

Fig. 2 Experimental and calculated (in the framework of the IBA model) level schemes for fission isomers ^{236m}U and ^{238m}U (taken from ref. (8)).

TABLE IV

Phenomenological level density parameters, deduced from microscopic NBCS calculations

Isotope^{+}	B_n(MeV)	$\overline{D}_{calc}$(eV)*	$\tilde{a}$(MeV^{-1})	γ(MeV^{-1})	$\Delta\gamma$(MeV^{-1})
^{244}Cm	6.80	0.98	27.0	0.148	0.013
^{245}Cm	5.52	11.0	27.5	0.181	0.033
^{246}Cm	6.45	1.25	27.0	0.148	0.015
^{247}Cm	5.16	21.8	27.5	0.176	0.041
^{248}Cm	6.21	1.24	27.0	0.154	0.016

*) obtained from NBCS calculations[4]; to be compared with the recommended values of Table III.

+) compound nucleus

As far as the optical model calculations are concerned, the parameters of ref.(10) were adopted. Cross section calculations were performed in the coupled-channel formalism by means of JUPITOR [11] and ADAPE [12] codes; this latter was utilized at incident neutron energies greater than 8-10 MeV, where the adiabatic approximation is valid and saves computer time.

The DOM parameters allow us to fairly reproduce the few available experimental data, total cross sections, scattering lengths and strength functions at low energy. Moreover, a reliable test is represented by a comparison of the calculated reaction cross section for compound nucleus formation with an empirical one deduced from the experimental fission cross sections and the fission probabilities measured by the Los Alamos group [13]:

$$\sigma_R(E) = \sigma_{nf}(E)/P_f(E) \qquad (2)$$

where σ_R is the reaction cross section for compound nucleus formation, σ_{nf} the total fission cross section and P_f the fission probability at an energy $E = E^* - B_n$.

A result of such a comparison is shown in fig. 3.

The statistical model calculations were performed with a modified version of the HAUSER code (14); no allowance was made for preequilibrium contributions, since they are negligible for heavy nuclei, as the Curium isotopes, at incident neutron energies below 15 MeV.

Particular care must be taken in linking together deformed optical and statistical Hauser-Feshbach calculations: in the Curium evaluations we simply added as incoherent sum the DOM and HF contributions to neutron cross sections. As pointed out by Ohsawa (priv. comm. to the Author of ref.(15)), this procedure might overestimate the inelastic scattering cross section. Strictly, one had to introduce the DOM transmission coefficients in a suitable way into the statistical HF code.

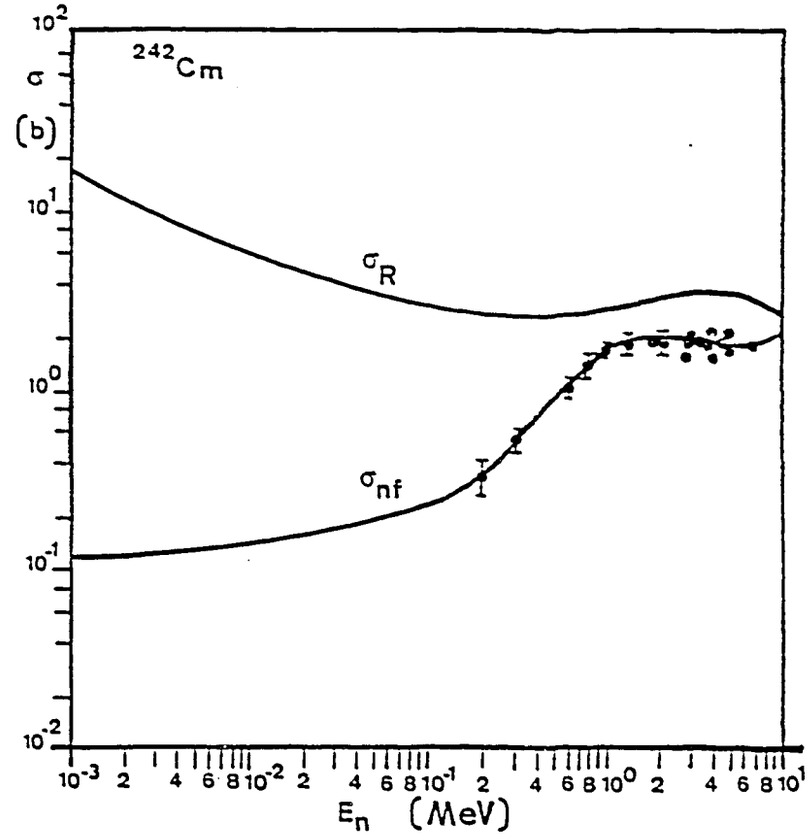

Fig. 3 Neutron cross section σ_R for formation of ^{243}Cm compound nucleus (^{242}Cm+n) and total fission cross section $\sigma_{nf} = P_f \cdot \sigma_R$, obtained by means of deformed optical model calculations with the parameters of ref. (10); the fission probabilities $P_f(E)$ and the experimental data are taken from ref. (13).

Our adopted method is just a practical compromise between such an exact treatment and an unphysical disregard of direct collective effects.

Another point to be outlined, lies in the reliable estimate of different contributions to total fission cross sections, due to the first and second chance fission processes in the energy range of interest here.

Our calculations predict a slightly increasing trend of the (n,f) cross section above the (n,n'f) reaction threshold [16].

In literature different behaviours are empirically deduced, that show a first chance fission cross section with a nearly constant or even decreasing trend. More dramatically, Tuttle [17] suggests

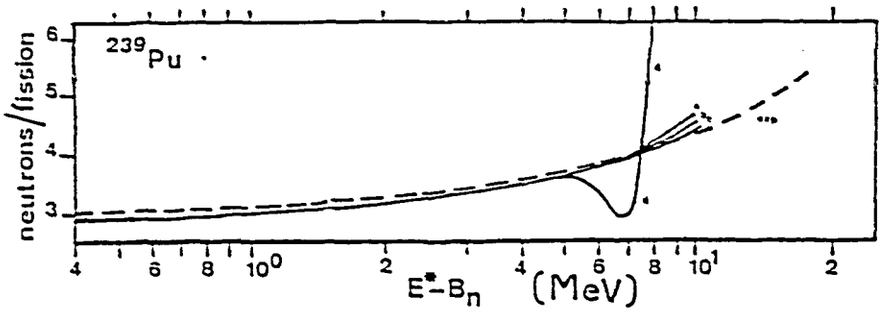

Fig. 4 ^{239}Pu yield of prompt neutrons per fission. Solid lines refer to calculations performed with different assumptions about the first-chance contribution to the total fission reaction, above the (n,n'f) threshold: a) (n,f) slightly decreasing; b) constant; c) slightly increasing (ref.(16)); d) vanishing (ref. (17)). The dashed line fits the experimental data of ref. (18).

a drastic reduction of the (n,f) cross section just above the (n,n'f) threshold and a subsequent greater contribution of the second-chance fission to the total cross section. This estimate is derived from considerations about the experimental number of delayed neutrons. According to Tuttle, a dominant second-chance fission is needed in order to reproduce the values at different excitation energies. However, the experimental data are quite scarce and the analysis of ref.(17) is based on some drastic approximations; for instance, a constant energy-independent yield value is assumed for each of the compound nuclei involved in the calculation. If we perform a similar analysis, but referred to the prompt neutrons in the fission reaction, instead of the delayed ones, we obtain close results of the only Pu-239 yield assuming first-chance contributions increasing, constant or slightly decreasing above the (n,n'f) threshold. Conversely, if we adopt the Tuttle's evaluation, the calculated trend is completely unrealistic. Fig. 4, referring to Pu-239, shows clearly these features. There, the letters a,b,c and d refer to Pu-239 yield calculation on the basis, respectively, of

decreasing, constant, increasing and nearly vanishing (Tuttle's estimate) first-chance fission; the dashed curve fits the experimental total average number of promot neutrons per fission[18].

Some further remarks have to be made about the HF calculations of the total fission cross section.

In our Curium evaluation, the parameters of the double-humped fission barriers were chosen as in ref. (13), where they are deduced from an analysis of measured fission probabilities. Since the outer saddle-point is lower than the inner one, fission cross sections were evaluated in a complete damping approximation, by neglecting the effect of quasibound states in the intermediate well.

Finally, the energy distributions of neutrons emitted in (n,2n), fission and inelastic scattering reactions are approximated by simple evaporative formulae.

For the first-chance fission spectrum a standard Maxwellian curve is adopted:

$$f(E,E') = \alpha\sqrt{E'}\, e^{-E'/\vartheta(E)} \qquad (3)$$

where E(E') is the incident (emitted) neutron energy and $\vartheta(E)$ is an effective temperature; α is a normalization constant.

The energy spectra for neutrons emitted in the reactions (n,n'γ) -- with excitation of the continuum -, (n,2n) and (n,n'f) are represented by evaporation formulae of the following kind:

$$g(E,E') = \beta E'\, e^{-E'/\vartheta(E)} \qquad (4)$$

$\vartheta(E)$ can be interpreted in these cases as the excitation temperature of the residual nucleus after emission of an $E' \simeq 0$ neutron; it has been calculated (4) microscopically in the framework of the finite-temperature NBCS model. For example, in fig. 5a,b,c,d,e and f, ϑ as a function of the excitation

energy E is shown for some reactions, from their effective thresholds up to 15 MeV.

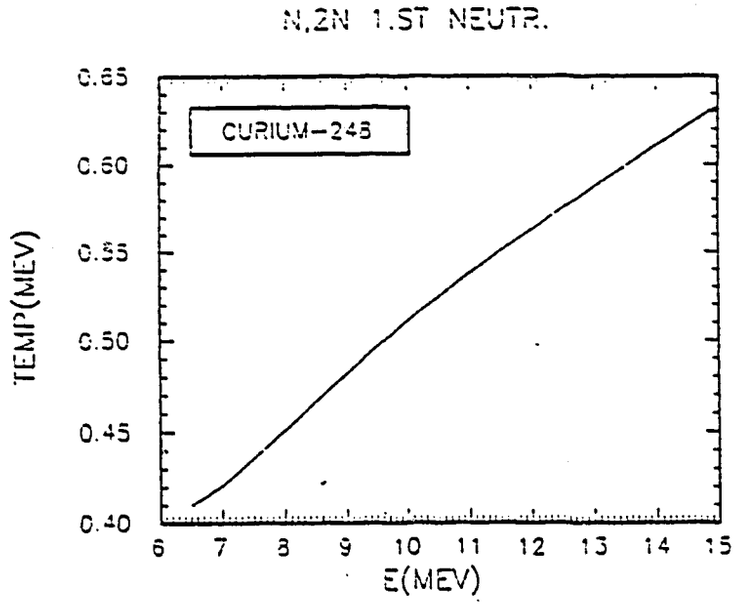

Fig. 5 a

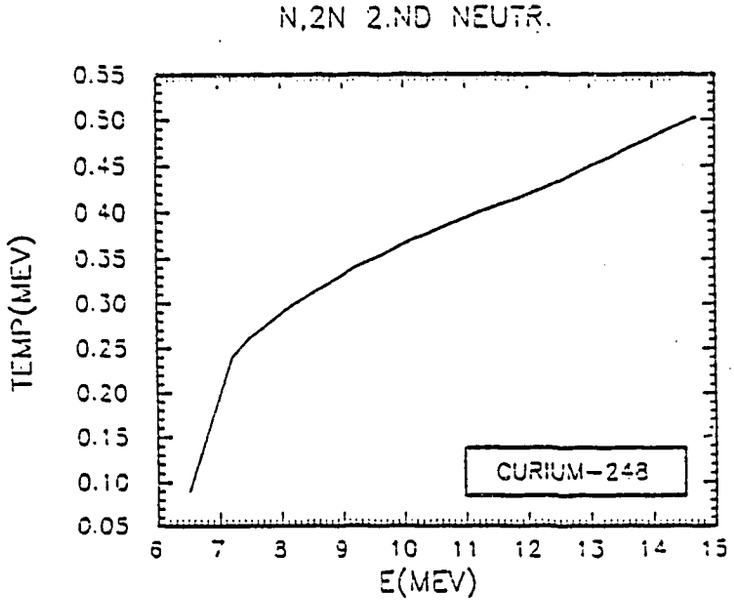

Fig. 5 b

Fig. 5a,b,c,d,e and f) Effective temperature $\vartheta(E)$ versus incident neutron energy E , relative to the energy spectra of emitted neutrons in (n,2n), (n,f), (n,n'f) and (n,n'γ) reactions, respectively.

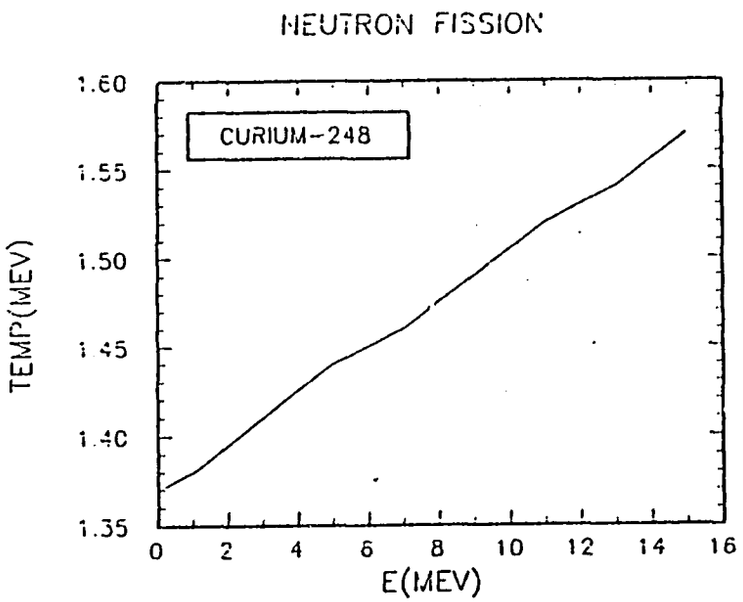

Fig. 5 c

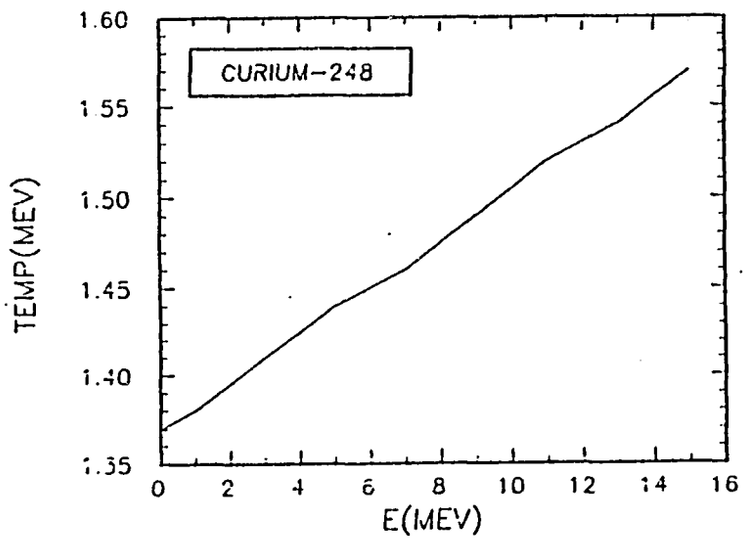

Fig. 5 d

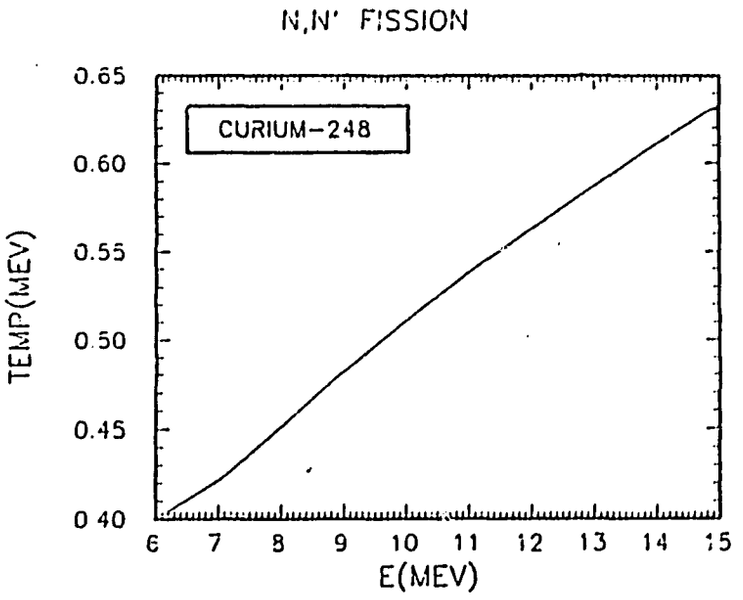

Fig. 5 e

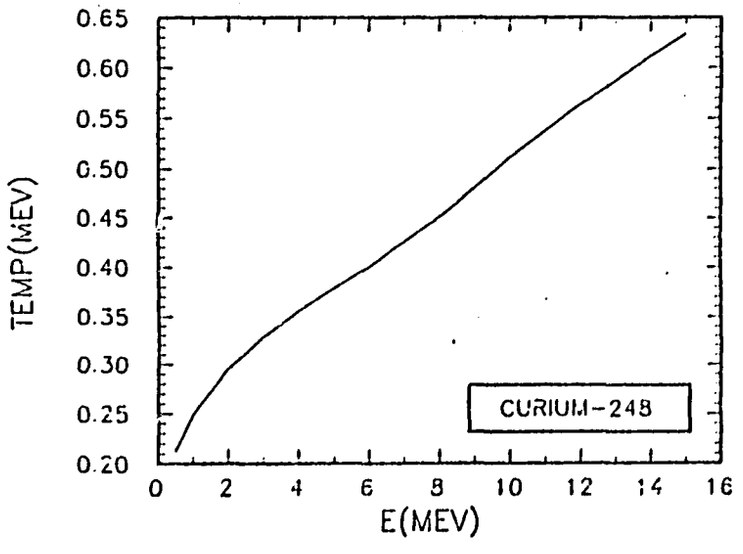

Fig. 5 f

Acknoledgment

We thank Dr. Pietro Santini for his help in performing calculations.

References

1) G. Maino, E. Menapace, M. Motta and M. Vaccari, "Evaluation of ^{242}Cm neutron cross sections from 10^{-5} eV to 15 MeV", report INDC(ITY)-7, May 1982;

G. Maino, T. Martinelli, E. Menapace, M. Motta, M. Vaccari and A. Ventura, "Evaluation of ^{243}Cm neutron cross sections from 10^{-5} eV to 15 MeV", report CNEN-RT/FI (81)23, October 1981;

G. Maino, T. Martinelli, E. Menapace, M. Motta and M. Vaccari, "Evaluation of ^{245}Cm neutron cross sections from 10^{-5} eV to 15 MeV", report CNEN-RT/FI(81)24, October 1981;

G. Maino, E. Menapace, M. Vaccari and A. Ventura, "Evaluation of ^{246}Cm neutron cross sections from 10^{-5} eV to 15 MeV", report INDC(ITY)-8, May 1982;

G. Maino, E. Menapace, M. Vaccari and A. Ventura, "Evaluation of ^{247}Cm neutron cross sections from 10^{-5} eV to 15 MeV", report INDC(ITY)-9, July 1982;

G. Maino, M. Rosetti, M. Vaccari and A. Ventura, "Evaluation of ^{248}Cm neutron cross sections from 10^{-5} eV to 15 MeV", report INDC(ITY)-10, November 1983.

2) G.C. Panini, report CNEN-RT/FI(81)30 (1981).

3) M. Stefanon, Nucl. Instr. and Meth. 174, 243 (1980).

4) G. Maino, M. Vaccari and A. Ventura, Comp. Phys. Comm. 29, 375 (1983).

5) G. Maino and E. Menapace, in Proceed. of the IAEA Advisory Group Meet. on Basic and Applied Problems of Nuclear Level Densities, Brookhaven Nat. Lab. 1983, M.R. Bhat (ed.), BNL-NCS-51694 UC-34c (June 1983), p. 75.

6) A. Arima and F. Iachello, Annu. Rev. Nucl. Part. Sci., 31, 75 (1981).

7) F. Iachello (ed.), "Interacting Bose-Fermi Systems in Nuclei", Plenum, New York (1981).

8) G. Maino, T. Martinelli, E. Menapace and A. Ventura, Lett. Nuovo Cimento 32, 235 (1981);

G. Maino and A. Ventura, Lett. Nuovo Cimento 34, 533 (1982).

9) G. Maino, E. Menapace and A. Ventura, Nuovo Cimento A57, 427 (1980);

V. Benzi, G. Maino and E. Menapace, Nuovo Cimento A66, 1 (1981).

10) L. Zuffi, Nucl. Sci. and Eng. 68, 356 (1978);

G. Maino, E. Menapace, M. Motta and A. Ventura, in Proceed. of the Int. Conf. on Nuclear Cross Sections and Technology, Knoxville 1979, NBS Spec. Publ. 594, p. 500 (1980).

11) T. Tamura, Rev. Mod. Phys. 37, 679 (1965).

12) F. Fabbri and L. Zuffi, report CNEN-RT/FI (69) 7 (1969).

13) B.B. Back, O. Hansen, H.C. Britt and J.D. Garrett, Phys. Rev.C9, 1924 (1974);

B.B. Back, H.C. Britt, O. Hansen and B. Leroux, Phys. Rev. C10, 1948 (1974);

A. Gavron, H.C. Britt, E. Konecny, J. Weber and J.B. Wilhelmy, Phys. Rev. C13, 2374 (1976).

H.C. Britt and J.B. Wilhelmy, Nucl. Sci. and Eng. 72, 222 (1979).

14) F.M. Mann, Hanford report HEDL-TME 76-80 (1976).

15) Y. Kikuchi, "Evaluation of Neutron Nuclear Data for ^{246}Cm and ^{247}Cm", report JAERI-M 83-236 and INDC(JAP)83/L, January 1984.

16) V. Benzi, G. Maino and E. Menapace, Lett. Nuovo Cimento 21, 231 (1978).

17) R.J. Tuttle, Nucl. Sci. and Eng. 56, 37 (1975); in Proceed. of the Consultants' Meeting on Delayed Neutron Properties, Vienna 1979, report INDC (NDS) - 107/G+Special, (August 1979), p. 29.

18) M. Soleilhac, J. Frehaut and J. Gauriau, J. Nucl. En. 23, 257 (1969).

Contributed Paper 17

INVESTIGATION OF NUCLEAR CHARACTERISTICS OF TRANSACTINIDE NUCLEI IN THE USSR

V.A. VUKOLOV
I.V. Kurchatov Institute of Atomic Energy,
Moscow, Union of Soviet Socialist Republics

Abstract

The paper presents a review of experimental results and evaluations of nuclear decay characteristics of transactinium isotopes performed in the Soviet Union in the last two years.

Introduction

A great contribution to systemization of extensive experimental data on nuclear characteristics of transactinides has been made by the International Atomic Energy Agency. Due to the IAEA activity requirements on the accuracy of the data for their usage in various atomic energy fields have been worked out, comparison has been made of the required accuracy with the attained one, and the lists of recommended data on the isotope's decay characteristics are periodically published.

In the Soviet Union a number of works was published for the last decade containing compilation, analysis and estimation of the experimental results on actinides and recommendations on improvement of some characteristics of individual isotopes. In spite of noticeable progress in expanding our knowledge of nuclear properties of actinides, the present state of affairs with these data cannot be considered satisfactory. Some data are either not accurate enough to be used in practice or their reliability is doubtful because of an insufficient number of measurements. Some earlier results require confirmation by using some newer technique.

The present report is a review of experimental results obtained in measuring nuclear characteristics of transactinide isotopes as well as of the data on evaluation (performed by the Soviet specialists for the last two years).

I. Measurement of Half-Lives of Transactinide Isotopes

Table 1 presents the results of measuring the half-lives. Given in the same table are: the decay type, the measurement method, error confidence level p and recent recommended values taken from ref. /8/. All the isotopes from Pu-246 to Es-253 were obtained by exposing the starting elements in the SM-2 high-flux reactor. The purification method used provided that the isotope purity of the samples under investigation was high. Various measurement methods were used. Their reliability was confirmed in a number of check experiments. For example, in measuring Cm-245 the Cm-244 half-life was taken equal to (18.099 $\pm$0.15) years but in the check experiment it turned out to be (18.23 $\pm$0.98) years. The results of the T measurements for Bk-249 agree within the 1.7% limit with earlier measurement data obtained using another method.

The aim of the presented experiments is the verification of the recommended values mostly based on measurements which were made 10 to 15 years ago. Comparisons showed that the results of the considered measurements whose accuracy is comparable with the uncertainty of the recommended values support the latter /8/ well.

Identification of the neutron-rich isotope of Pu-247 and determination of its half-life has been made for the first time. The only publication about the Am-247 production from the α-bombardment of Pu-244 and measurement of the half-life ((24 $\pm$3) min) was made in 1967 /17/.

The measurement of the T-values of U-236 and U-238 spontaneous fission has been made using relatively new method successfully employed in similar investigations. Spontaneous fission events have been detected by coincidence of pulses from fission neutrons in the ^{3}He-gas proportional counters. Within the experimental error the period of spontaneous fission of U-236 agrees with the results obtained from the only measurement made: T = = (2.43 $\pm$0.13)$\cdot 10^{16}$ years /9/. This value has been taken as a re-

Table 1

Isotope	Type of decay	Half-life period ($T \pm \Delta T$)	Measurement method	Notes	References	Recommended values /8/
1	2	3	4	5	6	7
U-236	α	$(2.7 \pm 0.4) \times 10^{16}$ years	By radiation multiplicity	p = 0.99	(1)	$(2.43 \pm 0.13) \times 10^{16}$ years
U-238	α	$(8.3 \pm 0.4) \times 10^{15}$ years	By radiation multiplicity	p = 0.99	(1)	$(8.08 \pm 0.26) \times 10^{15}$ years
Pu-246	β^-	(10.78 ±0.05) days	By fall of intensity of γ-lines with E_γ = = 43.81; 179.94; 223.75; 798.83; 1036.03; 1062.07; 1078.90 keV	p = 0.95	(2)	(10.85 ±0.02) days
Pu-247	β^-	(2.27 ±0.23) days	By fall of intensity of γ-lines with E_γ = = 226 and 285 keV belonging to Am-247	p = 0.95	(2)	-
Am-245	β^-	(122.5 ±0.8) min	By decay curve	Measurements of 7 samples; p = 0.95	(3)	(123.0 ±0.6) min
Am-246m	β^-	(24.7 ±0.7) min	By fall of intensity of γ-lines with E_γ = = 798.83; 1036.03; 1062.07; 1078.90 keV	p = 0.95	(2)	(25.0 ±0.2) min
Am-247	β^-	(23.0 ±1.3) min	By fall of intensity of γ-lines with E_γ = = 285 keV	p = 0.95	(2)	-
Cm-245	α	(8845 ±200) years	(1) By ratio of molar concentrations of isotopes of Cm-245/Cm-244 and their α-activities; (2) By specific α-activity of Cm-245; (3) By ratios of molar concentrations of isotopes of Cm-245/ /Cm-244 produced in their decay $Pu\text{-}240/Pu\text{-}241$ (4) By accumulation of Pu-241	Weighted average by 4 methods: T_α for Cm-244 was taken equal to (18.099 ± ±0.15) years; p = 0.95	(4)	(8500 ±100) years
Bk-249	β^-	(329 ±4) days	By decay curve	Measurements of 30 samples; p = 0.95	(5)	(320 ±6) days
Cf-249	α	(360 ±13) years	By rate of Bk-249 accumulation in sample	Taken: T_β for Bk-249 = (329 ± ±4) days; $I_\alpha / I_\beta = (1.48 \pm 0.12) \times 10^{-5}$; p = 0.95	(6)	(350.6 ±2.1) years
Es-253	α	(20.31 ±0.16) days	By decay curve	Measurements of 20 samples; p = 0.95	(7)	(20.4 ±0.1) days

commended one /8/. The number of the T-measurements of the U-238 spontaneous fission is great. It exceeds 40. These measurements were made by various methods. The data spread is $(6 - 11)\cdot 10^{15}$ years. The last two estimates /8, 10/ differ by 9%, the recommended accuracy being 3%. It is known that one of the main difficulties in determining the spontaneous fission constant for α-active isotopes is to make a correct allowance for light impuruty elements in the sample investigated. An incorrect allowance made for this factor results in a lower value of T due to induced fission by neutrons from the (α, n) reaction on light impurity elements. In the present work the influence of this factor has been checked experimentally by extrapolation of the effect measured using samples of various thickness to the zero thickness. The period value obtained is between the two recommended ones /8, 10/ and agrees with them within the experimental error. The foregoing indicates that the recommended values should be reestimated, the more so that the results of other measurements /11, 12/ are available at present.

II. Measurement of Transactinide Isotopes Radiation Intensity

Two works were carried out for this type of measurements. In ref. /13/ the spectrum of hard γ-radiation of Pu-238 was investigated. The sample activity was determined using the Ge (Li) detector. The absolute γ-ray intensity (with E_γ = 766.4 keV) was measured with a high accuracy and found to be $I_\gamma = (2.05 \pm 0.14)\cdot 10^{-7}$ γ/decay. This value was then used for determining the intensity of other γ-quanta. On the basis of the experimental data for I_γ the α-ray intensity values were calculated for nine levels of U-234 within the energy range of (786.28 - 1085.4) keV. The measurement results are listed in Table 2. The data for I_γ are essentially lower than the recommended values /8, 18/. For example, for the line with E_γ = 766.4 keV whose intensity was measured with

Table 2

E_γ (keV)	Intensity (%) I_γ (ΔI_γ) (13)	Intensity (%) I_γ (ΔI_γ) (8)	Energy of levels (keV)	Intensity (%) I_α (ΔI_α) (13)
99.86	$6.31(75)\cdot10^{-3}$	$7.24(20)\cdot10^{-3}$	786.28	$7.2(11)\cdot10^{-6}$
152.70	$8.57(78)\cdot10^{-4}$	$1.01(20)\cdot10^{-3}$	809.89	$6.7(13)\cdot10^{-5}$
705.6	$5\ (2)\cdot10^{-8}$	$1.4\ (2)\cdot10^{-7}$	849.3	$1.9(4)\cdot10^{-7}$
708.4	$3.5\ (7)\cdot10^{-7}$	$3.8\ (4)\cdot10^{-7}$	851.7	$2.2(2)\cdot10^{-6}$
742.8	$4.6\ (4)\cdot10^{-6}$	$7.6\ (7)\cdot10^{-6}$	926.71	$1.2(2)\cdot10^{-6}$
766.4	$2.05(14)\cdot10^{-5}$	$3.3\ (3)\cdot10^{-5}$	947.9	$1.2\ \cdot10^{-7}$
786.3	$2.8\ (2)\cdot10^{-6}$	$4.8\ (4)\cdot10^{-6}$	1023.84	$3.5\ \cdot10^{-7}$
805.6	$1.4\ (3)\cdot10^{-7}$	$1.8\ (2)\cdot10^{-7}$	1044.51	$1.2(2)\cdot10^{-6}$
808.2	$8\ (1)\cdot10^{-7}$	$1.1\ (1)\cdot10^{-6}$	1085.4	$8.1(11)\cdot10^{-7}$
851.7	$1.0\ (1)\cdot10^{-6}$	$1.9\ (2)\cdot10^{-6}$		
880.5	$1.3\ (3)\cdot10^{-7}$	$2.3\ (3)\cdot10^{-7}$		
883.2	$6.6\ (13)\cdot10^{-7}$	$1.1\ (1)\cdot10^{-6}$		
904.4	$5\ (2)\cdot10^{-8}$	$1.0\ (2)\cdot10^{-7}$		
926.7	$4.9\ (7)\cdot10^{-7}$	$8.3\ (8)\cdot10^{-7}$		
942.0	$3.9\ (9)\cdot10^{-7}$	$6.7\ (7)\cdot10^{-7}$		
946.1	$\leq 8\cdot10^{-8}$	$1.3\ (2)\cdot10^{-7}$		
1001.9	$8.4\ (12)\cdot10^{-7}$	$1.4\ (2)\cdot10^{-6}$		
1041	$2.7\ (6)\cdot10^{-7}$	$2.8\ (3)\cdot10^{-7}$		
1085.4	$1.0\ (3)\cdot10^{-7}$	$1.1\ (2)\cdot10^{-7}$		

special attention there was 1.5-times discrepancy from the recommended value. From the preliminary measurements /15/ a rather close value of $2.18/11/\cdot10^{-7}$ was obtained for the intensity of this line but, unfortunately, this result was absent from the final report /16/. For I_α in most cases a reasonable agreement with the data from the reference book /14/ is observed. The only exception is the level with the energy of 851.7 keV (E_α = 4662 keV) for which the new value is half of that given in ref. /14/.

In work /6/ the ratio of α - and β -probabilities of the Bk-249 decay was measured. The result was obtained by direct measurement of specific α - and β -activity of a radiochemically pure berkelium preparation and was found to be $(1.48 \pm 0.12)\cdot10^{-5}$ with confidence probability of 0.95. The recommended value /8/ is $(1.45 \pm 0.08)\cdot10^{-5}$.

III. Estimation of Nuclear Characteristics of Transactinide Isotopes

Within the framework of international cooperation the Soviet Union (CAJaD) is responsible for evaluation of the nuclear characteristics of nuclei with A = 238, 240, 242, 244. The data on evaluation of properties of nuclei with A = 238, 244 have been published in Nuclear Data Sheets. On the whole the evaluated characteristics of nuclide decay agree with the recommended ones /8/ except for the above-mentioned U-238 isotope. At present the evaluation of properties of nuclei with A = 240 (including the data known up to September, 1983) and with A = 242 (the data, up to October, 1983) has been prepared for publication. As compared to the recommended data /8/ the values of half-life periods for Pu-240, Np-240, Cm-242 have been defined more precisely:

Pu-240	T^{α} = 6.570/6/·10^3 years	T^{α} = 6.537/10/·10^3years/8/	
Np-240	T^{β^-} = 61.9/2/ min	T^{β^-} = 65/3/ min	/8/
Cm-242	T^{sf} = 7.2/2/·10^6 years	T^{sf} = 6.5/6/·10^6 years	/8/

REFERENCES

1. Belenkiy S.N., Skorokhvatov M.D., Etenko A.V. Atomnaya energiya, 1983, v. 52, No. 2, p. 97.
2. Popov Yu.S., Privalova P.A. et al. Radiokhimia, 1983, No. 4, p. 482.
3. Polukhova V.G., Timofeev G.A. et al. Radiokhimia, 1983, No. 4, p. 487.
4. Polukhov V.G., Timofeev G.A. et al. Radiokhimia, 1982, No. 4, p. 490.
5. Polukhov V.G., Timofeev G.A., Levakov B.I. Radiokhimia, 1981, No. 6, p. 884.
6. Polukhov V.G., Timofeev G.A., Levakov B.I. Radiokhimia, 1983, No. 1, p. 92.
7. Polukhov V.G., Timofeev G.A., Elesin A.A. Radiokhimia, 1982, No. 4, p. 494.
8. Lorenz A. Proposed Recommended List of Heavy Element Radionuclide Decay Data, December, 1983, INDC (NDS)-149/NE.
9. Van Gunten H. et al. Phys. Rev., 1981, v. C23, p. 1110.
10. Shurshikov E.N., Filchenkov M.F. et al. Nuclear Data Sheets, 1983, v. 38, No. 2, p. 277.

11. De Carvalho H.C. et al. NIM, 1982, p. 197.
12. Baptista Z.N.R. et al. An. Acad. Brasil. Sienc., 1981, p. 53.
13. Ovechkin V.A., Chesalin V.N., Shkabura I.A. Voprosy atomnoy nauki i tekhniki, ser. Yadernye konstanty, 1983, No. 2(51), p. 39.
14. Tables of Isotopes (ed. Lederer C.M., Shirley V.S.), New-York; Wiley J. and Sons, Inc., 1978.
15. Helmer R.G., Reich C.W. Reports to the DOE Nuclear Data Committee, DOE/NDC-27/U, May, 1982, p. 17.
16. Helmer R.G., Reich C.W. Reports to the DOE Nuclear Data Committee, DOE/NDC-30/U, May, 1983, p. 46.
17. Orth G.J., Daniels W.R. et al. Phys. Rev. Lett., 1967, v. 2, p. 209.
18. Ellis Y.A., Nuclear Data Sheets 21(4),1977,549.

LIST OF PARTICIPANTS

Dr. P. Andersson
University of Lund
Department of Nuclear Physics
Sölvegatan 14
S-223 62 Lund, Sweden

Dr. R. Arlt
IAEA Department of Safeguards
P.O. Box 100
A-1400 Vienna, Austria

Dr. F. Communeau
Service de Physique Neutronique
et Nucléaire
Centre d'Etudes Limeil Valenton
B.P. No. 27
F-941 90 Villeneuve-St.-George
France

Dr. H. Condé
Gustaf Werners Institute
Box 531
S-751 21 Uppsala, Sweden

Dr. N. Coursol
L.M.R.I.
CEA-CEN-Saclay
B.P. No. 2
F-911 90 Gif-sur-Yvette
France

Dr. S. Daroczy
Institute of Experimental Physics
Kossuth University
Bemter 18/A
H-4001 Debrecen, Hungary

Dr. H. Derrien
DRNR/SPCI Bât 320
Centre d'Etudes Nucléaires
de Cadarache
B.P. No. 1
F-131 15 St.-Paul-Lez-Durance
France

Dr. J.E. Frehaut
Commissariat à l'Energie Atomique
Service de Physique Neutronique
et Nucléaire
B.P. No. 12
F-916 80 Bruyères-le-Châtel
France

Dr. A.J. Fudge
Chemistry Division
Atomic Energy Research
Establishment
Harwell, Didcot, Oxfordshire
OX11 ORA, United Kingdom

Dr. S. Ganesan
311 GSB
Reactor Research Centre
Kalpakkam 603 102
Chengalpattu Dt.
Tamil Nadu, India

Dr. C.F. Højerup
Riso National Laboratory
DK-4000 Roskilde
Denmark

Dr. Sin-iti Igarasi
Nuclear Data Center
Japan Atomic Research Inst.
Tokai Research Establishment
Tokai-Mura, Naka-Gun
Ibaraki-Ken 319-11, Japan

Dr. N.B. Janeva
Inst. for Nuclear Research and
Nuclear Energy
Bulgarian Academy of Sciences
Blvd. Lenin 72
Sofia 1113, Bulgaria

Dr. H.H. Knitter
J.R.C. - Central Bureau for
Nuclear Measurements
Steenweg naar Retie
B-2440 Geel, Belgium

Dr. V.A. Konshin
Inst. for Nuclear Engineering of
the BSSR Academy of Sciences
Minsk, Sosny, USSR

Dr. H. Küsters
Kernforschungszentrum Karlsruhe
Institut für Neutronenphysik und
Reaktortechnik
Postfach 3640
D-7500 Karlsruhe, FRG

Dr. H.D. Lemmel
IAEA Nuclear Data Section
P.O. Box 100
A-1400 Vienna, Austria

Dr. A. Lorenz
IAEA Nuclear Data Section
P.O. Box 100
A-1400 Vienna, Austria

Dr. V.N. Manokhin
Centr Po Jad Dannym
Fiziko-Energeticheskij Institut
Obninsk, Kaluga Region, USSR

Dr. B. Neumann
NEA Data Bank
B.P. 9 Bâtiment 45
F-911 90 Gif-sur-Yvette
France

Dr. A.L. Nichols
UKAEA/A50
AEE Winfrith
Dorchester, Dorset
United Kingdom

Dr. R. Paviotti-Corcuera
Instituto de Estudos Avancados
IEAV/CTA
Rodovia dos Tamoios Km 5.5
12200-Sao Jose dos Campos, SP
Brazil

Dr. G. Reffo
C.R.E.E. Clementel
Via Mazzini 2
I-40138 Bologna, Italy

Dr. C.W. Reich
Idaho National Engineering Lab.
EG & G Idaho, Inc.
P.O. Box 1625
Idaho Falls, Idaho 83415, USA

Dr. J.R. Salvy
Commissariat à l'Energie Atomique
Service de Physique Neutronique
et Nucléaire
B.P. No. 12
F-916 80 Bruyères-le-Châtel
France

Dr. A.S. Santamarina
C.E.A./C.E.N. Cadarache
B.P. No. 1
Dept. des Réacteurs à Eau
F-13115 Saint-Paul-Lez-Durance
France

Dr. M. Schatz
Kraftwerksunion
Postfach 3220
Erlangen, FRG

Dr. A. Trkov
Institut Jožef Štefan
Jamova 39
YU-610 00 Ljubljana
Yugoslavia

Dr. B. Trostell
The Studsvik Science Research
Laboratory
S-611 82 Nyköping, Sweden

Dr. R. Vaninbroukx
Central Bureau for Nuclear
Measurements
Steenweg naar Retie
B-2440 Geel, Belgium

Dr. V.A. Vukolov
I.V. Kurchatov Inst. of Atomic
Energy
Ploshchad I.V. Kurchatova
SU-123182 Moscow D-182
USSR

Dr. Zhang Huanqiao
Institute of Atomic Energy
P.O. Box 275
Beijing
People's Rep. of China